TELLURIUM-CONTAINING HETEROCYCLES

This is the fifty-third volume in the series

THE CHEMISTRY OF HETEROCYCLIC COMPOUNDS

THE CHEMISTRY OF HETEROCYCLIC COMPOUNDS

A SERIES OF MONOGRAPHS

EDWARD C. TAYLOR, *Editor*

ARNOLD WEISSBERGER, *Founding Editor*

TELLURIUM-CONTAINING HETEROCYCLES

MICHAEL R. DETTY and (in Part)
MARIE B. O'REGAN

Office Imaging Research and Technical Development
Kodak Imaging Group
Eastman Kodak Company
Rochester, New York

AN INTERSCIENCE® PUBLICATION
JOHN WILEY & SONS, INC.
NEW YORK • CHICHESTER • BRISBANE • TORONTO • SINGAPORE

This text is printed on acid-free paper.

Library of Congress Cataloging in Publication Data:
Detty, Michael R., 1951–
Tellurium-containing heterocycles/Michael R. Detty and (in part) Marie B. O'Regan.
p. cm.—(The Chemistry of heterocyclic compounds; v. 53)
"An Interscience publication."
Includes bibliographical references and index.
ISBN 0–471–63395–X (acid-free)
1. Organotellurium compounds. 2. Heterocyclic compounds.
I. O'Regan, Marie B. II. Title. III. Series.
QD412.T4D48 1994
547'.59—dc20 93–50055

10 9 8 7 6 5 4 3 2 1

The Chemistry of Heterocyclic Compounds
Introduction to the Series

The chemistry of heterocyclic compounds constitutes one of the broadest and most complex branches of chemistry. The diversity of synthetic methods utilized in this field, coupled with the immense physiological and industrial significance of heterocycles, combine to make the general heterocyclic arena of central importance to organic chemistry.

The Chemistry of Heterocyclic Compounds, published since 1950 under the initial editorship of Arnold Weissberger, and later, until Dr. Weissberger's death in 1984, under our joint editorship, has attempted to make the extraordinarily complex and diverse field of heterocyclic chemistry as organized and readily accessible as possible. Each volume has dealt with syntheses, reactions, properties, structure, physical chemistry, and utility of compounds belonging to a specific ring system or class (e.g., pyridines, thiophenes, pyrimidines, three-membered ring systems). This series has become the basic reference collection for information on heterocyclic compounds.

Many broader aspects of heterocyclic chemistry are recognized as disciplines of general significance which impinge on almost all aspects of modern organic and medicinal chemistry, and for this reason we initiated several years ago a parallel series entitled *General Heterocyclic Chemistry*, which treated such topics as nuclear magnetic resonance, mass spectra, photochemistry of heterocyclic compounds, the utility of heterocyclic compounds in organic synthesis, and the synthesis of heterocyclic compounds by means of 1,3-dipolar cycloaddition reactions. These volumes are of interest to all organic and medicinal chemists, as well as to those whose particular concern is heterocyclic chemistry.

It has become increasingly clear that this arbitrary distinction created as many problems as it solved, and we have therefore elected to discontinue the more recently initiated series *General Heterocyclic Chemistry* and to publish all forthcoming volumes in the general area of heterocyclic chemistry in *The Chemistry of Heterocyclic Compounds* series.

Part of the fascination of heterocyclic chemistry, and the challenge in studying this discipline, is probing and understanding the role of the heteroatom(s) in determining chemical and physical properties. The impact of the heteroatom could not be more dramatically illustrated than in the case of tellurium, relative to its lighter chalcogens, as detailed so insightfully in this present volume by Michael R. Detty and his coauthor, Marie B. O'Regan.

EDWARD C. TAYLOR

Department of Chemistry
Princeton University
Princeton, New Jersey

Preface

For one of us (MRD), chemical efforts with organotellurium chemistry and tellurium heterocycles, in particular, have been a continual source of intellectual pleasure for the past 15 years. The numerous differences between the heterocyclic chemistry of tellurium-containing compounds and the heterocyclic chemistry of compounds containing the lighter chalcogens have challenged the mind to find utilities that exploit the differences. For the other of us (MBO'R), contributing a chapter to this work has enabled a transition-metal organometallic chemist to think about main-group organometallic chemistry. Both of us have enjoyed this opportunity to share our perspective.

The authors thank Barb Maxwell in the Kodak Research Libraries for her efforts to keep us as current as possible with respect to new references and Tim Frade for his efforts in copying many of the older references in the literature. The authors also respect the wishes of all those souls specifically requesting not to be acknowledged (but, thanks anyway).

While both authors work for the Eastman Kodak Company, the ideas expressed in this work should not be construed to define past, current, or future research directions of the Eastman Kodak Company. The ideas conveyed are the authors' alone.

MICHAEL R. DETTY AND MARIE B. O'REGAN

Rochester, New York
September, 1994

Contents

TELLURIUM-CONTAINING HETEROCYCLES

This is the fifty-third volume in the series

THE CHEMISTRY OF HETEROCYCLIC COMPOUNDS

Chemistry of Heterocyclic Compounds, Volume 53
Michael R. Detty, Marrie B. O'Regan

CHAPTER I

Tellurium-Containing Heterocycles: Reviews, Distinguishing Features, and Utility

I. HISTORY IN REVIEW(S)

The first organotellurium compound was reported more than 150 years ago with the synthesis of diethyltelluride in 1840.[1] (*Note*: Superscript reference numbers refer to references listed at end of chapter, under "References"; not references listed in text as here.) The area of organotellurium chemistry was slow to develop, but in the last 20 years, numerous reviews have appeared in order to

cover the thousands of papers dealing with organo- and organometallic tellurium compounds:

1. Irgolic, K. J. In *Houben-Weyl Methoden der Organischen Chemie: Organo tellurium Chemistry*, Klamann, D., ed., Georg Thieme, New York, 1990, Vol. E12b.
2. Patai, S., ed., *The Chemistry of Organic Selenium and Tellurium Compounds*, J. Wiley, New York, 1987, Vol. 2.
3. Patai, S.; Rappoport, Z., eds., *The Chemistry of Organic Selenium and Tellurium Compounds*, J. Wiley, New York, 1986, Vol. 1.
4. Irgolic, K. J. *The Organic Chemistry of Tellurium*, Gordon and Breach Science Publishers, New York, 1974.
5. Sadekov, I. D.; Rybalkina, L. E.; Movshovich, D. Ya; Bulgarevich, S. B.; Kogan, V. A. *Uspekhi Khimii* **1991**, *60*, 1229.
6. Petragnani, N.; Comasseto, J. V. *Synthesis* **1991**, 897.
7. Petragnani, N.; Comasseto, J. V. *Synthesis* **1991**, 793.
8. Sadekov, I. D.; Rivkin, B. B. *Khim. Geterostsikl. Soedin*, **1991**, 291.
9. Sadekov, I. D.; Abakarov, G. M.; Sadekova, Y. I.; Minkin, V. I. *Sulfur Reports* **1986**, *6*, 15.
10. Fringuelli, F.; Marino, G.; Taticchi, A. *Adv. Heterocycl. Chem.* **1977**, *21*, 119.

As the area of organotellurium chemistry has developed, the numbers of papers describing tellurium-containing heterocycles have increased as well. Saturated six-membered rings containing one tellurium atom (tellurane **1**) are among the oldest studied tellurium-containing heterocycles through the research of G. T. Morgan and colleagues in the 1920s.[2,3] Unsaturated analogs of the telluranes, however, were not prepared until the 1980s. Phenoxtellurine (**2**) was first prepared by Drew in 1926,[4] and tetrahydrotellurophene (**3**) was first prepared by Morgan and Burstall in 1931.[5] While these simple tellurium-containing heterocycles have been known for at least 50 years, other simple tellurium-containing heterocycles have only recently been prepared or remain unknown [e.g., monocyclic 1,3-tellurazole (**4**)].

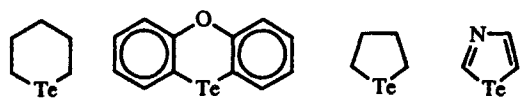

1 **2** **3** **4**

The vagaries of the syntheses of tellurium-containing heterocycles are illustrated by the development of the tellurophene nucleus. Although tetrahydrotellurophene (**3**) was first prepared in 1931[5] and dibenzotellurophene (**5**) was first prepared in 1936,[6] very few papers concerning these molecules have appeared in the ensuing 63 years. Tellurophene (**6**), on the other hand, was first prepared in

1966[7] and a major review (Fringuelli, et al., in the list above) appeared in 8 years. The benzo analog **7**, another simple heterocycle, was not prepared until 1971.[8]

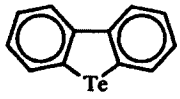

5

6

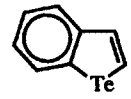

7

The development of the chemistry of tellurium-containing heterocycles in the last 25 years has been sufficiently rapid to warrant separate reviews as well as inclusion as discrete sections in other reviews. In the list presented above, the reviews devoted in their entirety to tellurium-containing heterocycles are Sadekov and Rivkin, Sadekov, et al., and Fringuelli, et al. and those with chapters dedicated to tellurium-containing heterocycles include Irgolic (Klamann, ed.); Patai, ed.; and Patai and Rappoport, eds. in the preceding list. The other reviews in the preceding list also describe tellurium-containing heterocycles and their reactions, but not in a systematic way. The series below contains chapters devoted to the synthesis, chemistry, and properties of tellurium- and selenium-containing heterocycles and is developed in a systematic way.

11. Katritzky, A. R.; Rees, C. W., eds.; *Comprehensive Heterocyclic Chemistry: The Structure, Reactions, Synthesis and Uses of Heterocyclic Compounds*, Pergamon, New York, 1984.

What is the need, then, for another review of tellurium-containing heterocycles? The field continues to develop rapidly, and numerous references have appeared since the more recent reviews in the lists presented above. The differences in the properties of series of heterocycles, where only the heteroatom varies, are rapidly becoming clear. Advances in organometallic chemistry have created new types of tellurium-containing heterocycles where tellurium is bonded to other metals and pseudo-metals. Finally, the "real-world use" of tellurium-containing heterocycles is beginning. This is perhaps reflected in the appearance of manuscripts devoted to the applications of tellurium-containing heterocycles and in the appearance of patents, where tellurium-containing heterocycles are not part of a boiler plate, but are described in detail. In these examples, the unique properties of tellurium are necessary for the application.

II. DISTINGUISHING CHARACTERISTICS OF THE TELLURIUM ATOM IN TELLURIUM-CONTAINING HETEROCYCLES

A. Electronegativity

Tellurium is the most electropositive of the chalcogen elements with a Pauling electronegativity of 2.1.[9] This value can be compared to electronegativities

of 3.5 for oxygen, 2.5 sulfur, and 2.4 for selenium.[9] One consequence of the low electronegativity of tellurium is an inverted polarization of the chalcogen–carbon bond as one moves down the periodic table from oxygen to tellurium. The tellurium–carbon bonds are polarized $Te^{\delta+}$—$C^{\delta-}$, while oxygen–carbon bonds are polarized $O^{\delta-}$—$C^{\delta+}$. Chemically, the difference in polarization of the bond is manifested in differing chemistry between telluro ethers and ethers. As an example, treating anisole with HBr gives phenol and bromomethane, while treating phenyl methyl telluride with HBr gives phenyltellurenyl bromide and methane.

B. Covalent and van der Waals Radii and Inter- and Intramolecular Interactions

Tellurium is significantly larger than the other chalcogen atoms with a covalent radius of 1.36 Å[9] and a van der Waals radius of 2.06 Å.[10] Because the tellurium atoms of tellurium-containing heterocycles are large and polarizable, intermolecular interactions between tellurium atoms tend to be strong, as found in 1,3-ditellurole (**8**). In crystal structures of 1,3-ditellurole (**8**),[11] Te···Te intermolecular interactions result in a three-dimensional polymeric array of tellurium atoms. The distances of the Te···Te interactions are 3.864 and 3.865 Å, which are significantly shorter than twice the van der Waals radius of tellurium: 4.12 Å. In 1,3-ditellurole (**8**), the interacting atoms are also in stereochemically significant positions. These two criteria have been given by Alcock as evidence for the formation of secondary bonds.[12]

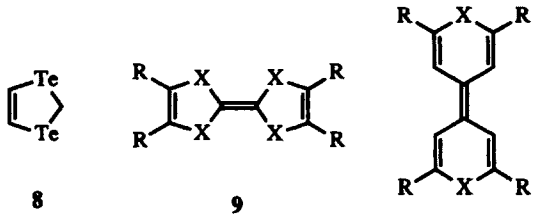

8 **9** **10**

X = O, S, Se, Te

The large size of tellurium also leads to less effective overlap of the heteroatom orbitals with an adjacent carbon π framework, which leads to higher orbital energies. In donor molecules such as the tetrachalcogenafulvalenes (**9**)[13–16] and (chalcogenopyranyl)chalcogenopyrans (**10**),[17,18] the first oxidation potential becomes more positive, and the difference between first and second oxidation potentials decreases as the heteroatom increases in size from oxygen to tellurium. These trends are opposite those expected from electronegativity differences among the heteroatoms, but are consistent with the premise that less effective overlap with the π framework both raises the energy of the first oxidation and promotes less effective communication between the heteroatoms.

In chromophores where the chalcogen atom is in the conjugation with π bonds, the wavelength of the tellurium-containing chromophore is at a longer wavelength than chromophores containing a lighter chalcogen atom. In dye molecules such as the chalcogenapyrylium dyes **11**[19,20] and the cyanine dyes **12**[21,22] raising the energy of the lone pair of electrons on the heteroatom leads to a lower-energy n–π^* transition, which leads to longer-wavelength-absorbing dyes. In dyes **11**, for example, the wavelength of the absorption maximum increases from 550 nm for the pyrylium dye to 650 nm for the telluropyrylium analogue.

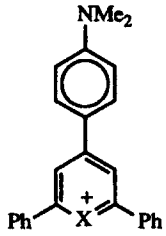

11

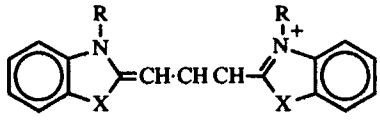

12

X = O, S, Se, Te

C. Hypervalent Bonding

The metallic character of tellurium dominates the geometry of organotellurium compounds. In organotellurium(II) compounds where one of the ligands is highly electronegative, tellurium(II) is stabilized by forming a bonding arrangement with an additional electronegative ligand to give a three-center, four-electron bond.[23–25] This bonding arrangement requires a nearly linear array of the metal and two ligands and results in approximately half of a covalent bond from tellurium to each ligand. The electronegative ligands occupy axial sites in a trigonal–bipyramidal array, while the equatorial sites are occupied by the bond to carbon and two lone pairs of electrons on tellurium. Such "hypervalent" bonding leads to molecules with cyclic geometry and long bonds, which constitute new classes of tellurium-containing heterocycles.[26] Illustrative examples of these heterocycles with a hypervalent bond in the ring are 2-acetylphenyltellurenyl bromide (**13**),[27] 1,5-diphenyl–dioxatellurapentalene **14**,[28] and oxatellurolylium chloride **15**.[29] Although hypervalent sulfur and selenium analogs are known, they are far fewer in number than the number of hypervalent organotellurium compounds.

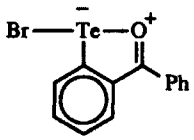

13

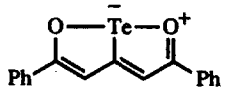

14

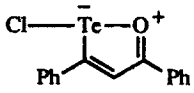

15

D. Higher Oxidation States, Ligand Exchange, and Reductive Elimination

The tellurium atom of tellurium-containing heterocycles is easily oxidized from tellurium(II) to tellurium(IV). A "diagnostic" reaction for the formation of a new tellurium-containing heterocycle is the oxidation of the tellurium atom of the ring with the halogens to give tellurium(IV) derivatives of the heterocyclic ring. The bonds from the halogens to tellurium are linear three-center, four-electron bonds. The geometry around tellurium is trigonal–bipyramidal with the halide ligands occupying axial sites and the ring bonds to tellurium and a lone pair of electrons occupying equatorial sites.

Unlike organosulfur and organoselenium compounds, which have isolable sulfoxide and selenoxide states, respectively, organotellurium compounds rarely have a discrete "oxide" state such as the telluroxide shown in Scheme 1. Typically, the telluroxide is hydrated to give the dihydroxytellurane, which shares the trigonal–bipyramidal geometry of other hypervalent organotellurium compounds.[30]

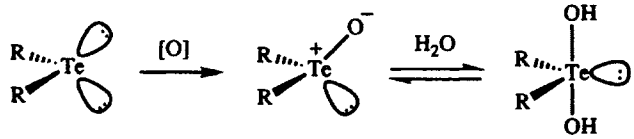

Scheme 1

Even the hypervalent heterocyles like **14** and **15** can be oxidized to tellurium(IV) derivatives. In the case of trigonal–bipyramidal complexes, oxidative addition of halogens generates an octahedral tellurium(IV) array such as that found in **16**[28] and **17**.[31] In these molecules, 2 three-center, four-electron bonds account for the bonding between the electronegative ligands and tellurium. The tellurium–carbon bond and one lone pair of electrons occupy the remaining octahedral sites.

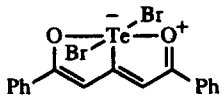

16

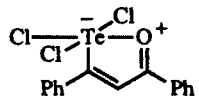

17

The electronegative ligands to tellurium in tellurium(IV) heterocyclic derivatives and in trigonal–bipyramidal tellurium(II) heterocyclic derivatives undergo nucleophilic ligand-substitution reactions. A variety of different kinds of ligands, which vary in electronegativity, size, thermal stability, and photochemical stability, can be incorporated in the ligand field of these heterocycles. Such variation in structure is not routinely found in analogous selenium- and sulfur-containing heterocyclic compounds.

Organotellurium(IV) compounds with highly electronegative ligands can exchange their ligands with a tellurium(II) compound to generate a new tellurium(IV) compound as illustrated in Scheme 2. This process was first observed in dihalodiaryltellurium(IV)/diaryltellurides[32,33] and was subsequently observed in 1,1-dihalotelluropyrans/telluropyrans[34] and 1,1-dihydroxytelluropyrans/telluropyrans.[35] The exchange of oxidation states and ligands in these systems was found to proceed via both first- and second-order processes as illustrated in Scheme 2. The order of the reaction is also dependent on the polarity of the solvent with more polar solvents promoting first-order behavior.

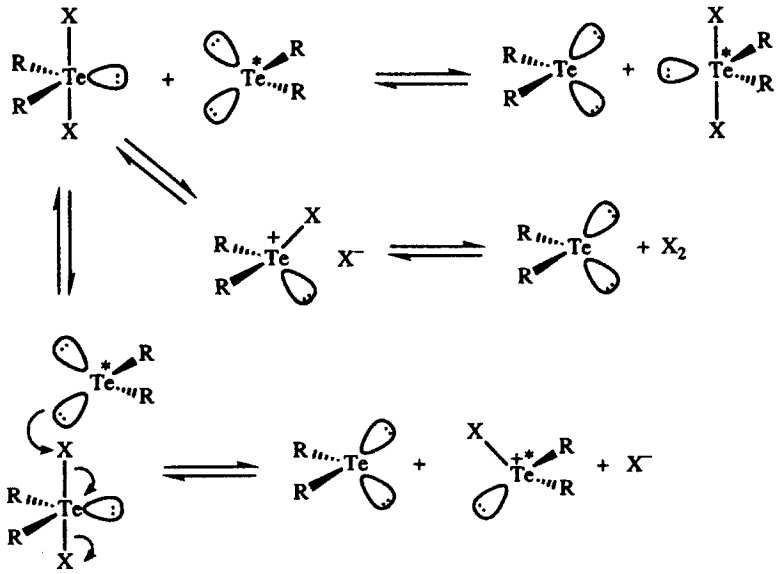

Scheme 2

In addition to exchange of ligands and transfer of oxidation state, tellurium-containing heterocycles with the tellurium(IV) oxidation state can also undergo thermal, reductive elimination of the electronegative ligands to give a tellurium(II) center and coupled, oxidized ligands. As shown in Scheme 3, 1,1-bis(dithiocarbamato)- and 1,1-bis(alkoxydithioxanthato)tetrahydrotellurophenes undergo reductive–elimination reactions on heating to generate tetrahydrotellurophene and a disulfide bond joining the two ligands.[36,37] Reductive elimination of chlorine from 1,1-dichlorotelluropyranyl groups[38] and reductive elimination of hydrogen peroxide from 1,1-dihydroxytelluropyranyl groups[35] generate telluropyrylium dyes as shown in Scheme 3. In the latter two systems, chloride and hydroxide, respectively, were found to act as catalysts for the reductive–elimination reactions. The mechanisms involved in thermal reductive elimination should be similar to the mechanisms of ligand exchange shown in

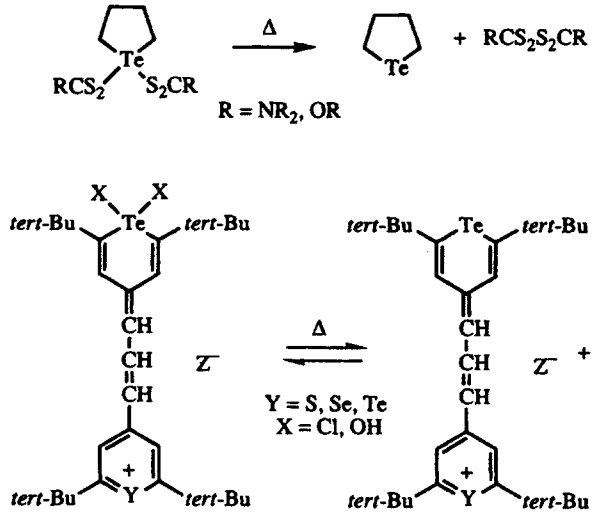

Scheme 3

Scheme 2. This rich chemistry is not found in heterocycles based on the lighter chalcogens.

Tellurium(IV) derivatives of heterocyclic systems with halide, hydroxide, or pseudohalide ligands are easily reduced electrochemically to the tellurium(II) analog of the heterocycle and two equivalents of halide, hydroxide, or pseudohalide.[28,31,34,39] The reductions as monitored by cyclic voltammetry are irreversible, two-electron waves.

Kinetically, tellurium-containing heterocycles react much more rapidly with oxidants such as chlorine, bromine, iodine, singlet oxygen, and ozone than the corresponding heterocycles incorporating the lighter chalcogens.[40,41] In the chalcogenopyrylium dye series **18**, the tellurium-containing dyes have second-order rate constants for reaction with these oxidants that are on the order of 10^9 L mol^{-1} s^{-1} or greater. Reaction is at the tellurium atoms to give oxidation to tellurium(IV). With those dyes that do not contain tellurium, second-order rate constants are orders of magnitude smaller and oxidation of the carbon π framework, not oxidation of the heteroatom, is observed.

E. Heavy-Atom Effects on Physical and Photophysical Properties

The spin–orbit coupling constant associated with an atom increases as a function of Z^4, where Z is the atomic number of the atom in question.[42] Obviously, then, the physical and photophysical properties of tellurium-containing heterocycles should reflect large contributions from spin–orbit effects relative to heterocycles containing only the lighter chalcogens. In measurements of excited-state lifetimes of chalcogenopyrylium dyes **18**, both singlet and triplet

lifetimes decrease as a function of increased spin–orbit effects.[41] The rates of intersystem crossing in these molecules are affected roughly two orders of magnitude more strongly than rates of internal conversion back to ground state. Thus, even though singlet and triplet lifetimes are short in telluropyrylium compounds relative to other chalcogenopyrylium compounds, triplet yields are large relative to analogs incorporating the lighter chalcogens because of accelerated rates of intersystem crossing.

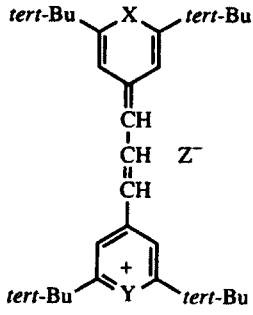

18

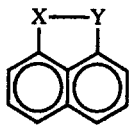

19

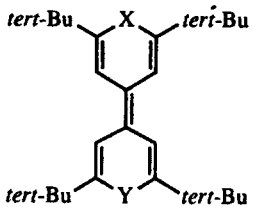

20

X, Y = O, S, Se, Te

The quenching of singlet oxygen by organochalcogen compounds was found to be a function of Z^4.[43] Interestingly, the quenching constants, k_Q, for these compounds and the rates of intersystem crossing, k_{isc}, for dyes **18** were found to be identical functions of Z^4 where rates increased with atomic number,[44] which is indicative that spin–orbit interactions are determining in both processes.

Spin–orbit parameters also appear in the EPR (electron paramagnetic resonance) spectra of tellurium-containing heterocycles. In two series of compounds, **19**[45] and **20**,[18] line widths and g values of the cation radicals increase as the atomic number of the chalcogen atoms in the molecules increases. The g values are linear functions of the spin–orbit coupling constants in these systems, which is indicative that the g values are also functions of Z^4. In most examples, EPR hyperfine structure from protons is lost in the line broadening of radical ions of tellurium-containing heterocycles.

F. Isotopes and Mass Spectral Fragmentation

In the mass spectra of tellurium-containing molecules, the tellurium-containing fragments are easy to recognize from the isotope pattern of tellurium. Six major isotopes are observed at m/e 122 (2.5% natural abundance), 124 (5%), 125 (7%), 126 (18%), 128 (32%), and 130 (34%) as shown in Figure 1. In tellurium-containing heterocycles incorporating more than one tellurium atom, the tellurium containing fragments have very complicated isotope clusters as illustrated in Figure 2 for Te_2-containing molecules and in Figure 3 for Te_4-containing molecules. The nominal mass in the parent-ion clusters is based on

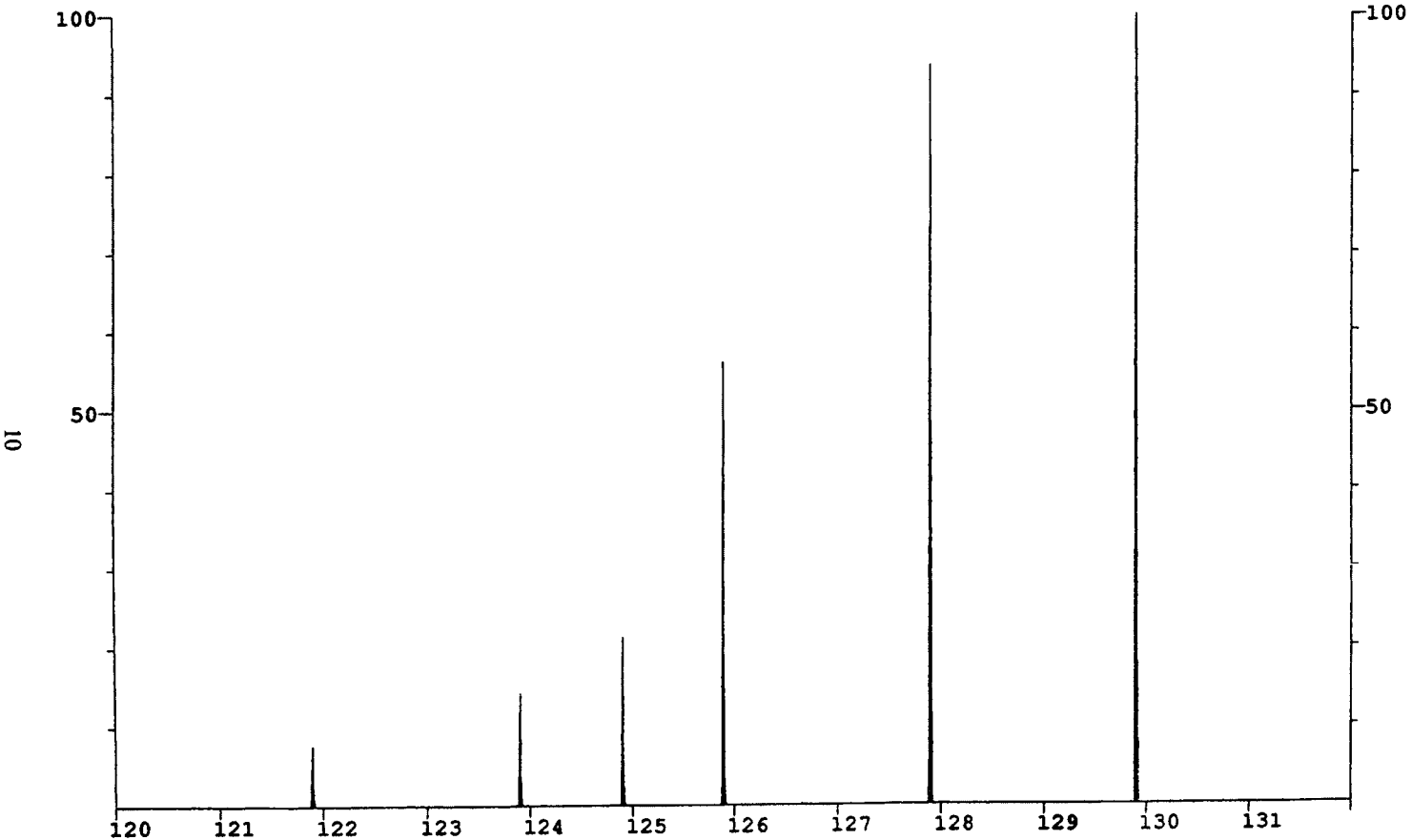

Figure 1. Tellurium isotope pattern for organotellurium compounds containing one tellurium atom.

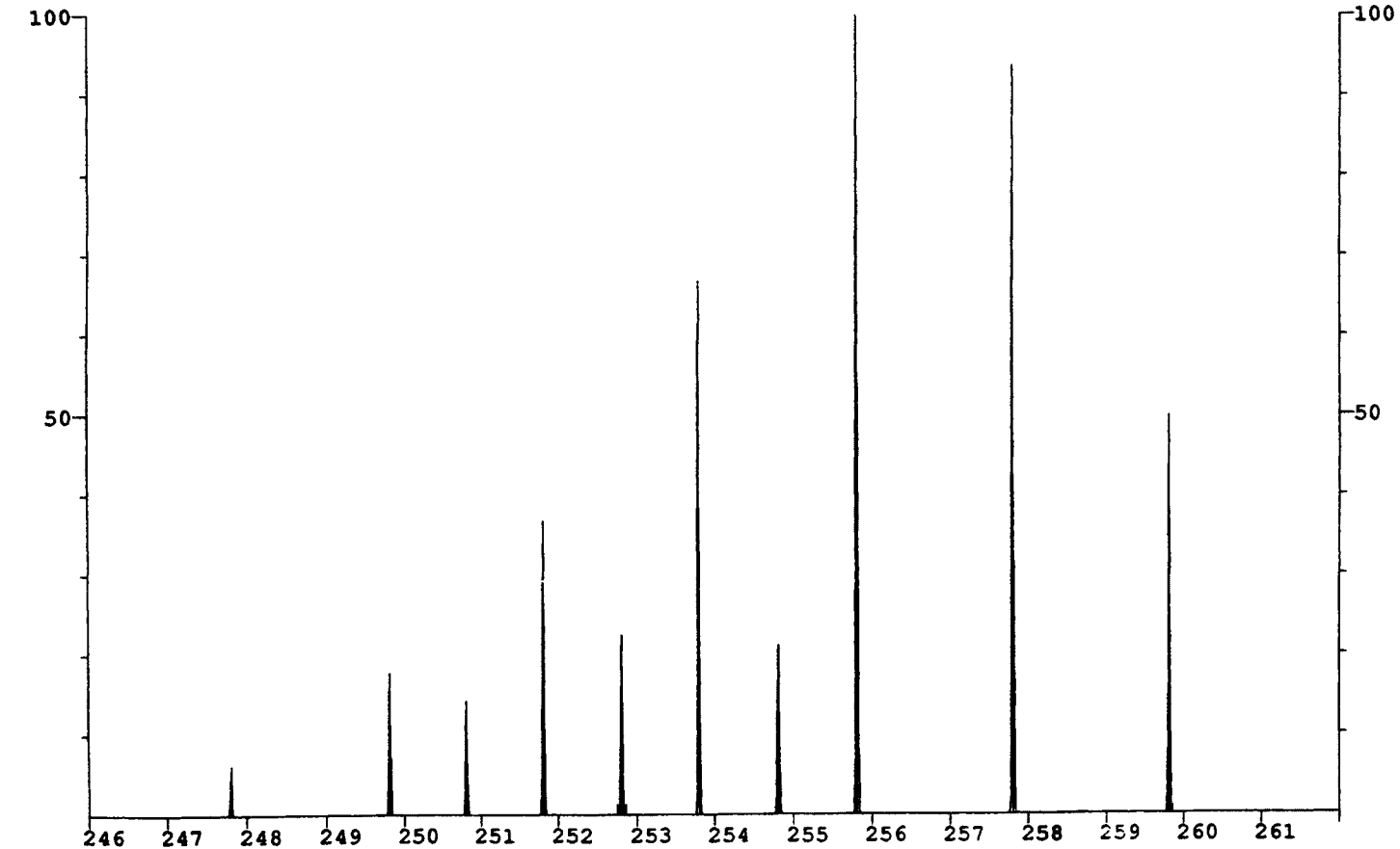

Figure 2. Tellurium isotope pattern for organotellurium compounds containing two tellurium atoms.

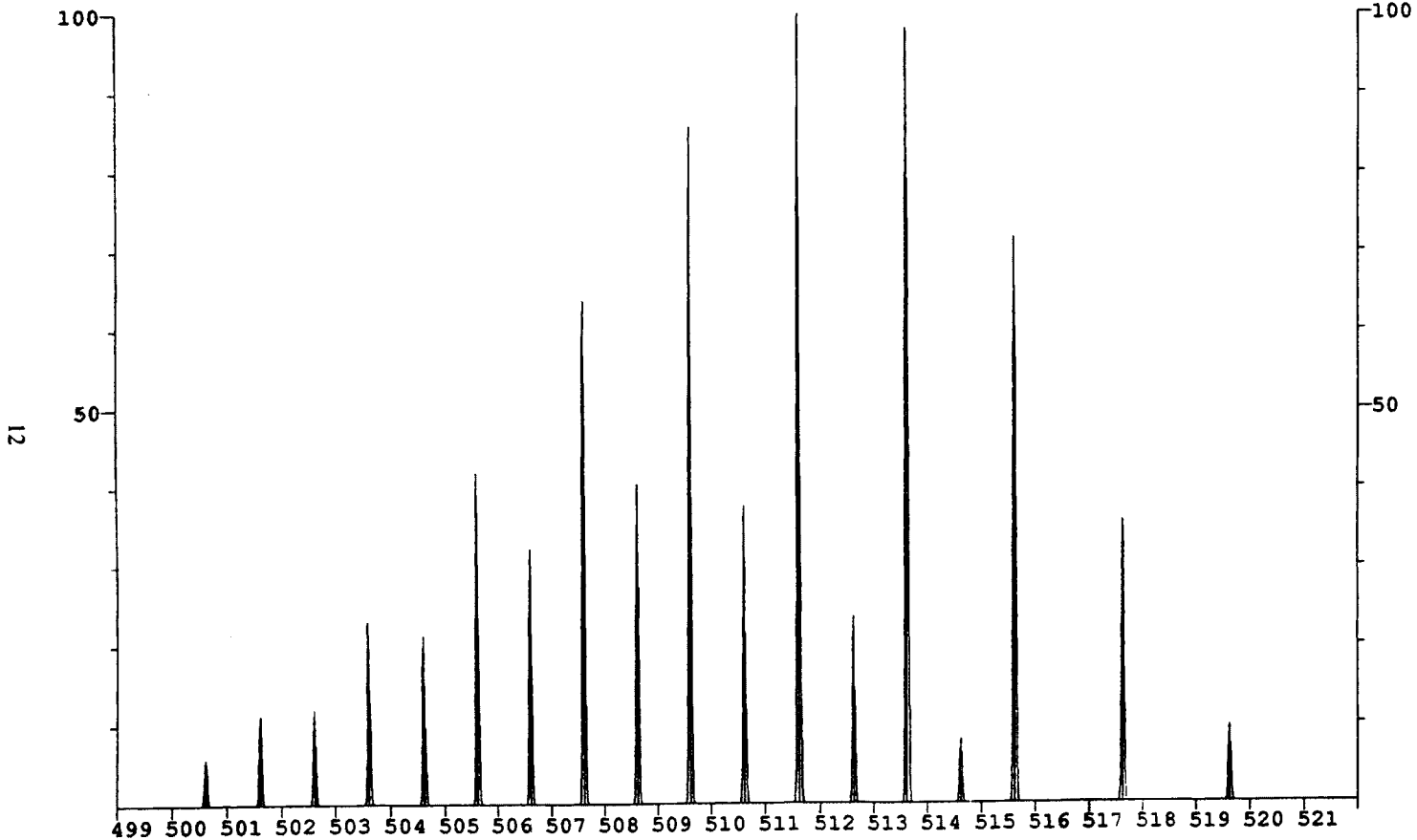

Figure 3. Tellurium isotope pattern for organotellurium compounds containing four tellurium atoms.

^{130}Te for all tellurium atoms in the molecule, but the intensity of this peak diminishes with increasing numbers of tellurium atoms in the molecule as illustrated sequentially in Figures 1–3.

G. Isotopes and Multinuclear Nuclear Magnetic Resonance (NMR)

Tellurium has two isotopes that are NMR-active: ^{123}Te and ^{125}Te.[46,47] The former is weakly radioactive (half-life of approximately 10^{13} years), has a spin $\frac{1}{2}$ nucleus, and is present in about 0.87% natural abundance. The latter is also a spin $\frac{1}{2}$ nucleus but present in nearly 7% natural abundance. The frequency of ^{125}Te is 0.28 that of ^{1}H and has a receptivity 12.5 times that of ^{13}C. In short, ^{125}Te is an easy nucleus to observe with both high receptivity and high natural abundance.

The ^{1}H NMR spectra of organotellurium compounds are characterized by small "side bands" associated with $^{2}J_{Te-H}$ coupling from the natural abundance of ^{125}Te for those molecules where tellurium is bonded to a proton-bearing carbon. The $^{3}J_{Te-H}$ coupling is also sometimes observed. In tellurium-containing heterocycles, the natural-abundance ^{125}Te satellites can help assign ^{1}H NMR chemical shifts. The $^{1}J_{Te-C}$ coupling constants are large (162–531 Hz)[46] and $^{2}J_{Te-C}$ coupling constants are an order of magnitude smaller, but both can be identified from the natural-abundance ^{125}Te satellites. Ditellurole **8** has been prepared in both mono- and di-^{125}Te-enriched forms, which allowed the detailed analysis of all tellurium couplings in these molecules, including the $^{2}J_{Te-Te}$ coupling of 260.3 Hz.[48]

8-^{125}*Te*

8-^{125}*Te*.^{125}*Te*

III. UTILITY OF TELLURIUM-CONTAINING HETEROCYCLES

In this section, the emerging utilities of tellurium-containing heterocycles are considered. Specifically excluded in this section are the synthetic uses of tellurium-containing heterocycles in organic and organometallic chemistry. These subjects are discussed in the appropriate chapters for the heterocycles.

A. Tellurium-Containing Heterocycles as Organic Conductors

Conducting complexes of tetratellurafulvalenes **9** have been found to display metallic behavior.[49–55] Although superconductivity has not yet been observed

in tellurium-containing heterocycles, the metallic behavior of complexes of tetratellurafulvalenes **9** is maintained to 5 K. The extremely short intermolecular tellurium–tellurium contacts in stacks of these molecular systems (3.54 Å for **21** as its 3 : 2 perchlorate complex) may be responsible for the high conductivities of some of these complexes.

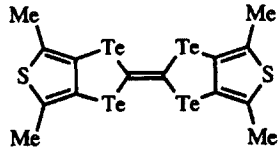

21

Although the perchlorate salt of **21** is a one-dimensional conductor, there are many contacts between heteroatoms in molecules of this type that are less than van der Waals radii. For the perchlorate complex of **21**, there are no fewer than 14 tellurium–tellurium contacts that are less than van der Waals radii apart. Although the 3 : 2 perchlorate complex is a one-dimensional conductor, the networks of intermolecular tellurium–tellurium contacts in molecules of this type may lead to two- and three-dimensional conductivity. Superconductivity has been observed in tetraselenafulvalenes with extended heteroatom interactions.[56,57]

Conducting polymers of organic and inorganic monomers have attracted considerable attention since the discovery of superconductivity in $(SN)_n$[58] and the insulator–metal transitions in doped polyacetylene $[(CH)_n]$[59]. Heterocyclic polymers such as polypyrrole, polythiophene, and polyselenophene have been prepared with a wide range of electrical properties.[60] The electrical conductivity of polythiophenes has been measured to be as high as $10^2\ S\,cm^{-1}$, while the electrical conductivity of polyselenophene was found to be relatively low. Polytellurophene (**22**) has been prepared, and doped films of this material have shown conductivities on the order of $10^{-6}\ S\,cm^{-1}$.[60] Polybenzotellurophene (**23**) has been prepared, and iodine-doped films have shown conductivities as high as $10^2\ S\,cm^{-1}$.[61] Again from the short, intermolecular tellurium–tellurium contacts, polymeric materials based on tellurium-containing heterocycles as monomers may show enhanced multidimensional conducting properties.

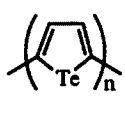

22

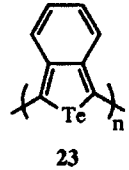

23

B. Applications of Infrared-Absorbing Dyes Based on Tellurium-Containing Heterocycles

Applications of infrared-absorbing dyes include heat generation in optical recording media and thermal printing, sensitization for charge-generation layers in electrophotographic applications, filter systems for near-infrared-emitting diode lasers, and sensitization for near-infrared silver halide photography and photodynamic therapy.[62] Infrared-absorbing dyes based on tellurium-containing heterocycles have been utilized in all these applications.

1. Optical Recording

Tellurium-containing dyes **18** (Te,Te; Te,Se; Te,S) have been utilized in write-once–read-many applications for optical recording.[63] These dyes have extremely high extinction coefficients in solution ($\varepsilon \geq 285{,}000$ L mol^{-1} cm^{-1}) with λ_{max} in the range 770–830 nm. Furthermore, increased spin–orbit interactions improve the efficiency of converting light energy into heat energy. The heat generated by absorption of light from the write laser heats a binder above its glass-transition temperature and creates a "pit." If this chemistry occurs on a highly reflective support, the "pit" changes the reflectivity of the medium and thus can be read as a dark mark on a highly reflective background.

A new method of optical recording in which an infrared-absorbing dye is generated on exposure to the write laser has been demonstrated only with tellurium-containing heterocycles.[64,65] Oxidative addition of chlorine or bromine to tellurium-containing dyes **18** gives the tellurium(IV) dyes **24**. The dyes **24** are coatable from organic solvents, and their absorption maxima are shifted approximately 300 nm to the blue as a consequence of removal of a tellurium *p* orbital from conjugation with the π framework. The oxidized dyes are transparent at wavelengths where gallium arsenide diode lasers emit. Consequently, optical recording media may be highly reflective at the operating wavelengths of the read laser.

Dyes **24** undergo thermal reductive elimination of halogen to generate the corresponding dyes **18** as shown in Scheme 4. At high concentrations in a binder such as those found in optical recording media, the write laser triggers the thermal reductive elimination reaction, and the released halogen is removed irreversibly by reaction with the trimethine bridge to generate the halogen-containing dyes **25**. The dyes **25** are shifted bathochromically by a few nanometers from the corresponding dyes **18** (Te,Y). Optical recording media based on these reactions require a single layer, are first-order in their kinetics with $\Delta H^{\ddagger}$ of approximately 20 kcal mol^{-1} and $\Delta S^{\ddagger}$ of approximately -10 cal mol^{-1} K^{-1},[38] and change reflectivity through increased absorption of the light from the read laser. As shown in Fig. 4 for a series of long and short recorded marks, the carrier : noise ratio is high (≥ 60 dB) with this method.

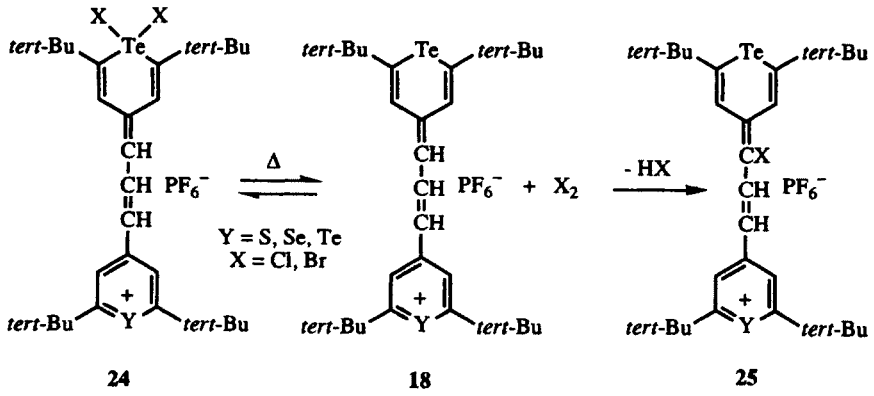

Scheme 4

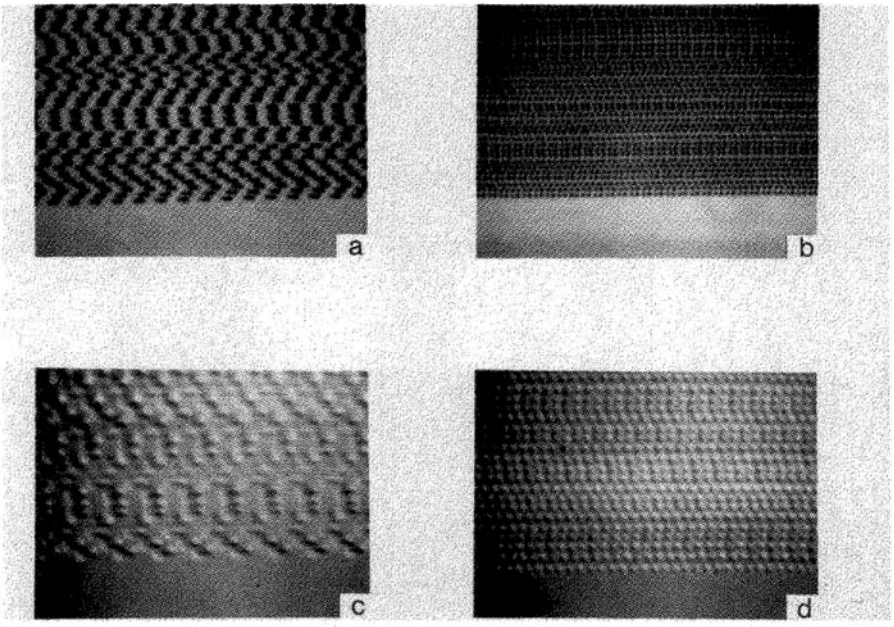

Figure 4. Recorded long [(*a*), 10–15 μm] and short [(*b*), 1–3 μm] marks created by irradiation of **24** (X = Br, Y = S) in a monomeric glass support on a gold reflective layer with a 788-nm diode laser as viewed by brightfield microscopy. The backside of the gold layer for (*a*) is shown in (*c*), and the backside of the gold layer in (*b*) is shown in (*d*) as viewed by DIC microscopy.

2. *Thermal Printing*

In thermal printing applications, three or four different near-infrared-emitting diode lasers are utilized to record the tricolor image. (The fourth is for

registration of a true black.) In such applications, good color separation is achieved by having a multilayer or dispersion package containing a series of nonoverlapping, infrared-absorbing dyes, which absorb specific wavelengths of light and convert light efficiently into heat. The squarylium dyes in general are characterized by narrow absorption bands and high extinction coefficients. The series of squarylium dyes **26** based on the 2,6-di-*tert*-butylchalcogenopyrylium nuclei provides excellent characteristics for multicolor, thermal printing based on the distinct bathochromic shifts observed as the chalcogen atoms increase in size.

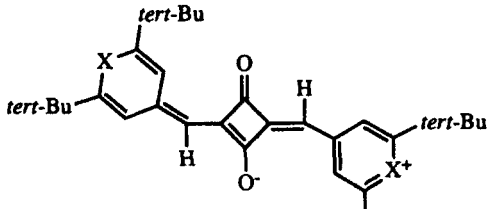

26a, X = O
26b, X = S
26c, X = Se
26d, X = Te

The pyrylium and thiopyrylium analogs **26a** and **26b**, respectively, have been known for several years and have found utility in a variety of applications, including thermal printing.[66,67] The wavelengths of absorption for these two dyes have maxima at 713 nm for **26a** and 804 nm for **26b** in dichloromethane solution with extinction coefficients greater than 300,000 $L\,mol^{-1}\,cm^{-1}$. The selenium analog **26c** has λ_{max} of 847 nm, and the tellurium analog **26d** has λ_{max} of 910 nm. Both dyes have extinction coefficients of greater than 300,000 $L\,mol^{-1}\,cm^{-1}$.[68] Both **26c** and **26d** have been found to be efficient sensitizers for thermal printing.[69] Increasing spin–orbit interactions as the heteroatoms increase in size give more efficient conversion of light energy to heat energy.

3. Sensitizers for Electrophotography

The diode lasers emitting in the near infrared near 720 nm (gallium phosphide) and in the 780–830-nm range (gallium arsenide) are convenient light sources for electrophotography or xerography. In this photochemical process, light allows a charged film (essentially a capacitor) to discharge. Tellurium-containing heterocycles have been utilized in two different capacities in electrophotography.[70–76] In one, the tellurium-containing heterocycle absorbs the incident light and the excited molecule serves to generate either an electron or a positively charged hole in a charge-transport material. The charged species then moves along the charge-transport material to the surface of the film to

complete the photoconduction process.[76a] Tellurium-containing heterocycles have also been utilized as electron-transport materials.[76]

The tellurium-containing heterocycles that function as electron-transport materials are shown below.[76] Although working examples of photoconductors have been constructed with these compounds, the transport properties are less desirable than those realized with other materials.[76a]

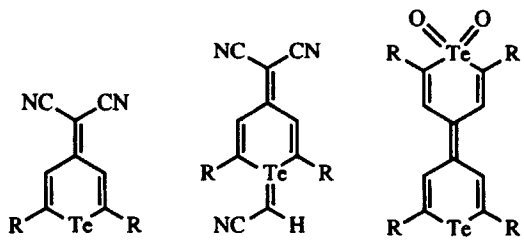

R = Ph, *tert*-Bu

A variety of different tellurium-containing heterocycles have been found to be efficient sensitizers for triarylamine photoconduction.[70–76] Perhaps the most interesting of these sensitizers are those based on the 2,6-diphenyltelluropyrylium nucleus such as dyes **27**–**29**.[70] These dyes absorb light of longer wavelengths with λ_{max} of 650 nm for **27**, λ_{max} of 760 nm for **28**, and λ_{max} of 885 nm for **29**. The telluropyrylium dye **27** forms an aggregate in polycarbonate binders and can function as a charge-generation layer sensitive to near-infrared radiation with λ_{max} of 760 nm for the aggregate.[70,76a]

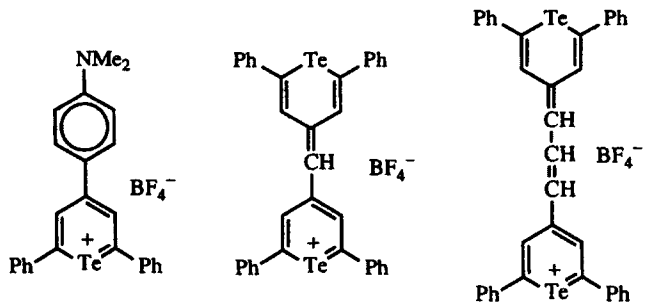

27 **28** **29**

In the excited state, the telluropyrylium dyes (and other dyes, as well) are stronger as both an oxidizing agent and as a reducing agent with two singly occupied molecular orbitals (SOMOs). If an electron is transferred from the lone pair of electrons on a triarylamine to the lowest SOMO of the excited state of the dye in a thin-film format in an applied field, then a radical cation of the triarylamine is formed and photoconduction is observed and the film discharges. Thin films containing telluropyrylium dyes **27**–**29** as sensitizers for triarylamine

photoconduction have similar electrophotographic responses to those films incorporating sulfur and selenium analogs of these dyes as photosensitizers.[71,72] The tellurium atoms allow the wavelengths of the gallium arsenide diode lasers to be reached with much shorter hydrocarbon π systems, which improves both the light and dark stability of the sensitizing dyes.

4. *Sensitizers for Silver Halide Photography*

The cyanine dyes **12** and close derivatives have been utilized for spectral sensitization of silver halide crystals. Native silver halide crystals have a sensitivity to blue and ultraviolet wavelengths of light. To make the silver halide crystals sensitive to other wavelengths of light, sensitizing dyes are placed on the surface of the silver halide grains. The sensitizing dyes then inject an electron into the conduction band of the silver halide crystal on absorbing a photon. The benzotellurazole nucleus **30** and derivatives such as the naphthotellurazole nucleus **31** give cyanine dyes of longer wavelength.[21,22,27] The cyanine dyes **12** with X equal to Te have been found to be efficient spectral sensitizers for silver halide film emulsions.[21,22]

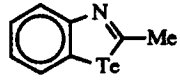

30

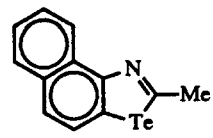

31

5. *Sensitizers for Photodynamic Therapy*

Photodynamic therapy (PDT) is an emerging area of medicine that utilizes light, biologically available oxygen, and a sensitizer to generate a cytotoxic species.[78–81] Often the biological targets are transformed cells in a tumor mass, cell clusters on a membrane or surface (bladder cancer, skin cancer), or free in the blood stream (leukemia). Non-life-threatening conditions such as psoriasis and other dermatological conditions are also treatable with PDT.

One advantage of PDT is that light can be used to generate cytotoxic species in a very localized area. Some of the criteria that define an ideal sensitizer for PDT are localization in or around the tumor mass, low toxicity toward normal tissue, activation by wavelengths of light that can penetrate deeply into both tumor and tumor-involved normal tissues, and efficient photochemical generation of the cytotoxic reagent.[82]

The issue of localization of the sensitizer in or around the tumor mass can be addressed through an understanding of some of the differences between normal and transformed cells. Cancer cells derive a significant fraction of their total

adenosine triphosphate (ATP) from mitochondrial oxidative phosphorylation. In fact, some tumor cells, *in vitro*, utilize very little glucose and instead rely on fatty acids and/or amino acids as fuel sources.[83] Consequently, mitochondrial oxidative phosphorylation is a major source of energy for transformed cells, and the mitochondrial structure is a suitable target for drug therapy against the transformed cell.

The numerous differences between the mitochondria of normal cells and transformed cells can be used to localize photosensitizers in the transformed cells. These differences include morphology, ultrastructure, ability to undergo configurational changes, and differences in matrix and/or membrane compositions.[84] Most neoplastic cells have less than 50% the number of mitochondria found in normal cells of the same cell type. Finally, tumor mitochondria more efficiently retain and accumulate calcium and other cations relative to normal cells. This accumulation of cationic species has been utilized to localize cationic photosensitizers in tumor cells.

Rhodamine-123 (Rh-123) is a dibenzopyrylium dye that is specifically taken up by the mitochondria of living cells, presumably via the pH gradient generated by the mitochondrial proton pump.[85,86] In general, differences in cell plasma membrane potentials of 59 mV and mitochondrial membrane potentials of 177 mV are sufficient to lead to a 10-fold increase in dye concentration in cytoplasm and a 10,000-fold increase in mitochondria relative to dye concentration in the culture medium *in vitro*.[87] It has further been demonstrated that Rh-123 accumulates more in carcinoma cells and muscle cells relative to other cell types[87] and shows some selective toxicity toward transformed cells.[88–90] Although studies with Rh-123 have established the groundwork for studies of the localization of other cationic photosensitizers, Rh-123 absorbs light of too short a wavelength for efficient tissue penetration in PDT. (The body is most transparent to light with wavelengths of between 700 and 1200 nm.[91]) Furthermore, Rh-123 is inefficient at producing photochemically generated cytotoxic species.[92,93]

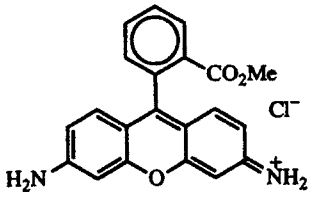

Rh-123

The photochemical generation of cytoxic species in PDT has been divided into two different classes. Type I processes are those that involve photoinduced electron transfer.[94] Type II processes are those that generate singlet oxygen.[95] The generation of singlet oxygen either *in vitro* or *in vivo* has proved to be an efficient cytotoxic process.[95]

Cationic dyes, such as Rh-123, are characterized by reversible one-electron oxidations and reductions in the ground state.[96] Following promotion of an electron in the excited state, both oxidation and reduction become more facile by approximately the energy of the absorbed photon. In the excited state, radicals can be generated by single-electron transfer from between the sensitizer and surrounding biological molecules while single electron transfer from the excited state of the dye and ground-state oxygen produces superoxide anion.

The singlet or S_1 state of the dye is short-lived, typically with lifetimes of less than 10 ns. If intersystem crossing is competitive with internal conversion, the triplet state of the dye is produced, which is typically much longer-lived than the singlet. The triplet state of the dye can react with ground-state oxygen via a spin-allowed process to produce ground-state dye and the first excited state of oxygen, singlet oxygen.[95] The energy of the triplet state should lie close to or higher than the 23-kcal mol^{-1} difference in energy of ground-state and singlet oxygen.[97] In pyrylium-type dyes, singlet-triplet splittings are reasonably small (8–12 kcal mol^{-1})[98] such that the energy of the absorbed photon need only be on the order of 31–35 kcal mol^{-1}, which corresponds to a wavelength of 900 nm or shorter.

The rate constants for intersystem crossing and internal conversion are influenced by spin–orbit interactions as described earlier in this chapter, which suggests that telluropyrylium dyes should be more efficient than pyrylium dyes at generating singlet oxygen. Tellurium-containing cationic dye **18** (Te,Se) functions as an efficient generator of singlet oxygen both in solution and *in vitro*[41,82] and has been found to be a good sensitizer for PDT both *in vitro* against human glioma cells[99] and *in vivo* against implanted brain tumors in rats.[100]

Shown in Figure 5 are two electronmicrographs of human U251 MG cells (malignant glioma). The first (Fig. 5*a*) is prior to treatment and the second (Fig. 5*b*) follows incubation with the chloride salt of **18** (Te,Se) and irradiation with 775-nm light.[82] In Figure 5a, the cristae of the mitochondria are clearly defined as indicated by the arrow. After exposure of the dye-treated cells to the 775-nm light, the mitochondrial membrane damage is extensive with complete disruption of the cristae (arrow in Fig. 5*b*) and swelling of the mitochondria.

An ideal photosensitizer, following photoproduction of a cytotoxic amount of reactive species, should be bleached during PDT or converted temporarily to a form that no longer absorbs the activating wavelengths of light. This is necessary in order that the sensitizer at the surface of the tumor mass does not shield the inner tumor mass from the activating wavelengths of light. The phenomenon of the photosensitizer limiting the depth of tissue treated by PDT has been described for hematoporphyrin derivative and is called the *shielding effect*.[101]

In an aqueous environment, singlet oxygen and telluropyrylium dye **18** (Te,Se) react to give the dihydroxy-tellurane **32** as shown in Scheme 5. Dihydroxytellurane **32** has a maximum of absorption around 500 nm and is transparent at 785 nm, which is the wavelength of light used for PDT with **18**

(Te,Se).[41,82] Oxidation of the sensitizer as singlet oxygen is produced and serves to bleach temporarily the long-wavelength absorption of the sensitizer. While **18** (Te,Se) produces singlet oxygen via a type II process, irradiation of **32** at 500 nm produces hydroxy radicals, which are also cytotoxic, via a type I process and regenerates dye **18** (Te,Se) allowing multiple treatments from a single dye injection.[102] This dual-action behavior as a photosensitizer is unprecedented with other sensitizers for PDT.

The localization of the sensitizer **18** (Te,Se) in the mitochondria of transformed cells as well as the oxidation to **32** is illustrated in Figure 6.[82] Epifluorescence microscopy of a human U251MG cell treated with 10^{-7} *M* **18** (Te,Se) and light shows the granular fluorescence typical of mitochondrial staining. The emission maximum of 560 nm observed in Figure 6 is the emission maximum of the oxidized dye **32**.

Tellurium analogs of Rh-123[92,93] and other cationic dyes such as the Nile Blue dyes[103] have not been prepared. The lighter chalcogen analogs of these materials show some activity in PDT, and one would expect heavy-atom analogs to be far more efficient at producing singlet oxygen.

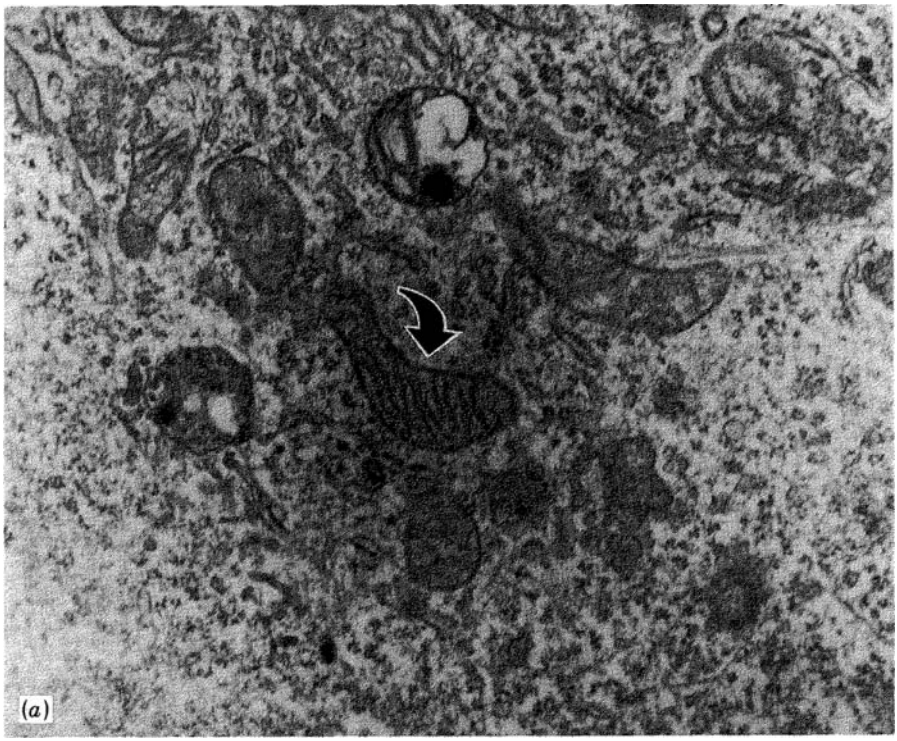

Figure 5. (*Continued*)

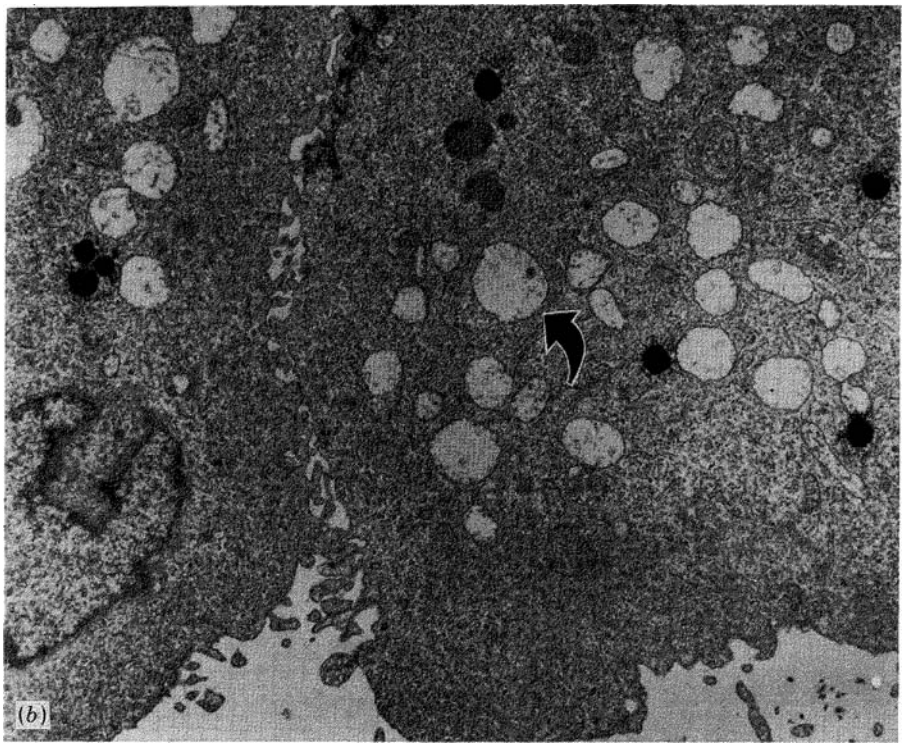

Figure 5. (*a*) Electronmicrograph of an untreated human U251MG malignant glioma cell. Note that the arrow indicates the clearly defined cristae within the mitochondria. (*b*) Electronmicrograph of a human U251MG malignant glioma cell incubated for 15 min with **18** (Te,Se) at 10^{-6} *M* concentration and irradiated for 5 min with 775-nm light. Note that the arrow indicates disruption of the cristae and internal mitochondrial membranes in addition to swelling of the mitochondria. (Reprinted with permission from *Journal of Medicinal Chemistry*, **1990**, *33*, 1108. Copyright 1990 the American Chemical Society.)

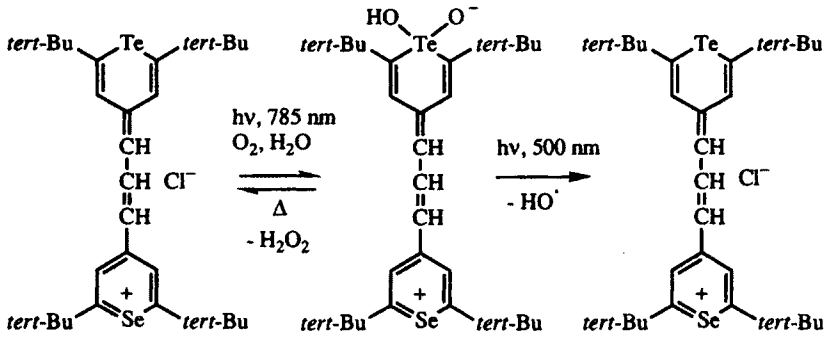

Scheme 5

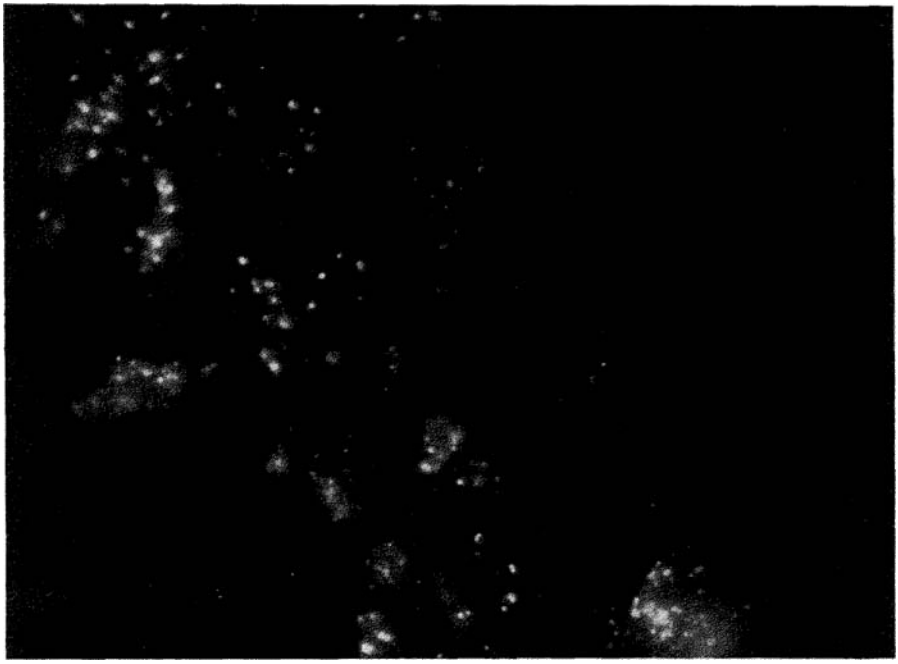

Figure 6. Epifluorescence microscopy of a human U251MG cell treated with 10^{-7} *M* **18** (Te, Se) as the chloride salt and with light. The granular fluorescence is presumably from the mitochondria and the emitting species is oxidized dye **32**. (Reprinted with permission from *Journal of Medicinal Chemistry*, **1990**, *33*, 1108. Copyright 1990 the American Chemical Society.)

C. Applications Using Tellurium-Containing Heterocycles as Catalysts

The tellurium(II)–tellurium(IV)–tellurium(II) shuttle has found utility in different applications where hydrogen peroxide is produced and/or consumed.[35,104–106] This chemistry has no precedent in the chemistry of organosulfur and organoselenium chemistry. Hopefully, the utility of this shuttle will be more fully developed in the future.

1. Solar Energy Storage via Photochemical–Thermal Generation of Hydrogen Peroxide

The development of methods to convert light to chemical energy has acquired importance in humankind's quest to store solar energy for use as a fuel source. While the major emphasis in light-to-chemical-energy conversion has been the splitting of water for the production of hydrogen,[104–108] photoprocesses to make other energy-rich compounds such as hydrogen peroxide (23 kcal mol^{-1}

for conversion to oxygen and water) have also received attention.[105,109–115] In all these systems, whether metal-based or dye-mediated or hydrogen- or hydrogen-peroxide-producing, a sacrificial electron donor is required to minimize back-electron transfer from the electron relay.

The tellurium(II)–tellurium(IV)–tellurium(II) shuttle in telluropyrylium dyes has been utilized to convert light, oxygen, and water to hydrogen peroxide as shown in Scheme 6.[35,116–118] Because the overall catalytic cycle is a reversible two-electron process, no sacrificial electron donor is required in the process and the system is truly catalytic. The price paid with the systems utilized to date is that a slow thermal reaction is coupled to the photochemical process, and this process is the rate-limiting step.

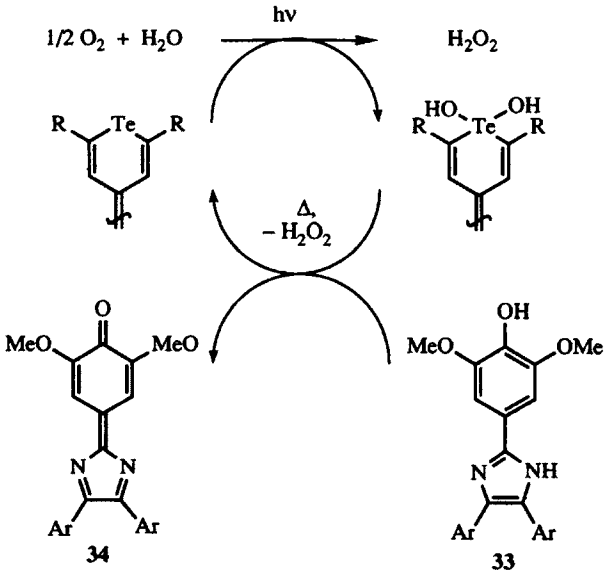

Scheme 6

The thermal reductive elimination reaction can be removed from the cycle if the reduction of the dihydroxy telluranes is coupled with a much faster (relative to reductive elimination) oxidation of another substrate. The oxidation of leucodyes **33** to dyes **34** is one such reaction.[35,116–118] This particular oxidation at 10^{-5} *M* concentration of telluropyrylium dye is several orders of magnitude faster than reductive elimination of hydrogen peroxide from the dihydroxy tellurane. Turnover numbers of ≥ 100 have been observed for the tellurium(II)–tellurium(IV)–tellurium(II) shuttle in these systems. Again, this chemistry is not observed with pyrylium, thiopyrylium, and selenopyrylium dyes.

2. *Catalysts for Oxidations with Hydrogen Peroxide*

Hydrogen peroxide is a strong oxidant thermodynamically (23 kcal mol^{-1} for conversion to oxygen and water) but is kinetically slow to react. The tellurium(II)–tellurium(IV)–tellurium(II) shuttle with telluropyrylium dyes has been utilized to catalyze oxidations with hydrogen peroxide.[117–119] Oxidation of leucodyes **33** to dyes **34** and oxidation of aromatic thiols to disulfides are slow with hydrogen peroxide. For the leucodye systems, second-order rate constants for oxidation with hydrogen peroxide are on the order of $\leq 10^{-5}$ L mol^{-1} s^{-1}, while for the thiol systems, second-order rate constants for oxidation with hydrogen peroxide are on the order of 10^{-2} L mol^{-1} s^{-1}. In the presence of telluropyrylium dyes at 10 mol% or less in concentration, both oxidations are accelerated with values of k_{cat}, the rate constant for catalysis, of $\geq 10^{4}$ L^{2} mol^{-2} s^{-1} being observed. Turnover numbers of greater than 330 have also been observed.

IV. SUMMARY

Tellurium-containing heterocycles are distinguished from their oxygen-, sulfur-, and selenium-containing analogues by distinct differences in properties primarily from the increased metallic character of tellurium. Technical applications that exploit these differences are emerging and should continue to develop in the future. In the remaining chapters of this work, the syntheses and properties of tellurium-containing heterocycles are described. The application of this knowledge is limited only by our imaginations.

REFERENCES

1. Wohler, F. *Ann. Chem.* **1840**, *35*, 111.
2. Morgan, G. T.; Drew, H. D. K. *J. Chem. Soc.* **1920**, *117*, 1456.
3. Morgan, G. T.; Burgess, H. *J. Chem. Soc.* **1928**, *133*, 321.
4. Drew, H. D. K. *J. Chem. Soc.* **1926**, *129*, 223.
5. Morgan, G. T.; Burstall, F. H. *J. Chem. Soc.* **1931**, 180.
6. Courtot, C.; Bastani, M. G. *C. R. Acad. Sci.* **1936**, *203*, 197.
7. Mack, W. *Angew. Chem., Int. Ed. Engl.* **1966**, *5*, 896.
8. Piette, J. L.; Renson, M. *Bull. Soc. Chim. Belg.* **1971**, *80*, 521.
9. Pauling, L. *The Nature of the Chemical Bond*, 3rd ed., Cornell University Press; Ithaca, NY, 1960.
10. Bondi, A. J. *Phys. Chem.* **1964**, *68*, 441.
11. Detty, M. R.; Haley, N. F.; Eachus, R. S.; Hassett, J. W.; Luss, H. R.; Mason, M. G.; McKelvey, J. M.; Wernberg, A. A. *J. Am. Chem. Soc.* **1985**, *107*, 6298.
12. Alcock, N. W. *Adv. Inorg. Chem. Radiochem.* **1972**, *15*, 1.

13. Wudl, F.; Aharon-Shalom, E. *J. Am. Chem. Soc.* **1982**, *104*, 1154.
14. Lerstrup, K.; Talham, D.; Bloch, A.; Poehler, T.; Cowan, D. *J. Chem. Soc., Chem. Commun.* **1982**, 336.
15. McCullough, R D.; Kok,. G. B.; Lerstrup, K.; Cowan, D. O. *J. Am. Chem. Soc.* **1987**, *109*, 4115.
16. Bailey, A. B.; McCullough, R. D.; Mays, M. D.; Cowan, D. O.; Lerstrup, K. *Synth. Met.* **1988**, *27*, B425.
17. Detty, M. R.; Murray, B. J.; Perlstein, J. H. *Tetrahedron Lett.* **1983**, *24*, 1239.
18. Detty, M. R.; Hassett, J. W.; Murray, B. J.; Reynolds, G. A. *Tetrahedron* **1985**, *45*, 4853.
19. Detty, M. R.; Murray, B. J. *J. Org. Chem.* **1982**, *47*, 5235.
20. Detty, M. R.; McKelvey, J. M.; Luss, H. R. *Organometallics* **1988**, *7*, 1131.
21. Günther, W. H. H.; Lok, R. US Patent 4,607,000 (1986).
22. Przyklek-Elling, R.; Günther, W. H. H.; Lok, R. US Patent 4,661,438 (1987).
23. Gillespie, R. J. *J. Chem. Educ.* **1970**, *47*, 18.
24. Drago, R. S. *J. Chem. Educ.* **1973**, *50*, 244.
25. Rundle, R. E. *Rec. Chem. Prog.* **1962**, *50*, 3677.
26. Sadekov, I. D.; Rybalkina, L. E.; Movshovich, D. Ya; Bulgarevich, S. B.; Kogan, V. A. *Uspekhi Khimii* **1991**, *60*, 1229.
27. Piette, J.-L.; Thibaur, P.; Renson, M. *Tetrahedron* **1978**, *34*, 655.
28. Detty, M. R.; Luss, H. R. *J. Org. Chem.* **1983**, *48*, 5149.
29. Detty, M. R.; Murray, B. J.; Smith, D. L.; Zumbulyadis, N. *J. Am. Chem. Soc.* **1983**, *105*, 875.
30. Detty, M. R. *J. Org. Chem.* **1980**, *45*, 274.
31. Detty, M. R.; Luss, H. R.; McKelvey, J. M.; Geer, S. M. *J. Org. Chem.* **1986**, *51*, 1692.
32. Nefedov, V. D.; Sinotova, E. N.; Sarbash, A. N.; Kolobov, E. A.; Kapustin, V. K. *Radiokhimiya* **1971**, *13*, 435.
33. Nefedov, V. D.; Sinotova, E. N.; Sarbash, A. N.; Timofev, S. A. *Radiokhimiya* **1969**, *11*, 154.
34. Detty, M. R.; Luss, H. R. *Organometallics* **1986**, *5*, 2250.
35. Detty, M. R. *Organometallics* **1991**, *10*, 702.
36. Schmidt, E. *Phosphorus Sulfur* **1988**, *35*, 223.
37. Srivastava, T. N.; Srivastava, R. C.; Bhargava, A. *Ind. J. Chem.* **1979**, *18A*, 236.
38. Detty, M. R.; Frade, T. M. *Organometallics* **1993**, *12*, 2496.
39. Detty, M. R.; Murray, B. J. *J. Org. Chem.* **1987**, *52*, 2123.
40. Detty, M. R.; Friedman, A. E. *Organometallics* **1994**, *13*, 533.
41. Detty, M. R.; Merkel, P. B. *J. Am. Chem. Soc.* **1990**, *112*, 3845.
42. Wittel, K.; Manne, R. *Theor. Chim. Acta* **1974**, *33*, 347.
43. Corey, E. J.; Kahn, A. U.; Ha, D.-C. *Tetrahedron Lett.* **1990**, *31*, 1389.
44. Detty, M. R. *Organometallics* **1992**, *11*, 2310.
45. Bock, H.; Brahler, G.; Dauplaise, D.; Meinwald, *J. Chem. Ber.* **1981**, *114*, 2622.
46. McFarlane, H. C. E.; McFarlane, W. In *NMR of Newly Accessible Nuclei*, Laszlo, P., ed., Academic Press, New York, 1983, Vol. 2, Ch. 10.
47. Lutz, O. In *The Multinuclear Approach to NMR spectroscopy*, Lambert, J. B.; Riddell, F. G., eds., Reidel, Boston, 1983, Ch. 19.
48. Detty, M. R.; Henrichs, P. M.; Whitefield, J. A. *Organometallics* **1986**, *5*, 1544.
49. Saito, G.; Enoki, T.; Inokuchi, H.; Kumagai, H.; Tanaka, J. *Chem. Lett.* **1983**, 503.
50. Saito, G.; Kumagai, H.; Tanaka, J.; Enoki, T.; Inokuchi, H. *Mol. Cryst. Liq. Cryst.* **1985**, *120*, 337.
51. Matsuzaki, S.; Li, Z. S.; Sano, M. *Synth. Met.* **1987**, *19*, 399.

52. Mays, M. D.; McCullough, R. D.; Bailey, A. B.; Cowan, D. O.; Bryden, W. A.; Poehler, T. O.; Kistenmacher, T. J. *Synth. Met.* **1988**, *27*, B493.

53. Mays, M. D.; McCullough, R. D.; Cowan, D. O.; Poehler, T. O.; Bryden, W. A.; Kistenmacher, T. J. *Solid State Commun.* **1988**, *65*, 1089.

54. Cowan, D. O.; Mays, M. D.; Kistenmacher, T. J.; Poehler, T. O.; Beno, M. A.; Kini, A. M.; Williams, J. A.; Kwok, Y. K.; Carlson, K. D.; Xiao, L.; Novoa, J. J.; Whangbo, M.-H. *Mol. Cryst. Liq. Cryst.* **1990**, *181*, 43.

55. Kobayashi, K.; Kikuchi, K.; Koide, A.; Ishikawa, Y.; Saito, K.; Ikemoto, I. *J. Chem. Soc., Chem. Commun.* **1992**, 1198.

56. Williams, J. M.; Ferraro, J. R.; Thorn, R. J.; Carlson, K. D.; Geiser, U.; Wang, H. H.; Kini, A. M.; Whangbo, M.-H. *Organic Superconductors*, Prentice Hall, Englewood Cliffs, NJ, 1992.

57. Kobayashi, H.; Udagawa, T.; Tomita, H.; Bun, K.; Naito, T.; Kobayashi, A. *Chem. Lett.* **1993**, 1559.

58. Greene, R. L.; Street, G. B.; Siuter, L. J. *Phys. Rev. Lett.* **1975**, *34*, 577.

59. Chiang, C. K.; Fincher, C. R., Jr.; Park, Y. W.; Heeger, A. J.; Shirakawa, H.; Louis, E. J.; Gau, S. C.; MacDiarmid, A. G. *Phys. Rev. Lett.* **1977**, *39*, 109.

60. Sugimoto, R.; Yoshino, K.; Inoue, S.; Tsukagoshi, K. *Jpn. J. Appl. Phys. Part 2*, **1985**, *24*, 425.

61. Kubota, F. Jpn. Kokai Tokkyo Koho Jpn. Patent 02,263,824 [90,263,823] (1990); *Chem. Abstr.* **1991**, *115*, 20291s.

62. Matsuoka, M., ed., Infrared Absorbing Dyes, Plenum Press, New York, 1990.

63. Detty, M. R.; Thomas, H. T. U.S. Patent 4,584,258 (1986).

64. Detty, M. R.; Fleming, J. C. *Adv. Mat.* **1994**, *6*, 48.

65. Detty, M. R.; Fleming, J. C. U.S. Patent *5*, 300,385 (1994).

66. Yamaguchi, C.; Hiraoka, Y.; Kageyama. H.; Ando, T.; Matsuoka, S.; Endo, T. Jpn. Kokai Tokkyo Koho Jpn. Patent 62,257,890 [87,257,890] (1987); *Chem. Abstr.* **1987**, *107*, 187518t.

67. Kellogg, R. F.; Laganis, E. D. U.S. Patent 5,019,549 (1991).

68. Detty, M. R.; Henne, B. *Heterocycles* **1993**, *35*, 1149.

69. Burberry, M. S.; Tutt, L. W.; Detty, M. R. U.S. Patent *5*, 256,620 (1992).

70. Detty, M. R.; Murray, B. J. U.S. Patent 4,279,365 (1981).

71. Detty, M. R.; Murray, B. J.; Perlstein, J. H. U.S. Patent 4,365,017 (1982).

72. Detty, M. R.; Murray, B. J.; Perlstein, J. H. U.S. Patent 4,365,016 (1982).

73. Detty, M. R.; Goliber, T. E.; Murray, B. J.; Perlstein, J. H. U.S. Patent 4,329,284 (1982).

74. Detty, M. R.; Perlstein, J. H. U.S. Patent 4,450,217 (1984).

75. Detty, M. R.; Perlstein, J. H. U.S. Patent 4,525,443 (1985).

76. Detty, M. R.; Murray, B. J.; Scozzafava, M. 4,634,553 (1987).

76a. Borsenberger, P. M.; Weiss, D. S. *Organic Photoreceptors for Imaging Systems*, Marcel Dekker, New York, 1993, Ch. 11.

77. Junk, T.; Irgolic, K. J. *Phosphorus Sulfur* **1988**, *38*, 121.

78. *Progress in Clinical and Biological Research*, Vol. 170, *Porphyrin Localization and Treatment of Tumors*, Doiron, D. R.; Gomer, C. J., eds., Alan R. Liss; New York, 1984.

79. *Advances in Experimental Medicine and Biology*, Vol. 193, *Methods in Porphyrin Photosensitization*, Kessel, D., ed., Plenum Press; New York, 1985.

80. Sternberg, E.; Dolphin, D. In *Infrared Absorbing Dyes*, Matsuoka, M., ed., Plenum Press; New York, 1990, Ch. 15.

81. Powers, S. K.; Detty, M. R. In *Photodynamic Therapy of Neoplastic Disease*, Kessel, D., ed., CRC Press, Boca Raton, FL, 1990, pp. 308–328.

82. Detty, M. R.; Merkel, P. B.; Hilf, R.; Gibson, S. L.; Powers, S. K. *J. Med. Chem.* **1990**, *33*, 1108.

83. Walstad, D. L.; Brown, J. T.; Powers, S. K. *Photochem. Photobiol.* **1989**, *49*, 285.
84. Pederson, P. L. *Prog. Exp. Tumor Res.* **1978**, *22*, 190.
85. Johnson, L. V.; Walsh, M. L.; Chen, L. B. *Proc. Natl. Acad. Sci* (USA) **1980**, *77*, 990.
86. Mitchell, P. *Chemiosmotic Coupling in Oxidative and Photosynthetic Phosphorylation*, Glynn Research Ltd.; Bodmin, 1966, pp. 1–205.
87. Summerhayes, I. C.; Lampidis, T. J.; Bernal, S. D.; Chen, L. B. *Proc. Natl. Acad. Sci* (USA) **1982**, *79*, 5292.
88. Lampidis, T. J.; Bernal, S. D.; Summerhayes, I. C.; Chen, L. B. *Ann. N. Y. Acad. Sci.* **1982**, *395*, 299.
89. Lampidis, T. J.; Bernal, S. D., Summerhayes, I. C.; Chen, L. B. *Cancer Res.* **1983**, *43*, 716.
90. Bernal, S. D.; Lampidis, T. J.; Summerhayes, I. C.; Chen, L. B. *Science (Washington, D.C.)* **1982**, *218*, 1117.
91. Wan, S.; Parrish, J. A.; Anderson, R. R.; Madden, M. *Photochem. Photobiol.* **1981**, *34*, 679.
92. Powers, S. K.; Pribil, S.; Gillespie, G. Y.; Watkins, P. J. *J. Neurosurg.* **1986**, *64*, 918.
93. Beckman, W. C., Jr., Powers, S. K.; Brown, J. T.; Gillespie, G. Y.; Bigner, D. D.; Camps, J. L. Jr. *Cancer* **1987**, *59*, 266.
94. Kapinus, E. I.; Weksankia, M. M.; Starzi, V. P.; Boghillo, V. I.; Dilung, I. I. *J. Chem. Soc., Faraday Trans. II* **1985**, *81*, 361.
95. Foote, C. S. In *Progress in Clinical and Biological Research*, Vol. 170, *Porphyrin Localization and Treatment of Tumors*, Doiron, D. R.; Gomer, C. J., eds., Alan R. Liss, New York, 1984.
96. Detty, M. R.; McKelvey, J. M.; Luss, H. R. *Organometallics* **1988**, *7*, 1131.
97. Firey, P. A.; Ford, W. E.; Sounik, J. R.; Kenney, M. E.; Rogers, M. A. G. *J. Am. Chem. Soc.* **1988**, *110*, 7626.
98. McGlynn, S. P.; Azumi, T.; Kinoshita, M. In *Molecular Spectroscopy of the Triplet State*, Prentice-Hall, Englewood Cliffs, NJ, 1969, pp. 172–174.
99. Powers, S. K; Walstad, D. L.; Brown, J. T.; Detty, M. R.; Watkins, P. J. *J. Neuro-Oncol.* **1989**, *7*, 179.
100. Detty, M. R.; Powers, S. K. U.S. Patent 5,047,419 (1991).
101. Dorion, D. R.; Svaasand, L. O.; Profio; A. E. *Adv. Exp. Med. Biol.* **1981**, *160*, 63.
102. Detty, M. R.; Merkel, P. B.; Gibson, S. L.; Hilf, R. *Oncol. Res.* **1992**, *4*, 367.
103. Oseroff, A. R.; Ohuoha, D.; Ara, G.; McAuliffe, D.; Foley, J.; Cincotta, L. *Proc. Natl. Acad. Sci* (USA) **1986**, *83*, 9729.
104. Harriman, A.; West, M. A., eds., *Photogeneration of Hydrogen*, Academic Press, London, 1982.
105. Gratzel, M., ed., *Energy Resources through Photochemistry and Catalysis*, Academic Press, New York, 1983.
106. Frank, A. J.; Willner, I.; Goren, Z.; Degani, Y. *J. Am. Chem. Soc.* **1987**, *109*, 3568.
107. Pelizett, E.; Serpone, N. eds., *Homogeneous and Heterogeneous Photocatalysis*, Reidel, Dordrecht (The Netherlands), 1986.
108. Gouterman, M. In *The Porphyrins*, Dolphin, D., ed., Academic Press, New York, 1978; Vol. IIIa, Ch. 1.
109. Connolly, J. S., ed., *Photochemical Conversion and Storage of Solar Energy*, Academic Press, New York, 1981.
110. Hall, D. O.; Palz, W.; Pirrwitz, D., eds., *Photochemical, Photoelectrochemical and Photobiological Processes*, Reidel, Dordrecht, The Netherlands, 1983, Series D, Vol. 2.
111. Martin, J. P.; Logsdon, N. *Arch. Biochem. Biophys.* **1987**, *256*, 39.
112. Albery, W. J.; Foulds, A. W.; Daruent, J. R. *J. Photochem.* **1982**, *19*, 37.
113. Navarro, J. A.; Roncel, M.; De la Rosa, F. F.; De la Rosa, M. A. *Photochem. Photobiol.* **1987**, *40*, 279.

114. Kurimura, Y.; Katsumata, K. *Bull. Chem. Soc. Jpn.* **1982**, *55*, 2560.
115. Kurimura Y.; Nagashima, M.; Takato, K.; Tsuchida, E.; Kaneko, M.; Yamada, A. *J. Phys. Chem.* **1982**, *86*, 2432.
116. Detty, M. R.; Gibson, S. L. *J. Am. Chem. Soc.* **1990**, *112*, 4086.
117. Detty, M. R. *Phosphorus Sulfur Silicon* **1992**, *4*, 367.
118. Detty, M. R., Gibson, S. L. *Organometallics* **1992**, *11*, 2147.
119. Engman, L.; Stern, D.; Pelcman, M. *J. Org. Chem.* **1994**, *59*, 1973.

Chemistry of Heterocyclic Compounds, Volume 53
Michael R. Detty, Marrie B. O'Regan

CHAPTER II

Tellurophenes, Dihydrotellurophenes, and Tetrahydrotellurophenes and Their Benzo and Dibenzo Analogs

The first five-membered heterocyclic ring containing a tellurium atom was a tetrahydrotellurophene derivative reported in 1931 by Morgan and Burstall.[1] The first aromatic tellurophene derivative was reported in 1961 by Braye et al.[2] Numerous derivatives of these systems as well as their benzo and dibenzo analogs have been described.

I. NOMENCLATURE

Both IUPAC (International Union of Pure and Applied Chemistry) rules and *Chemical Abstracts* conventions suggest the name *tellurophene* for the fully unsaturated five-membered ring containing one tellurium atom. The numbering of the tellurophene ring begins with the tellurium atom as the 1-position. The addition of a benzo group gives benzotellurophene, while the fusion of two benzo groups gives dibenzotellurophene as shown in Figure 1.

The dihydro and tetrahydro analogs of tellurophene have many more descriptors: 2,5-dihydrotellurophene is synonymous with 4-telluracyclopentene; 2,3-dihydrotellurophene is synonymous with 3-telluracyclopentene; and tetrahydrotellurophene is synonymous with telluracyclopentane, tellurolane, and, in the convention of the 1920s and 1930s, cyclotellurobutane. IUPAC rules of nomenclature suggest naming the saturated systems as the hydrocarbon with "tellura-" as the descriptor for the heteroatom substitution. Benzo analogs of the dihydrotellurophenes have been trivially described as telluraindanes.

II. SYNTHESIS OF THE DIHYDRO- AND TETRAHYDROTELLUROPHENES AND BENZO-FUSED ANALOGS

The majority of dihydro- and tetrahydrotellurophenes have been prepared via two different synthetic routes. In one approach, electrophilic species such as tellurium tetrachloride add to 1,3- or 1,5-dienes to give tellurium(IV) analogs of dihydro- and tetrahydrotellurophenes. In a second approach, tellurium

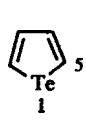

tellurophene

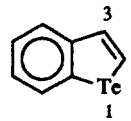

benzotellurophene

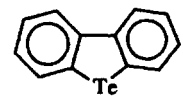

dibenzotellurophene

2,5-dihydrotellurophene
4-telluracyclopentene

2,3-dihydrotellurophene
3-telluracyclopentene

tetrahydrotellurophene
telluracyclopentane
cyclotellurobutane

Figure 1. Nomenclature for tellurophene derivatives and benzo analogs.

nucleophiles displace, 1,4-dihalides or pseudohalides to form five-membered, tellurium-containing rings. Numerous derivatives of dihydro- and tetrahydrotellurophenes have been prepared by ligand exchange reactions.

A. Synthesis of Tetrahydrotellurophene Derivatives

A single example of a third approach to tetrahydrotellurophenes has been described in which the thermolysis of di-4-pentenyltelluride leads to low yields of 2-methyltetrahydrotellurophene (**1**) and a derivative as shown in Scheme 1.[3] This reaction proceeds via homolysis of a tellurium–carbon bond to give a tellurium-centered radical, which then cyclizes. All other approaches to ring construction in tetrahydrotellurophenes discussed in this section follow one of the two reaction types described above.

Morgan and Burstall found that 1,1-diiodotetrahydrotellurophene (**2**) was formed on heating 1,4-diiodobutane with tellurium metal as shown in Scheme 2.[1] The parent tetrahydrotellurophene **3** is prepared by sulfur dioxide reduction

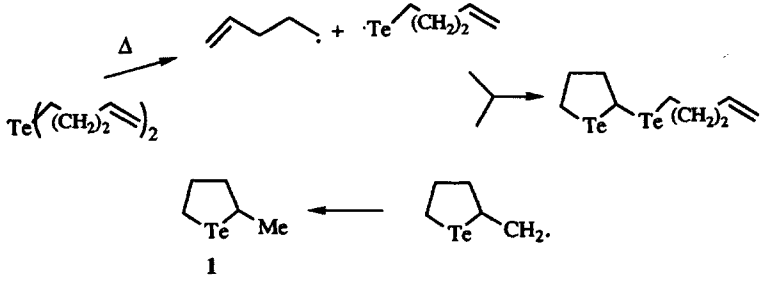

1

Scheme 1

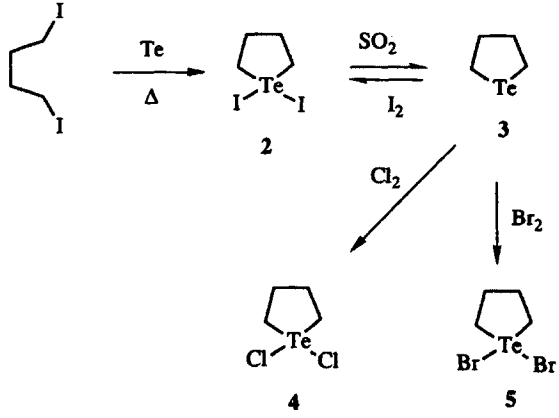

2 **3** **4** **5**

Scheme 2

of **2** followed by isolation of **3** via steam distillation. Oxidative addition of chlorine, bromine, and iodine gives 1,1-dihalotetrahydrotellurophenes **4**, **5**, and **2**, respectively.

Similar chemistry has been used to prepare 2-methyltetrahydrotellurophene as shown in Scheme 3.[4] Refluxing a mixture of 1,4-dibromopentane, sodium iodide, and tellurium metal in 2-butoxyethanol gives 1,1-diodo-2-methyltetrahydrotellurophene (**6**). Sodium borohydride reduction of **6** gives 2-methyltetrahydrotellurophene (**1**) *in situ*, which can then be converted to telluronium species **7** by the addition of alkyl halides.

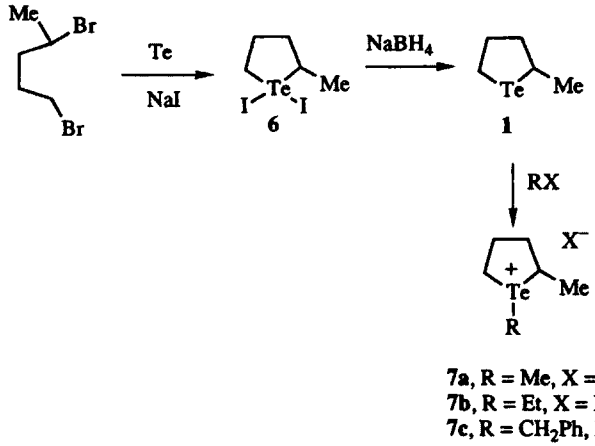

7a, R = Me, X = I
7b, R = Et, X = I
7c, R = CH_2Ph, X = Br

Scheme 3

The telluronium species **7** are described as a *cis–trans* mixture of stereoisomers with tetrahedral tellurium and strongly covalent tellurium–halogen bonds. This description is deduced from the ^1H NMR spectra of these compounds in dimethyl sulfoxide-d_6.[4] While this is clearly one possible explanation for the two observed sets of NMR signals, to this author, complexation of the telluronium species with the sulfoxide oxygen of the solvent to give a tetrahedral tellurium with ionic bromide is also a plausible alternative explanation as shown in Figure 2. In deuterochloroform as solvent, the chemical shifts of the telluronium species are quite different from those observed in dimethyl sulfoxide-d_6, suggesting yet another structure in this solvent, which is also shown in Figure 2. A dimeric telluronium species in deuterochloroform would have distinctly different NMR environments for the stereoisomers.

The addition of tellurium tetrachloride and tellurium tetrabromide to 1,5-hexadiene in ether give tetrahalides **8** and **9** in 34 and 6% isolated yields, respectively, as shown in Scheme 4.[5] A similar reaction of tellurium tetrachloride with cyclopentenylcyclopentene **10** gives tricyclic tetrahydrotellurophene tetrachloride **11**.[6] In the reports describing all three of the reactions in Scheme 4, the stereochemistry of tellurium tetrahalide addition has not been rigorously defined.

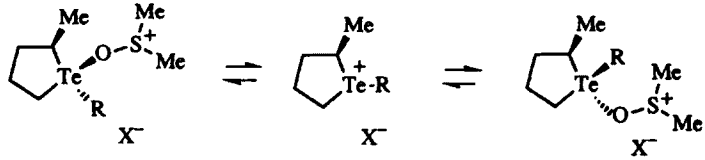

Solvent Participation

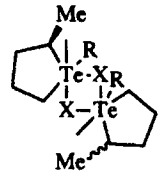

Dimer

Figure 2. Possible solution structures for telluronium salt 7 in dimethyl sulfoxide-d_6.

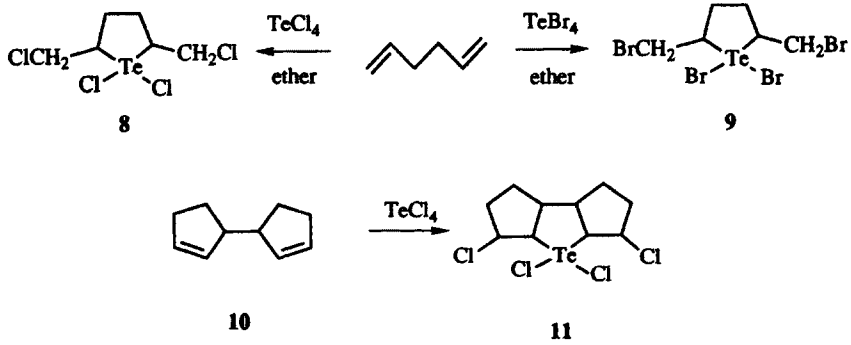

Scheme 4

The nucleophilic displacement of halides with tellurides has been the most common route for synthesis of tetrahydrotellurophenes. The first synthesis of this type was reported by Farrar and Gulland in 1945 and is illustrated in Scheme 5.[7] Sodium telluride is prepared by the reduction of tellurium metal with sodium formaldehydesulphoxylate. 1,4-Dibromobutane is then added to give tetrahydrotellurophene (**3**), which can then be isolated as dichloride **4** or dibromide **5** on oxidative addition of halogen (as shown in Scheme 2).

The addition of excess sodium telluride to tetraiodide **12** gives ditetrahydrotellurophene **13** in 62% isolated yield.[8] Similarly, the addition of sodium telluride to dibromides **14**[9] and **15**[10] gives tellurasteroids **16** and **17**, which both contain tetrahydrotellurophene rings, in < 20% isolated yields, respectively.

Other forms of nucleophilic tellurium have also been employed in the construction of tetrahydrotellurophenes as shown in Scheme 6. The addition of lithium methyltelluride to 1,4-dichlorobutane gives tetrahydrotellurophene **3** in

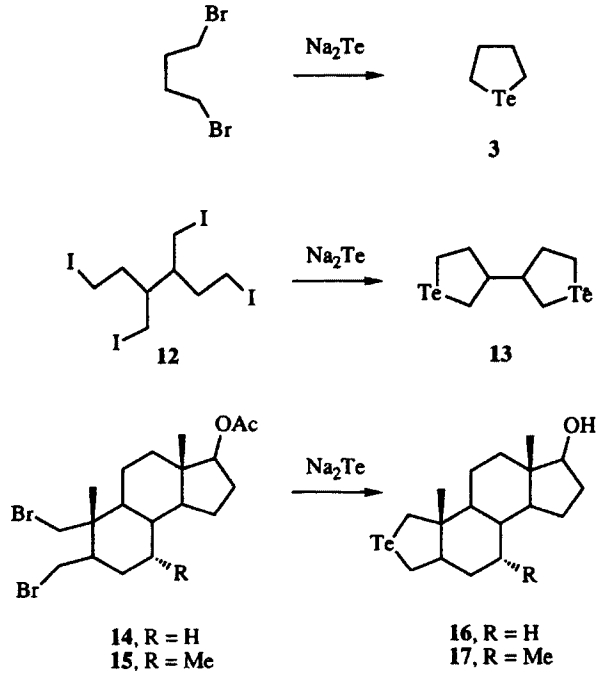

Scheme 5

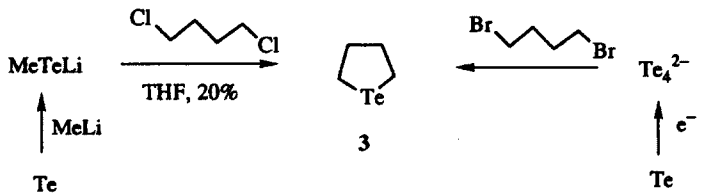

Scheme 6

20% yield in addition to other products.[11] Electrochemical reduction of tellurium metal to the tetrameric tellurium cluster dianion followed by introduction of 1,4-dibromobutane gives **3**.[12] In this example, the addition of bromine gives 1,1-dibromotetrahydrotellurophene (**5**) in 50% isolated yield overall.

1-Aryltetrahydrotellurophene salts have been prepared from 1,4-dichloro- and 1,4-dibromobutanes and aryltelluride anions as shown in Scheme 7.[13] Sodium borohydride reduction of diaryl ditellurides gives sodium aryltellurides. Introduction of 1,4-dichloro- and 1,4-dibromobutane to the telluride anions gives telluronium chlorides **18** and bromides **19**, respectively, in 70–80% yields. In these examples, the tetrahydrotellurophene is formed as a telluronium salt in the ring-closure step.

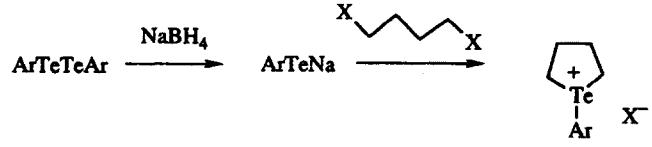

18, Ar = 4-$EtOC_6H_4$, X = Cl
19a, Ar = Ph, X = Br
19b, Ar = 4-$EtOC_6H_4$, X = Br

Scheme 7

Most of the derivatives of **3** that have been described in the literature have been prepared by ligand substitution reactions on 1,1-diiodotetrahydrotellurophene (**2**). The use of silver salts to drive substitution reactions in 1,1-diiodotetrahydrotellurophene (**2**) has been described in several studies. The addition of silver chloride or silver bromide to solutions of **3** gives **4** and **5**, respectively, in greater than 80% yield as shown in Scheme 8.[14,15] The addition of silver oxide followed by aqueous hydrofluoric acid gives 1,1-difluorotetrahydrotellurophene (**20**) in 82% isolated yield.[15] Silver isocyanate, isothiocyanate, and isoselenocyanate give the corresponding 1,1-disubstituted tetrahydrotellurophenes **21–23** in 80, 40, and 40% isolated yields, respectively.[15]

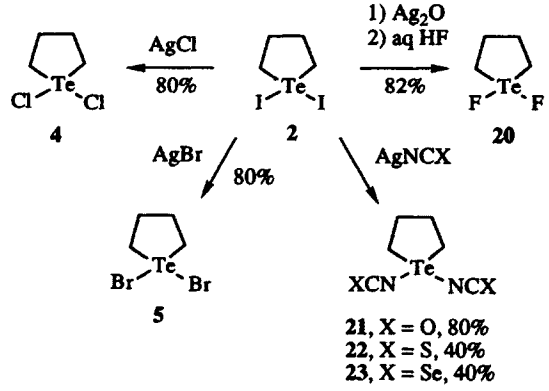

21, X = O, 80%
22, X = S, 40%
23, X = Se, 40%

Scheme 8

Silver carboxylate salts and other silver salts also give good yields of substitution products with **2** as shown in Scheme 9. Silver acetate,[15] benzoate,[15] trichloroacetate,[15] and butyl maleate[16] give the corresponding 1,1-dicarboxyltetrahydrotellurophenes **24**. The reaction of silver cyanide with 1,1-diiodotetrahydrotellurophene (**2**) gives 1,1-dicyanotetrahydrotellurophene (**25**) in 63% isolated yield. Similarly, the addition of an excess of silver azide to **2** gives a nearly quantitative yield of diazide **26**.

Ligand substitution in 1,1-diiodotetrahydrotellurophene (**2**) gives different types of substitution products with silver perchlorate as illustrated in Scheme

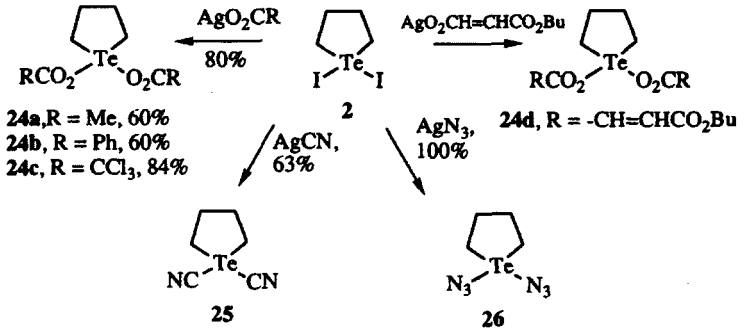

Scheme 9

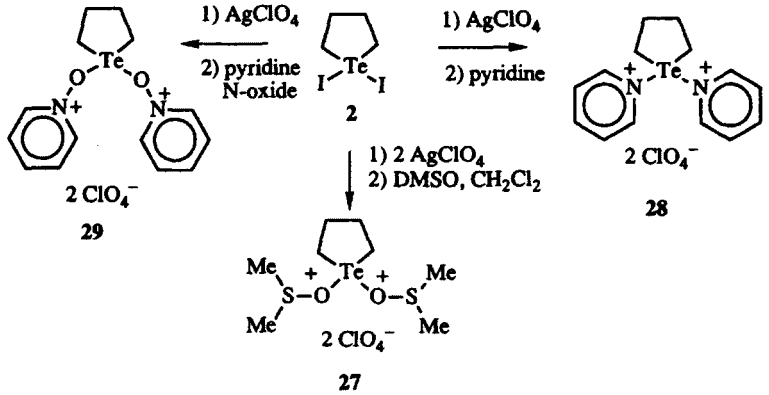

Scheme 10

10.[17,18] The addition of dimethyl sulfoxide,[17] aromatic amines,[18] and aromatic amine *N*-oxides[18] to premixed suspensions of **2** or **4** and silver perchlorate in dichloromethane gives isolable microcrystalline powders described as **27–29**, respectively, in 50–70% yields. The ionic nature of these complexes was confirmed by conductance measurements in solution. X-ray structural data are absent for complexes of these types, and detailed ^{1}H NMR work is also absent. However, bands at 1100 and 625 cm^{-1} in infrared spectra of these complexes suggest ionic perchlorates in these structures.[19]

Nonsilver salts of other nucleophiles also give ligand substitution products in reactions with **2**. 1,1-Di-(alkylxanthato)tetrahdyrotellurophenes **30** have been prepared from the sodium salts of the alkylxanthates as shown in Scheme 11.[20] Alternatively, carbon disulfide thermally inserts into tellurium–oxygen bonds of 1,1-dialkoxytetrahydrotellurophenes **31** to give **30**. Compounds **31** are thermally unstable relative to reductive elimination to give tetrahydrotellurophene (**3**) and the corresponding dixanthates **32**.

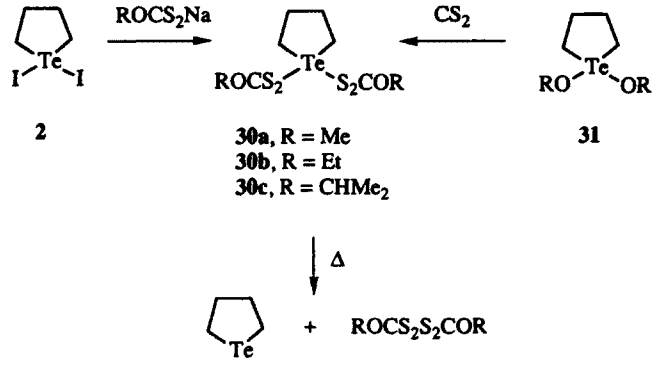

Scheme 11

Ammonium and sodium salts of dithiocarbamates also react with 1,1-diiodotetrahydrotellurophene (**2**) to give ligand substitution reactions as shown in Scheme 12.[21] The dithiocarbamates **33** undergo reductive elimination of the ligands at 180°C to give tetrahydrotellurophene (**3**), carbon disulfide, and the appropriate thiourea **34**.

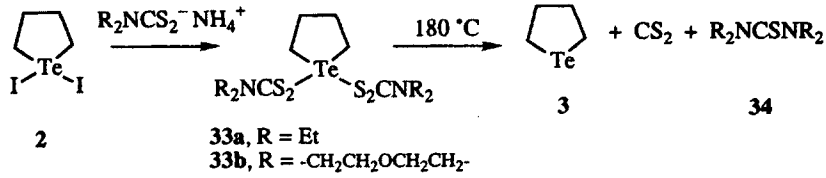

Scheme 12

The addition of iodonium chloride, iodonium bromide, or iodine to 1,1-diiodotetrahydrotellurophene (**2**) in chloroform solution gives 1 : 1 complexes with **2** that can be isolated as the crystalline solids **35** as shown in Scheme 13.[14] Spectroscopic examination of these complexes suggests that the iodine–chlorine, iodine–bromine, and iodine–iodine bonds are still intact in these complexes and that they are not octahedral via oxidative addition across tellurium. Similar complexes are not formed on the addition of chlorine or bromine to **2**, nor are complexes formed on the additions of halogen to 1,1-dichlorotetrahydrotellurophene (**4**) or 1,1-dibromotetrahydrotellurophene (**5**).

The hydrolysis of the iodine complex **35c** has been described.[14] The product is best described as a protonated telluroxide **36** with a triiodide counterion, according to the authors, which is analogous to the product described for hydrolysis of tellurane tetraiodide.[1]

The telluroxide of **3** has been prepared by either air oxidation of **3** or by the basic hydrolysis of the 1,1-dihalotetrahydrotellurophenes **2**, **4**, and **5** as shown in Scheme 14.[1,22] The 1,1-dihalo compounds are regenerated on treating **37** with

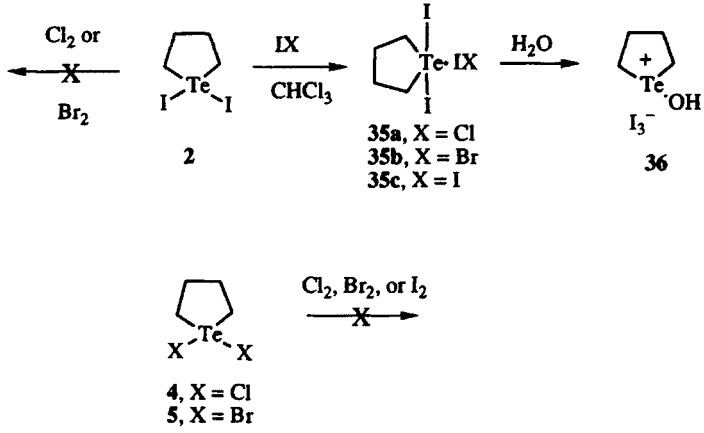

Scheme 13

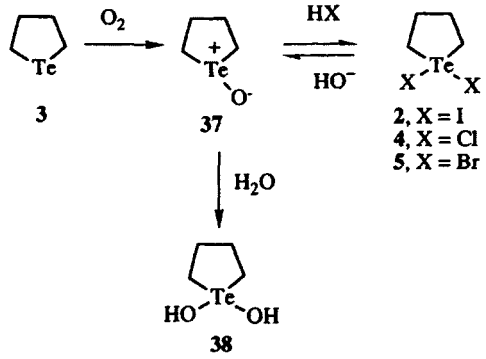

Scheme 14

the appropriate halogen acid. While this product is described as the telluroxide, it most likely is the 1,1-dihydroxytellurophene **38** formed by the addition of water to **37**.[23]

The addition of tetra-*n*-alkylammonium, tetraphenylphosphonium, tetraphenylarsonium, and tetraphenylantimonium halides to 1,1-diiodotetrahydrotellurophene (**2**) gives octahedral 1,1,1,1-tetrahalotetrahydrotellurophenes **39** as isolable, crystalline solids as shown in Scheme 15.[24] The dichlorodiiodo and dibromdiiodo products are converted to the corresponding tetraiodo complexes with potassium iodide and to the corresponding diiododiisothiocyanato or diiododicyanato complexes with silver (or potassium) thiocyanate or silver (or potassium) cyanate, respectively.

The tetraiodo complexes are converted to the corresponding tetraisothiocyanate, tetraazido, or tetracyanato complex with either the silver or potassium salt of the respective ligand as shown in Scheme 15.[24] The tetraiiodocomplex is

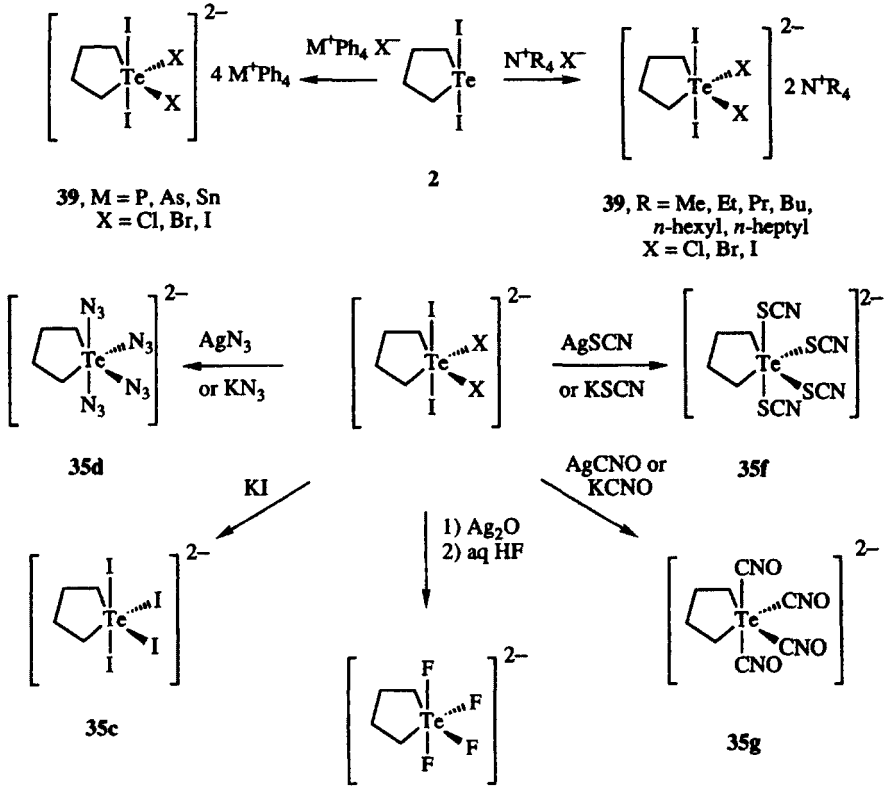

Scheme 15

converted to the tetrafluoride via sequential treatment with silver oxide followed by aqueous hydrofluoric acid.[24]

The reaction of 1,1-diiodotetrahydrotellurophene (**2**) with two equivalents of sodium tetraphenylborate gives a different type of substitution product as shown in Scheme 16. One iodo ligand has been replaced with a phenyl group from the tetraphenyl borate to give 1-phenyl telluronium salt **40a**.[25] The same substitution reaction has also been observed with 1,1-diiodo-2-methyl-tetrahydrotellurophene (**6**) to give 1-phenyltelluronium salt **40b**.[26]

1-Alkyl-tetrahydrotellurophenium halides have been converted to their tetraphenylborate salts with sodium tetraphenylborate as shown in Scheme 16.[25,26] The 1-alkyl-tetrahydrotellurophenium halides in turn are prepared by the addition of alkyl halides to tetrahydrotellurophene (**3**). Conductance studies suggest that these complexes approach the solution behavior of 1 : 1 electrolytes but ^{1}H NMR studies suggest that some ion pairing occurs. In contrast, conductance studies of **6** and dichloride and dibromide analogs of **6** suggest

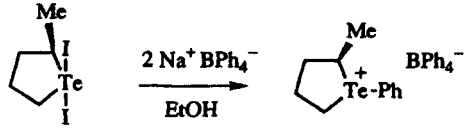

2, R = H
6, R = Me

40a, R = H
40b, R = Me

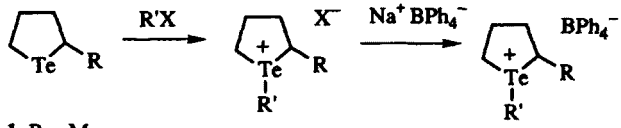

1, R = Me
3, R = H

7a, R' = Me, R = Me, X = I
7b, R' = Et, R = Me, X = I
7c, R' = CH_2Ph, R = Me, X = Br
7d, R' = Me, R = Me, X = Cl
7e, R' = $CH_2CH{=}CH_2$, R = Me, X = Br
7f, R' = $CH_2CH{=}CH_2$, R = Me, X = I
41a, R' = Et, R = H, X = I
41b, R' = Et, R = H, X = Br
41c, R' = CH_2Ph, R = H, X = Br
41d, R' = CH_2Ph, R = H, X = Cl
41e, R' = Me, R = H
41f, R' = $CH_2CH{=}CH_2$, R = H, X = I
41g, R' = $CH_2CH{=}CH_2$, R = H, X = Br
41h, R' = $CH_2CH{=}CH_2$, R = H, X = Cl

42a, R' = Me, R = Me
42b, R' = Et, R = Me

Scheme 16

mostly covalent character in both dimethyl sulfoxide (DMSO) and dimethyl formamide (DMF).[26]

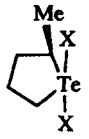

6, X = I
6, X = Cl
6, X = Br

Charge-transfer complexes of tetrahydrotellurophene (**3**) and organic acceptors tetracyanoquinodimethane (TCNQ) and 2,3-dichloro-5,6-dicyano-1,4-benzoquinone (DDQ) have been prepared.[27,28] These materials (**3-TCNQ** and **3-DDQ**) are highly ionic in the ground state and probably show semiconductor properties.

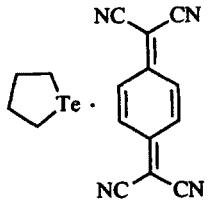

3-TCNQ

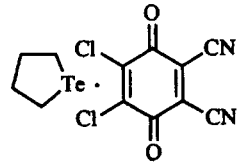

3-DDQ

B. Synthesis of 2,5-Dihydrotellurophenes and Derivatives

The addition of tellurium tetrachloride to two equivalents of 1,3-butadiene gives 1,1-dichloro-2,5-dihydrotellurophene (**43a**) in 62% yield and 1,4-dichloro-2-butene as shown in Scheme 17.[29] Similar reactions with 2-methyl- and 2,3-dimethyl-1,3-butadiene give 1,1-dichloro-3-methyl-2,5-dihydrotellurophene (**43b**) and 1,1-dichloro-3,4-dimethyl-2,5-dihydrotellurophene (**43c**), respectively, in 46 and 53% yields. 2,3-Diphenyl-1,3-butadiene does not react with tellurium tetrachloride under the reaction conditions, while *cis*-2,*trans*-4-hexadiene produces large amounts of tellurium metal under the same reaction conditions.

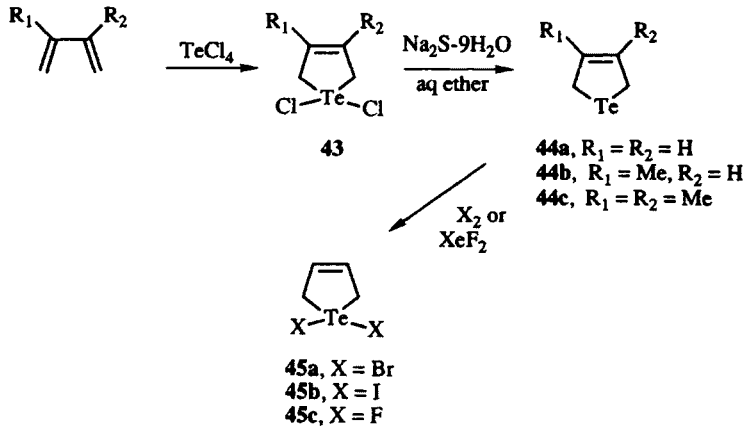

43

44a, $R_1 = R_2 = H$
44b, $R_1 = Me$, $R_2 = H$
44c, $R_1 = R_2 = Me$

45a, X = Br
45b, X = I
45c, X = F

Scheme 17

The 1,1-dichloro compounds **43** were reduced with disodium sulfide nonahydrate in ether (5% aqueous) to 2,5-dihydrotellurophenes **44** in 84% isolated yield for **44a** and in nearly quantitative yield for **44b** and **44c**.[29] Although the original preparation of compounds **44** describes them as heavy oils, a later report describes ultrapure **44a** as being crystalline at room temperature.[30]

The oxidative addition of bromine and iodine to **44** gives 1,1-dihalo-2,5-dihydrotellurophenes **45a** and **45b** in 88 and 90% isolated yields, respectively.[29]

The addition of xenon difluoride to **44a** gives 1,1-difluoro-2,5-dihydrotellurophene (**45c**) in 97% isolated yield.

The reaction products of tellurium tetrachloride with 1,3-butadiene had been described in earlier reports, but the product described by Bergman and Engman is bis(4-chloro-2-butenyl)tellurium dichloride (**46**).[29] Refluxing **46** in toluene for an hour gives 1,1-dichloro-2,5-dihydrotellurophene (**43a**), which suggests that **46** might be an intermediate in the reaction depicted in Scheme 17.

$(ClCH_2CH{=}CHCH_2)_2TeCl_2$

46

The oxidation of 2,5-dihydrotellurophene (**44a**) with hydrogen peroxide gives a white crystalline solid, which does not appear to be the telluroxide analog or a hydrate.[29] When dry, the product of this reaction is explosive, suggesting peroxy derivatives such as **47** as shown in Scheme 18.

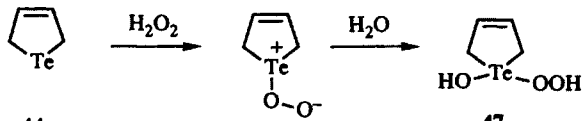

44a **47**

Scheme 18

Charge-transfer complexes of 2,5-dihydrotellurophenes **44** with organic donors TCNQ and tetrachlorobenzoquinone (TCB) have been described.[32] Compounds **44** fail to give complexes with *p*-dinitrobenzene (DNB). The complexes show semiconducting behavior and, with respect to the TCNQ complexes, the relative donor power with TCNQ is **44a** > **44b** > **44c**.

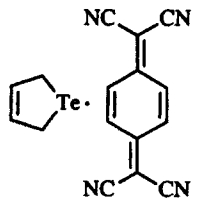

44-TCNQ

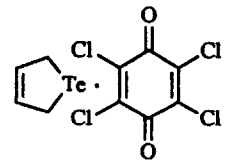

44-TCB

C. Benzodihydrotellurophenes

The first synthesis of a benzo analog of 2,5-dihydrotellurophene employed the nucleophilic attack of disodium telluride on α,α′-dibromo-*o*-xylene as shown in Scheme 19.[33] 1,3-dihydrobenzo[*c*]tellurophene (**48**) is isolated in moderate yield

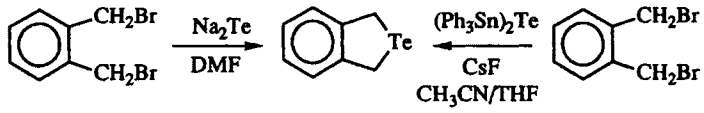

48

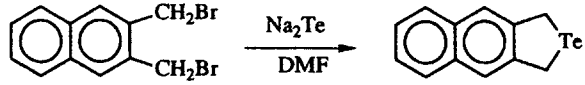

Scheme 19

from this reaction. The addition of disodium telluride to 2,3-di-(bromomethyl)naphthalene under the same reaction conditions gives a moderate yield of 1,3-dihydronaphtho[2,3-*c*]tellurophene (**49**).[33]

A variation on the source of nucleophile in Scheme 19 has been reported.[34] The addition of cesium fluoride to an acetonitrile–THF solution of α,α′-dibromo-*o*-xylene, and bis(triphenylstannyl)telluride gives **48** in 50% isolated yield.

2,2-Diiodo-1,3-dihydrobenzo[*c*]tellurophene (**50**) has been prepared from α,α′-dichloro-*o*-xylene, sodium iodide, and tellurium powder in 83% yield in 2-methoxyethanol as shown in Scheme 20.[35] Hydrazine reduction of **50** in aqueous ethanol gives 1,3-dihydrobenzo[*c*]tellurophene (**48**) in 60% yield.[36]

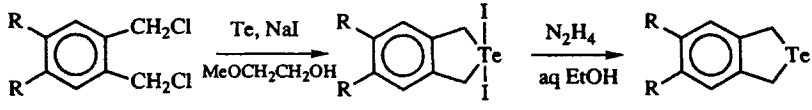

50, R = H
51, R = Me

48, R = H
52, R = Me

Scheme 20

Similar chemistry has been reported starting with 1,2-di-(chloromethyl)-4,5-dimethylbenzene.[37] Tellurium and sodium iodide give 2,2-diiodo-5,6-dimethyl-1,3-dihydrobenzo[*c*]tellurophene (**51**), and hydrazine reduction of **51** gives 5,6-dimethyl-1,3-dihydrobenzo[*c*]tellurophene (**52**).

Tellurium(IV) analogs of 1,3-dihydrobenzo[*c*]tellurophene derivatives **48** and **52** have been prepared by oxidative addition of halogens as shown in Scheme 21. Oxidative addition of iodine or bromine to ether solutions of 1,3-dihydrobenzo[*c*]tellurophene (**48**) gives 2,2-diiodo-1,3-dihydrobenzo[*c*] tellurophene (**50**) or 2,2-dibromo-1,3-dihydrobenzo[*c*]tellurophene (**53**) in nearly quantitative yield.[36] The addition of thionyl chloride to **48** gives 2,2-dichloro-1,3-dihydrobenzo[*c*]tellurophene (**54**).[36] The oxidative addition of iodine, bromine, or chlorine to 5,6-dimethyl-1,3-dihydrobenzo[*c*]tellurophene

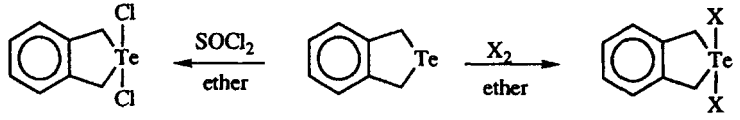

54 48 50, X = I
53, X = Br

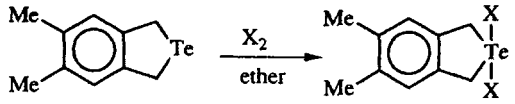

52 51, X = I
55, X = Br
56, X = Cl

Scheme 21

(52) gives 2,2-diiodo- (51), 2,2-dibromo- (55), or 2,2-diiodo-5,6-dimethyl-1,3-dihydrobenzo[*c*]tellurophene (56), respectively.[38]

Telluronium salts of 5,6-dimethyl-1,3-dihydrobenzo[*c*]tellurophene (52) have been prepared by the addition of alkyl halides as shown in Scheme 22.[38] Anion exchange reactions of the halide salts of 57 with silver isothiocyanate, silver acetate, and sodium *N*,*N*-diethyldithiocarbamate gave these salts of compounds 57. The addition of two equivalents of sodium tetraphenylborate to 2,2-diiodo-5,6-dimethyl-1,3-dihydrobenzo[*c*]tellurophene (51) gives the phenyl telluronium salt 58.[37] Conductance studies of 57 and 58 suggest considerable ionic character to these compounds in DMSO and DMF.[38]

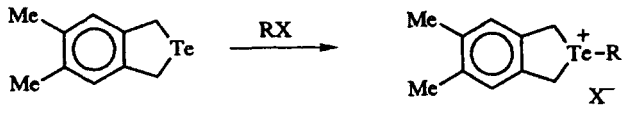

52

57, R = Me, Et, -$CH_2CH{=}CH_2$, CH_2Ph
X = NCS, Cl, Br, I, OAc, S_2CNEt_2

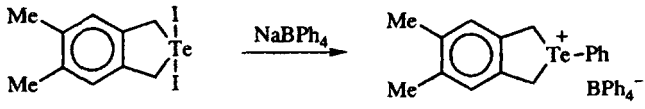

51 58

Scheme 22

Some unusual tellurium(IV) derivatives of 1,3-dihydrobenzo[*c*]tellurophenes have been prepared from 2,2-diiodo-1,3-dihydrobenzo[*c*]tellurophene (**50**) and sodium *N*,*N*-diethyldithiocarbamate, potassium *O*,*O*-diethyldithiophosphite, and potassium *O*-ethyldithioxanthate as shown in Scheme 23.[39] Compounds **59**–**61** are neutral, pseudooctahedral complexes of tellurium(IV).

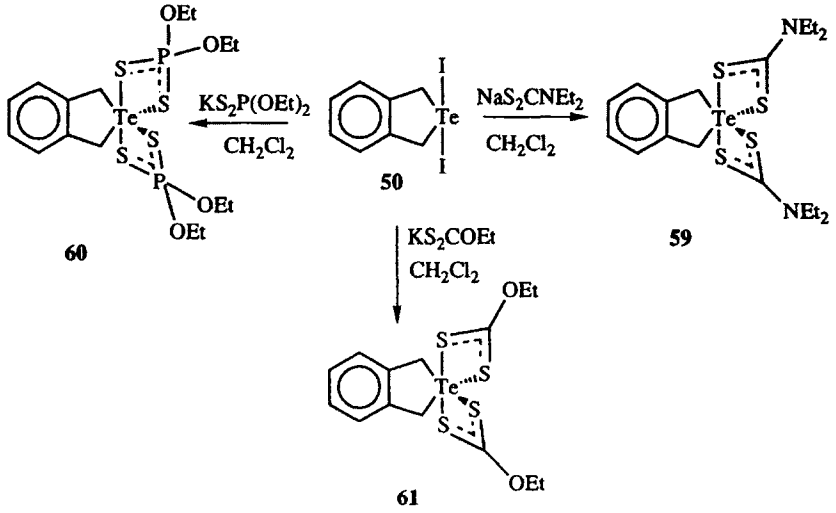

Scheme 23

The only examples of 2,3-dihydrotellurophenes are fused to quinoline rings.[40] The nucleophilic displacement of two chlorides from 2-chloro-3-(2′-chloroethyl)quinolines with sodium hydrogentelluride in ethanol gives 2,3-dihydroquinolino[2,3-*b*]tellurophenes **62** in 30–49% isolated yields as shown in Scheme 24.

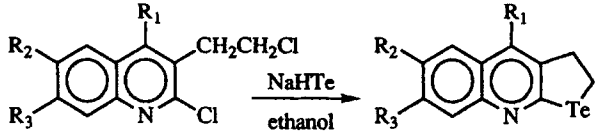

62a, R_1 - R_3 = H
62b, R_1 = R_3 = H, R_2 = Me
62c, R_1 = Ph, R_2 = R_3 = H
62d, R_1 = R_2 = H, R_3 = Me

Scheme 24

The addition of tellurium and sodium iodide to a 2-methoxyethanol solution of 2,3-bis(bromomethyl)quinoxaline gives 2,2-diiodo-1,3-dihydroquinoxalino [3,4-*b*]tellurophene (**63a**) in 60% yield as shown in Scheme 25.[41] Similarly, the addition of tellurium and sodium iodide to a 2-methoxyethanol solution of 2,3-

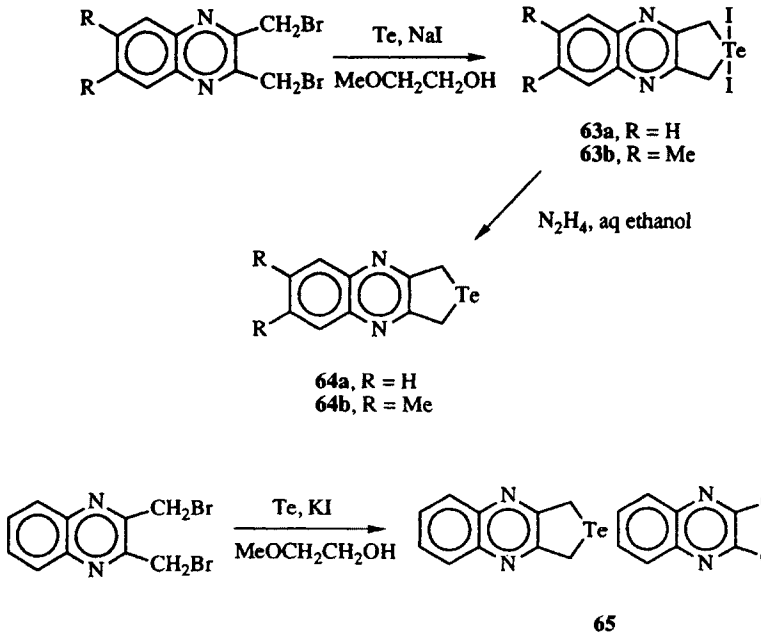

Scheme 25

bis(bromomethyl)-6,7-dimethylquinoxaline gives 2,2-diiodo-7,8-dimethyl-1,3-dihydroquinoxalino[3,4-*b*]tellurophene (**63b**) in 53% yield.[32] The 1,1-diiodides were reduced to the hydrocarbons **64** with ethanolic hydrazine.[41]

The use of potassium iodide with tellurium and 2,3-bis(bromomethyl) quinoxaline in methoxyethanol gives a different product.[41] The 1 : 1 complex of **63a** and 2,3-bis(iodomethyl)quinoxaline (**65**) is isolated in 75% yield.

The reaction of tellurium metal and potassium iodide in 2-methoxyethanol with 1,2,4,5-tetra(bromomethyl)benzene gives 1,2,4,5-bis(diiodotelluracyclopentano)benzene (**66**) as a yellow crystalline solid as shown in Scheme 26.[27] Hydrazine reduction of **66** does not give 1,2,4,5-bis(telluracyclopentano)benzene (**67**).

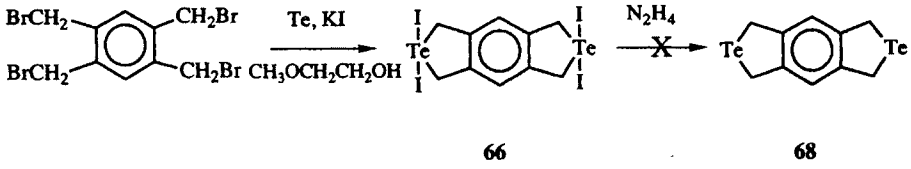

Scheme 26

Donor–acceptor complexes have been formed with several of the dihydrobenzotellurophenes. TCNQ complexes of both **64a** and **64b** have been described,[32,41] as have the TCNQ complexes of **48** and **52**.[42] The DNB complex of

48 has been described.[32] 5,6-Dimethyl-1,3-dihydrobenzo[*c*]tellurophene (**52**) has formed complexes with *p*-benzoquinone, 1,4-naphthoquinone, and 2,3-dimethylanthraquinone.[43] Tellurophthalic anhydride (**68**)[44]—a 1,3-dioxo-1,3-dihydrobenzotellurophene—failed to give a complex with TCNQ.[27] In all these complexes, the materials are either insulators or at best semiconducting with specific conductances of $< 10^{-8}\ \Omega^{-1}\,cm^{-1}$.

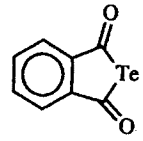

68

Electrochemical oxidation of 1,3-dihydrobenzo[*c*]tellurophene (**48**) has given different structures not prepared by other means as shown in Scheme 27.[45] Oxidation at a platinum electrode in dichloromethane in the presence of tetra-*n*-butylammonium perchlorate gives 1,3-dihydrobenzo[*c*]tellurophene 2,2-bisperchlorate **69**. At a mercury pool electrode, two different oxidation processes are described. The first, with $E^\circ = 0.26$ V (vs. Ag/AgCl), requires 0.65 electrons per molecule of **48** and corresponds to mercury complex **70**. The second oxidation with $E^\circ = 0.61$ V (vs. Ag/AgCl) gives a different product that has been assigned the mercury-rich structure **71**.[45]

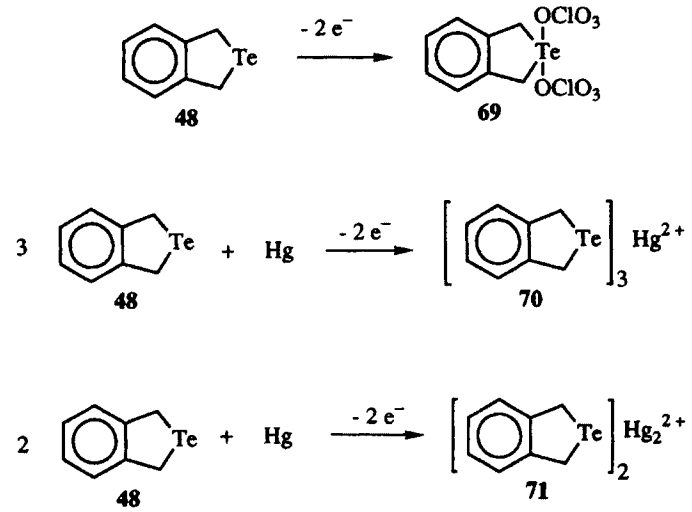

Scheme 27

D. Oxodihydrobenzotellurophenes

1. 2-Oxo-2,5-dihydrobenzotellurophenes

Oxo derivatives of the benzodihydrotellurophenes have been prepared via nucleophilic displacements of halides with telluride anions as shown in Scheme 28. The addition of sodium hydrogentelluride to either *o*-bromomethylbenzoyl chloride[46,47] or *o*-bromomethylbenzoyl bromide[47] gives 2-oxo-2,5-dihydrobenzotellurophene (**72**) or, as an alternative naming, 2,5-dihydrobenzo[*c*]-tellurophene-2-one. The tellurium analog of phthallic anhydride—compound **68**—can be prepared by the addition of disodium telluride to phthaloyl chloride.[44]

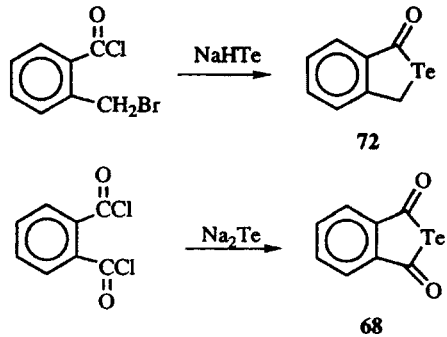

Scheme 28

The telluroester fragment of compounds **68** and **72** make them somewhat reactive toward both nucleophiles and electrophiles. Unlike compounds **48**, **49**, and **52**, which undergo oxidative addition reactions at tellurium (Scheme 21) with halogens, compound **72** reacts with thionyl chloride, bromine, and iodine to give products derived from cleavage of the tellurium–carbonyl bond as shown in Scheme 29.[46,47] In the presence of two equivalents of bromine, tellurium tribromide derivatives are isolated.

Nucleophilic addition reactions can also be problematic with **72** as shown in Scheme 30.[47] The addition of phenylmagnesium bromide to **72** leads to diphenyl ditelluride with destruction of the benzotellurophene ring. However, the carbonyl group can be converted to a thione group with the Lawessen reagent to give benzotellurophene derivative **73** in nearly quantitative yield.

2. 3-Oxo-2,3-dihydrobenzotellurophenes

3-Oxo-2,3-dihydrobenzotellurophene (**74**) was first prepared[48] by the cyclization of 2-acetylphenyl tellurenyl bromide (**75**) with potassium hydroxide or

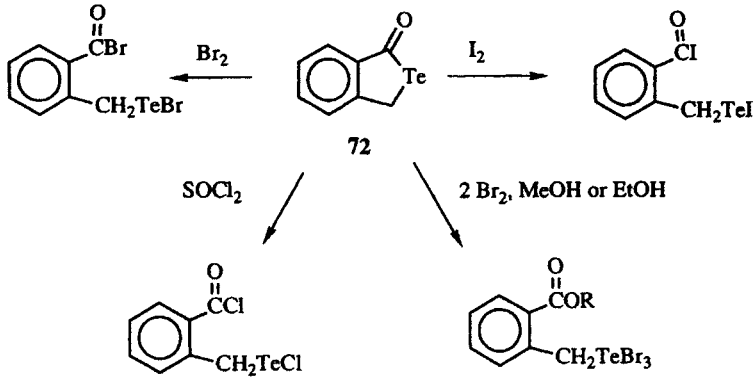

Scheme 29

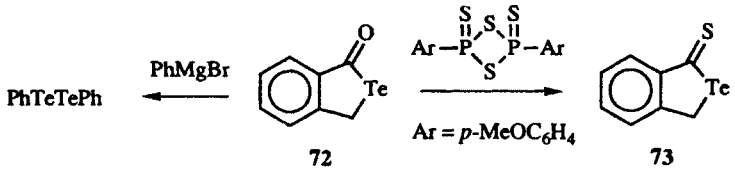

Scheme 30

ammonia[49] in ethanol. An improvement in yield and product purity is realized by the use of potassium acetate as base.[50] The synthesis of **74** via the last route is shown in Scheme 31, in which the cyclization step proceeded in 53% isolated yield.[50] The use of a copper oxide–induced decomposition of diazocompound **76** has also been utilized to prepare **74** in 30–40% isolated yield.[51]

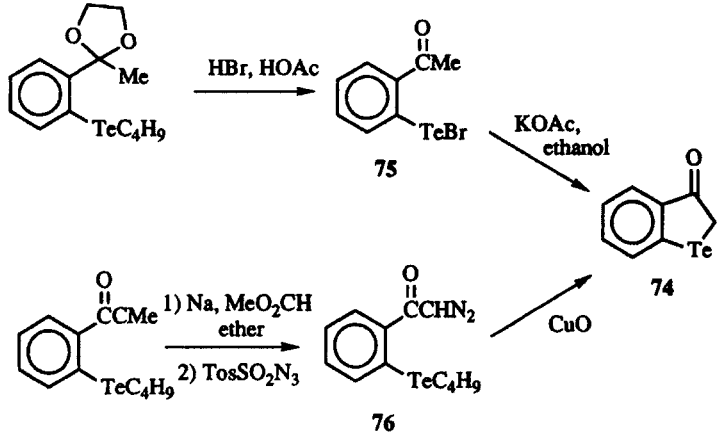

Scheme 31

The hydrolysis of certain 3-halobenzotellurophenes has given 3-oxo-2,3-dihydrobenzotellurophene (**74**).[52] Refluxing 3-chlorobenzotellurophene in trifluoroacetic acid gives **74** in 84% isolated yield as shown in Scheme 32. Under similar conditions, 3-bromobenzotellurophene gives **74** in only 7% yield. 3-Halo-2-methylbenzotellurophenes fail to give any 3-oxo-2,3-dihydrobenzotellurophene derivatives in refluxing acetic acid.

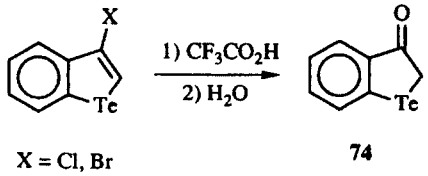

Scheme 32

3-Oxo-2,3-dihydrobenzotellurophene (**74**) is a versatile intermediate for preparing 2-substituted derivatives via condensation reactions as shown in Scheme 33.[48,50,53] Oxidation with either air[48] or potassium ferricyanide gives telluroindigo **77** (in 73% isolated yield in the latter reaction).[50] The condensation of **74** with aromatic aldehydes gives the 2-arylidene derivatives **78**,[48] with dimethylformamide[53] or its diethoxy ketal[48] gives 2-aminomethylidene derivative **79**, and with 4-nitroso-*N*,*N*-dimethylaniline gives 2-imino derivative **80**.

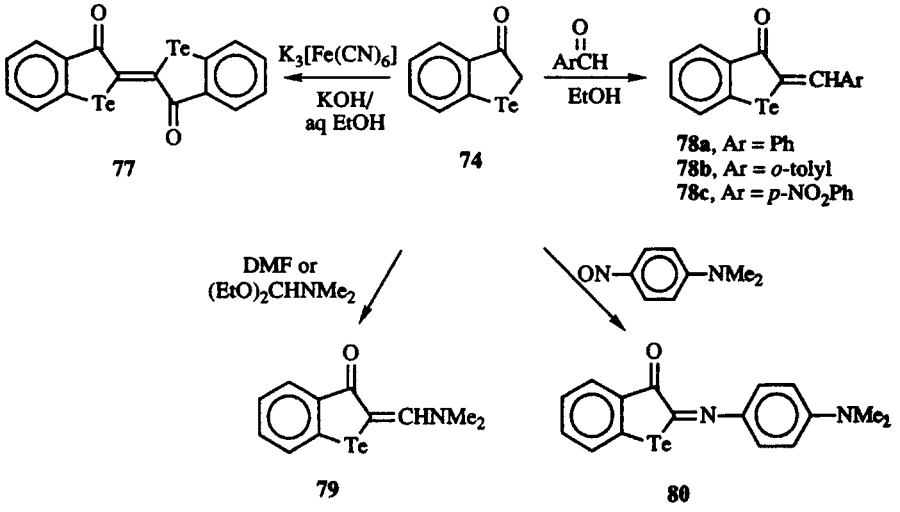

Scheme 33

The arylidene derivatives **78** have also been prepared via the condensation of aldehydes with 2-acetylphenyltellurenyl bromide (**75**) in the presence of piperdine in refluxing acetic acid.[54] Presumably, the condensation of the aldehyde with **75** gives **81** as an intermediate which then cyclizes and loses HBr to give telluroaurones **78** in approximately 80% isolated yields as shown in Scheme 34.

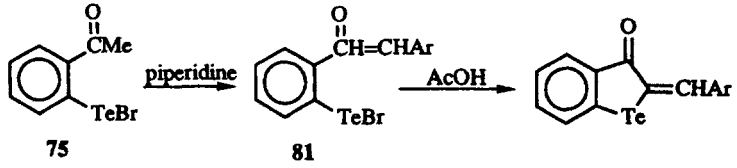

75 81

78a, Ar = Ph
78d, Ar = *p*-MeOPh
78e, Ar = *p*-MePh
78f, Ar = *p*-ClPh
78g, Ar = *o*-ClPh
78h, Ar = *p*-IPh
78i, Ar = *p*-Me_2NPh
78j, Ar = α-naphthyl

Scheme 34

The carbonyl of **74** is "normal" in the sense that condensations with various nucleophiles give expected products. Thus, hydroxylamine gives the oxime **81**, 2,4-dinitrophenylhydrazine gives the 2,4-dinitrophenylhydrazone **82**, and semicarbazide gives the corresponding semicarbazone **83**.[48]

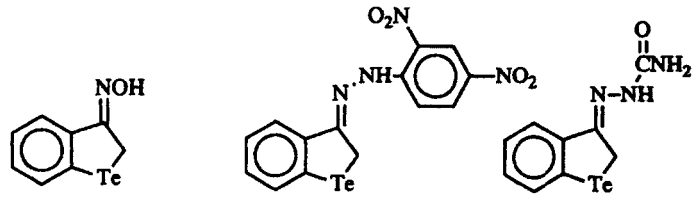

81 **82** **83**

The tellurium atom of **74** reacts with halogens to give products derived from oxidative addition as shown in Scheme 35.[48] The tellurium(IV) analogs **84** are isolable, crystalline solids. Similarly, the addition of methyl iodide to **74** gives the

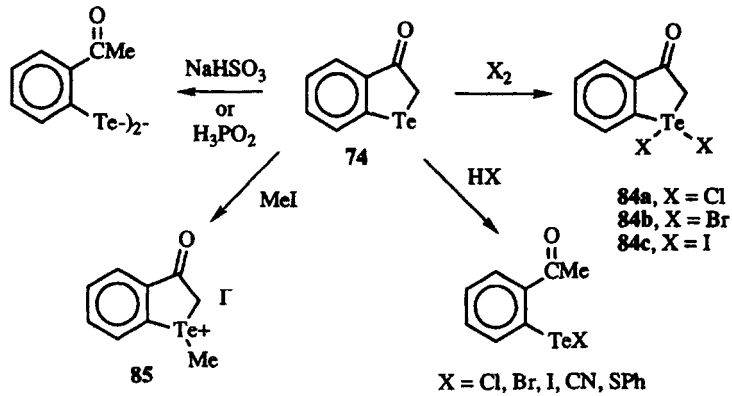

84a, X = Cl
84b, X = Br
84c, X = I

85

X = Cl, Br, I, CN, SPh

Scheme 35

methyl telluronium salt **85** in nearly quantitative yield.[48] In contrast, the addition of hydrohalic acids, hydrogen cyanide, or thiophenol to **74** gives cleavage of the bond between tellurium and the methylene carbon to give 2-acetylphenyl tellurenyl halides or pseudohalides (Scheme 35).[48,54] Reductive cleavage of the tellurium–methylene carbon bond is observed with either sodium bisulfite or hypophosphoric acid to give 2-acetylphenyl ditelluride.[55]

III. TELLUROPHENE AND DERIVATIVES

A. Tellurophenes from Diynes, Dienes, or Derivatives

The tellurophene nucleus was an elusive heterocycle for 30 years following the first documented efforts to prepare it.[56] Other unsuccessful efforts have been reported as well.[57]

The first reported synthesis of the tellurophene nucleus incorporated the addition of tellurium tetrachloride to 1,4-dilithiotetraphenyl-1,3-butadiene to give 2,3,4,5-tetraphenyltellurophene (**86**) in 56% isolated yield (Scheme 36).[58] Alternatively, the addition of dilithium telluride to 1,4-diiodotetraphenyl-1,3-butadiene gives **86** in 82% yield. Tetraphenyltellurophene **86** reacts with bromine in carbon tetrachloride to give the 1,1-dibromotetraphenyltellurophene **87** in 92% isolated yield.

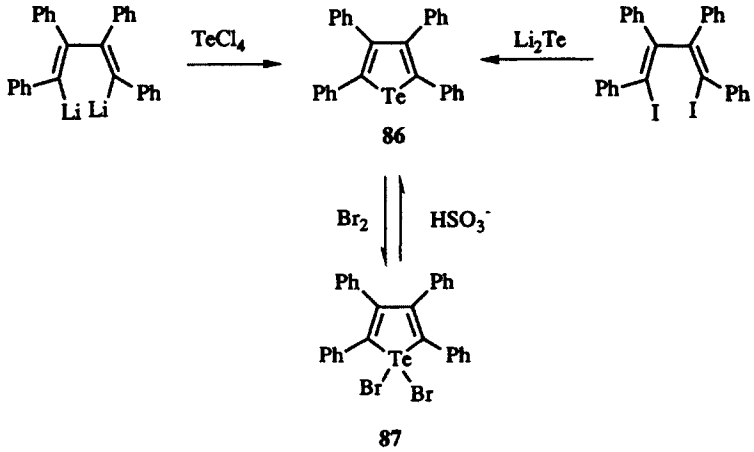

Scheme 36

A variation of this procedure was used to prepare 2,3,4,5-tetrachlorotellurophene (**88**) as shown in Scheme 37.[59] A stirred suspension of tellurium metal and hexachloro-1,3-butadiene gives tellurium tetrachloride and **88**, the latter compound in 14% isolated yield. The oxidative addition of chlorine to **88** gives hexachlorotellurophene **89**, which can be reduced with sodium bisulfite to regenerate **88**.

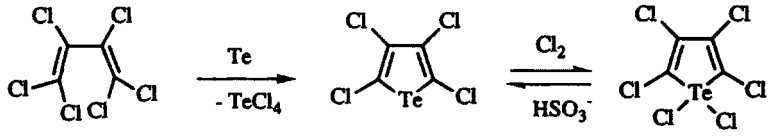

88 89

Scheme 37

The parent tellurophene was first prepared by the addition of disodium telluride to 1,3-butadiyne in methanol to give **90** in 69% isolated yield (Scheme 38).[60] The addition of a solution of bromine in methanol to **90** gives the 1,1-dibromo compound **91**, which can be reduced back to tellurophene (**90**) in nearly quantitative yield with sodium bisulfite. The same procedure with 1,6-dihydroxyhexa-2,4-diyne gives 2,5-bis(hydroxymethyl)tellurophene (**92**) in 25% yield and with 1,7-dihydroxy-1,7-dimethylocta-3,5-diyne gives 2,5-bis-(dimethylhydroxymethyl)tellurophene (**93**) in almost quantitative yield.[60]

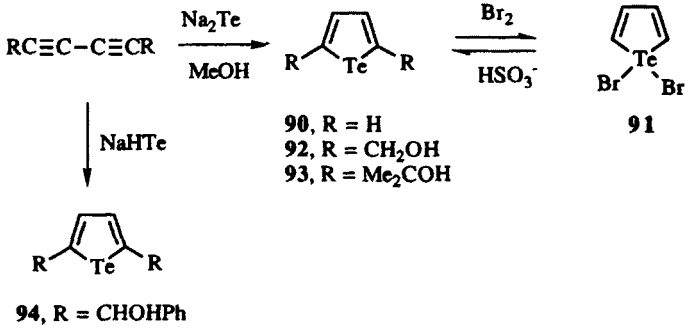

90, R = H
92, R = CH_2OH
93, R = Me_2COH

91

94, R = CHOHPh

Scheme 38

The basic procedure shown in Scheme 38 has been modified by others to optimize yields and to provide other derivatives. Fringuelli and Taticchi describe in great detail steps to be taken in the preparation of sodium telluride from sodium in liquid ammonia and the isolation of the tellurophene product (**90**).[61,62] Others have used sodium hydrogentelluride in the presence of silver acetate to give **94** in 52% isolated yield.[63]

Unsymmetrical 1,3-diacetylenes also work in this reaction sequence as shown in Scheme 39. The addition of phenyl-1,3-butadiyne to disodium telluride in

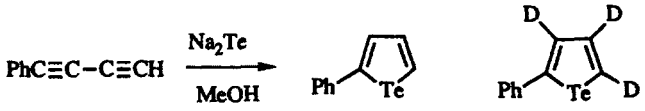

95 **95-d_3**

Scheme 39

methanol gives 2-phenyltellurophene (**95**) in 58% isolated yield.[64] This approach has also been utilized with 1-phenyl-5-deutero-1,3-butadiyne in methanol-*O*-d_1 to give 2-phenyl-3,4,5-trideuterotellurophene (**95**-d_3). [2,3,4,5-Tetradeuterotellurophene (**90**-d_4) has been prepared as shown in Scheme 38 via the use of methanol-*O*-d_1 with 1,3-butadiyne and disodium telluride.[65]]

Tellurophene (**90**) has been isolated in 3% yield from the reaction of tellurium and acetylene in the presence of aqueous potassium hydroxide and stannous chloride.[66] Similarly, the reaction of 1,3-butadiyne with tellurium in the presence of aqueous potassium hydroxide–DMSO–hydrazine hydrate gives tellurophene (**90**) in 15–20% isolated yield.[67] Neither of these reactions has practical synthetic utility for the preparation of **90** and derivatives.

A more practical modification of the butadiyne approach to tellurophenes is shown in Scheme 40. 1,4-bis(trimethylsilyl)-1,3-butadiyne reacts with disodium telluride to give tellurophene (**90**) in 37% isolated yield.[68] A modification of this approach using disodium telluride generated *in situ* from tellurium and sodium formaldehyde sulfoxylate gives **90** in 59% isolated yield.[69] Presumably, 2,5-bis(trimethylsilyl)tellurophene (**96**) is the first-formed product in both reactions that loses the trimethylsilyl groups under the reaction conditions.

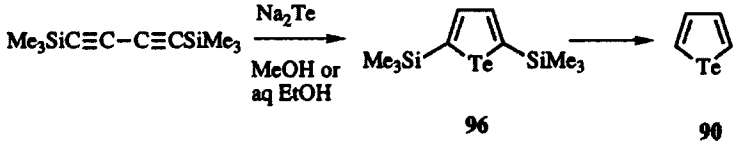

96 **90**

Scheme 40

3-Methylbut-3-en-1-yne (**97**) has been employed as a four-carbon unit for the synthesis of 3-methyltellurophene (**98**) as shown in Scheme 41.[70] The addition of *n*-butyl lithium and potassium *tert*-butoxide to a THF–hexane solution of **97** in the presence of lithium bromide gives the dilithio salt **99**. The allyl lithium moiety reacts with tellurium metal and the resulting species cyclizes in the

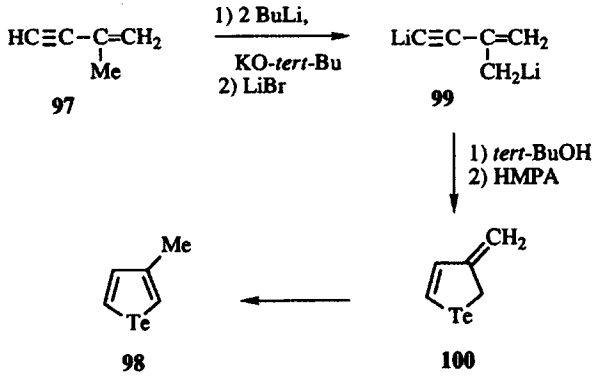

97 **99** **98** **100**

Scheme 41

presence of *tert*-butanol and HMPA to give 3-methylene-2,3-dihydrotellurophene (**100**) in 51% isolated yield. 3-Methyltellurophene (**98**) is isolated in 90% yield when **100** is heated with a mixture of potassium *tert*-butoxide, *tert*-butanol, HMPA, and THF.

A similar approach has utilized acetylenic chlorohydrins **101** instead of but-3-en-1-ynes as shown in Scheme 42.[71] The addition of sodium hydrogen telluride to **101** gives tellurophene (**90**) in 10% isolated yield, 3-methyltellurophene (**98**) in 40% isolated yield, and 2,4-dimethyltellurophene (**102**) in 50% isolated yield.

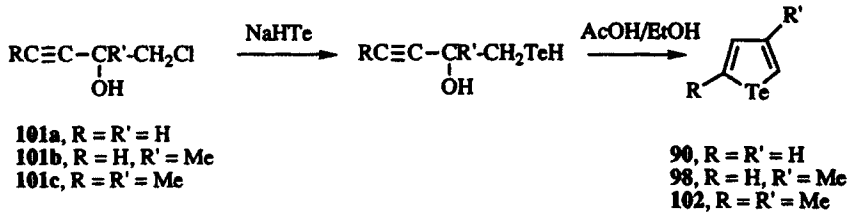

101a, R = R' = H
101b, R = H, R' = Me
101c, R = R' = Me

90, R = R' = H
98, R = H, R' = Me
102, R = R' = Me

Scheme 42

Acetylenic epichlorohydrins also react with disodium telluride to give tellurophene derivatives **103** and enynols **104** as shown in Scheme 43.[72] The yields of tellurophenes are between 59 and 73% in these reactions when the disodium telluride is produced via the reduction of tellurium metal with sodium borohydride in aqueous methanol. When tellurium is reduced by other reagents such as sodium formaldehydesulphoxylate, the yields of tellurophene products are less than 10% and the major products are enynols **104**.

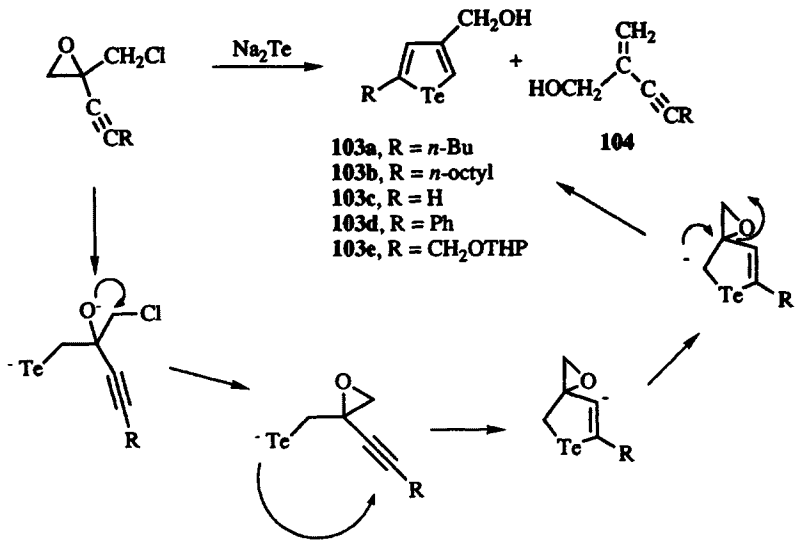

103a, R = *n*-Bu
103b, R = *n*-octyl
103c, R = H
103d, R = Ph
103e, R = CH_2OTHP

104

Scheme 43

B. Tellurophenes from Metallocyclopentadienes

Metallocyclopentadienes have also been used as precursors to tellurophenes.[73–75] The addition of rhodium(I) tris(triphenylphosphine)chloride to a benzene or toluene solution of phenylpropargyl ether gives the rhodium metallocycle **105** in 91% isolated yield as shown in Scheme 44. The addition of black, amorphous tellurium to a toluene solution of **105** gives tellurophene **106** in 14% isolated yield.[73] Tellurophenes fused to quinones have also been prepared by this route as shown in Scheme 44.[74,75] The addition of rhodium(I) tris(triphenylphosphine)chloride to bis(arylacetylenic)ketones gives quinones **107** and related structures. The addition of black, amorphous tellurium to these compounds gives tellurophenes **108–111** in yields varying from 10% for **109b** to 63% for **108a**.

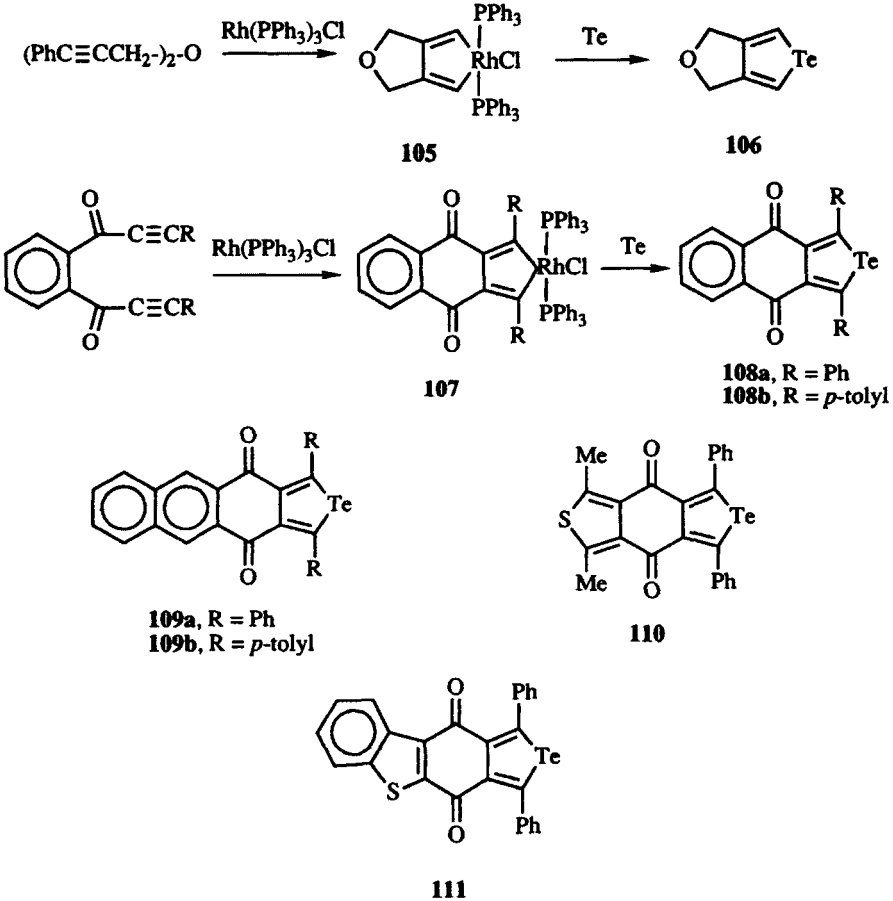

Scheme 44

C. Other Cyclization Routes to Tellurophenes

The addition of disodium telluride to a three-carbon unit followed by addition of a one-carbon unit has been employed to prepare a variety of substituted tellurophenes as illustrated in Scheme 45.[76,77] The initial Michael addition followed by chloride elimination generates a propenal derivative **112** with a 3-telluride anion substituent. The one-carbon unit as a methylene halide must bear an anion stabilizing group. Nucleophilic displacement of the halide generates vinyl tellurides **113**, which generate tellurophenes **114–117** via intramolecular condensation. The yields in this reaction appear to be somewhat variable. Tellurophene **114d** was isolated in 47% yield[76] while tellurophenes **114e** and **114f** were isolated in 12 and 10% yields, respectively.[77]

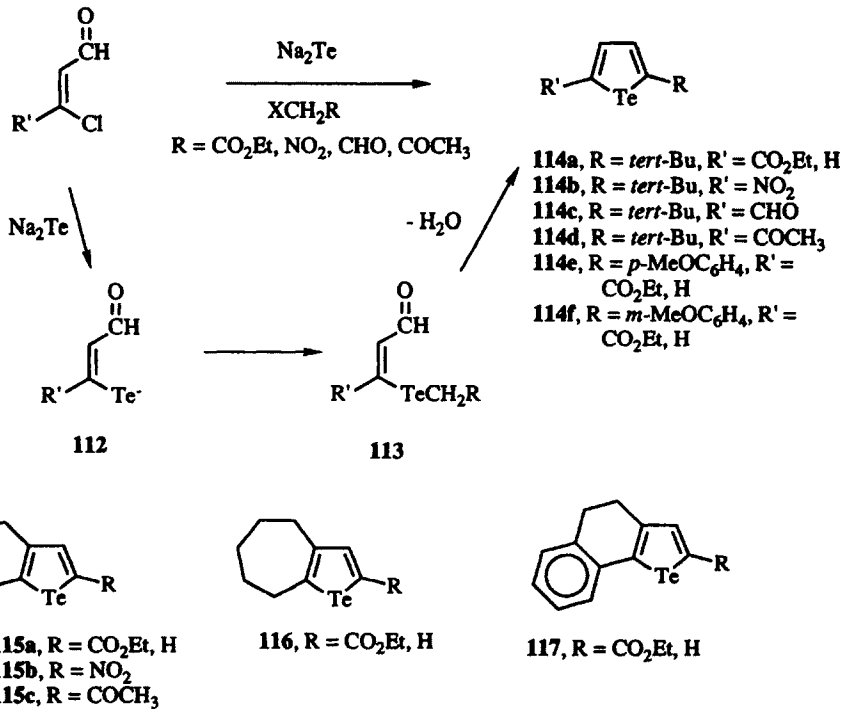

Scheme 45

The addition of tellurium metal to sodium phenylacetylenide generates sodium phenylethynyltelluride in DMSO as shown in Scheme 46.[78] The addition of a DMSO solution of dimethylacetylene dicarboxylate gives 2,3-bis(carbomethoxy)-5-phenyltellurophene (**118**) in 7% isolated yield.

Pyrolysis of divinyltelluride at 420–450°C in the presence of acetylene gives tellurophene (**90**) in 30% yield.[79] As shown in Scheme 47, the reaction presumably proceeds via a vinyltelluride radical that adds to acetylene.

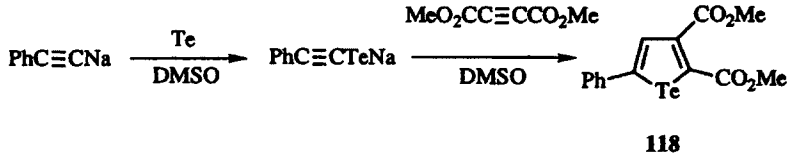

118

Scheme 46

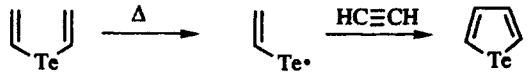

90

Scheme 47

D. Transformations of Tellurophene Rings

The reactivity of the tellurophene ring toward various reagents involves not only the ring but also the tellurium atom. The tellurium atom undergoes oxidation and reduction reactions from tellurium(II) to tellurium(IV) and back. Transformations of thiophene and selenophene nuclei to other derivatives may not be possible with the tellurophene nucleus.

The tellurophene ring **90** is more reactive than thiophene and selenophene but less reactive than furan toward Vilsmeier–Haack formylation, acetylation with a mixture of acetic anhydride and tin(IV) chloride, and trifluoroacetylation with trifluoroacetic anhydride.[80,81] The products are 2-formyltellurophene (**119**), 2-acetyltellurophene (**120**, isolated in 30% yield),[61] and 2-trifluoroacetyltellurophene (**121**, isolated in 18% yield),[81] respectively, as shown in Scheme 48.

Bromination of the tellurophene ring is not observed on treating tellurophene (**90**) with bromine as shown in Scheme 38. Tellurium(IV) analog **91** is formed in

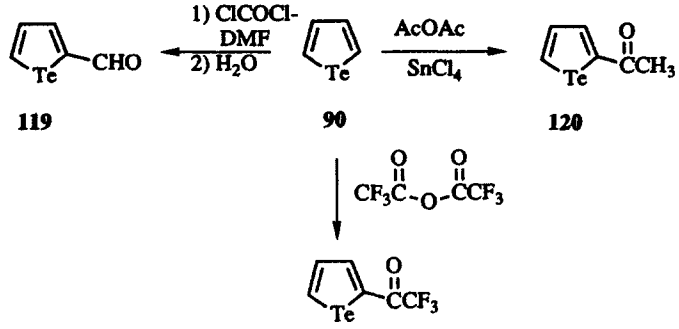

Scheme 48

excellent yield. Reduction with bisulfite regenerates **90** with no detectable ring-bromination products.[60,82] The tellurophene ring is reactive toward electrophiles as illustrated by the electrophilic deuterium–hydrogen exchange between tellurophene (**90**) and sulfuric acid-d_2 in methanol-O-d_1 to give 2,5-dideuterotellurophene (**90**-d_2).[82]

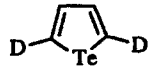

90-d_2

Electrophilic chloromethylation of 2,5-diphenyltellurophene (**122**), prepared from disodium telluride and 1,4-diphenyl-1,3-butadiyne in 55% yield,[82] with formaldehyde and hydrochloric acid in acetic acid gives 3,4-bis(chloromethyl)-2,5-diphenyltellurophene (**123**) in 61% isolated yield as shown in Scheme 49.[83] Compound **123** serves as a versatile intermediate for the preparation of other tellurophenes. The addition of either methoxide or ethoxide to **123** gives the corresponding ethers **124** in 83 or 45% isolated yields, respectively.[83] Similarly, the reaction of hydroxide with **123** gives diol **125** in 49% isolated yield.[83] The addition of disodium sulfide or disodium selenide to **123** gives the corresponding heterocycles **126** in 82 or 60% isolated yield, respectively.[84] The addition of

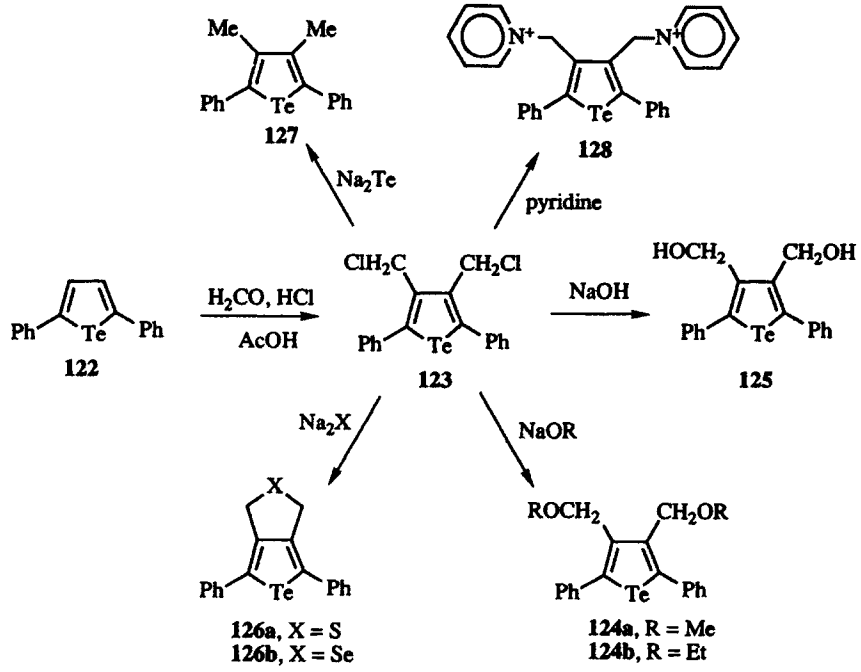

Scheme 49

disodium telluride to **123** gives 2,5-diphenyl-3,4-dimethyl-tellurophene (**127**) in 30% isolated yield via reduction of the chloromethylsubstituents.[84] Finally, the addition of excess pyridine to **123** gives bispyridinium salt **128** in 98% isolated yield.[83]

Diol **125** is also easily transformed to other products as shown in Scheme 50. Reaction with phosphorus tribromide in benzene gives dibromide **129** in 77% isolated yield.[83] Oxidation of **125** with selenium dioxide gives 3,4-diformyl-2,5-diphenyltellurophene (**130**) in 70% isolated yield.[83] Dialdehyde **130** reacts via double condensation reactions to form rings: with hydrazine to give **131a** in 40% isolated, with biscarbomethoxy acetone to give **131b** in 40% yield, with diphenylacetone to give **131c** in 68%, and with thiodiacetic acid ester to give **131d** in 11% yield.[85] A similar condensation reaction with *o*-phenylene diamine gives **132** in 40% yield.[85]

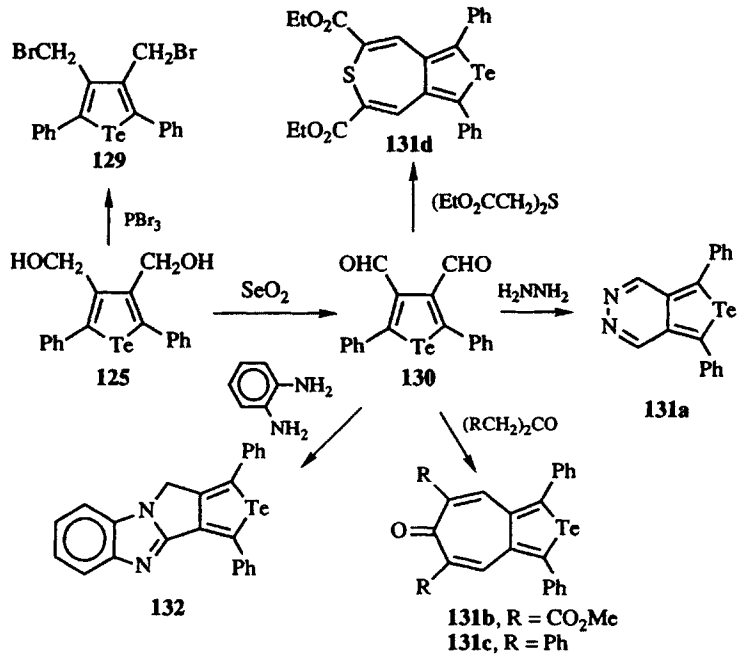

Scheme 50

E. Tellurophene Transformations Involving Metallation of the Ring

The metallation of the tellurophene ring has given metal-substituted intermediates that have been converted to a variety of different products. The addition of mercury(II) acetate to an ethanol solution of tellurophene (**90**) gives 2,5-bis(acetoxymercury)tellurophene (**133**) as shown in Scheme 51.[82] The addition of *n*-butyl lithium to a solution of tellurophene (**90**) in ether gives

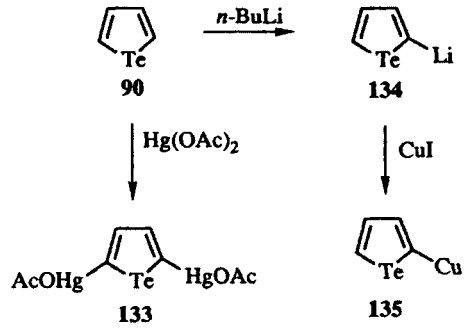

Scheme 51

2-lithiotellurophene (**134**).[61,65] The addition of copper(I) iodide to **134** gives the corresponding organocopper species **135**.[77]

2-Lithiotellurophene (**134**) has been converted to several different products as shown in Schemes 52 and 53. As shown in Scheme 52, the addition of deuterium oxide to **134** gives 2-deuterotellurophene (**90**-d_1).[65] The addition of carbon dioxide to **134** gives tellurophene carboxylic acid **136** in 37% isolated yield.[61] The acid **136** is converted to the methyl ester **137** with diazomethane in nearly quantitative yield.[61] The addition of *N*-methylformanilide to **134** gives tellurophene carboxaldehyde **119** in 25% isolated yield.[61] The addition of dimethyl sulfate to **134** gives 2-methyltellurophene (**138**) in 35% isolated yield.[61] The addition of acetaldehyde to **134** gives alcohol **139** in 65% isolated yield.[61]

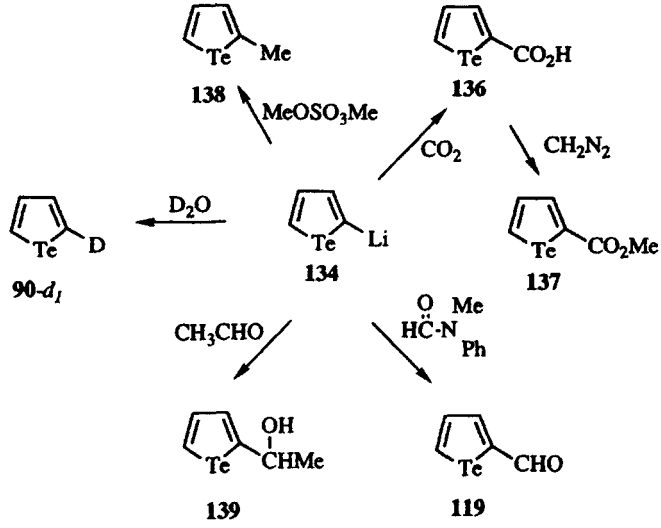

Scheme 52

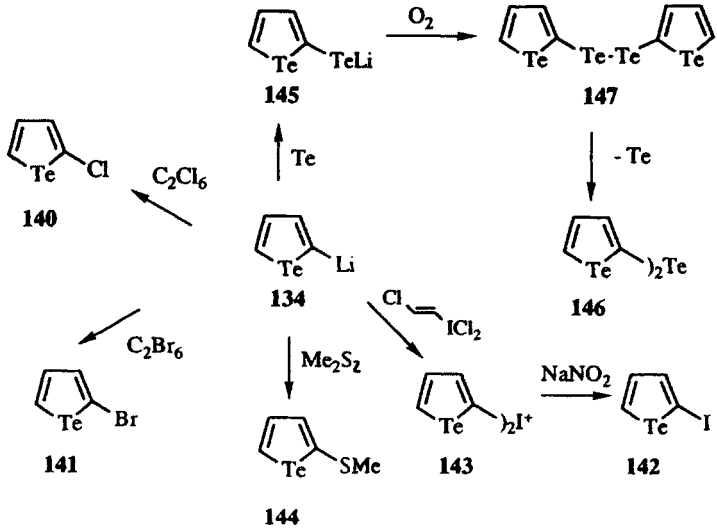

Scheme 53

2-Lithiotellurophene (**134**) can be converted to halogen- and chalcogen-substituted tellurophenes as shown in Scheme 53. The addition of hexachloroethane to **134** gives 2-chlorotellurophene (**140**) in 53% isolated yield, while the addition of hexabromoethane to **134** gives 2-bromotellurophene (**141**) in 44% isolated yield.[86] 2-Iodotellurophene (**142**) is prepared via the iodonium salt **143**, which in turn is prepared from **134** and *trans*-2-chloroethylene-1-iodoso dichloride.[86] Decomposition of the iodonium salt **143** with sodium nitrite does not give any evidence for the formation of nitrotellurophenes. The addition of dimethyl disulfide to **134** gives 2-methylthiotellurophene (**144**).[87] The addition of tellurium metal to **134** gives lithium telluride **145**, which is oxidized on workup to give bis(2-tellurophenyl)telluride (**146**).[86] Compound **146** is presumably formed by loss of tellurium from ditelluride **147**, which would be the first-formed product on oxidation of **145**.

The addition of carbon dioxide to **134** also gives a second product in addition to carboxylic acid **136**.[88] After stirring for 2 h at room temperature, a mixture of **134** and carbon dioxide in ether gives a 6% yield of ketone **148** as shown in Scheme 54.

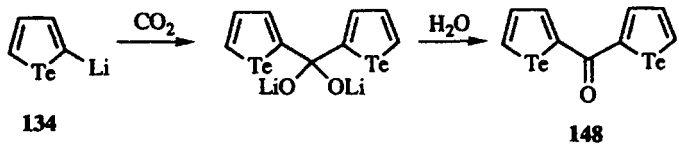

Scheme 54

2-Substituted tellurophenes are also metallated at the ring carbon adjacent to the tellurium atom as shown in Scheme 55. The addition of *n*-butyl lithium to 2-methyltellurophene (**138**) gives 2-lithio-5-methyltellurophene (**149**), which reacts with carbon dioxide to give carboxylic acid **150** in 35% isolated yield.[61] The addition of *n*-butyl lithium to 2-phenyltellurophene (**95**) gives 2-lithio-5-phenyltellurophene (**151**), which then reacts with deuterium oxide to give 2-deutero-5-phenyltellurophene (**95**-d_1).[64]

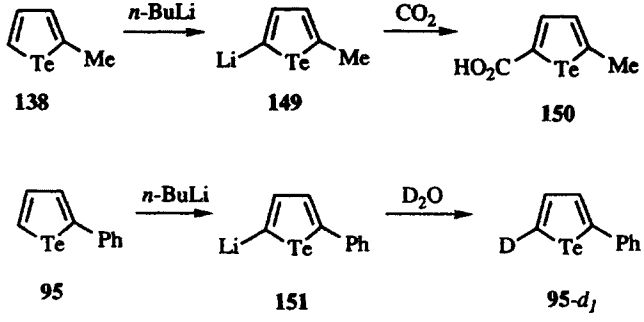

Scheme 55

F. Functional-Group Manipulations to Generate New Tellurophenes

Many common functional-group transformations are compatible with the tellurophene ring system. Tellurophene esters are saponified to the corresponding carboxylic acids in nearly quantitative yield as shown in Scheme 56. Ethyl esters **144a**,[76] **114e**,[77] **144f**,[77] and **115–117**[76] give the corresponding carboxylic acids **152–157**, respectively, in greater than 91% yield.

Tellurophene esters are still reactive toward electrophilic acylation as shown in Scheme 57 for the preparation of **158**. Methyl ester **158** is prepared in 47% isolated yield via acylation of 2-carbomethoxytellurophene (**137**) with acetic anhydride and tin(IV) chloride.[61] Saponification with sodium hydroxide gives carboxylic acid **159** in 95% isolated yield.[61] Ester **158** reacts with pyridine and iodine to give the pyridinium iodide **160**, which is then hydrolyzed to dicarboxylic acid **161** with sodium hydroxide.[89]

Tellurophene carboxylic acids react with diazomethane to give methyl esters as shown in Scheme 58 for the conversion of acid **136** to ester **137**.[61] Tellurophene-2,5-dicarboxylic acid is converted to the diester **162** with diazomethane.[89] The diester **162** is saponified to the diacid **161** with sodium hydroxide without degradation of the tellurophene ring.[89]

Tellurophene carboxylic acids can be decarboxylated with copper chromite as catalyst in the presence of quinoline as shown in Scheme 59.[77] Acid **153** is decarboxylated to give 2-(4-methoxyphenyl)tellurophene (**163**) in 83% yield and

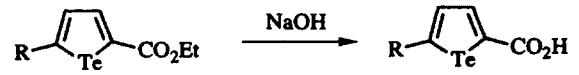

114a, R = *tert*-Bu
114e, R = *p*-$MeOC_6H_4$
114f, R = *m*-$MeOC_6H_4$

152, R = *tert*-Bu
153, R = *p*-$MeOC_6H_4$
154, R = *m*-$MeOC_6H_4$

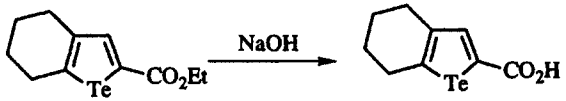

115a **155**

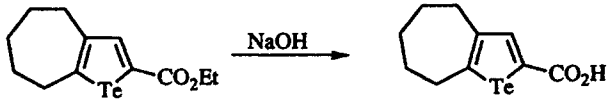

116 **156**

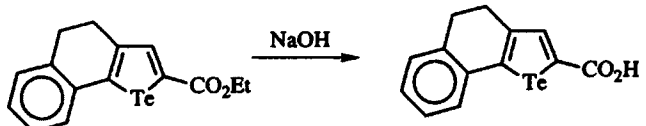

117 **157**

Scheme 56

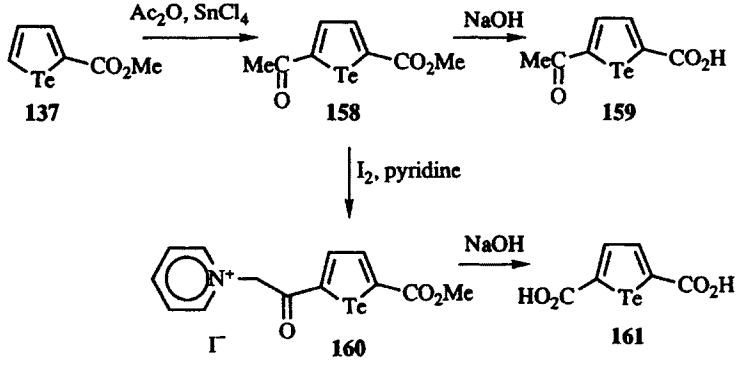

137 **158** **159**

160 **161**

Scheme 57

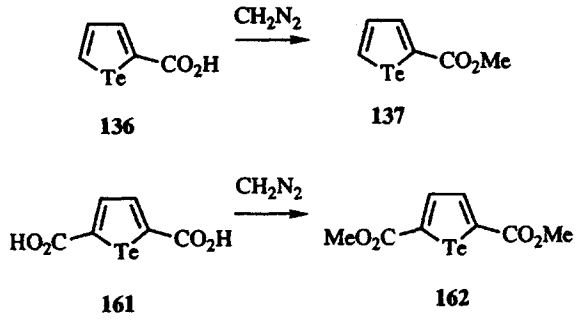

Scheme 58

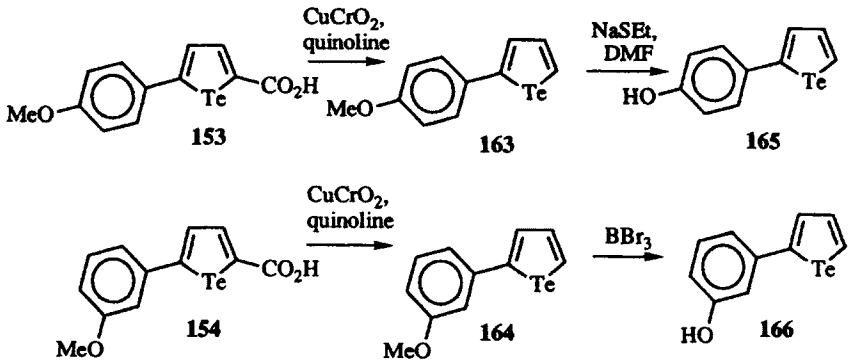

Scheme 59

acid **154** is decarboxylated to give 2-(3-methoxyphenyl)tellurophene (**164**) in 80% yield.

The anisole substituents of **163** and **164** can be converted to the corresponding phenols in low yields as shown in Scheme 59.[77] The reaction of sodium ethylthiolate with **163** in DMF gives the phenol-substituted tellurophene **165** in 25% isolated yield. The addition of boron tribromide to a dichloroethane solution of **164** gives phenol-substituted tellurophene **166** in 10% isolated yield. In the latter reaction, boron tribromide reacts with **164** for 10 h at room temperature, which may cause degradation of the tellurophene ring by attack of the tellurium atom and the tellurium–carbon bonds.

Tellurophene carboxylic acids **152** and **155–157** are decarboxylated by heating with quinoline to give the corresponding 2-*tert*-butyltellurophene (**167**) in 90% yield and tellurophenes **168–170**, respectively, as shown in Scheme 60.[176] Tellurophene **170** is dehydrogenated in 90% yield with DDQ to give the naphthotellurophene **171**.

Tellurophene-2-carboxaldehyde (**119**) and 2-acetyltellurophene (**120**) undergo standard transformations without degredation of the tellurophene ring as

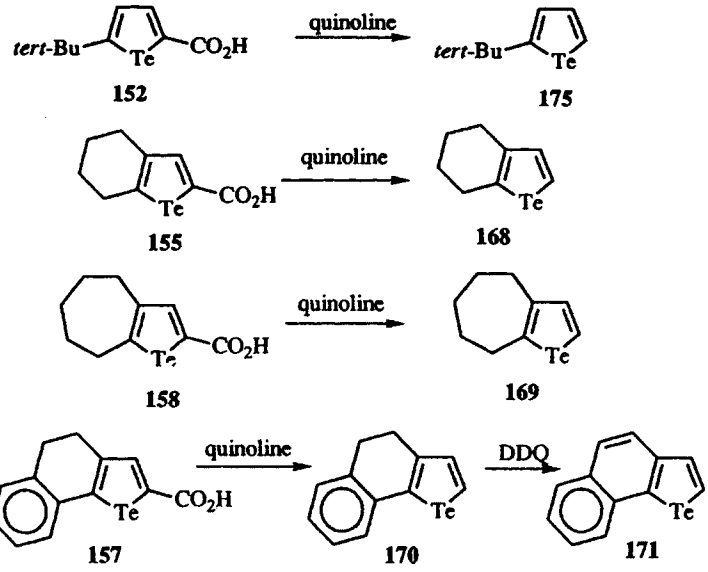

Scheme 60

shown in Scheme 61.[61] Wolff–Kishner reduction of **119** (hydrazine hydrate, ethylene glycol, potassium hydroxide) gives 2-methyltellurophene (**138**) in 40% yield. Lithium aluminium hydride reduction of **119** gives 2-(hydroxymethyl)tellurophene (**167**). Compound **167** is also obtained by lithium aluminium hydride reduction of ester **137** (Scheme 61). Lithium aluminum hydride reduction of 2-acetyltellurophene (**120**) gives 2-(1-hydroxyethyl)tellurophene (**139**).

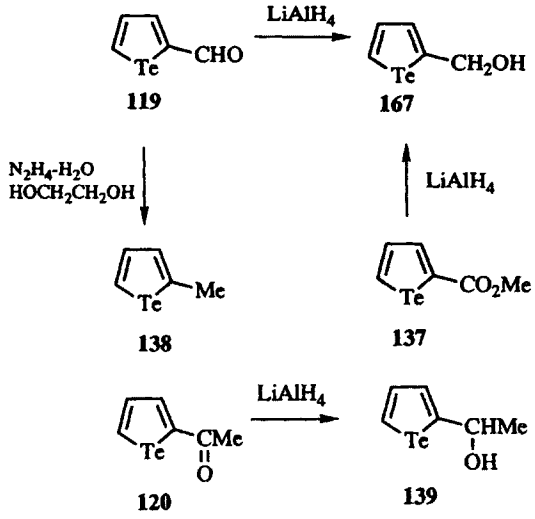

Scheme 61

Tellurophene **94** reacts with pyrrole in refluxing benzene in the presence of 2% chloroacetic acid to give bispyrrolo tellurophene **173** as shown in Scheme 62.[63] Electrophilic cyclization of **173** with 2,5-bis(phenylhydroxymethyl)thiophene (**172**) gives the tellurophene-containing tetraphenylporphyrin analog **174**.

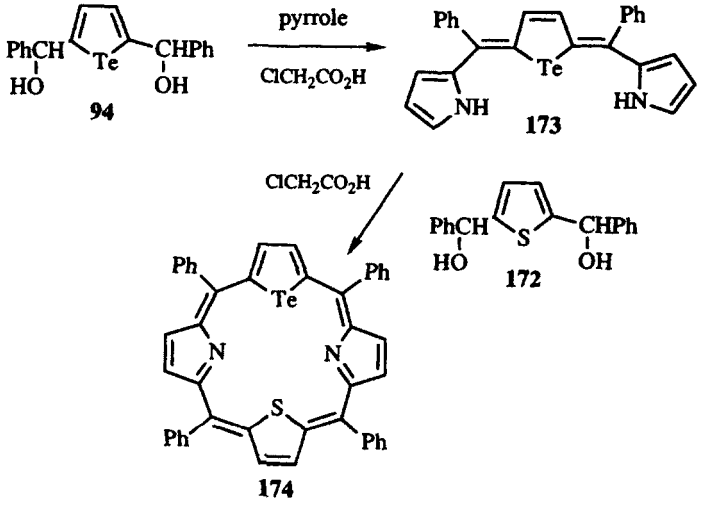

Scheme 62

G. Tellurophenes from Ring-Contraction Reactions

The dihydroxytelluranes **175** undergo intramolecular nucleophilic addition of a telluroxide oxygen or addition of peroxide anion to the 2-position of the tellurane ring.[90] Ring contraction with net loss of hydrogen peroxide from **175**

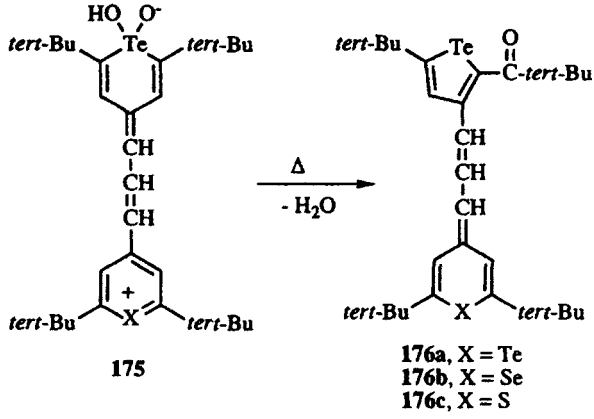

Scheme 63

gives the 2,3,5-substituted tellurophenes **176** in 25–59% isolated yield as shown in Scheme 63.

IV. BENZOTELLUROPHENES AND DERIVATIVES

A. Preparation of the Parent Benzotellurophene

The first synthetic route to benzotellurophene (**177**) involved the intramolecular aldol condensation of acetic acid derivative **178** to give benzotellurophene-2-carboxylic acid (**191**) as shown in Scheme 64.[91] Decarboxylation of **191** with copper powder and quinoline gives **177**. Alternatively, the ethyl ester of **178** (compound **180**) is converted directly to **177** on heating in pyridine as shown in Scheme 64.[92] In both of these reactions, the addition of an α-bromo acid or ester to 2-(methyltelluro)benzaldehyde gives an unstable telluronium salt that loses bromomethane to give **178** or **180**, respectively. It is interesting to note that methyl telluronium salts **181**, which are generated by the addition of either α-bromoacetic acid or ethyl α-bromoacetate to a solution of 2-(methyltelluro)acetophenone, do not undergo similar loss of bromomethane and intramolecular condensation to give 3-methylbenzotellurophenes.[92]

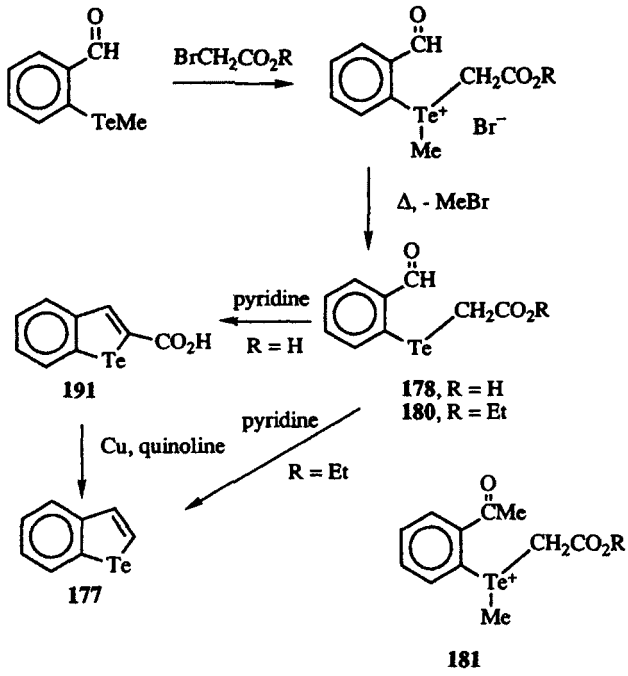

Scheme 64

The thermolysis of phenyl allyltelluride at 500–570°C in the presence of acetylene gives rise to small amounts of benzotellurophene (**177**) as shown in Scheme 65.[93] The yields of benzotellurophene produced in this manner are on the order of 3–4%.

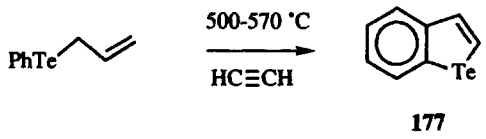

177

Scheme 65

Perhaps the best synthetic route to benzotellurophene (**177**) involves the addition of tellurium metal to dilithiated phenylacetylene followed by the addition of *tert*-butanol and hexamethylphosphortriamide (HMPT) as shown in Scheme 66.[94] Yields of up to 85% are described for this reaction. The critical feature of this reaction is the generation of the dilithio species **182**. The addition of two equivalents of *n*-butyllithium to a hexane solution of phenylacetylene and tetramethylethylene diamine (TMEDA) gives the dilithio **182** directly, but as only 80% of the product mixture (Scheme 66). A more regioselective route to **182** involves the initial generation of lithium phenylacetylenide from phenylacetylene and *n*-butyllithium followed by the addition of potassium *tert*-butoxide

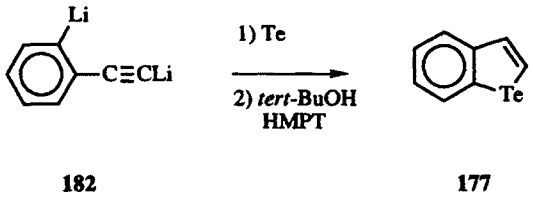

182 **177**

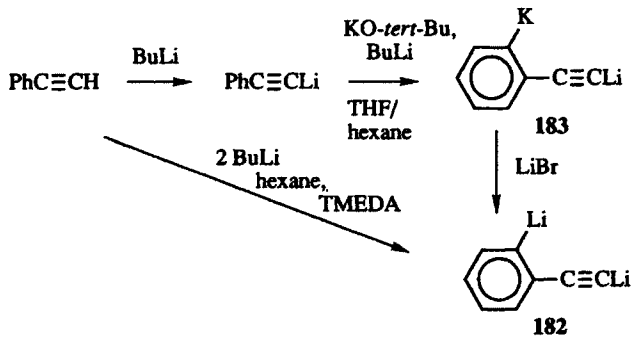

Scheme 66

and *n*-butyllithium to give the mixed-metal species **183**. Potassium–lithium exchange following the addition of lithium bromide gives **182** with excellent regiospecificity.

The addition of tellurium metal to another dilithiated species has also been utilized to prepare benzotellurophene (**177**) as shown in Scheme 66a.[94a] The addition of diisobutylaluminium hydride to trimethylsilyl phenylacetylene at room temperature followed by bromination with *N*-bromosuccinimide at − 20°C gives 1-bromo-1-trimethylsilylstyrene in 92% yield. Metal–halogen exchange and metallation of the *ortho* position of the ring with *n*-butyllithium in ether at reflux generates 1-trimethylsilyl-1,3-dilithiostyrene. The addition of tellurium metal gives 2-trimethylsilylbenzotellurophene in 90% isolated yield. Heating with potassium hydroxide in methanol removes the trimethylsilyl group quantitatively to give benzotellurophene (**177**).

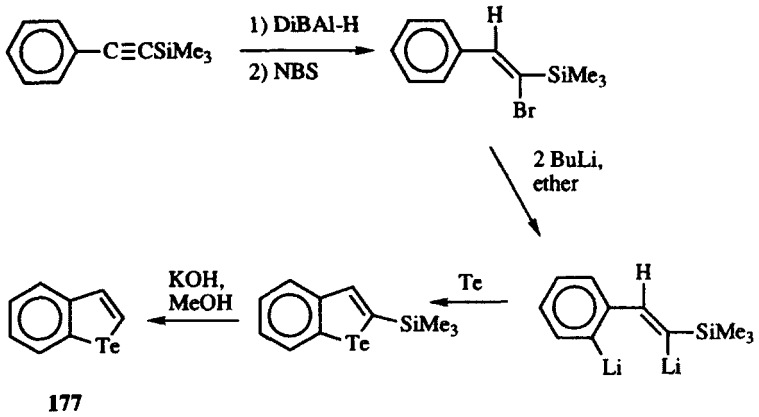

177

Scheme 66a

The tellurium atom of benzotellurophene (**177**) reacts with the halogens in chloroform to give the expected products of oxidative addition as shown in Scheme 67.[91] The 1,1-dihalobenzotellurophenes **184–186** are isolated in excellent yield as crystalline solids. The addition of bromomethane to **177** in chloroform solution gives telluronium salt **187** as shown in Scheme 67.[91]

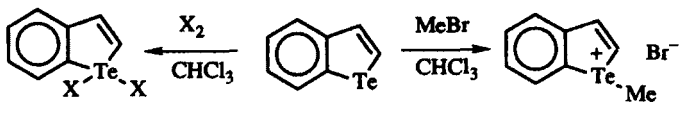

184, X = Cl
185, X = Br
186, X = I

177

187

Scheme 67

B. 2-Substituted Benzotellurophenes

The benzotellurophene nucleus is reactive to electrophiles in Friedel–Crafts-type reactions as shown in Scheme 68.[92] The yield of 2-acetylbenzotellurophene (**188**) from acylation of **177** is low in part because of the reactivity of tellurium and the ease of tellurium–carbon bond cleavage. Metallation of **177** with *n*-butyllithium in ether at 0°C gives 2-lithiobenzotellurophene (**189**) as shown in Scheme 68.[92,95]

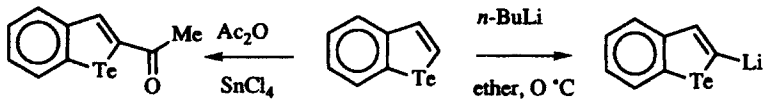

188 **177** **189**

Scheme 68

2-Lithiobenzotellurophene (**189**) is converted to a variety of other 2-substituted benzotellurophenes as shown in Scheme 69. The addition of iodomethane to **189** gives 2-methylbenzotellurophene (**190**) in 88% yield.[95] If the lithiated species is quenched with deuterium oxide, 2-deuterobenzotellurophene **177**-d_1) is produced in good yield with excellent regiochemical control.[95] The addition of carbon dioxide to **189** gives carboxylic acid **191** while the addition of *N*,*N*-dimethylformamide to **189** gives 2-formylbenzotellurophene (**192**) in 60% yield.[92]

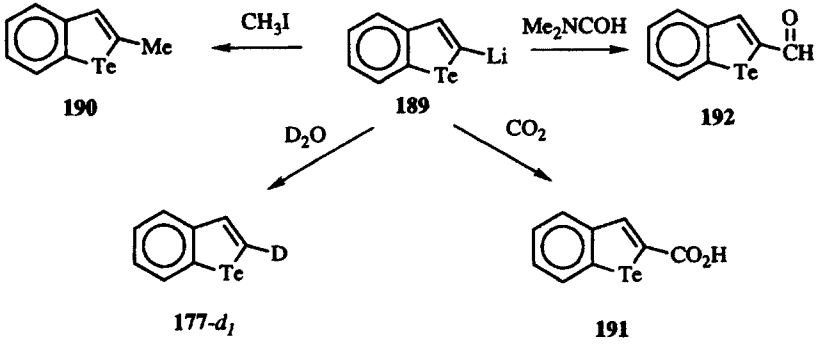

190 **189** **192**

177-d_1 **191**

Scheme 69

Carboxylic acid **191**, the synthesis of which is shown in Scheme 64, is a versatile intermediate for the preparation of 2-substituted benzotellurophenes as shown in Scheme 70. Lithium aluminum hydride reduction of **191** gives 2-(hydroxymethyl)benzotellurophene (**193**) in 62% yield.[92] Carboxylic acid **191** is converted to the corresponding acid chloride **194** in 80% yield by the action of

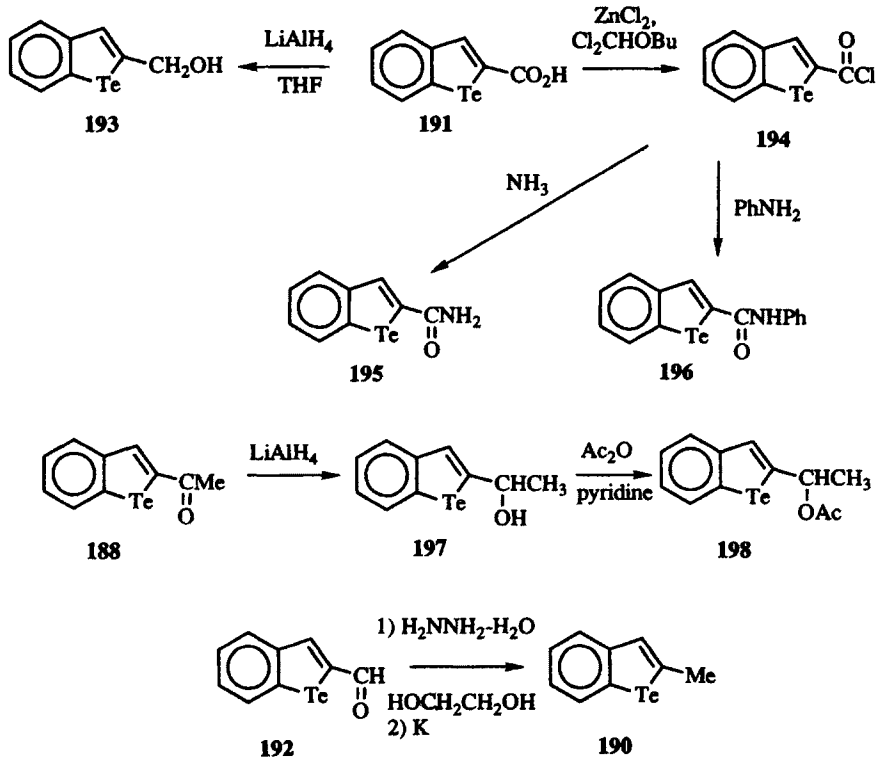

193 191 194 195 196 188 197 198 192 190

Scheme 70

zinc chloride and dichloromethyl butyl ether. The addition of ammonia to **194** gives benzotellurophene amide **195**, while the addition of aniline to **194** gives formanilide derivative **196**.[92]

Reduction of 2-acetylbenzotellurophene (**188**) with lithium aluminum hydride gives alcohol **197**, which is acylated with acetic anhydride in pyridine to give acetate **198** as shown in Scheme 70.[96] Wolff–Kischner reduction of 2-formylbenzotellurophene (**192**), with hydrazine in ethylene glycol followed by the addition of potassium metal, gives 2-methylbenzotellurophene **190** in 80% isolated yield as shown in Scheme 70.

Various 2-substituted benzotellurophenes can be prepared from 2-(methyltelluro)benzaldehyde as shown in Scheme 71.[92] Wittig condensation with the aldehyde functionality generates 2-(methyltelluro)styrene derivatives **199** in 89–100% yields. The addition of bromine to **199** generates the corresponding tellurium(IV) derivatives that react with pyridine to give 2-substituted benzotellurophenes **200–203** in 90, 70, 70, and 90% yields, respectively.

The 2-substituted benzotellurophenes react with halogens to give the corresponding 1,1-dihalo-2-substituted benzotellurophenes as shown in Scheme 72.[92] The addition of bromine to solutions of **190** and **191** gives the corresponding

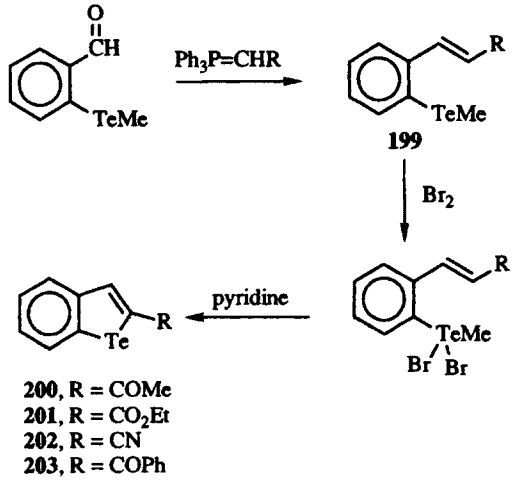

Scheme 71

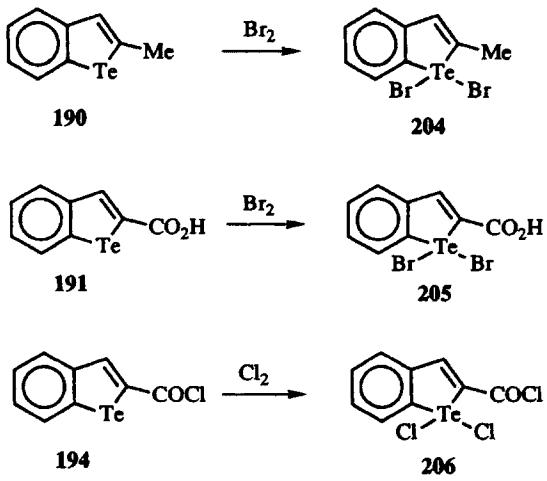

Scheme 72

1,1-dibromo derivatives **204** and **205**, respectively. Similarly, the addition of chlorine to **194** gives 1,1-dichloro derivative **206**.

C. 3-Substituted Benzotellurophenes

The reaction of arylacetylenes with tellurium dioxide in acetic acid in the presence of lithium halides yields 3-substituted benzotellurophenes **207–211** as shown in Scheme 73.[52] The benzotellurophenes are most easily isolated from the

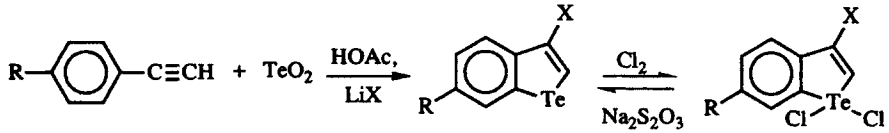

207, R = H, X = Cl
208, R = H, H = Br
209, R = H, X = I
210, R = Me, X = Cl
211, R = Br, X = Cl

212, R = H, X = Cl
213, R = H, H = Br
214, R = H, X = I
215, R = Me, X = Cl
216, R = Br, X = Cl

Scheme 73

reaction mixtures by the addition of chlorine to yield the 1,1-dichloro-3-substituted benzotellurophenes **212–216**, respectively. Via this two-step process, compounds **212–216** are isolated in 52, 92, 21, 39, and 77% yields, respectively. The 3-substituted benzotellurophenes **207–211** are produced in nearly quantitative yield by sodium bisulfite reduction of the 1,1-dichloro derivatives.

D. 2,3-Disubstituted Benzotellurophenes

The first synthesis of a 2,3-disubstituted benzotellurophene utilized an intramolecular electrophilic substitution with a tellurium trichloride to generate the benzotellurophene.[97] The addition of tellurium tetrachloride to diphenylacetylene generates the 1-trichlorotellurium-2-chlorostilbene (**217**) as shown in Scheme 74.[98] A mixture of **217** and 1,2,4-trichlorobenzene is heated at reflux to give a 52% yield of 1,1,3-trichloro-2-phenylbenzotellurophene (**218**).[97] Compound **218** is reduced to 3-chloro-2-phenylbenzotellurophene (**219**) in 95% isolated yield with disodium sulfide nonahydrate.

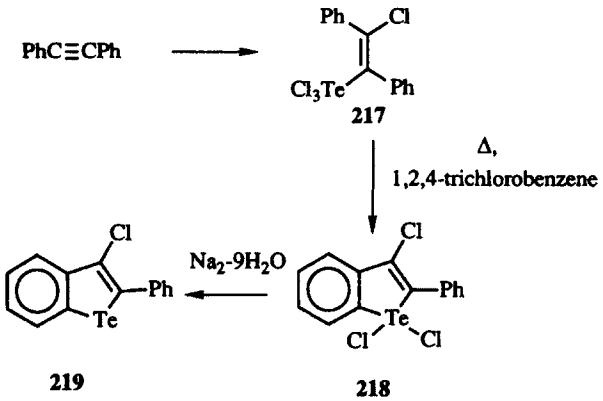

219 **218**

Scheme 74

A similar cyclization reaction has been utilized for the preparation of 3-halo-2-(aminomethyl)benzotellurophenes **220–224** as shown in Scheme 75.[99] The addition of tellurium tetrachloride to 3-amino-1-phenyl-1-propyne derivatives followed by sodium bicarbonate to deprotonate the amine gives **220–224** in 83, 70, 40, 66, and 68% yields.

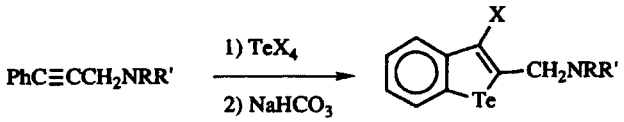

220, X = Br, R = H, R' = Me
221, X = Br, R = R' = Et
222, X = Cl, R = R' = Et
223, X = Br, R,R' = -$(CH_2CH_2)_2O$
224, X = Cl, R,R' = -$(CH_2CH_2)_2O$

Scheme 75

One 2,3-disubstituted benzotellurophene has been prepared by the condensation of phenylhydrazine with 3-oxo-2,3-dihydrobenzotellurophene (**74**) in acetic acid as shown in Scheme 76.[48] The product of this reaction is the indole-fused benzotellurophene **225**.

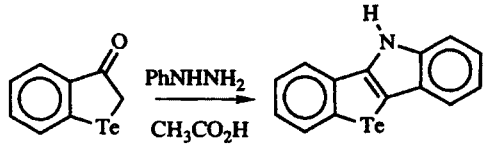

74 **225**

Scheme 76

E. Routes to Benzo-Substituted Benzotellurophenes

Ring-contraction reactions of tellurochromenes on reaction with selenium dioxide have generated a number of benzotellurophene derivatives as shown in Scheme 77.[100,101] The ring-contraction mechanism is thought to be initiated by selenium dioxide attack at the 2-position of the tellurochromenes **226**. Decomposition of the resulting selenous acid derivative and ring opening give tellurenyl species **227**. Electrophilic addition and proton loss generate the benzotellurophene derivatives **228–330** in 60, 25, and 40% yields, respectively.[100] 2-Acetylbenzotellurophene is produced in 10–15% yield via this procedure.[100] Similarly, the preparation of 2-formylbenzotellurophene (**192**) via this

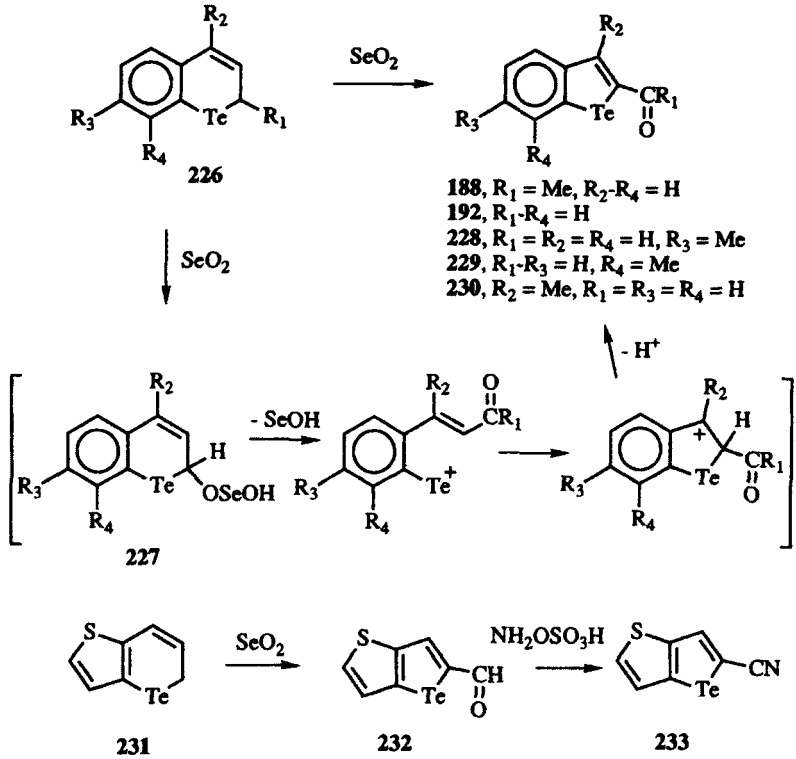

Scheme 77

route in 19% yield is also claimed.[101] Thiophene-fused telluropyran **231** is converted to thiophene-fused tellurophene **232** in 66% isolated yield.[100] Compound **232** is converted to the corresponding 2-cyano compound **233** via reaction with hydroxylamine sulfonic acid.

2,3-Dihydrobenzotellurophenes have been dehydrogenated to give benzotellurophene derivatives as shown in Scheme 78.[102] The dehydrogenation of

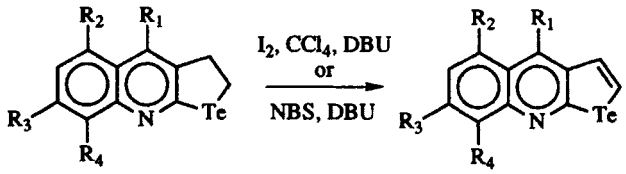

234, R_1-R_4 = H
235, R_1-R_3 = H, R_4 = Me
236, R_1 = R_3 = H, R_2 = R_4 = Me
237, R_1 = R_2 = R_4 = H, R_3 = Cl
238, R_1 = Ph, R_2-R_4 = H

Scheme 78

quinoline-fused dihydrotellurophenes **62** with iodine and DBU (diazabicycloundecane) in carbon tetrachloride gives quinoline-fused tellurophenes **234–238** in low yields (18–35%). The same transformation is accomplished in even poorer yield (12–16%) with *N*-bromosuccinimide and DBU (Scheme 78).

V. DIBENZOTELLUROPHENES AND DERIVATIVES

A. Cyclization Routes to Dibenzotellurophenes

The first synthetic routes to dibenzotellurophene (**239**) utilized the electrophilic addition of tellurium tetrahalides to biphenyl as shown in Scheme 79.[103] The initially formed products are the *Te,Te*-dihalodibenzotellurophenes **240**, which are reduced to **239** with bisulfite. Yields as high as 75% have been reported for this reaction sequence.[104] As shown in Scheme 79, the electrophilic cyclization is thought to proceed via the tellurium trihalide species **241**. Both the tellurium trichloride **241a**[105] and the tellurium tribromide **241b**[106] have been prepared independently and have been shown to react thermally to give the 1,1-dihalodibenzotellurophenes **240**. The crystal structure of **241b** shows an unusually short tellurium–C12 (of the biphenyl) nonbonding distance, which is perhaps related to the ease with which this compound reacts to give **240b**. Trichloride **241a** is prepared by the addition of tellurium tetrachloride to either a mercury biphenyl derivative or to *o*-lithiobiphenyl.[105] The tribromide **241b** is prepared by the addition of bromine to a solution of di-*o*-biphenyl ditelluride.[106]

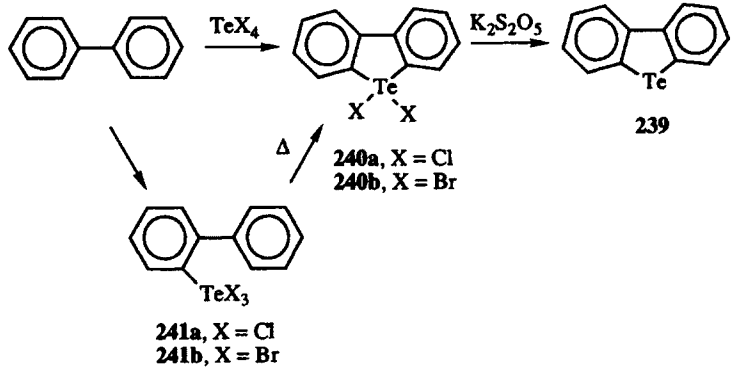

Scheme 79

Dibenzotellurophene (**239**) has been prepared via a variety of other routes as shown in Scheme 80. The addition of tellurium metal to *o,o'*-biphenylenyl mercury gives **239** in 82% isolated yield.[107,108] The same procedure with 3,10-dimethyl-*o,o'*-biphenylenyl mercury gives dimethylbenzotellurophene **242** in

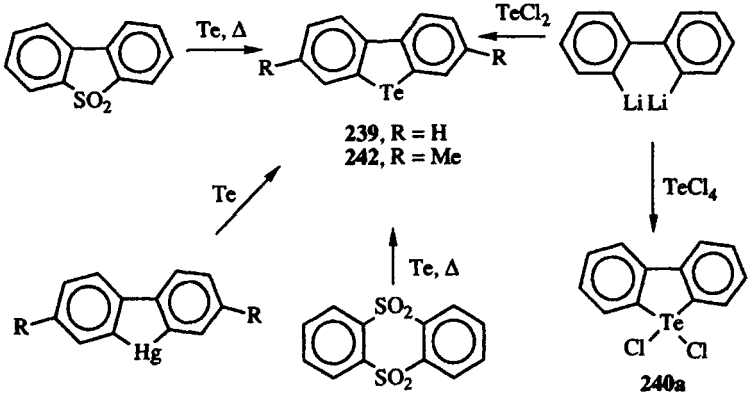

Scheme 80

79% yield.[109] The addition of tellurium dichloride to *o,o'*-dilithiobiphenyl gives **239** in 52% isolated yield, while the addition of tellurium tetrachloride gives **240a** in 30–40% yield.[107] Heating a mixture of dibenzothiophene sulfone and tellurium powder gives loss of sulfur dioxide and approximately a 10% yield of **239**.[110] In a related reaction, heating a mixture of thianthrene tetroxide and tellurium metal gives loss of two equivalents of sulfur dioxide and a poor yield of **239**.[111]

The dibenzotellurophene ring system has been constructed via the intermediacy of telluronium salts, which undergo electrophilic ring closure to give *Te*-(trifluoromethyl)dibenzotellurophenium triflate (**243**) as shown in Scheme 81.[112] The addition of DMSO and triflic anhydride to 1-(trifluromethyl)biphenyl (**244**) gives **243** presumably via the intermediacy of **245**. Dimethylsulfide is detected as a reaction product in this reaction. Alternatively, **243** can be formed via the addition of bromine to **244** followed by triflic acid.[112]

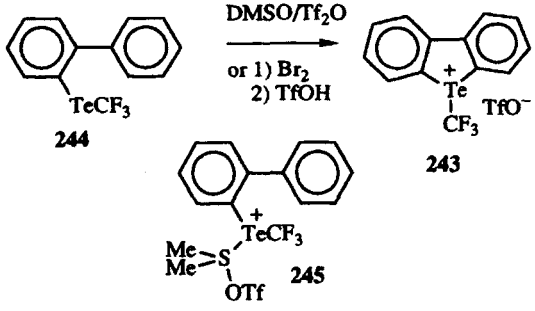

Scheme 81

These approaches to the dibenzotellurophene nucleus also work with more highly substituted derivatives 2,3,6,7-Tetramethoxydibenzotellurophene (**246**) is

prepared in 3% isolated yield via the addition of tellurium tetrachloride to *o,o'*-dilithiobiphenyl **247** followed by reduction of the tellurium(IV) intermediate with sodium bisulfite as shown in Scheme 82.[113] Alternatively, the addition of tellurium metal to **247** followed by oxidation with a stream of oxygen gives **246** in 16% isolated yield. In a third variation, the addition of 1,1-dichloro-2,5-dihydrotellurophene (**43a**) to **247** gives **246** in 13% isolated yield.

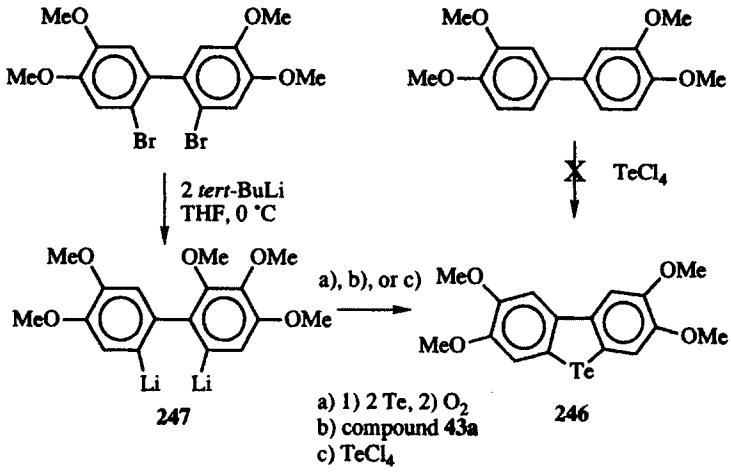

Scheme 82

Octaflurodibenzotellurophene (**248**) has been prepared via several different routes as shown in Scheme 83.[114-116] The addition of powdered tellurium metal to *o,o'*-diiodooctafluorobiphenyl at 325°C gives **248** in 66% isolated yield.[114,115] The addition of tellurium tetrachloride to *o,o'*-dilithio-

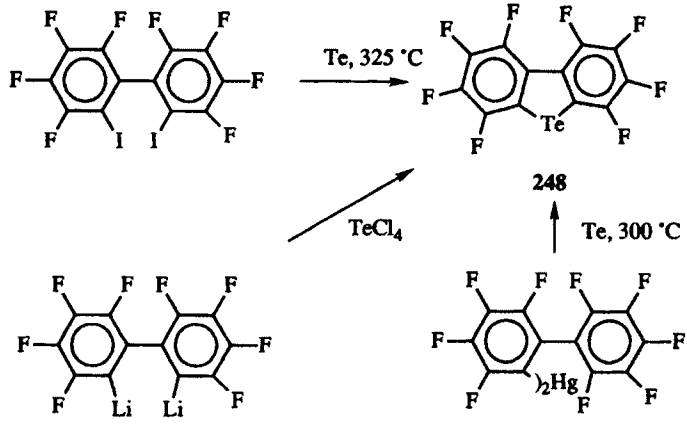

Scheme 83

octafluorobiphenyl gives **248** in 17% isolated yield.[115] The thermal reaction of *o*-nonafluorobiphenyl mercury and tellurium metal at 300°C gives **248** in 10% isolated yield.[116]

B. Reactions of the Benzo Groups in Dibenzotellurophenes

The dibenzotellurophenes **239** and **243** are susceptible to electrophilic aromatic substitution as shown in Scheme 84. Nitration of **239** with concentrated nitric acid gives the 2-nitrodibenzotellurophene–*Te*,*Te*-dinitrate (**249**), which is reduced to 2-nitrodibenzotellurophene (**250**).[111] The telluronium salt **243** is nitrated with excess nitronium triflate to give *Te*-trifluoromethyl-2,7-dinitrodibenzotellurophenium triflate (**251**).[112]

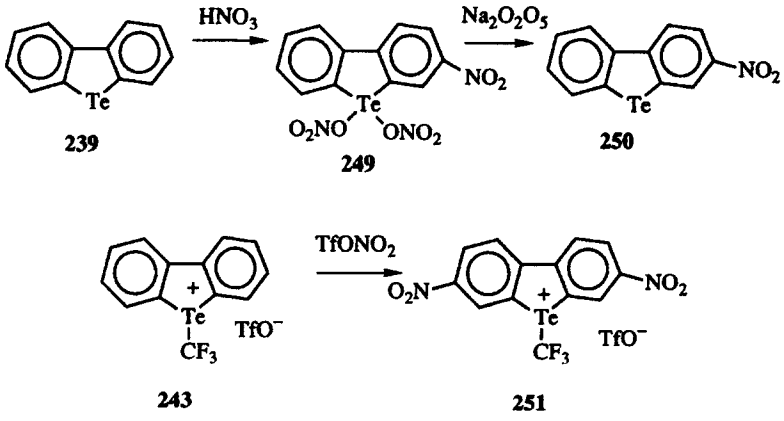

Scheme 84

Other reactions of the dibenzotellurophene system have been observed as shown in Scheme 85. The dibenzotellurophene nucleus is susceptible to tellurium–sulfur exchange. Heating a mixture of **239** and elemental sulfur gives dibenzothiophene.[103] Reaction of excess butyllithium with **239** gives *o*,*o*′-dilithiobiphenyl.

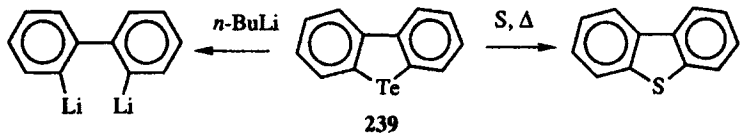

Scheme 85

C. Reactions at the Tellurium Atom of Dibenzotellurophenes

The tellurium atom of dibenzotellurophene (**239**) undergoes typical oxidative addition reactions with the halogens to give the corresponding tellurium(IV) adducts **240** as shown in Scheme 86.[105, 107, 117] Reduction of the tellurium(IV) adducts with bisulfite regenerates **239**. Chloramine-T also oxidizes **239** to the tellurium(IV) derivative **252**, which can then be hydrolyzed to the corresponding telluroxide (or its hydrate).[109] The addition of methyl iodide to **239** gives the methyl telluronium salt **253**.[118]

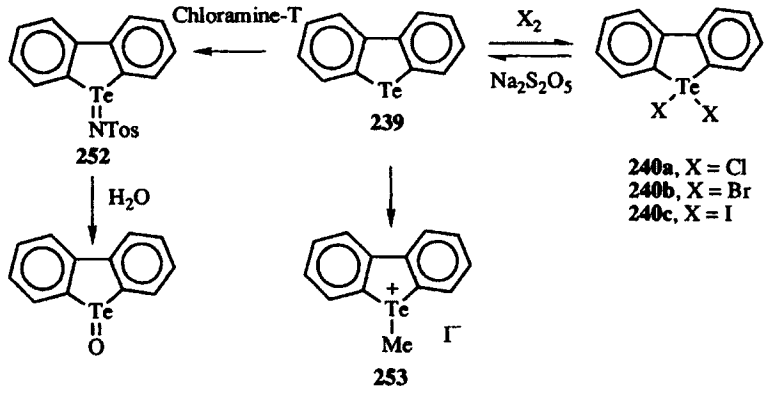

Scheme 86

The tellurium(IV) adducts **240** undergo a variety of different chemical reactions. The addition of tellurium tetrachloride to **240a** gives ring opening and the formation of a bis(trichlorotellurium)-containing molecule **254** as shown in Scheme 87.[117] Bisulfite reduction of **254** produces low yields of **239** and various

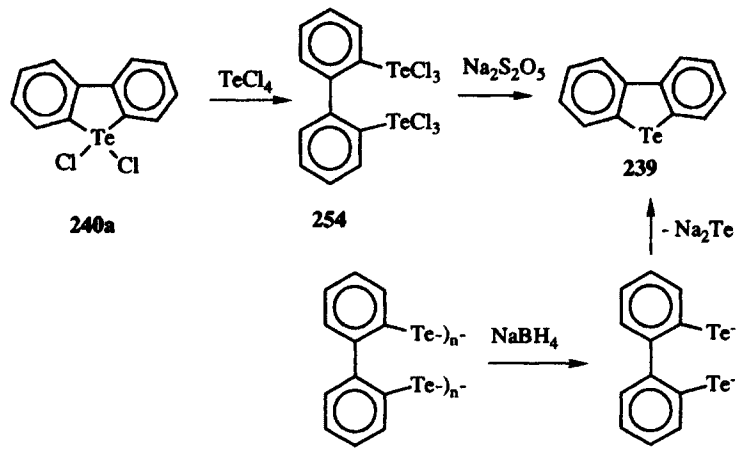

Scheme 87

polytellurides, which can be reduced with sodium borohydride to give low yields of **239** and disodium telluride.

Expansion of the coordination sphere of tellurium in **240a** has also given a number of dibenzotellurophene derivatives as shown in Scheme 88.[104, 119, 120] Oxinate **255** and salicylate **256** have been prepared from **240a** with the appropriate sodium salt of the ligand.[118, 119] The addition of tetraethylammonium chloride to **240a** gives octahedral complex **257**, while the addition of *N,N*-dimethylacetamide to **240a** presumably gives neutral octahedral complex **258**.[104] Chloride exchange in **240a** with silver nitrate gives bisnitrate **259**, while the addition of mercuric chloride to **240a** gives a mercury complex, represented here as **260**.[104]

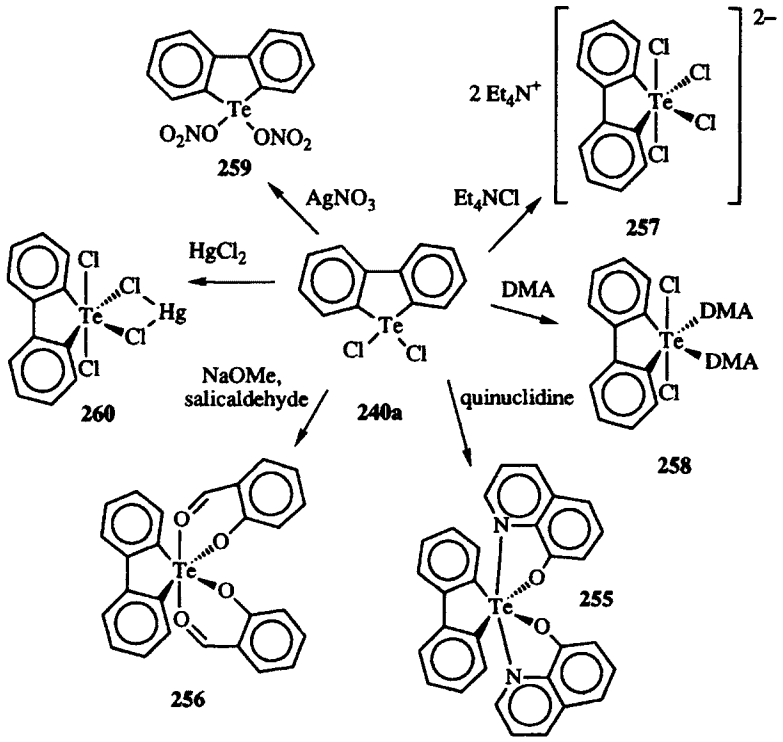

Scheme 88

The addition of *o,o'*-dilithiobiphenyl to **240a**,[109] **252**,[109] or telluronium salt **253**[118] gives the tellurium(IV) spirane **261** in yields of 36, 44, and 52%, respectively, as shown in Scheme 89.[109] Spirane **261** can also be prepared from the reaction of *o,o'*dilithiobiphenyl with tellurium tetramethoxide (49%), tellurium hexamethoxide (48%), or tellurium tetrachloride (44%).[107, 109] The addition of tellurium tetrachloride to 3,10-dimethyl-*o,o'*-dilithiobiphenyl gives the tetramethyl spirane **262**.[109] In all these reactions, it is assumed that a

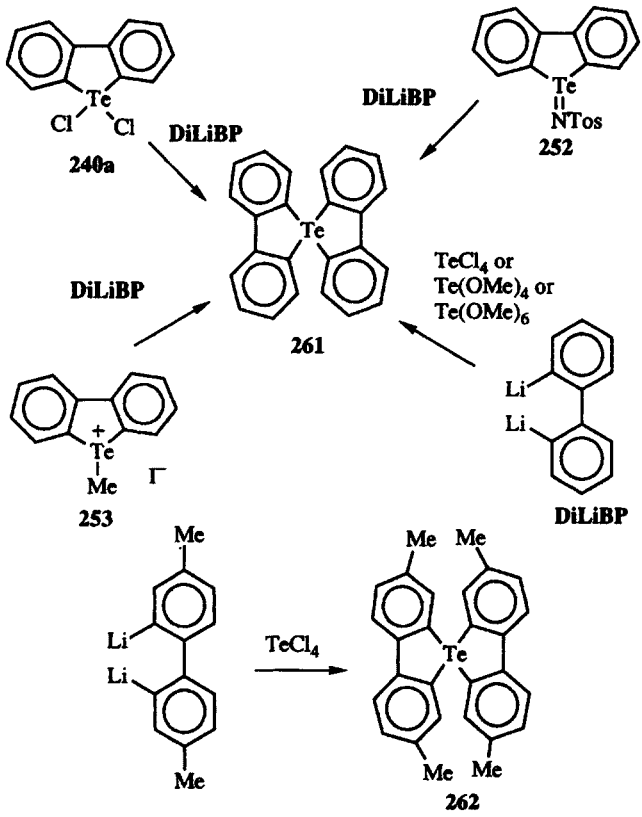

Scheme 89

tellurium(IV) analog of a dibenzotellurophene (such as **240a**) is an intermediate on the path to the spiranes **261** and **262**.

The tellurium–carbon bonds of spiranes **261** and **262** are fragile to a variety of reagents as shown in Scheme 90. The addition of four equivalents of butyllithium to **261** gives tetrabutyl tellurium and *o,o'*-dilithiobiphenyl.[118] The tetrabutyl tellurium can be hydrolyzed with hydroiodic acid to give tributyltelluronium iodide. The tellurium–carbon bonds are susceptible to hydrolysis to give *Te*-1-biphenyl telluronium salts **263** with protic cleavage of the bond.[109] The addition of chlorine or iodine to **261** gives halogen addition across the tellurium–carbon bond to give telluronium salts **264**.[109] The addition of hydrochloric acid to **262** gives telluronium salt **265a**, while the addition of bromine gives telluronium salt **265b** via addition of bromine across the tellurium–carbon bond.[109]

D. Heteroaryl Analogs of Dibenzotellurophene

A bisthiophene analog of bibenzotellurophene (**239**) has been prepared as shown in Scheme 91.[121] Selective lithium–bromine exchange on addition of

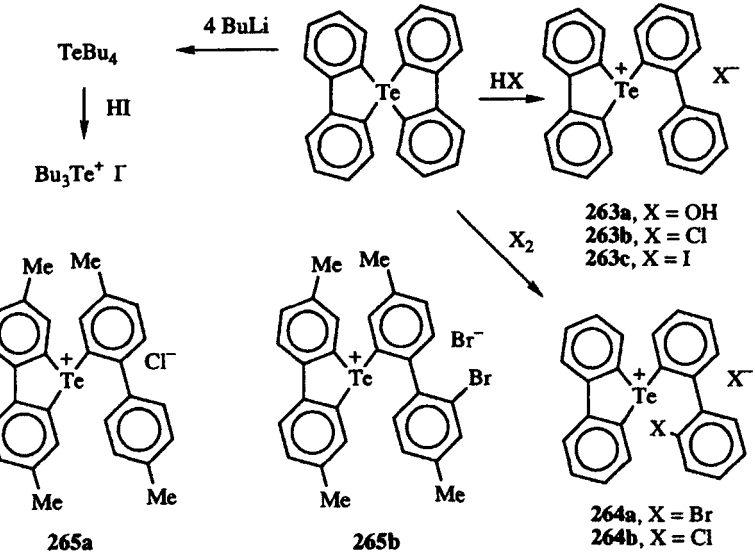

Scheme 90

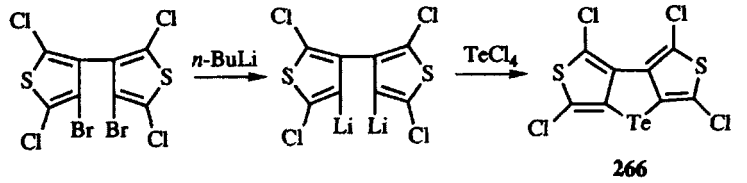

Scheme 91

butyllithium to bi-3,3′-dibromo-2,2′,5,5′-tetrachloro-2-thiophene gives the dilithiotetrachlorobithiophene. The addition of tellurium tetrachloride to a cold ether–hexane solution of the dilithio compound gives dithienotellurophene **266** in 90% yield.

VI. SYNTHETIC TRANSFORMATIONS OF TELLUROPHENES AND ANALOGS WITH DESTRUCTION OR POLYMERIZATION OF THE RING

A. Thermal Extrusion of Tellurium

Thermolysis of spirane **261** at 260°C gives dibenzocyclobutadiene in 51% yield and dibenzotellurophene (**239**) in greater than 90% yield as shown in Scheme 92.[109] The low reaction temperature for homolysis of the tellurium–carbon bonds prompted other thermal extrusion reactions based on loss of tellurium. Thermolysis of dihydrobenzotellurophene **48** at 500°C gives

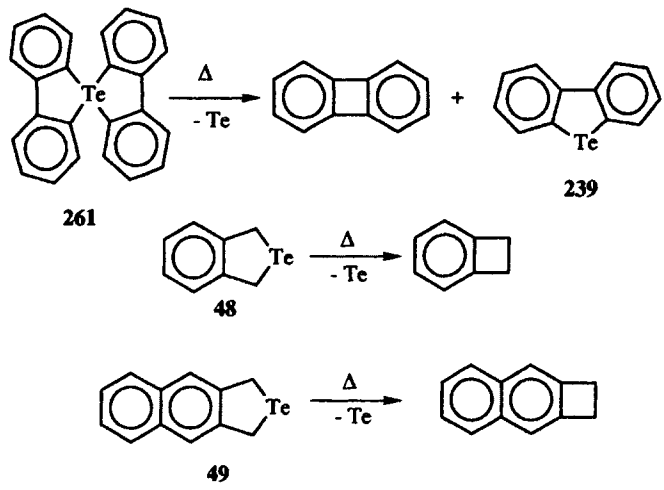

Scheme 92

benzocyclobutene in 74% yield, and thermolysis of 2,5-dihydronaphthotellurophene **49** under similar conditions gives naphthocyclobutene in good yield.[33]

Tellurium extrusion from singlet-oxygen-addition products have given the net oxidation of the 2- and 5-carbon atoms of tellurophenes to ketones as shown in Scheme 93.[85] The authors of reference 85 suggest that compounds **131a** and **131c**, when irradiated in oxygenated chloroform, generate singlet oxygen, which

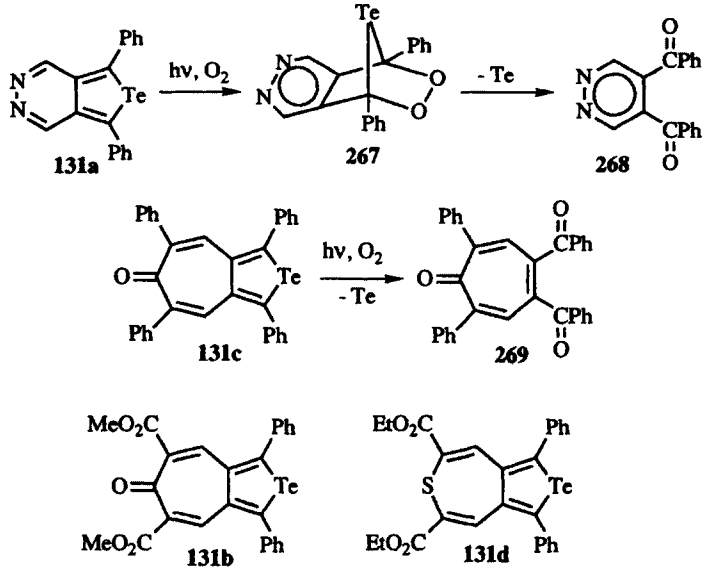

Scheme 93

adds to the tellurophene nucleus via [4 + 2] cycloaddition reactions. The intermediate 2,3-dioxa-7-tellurabicyclo[2·2·1]heptanes (such as **267**) lose tellurium on silica gel to generate dibenzoyl compounds **268** and **269** in 40 and 43% isolated yields, respectively. Diesters **131b** and **131d** do not undergo the photochemical oxidation (at least not at a synthetically useful rate), and diester **131d** does not undergo thermal loss of either sulfur or tellurium.[85]

B. Photochemical Extrusion of Tellurium

The observed photochemical oxidations of **131** may be a direct function of tellurophene photochemistry and not of singlet-oxygen cycloaddition reactions. Irradiation of 2,5-diphenyltellurophene leads to recovery of unreacted starting material.[122] Furthermore, Diels–Alder reactions of **177** have not been observed under even forcing conditions.[122] However, irradiation of 2-phenyltellurophene (**95**) (λ_{max} 292 nm, ε 12,600) through Pyrex in argon-degassed ether leads immediately to the formation of a black precipitate of tellurium with subsequent formation of a tellurium mirror around the reaction vessel.[64] From the reaction mixture, phenylvinylacetylene is isolated in 46% yield as shown in Scheme 94. From deuterium labeling studies with **95**, phenylvinylacetylene is produced via hydrogen abstraction from ether, which implicates free-radical intermediates. If irradiation of tellurophenes were to form a reactive vinyl radical, addition of oxygen would form hydroperoxy radicals, which might produce the products observed in Scheme 93 and not involve the proposed dioxatellurabicycloheptane intermediates such as **267**.

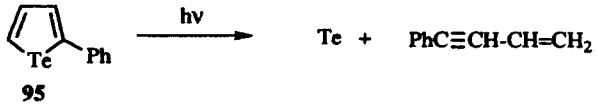

95

Scheme 94

Irradiation of 3-methyl-2,5-dihydrotellurophene (**43b**) in ethanol at 300 nm gives two products: tellurium metal and isoprene.[29] If simple homolysis of the tellurium–carbon bonds were involved, the expected product would be 1-methylcyclobutene, which was not observed.

C. Metallation of the Tellurium–Carbon Bonds

When 2,5-dihydrotellurophene (**44a**) is treated with two equivalents of butyllithium, butadiene is formed and dibutyl ditelluride.[29] Mechanistically, the addition of butyllithium across tellurium to give an "ate" complex would lead to lithium butyltelluride (as a leaving group) and butadiene. Air oxidation on

workup would give the ditelluride. In a similar reaction, 1,1-dichloro-2,5-dihydrotellurophene (**43a**) reacts with two equivalents of a Grignard reagent to give butadiene and diorganotellurides.[29] A similar mechanistic route might be operative although the timing of the formation of the second, new tellurium–carbon bond is uncertain.

When dibenzotellurophene (**239**) is treated with two equivalents of butyllithium, dibutyltelluride, and *o,o'*-dilithiobiphenyl are formed as shown in Scheme 95.[118] The dilithiobiphenyl can be captured with benzophenone to give diol **270**. Similar chemistry is observed on treatment of spirane **261** with four equivalents of butyllithium. Tetrabutyltellurium is produced (which can be isolated as a tributyltelluronium salt) as well as *o,o'*-dilithiobiphenyl. While these particular reactions are synthetically trivial in that it is an expensive route to the dilithiobiphenyl, the use of tellurophenes as masked dimetallated compounds has found some synthetic utility.

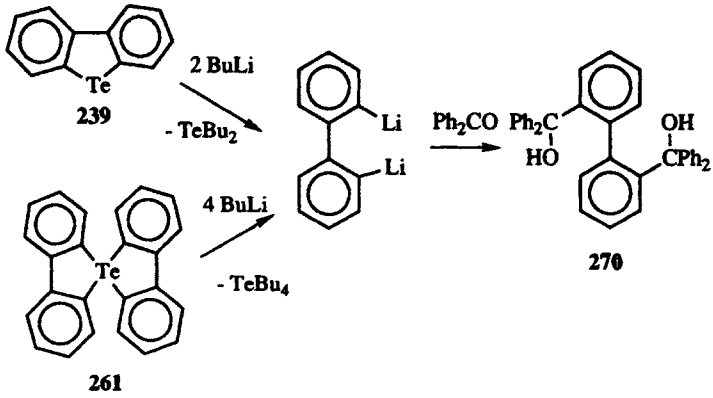

Scheme 95

One such reaction is the addition of two equivalents of butyllithium to a hexane solution of benzotellurophene (**177**) at 20°C, which gives dilithiostyrene **271** as a beige powder in 94% isolated yield and dibutyltelluride as shown in Scheme 96.[95] The metallation is stereospecific in that only the *cis* isomer is formed. The addition of either methyl iodide or dimethylsulfate to a hexane suspension of **271** gives pure *cis*-styrene **272**. Similarly, the addition of dibutyldichlorostannane to **271** in hexane gives the dibutylbenzostannophene **273** in 82% isolated yield. It should be noted that **273** does not serve as a precursor to **271**. This chemistry provides synthetic entry to a variety of stereospecific dilithiostyrene derivatives limited only by the availability of the benzotellurophene precursor.

2,5-Diphenyltellurophene (**122**) is metallated with butyllithium/tetramethylethylene diamine complex (BuLi/TMEDA) to give 1,4-dilithio-1,4-diphenyl-1,3-butadiene (**274**).[123] A variety of electrophiles react regiospecifically with the

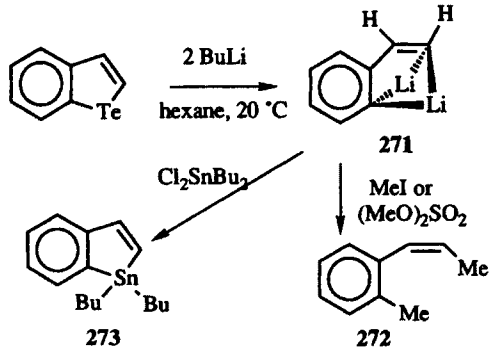

Scheme 96

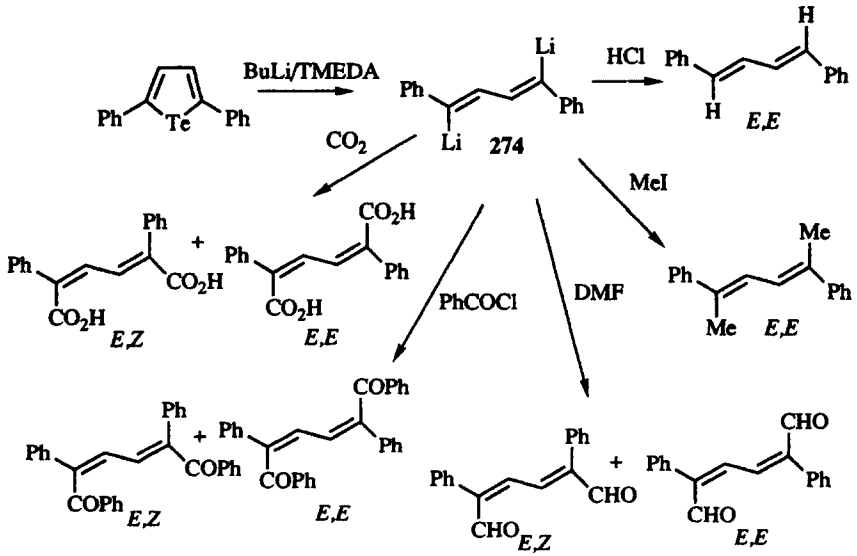

Scheme 97

dianion as shown in Scheme 97 but with varying degrees of stereoselectivity. The addition of hydrochloric acid to the dianion **274** gives *E,E*-1,4-diphenyl-1,3-butadiene stereospecifically in 58% yield, and the addition of iodomethane gives *E,E*-2,5-diphenyl-2,4-hexadiene stereospecifically in 47% yield. The addition of *N,N*-dimethylformamide to the dianion **274** gives both the *E,Z* and *E,E* isomers of 2,5-diphenyl-2,4-hexadiene-1,6-dial in a 19 : 2 ratio. The addition of carbon dioxide or benzoyl chloride to **274** gives mixtures of stereoisomers for products.

Tellurophene (**90**) can function as a precursor for the preparation of *Z,Z*-dienes as shown in Scheme 98.[124] The addition of two equivalents of Grignard reagent to tellurophene in the presence of 10 mol% nickel catalyst gives *Z,Z*-diene derivatives stereoselectively. Phenylmagnesium bromide gives a mixture

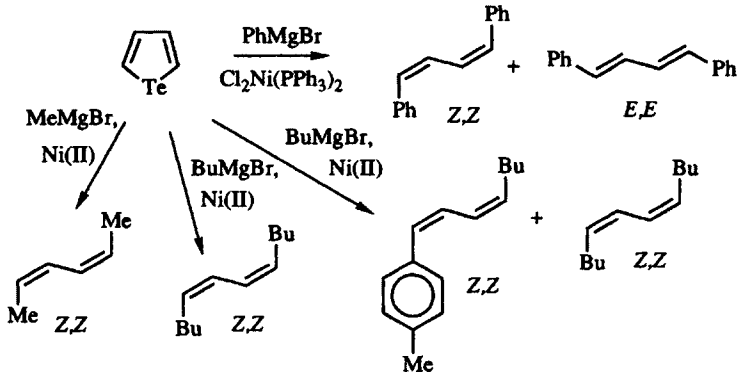

Scheme 98

of *Z,Z* and *E,E* isomers in 88% isolated yield. Methylmagnesium bromide gives *Z,Z*-2,4-hexadiene in 88% yield, and butylmagnesium bromide gives *Z,Z*-5,7-decadiene in 66% yield. Aryl groups from the nickel catalyst can be incorporated in the diene product as shown by the 6% yield of *Z,Z*-1-(*p*-tolyl)-1,3-octadiene in addition to the 52% yield of *Z,Z*-5,7-decadiene when butylmagnesium bromide is added to tellurophene in the presence of 1,3-bis(di-*p*-tolylphosphino)propanenickel dichloride.

D. Polymerization of Tellurophene and Derivatives

Polytellurophene has been prepared by the use of ferric chloride as catalyst.[125] Polytellurophene prepared in this manner is obtained in a powder form—not as thin films. Compressed pellets of polytellurophene show very low conductivity (10^{-12} S cm^{-1}) at room temperature and conductivity as high as 10^{-6} S cm^{-1} with iodine doping. While the conductivity of the undoped state is similar to that found for undoped polythiophene and polyselenophene, the doped conductivity of polytellurophene is much lower than that of similarly doped polythiophene and polyselenophene.

VII. TRANSITION-METAL COMPLEXES OF TELLUROPHENE AND RELATED COMPOUNDS

Complexes of tellurophene with transition metals can be divided into three categories consisting of complexes using the tellurium atom of tellurophene ligands as a two-electron donor, complexes derived from metal insertion into a carbon–tellurium bond, and complexes derived from utilizing tellurophene as a six-electron π donor to the metal. The literature of these complexes is not extensive.

A. Tellurophenes as Two-Electron Donors

Planar cobalt(II) complexes of Schiff-base ligands form adducts with electron-pair donors such as tetrahydrotellurophene (**3**).[126] While many of these complexes with electron-pair donors are one-to-one complexes, the complex with **3** is a one-to-two complex **275a** with tetrahydrotellurophene occupying both axial sites. Displacement with oxygen is possible to give the one-to-two complex **275b** with oxygen occupying the second axial site.[127]

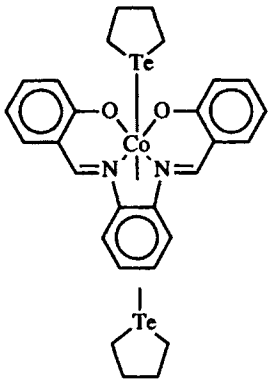

275a

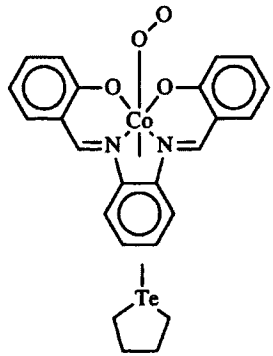

275b

Tetrahydrotellurophenes, dihydrotellurophenes, and benzotellurophenes have been utilized as ligands to form rhodium complexes.[128,129] The complexes **276–280** were prepared as shown in Scheme 99 from rhodium(III) trichloride trihydrate and the appropriate tellurophene.[128] Thermogravimetric analysis[129] and elemental analyses[128] of these complexes suggest that the complexes are octahedral (as shown in Scheme 99) and that two tellurium heterocycles are lost on heating to give a square-planar complex.[129] Complex **280** is best described as an octahedral trichlorotriiodo rhodium trianion with three telluronium cations.

Some interesting comparisons of the ligand properties of tetrahydrofuran, tetrahydrothiophene, tetrahydroselenophene, and tetrahydrotellurophene have come from niobium cyclopentadienide complexes of these ligands.[130] All the complexes were prepared as illustrated in Scheme 100 for the preparation of the tetrahydrotellurophene complex **281**. Irradiation of a solution of tetrahydrotellurophene (**3**) and niobium cyclopentadienide tetracarbonyl gives complex **281** as red crystals in 53% isolated yield.

When complex **281** is heated with various phosphines, phosphine substitution for tetrahydrotellurophene (**3**) is observed.[130] The kinetics of this process can be resolved to both a first-order process, which involves dissociation of the tellurium–niobium bond, and a second-order process in which the phosphine is incorporated into the ligand sphere of **281** followed by loss of tetrahydrotellurophene (**3**) as shown in Scheme 100. The dissociation of tetrahydrotellurophene

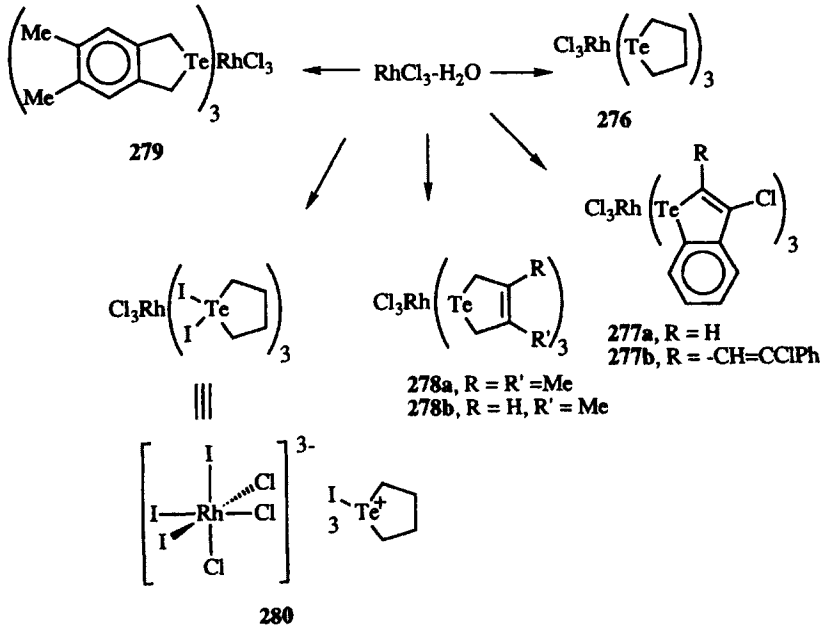

Scheme 99

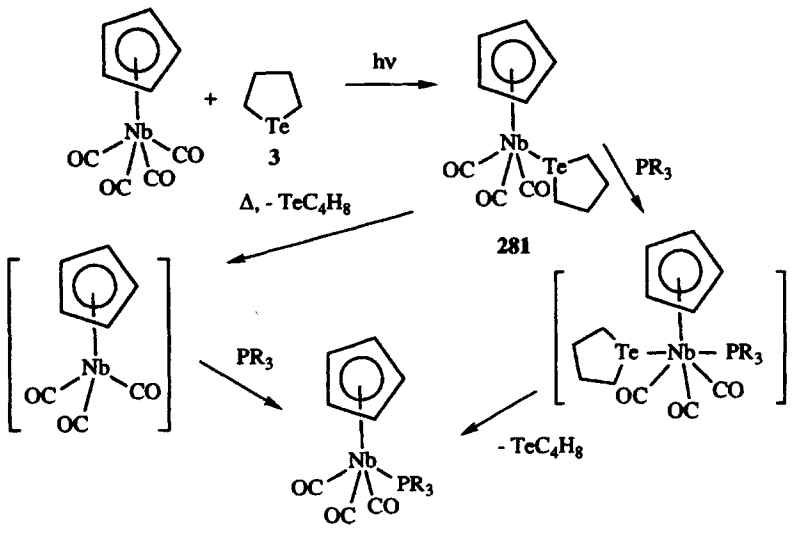

Scheme 100

via the first-order process proceeds with $\Delta H^{\ddagger}$ of 31.6 kcal mol^{-1} and $\Delta S^{\ddagger}$ of 8.2 cal mol^{-1} K^{-1}. This value of $\Delta H^{\ddagger}$ is more than 5 kcal mol^{-1} more positive than dissociation of tetrahydrofuran, tetrahydrothiophene, and tetrahydroselenophene from similar niobium complexes, and the value of $\Delta S^{\ddagger}$ is at least

7 cal mol^{-1} K^{-1} more positive than for dissociation of the other ligands. Addition of phosphines to the ligand sphere of **281** via the second-order process proceeds with a $\Delta H^{\ddagger}$ that is at least 4 kcal mol^{-1} more positive than for the complexes with the lighter chalcogen ligands. In the second-order process, all values of $\Delta S^{\ddagger}$ are comparable (approximately 20 cal mol^{-1} K^{-1}).

These data are consistent with a stability of O < S < Se < Te for niobium complexes of the tetrahydrochalcogenophenes. This increase in stability is probably due to the greater σ-donating ability of tellurium relative to the other chalcogens. Evidence for the increasing σ-donor ability comes from the frequency of the carbonyl bands in the infrared spectra of these complexes. This trend has also been observed in other series with dialkylchalcogenide and dialkyl dichalcogenide ligands such as $CpV(CO)_3(EMe_2)$[131] and $M_2(CO)_6(\mu\text{-}E_2Ph_2)$ where M is manganese or rhenium.[132]

Tellurophene (**90**) and tetrachlorotellurophene (**88**) have been utilized as a two-electron donor ligand in complexes of palladium as shown in Scheme 101.[133] Heating a mixture of disodium tetrachloropalladium and tellurophene (**90**) gives two products that are isolated as crystalline solids in 70 and 27% yields. The major product is monomeric with respect to palladium and is assigned the *cis* stereochemistry as in **282** on the basis of palladium–chloride stretching frequencies of 287 and 303 cm^{-1} in the infrared spectrum. The minor product is assigned the structure of the dimer **283**. Similarly, the reaction of palladium chloride and tetrachlorotellurophene (**88**) in refluxing methanol gives *trans* complex **284** as a crystalline solid in 61% yield. The *trans* stereochemistry in **284** is assigned on the basis of a palladium–chloride stretching frequency of 354 cm^{-1} in the infrared spectrum.

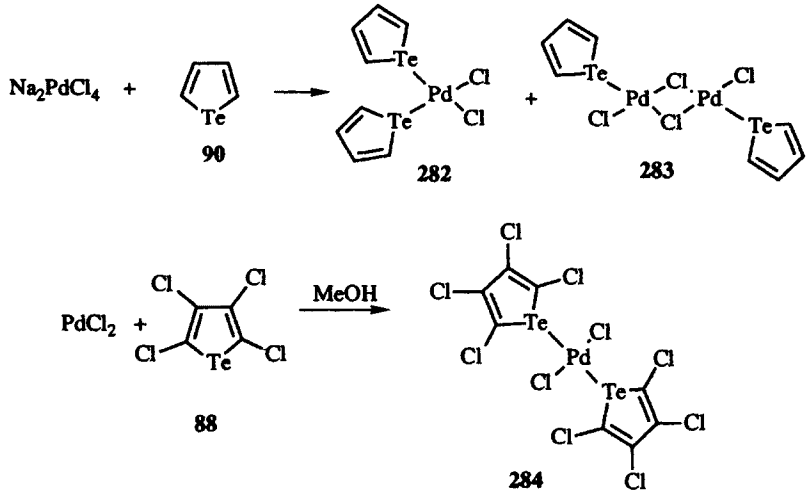

Scheme 101

B. Metal Complexes with Insertion into the Tellurium–Carbon Bond

The oxidative addition of metal complexes across the tellurium–carbon bonds of tellurophenes have been observed for several clusters.[134,135] In the reaction of tellurophene (**90**) with $Os_3(CO)_{10}(MeCN)_2$ in dichloromethane, the acetonitrile ligands are lost and the elements of the tellurophene nucleus are gained and a crystalline complex is isolated in 38% yield as shown in Scheme 102. The spectroscopic properties of the complex with tellurophene are very similar to those of the osmium complex with selenophene, which has been characterized by single-crystal X-ray crystallography.[135] On the basis of the structure with selenophene, the structure **285** is assigned to the tellurophene complex where oxidative addition across one tellurium–carbon bond is observed.

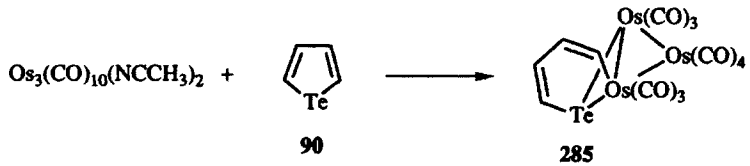

Scheme 102

Similar chemistry has been observed for the reaction of $Fe_3(CO)_{12}$ with tellurophene as shown in Scheme 103. In both cyclohexane[135] and benzene,[133] the major complex isolated is $Fe_2(CO)_6C_4H_4$ (**286**). However, in benzene solution two other products are also isolated.[133] One is $Te_2Fe_3(CO)_9$, and the other appears to be the product of oxidative addition of iron across the tellurium–carbon bond to give **287**, which is structurally quite similar to the osmium cluster **285**. Complex **287** may well be an intermediate in the reaction path to give **286**. In this path, tellurium extrusion would arise from

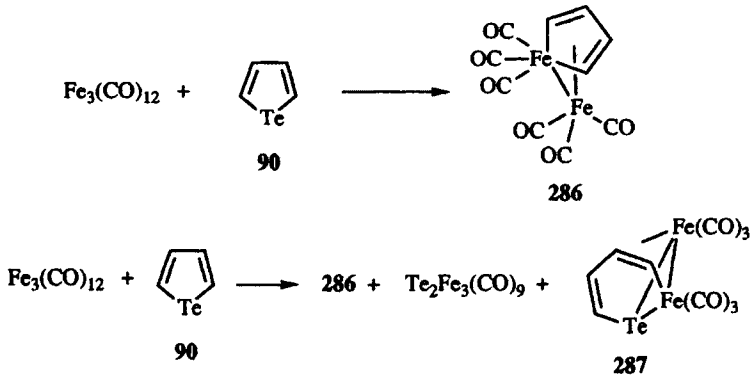

Scheme 103

sequential oxidative addition across both tellurium–carbon bonds of tellurophene.

The reaction of tetraphenyltellurophene (**86**) with $Fe_3(CO)_{12}$ has been described to give a small amount of a complex.[58] Although an empirical formula of $C_{28}H_{20}Te\text{-}Fe(CO)_3$ was suggested by the authors of reference 58 on the basis of the carbonyl stretching frequencies in the infrared spectrum of the complex, no other structural information is available to identify this complex.

The reaction of $Ru_3(CO)_{10}(MeCN)_2$ with tellurophene (**90**) gives a complex in 40% yield, which contains no tellurium as shown in Scheme 104.[135] The structure **288** is assigned to this complex on the basis of spectroscopic properties and a molecular formula of $Ru_2(CO)_6C_4H_4$. On the basis of the chemistry observed to generate the various osmium and iron complexes with tellurophene, complex **288** arises via tellurium extrusion from tellurophene through sequential oxidative additions across the tellurium–carbon bonds.

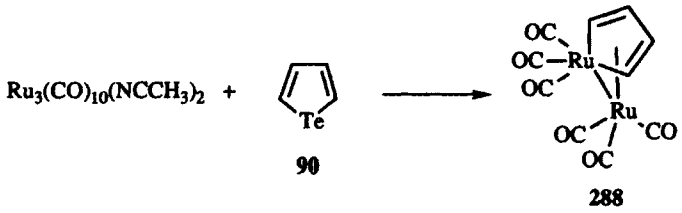

Scheme 104

C. Pi Complexes of Tellurophenes

The π complex of tellurophene (**90**) with chromium tricarbonyl has been prepared as shown in Scheme 105. The reaction of tellurophene (**90**) with $(MeCN)_3Cr(CO)_3$ at 50–60°C in butyl ether gives the π-heteroarene complex **289** in 80% isolated yield.[133] The heat-capacity curves of **289** and the corresponding selenophene–chromium tricarbonyl complex show no anomalies when compared to that of benzene–chromium tricarbonyl.[136]

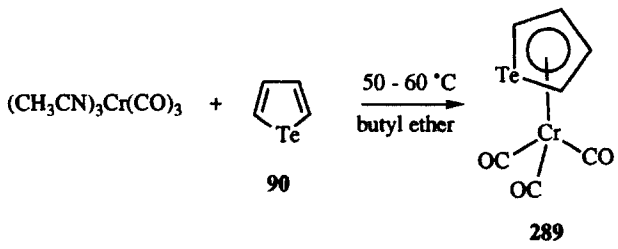

Scheme 105

D. Miscellaneous Metal Complexes with Tellurophene

The photochemical or thermal reaction of tellurophene with 2,4-dibromo-3-pentanone in the presence of $Fe_2(CO)_9$ gives a mixture of products consisting of all three stereoisomers of the 2,4-dimethyl-8-tellurabicyclo[3.2.1]oct-6-en-3-one (**290**) and tellurophene **291** as shown in Scheme 106.[137] Although convention might suggest the operation of an oxallyl cation in this reaction process,[138] the presence of **291** in the product mixture (similar products are not observed with furan) and the reactivity of tellurophene with iron carbonyls[58,133,135] suggest that the reaction pathway may be more complicated than formation of a simple iron–oxallyl complex with 2,4-dibromo-3-pentanone.

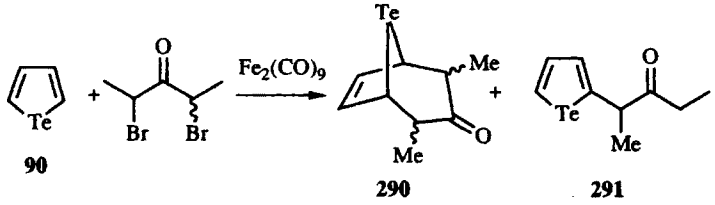

90 **290** **291**

Scheme 106

VIII. STRUCTURAL, PHYSICAL, AND SPECTROSCOPIC PROPERTIES OF TELLUROPHENES AND RELATED COMPOUNDS

A. Tetrahydrotellurophenes and Related Chalcogen Analogs

1. X-ray Crystallographic Analysis

Tetrahydrotellurophene (**3**) and its oxygen, sulfur, and selenium analogs are liquid compounds. The X-ray-derived structure of a telluronium analog of **3** [1-phenyltetrahydrotellurophene tetraphenylborate (**290**)] has been reported in the literature.[139] The numbering scheme used for **290** is shown in Figure 3, and bond lengths and angles are compiled in Table 1 (at the end of this chapter).

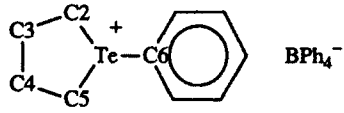

290

Figure 3. Numbering scheme for telluronium salt **290**.

For clarity, the tetraphenylborate anion is excluded from the discussion. The tellurium-carbon bond lengths of 2.172 and 2.113 Å in the heterocyclic ring and 2.109 Å to the telluronium methyl group are of the expected length based on a value of 2.14 Å for the sum of covalent radii.[140] The carbon–carbon bond lengths are typical of sp^3–sp^3 hybridized bonds. The five-membered ring is nonplanar with a twist at C3 and C4. The geometry about tellurium is best described as tetrahedral with the phenyl group occupying one tetrahedral site and a lone pair of electrons occupying another. The lone pair of electrons is stereochemically active as viewed in the distortion of the tetrahedral angles from C6 in the phenyl group through the tellurium atom to C2 and C5 to give angles of 95.7° and 99.5°, respectively.[141] The C2–Te–C5 angle of 84.9° also reflects compression from a tetrahedral angle due to both the phenyl group and the lone pair of electrons.

2. *Infrared and Vibrational Spectra*

Comparisons of the infrared spectra of tetrahydrotellurophene and its lighter chalcogen counterparts tetrahydroselenophene (**291a**) and tetrahydrothiophene (**291b**) in both the solid and liquid phases have been made as well as comparisons of the liquid Raman spectra.[142] On the basis of the ring and the elements of the ring, 33 bands have been predicted and assigned as shown in Table 2. The assignments are consistent with C_2 symmetry in these molecules. The methylene groups give rise to 24 normal modes of vibration, which are four symmetric stretching bands, 4 asymmetric stretching bands, 4 scissoring bands, and 12 C—C—H deformations. All vibrations are active and decrease in frequency in the order **291b** > **291a** > **3**.

3, X = Te
291a, X = Se
291b, X = S
291c, X = O

3. *Dipole Moments*

The dipole moments of the tetrahydrochalcogenophenes have been measured in benzene at 25°C. The values vary from 1.63 D (Debeye) for tetrahydrotellurophene (**3**) to 1.89 D for tetrahydrothiophene (**291b**) as shown in Table 3.[143] The dipole moments do not track electronegativity, which increases in the order Te < Se < S < O.

4. *Ionization Potentials*

One trend that does track electronegativity is the trend in ionization potentials (IP) as measured by gas-phase photoelectron spectroscopy.[144] A plot of the first IP as a function of the Pauling electronegativity is linear and shows that IP increases with increasing electronegativity of the heteroatom. Thus, tetrahydrotellurophene (**3**) has the lowest value of first IP in this series (7.73 eV) and tetrahydrofuran (**291c**) has the highest (9.53 eV) as shown in Table 3. The first three IPs of these compounds were measured and are compiled in Table 3.

5. *Mass Spectral Fragmentation*

The mass spectral fragmentation of the tetrahydrochalcogenophenes has been studied.[145] On electron impact, the parent ions are increasingly stabilized by the heteroatom in the order O < S < Se < Te.

6. *NMR Parameters*

The proton NMR spectra of all four tetrahydrochalcogenophenes are compiled in Table 4.[146,147] The protons of the methylenes adjacent to the heteroatom are at increasing field in the order **291b** > **291a** > **3** > **291c**, while the protons of the methylenes beta (β) to the heteroatom are at increasing field in the order **291c** > **291b** > **291a** > **3**. In all four compounds, the protons of the methylenes adjacent to the heteroatom are at lower field than the protons of the methylenes β to the heteroatom. The chemical shifts of the protons of the methylenes β to the heteroatom vary systematically with the heteroatom electronegativity.

The chemical shifts of the protons of the methylenes adjacent to the heteroatom vary as a more complicated function of the heteroatom. The heteroatom size and polarizability become important in the mixing of the nonbonding electrons of the heteroatom with the σ bonds of the α-methylenes. While electronegativity differences should deshield the α protons with increasing electronegativity, increasing electronegativity corresponds to smaller heteroatom size and more effective interaction of the heteroatom lone pairs with the C—H σ bonds. Thus, the α-methylenes in tetrahydrotellurophenes should be shielded relative to tetrahydrofuran on the basis of polarization of the carbon–heteroatom bond but deshielded because of poorer hyperconjugation.

Within the series of compounds comprising tetrahydrotellurophenes, 1,1-dihalotetrahydrotellurophenes, 1-alkyl or 1-aryltetrahydrotellurophenium halides, and hexacoordinate tetrahydrotellurophene species, a variety of different structural features can be evaluated by a comparison of ^{125}Te, ^{1}H, and

^{13}C NMR parameters. Table 5 contains chemical-shift values for these nuclei for tetrahydrotellurophene (**3**),[11] 1,1-diiodotetrahydrotellurophene (**2**),[25] 1-(*p*-ethoxyphenyl)tetrahydrotellurophenium chloride (**18**)[13], 1-methyltetrahydrotellurophenium iodide (**41e**),[25] 1-allyltetrahydrotellurophenium iodide (**41f**),[25] 1,1,1,1-tetraiodotetrahydrotellurophene (**35c**),[14] tetrahydrotellurophene DMSO–perchlorate complex (**27**),[7] and tetrahydrotellurophene pyridine–perchlorate complex (**28**).[7] Compounds **3**, **18**, **41e**, and **41f** are formally tellurium(II) species, although the latter three compounds are telluronium species with a formal positive charge. Tellurium NMR chemical shifts are sensitive to both the oxidation state of the tellurium atom and the net charge at tellurium.[36] The ^{125}Te chemical shifts of all three telluronium compounds are similar (δ 634–761) and are several hundred parts per million (ppm) upfield of the ^{125}Te chemical shift of tetrahydrotellurophene (δ 234). Neutral tellurium(IV) species **2** is further upfield (δ 929) than any of the telluronium salts, which is indicative that the ^{125}Te chemical shift is more sensitive to oxidation state than to charge.

The shielding of the carbon atoms adjacent to tellurium is sensitive to both charge and oxidation state. The reversal of the heteroatom–carbon polarization in proceeding from tetrahydrofuran to tetrahydrotellurophene is reflected in the ^{13}C NMR chemical shifts of tetrahydrotellurophenes. The α carbons of **3** are greatly shielded by the $Te^{\delta+}$—$C^{\delta-}$ polarization of the tellurium–carbon σ bond (δ 5.8), while the β carbons fall in a typical aliphatic range (δ 35.8). In telluronium salts **18**, **41e**, and **41f**, the α carbons are not deshielded (perhaps because of increased effective electronegativity for tellurium, the presence of the positive charge, and/or removal of a lone pair of electrons). In the telluronium salts, both the α- and β-carbon chemical shifts are in the δ 30–35 range. In tellurium(IV) compound **2**, the chemical shift of the α carbon is deshielded even further (δ 42.9), perhaps because of increased effective electronegativity of the I—Te—I moiety and removal of the axial lone pair of electrons on tellurium.

In the proton NMR spectra of these compounds, the β-protons are at higher field than the α protons in every case by approximately 1 ppm. Values of these chemical shifts are not diagnostic for either oxidation state or net charge at tellurium. The ^{1}H NMR spectra of 1,1-diiodo-2-methyltetrahydrotellurophene (**6**), 1,1-dichloro-2-methyltetrahydrotellurophene (**6b**), 1,2-dimethyltetrahydrotellurophenium iodide (**7a**), and 1,2-dimethyltetrahydrotellurophenium tetraphenylborate (**42a**) follow similar trends as compiled in Table 6.[4,26] Although the β protons are at higher field than the α protons, the differences are not diagnostic between the telluronium compounds and the tellurium(IV) compounds.

The most interesting data in Table 6 are the apparent shielding of the ring protons by the tetraphenylborate counterion in **42a** relative to the iodide salt **7a**.[26] The chemical shifts of the protons at the tellurium-containing end of the molecule are shielded by 0.1–0.3 ppm in the tetraphenylborate salt **42a** relative to the iodide salt **7a**. The shielding cones of the aromatic rings in the counterion may be oriented in such a way as to shield the end of the molecule containing tellurium (the site of the positive charge, which might promote ion pairing).

The halide counterions show little difference in the shielding of either the tellurium nucleus or the α carbons as shown in Table 7 for the 1-allyltetrahydrotellurophenium halides **41f–h**.[11] Both the ^{125}Te and ^{13}C NMR chemical shifts vary by less than 2 ppm as the halide changes from chloride to bromide to iodide.

Tellurium Mössbauer studies have been carried out on a few tetrahydrotellurophene derivatives.[148] Bonding from tellurium to its attached carbons is best explained in terms of tellurium *p* orbitals, which leads to the roughly 90° bond angles observed for the C—Te—C angles in X-ray structures.

B. 2,5-Dihydrotellurophenes and Related Chalcogen Analogs

1. Reactivity

Two of the more interesting features of 2,5-dihydrotellurophenes are their photolytic instability (**44b** decomposes with formation of isoprene and elemental tellurium) and their reactivity toward organometallic bases such as butyllithium (**44a** decomposes with formation of butadiene and dibutyl ditelluride).[29] Similarly, 1,1-dichloro-2,5-dihydrotellurophene (**43a**) reacts with Grignard reagents to form diorganotellurides and butadiene.[29] It is somewhat surprising then that the double bond of **43a** is inert to the addition of either chlorine or bromine.

2. Mass Spectral Fragmentation

The parent ions of 2,5-dihydrotellurophenes (**44**) can be recorded in spite of the instability of these molecules.[29] In the case of the parent compound **44a**, dehydrogenation of the parent ion (m^+/e 184) occurs in the mass spectrometer to give tellurophene (m^+/e 182). In the case of 1,1-dichlor-2,5-dihydrotellurophene (**43a**), strong peaks corresponding to **44a** (m^+/e 184) and tellurophene (m^+/e 182) are also observed.

3. NMR Parameters

The proton NMR spectra of 2,5-tetrahydrotellurophene (**44a**)[29] and its lighter chalcogen analogs **292**[149,150] have been reported and are compiled in Table 8. The chemical shifts of the α protons do not follow electronegativity trends for the dihydrofuran **292c**, dihydrothiophene **292b**, dihydroselenophene **292a**, and dihydrotellurophene **44a** analogs. The same reasons as those cited for the tetrahydrochalcogenophenes are applicable here as well. The olefinic protons are much less sensitive to the nature of the heteroatom. The chemical shifts for the protons of the 1,1-dihalo-2,5-dihydrotellurophenes **43a** and **45** are compiled

in Table 8 as well.[29] The olefinic protons and the α-methylene protons show opposite trends as the electronegativity of the halogen increase. Thus, the chemical shifts of the α-methylene protons move to lower field as the electronegativity of the halide ligands decreases, while those of the olefinic protons move to higher field as the electronegativity decreases. Interestingly, the ^{13}C NMR chemical shifts of **43a** and **45** are little affected by the nature of the halide ligands to tellurium.

44a, X = Te
292a, X = Se
292b, X = S
292c, X = O

43a, X = $TeCl_2$
45a, X = $TeBr_2$
45b, X = TeI_2
45c, X = TeF_2

In the ^1H NMR spectra of methyl-substituted dihydrotellurophenes **44b** and **44c** and 1,1-dichlorodihydrotellurophenes **43b** and **43c**, fortuitous overlap of the methylene signals occurs in the unsymmetrical compounds as shown in Table 9.[29] The methylene protons appear as a narrow singlet in all four systems. The methyl groups in these compounds appear at slightly lower field in the tellurium(IV) analogs relative to the tellurium(II) analogs.

C. 2,5-Dihydrobenzotellurophenes

1. X-Ray Crystallographic Analysis

X-ray structural data are available for many 2,5-dihydrobenzotellurophenes or closely related derivatives. The experimentally determined bond lengths and angles for 3,4-quinoxaline derivative **64a**[151] and its 1,1-diiodo derivative **63a**[152] are compiled in Table 10. Bond lengths and angles for a telluronium salt—1-methyl-2,5-dihydrobenzotellurophenium tetraphenylborate (**293**)[139]—are compiled in Table 10 as well. The numbering schemes for these three molecules are shown in Figure 4. This series allows the comparison of differences between tellurium(II) and tellurium(IV) states and differences among the various coordination numbers at tellurium on bond lengths and angles.

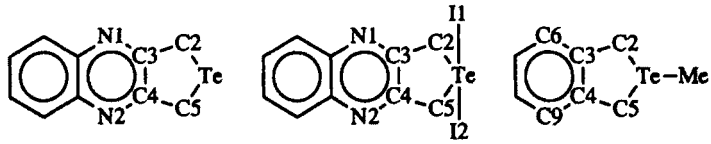

64a **63a** **293**

Figure 4. Numbering schemes for compounds **63a**, **64a**, and **293**.

From the data in Table 10, the tellurium–carbon and carbon–carbon bond lengths are similar in the three molecules **63a**, **64a**, and **293**, but some differences are noted. In the telluronium salt **293**, the average of the three tellurium–carbon bond lengths (2.099 Å) is approximately 0.04 Å shorter than the average tellurium–carbon bond lengths (2.138 Å) in **63a** and **64a**. The C2—C3 and C4—C5 bond lengths vary from 1.47 Å in **64a** to 1.54 Å in **293**, while the C3—C4 bond lengths vary from 1.38 Å in **293** to 1.42 Å in **63a**.

Bond angles are similar in the three molecules **63a**, **64a**, and **293**; the major differences are observed in the C2—Te—C5 angle. From the data in Table 10, the tellurium(II) derivative **64a** has an angle of 80.7°, which is significantly smaller than the 86.4° and 86.6° angles observed in **63a** and **293**, respectively. In **64a**, both lone pairs of electrons around tellurium should be stereochemically active according to VSEPR (Valence Shell Electron Pair Repulsion) theory[142] and should compress the C—Te—C angle from the tetrahedral angle of approximately 109°. Alternatively, the construction of tellurium–carbon bonds with nearly pure *p* orbitals on tellurium would place the C—Te—C angle at 90° to start. In telluronium salt **293**, one lone pair of electrons has been removed by formation of a tellurium–carbon bond. According to VSEPR theory, lone pair repulsion would be diminished and the C—Te—C angle relaxed. Alternatively, all three C—Te—C angles in **293** are approximately 90° and presumably are constructed of pure *p* orbitals on tellurium. In tellurium(IV) derivative **63a**, the geometry about tellurium is trigonal bipyramidal with the iodide ligands occupying the two axial sites and the tellurium lone pair occupying the third equatorial site. The C2—Te—C5 bond angle should be slightly larger in this geometry relative to the tetrahedral geometry of **64a** but compressed by the lone pair from the ideal angle of 120°. The stereochemical activity of the lone pair of electrons is observed in the I—Te—I angle of 176.5°, which is compressed from the ideal of 180°.

The X-ray crystal structures of single crystals of the 1,1-bidentate-ligand-disubstituted-2,5-dihydrobenzotellurophenes **59–61** have also been determined.[39] The numbering system used for these molecules is shown in Figure 5. The dihydrobenzotellurophene moiety is planar in these molecules. Selected bond lengths and angles for these compounds are compiled in Table 11 and are similar for all three compounds. The average tellurium–carbon bond length is 2.34 Å, and the average C—Te—C bond angle is 85.4°. Structurally, all three

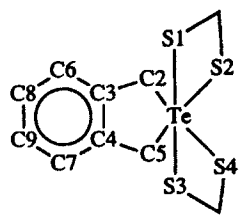

59-61

Figure 5. Numbering scheme for compounds **59–61**.

complexes have axial sulfur ligands to tellurium. Although the expected angle is 180°, the observed angles are near the average of 165.6°. These molecules can be viewed as having a trigonal–bipyramidal structure in which the second sulfur atoms of the bidentate ligands are roughly in the same plane as the axial sulfur atoms but 60° away. This array has been described as a 1 : 2 : 2 : 2 structure in which the tellurium lone pair is at the apex or, alternatively, as an octahedral complex in which the tellurium lone pair is stereochemically inert.[39]

2. *NMR Parameters*

The α-methylenes to the tellurium atom in 2,5-dihydrobenzotellurophene (**48**) appear as singlet at δ 4.69 and in 2,5-dihydronaphthotellurophene (**49**), as a singlet at δ 4.68. The aromatic protons in these molecules appear as multiplets between δ 7.0 and 7.6 for **48** and δ 7.2 and 7.9 for **49**.[33]

The ^{125}Te NMR spectra of a variety of 2,5-dihydrobenzotellurophenes have been described, and the data are compiled in Table 12.[13,36,39] The ^{125}Te NMR chemical shift of the tellurium(II) derivative **48** is δ269. The telluronium salts **294** are still formally tellurium(II) compounds, but the positive charge deshields the tellurium nucleus, and ^{125}Te NMR chemical shifts of δ651–722 are observed. In the 1,1-dihalo tellurium(IV) derivatives **50**, **53**, and **54**, the ^{125}Te NMR chemical shifts are in the range 830.5–994. The chemical shift becomes more positive with increasing electronegativity of the axial ligands, which is in the direction expected with increased deshielding of tellurium with more electronegative ligands. In the dithiolato complexes **59–61**, the tellurium(IV) nucleus is shielded by the added electrons of the second sulfur donor ligand. As a consequence, the ^{125}Te NMR chemical shifts of **59–61** are in the range δ 605–727 (when referenced to Me_2Te).

The ^{13}C NMR spectrum of the parent compound **48** has not been described in the literature. Some ^{13}C NMR data are available for telluronium salts and tellurium(IV) derivatives and are compiled in Table 13 utilizing the numbering scheme shown in Figure 6.[13,39] The carbon atoms attached to tellurium are shielded by 10 ppm in the tellurium(II) derivatives **294** relative to the tellurium(IV) derivatives **59–61**, even though the tellurium(II) compounds are telluronium species and bear a positive charge.

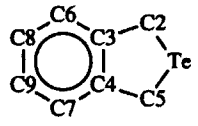

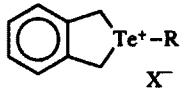

294a, R = Me, X = I
294b, R = $CH_2CH{=}CH_2$, X = Br
294c, R = CH_2Ph, X = Br

Figure 6. Numbering scheme for compounds **59–61** and **294** and chemical structures of compounds **294**.

D. 2,3-Dihydrobenzotellurophenes

1. NMR, IR, and UV–Visible Spectral Properties

Most of the structural and spectroscopic information available for 2,3-dihydrobenzotellurophenes is compiled for 3-oxo-2,3-dihydrobenzotellurophene (**74**) and for its aurone analog **78a**.[48,153] Lighter chalcogen analogs of these materials are also known as represented by compounds **295** and **296**.

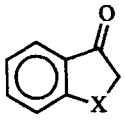

74, X = Te
295a, X = Se
295b, X = S
295c, X = O

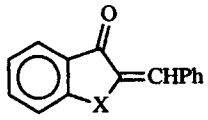

78a, X = Te
296a, X = Se
296b, X = S
296c, X = O

The ^{125}Te NMR signal of **74** is observed at δ 383, and the methylene protons are observed at δ 4.18 in the ^{1}H NMR spectrum of **74**. The tellurium–proton coupling constant ($J_{Te\text{-}CH_2}$) is 26 Hz, which is quite similar to the 23 Hz observed for **48**.

In telluroaurone **78a**, the ^{125}Te NMR signal is observed at δ 500,[153] and the olefinic proton is observed at δ 8.56 in the ^{1}H NMR spectrum of **78a** as shown in Table 14.[48] In the lighter chalcogen analogs **296**,[48,154] the chemical shift of the olefinic proton moves to higher field with increasing electronegativity of the heteroatom (Te < Se < S < O). Thus the chemical shift of the olefinic proton decreases from δ 8.56 for **78a** to δ 6.95 for **296c**.

The carbonyl stretching frequency (ν_{co}) also varies systematically with the heteroatom in both the **78/295** and **78a/296** series.[48,154] As the electronegativity of the heteroatom increases, the carbonyl stretching frequency increases. For **74**, ν_{co} is 1670 cm^{-1}, and for selenium analog **295a**, ν_{co} increases to 1685 cm^{-1}. In the **78a/296** series, ν_{co} increases from 1645 cm^{-1} for telluroaurone **78a** to 1685 cm^{-1} for aurone **296c** as illustrated in Table 14.

The series of chalcogenopyranones **297** shows the same trend with respect to ν_{co} as is observed in the **78a/296** series.[155] Although X-ray crystallographic data are absent for the **78a/296** series, X-ray structural data for compounds **297** show

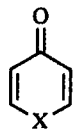

297a, X = Te
297b, X = Se
297c, X = S
297d, X = O

that the C=O bond length in telluropyranone **297** is 0.03 Å longer than observed in selenopyranone **297b** or thiopyranone **297c**, which is consistent with a weaker C=O stretch and a lower-frequency value of ν_{CO}.

The absorption spectra of the **78a/296** series also vary as a function of the heteroatom. As the electronegativity of the heteroatom increases and/or as the size of the heteroatom decreases, the absorption maximum shifts to shorter wavelengths as shown in Table 14. Thus λ_{max} is observed at 472 nm in telluroaurone **78a** and decreases to 422 nm in thioaurone **296b**. The oscillator strength is similar in all three compounds. This transition in the absorption spectrum is an n–π^* transition. As the electronegativity of the heteroatom increases, the lone pair of electrons is bound more tightly and is at lower orbital energy. Thus, the n–π^* transition is higher in energy and is observed at shorter wavelengths as electronegativity increases.

E. Tellurophenes and Related Chalcogen Analogs

1. Reactivity and Aromaticity

The aromaticity of the chalcogenophene series tellurophene (**90**), selenophene (**298a**), thiophene (**298b**), and furan (**298c**) has been the subject of numerous papers. One ranking of aromaticity has been based on rate constants for electrophilic aromatic substitution.[80,81] Rate constants for formylation and relative rate constants for acetylation and trifluroacetylation have been determined for the entire **90/298** series and are compiled in Table 15. In this series of reactions, the relative ordering of aromaticity of the heterocyclic systems is thiophene (**298b**) > selenophene (**298a**) > tellurophene (**90**) > furan (**298c**). In terms of Eyring activation parameters, Vilsmeier–Haack formylation is 2.4 kcal mol^{-1} more facile for furan (**298c**) relative to thiophene (**298b**). Although these parameters were determined only for formylation, plots of relative reactivities for acetylation and trifluoroacetylation as a function of relative reactivities for formylation are linear, which suggests similar behavior for all three reactions.

90, X = Te
298a, X = Se
298b, X = S
298c, X = O

Theoretical chemistry has also attempted to evaluate the aromaticity of the chalcogenophenes. A statistical evaluation of deviations in peripheral bond order has been utilized to develop an aromaticity index in which the order of chalcogenophene aromaticity is thiophene (**298b**) > selenophene

(**298a**) > tellurophene (**90**) > furan (**298c**).[156] This approach was described as a simplification of the sum of bond-order differences, which gives a similar ordering for these molecules but becomes cumbersome with unsymmetrical derivatives.[157,158] A configuration analysis of the state functions determined by MO-LCAO (molecular orbital–linear combination of atomic orbitals) theory (PPP-CA Pariser–Parr–Pople Correlation Analysis calculations) gives a somewhat different ordering of aromaticity: thiophene (**298b**) > furan (**298c**) > selenophene (**298a**) > tellurophene (**90**).[159]

Force fields and mean amplitudes of vibrations from the fundamental frequencies of the chalcogenophenes have been utilized to evaluate the ground-state aromaticity of these molecules.[160] An aromaticity ordering of thiophene (**298b**) > selenophene (**298a**) > tellurophene (**90**) > furan (**298c**) was determined by this method.

2. *Tellurophenes and Lighter Chalcogen Analogs as Substituents*

Hammett-type substituent constants have been determined for the chalcogenophenes attached at the 2-position from ionization constants and ^{1}H NMR chemical shifts for chalcogenophene-substituted phenols **165/299** and **166/300**.[77,161,162] As shown in Table 16, Hammett σ_p substituent constants are quite similar for the chalcogenophene series. However, σ_m constants increase slightly with increasing heteroatom electronegativity (from 0.06 for the 2-tellurienyl substituent to 0.09 for the 2-furyl substituent). The σ_p^- constants are numerically larger than the σ_p constants and increase slightly with decreasing heteroatom electronegativity (from 0.25 for the 2-tellurienyl substituent to 0.21 for the 2-furyl substituent). The σ_m^- constants are nearly identical for the 2-tellurienyl, 2-thienyl, and 2-furyl substituents (approximately 0.11), and these values are slightly smaller than the σ_m^- value of 0.16 measured for the 2-selenienyl substituent. On net, these substituents are weakly, inductively electron-withdrawing and show a slightly greater ability to delocalize a negative charge through resonance effects.

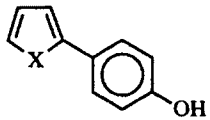

165, X = Te
299a, X = Se
299b, X = S
299c, X = O

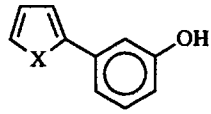

166, X = Te
300a, X = Se
300b, X = S
300c, X = O

The ability of the chalcogen atom to affect the pK_a of 2-chalcogenophene carboxylic acids has also been studied.[89,163–166] In water at 25°C for the series of carboxylic acids **136/301**, the pK_a decreases with increasing electronegativity from 3.97 for **136**[89] to 3.60 for **301a**[164] to 3.53 for **301b**[165] to 3.16 for **301c**.[166] In

50% aqueous ethanol, the same trend is observed, with the pK_a decreasing from 5.48 for **136** to 5.14 for **301a** to 5.05 for **301b** to 4.54 for **301c**.[163] These trends are somewhat surprising in view of the substituent constants for 2-chalcogenopheneyl systems compiled in Table 16, which would predict the opposite trend. The magnitude of the substituent constants is sufficiently small such that minimal differences in pK_a would be expected within the series.

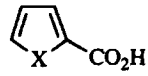

136, X = Te
301a, X = Se
301b, X = S
301c, X = O

3. *X-Ray Crystallographic Analysis*

Tellurophene (**90**) is a liquid at room temperature (bp 91–92°C at 100 torr) with a melting point of approximately − 36°C.[167] Although X-ray crystallography has not been applied to the parent nucleus, the X-ray crystal structures of two crystalline tellurophene derivatives, **136**[168] and **302**,[169] have been reported.

Bond lengths and bond angles for **136** and **302** are compiled in Table 17 according to the numbering scheme shown in Figure 7. Two crystallographically nonequivalent molecules (**136a** and **136b**) are found in the unit cell of **136**, and data for both molecules are included in Table 17. Both **136** and **302** are unsymmetrical molecules through substituent placements, but this asymmetry is not reflected in the bond lengths and angles, which are essentially identical in both halves of the molecules. Both **136** and **302** are planar molecules with no detectable twist from planarity. The C2—Te—C5 bond angles are approximately 82° in both molecules, and the Te—C bond lengths are roughly 2.06 Å in length. These values can be compared to the X-ray structures of the tetrahydrotellurophenium compound **290**, 2,5-dihydrobenzotellurophene derivatives **59–61**, **63a**, **64a**, and **293**. In tellurophene derivatives **136** and **302**, Te—C bond lengths are 0.060 Å or more shorter than in the dihydro and tetrahydro species.

The C2—C3 and C4—C5 bond lengths are slightly shorter than the C3—C4 bond length, and all three bonds are shorter than a C—C single bond. The

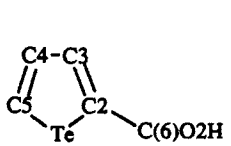

136

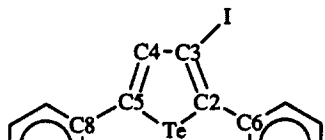

302

Figure 7. Numbering scheme for compounds **136** and **302**.

C2—Te—C5 angle is 3° smaller than in the dihydro- and tetrahydrotellurophene derivatives. The C2—C3—C4 and C3—C4—C5 bond angles are approximately 120° in both molecules, while the Te—C2—C3 and Te—C5—C4 angles are approximately 110°. The C3—I bond does not bisect the C2—C3—C4 angle. The iodine is pushed away from the C2—C3 bond, presumably via the steric influence of the 2-phenyl substituent.

4. *Other Approaches to Molecular Structure in Chalcogenophenes*

Several approaches to elucidate structural information for the liquid chalcogenophenes **90**/**298** have been reported. Microwave spectroscopy has been utilized to characterize the structure of the chalcogenophene series tellurophene (**90**),[170] selenophene (**298a**),[171] thiophene (**298b**),[172] and furan (**298c**).[173] The structural data are compiled in Table 18 utilizing the numbering scheme shown in Figure 8.

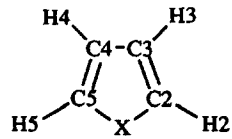

90, X = Te
298a, X = Se
298b, X = S
298c, X = O

Figure 8. Numbering scheme for compounds **90** and **298**.

As compiled in Table 18, the Te—C bond lengths in **90** of 2.055 Å are nearly identical to the 2.06-Å average Te—C bond lengths in the X-ray structures of **136** and **302**. The C2—Te—C5 bond angle of 82.5° in **90** is again nearly identical to the 82° average bond angle for **136** and **302**. Carbon–carbon bond lengths and other ring angles are virtually identical for **90** by microwave spectroscopy and **136** and **302** by X-ray crystallography.

As the heteroatoms change in the five-membered ring, the expected changes in the C2—X and C5—X bond lengths and the C2—X—C5 angles are observed. The bond lengths increase from 1.36 Å for **298c** to 2.06 Å for **90**, while the C—X—C angle decreases from 106.5° in **298c** to 82.5° in **90**. The C3—C2—X and C4—C5—X angles are little affected by heteroatom substitution, varying from 110.7° to 111.6°. Most of the imposed angle changes from the increased bond length (other than the C2—X—C5 angle) appear in the C2—C3—C4 and C3—C4—C5 angles, which vary sequentially from 106.1° in **298c** to 117.9° in **90**. The carbon–carbon bond lengths in the four molecules are little affected by heteroatom substitution, which seems to suggest that no localizing of double-bond character occurs because of decreased aromatic character.

Ab initio computational methods also give a good prediction of experimental geometry.[174,175] Theoretical geometries for tellurophene (**90**) at the 3-21G and 3-21G* levels are compiled in Table 19. The fit to experiment is quite good with Te—C bond lengths of 2.10 Å predicted (2.06 Å observed experimentally) and a C—Te—C angle of 80.7° predicted (82.5° observed experimentally). The remaining internal angles of 111° and 118° are identical to the same values observed experimentally. Carbon–carbon bond lengths of 1.34 and 1.45 Å are predicted, while values of 1.37 and 1.42 Å are observed experimentally.

The r^a structures of tellurophene (**90**) and tellurophene-2-carboxaldehyde (**119**) have been determined from ^{1}H NMR spectra in oriented phases through the inclusion of ^{13}C and ^{125}Te satellites. From a fixed carbon–carbon distance (1.45 Å for C3—C4), the bond lengths and angles compiled in Table 20 have been determined for tellurophene-2-carboxaldehyde (**119**) utilizing the numbering scheme shown in Figure 9.[176] The r^a structure of tellurophene (**90**) has been the subject of several papers,[177–179] and the structural parameters for one of them are included in Table 20.[179] The coupling constants of the various nuclei in these molecules is discussed in the NMR section below.

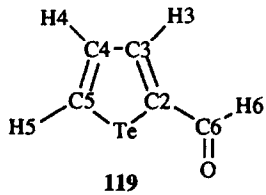

119

Figure 9. Numbering scheme for compound **119**.

The r^a structure of tellurophene (**90**), when the C3—C4 bond length is fixed, is in remarkable agreement with the tellurophene structures from other measurements: the Te—C bond lengths are 2.07 Å, the C—Te—C angle is 80.3°, and the remaining two internal angles are 117.5° for C2—C3—C4 and 112.3° for Te—C2—C3. The r^a structure of tellurophene-2-carboxaldehyde (**119**), when the C3—C4 bond length is fixed, has Te—C bond lengths of 2.10 Å, a C—Te—C angle of 77.3°, and four remaining internal angles of approximately 115° each. The fit of the data for tellurophene-2-carboxaldehyde (**119**) is most consistent with an aldehyde structure with the carbonyl oxygen *syn* to the tellurium atom.[176]

5. *Vibrational and Infrared Spectra of Tellurophenes and Related Chalcogen Analogs*

In the chalcogenophenes **90**/**298**, there are 21 normal vibrations.[180–183] All are active, and all have been observed through a combination of infrared and Raman spectroscopy. In tellurophene (**90**), full assignment has been made

through the use of deuterated tellurophenes. It was assumed in these assignments that the tellurophene nucleus is planar and that the molecule possesses C_{2v} symmetry. These assignments are summarized in Table 21, and frequencies are listed for all four chalcogenophenes **90/298**.[180–183]

Of the four chalcogenophenes, the behavior of furan (**298c**) is somewhat different from that of the other three.[180] In the tellurophene (**90**), selenophene (**298a**), thiophene (**298b**) series, several normal modes appear at nearly identical frequencies (ν_6, ν_{10}, ν_{15}, and ν_{16}), several modes show sequential lowering of frequency with increasing heteroatom size (ν_1, ν_2, ν_4, ν_7, ν_{11}, ν_{12}, ν_{13}, and ν_{19}), several modes show a slight sequential increase in frequency with increasing heteroatom size (ν_5, ν_9, ν_{614}, and ν_{20}), and the remaining frequencies show a large decrease in frequency with increasing heteroatom size (ν_3, ν_8, ν_{17}, ν_{18}, and ν_{21}). In the last group of frequencies, the large changes are a function of the mass and geometric effects imposed by the size of the heteroatoms, which directly determine the symmetric and asymmetric C—X—C stretching (ν_3 and ν_{17}, respectively) and ring-deformation modes involving the heteroatom (ν_8, ν_{18}, and ν_{21}). The increase in ν_5 (a C=C stretch) with increasing heteroatom size may be a function of increased double-bond character with lower aromaticity. In this context, the frequency of ν_5 in furan (**298c**) is much higher at 1483 cm^{-1}, which is consistent with this argument.

Force-field calculations have been determined for the 8 A_1 and 7 B_1 in-plane vibrations[184] of tellurophene (**90**) and selenophene (**298a**) and for the A_2 and B_2 out-of-plane modes for these same molecules.[185] The calculations were performed with the G–F matrix method,[186] assuming a general valence force field (GVFF) as zeroth-order force field. In these calculations, the ring-stretching force constants show a monotonic variation toward pure C—C and C=C character as the heteroatom changes from sulfur to selenium to tellurium, and that the X—C force constant is involved in the same trend. In this analysis (and intuitively), the overlap of the heteroatom and carbon p orbitals shows the trend S > Se > Te, which is in the same order as the aromaticity of the heterocyclic rings [thiophene (**298b**) > selenophene (**298a**) > tellurophene (**90**)].

A similar analysis of the vibrational spectra and assignments for 2-chlorotellurophene (**140**) and 2-bromotellurophene (**141**) and their corresponding selenophene (**303a** and **304a**, respectively) and thiophene (**303b** and **304b**, respectively) analogs has been made.[187] Identical trends were observed in these substituted derivatives as were observed in the parent heterocycles (**90/298a/298b**) with respect to increasing mass and size of the heteroatom and observed changes in C—C and C=C stretching behavior. Force-field calculations assuming a

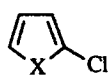

140, X = Te
303a, X = Se
303b, X = S
303c, X = O

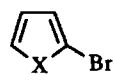

141, X = Te
304a, X = Se
304b, X = S
304c, X = O

GVFF were less satisfactory in these series of molecules in explaining the observed trends (or lack of trends).[188]

The chalcogenophene rings, as substituents, influence the infrared bands of carbonyl groups attached to them as shown in Table 22. In carboxylic acids **136** and **301**, the carbonyl stretching frequency decreases from 1755 cm^{-1} in furan-2-carboxylic acid (**301c**) to 1721 cm^{-1} in tellurophene-2-carboxylic acid (**136**).[163] Similarly, the bis-3-chalcogenopheneyl ketones **148/305**[88] show a decrease in carbonyl stretching frequency from 1632 cm^{-1} for furan derivative **305c** to 1600 cm^{-1} for tellurophene derivative **148**. One explanation for these trends is increasing dipolar character to the carbonyl group as the heteroatom becomes more electropositive. This would give more single-bond character to the carbonyl group and a lower stretching frequency.

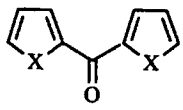

148, X = Te
305a, X = Se
305b, X = S
305c, X = O

6. *Dipole Moments of Tellurophenes and Related Chalcogen Compounds*

The dipole moments of tellurophene (**90**) and a variety of 2-substituted derivatives have been determined and compared to the corresponding lighter chalcogen analogs (Table 23).[189] For the unsubstituted ring systems **90/298**, the dipole moments are small and similar (0.46–0.72 D) and show much less variation than those for the tetrahydrochalcogenophenes **3/291** (Table 3). Introduction of polar substituents into the 2-position of the ring dominates the dipole moment of the resulting molecules.

7. *Mass Spectral Fragmentation of Tellurophenes and Related Compounds*

The electron-impact mass spectral fragmentation patterns of the four chalcogenophenes have been characterized and are compiled in Table 24.[190–192] The isotope patterns associated with selenium and tellurium make the identification of fragments containing these heteroatoms far more facile than for furan and thiophene derivatives. The fragmentation patterns are summarized in Scheme 107.

As shown in Table 24, all four molecules have significant parent ions (M^+)—a tendency that is shared by substituted tellurophene derivatives. In the cases of

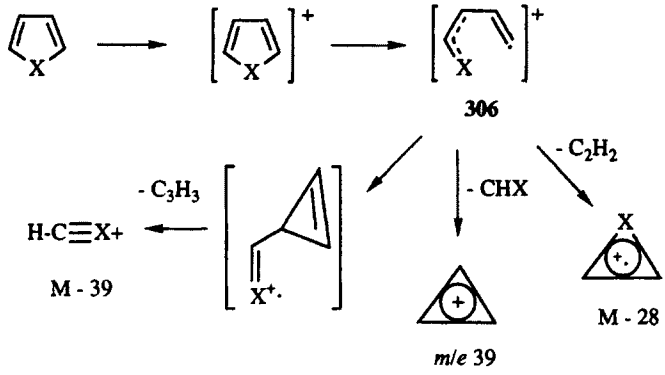

Scheme 107

selenophene and tellurophene, the X^+ fragment is also significant. Fission of one C—X bond in M^+ leads to a metastable ion **306**, which can lose —CHX, acetylene (C_2H_2), or the cyclopropenium radical (C_3H_3) to give fragments with *m/e* of 39, M—C_2H_2, and M—39, respectively. For selenophene (**298a**) and tellurophene (**90**), two additional fragmentation routes from **306** are observed, which correspond to loss of X and HX to give ions with *m/e* of 52 and 51, respectively. Some of the factors influencing the changes in fragmentation patterns observed in changing the heteroatom within these molecules are the strength of the C—X bond, which decreases from oxygen to tellurium, and the different geometrical constraints imposed as the heteroatom becomes larger.[190]

8. *NMR Parameters for Tellurophenes and Related Chalcogen Analogs*

The NMR parameters of the chalcogenophenes have been the subject of numerous studies, which have attempted to quantify the differences among the systems and to predict the chemical shifts of various nuclei in the molecules. A study of similarly substituted tellurophenes and selenophenes show that the ^{125}Te nucleus is 2.44 times as sensitive to substituent effects as the ^{77}Se nucleus.[193] A quantitative measure of π-electron deficiency and π-electron excessiveness ($^{\pi}\Delta$) has been developed that allows the prediction of ^{13}C NMR chemical shifts based on the difference between a given substituted chalcogenophene and its parent and the identically substituted benzene derivative.[194] The effects of substituents on ^{1}H and ^{13}C chemical shifts in 2- and 3-substituted chalcogenophenes has been studied by principal-components analysis and by partial-least-squares analysis.[195] The substituent effects are grouped into four distinct groups depending on the heteroatom present in the ring. Furthermore, the substituent-heteroatom interactions follow the same trends in all four groups allowing the prediction of both ^{1}H and ^{13}C NMR chemical shifts.

The ^1H and ^{13}C NMR shifts of the chalcogenophenes **90** and **298** are compiled in Table 25.[196] The ^{125}Te NMR chemical shift of tellurophene has been measured at δ 782.[197] The two different protons in the ring system appear at lowest field in tellurophene (**90**) and at highest field in thiophene (**298b**) for H2(5) and in furan (**298c**) for H3(4). In the ^{13}C NMR spectra of these compounds, C3(4) moves to lower field with increasing heteroatom electronegativity while C2(5) follows no trend at all. For sp^3-hybridized carbon atoms attached to tellurium, the ^{13}C NMR chemical shift displays marked shielding from the $Te^{\delta+}—C^{\delta-}$ polarization of the bonds. Similar shielding is not observed in the ^{13}C NMR chemical shifts of sp^2-hybridized carbon atoms (C2,C5) attached to tellurium in the tellurophenes. In fact, carbon atoms bound to sulfur, which is more electronegative than tellurium, appear at higher field than in the corresponding tellurophene.

The observed coupling constants in the chalcogenophenes **90** and **298** are compiled in Table 26 using the numbering scheme of Figure 8. The J_{H2-H3} and J_{H3-H4} coupling constants increase monotonically from furan (**298c**) through tellurophene (**90**). The proton–carbon coupling constants J_{C2-H2} and J_{C3-H3} decrease from furan (**298c**) through tellurophene (**90**).

The proton and tellurium coupling constants in tellurophene (**90**)[179,198,199] and tellurophene-2-carboxaldehyde (**119**)[176,199] have been fully analyzed. Values of these coupling constants, including signs, are compiled in Table 27 for tellurophene (**90**) and in Table 28 for tellurophene-2-carboxaldehyde (**119**). The signs of two- and three-bond couplings of tellurium to protons are negative, while one-bond couplings of tellurium to carbon are positive, as determined by selective-population-transfer experiments.[198] A comparison of the data in Tables 27 and 28 shows that spin–spin coupling constants are quite similar in the two molecules, even though a very polar substituent has been added in **119**.

The ^1H and ^{13}C NMR chemical shifts of various 2-substituted tellurophenes have been measured, and illustrative examples are compiled in Table 25.[200] Electron-donating substituents at C2 (Me in **138**, SMe in **144**, CH_2OH in **167**) lead to higher-field chemical shifts for all three protons. Electron-withdrawing substituents (the halogens in **140–141**, formyl in **119**, acetyl in **120**, carboxy groups in **136** and **137**) lead to lower-field shifts for H5. However, carbonyl- and carboxy-containing substituents give lower-field shifts for H3 and H4, while halogen substituents give higher-field shifts for these protons (with the exception of iodine, where δ H5 is shifted to lower field). The ^{13}C NMR chemical shifts are also sensitive to substituents. Electron-donating substituents in this series lead to lower-field shifts for C2 and higher-field shifts for C3—C5. All the electron-withdrawing substituents lead to higher-field shifts for C3—C5, but C2 is subject to both electronic and inductive effects from the substituent (δ 68.9 for an iodine substituent to δ 153.5 for the acetyl substituent).

The various proton–proton and proton–carbon coupling constants for 2-substituted tellurophenes have been measured,[200] and selected data are compiled in Table 26. Not unexpectedly, the proton–proton coupling constants

are quite similar for the parent tellurophene (**90**) and the 2-substituted derivatives. The largest variation is observed in 2-chlorotellurophene (**140**), where the proton–proton couplings are all roughly 0.5 Hz larger than in **90**. The $^1J_{CH}$ coupling constants and the $^2J_{CH}$ coupling constants (data not shown) are virtually identical in the parent (**90**) and 2-substituted tellurophenes.

The ^{125}Te NMR chemical shifts and one- and two-bond tellurium–carbon coupling constants in various 2-substituted tellurophenes have been measured.[199] These data are compiled in Table 29. The values of J_{Te-C3}, J_{Te-C4}, J_{Te-C5}, and J_{Te-C6} (the carbon atom on the substituent bound to the ring) are quite similar in the eight molecules. However, values of J_{Te-C2} are quite sensitive to substituent changes varying from 274 Hz in **120** to 374 Hz in **141**. Although the various tellurium–carbon coupling constants are similar in the eight compounds of Table 29, the ^{125}Te NMR chemical shifts vary by nearly 200 ppm, which illustrates the sensitivity of this nucleus to changes in its environment.

Theoretically determined coupling constants and their signs are in reasonable agreement with the experimental values in both the parent tellurophene (**90**) and various 2-substituted derivatives.[201–203] The IPPP method (inner projections of the polarization propagator) implemented at the RPA level (random-phase approximation), and using an INDO (intermediate neglect of differential overlap) ground-state wavefunction has proved to be the most versatile.[203] This method has proved useful for studying through-space transmissions of spin–spin coupling constants.

9. *Electronic Structures of Tellurophenes and Lighter Chalcogen Analogs: Ionization Potentials and Electron Affinities*

The electronic structures of tellurophene (**90**) and its lighter chalcogen analogs (**298**) have received considerable scrutiny, in part because of the aromatic character of these heterocyclic systems. The ionization potentials of these systems have been measured by both photoelectron spectroscopy[204,205] and by electron-impact spectroscopy (mass spectrometry).[205] Values of the experimental ionization potentials for the entire series as measured by photoelectron spectroscopy are compiled in Table 30.[204] This technique allows the observation of energy levels associated with the occupied molecular orbitals of the heterocyclic systems. The lowest π orbital, π^1, has the most significance for the aromaticity of the chalcogenophene systems but is difficult to assign experimentally. The π^2 and π^3 orbitals are easier to assign. In particular, the energy of the π^3 orbital, which is assigned the $1a_2$ symmetry shown in Figure 10, remains fairly constant across all four systems, varying from 8.87 to 8.92 eV. This assignment allows the trend in the energy of the π^2 orbital, which is assigned the $2b_1$ symmetry in Figure 10, to be observed unambiguously as the ionization potential decreases monotonically as the electronegativity of the heteroatom decreases. From selenophene (**298a**) to tellurophene (**90**), the HOMO (highest occupied molecular orbital) changes from π^3 to π^2 as these energy levels cross

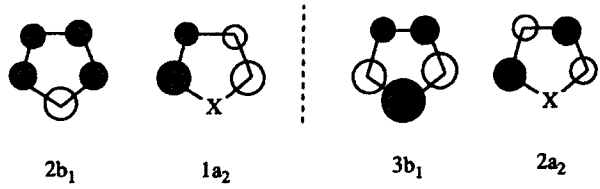

Figure 10. Symmetries of two highest occupied molecular orbitals and two lowest unoccupied molecular orbitals for the chalcogenophenes **90** and **298**.

(Table 30). The symmetry of the HOMO changes as well from the $1a_2$ state for furan (**298a**), thiophene (**298b**), and selenophene (**298c**) to the $2b_1$ state for tellurophene.

Ionization potentials as determined by photoelectron spectroscopy have also been measured for a variety of 2-substituted tellurophenes and their lighter chalcogen analogs.[204] Qualitatively, the trends are the same with a crossing of π^2 and π^3 observed in the tellurophenes relative to the lighter chalcogenophenes. Electron-donating substituents contribute to lower energies for the ionization potential, while electron-withdrawing substituents contribute to higher values for the ionization potential.

The energies of the unoccupied molecular orbitals in these systems are discerned from the experimental electron affinities, which have been measured for the parent chalcogenophenes **90** and **298** and are compiled in Table 30.[206] Both the π^{2*} and π^{3*} orbitals decrease in energy with decreasing heteroatom electronegativity and are assigned the symmetries $2a_2$ and $3b_1$, respectively, in Figure 10. Furthermore, these orbitals do not cross. However, the energy of the lowest σ^* orbital decreases with decreasing electronegativity and is discernible in selenophene (**298a**) at 1.53 eV and in tellurophene (**90**) at 0.23 eV. The consequence of this lowering of the σ^* orbital is that the nature of the LUMO (lowest unoccupied molecular orbital) changes from π^{3*} in furan (**298a**), thiophene (**298b**), and selenophene (**298c**) to a σ^* orbital in tellurophene (**90**).

The experimental values have been correlated quite well with theory in several different sets of calculations.[175,206-208] In one group of calculations,[206,207] SCF (self-consistent field) X_α calculations[209] predict the crossings of both the π^2 and π^3 orbitals in the occupied orbitals[206,207] and the σ^* and π^{3*} orbitals in the unoccupied orbitals[206] as the heteroatom is changed from the lighter chalcogens to tellurium. Values of ionization potentials and electron affinities (utilizing Koopman's theorem) as determined by the SCF X_α calculations in reference 206 are compiled in Table 31. Calculations at the CNDO (complete neglect of differential overlap) level[208] do not correlate as effectively with the experimental results, although the crossing of π^2 and π^3 is predicted. Calculations using *ab initio* methods utilizing the 3-21G (Table 31) and 3-21G* basis sets give ionization potentials that correlate well with experiment,[175] in that the crossing of the energy levels of π^2 and π^3 is predicted with these methods.

10. Electronic Structure of Tellurophene and Lighter Chalcogen Analogs: EPR Studies

The radical cations and radical anions of 2,5-diphenyltellurophene (**122**) and its lighter chalcogen analogues **307** have been generated and their EPR spectra recorded.[210] The heterocycles were oxidized with either sulfuric acid or thallium(III) trifluroacetate and were reduced by the action of alkali metal in dimethoxyethane. Hyperfine coupling constants and g values are listed in Table 32 according to the numbering scheme of Figure 11. The assignments in these systems were based on INDO calculations for the cation radical and anion radical of the furan **307c** and the observed trends in the experimental spectra.

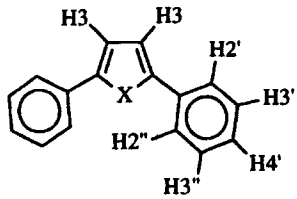

122, X = Te
307a, X = Se
307b, X = S
307c, X = O

Figure 11. Numbering scheme for 2,5-diphenylchalcogenophenes **122** and **307**.

As shown in the data of Table 32, the cation and anion radicals of **122** and **307** are not freely rotating systems on the EPR time scale as observed in the two different sets of *ortho*- and *meta*-proton hyperfine coupling constants. PM3 calculations[211,212] estimate the rotational barriers to be 1.2 kcal mol^{-1} for the ground state of **307c** and 7.2 and 9.6 kcal mol^{-1} for the cation radical and anion radical, respectively.[210]

From furan **307c** to thiophene **307b** to selenophene **307c**, little change in either the hyperfine coupling constants or the overall spectral width (19.0–20.0 G) is observed, although the hyperfine couplings decrease slightly with increasing heteroatom electronegativity. The EPR spectra of the cation radical and anion radical of tellurophene **122** show significant differences from those of their lighter chalcogen analogs. In the anion radical of **122**, the overall spectral width increases to 25.7 G, which indicates a shift of electron density away from the nonobservable positions, and, consistent with this observation, the hyperfine couplings to the H3 protons of the tellurophene ring and the *ortho* and *para* protons of the phenyl substituents increase (Table 32). A tellurium hyperfine coupling of 13.5 G is also observed. Similar trends are observed in the cation radicals of these systems. From furan **307c** to selenophene **307a**, little change is observed in spectral widths and hyperfine coupling constants. In the radical

cation of tellurophene **122**, the hyperfine coupling constants to H3 and protons of the phenyl substitutents increase (Table 32).

These observations have been rationalized in terms of the heteroatom effects on the HOMO and LUMO of the neutral heterocycles, which translates to the SOMO of the cation radicals and anion radicals.[210] In the case of the LUMOs, increasing electronegativity in the heteroatom increases the coefficient of the LUMO—the MO of $3b_1$ symmetry in the parent chalcogenophenes—and diminishes the electron density at other positions. This rationalization is consistent with the experimental results on the anion radicals with a_{H3} increasing with decreasing electronegativity of the heteroatom. In the HOMOs, the heteroatom is at a node in the MO of $1a_2$ symmetry in the parent chalcogenophenes and in the 2,5-diphenyl-substituted derivatives. Consequently, very little change is observed in the proton hyperfine couplings in the cation radicals of the lighter chalcogenophenes **307**. Photoelectron spectroscopy[204,205] and MO calculations on the chalcogenophenes[206-208] suggest a crossing of the π^2 and π^3 orbitals from selenophene (**298a**) to tellurophene (**90**), which would make the HOMO an MO of $2b_1$ symmetry in tellurophenes **90** and **122**. With a large coefficient at the heteroatom and the electropositive character of tellurium, electron density should be pushed toward H3 and the substituent protons as is observed in the increased proton hyperfine couplings of the radical cation of **122** relative to the radical cations of the lighter chalcogenophenes **307**.

F. Benzotellurophenes and Related Chalcogen Analogs

1. Properties and Reactivity

In many respects, the benzochalcogenophenes follow the same trends as the monocyclic chalcogenophenes. One such similarity is the ability of the chalcogen atom to affect the pK_a of benzochalcogeneophene-2-carboxylic acids.[163] In 50% aqueous ethanol at 25°C for the series of carboxylic acids **191**/**308**, the pK_a decreases with increasing electronegativity from 5.13 for **191** to 4.79 for **308a** to 4.67 for **308b** to 4.20 for **308c**. These molecules were too insoluble for pK_a measurements in water. The benzo derivatives are slightly stronger acids than their monocyclic counterparts, but the heteroatom effects on pK_a values in the two series of compounds are nearly identical.

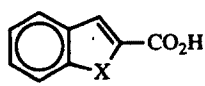

191, X = Te
308a, X = Se
308b, X = S
308c, X = O

2. *Ionization Potentials of Benzotellurophene and Related Chalcogen Analogs*

The ionization potentials of benzotellurophene (**177**) and the benzochalcogenophenes **309** have been measured by photoelectron spectroscopy, and values for the first ionization are compiled in Table 33.[213] The ionization potentials follow the electronegativity of the heteroatoms with ionization occurring at higher energy as the electronegativity increases. There is no observed crossing of π orbitals with benzotellurophene (**177**) as was observed in the photoelectron spectrum of tellurophene (**90**).

3. *Spectral Properties of Benzotellurophenes and Related Chalcogen Analogs*

Representative spectral data for benzotellurophene (**177**) and its lighter chalcogen analogs **309** are compiled in Table 33 utilizing the numbering scheme of Figure 12. The ^{125}Te NMR chemical shift of benzotellurophene has been measured at δ 727,[214] which is similar to the chemical shifts observed for other organotellurium compounds with tellurium bonded to an aromatic group ($Ph_2{}^{125}Te$, δ 688). The ^{1}H NMR spectra of benzotellurophene (**177**) and its lighter chalcogen analogs have been assigned completely.[215–218] Chemical-shift values are compiled in Table 33, and proton–proton coupling constants are compiled in Table 34. The electronic spectra of this series of molecules have only been evaluated in a qualitative way. From values of λ_{max} compiled in Table 33, the wavelength of absorption becomes shorter as the electronegativity of the heteroatom increases.

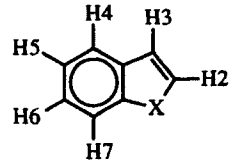

177, X = Te
309a, X = Se
309b, X = S
309c, X = O

Figure 12. Numbering scheme for benzochalcogenophenes **117** and **309**.

The heteroatom effects on the ^{1}H NMR spectra of the chalcogenophene ring of benzotellurophene (**177**) and its lighter chalcogen analogs **309** are comparable to those observed in the chalcogenophene **90**/**298** series. The chemical shifts of the benzo protons H4, H5, and H6 are little affected by changes in the heteroatom. The chemical shift of the *peri* proton H7, however, is sensitive

to the electronegativity of the heteroatom, shifting monotonically 0.4 ppm to higher field as the heteroatom increases in electronegativity from tellurium to oxygen. In the tellurophene ring, the same trend is observed for H3, which is also three bonds removed from the heteroatom, but the shift is nearly 1.2 ppm. The chemical shift of H2 experiences opposing influences from the heteroatoms with no apparent trend. The chemical shift of H2 in benzotellurophene (**177**) is roughly 1 ppm to lower field of the other benzochalcogenphenes **309**. The geometry of the five-membered ring changes significantly as the heteroatom becomes larger. These changes in geometry result in systematic changes in some of the observed proton–proton coupling constants (Table 34). The H2–H3 coupling is most sensitive to the identity of the heteroatom, increasing from 2.19 Hz in benzofuran (**309c**) to 6.95 Hz in benzotellurophene (**177**). The long-range coupling between H3 and H7 also appears to be sensitive to geometry, decreasing monotonically from 0.87 Hz for benzofuran (**309c**) to 0.43 Hz for benzotellurophene (**177**).

The ^{1}H NMR chemical shifts of 2- and 3-substituted benzotellurophenes have been reported.[52,92] Chemical shifts for the protons of the substituents and the five-membered ring are compiled in Table 35. Substitutents at the 2-position move the chemical shift of H3 to higher field if they are electron-donating and to lower field if they are electron-withdrawing. Halogen substitutents at the 3-position shield H2 by 0.6 ppm as the electronegativity of the halogen increases from iodine to bromine to chlorine.

As substituents, the benzochalcogenophenes **17** and **309** affect carbonyl stretching frequencies similarly to their monocyclic analogues.[92,163] In the carboxylic acid series **191/308**, the carbonyl stretching frequency decreases monotonically from 1758 cm^{-1} for benzofuran derivative **308c** to 1733 cm^{-1} for benzothiophene derivative **308b** to 1731 cm^{-1} for benzoselenophene derivative **308a** to 1716 cm^{-1} for benzotellurophene derivative **191**.[163] The benzotellurophene nucleus shifts carbonyl stretching frequencies to lower values than the lighter chalcogen analogs in other 2-substituted benzotellurophenes as shown in Table 35.[92]

Benzotellurophene (**177**) and 2- and 3-substituted derivatives show strong parent ions by electron-impact mass spectroscopy. This tendency is observed in the monocyclic tellurophene derivatives as well.

G. Dibenzotellurophenes and Lighter Chalcogen Analogs

The structures of dibenzotellurophene (**239**) and its lighter chalcogen analogs **310** have been determined unambiguously by X-ray crystallography.[219–222] The X-ray structure of 1,1-diiodobenzotellurophene (**240c**) has also been reported.[223] Selected bond lengths and angles for these compounds are compiled in Table 36. The numbering scheme shown in Figure 13 is used in the table to facilitate comparison with the structures of monocyclic chalcogenophenes and bicyclic benzochalcogenophenes.

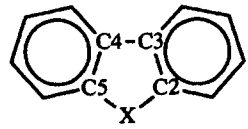

239, X = Te
240c, X = TeI_2
310a, X = Se
310b, X = S
310c, X = O

Figure 13. Numbering scheme for dibenzochalcogenophenes **239**, **240c**, and **310**.

As the heteroatom increases in size, the C2—X—C5 angles decrease and the C2—C3—C4 and C3—C4—C5 angles expand to accommodate the longer C—X bonds. The C3—C2—X and C4—C5—X angles are not affected by the change in heteroatom. In a comparison of the C—C bond lengths of **239** and **240c**, removing the tellurium *p* orbital from conjugation with the π framework via oxidative addition of iodine, gives more double-bond character to the C2—C3 and C3—C4 bond lengths and more single-bond character to the C3—C4 bond length. The tellurium lone pair of electrons distorts the I—Te—I angle only slightly from 180° (178.47°).

TABLES

TABLE 1. BOND LENGTHS (Å) AND ANGLES (°) AS DETERMINED BY SINGLE-CRYSTAL X-RAY CRYSTALLOGRAPHIC ANALYSIS OF **290**[a]

Bond (Å)		Angle (°)	
Te—C2	2.172	Te—C2—C3	105.7
Te—C5	2.113	C2—C3—C4	109.6
Te—C6	2.109	C3—C4—C5	111.2
C2—C3	1.517	C4—C5—Te	105.7
C3—C4	1.521	C5—Te—C2	84.9
C4—C5	1.514	C5—Te—C6	99.5
		C2—Te—C6	95.7

[a] Reference 139.

TABLE 2. VIBRATIONAL SPECTRA FOR TETRAHYDROTELLUROPHENE (3), TETRAHYDROSELENOPHENE (291a), AND TETRAHYDROTHIOPHENE (291b)[a]

ν_i	Description	3	291a	291b
ν_1	Ring def. (deformation)	310	363	471
ν_2	C—M—C stretch	561	616	684
ν_3	C—C stretch	761	800	819
ν_4	C—C stretch	942	985	1020
ν_5	CH_2 wag	1233	1254	1275
ν_6	CH_2 wag	1324	1326	1323
ν_7	CH_2 scissor	1412	1424	1433
ν_8	CH_2 scissor	1449	1457	1461
ν_9	C—H stretch	2903	2900	2910
ν_{10}	C—H stretch	2930	2944	2948
ν_{11}	Ring def.	297		
ν_{12}	CH_2 rock	756	757	790
ν_{13}	CH_2 rock	850	831	888
ν_{14}	CH_2 twist	1189	1204	1215
ν_{15}	CH_2 twist	1079	1014	1033
ν_{16}	C—H stretch	2836	2847	2858
ν_{17}	C—H stretch	2880	2866	
ν_{18}	Ring def.	442	481	515
ν_{19}	C—M—C stretch	543	588	675
ν_{20}	C—C stretch	1131	1168	1197
ν_{21}	CH_2 wag	1241	1247	1258
ν_{22}	CH_2 wag	1309	1308	1308
ν_{23}	CH_2 scissor	1422	1433	1441
ν_{24}	CH_2 scissor	1436	1439	1448
ν_{25}	C—H stretch	2913	2927	2932
ν_{26}	C—H stretch	2975	2976	2964
ν_{27}	Ring def.	160	260	294
ν_{28}	CH_2 rock	799	849	883
ν_{29}	CH_2 rock	948	957	958
ν_{30}	CH_2 twist	1042	1040	1059
ν_{31}	CH_2 twist	1105	1117	1134
ν_{32}	C—H stretch		2963	2848
ν_{33}	C—H stretch			

[a] Reference 142.

TABLE 3. DIPOLE MOMENTS (μ) IN BENZENE AT 25°C AND IONIZATION POTENTIALS (IP) BY PHOTOELECTRON SPECTROSCOPY FOR TETRAHYDROTELLUROPHENE (3), TETRAHYDROSELENOPHENE (**291a**), TETRAHYDROTHIOPHENE (**291b**), AND TETRAHYDROFURAN (**291c**)

Compound	X	μ (D)[a]	$n\pi$ (b_1)	IP (eV)[b] C_2X (a_1)	C_2X (b_2)	Pauling Electronegativity
3	Te	1.63	7.73	10.0	10.7	2.1
291a	Se	1.81	8.14	10.5	$\geq$ 11.4	2.4
291b	S	1.89	8.42	10.9	$\geq$ 11.9	2.5
291c	O	1.75	9.53, 9.65	11.4	13.0	3.5

[a] Reference 143.
[b] Reference 144.

TABLE 4. ^{1}H NMR SPECTRA OF TETRAHYDROTELLUROPHENE (3), TETRAHYDROSELENOPHENE (**291a**), TETRAHYDROTHIOPHENE (**291b**), AND TETRAHYDROFURAN (**291c**)

Compd.	X	H2 (δ ppm)	H3 (δ ppm)	Ref.
3	Te	3.10	2.03	146
291a	Se	2.79	1.96	146
291b	S	2.75	1.91	147
291c	O	3.61	1.79	147

TABLE 5. ^{1}H, ^{13}C, AND ^{125}Te NMR SPECTRA FOR TETRAHYDROTELLUROPHENE (**3**), 1,1-DIIODOTETRAHYDROTELLUROPHENE (**2**), 1-(*p*-ETHOXYPHENYL)TETRAHYDROTELLUROPHENIUM CHLORIDE (**18**), 1-METHYLTETRAHYDROTELLUROPHENIUM IODIDE (**41e**), 1-ALLYL-TETRAHYDROTELLUROPHENIUM IODIDE (**41f**), 1,1,1,1-TETRAIODOTETRAHYDROTELLUROPHENE (**35c**), TETRAHYDROTELLUROPHENE DMSO–PERCHLORATE COMPLEX (**27**), AND TETRAHYDROTELLUROPHENE PYRIDINE–PERCHLORATE COMPLEX (**28**)

			H2	H3	H_{Me}	C2	C3	C_{Me}	
Compd.	^{125}Te, δ ($Me_2Te = O$)	J_{Te-H2} (Hz)	(δ, $Me_4Si = O$)						J_{Te-C2} (Hz)
3[a]	234	25.5	3.02	2.05	—	5.8	35.8	—	126 (28)
2[b]	929	—	3.20	2.23	—	42.9	32.8	—	138
18[c]	761	—	—	—	—	35.7	31.4	—	—
41e[b]	634	25.2	3.25	2.7	2.51	31.2	31.2	5.1	136.5
41f[b]	661	—	—	—	—	32.0	33.0	—	—
35c[d]	—	—	3.68	2.88	—	—	—	—	—
27[e]	—	—	3.28	2.50	—	—	—	—	—
28[e]	—	—	3.30	2.40	—	—	—	—	—

[a] Reference 11.
[b] Reference 25.
[c] Reference 13.
[d] Reference 14.
[e] Reference 17.

TABLE 6. ^{1}H NMR SPECTRA OF 1,1-DIIODO-2-METHYLTETRAHYDROTELLUROPHENE (**6**), 1,1-DICHLORO-2-METHYLTETRAHYDROTELLUROPHENE (**6b**), 1,2-DIMETHYLTETRAHYDROTELLUROPHENIUM IODIDE (**7a**), AND 1,2-DIMETHYLTETRAHYDROTELLUROPHENIUM TETRAPHENYLBORATE (**42a**)

	H_{Me}	H2	H3	H4	H5	
Compd.	(δ ppm, DMSO-d_6)					Ref.
6	1.90	4.12	2.38	3.03	4.12	4
6b	1.75	3.94	2.12	2.80	3.81	4
7a (*cis*)	1.45, 2.10	3.75	2.28	2.28	3.05	26
7a (*trans*)	1.60, 2.20	3.75	2.28	2.28	3.05	26
42a (*cis*)	1.33, 1.90	3.49	2.28	2.28	2.88	26
42a (*trans*)	1.47, 2.20	3.49	2.28	2.28	2.88	26

TABLE 7. ^{125}Te AND ^{13}C NMR SPECTRA OF 1-ALLYL-TETRAHYDROTELLUROPHENIUM HALIDES (41) TO ILLUSTRATE COUNTERION EFFECT ON CHEMICAL SHIFT[a]

Compd.	X	^{125}Te	C1	C2	C3	C4	C5
		(δ ppm, DMSO-d_6)					
41f	I	662	33.0	32.0	130.3	121.3	121.3
41g	Br	663	32.0	32.9	31.2	130.4	121.1
41h	Cl	663	33.0	32.0	30.2	130.4	120.8

[a] Reference 11.

TABLE 8. ^{1}H AND ^{13}C NMR SPECTRA FOR 2,5-DIHYDROTELLUROPHENE (**44a**), 2,5-DIHYDROSELENOPHENE (**292a**), 2,5-DIHYDROTHIOPHENE (**292b**), AND 2,5-DIHYDROFURAN (**292c**)

Compd.	X	CH_2	CH	C2	C3	Ref.
				(δ $CDCl_3$)		
44a	Te	4.02	5.70	10.59	133.14	29
292a	Se	3.76	5.82	30.7	130.2	149
292b	S	3.66	5.79	—	—	150
292c	O	4.51	5.85	—	—	150
45c	TeF_2	3.93	6.49	53.98	129.29	29
43a	$TeCl_2$	4.53	6.41	58.33	129.41	29
45b	$TeBr_2$	4.73	6.30	56.88	129.77	29
45a	TeI_2	4.83	6.12	—	—	29

TABLE 9. ^{1}H NMR SPECTRA OF 3-METHYL- AND 3,4-DIMETHYL-2,5-DIHYDROTELLUROPHENES (**44b** AND **44c**) AND THEIR 1,1-DICHLORO ANALOGS (**43b** AND **43c**)[a]

Compd.	CH_2	CH_2	CH	Me
44b[b]	3.91	3.91	5.55	1.82
44c	4.00	—	—	1.60
43b	4.40	4.40	6.20	2.00
43c	4.30	—	—	1.90

[a] Reference 29.
[b] C NMR δ 8.57 (CH_2), 13.16 (CH_2), 18.45 (Me), 127.51, 142.39

TABLE 10. X-RAY CRYSTALLOGRAPHIC DATA FOR 3,4-QUINOXALINE DERIVATIVES **63a** AND **64a** AND 1-METHYL-2,5-DIHYDROBENZOTELLUROPHENIUM TETRAPHENYLBORATE (**293**)

	Bond lengths (Å) and Angles (°)		
Compd.	**64a**[a]	**63a**[b]	**293**[c]
Te—C2	2.145	2.136	2.136
Te—C5	2.123	2.140	2.088
C2—C3	1.469	1.51	1.51
C3—C4	1.405	1.42	1.38
C4—C5	1.473	1.51	1.57
Te—I1		2.886	
Te—I2		2.911	
Te—Me			2.074
C2—Te—C5	80.7	86.4	86.6
C3—C2—Te	103.9	107	107
C2—C3—C4	118.8	119	120
C4—C3—N1(C6)	120.9	123	119
C4—C5—Te	105.5	106	107
C3—C4—N2(C9)	123.9	122	119
I1—Te—I2		176.5	
C2—Te—I1(Me)		90.3	95.7
C5—Te—I1(Me)		89.3	94.0
C2—Te—I2		87.9	
C5—Te—I2		87.6	

[a] Reference 151.
[b] Reference 152.
[c] Reference 139.

TABLE 11. X-RAY CRYSTALLOGRAPHIC DATA FOR 2,5-DIHYDROBENZOTELLUROPHENE DERIVATIVES **59–61**[a]

	Bond Lengths (Å) and Angles (°)		
Compd.	**59**	**60**	**61**
Te—C2	2.150	2.133	2.125
Te—C5	2.143	2.109	2.143
C2—Te—C5	84.9	85.6	85.6
C3—C2—Te	107.2	107.7	106.6
C2—C3—C4		119.6	
C4—C5—Te	107.3	106.8	107.1
C3—C4—C7		120.0	
S1—Te—S2	60.89	64.35	59.08
S3—Te—S4	59.74	64.13	59.80
S1—Te—S3	168.55	163.6	164.63

[a] Reference 39.

TABLE 12. ^{125}Te NMR CHEMICAL SHIFTS FOR 2,5-DIHYDROBENZOTELLUROPHENE] (**48**), 1-ALKYL-2,5-DIHYDROTELLUROPHENIUM HALIDES (**294**)], 1,1-DIHALO-2,5-DIHYDROTELLUROPHENES (**50**, **53**, AND **54**), AND 1,1-DITHIOLATO-2,5-DIHYDROTELLUROPHENES **59–61**

Compd.	R	X	^{125}Te $\delta(Me_2Te = O)$	J_{Te-CH}	Ref.
48	—	—	269	23	36
50	—	I	830.5	34	36
53	—	Br	940	40	36
54	—	Cl	994	40	36
59	—	S_2CNEt_2	605	—	39
60	—	$S_2P(OEt)_2$	727	—	39
61	—	S_2COEt	660	—	39
294a	Me	I	651	—	13
294b	$CH_2CH{=}CH_2$	Br	688	—	13
294c	CH_2Ph	Br	722	—	13

TABLE 13. ^{13}C NMR CHEMICAL SHIFTS FOR 1-ALKYL-2,5-DIHYDROTELLUROPHENIUM HALIDES (**294**) AND 1,1-DITHIOLATO-2,5-DIHYDROTELLUROPHENES **59–61**

Compd.	C2,C5	C3,C4	C6,C7	C8,C9	Ref.
	$\delta(Me_4Si = O)$				
294a	34.4	—	—	—	13
294b	34.3	—	—	—	13
59	44.6	140.7	127.6	130.6	39
60	44.7	139.0	127.9	130.0	39
61	44.7	140.2	128.3	130.7	39

TABLE 14. SELECTED SPECTRAL PROPERTIES FOR TELLUROAURONE **78a** AND ITS LIGHTER CHALCOGEN ANALOGS **296**

Compd.	X	$=CHPh^a$ δ	ν_{CO} (cm^{-1})	λ_{max} (ε)	Ref.
78a	Te	8.56	1645	472 (4470)	48
296a	Se	8.21	1660	438 (6920)	48
296b	S	7.98	1675	422 (5500)	154
296c	O	6.95	1685	—	154

[a] ^{1}H NMR data from reference 48.

TABLE 15. RATE CONSTANTS AND EYRING ACTIVATION PARAMETERS FOR ELECTROPHILIC FORMYLATION AND RELATIVE RATE CONSTANTS FOR ELECTROPHILIC FORMYLATION, ACYLATION, AND TRIFLUORACYLATION OF TELLUROPHENE (**90**), SELENOPHENE (**298a**), THIOPHENE (**298b**), AND FURAN (**298c**)

Compd.	X	k (30°C) (s^{-1}) (—CHO)[a]	k_{rel} (30°C) (—CHO)[a]	k_{rel} (25°C) [—C(=O)CH_3][b]	k_{rel} (75°C) [—C(=O)CF_3][c]	$\Delta H^{\ddagger}$[d] (—CHO)[a]	$\Delta S^{\ddagger}$[e] (—CHO)[a,f]
90	Te	4.08×10^{-5}	36.8	7.55	46.4	15.5	−27.5
298a	Se	4.04×10^{-6}	3.64	2.28	7.33	16.5	−28.8
298b	S	1.11×10^{-6}	1	1	1	17.1	−29.5
298c	O	1.19×10^{-4}	107	11.9	140	14.7	−27.7

[a] $COCl_2$—$HCONMe_2$.
[b] Ac_2O—$SnCl_4$.
[c] $(CF_3CO)_2O$.
[d] kcal mol^{-1}.
[e] cal mol^{-1} k^{-1}.
[f] Reference 81.

TABLE 16. HAMMETT σ_p, σ_m, σ_p^-, AND σ_m^- SUBSTITUENT CONSTANTS FOR 2-TELLURIENYL, 2-SELENIENYL, 2-THIENYL, AND 2-FURYL SUBSTITUENTS

Substituent	X	σ_p	σ_m	σ_p^-	σ_m^-	Ref.
2-Tellurienyl	Te	0.03	0.06	0.25	0.10	77
2-Selenienyl	Se	0.04	0.06	0.22	0.16	77
2-Thienyl	S	0.05	0.09	0.19	0.11	161
2-Furyl	O	0.02	0.06	0.21	0.11	162

TABLE 17. X-RAY CRYSTALLOGRAPHIC DATA FOR 2-TELLUROPHENE CARBOXYLIC ACID (**136**) AND 3-IODO-2,5-DIPHENYLTELLUROPHENE (**302**)

	Bond Lengths (Å) and Angles (°)		
Compd.	**136a**[a]	**136b**[a]	**302**[b]
Te—C2	2.056	2.058	2.077
Te—C5	2.069	2.025	2.070
C2—C3	1.394	1.375	1.34
C3—C4	1.380	1.445	1.45
C4—C5	1.339	1.375	1.35
C2—C6	1.415	1.431	1.47
C5—C7			1.49
C3—I			2.108
C2—Te—C5	81.1	81.9	82.7
C3—C2—Te	110.6	112.8	108.9
C2—C3—C4	117.6	114.9	120.7
C3—C4—C5	119.3	118.3	116.7
C4—C5—Te	111.4	112.0	110.9
C3—C2—C6	125.2	124.5	131.0
C4—C5—C7			126.1
C2—C3—I			123.3
C4—C3—I			115.8

[a] Reference 168.
[b] Reference 169.

TABLE 18. MOLECULAR GEOMETRIES OF THE CHALCOGENOPHENES **90** AND **298** AS DETERMINED BY MICROWAVE SPECTROSCOPY

	Bond Lengths (Å) and Angles (°)			
Compd.	**298c**[a] (X = O)	**298b**[b] (X = S)	**298a**[c] (X = Se)	**90**[d] (X = Te)
X—C2	1.362	1.714	1.855	2.055
X—C5	1.362	1.714	1.855	2.055
C2—C3	1.361	1.370	1.369	1.375
C3—C4	1.431	1.423	1.433	—
C4—C5	1.361	1.370	1.369	1.375
C2—X—C5	106.55	92.17	87.76	82.53
C3—C2—Te	110.68	111.47	111.56	110.81
C2—C3—C4	106.06	112.45	114.55	117.93
C3—C4—C5	106.06	112.45	114.55	117.93
C4—C5—Te	110.68	111.47	111.56	110.81

[a] Reference 173.
[b] Reference 172.
[c] Reference 171.
[d] Reference 170.

TABLE 19. MOLECULAR GEOMETRIES OF TELLUROPHENE (90) DERIVED FROM AB INITIO CALCULATIONS USING SPLIT-VALENCE 3-21G AND SCF/3-21G*

	Bond Lengths (Å) and Angles (°)		
Compd.	3-21G[a]	3-21G*[a]	3-21G*[b]
Te—C2	2.106	2.100	2.101
Te—C5	2.106	2.100	2.101
C2—C3	1.335	1.339	1.339
C3—C4	1.456	1.453	1.454
C4—C5	1.335	1.339	1.339
C2—H2		1.069	1.069
C3—H3		1.073	1.073
C2—Te—C5	80.3	80.7	80.7
C3—C2—Te	111.8	111.4	111.4
C2—C3—C4	118.1	118.2	118.8
C3—C4—C5	118.1	118.2	118.8
C4—C5—Te	111.8	111.4	111.4
C2—C3—H3	121.8	121.8	119.5
C3—C2—H2	124.7	125.1	125.2

[a] Reference 175.
[b] Reference 174.

TABLE 20. GEOMETRIES OF 2-TELLUROPHENE CARBOXALDEHYDE (**119**) AND TELLUROPHENE (**90**) AS DETERMINED BY NMR IN AN ORIENTED PHASE

	Bond Lengths (Å) and Angles (°)		
Compd.	**119**[a,c]	**119**[a,d]	**90**[b]
Te—C2	2.198	2.108	2.073
Te—C5	2.062	2.091	2.073
C2—C3	1.391	1.365	1.356
C3—C4	1.450[e]	1.450[e]	1.429
C4—C5	1.383	1.363	1.356
C2—C6(H2)	—	1.49	1.060
C3—H3	1.093	1.083	1.067
C4—H4	1.077	1.081	1.067
C5—H5	1.081	1.080	1.060
C2—Te—C5	77.3	79.9	80.3
C3—C2—Te	113.0	112.3	112.3
C2—C3—C4	115.3	117.7	117.5
C3—C4—C5	115.8	116.7	117.5
C4—C5—Te	117.9	112.3	112.3
C2—C3—H3	121.5	121.4	120.8
C3—C2—H2	—	—	120.8
C5—C4—H4	121.8	122.1	120.8
C4—C5—H5	116.7	120.2	120.8

[a] Reference 176.
[b] Reference 179.
[c] Data fitting with only dipolar couplings from the ring considered.
[d] Data fitting with all dipolar couplings fitted simultaneously.
[e] Fixed distance.

TABLE 21. VIBRATIONAL SPECTRA FOR TELLUROPHENE (90), SELENOPHENE (298a), THIOPHENE (298b), AND FURAN (298c)

ν_n	Description	C_{2v}	3[a]	291a[b]	291b[c]	291c[d]
ν_1	C—H stretch	A_1	3084	3110	3110	3159
ν_2	C—H stretch		3045	3063	3086	3128
ν_5	Ring stretch		1432	1419	1408	1483
ν_4	Ring stretch		1316	1341	1360	1380
ν_6	C—H def. in plane		1079	1080	1081	1140
ν_7	C—H def. in plane		984	1010	1033	1061
ν_3	Ring stretch (sym. CXC)		687	758	833	986
ν_8	Ring def. in plane		380	456	606	873
ν_9	C—H def. out of plane	A_2	912	905	900	863
ν_{10}	C—H def. out of plane		690	685	686	728
ν_{11}	Ring def. out of plane		507	541	565	613
ν_{12}	C—H stretch	B_1	3084	3100	3110	3148
ν_{13}	C—H stretch		3030	3054	3073	3120
ν_{14}	Ring stretch		1516	1515	1506	1556
ν_{15}	C—H def. in plane		1246	1243	1250	1270
ν_{16}	C—H def. in plane		1079	1080	1081	1171
ν_{17}	Ring stretch (asym. CXC)		797	820	871	1040
ν_{18}	Ring def. in plane		552	623	750	873
ν_{20}	C—H def. out of plane	B_2	884	870	864	839
ν_{19}	C—H def. out of plane		674	700	712	745
ν_{21}	Ring def. out of plane		354	394	453	601

[a] Reference 180.
[b] Reference 181.
[c] Reference 182.
[d] Reference 183.

TABLE 22. EFFECT OF HETEROATOM CHANGES ON CARBONYL STRETCHING FREQUENCIES IN CHALCOGENOPHENE-2-CARBOXYLIC ACIDS (136/301) AND BIS-2-CHALCOGENOPHENEYLKETONES (148/304)

Compd.[a]	X	ν_{CO_2}	Compd.[b]	X	ν_{CO}
136	Te	1721	**148**	Te	1600
301a	Se	1728	**304a**	Se	1600
301b	S	1734	**304b**	S	1615
301c	O	1755	**304c**	O	1632

[a] Reference 163.
[b] Reference 88.

TABLE 23. DIPOLE MOMENTS (μ, D) AS MEASURED FOR THE PARENT CHALCOGENOPHENES (R = H) AND FOR 2-SUBSTITUTED DERIVATIVES[a]

R (X)	μ (D)					
	H	Br	Me	SMe	CHO	Ac
Te	0.46	1.44	0.64	1.30	3.18	2.97
Se	0.52	1.37	0.56	1.37	3.25	3.18
S	0.54	1.35	0.67	1.47	3.48	3.37
O	0.72	1.46	0.72	1.60	3.54	3.23

[a] Reference 189.

TABLE 24. MASS SPECTRAL FRAGMENTATION PATTERNS FOR CHALCOGENOPHENES **90** AND **298** EXPRESSED IN PERCENT OF TOTAL IONIZATION

Fragment	**298c**[a] (X = O)	**298b**[a] (X = S)	**298a**[b] (X = Se)	**90**[b] (X = Te)
M^+	26.8	30.4	44.8	44.4
M—CHX (*m/e* 39)	43.2	8.3	3.3	0.4
M—39	6.8	17.5	5.2	1.1
M—C_2H_2	3.0	19.7	16.6	4.1
M—HX (*m/e* 51)		1.1	5.7	6.6
X^+			4.8	21.6
M—X (*m/e* 52)			0.8	3.8

[a] References 191 and 192.
[b] Reference 190.

TABLE 25. ^1H AND ^{13}C NMR CHEMICAL SHIFTS FOR THE CHALCOGENOPHENES **90** AND **298** IN ACETONE-d_6[a]

Compd.	X, R	δ (acetone-d_6)						
		H2,H5	H3	H4	C2	C3	C4	C5
90	Te	8.97	7.79	7.79	127.3	138.0	138.0	127.3
298a	Se	8.10	7.33	7.33	131.0	128.8	131.0	131.0
298b	S	7.40	7.10	7.10	125.6	127.3	127.3	125.6
298c	O	7.46	6.36	6.36	143.6	110.4	110.4	143.6
119	Te, CHO	9.56	8.62	8.05	151.5	148.1	139.4	138.7
120	Te, COMe	9.41	8.44	8.00	153.5	143.4	139.8	137.8
136	Te, CO_2H	9.40	8.53	7.93	137.6	144.7	138.6	138.1
137	Te, CO_2Me	9.38	8.49	7.92	139.0	144.5	138.6	137.4
138	Te, Me	8.64	7.23	7.47	144.6	137.5	136.8	124.9
140	Te, Cl	8.75	7.33	7.34	136.4	139.1	136.0	128.7
141	Te, Br	8.91	7.72	7.41	110.0	142.6	137.4	131.5
142	Te, I	9.13	8.11	7.32	68.9	149.2	139.4	135.0
144	Te, SMe	8.81	7.42	7.55	142.1	136.3	137.8	125.6
167	Te, CH_2OH	8.77	7.41	7.72	155.3	132.2	137.4	124.9

[a] See reference 196 for unsubstituted derivatives and reference 200 for 2-substituted tellurophenes.

TABLE 26. COUPLING CONSTANTS (IN Hz) IN THE CHALCOGENOPHENES **90** AND **298** AND 2-SUBSTITUTED TELLUROPHENES[a]

Compd.	X, R	J_{H2-H3}, J_{H4-H5}	J_{H2-H4}, J_{H3-H5}	J_{H2-H5}	J_{H3-H4}	J_{C2-H2}	J_{C3-H3}	J_{C4-H4}	J_{C5-H5}
90	Te	6.58	1.12	1.82	3.76	183	159	159	183
298a	Se	5.40	1.46	2.34	3.74	189	166	166	189
298b	S	4.90	1.04	2.84	3.50	185	168	168	185
298c	O	1.75	0.85	1.40	3.30	201	175	175	201
119	Te, CHO	6.77	1.32	—	4.10	—	161	163	184
120	Te, COMe	6.78	1.16	—	4.22	—	161	163	182
136	Te, CO_2H	6.76	1.34	—	4.20	—	159	161	183
137	Te, CO_2Me	6.79	1.33	—	4.11	—	164	163	184
138	Te, Me	7.14	1.27	—	3.90	—	—	—	—
140	Te, Cl	7.33	1.47	—	4.26	—	165	164	185
141	Te, Br	7.28	1.49	—	4.27	—	166	164	187
142	Te, I	7.10	1.54	—	4.06	—	—	—	—
144	Te, SMe	6.93	1.28	—	4.03	—	161	161	185

[a] See reference 196 for unsubstituted derivatives and reference 200 for 2-substituted tellurophenes.

TABLE 27. EXPERIMENTAL INDIRECT COUPLING CONSTANTS OF TELLUROPHENE (90)

Coupling[a]	Hz	Coupling[a]	Hz
$^1J_{H2-C2}$	183.84	$^1J_{Te-C2}$[b]	302.4
$^2J_{H2-C3}$	3.09	$^2J_{Te-H2}$	− 100
$^3J_{H2-C4}$	11.68	$^2J_{Te-C3}$[b]	5.6
$^3J_{H2-H3}$	6.62	$^3J_{Te-H3}$	− 20.05
$^3J_{H2-C5}$	2.14		
$^4J_{H2-H4}$	1.14		
$^4J_{H2-H5}$	1.85		
$^1J_{H3-C3}$	161.13		
$^2J_{H3-C2}$	4.85		
$^3J_{H3-H4}$	3.84		
$^3J_{H3-C4}$	6.09		
$^3J_{H3-C5}$	10.50		

[a] Reference 179.
[b] Reference 199.

TABLE 28. EXPERIMENTAL INDIRECT COUPLING CONSTANTS FOR TELLUROPHENE-2-CARBOXALDEHYDE (119)

Coupling[a]	Hz	Coupling[a]	Hz
$^1J_{H5-C5}$	183.7	$^1J_{Te-C2}$[b]	290.2
$^2J_{H5-C4}$	2.9	$^1J_{Te-C5}$[b]	321.6
$^3J_{H5-C3}$	11.0	$^2J_{Te-C3}$[b]	− 3.5
$^3J_{H5-H4}$	6.6	$^2J_{Te-C4}$[b]	− 15.1
$^3J_{H5-C2}$	2.1	$^2J_{Te-C6}$[b]	− 34.0
$^4J_{H5-H3}$	1.2	$^2J_{Te-H5}$	− 93.8
$^5J_{H5-H6}$	1.2	$^3J_{Te-H4}$	− 9.2
		$^3J_{Te-H3}$	− 13.1
$^1J_{H4-C4}$	164.4	$^3J_{Te-H6}$	− 10.5
$^2J_{H4-C3}$	5.8		
$^3J_{H4-H3}$	4.2		
$^2J_{H4-C5}$	4.5		
$^3J_{H4-C2}$	10.50		
$^1J_{H3-C3}$	161.7		
$^2J_{H3-C2}$	4.9		
$^2J_{H3-C4}$	4.1		
$^3J_{H3-C5}$	11.1		
$^3J_{H3-C6}$	5.3		
$^4J_{H3-H6}$	− 0.1		

[a] Reference 176.
[b] Reference 199.

TABLE 29. ^{125}Te NMR CHEMICAL SHIFTS (δ) AND $^{1}J_{Te-C}$ and $^{2}J_{Te-C}$ COUPLING CONSTANTS (Hz) FOR VARIOUS 2-SUBSTITUTED TELLUROPHENES[a]

Compd.	R	^{125}Te	J_{Te-C2}	J_{Te-C3}	J_{Te-C4}	J_{Te-C5}	J_{Te-C6}
90	H	793	302.4	5.6	5.6	302.4	—
119	CHO	804	290.2	− 3.5	15.1	321.6	− 34.0
120	$COCH_3$	825	274.3	− 5.4	14.0	317.7	− 33.1
136	CO_2H	861	297.6	− 5.4	13.9	317.6	− 39.0
137	CO_2Me	862	299.6	− 5.3	13.5	317.8	− 36.7
141	Br	960	373.8	± 4.7	7.0	310.5	—
144	SMe	886	335.4	| < 3|	6.7	304.5	—
167	CH_2OH	775	289.2	| < 3|	7.0	297.5	− 31.7

[a] Reference 199.

TABLE 30. EXPERIMENTAL IONIZATION POTENTIALS (IP) FOR SELECTED OCCUPIED MOLECULAR ORBITALS AND ELECTRON AFFINITIES (EA) FOR SELECTED UNOCCUPIED MOLECULAR ORBITALS IN GROUND STATE OF CHALCOGENOPHENES **90** AND **298**

	IP or EA (eV)			
MO	**298c**[a] (X = O)	**298b**[a] (X = S)	**298a**[b] (X = Se)	**90**[b] (X = Te)
$2a_2\ \pi_2^*$	3.15	2.63	2.72	2.62
$3b_1\ \pi_3^*$	1.76	1.15	0.90	0.55
σ^*	—	—	1.53	0.23
$1a_2\ \pi^3$	8.89	8.87	8.92	8.88
$2b_1\ \pi^2$	10.32	9.49	9.18	8.40
π^1	14.4	12.1	12.0	11.8

TABLE 31. CALCULATED IONIZATION POTENTIALS (IP) FOR SELECTED OCCUPIED MOLECULAR ORBITALS AND ELECTRON AFFINITIES (EA) FOR SELECTED UNOCCUPIED MOLECULAR ORBITALS IN GROUND STATE OF CHALCOGENOPHENES **90** AND **298** AS DETERMINED BY SCF X_α (STO 3-21G)[b] CALCULATIONS[a]

	IP or EA (eV)			
MO	**298c** (X = O)	**298b** (X = S)	**298a** (X = Se)	**90** (X = Te)
$2a_2\ \pi^{2*}$	3.19	2.81	2.76	2.67
$3b_1\ \pi^{3*}$	1.82	1.57	1.53	1.02
σ^*	—	—	1.72	0.90
$1a_2\ \pi^3$	8.28 (9.01)	8.40 (9.31)	8.22 (9.13)	9.19 (9.09)
$2b_1\ \pi^2$	9.90 (10.80)	9.11 (9.55)	8.62 (8.87)	8.21 (8.16)

[a] Reference 206.
[b] Reference 175.

TABLE 32. EPR HYPERFINE COUPLINGS AND g VALUES FOR ANION RADICALS AND CATION RADICALS OF 2,5-DIPHENYLTELLUROPHENE (122) AND ITS LIGHTER CHALCOGEN ANALOGS 307[a]

Compd.	X	^{a}H3	^{a}2′,H2″	^{a}3′,H3″	^{a}H4′	^{a}X	g Value
122	$Te^{-\cdot}$	1.61	2.42, 3.18	0.31, 0.51	4.82	13.5	2.0027
307a	$Se^{-\cdot}$	1.29	1.95, 2.20	0.50, 0.63	3.07	—	2.0064
307b	$S^{-\cdot}$	1.20	1.85, 2.26	0.42, 0.62	3.13	—	2.0036
307c	$O^{-\cdot}$	0.80	2.00, 2.41	0.40, 0.60	3.81	—	2.0025
122	$Te^{+\cdot}$	2.99	2.22, 2.37	0.78, 0.93	3.80	—	2.0025
307a	$S^{+\cdot}$	2.40	2.38	0.73	3.40	—	2.0007
307b	$S^{+\cdot}$	2.48	2.42	0.73	3.48	—	2.0023
307c	$O^{+\cdot}$	2.78	2.41, 2.42	0.69, 0.77	3.38	—	2.0025

[a] Reference 210.

TABLE 33. REPRESENTATIVE SPECTRAL DATA AND IONIZATION POTENTIALS (IP) FOR BENZOTELLUROPHENE (177) AND ITS LIGHTER CHALCOGEN ANALOGS 309

		H2	H3	H4	H5	H6	H7			
Compd.	X	(δ)						λ_{max} (nm)[d]	^{125}Te (δ)[e]	IP (eV)[f]
177	Te[a]	8.55	7.84	7.71	7.26	7.03	7.82	318	727	7.76
309a	Se[a]	7.79	7.42	7.69	7.24	7.14	7.77	304	—	8.03
309b	S[b]	7.27	7.19	7.70	7.25	7.22	7.77	298	—	8.40
309c	O[c]	7.52	6.66	7.49	7.13	7.19	7.42	282	—	—

[a] Reference 215.
[b] Reference 216.
[c] Reference 217.
[d] Reference 91.
[e] Reference 214.
[f] Reference 213.

TABLE 34. OBSERVABLE PROTON–PROTON COUPLING CONSTANTS (J_{nm}) FOR BENZOTELLUROPHENE (177) AND ITS LIGHTER CHALCOGEN ANALOGS 309

		J_{23}	J_{37}	J_{45}	J_{46}	J_{47}	J_{56}	J_{57}	J_{67}
Compd.	X	(Hz)							
177	Te[a]	6.96	0.43	7.97	1.07	0.51	7.24	1.08	8.00
309a	Se[a]	5.57	0.65	7.97	1.02	0.48	7.22	1.17	8.27
309b	S[b]	5.57	0.86	8.09	1.16	0.73	7.22	1.17	8.06
309c	O[c]	2.19	0.87	7.89	1.28	0.80	7.27	0.92	8.43

[a] Reference 215.
[b] Reference 216.
[c] Reference 217.

TABLE 35. ^{1}H NMR CHEMICAL SHIFTS OF THE TELLUROPHENE RING PROTONS AND SUBSTITUENT PROTONS IN 2- AND 3-SUBSTITUTED BENZOTELLUROPHENES AND CARBONYL STRETCHING FREQUENCIES FOR CARBONYL-CONTAINING GROUPS

Compd.	R	R	H2[a]	H3[b]	ν_{CO} (cm^{-1})
		(δ)			
177	H	—	8.55	7.84	—
188	$COCH_3$	2.63	—	8.45	1630
190	Me	2.58	—	7.26	—
191	CO_2H	—	—	8.50	1716
192	CHO	9.63	—	8.47	1660
193	CH_2OH	4.90	—	7.63	—
201	CO_2Et	—	—	8.50	1680
203	COPh	—	—	8.27	1610
207	Cl	—	8.40	—	—
208	Br	—	8.60	—	—
209	I	—	9.00	—	—

[a] Reference 92.
[b] Reference 52.

TABLE 36. MOLECULAR GEOMETRIES OF THE DIBENZOCHALCOGENOPHENES **239** AND **310** AND 1,1-DIIODODIBENZOTELLUROPHENE (**240c**) AS DETERMINED BY X-RAY CRYSTALLOGRAPHY

Compd.	Bond Lengths (Å) and Angles (°)				
	310c[a] (X = O)	**310b**[b] (X = S)	**310a**[c] (X = Se)	**239**[d] (X = Te)	**240c**[e] (X = TeI_2)
X—C2	1.404	1.740	1.899	2.087	2.112
X—C5	1.404	1.740	1.899	2.087	2.112
C2—C3	—	—	—	1.394	1.409
C3—C4	—	—	—	1.460	1.469
C4—C5	—	—	—	1.394	1.409
Te—I	—	—	—	—	2.936
C2—X—C5	104.1	91.5	86.7	81.7	81.8
C3—C2—X	112.3	112.3	112.3	112.1	114.5
C2—C3—C4	105.3	111.9	114.3	117.1	117.6
C3—C4—C5	105.3	111.9	114.3	117.1	117.6
C4—C5—X	112.3	112.3	112.3	112.1	114.5
I—Te—I	—	—	—	—	178.47

[a] Reference 222.
[b] Reference 221.
[c] Reference 220.
[d] Reference 219
[e] Reference 223.

REFERENCES

1. Morgan, G. T.; Burstall, F. H. *J. Chem. Soc.* **1931**, 180.
2. Braye, E. H.; Hubel, W.; Caplier, I. *J. Am. Chem. Soc.* **1961**, *83*, 4406.
3. Bell, W.; McQueen, A. E. D.; Walton, J. C.; Foster, D. F.; Cole-Hamilton, D. J. *J. Crystal Growth* **1992**, *117*, 58.
4. Al-Rubaie, A. Z.; Alshirayda, H. A. Y. *J. Organomet. Chem.* **1985**, *294*, 315.
5. Migalina, Yu. V.; Balog, I. M.; Lendel, V. G.; Koz'min, A. S.; Zefirov, N. S. *Khim. Geterotsikl. Soedin.* **1978**, 1212.
6. Albeck, M.; Tamary, T. *J. Organomet. Chem.* **1979**, *164*, C23.
7. Farrar, W. V.; Gulland, J. M. *J. Chem. Soc.* **1945**, 11.
8. Buchta, E.; Greiner, K. *Chem. Ber.* **1961**, *94*, 1311.
9. Knapp, F. F., Jr. *J. Labelled Compd. Radiopharm.* **1980**, *17*, 81.
10. Zanati, G.; Gaare, G.; Wolff, M. E. *J. Med. Chem.* **1974**, *17*, 561.
11. Hope, E. G.; Kemmitt, T.; Levason, W. *Organometallics* **1988**, *7*, 78.
12. Merkel, G.; Berge, H.; Jeroschavski, P. *J. Prakt. Chem.* **1984**, *326*, 467.
13. Desilva, K. G. K.; Monsef-Mirzai, Z.; McWhinnie, W. R. *J. Chem. Soc., Dalton Trans.* **1983**, 2143.
14. Srivastava, T. N.; Srivastava, R. C.; Singh, M. *Ind. J. Chem.* **1979**, *17A*, 615.
15. Srivastava, T. N.; Srivastava, R. C.; Singh, H. B.; Singh, M. *Ind. J. Chem.* **1979**, *18A*, 367.
16. Abed-Ali, S. S.; McWhinnie, W. R. *J. Organomet. Chem.* **1984**, 365.
17. Srivastava, T. N.; Srivastava, V. K.; Srivastava, R. C. *Polyhedron* **1985**, *4*, 1223.
18. Srivastava, T. N.; Siddiqui, M. A.; Srivastava, S. K. *Ind. J. Chem.* **1988**, *27A*, 550.
19. Mathaway, B. J.; Underhill, A. E. *J. Chem. Soc.* **1961**, 3091.
20. Schmidt, E. *Phosphorus Sulfur* **1988**, *35*, 223.
21. Srivastava, T. N.; Srivastava, R. C.; Bhargava, A. *Ind. J. Chem.* **1979**, *18A*, 236.
22. Gilbert, F. L.; Lowry, T. M. *J. Chem. Soc.* **1928**, 2658.
23. Detty, M. R. *J. Org. Chem.* **1980**, *45*, 924.
24. Srivastava, T. N.; Srivastava, R. C.; Singh, M. *J. Organomet. Chem.* **1978**, *157*, 405.
25. Al-Rubaie, A. Z.; Alshirayda, H. A. Y.; Granger, P.; Chapelle, S. *J. Organomet. Chem.* **1985**, *287*, 321.
26. Al-Rubaie, A. Z.; Al-Shirayda, H. A.; Auoob, A. I. *J. Organomet. Chem.* **1988**, *356*, 49.
27. Singh, H. B.; Khanna, P. K.; Kumar, S. K. *J. Organomet. Chem.* **1988**, *338*, 1.
28. Kumar, S. K.; Khanna, P. K.; Singh, H. B. *Ind. J. Chem.* **1991**, *30A*, 720.
29. Bergman, J.; Engman, L. *J. Am. Chem. Soc.* **1981**, *103*, 2715.
30. Lichtmann, L. S.; Parsons, J. D.; Cirlin, E. H. *J. Cryst. Growth* **1988**, *86*, 217.
31. Arpe, H. J.; Kuckertz, H. *Angew. Chem., Int. Ed. Engl.* **1971**, *10*, 73.
32. Abid, K. Y.; McWhinnie, W. R. *J. Organomet. Chem.* **1987**, *330*, 337.
33. Cuthbertson, E.; MacNicol, D. D. *Tetrahedron Lett.* **1975**, 1893.
34. Li, C. J.; Harpp, D. N. *Tetrahedron Lett.* **1990**, *31*, 6291.
35. Ziolo, R. F.; Gunther, W. H. H. *J. Organomet. Chem.* **1978**, *146*, 245.
36. Zumbulyadis, N.; Gysling, H. J. *J. Organomet. Chem.* **1980**, *192*, 183.
37. Al-Rubaie, A. Z. *J. Organomet. Chem.* **1990**, *382*, 383.
38. Al-Rubaie, A. Z.; Al-Masoudi, E. A. *Heteroat. Chem.* **1991**, *2*, 417.

39. Dakternieks, D.; Di Giacomo, R.; Gable, R. W.; Hoskins, B. F. *J. Am. Chem. Soc.* **1988**, *110*, 6753.
40. Ramasamy, K.; Shanmugam, P. *Z. Naturforsch. B: Anorg. Chem., Org. Chem.* **1977**, *32B*, 605.
41. Singh, H. B.; McWhinnie, W. R. *J. Chem. Soc., Dalton Trans.* **1984**, 23.
42. Singh, H. B.; McWhinnie, W. R.; Ziolo, R. F.; Jones, C. H. *J. Chem. Soc., Dalton Trans.* **1984**, 1267.
43. Al-Rubaie, A. Z.; Al-Masoudi, E. A. *Polyhedron* **1990**, *9*, 847.
44. Bergman, J.; Engman, L. *Org. Prep. Proceed. Int.* **1978**, *10*, 289.
45. Bond, A. M.; Dakternieks, D.; Di Giacomo, R.; Hollenkamp, A. F. *Organometallics* **1991**, *10*, 3510.
46. Loth-Compere, M.; Luxen, A.; Thibaut, P.; Christiaens, L.; Guillaume, M.; Renson, M. *J. Heterocycl. Chem.* **1981**, *18*, 343.
47. Engman, L.; Cava, M. *J. Org. Chem.* **1981**, *46*, 4194.
48. Talbot, J.-M.; Piette, J.-L., Renson, M. *Bull. Soc. Chim. Fr.* **1976**, 294.
49. Weber, R.; Piette, J. L.; Renson, M. *J. Heterocycl. Chem.* **1978**, *15*, 865.
50. Lohner, W.; Praefcke, K. *J. Organomet. Chem.* **1981**, *208*, 35.
51. Lohner, W.; Praefcke, K. *J. Organomet. Chem.* **1980**, *194*, 173.
52. Bergman, J.; Engman, L. *J. Organomet. Chem.* **1980**, *201*, 377.
53. Dereu, N.; Renson, M. *J. Organomet. Chem.* **1981**, *208*, 11.
54. Piette, J.-L.; Petit, A.; Renson, M. *C. R. Acad. Sci. Ser. C* **1973**, *276*, 1035.
55. Weber, R.; Christiaens, L.; Renson, M. *Chem. Scr.* **1975**, *8A*, 116.
56. McMahon, F. A.; Pearson, T. G.; Robinson, P. L. *J. Chem. Soc.* **1933**, 1644.
57. Zoellner, W. G. *Dissertation Abstr.* **1959**, *19*, 3139; *Chem. Abstr.* **1959**, *53*, 17141i.
58. Braye, E. H.; Hubel, W.; Caplier, I. *J. Am. Chem. Soc.* **1961**, *83*, 4406.
59. Mack, W. *Angew. Chem., Int. Ed. Engl.* **1965**, *4*, 245.
60. Mack, W. *Angew. Chem., Int. Ed. Engl.* **1966**, *5*, 896.
61. Fringuelli, F.; Taticchi, A. *J. Chem. Soc., Perkin I* **1972**, 199.
62. Fringuelli, F.; Taticchi, A. *Ann. Chim.* (Rome) **1972**, *62*, 777.
63. Ulman, A.; Manassen, J.; Frolow, F.; Rabinovich, D. *Tetrahedron Lett.* **1978**, 1885.
64. Barton, T. J.; Tully, C. R.; Roth, R. W. *J. Organomet. Chem.* **1976**, *108*, 183.
65. Paliani, G.; Cataliotti, R.; Poletti, A.; Fringuelli, F.; Taticchi, A.; Giorgini, M. G. *Spectrochem. Acta* **1976**, *32A*, 1089.
66. Gusarova, N. K.; Trofimov, B. A.; Tatarinova, A. A.; Potapov, V. A.; Gusarov, A. V.; Amosova, A. V.; Voronkov, M. G. *Zh. Org. Khim.* **1989**, *25*, 39.
67. Potapov, V. A.; Amosova, S. V. *Metalloorg. Khim.* **1990**, *3*, 1197.
68. Barton, T. J.; Roth, R. W. *J. Organomet. Chem.* **1972**, *39*, C66.
69. Lohner, W.; Praefcke, K. *Chem. Ber.* **1978**, *111*, 3745.
70. Kulik, W.; Verkruijsse, H. D.; de Jong, R. L. P.; Hommes, H.; Brandsma, L. *Tetrahedron Lett.* **1983**, *24*, 2203.
71. Catel, J.-M.; Mahatsekake, C.; Andrieu, C.; Mollier, Y. *Phosphorus Sulfur* **1987**, *34*, 119.
72. Discordia, R. P.; Dittmer, D. C. *Tetrahedron Lett.* **1988**, *29*, 4923.
73. Scheller, A.; Winter, W.; Muller, E. *Liebigs Ann. Chem.* **1976**, 1448.
74. Muller, E.; Luppold, E.; Winter, W. *Synthesis* **1975**, 265.
75. Muller, E.; Luppold, E.; Winter, W. *Chem. Ber.* **1975**, *108*, 237.
76. Cagniant, P.; Close, R.; Kirsch, G.; Gagniant, D. *C. R. Acad. Sci., Ser. C* **1975**, *281*, 187.

77. Fringuelli, F.; Serena, B.; Taticchi, A. *J. Chem. Soc., Perkin II* **1980**, 971.
78. Laishev, V. Z.; Petrov, M. L.; Petrov, A. A. *Zh. Org. Khim.* **1981**, *17*, 2064.
79. Korchevin, N. A.; Zhnikin, A. R.; Ivanova, N. D.; Sukhomazova, E. N.; Tatarinova, A. A.; Trofimov, B. A.; Deryagina, E. N.; Voronkov, M. G. *Metalloorg. Khim.* **1990**, *3*, 1189.
80. Fringuelli, F.; Marino, G.; Savelli, G.; Taticchi, A. *J. Chem. Soc., Chem. Commun.* **1971**, 1441.
81. Clementi, S.; Fringuelli, F.; Linda, P.; Marino, G.; Savelli, G.; Taticchi, A. *J. Chem. Soc., Perkin II* **1973**, 2097.
82. Mack, W. *Angew. Chem.* **1966**, *78*, 940. (*Author's note*: The experimental results in reference 60, the *International Edition*, are less extensive than those in reference 82.)
83. Muller, E.; Luppold, E.; Winter, W. *Z. Naturforsch., B: Anorg. Chem., Org. Chem.* **1976**, *31B*, 367.
84. Luppold, E.; Winter, W. *Chem.-Zeit.* **1977**, *101*, 303.
85. Luppold, E.; Winter, W.; Muller, E. *Chem. Ber.* **1976**, *109*, 3886.
86. Fringuelli, F.; Gronowitz, S.; Hornfeldt, A.-B.; Johnson, I.; Taticchi, A. *Acta Chem. Scand.* **1976**, *30B*, 605.
87. Fringuelli, F.; Gronowitz, S.; Hornfeldt, A.-B.; Johnson, I.; Taticchi, A. *Acta Chem. Scand.* **1974**, *28B*, 175.
88. Lohner, W.; Praefcke, K. *J. Organomet. Chem.* **1981**, *208*, 43.
89. Fringuelli, F.; Marino, G.; Taticchi, A. *J. Chem. Soc., Perkin II* **1972**, 1738.
90. Detty, M. R. *Organometallics* **1991**, *10*, 702.
91. Piette, J. L.; Renson, M. *Bull. Soc. Chim. Belges* **1971**, *80*, 521.
92. Piette, J. L.; Talbot, J. M.; Genard, J.-C.; Renson, M. *Bull. Soc. Chim. Fr.* **1973**, 2468.
93. Russavskaya, N. V.; Korchevin, N. A.; Sukhomazova, E. N.; Turchaninova, L. P.; Deryagina, E. N.; Voronkov, M. G. *Zh. Org. Khim.* **1991**, *27*, 359.
94. Brandsma, L.; Hommes, H.; Verkruijsse, H. D.; de Jong, R. L. P. *Recl. Trav. Chim. Pays-Bas* **1985**, *104*, 226.
94a Kurita, J.; Yasuike, S.; Tsuchiya, T. *J. Chem. Soc. Chem. Commun.* **1993**, 1309.
95. Maercker, A.; Bodenstedt, H.; Brandsma, L. *Angew. Chem. Int. Ed. Engl.* **1992**, *31*, 1339.
96. Clementi, S.; Fringuelli, F.; Linda, P.; Marino, G.; Savelli, G.; Tatichhi, A.; Piette, J. L. *Gazz. Chim. Ital.* **1977**, *107*, 339.
97. Sadekov, I. D.; Minkin, V. I. *Khim. Geterotsikl. Soedin.* **1971**, 138.
98. Campos, M. de M.; Petragnani, N. *Tetrahedron* **1962**, *18*, 527.
99. Lendel, V. G.; Pak, V. I.; Petrus, V. V.; Kiyak, M. Yu.; Migalina, Yu. V. *Khim. Geterotsikl. Soedin.* **1990**, 1331.
100. Dereu, N.; Renson, M. *J. Organomet. Chem.* **1983**, *258*, 163.
101. Sadekov, I. D.; Nivorozhkin, V. L.; Ladatko, A. A.; Minkin, V. I. *Khim. Geterotskil. Soedin.* **1988**, 1050.
102. Ramasamy, K.; Murugesan, M.; Shanmugam, P. *Synthesis* **1978**, 842.
103. Courtot, C.; Bastani, M.-G. *C. R. Hebd. Seances Acad. Sci.* **1936**, *203*, 197.
104. Srivastava, T. N.; Mehrotra, S. *Synth. React. Inorg. Met.-Org. Chem.* **1985**, *15*, 709.
105. McCullough, J. D. *Inorg. Chem.* **1975**, *14*, 2285.
106. Knobler, C.; McCullough, J. D. *Inorg. Chem.* **1977**, *16*, 612.
107. Hellwinkel, D.; Fahrbach, G. *Tetrahedron Lett.* **1965**, 1823.
108. Hellwinkel, D. *Ann. N. Y. Acad. Sci.* **1972**, *192*, 158.
109. Hellwinkel, D.; Fahrbach, G. *Liebigs Ann. Chem.* **1968**, *712*, 1.
110. Cullinane, N. M.; Rees, A. G.; Plummer, C. A. J. *J. Chem. Soc.* **1939**, 151.
111. Passerini, R.; Purello, G.; *Ann. Chim.* (Rome) **1958**, *48*, 738.

112. Umemoto, T.; Ishihara, S. *J. Am. Chem. Soc.* **1993**, *115*, 2156.
113. Engman, L. *J. Heterocycl. Chem.* **1984**, *21*, 413.
114. Cohen, S. C.; Reddy, M. L. N.; Massey, A. G. *J. Chem. Soc. Chem. Commun.* **1967**, 451.
115. Cohen, S. C.; Reddy, M. L. N.; Massey, A. G. *J. Organomet. Chem.* **1968**, *11*, 563.
116. Woodard, C. M.; Hughes, G.; Massey, A. G. *J. Organomet. Chem.* **1976**, *112*, 9.
117. Sadekov, I. D.; Rivkin, B. B.; Maslakov, A. G.; Minkin, V. I. *Khim. Geterotsikl. Soedin.* **1987**, 420.
118. Hellwinkel, D.; Fahrbach, G. *Chem. Ber.* **1968**, *101*, 574.
119. Srivastava, T. N.; Singh, J. D.; Mehrotra, S. *Ind. J. Chem.* **1986**, *25A*, 480.
120. Srivastava, T. N.; Singh, J. D.; Mehrotra, S. *Ind. J. Chem.* **1985**, *24A*, 849.
121. Earle, M. J.; Massey, A. G.; Al-Soudani, A.-R.; Zaidi, T. *Polyhedron* **1989**, *8*, 2817.
122. Barton, T. J.; Nelson, A. J. *Tetrahedron Lett.* **1969**, 5037.
123. Luppold, E.; Mueller, E.; Winter, W. *Z. Naturforsch., B: Anorg. Chem., Org. Chem.* **1976**, *31B*, 1654.
124. Wenkert, E.; Leftin, M. H.; Michelotti, E. L. *J. Chem. Soc., Chem. Commun.* **1984**, 617.
125. Sugimoto, R.; Yoshino, K.; Inoue, S.; Tsukagoshi, K. *Jpn. J. Appl. Phys., Part 2* **1985**, *24*, 425.
126. Haas, O.; von Zelewsky, A. *J. Chem. Research (M)* **1980**, 1201.
127. Haas, O.; von Zelewsky, A. *J. Chem. Research (M)* **1980**, 1228.
128. Al-Rubaie, A. Z.; Al-Obaidi, Y. N.; Yousif, L. Z. *Polyhedron* **1990**, *9*, 1141.
129. Al-Rubaie, A. Z.; Al-Obaidi, Y. N.; Yousif, L. Z. *Thermochemica Acta* **1990**, *162*, 409.
130. Freeman, J. W.; Basolo, F. *Organometallics* **1991**, *10*, 256.
131. Belforte, A.; Calderazzo, F.; Zanazzi, P. F. *Gazz. Chimi. It.* **1985**, *115*, 71.
132. Atwood, J. L.; Bernal, I.; Calderazzo, F.; Canada, L. G.; Rogers, R. D.; Veraeini, C. A.; Vitali, D.; Poli, R. *Inorg. Chem.* **1983**, *22*, 1797.
133. Ofele, K.; Dotzauer, E. *J. Organomet. Chem.* **1972**, *42*, C87.
134. Arce, A. J.; Deeming, A. J.; De Sanctis, Y.; Machado, R.; Manzur, J.; Rivas, C. *J. Chem. Soc., Chem. Commun.* **1990**, 1568.
135. Arce, A. J.; Machado, R.; Rivas, C.; De Sanctis, Y.; Deeming, A. J. *J. Organomet. Chem.* **1991**, *419*, 63.
136. Chhor, K.; Pommier, C.; Berear, J. F.; Calvarin, G.; Diot, M. *Mol. Cryst. Liq. Cryst.* **1981**, *71*, 3.
137. Pacheco, D.; Vargas, F.; Rivas, C. *Phosphorus and Sulfur* **1985**, *25*, 245.
138. Hoffman, H. M. R.; Clemens, K. E.; Smithers, R. H. *J. Am. Chem. Soc.* **1972**, *94*, 3940.
139. Jones, R. H.; Hamor, T. A. *J. Organomet. Chem.* **1984**, *269*, 11.
140. Pauling, L. *The Nature of the Chemical Bond*, 3rd ed., Cornell University Press, Ithaca, NY, 1960.
141. Gillespie, R. J.; Nyholm, R. S. *Q. Rev. Chem. Soc.* **1957**, *11*, 339.
142. Giorgini, M. G.; Paliani, G.; Cataliotti, R. *Spectrochim. Acta* **1977**, *33A*, 1083.
143. Lumbroso, H.; Bertin, D. M.; Fringuelli, F.; Taticchi, A. *Comp. Rend. Acad. Sc. Paris* **1973**, *277*, 203.
144. Pignataro, S.; Distefano, G. *Chem. Phys. Lett.* **1974**, *26*, 356.
145. Duffield, A. M.; Budzikiewicz, L.; Djerassi, C. *J. Am. Chem. Soc.* **1965**, *87*, 2920.
146. Fringuelli, F.; Gronowitz, S.; Hornfeldt, A.-B.; Taticchi, A. *J. Heterocycl. Chem.* **1974**, *11*, 827.
147. Barton, T. J.; Roth, R. W.; Verkade, J. G. *J. Am. Chem. Soc.* **1972**, *94*, 8854.
148. Jones, C. H. W.; Schultz, R.; McWhinnie, W. R.; Dance, N. S. *Can. J. Chem.* **1976**, *54*, 3234.
149. Braillon, B.; Caire, J.-C.; Saquet, M.; Thuillier, A. *J. Chem. Res. (S)* **1986**, 98.
150. Lozac'h, R.; Braillon, B. *J. Magn. Reson.* **1973**, *12*, 244.

151. McCarthy, A. E.; Singh, H. B. *J. Organomet. Chem.* **1984**, *275*, 57.
152. Singh, H. B.; McWhinnie, W. R.; Hamor, T. A.; Jones, R. H. *J. Chem. Soc. Dalton Trans.* **1984**, 23.
153. Lohner, W.; Praefcke, K. *J. Organomet. Chem.* **1981**, *208*, 39.
154. Wadsworth, D. H.; Detty, M. R. *J. Org. Chem.* **1980**, *45*, 4611.
155. Detty, M. R.; Luss, H. R. *Organometallics* **1992**, *11*, 2157.
156. Bird, C. W. *Tetrahedron* **1985**, *41*, 1409.
157. Fringuelli, F.; Marino G.; Taticchi, A.; Grandolini, G. *J. Chem. Soc., Perkin Trans. II* **1974**, 332.
158. Fringuelli, F.; Marino, G.; Taticchi, A. *Gazz. Chim. Ital.* **1973**, *103*, 1041.
159. Fabian, J. *Z. Phys. Chem.* (Leipzig) **1979**, *260*, 81.
160. Campos-Vallette, M. M.; Clavijo C., R. E. *Spectrosc. Lett.* **1985**, *18*, 759.
161. Fringuelli, F.; Marino, G.; Taticchi, A. *J. Chem. Soc.* (*B*) **1970**, 1595.
162. Fringuelli, F.; Marino, G.; Taticchi, A. *J. Chem. Soc.* (*B*) **1971**, 2304.
163. Fringuelli, F.; Taticchi, A. *J. Heterocycl. Chem.* **1973**, *10*, 89.
164. Spinelli, D.; Guanti, G.; Dell'Erba, C. *Ric. Sci.* **1968**, *38*, 1048.
165. Butler, A. R. *J. Chem. Soc.* (*B*) **1970**, 867.
166. Lumme, P. O. *Suomen. Kemistil.* **1960**, *B33*, 87.
167. Marino, G. *Chem. Scr.* **1975** *8A*, 23.
168. Fanfani, L.; Nunzi, A.; Zanazzi, P. F.; Zanzari, A. R.; Pellinghelli, M. A. *Cryst. Struct. Commun.* **1972**, *1*, 273.
169. Zukerman-Schpector, J.; Dabdoub, M. J.; Daddoub, V. B.; Pereira, M. A. *Acta Crystallogr., Sect. C: Cryst. Struct. Commun.* **1992**, *C48*, 767.
170. Brown, H. D.; Crofts, J. G. *Chem. Phys.* **1973**, *110*, 4204.
171. Pozdeev, N. M.; Akulinin, O. B.; Shapkin, A. A.; Magdesieva, N. N. *Dokl. Akad. Nauk SSSR* **1969**, *185*, 384.
172. Bak, B.; Christensen, D.; Hansen-Nygaard, L.; Rastrup-Andersen, J. *J. Mol. Spectrosc.* **1961**, *7*, 58.
173. Bak, B.; Christensen, D.; Dixon, W. B.; Hansen-Nygaard, L.; Rastrup-Andersen, J.; Schottlander, M. *J. Mol. Spectrosc.* **1962**, *9*, 124.
174. Baldridge, K. K.; Gordon, M. S. *J. Am. Chem. Soc.* **1988**, *110*, 4204.
175. Yadav, V. K.; Yadav, A.; Poirier, R. A. *J. Mol. Struct.* **1989**, *186*, 101.
176. Catalano, D.; Caporusso, A. M.; Da Settimo, F.; Forte, C.; Veracini, C. A. *Gazz. Chim. Ital.* **1988**, *118*, 529.
177. Chidichimo, G.; Bucci, P.; Lelj, F.; Longeri, M. *Mol. Phys.* **1981**, *43*, 887.
178. Jokisaari, J.; Vääänänen, T. *Mol. Phys.* **1986**, *58*, 959.
179. Diehl, P.; Kellerhals, M.; Lounila, J.; Wasser, R.; Hiltunen, Y.; Jokisaari, J.; Vääänänen, T. *Magn. Reson. Chem.* **1987**, *25*, 244.
180. Palianai, G.; Cataliotti, R.; Poletti, A.; Fringuelli, F.; Taticchi, A.; Giorgini, M. G. *Spectrochim. Acta* **1976**, *32A*, 1089.
181. Magdesieva, N. N. In *Advances in Heterocyclic Chemistry*, Katritzky, A. R.; Boulton, A. J., eds., Academic Press, New York, 1970, Vol. 12, Ch. 1.
182. Rico, M.; Orza, J. M.; Morcillo, J. *Spectrochim. Acta* **1965**, *21*, 689.
183. Rico, M.; Barrachina, M.; Orza, J. M. *J. Mol. Spectrosc.* **1967**, *24*, 133.
184. Santucci, A.; Paliani, G.; Cataliotti, R. S. *Spectrochim. Acta* **1985**, *41A*, 679.
185. Santucci, A.; Paliani, G.; Cataliotti, R. S. *Chem. Phys. Lett.* **1987**, *138*, 244.
186. Wilson, E. B.; Decius, J. C.; Cross, P. C. *Molecular Vibrations*, McGraw-Hill, New York, 1955.
187. Paliani, G.; Cataliotti, R. *Spectrochim. Acta* **1981**, *37A*, 707.

188. Santucci, A.; Murgia, S. M.; Paliani, G.; Cataliotti, R. S. *Spectrosc. Lett.* **1988**, *21*, 243.
189. Lumbroso, H.; Bertin, D. M.; Fringuelli, F.; Taticchi, A. *J. Chem. Soc., Perkin II* **1977**, 775.
190. Fringuelli, F.; Taticchi, A. *J. Heterocycl. Chem.* **1978**, *15*, 137.
191. Budzikiewicz, H.; Djerassi, C.; Williams, D. H. *Interpretation of Mass Spectra of Organic Compounds*, Holden-Day, San Francisco, 1964.
192. Spiteller, G. In *Physical Methods in Heterocyclic Chemistry*, Katritzky, A. R., ed., Academic Press, London, 1971, Vol. 3, p. 223.
193. Drakenberg, T.; Fringuelli, F.; Gronowitz, S.; Hornfeldt, A. B.; Johnson, I.; Taticchi, A. *Chem. Scr.* **1976**, *10*, 139.
194. Paudler, W. W.; Jovanovic, M. V. *Org. Magn. Reson.* **1982**, *19*, 192.
195. Ebert, C.; Gianferrara, T.; Linda, P.; Masotti, P. *Magn. Reson. Chem.* **1990**, *28*, 397.
196. Fringuelli, F.; Gronowitz, S.; Hornfeldt, A. B.; Johnson, I.; Taticchi, A. *Acta Chem. Scand.* **1974**, *B28*, 175.
197. Kalabin, G. A.; Valeev, R. B. *Zh. Org. Khim.* **1981**, *17*, 947.
198. Martin, M. L.; Trierweiler, M.; Galasso, V.; Fringuelli, F.; Taticchi, A. *J. Magn. Reson.* **1981**, *42*, 155.
199. Martin, M. L.; Trierweiler, M.; Galasso, V.; Fringuelli, F.; Taticchi, A. *J. Magn. Reson.* **1982**, *47*, 504.
200. Fringuelli, F.; Gronowitz, S.; Hornfeldt, A.-B.; Johnson, I.; Taticchi, A. *Acta Chem. Scand.* **1976**, *B30*, 605.
201. Galasso, V.; Martin, M. L.; Trierweiler, M.; Fringuelli, F.; Taticchi, A. *J. Mol. Struct. THEOCHEM* **1982**, *90*, 53.
202. Natiello, M. A.; Scuseria, G. E.; Contreras, R. H. *J. Mol. Struct. THEOCHEM* **1983**, *14*, 233.
203. Turfo, M. F.; Contreras, R. H. *Z. Phys. Chem.* (Leipzig) **1986**, *267*, 873.
204. Fringuelli, F.; Marino, G.; Taticchi, A.; Distefano, G.; Colonna, F. P.; Pignataro, S. *J. Chem. Soc., Perkin Trans II* **1976**, 276.
205. Distefano, G.; Pignataro, S.; Innorta, G.; Fringuelli, F.; Marino, G.; Taticchi, A. *Chem. Phys. Lett.* **1973**, *22*, 132.
206. Modelli, A.; Guerra, M.; Jones, D.; Distefano, G.; Irgolic, K. J.; French, K.; Pappalardo, G. C. *Chem. Phys.* **1984**, *88*, 455.
207. De Alti, G.; DeCleva, P. *Chem. Phys. Lett.* **1981**, *77*, 413.
208. Galasso, V. *THEOCHEM* **1982**, 231.
209. Slater, J. C. *Adv. Quantum. Chem.* **1972**, *6*, 1.
210. Davies, A. G.; Schiesser, C. H. *J. Organomet. Chem.* **1990**, *389*, 301.
211. Stewart, J. J. P. *J. Comput. Chem.* **1989**, *10*, 209.
212. Stewart, J. J. P. *J. Comput. Chem.* **1989**, *10*, 221.
213. Muller, J.-F. *Helv. Chim. Acta* **1975**, *58*, 2646.
214. Baiwir, M.; Llabres, G.; Luxen, A.; Christiaens, L.; Piette, J.-L. *Org. Magn. Reson.* **1984**, *22*, 312.
215. Llabres, G.; Baiwir, M.; Denoel, J.; Piette, J.-L.; Christiaens, L. *Tetrahedron Lett.* **1972**, 3177.
216. Bartle, K. D.; Jones, D. W.; Matthesis, R. S. *Tetrahedron* **1971**, *27*, 5177.
217. Black, P. J.; Hofferman, M. L. *Aust. J. Chem.* **1965**, *18*, 353.
218. Faller, P.; Weber, J. *Bull. Soc. Chim. Fr.* **1972**, 3193.
219. McCullough, J. D. *Inorg. Chem.* **1975**, *14*, 2639.
220. Hope, H.; Knobler, C.; McCollough, J. D. *Acta Crystallogr., Sect. B.* **1970**, *B26*, 628.
221. Schaffrin, R. M.; Trotter, J. *J. Chem. Soc.* **1970**, 1561.
222. Dideberg, O.; Dupont, L.; Andre, J. M. *Acta Crystallogr., Sect. B.* **1972**, *B28*, 1002.
223. McCullough, J. D. *Inorg. Chem.* **1975**, *14*, 1142.

Chemistry of Heterocyclic Compounds, Volume 53
Michael R. Detty, Marrie B. O'Regan

CHAPTER III

Telluranes, Tellurins, and Other Six-Membered Rings Containing One Tellurium Atom

Six-membered rings containing one tellurium atom are among the oldest studied tellurium-containing heterocycles. The telluranes were first studied by G. T. Morgan and colleagues in the 1920s.[1,2] Since these pioneering studies, most combinations of unsaturation and tellurium–atom placement have been achieved synthetically. The telluranes, their unsaturated analogs, and benzo-fused derivatives have been compared to their lighter chalcogen analogs, and the consequences of heteroatom substitution with respect to properties and reactivity have been defined. Unlike their lighter chalcogen analogs, the tellurium-containing heterocycles readily form tellurium(IV) analogs via oxidative addition of halogens and pseudohalogens. In terms of applications to technology, the six-membered rings containing one tellurium atom have served as precursors to other compounds such as the telluropyrylium compounds (Chapter 4) or electron-donating tellurium analogs of (pyranyl)pyrans (Chapter 5). However, the construction of the six-membered ring for all these latter compounds began with the construction of a tellurane.

I. NOMENCLATURE

IUPAC and *Chemical Abstracts* conventions suggest the name *tellurane* for the fully saturated six-membered ring containing one tellurium atom. As shown in structure **1** (Fig. 1), the numbering scheme begins with the heteroatom and proceeds around the ring. Under the *Chemical Abstracts* convention, the addition of unsaturation to the ring changes the name to *tellurin*, and the site of

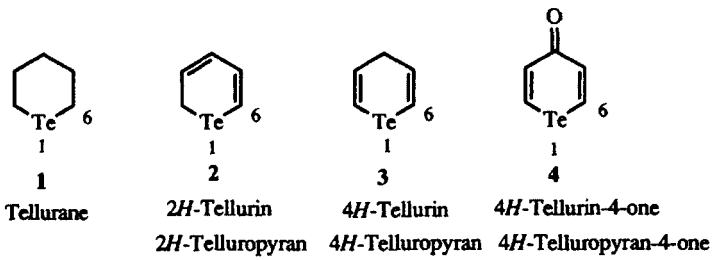

Figure 1. Nomenclature for telluranes and related compounds.

saturation is numbered as in 2*H*-tellurin **2** and 4*H*-tellurin **3**. Under the IUPAC convention, compounds **2** and **3** are described as telluropyrans as an extension of the pyran–thiopyran nomenclature. Further unsaturation as in the addition of a carbonyl group in **4** is described in the *Chemical Abstracts* convention as either a 4*H*-tellurin-4-one or as a 4-oxo-4*H*-tellurin. Under IUPAC nomenclature, these compounds are described as telluropyranones as an extension of the pyranone–thiopyranone nomenclature.

The addition of a benzo-fused ring system to the tellurane nucleus has given many more trivial names to the corresponding tellurium heterocycles. Benzotellurane **5** (Fig. 2) is trivially known as *tellurochromane*, while 2*H*-benzotellurin **6** and 4*H*-benzotellurin **7** are trivially known as 2-*tellurochromene* and 4-*tellurochromene*, respectively. The addition of a carbonyl group to the heterocyclic ring of **6** gives 2*H*-benzotellurin-2-one (**8**, or 2*H*-benzotelluropyran-2-one) and the addition of a carbonyl group to **7** gives 4*H*-benzotellurin-4-one (**9**, or 4*H*-benzotelluropyran-4-one). The trivial name for **8** is tellurocoumarin as an extension of the coumarin–thiocoumarin nomenclature, while the trivial name for **9** is tellurochromone after the chromone–thiochromone nomenclature. The placement of a 2-aryl substituent in **9** gives the trivial name of telluroflavone. The benzogroup of **6** and the double bond can be interchanged to give the 1*H*-benzo-2-tellurin system. 1-Oxo-1*H*-benzo-2-tellurin or 1*H*-benzo-2-tellurin-1-one (**10**) has the trivial name of telluroisocoumarin.

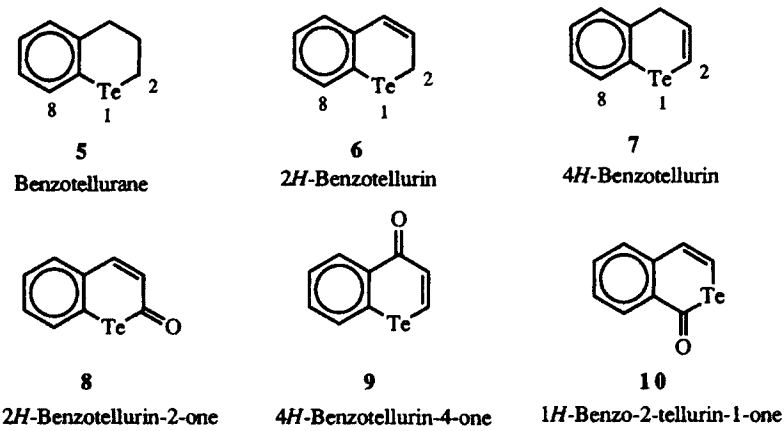

Figure 2. Nomenclature for benzotelluranes and related compounds.

The 4*H*-tellurin nucleus fused to two benzo groups has the *Chemical Abstracts*—suggested and IUPAC-suggested name of telluroxanthene (**11**) (Fig. 3). The addition of a carbonyl group to the 9-position leads to the *Chemical Abstracts*—suggested and IUPAC-suggested name of telluraxanthone (**12**). These molecules have also been referred to with the trivial names of telluraxanthene and telluraxanthone.

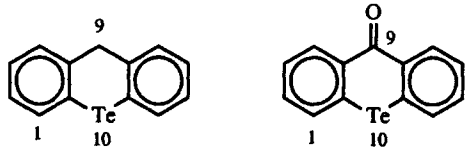

11 **12**

Telluraxanthene
Telluroxanthene

Telluraxanthone
Telluroxanthone

Figure 3. Nomenclature for dibenzotelluranes and related compounds.

II. SYNTHESES OF THE TELLURANE AND TELLURIN NUCLEI AND THEIR BENZO-FUSED ANALOGS

The syntheses of the tellurane and tellurin nuclei as well as their benzo-fused analogs involve three types of ring-forming reactions. In one type of reaction, cyclization of a six-atom sequence gives rise to the six-membered ring. In another cyclization reaction, tellurium is added as a one-atom unit to a five-atom carbon framework to give a six-membered ring. This reaction can involve either nucleophilic or electrophilic tellurium species. In a third type of reaction, a covalently bound tellurium atom–carbon atom pair adds as a two-atom unit to a four-atom carbon framework to give a six-membered ring. Alternatively, a two-carbon unit can add to a tellurium-containing four-atom sequence to give the six-membered ring.

A. Synthesis of the Tellurane Nucleus

1. The Tellurane Nucleus and Tellurium(IV) Derivatives

The initial work of Morgan and Burgess[23] and Morgan and Burstall[3] describes the thermal reaction of aluminum telluride with 1,5-dihalopentanes to give the 1,1-dihalotelluranes **13** as shown in Scheme 1. Distillation of the dihalides **13** gives tellurane (**1**) presumably via reductive elimination of halogen

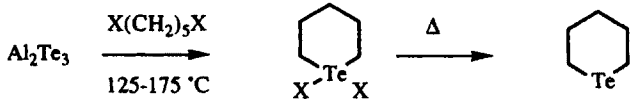

13a, X = Cl
13b, X = Br
13c, X = I

1

Scheme 1

from the tellurium(IV) species. Although the initial papers claim that the reaction was unsuccessful with 1,5-diiodopentane,[2,3] Farrar and Gulland have shown that the reaction is successful even with the diiodide to give 1,1-diiodotellurane (**13c**) in 63% yield.[4]

Farrar and Gulland introduced the use of rongalite (sodium formaldehydesulfoxylate) in these reactions as a reducing agent for tellurium in aqueous sodium hydroxide solution to produce sodium hydrogen telluride.[4] This procedure has been more recently used as shown in Scheme 2 to produce 3,3-dimethyltellurane (**14**) in 60% isolated yield.[5]

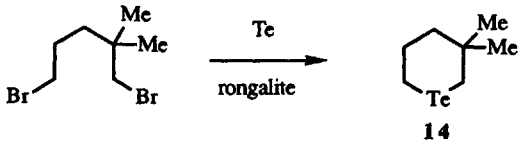

14

Scheme 2

The 1,1-dihalogroups of the telluranes with a tellurium(IV) oxidation state are easily exchanged for other ligands.[6] Various silver salts have been employed in these reactions as shown in Scheme 3 for ligand exchange with diodide **13c**. Other examples of this reaction are compiled in Table 1.

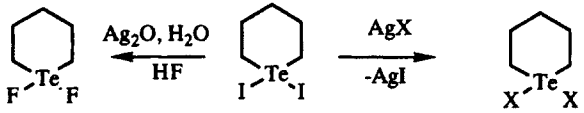

13d **13c** **13e-n**

Scheme 3

Sulfonyl chlorides have been found to react with tellurane to give 1,1-dichlorotellurane in good yield.[7] Both alkyl (methyl, ethyl, propyl) and aryl (phenyl, *p*-tolyl) sulfonyl halides have given this reaction.

The sulfonium–salt analog in tellurium chemistry is the telluronium salt. Telluronium salt analogs of telluranes are known and have been prepared by either the reaction of aryltelluride anions with 1,5-dibromopentanes (Scheme 4) or the addition of reactive alkyl halides to telluranes.[8-10] In these reactions, the aryltelluride reacts with one end of the dihalopentane to give an alkylaryltelluride. Intramolecular cyclization reactions then produce the cyclic telluronium species. Intermolecular reactions to give bistelluronium salts and/or to give 1,5-bis(phenyltelluro)pentanes are complicating side reactions.[9]

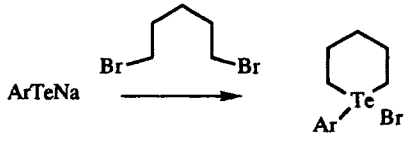

Scheme 4

2. *Tellurane-4-one and Tellurane-3,5-diones and Derivatives*

The preparation of tellurane-4-one (**15**) follows a path similar to the preparation of the fully saturated telluranes. As shown in Scheme 5, the nucleophilic addition of sodium hydrogen telluride to *N,N*-dimethylpiperidinium salt **16** gives tellurane-4-one (**15**) in 38% isolated yield.[11] This reaction can be compared to the addition of disodium selenide to **16**, which gives selenane-4-one **17** in 61% isolated yield.[11]

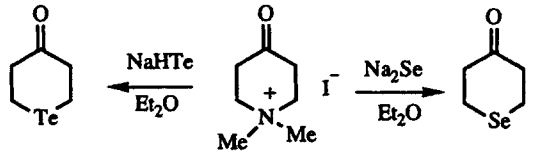

15 **16** **17**

Scheme 5

The tellurane-3,5-diones were among the first tellurium-containing heterocycles synthesized in the laboratory. As shown in Scheme 6, the electrophilic addition of tellurium tetrachloride to 2,4-pentanedione and derivatives leads to good yields of the 1,1-dichlorotellurane-3,5-diones **18** (Table 2).[1,12-18] Sodium bisulphite reduction of tellurium(IV) to tellurium(II) gives the tellurane-3,5-diones **19**. This reaction of tellurium tetrachloride is somewhat surprising in that most metals and semimetals react through the carbonyl oxygens of 3,5-pentanediones to give chelates. The chemical structure of compounds, **19** was first suggested by their ability to form dioximes, which was indicative that both carbonyl groups were still intact.[15,17]

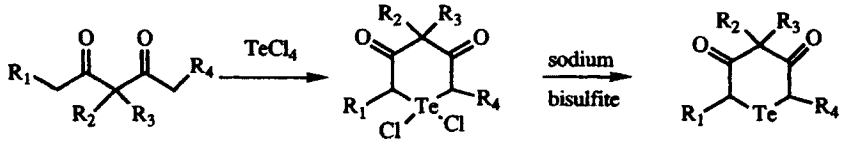

18 **19**

Scheme 6

The oxidative addition of halogens to the telluranediones **19** regenerates the tellurium(IV) analogs **18**.[12] Thus, the addition of chlorine to 4-ethyltellurane-3,5-dione **19c** regenerates tellurium(IV) dichloride **18c**, while the additions of bromine and iodine give the dibromide and diiodide, respectively. Similarly, oxidative additions of bromine and iodine to 4-methyltellurane-3,5-dione give the corresponding tellurium(IV) dibromide and diiodide, respectively.

B. Synthesis of the Tellurin Nucleus

The introduction of one or more double bonds to the tellurane nucleus produces a dihydrotellurin. The introduction of unsaturation to the tellurane nucleus is limited by the ease of oxidation of tellurium(II) to tellurium(IV). As a consequence, tellurins have been prepared only by the formal addition of tellurium to a five-carbon unit, by [4 + 2] cycloaddition reactions, and by reactions of other tellurins.

1. The 3,5-Dihydro-2H-tellurin Nucleus and Derivatives

The 3,5-dihydro-2*H*-tellurin nucleus (**20**) has been prepared by [4 + 2] cycloaddition reactions of a tellurocarbonyl with a butadiene unit as shown in Scheme 7.[19-22] The tellurocarbonyl species can be either metal-complexed or can be transiently stable if generated in the presence of a diene.

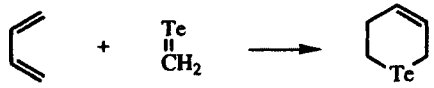

20

Scheme 7

The tellurocarbonyl group was long thought to be too unstable to isolate. However, telluroesters,[23-25] telluroamides,[26] telluroketenes,[27-29] and stable tellurocarbonyl compounds coordinated to transition metals[19,22,30-37] have been known since 1979. The addition of tellurium to pentacarbonyl(diphenylmethylidene)tungsten gives the tungsten-coordinated diphenyltelluroketone **21**.[31] The first 3,5-dihydro-2*H*-tellurins were prepared by the cycloaddition of **21** with either 2,3-dimethyl-1,3-butadiene or cyclopentadiene as shown in Scheme 8.[19] Pentacarbonyl(2,2-diphenyl-4,5-dimethyl-3,5-dihydro-2*H*-tellurin) tungsten (**22**) was isolated in 12% yield and pentacarbonyl(3,3-diphenyl-2-tellurabicyclo [2.2.1]hept-5-ene)tungsten (**23**, a tellurin with a bridging methylene unit) was isolated in 24% yield via these reactions.

Similar chemistry can be employed to prepare tungsten-coordinated tellurobenzaldehyde complexes.[22] The reaction of benzylidene(pentacarbonyl) tungsten with tellurocyanate gives pentacarbonyl(tellurobenzaldehyde)tungsten(**24**) via insertion of the tellurium atom of tellurocyanate into the benzylidene–tungsten bond. The tungsten-coordinated tellurobenzaldehyde is thermally very labile relative to the tungsten-coordinated diphenyltelluroketone **21**. The addition of excess 2,3-dimethyl-1,3-butadiene to **24** in dichloromethane at $-90°C$ gives isomers of pentacarbonyl(2-phenyl-4,5-dimethyl-3,5-dihydro-2*H*-tellurin)tungsten (**25**) in 8% isolated yield. ^1H NMR analysis of the product

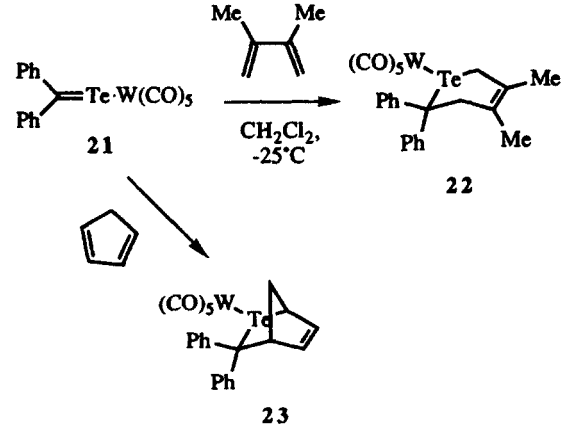

Scheme 8

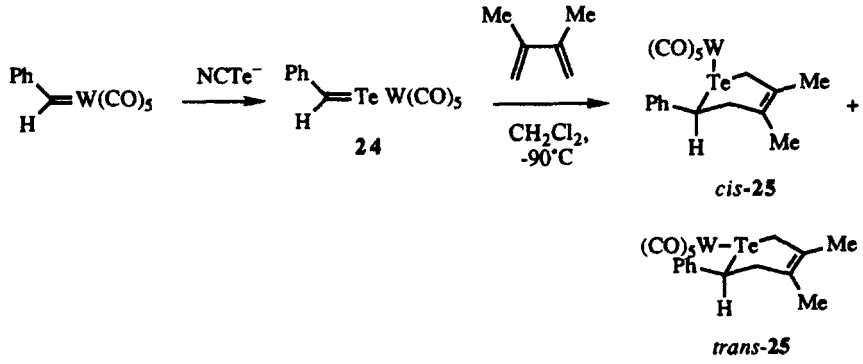

Scheme 9

mixture of **25** was indicative of a 1.4 : 1 ratio of isomers with the 2-phenyl group occupying an equatorial position in each as shown in Scheme 9.

The cycloaddition reaction of cyclopentadiene with **24** gives isomers of pentacarbonyl(3-phenyl-2-tellurabicyclo[2.2.1]hept-5-ene)tungsten **26** in an 11 : 1 ratio in greater than 35% isolated yield (Scheme 10).[22] The structure of the *exo* isomer of **26** [phenyl, *exo*; (pentacarbonyl)tungsten, *endo*] was assigned

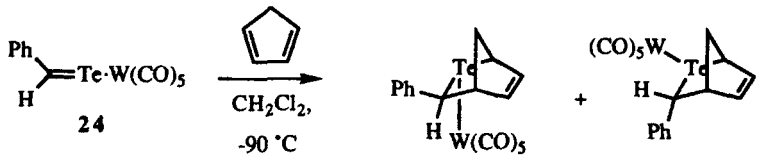

Scheme 10

unambiguously through single-crystal X-ray crystallographic analysis, while the structure of the *endo* isomer [phenyl, *endo*; (pentacarbonyl)tungsten, *exo*] was assigned via ^{1}H NMR spectroscopy.

While many of the transition-metal-coordinated complexes of tellurocarbonyl compounds can be isolated, the free telluroaldehydes and telluroketones are only transiently stable.[20,21] These materials can be captured by 1,3-dienes to give 3,5-dihydro-2*H*-tellurin compounds. Benzylidene triphenylphosphorane reacts with tellurium metal (treated with triphenylphosphine) in toluene to give tellurobenzaldehyde.[20] The tellurobenzaldehyde can be trapped with 2,3-dimethyl-1,3-butadiene to give 4,5-dimethyl-3,5-dihydro-2*H*-tellurin (**27a**) in 11% isolated yield as shown in Scheme 11 and Table 4.

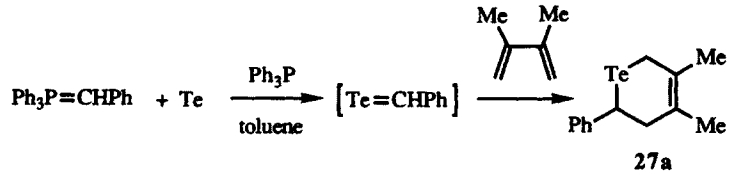

Scheme 11

Bis(dimethylaluminum)telluride is an efficient tellurating agent for the direct conversion of aldehydes and ketones to tellurocarbonyl compounds.[21] The reagent is prepared by the transmetallation of bis(tributyltin)telluride with

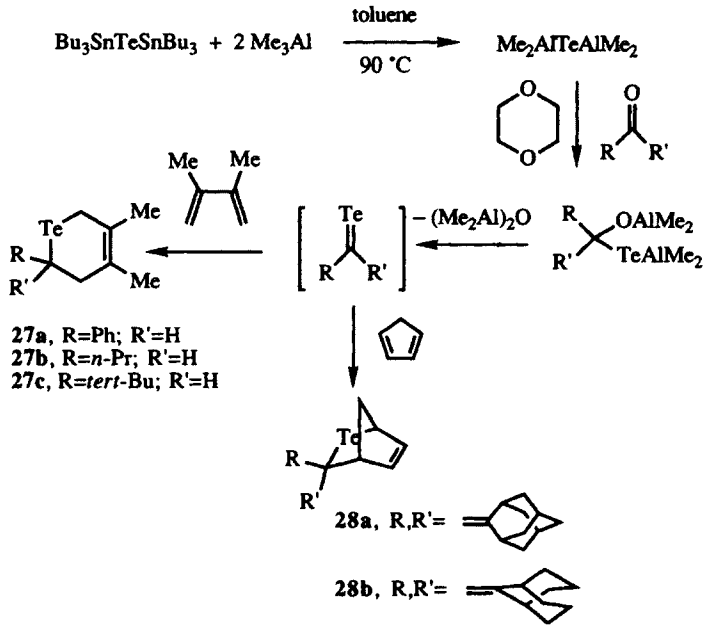

Scheme 12

trimethylaluminum in toluene. Toluene is removed and replaced with dioxane to give a soluble reagent. The generation of the tellurocarbonyl compounds is accomplished in refluxing dioxane in the presence of a diene to capture the tellurocarbonyl compound as it is formed (Scheme 12). The yields of these reactions are compiled in Table 3. Telluroaldehydes were captured with 2,3-dimethyl-1,3-butadiene to give tellurins **27**, and telluroketones were captured with cyclopentadiene to give bicyclo[2.2.1]telluraheptenes **28**. In these reactions, the use of 1,4-dioxane as solvent gave much better yields than the use of tetrahydrofuran.

2. *4H-Tellurin-4-ones and Derivatives*

The 4*H*-tellurin-4-ones **29** have been prepared by what is formally the double Michael addition of disodium telluride to a 1,4-pentadiyn-3-one **30**.[38–44] This approach has been used with varying degrees of success for the preparation of 2,6-dimethyl-,[41,45] 2,6-di-*tert*-butyl-,[41] and 2,6-diphenylthiopyran-4-one[41,45,46] and for the preparation of the corresponding selenopyran-4-ones.[41,47] In practice, the preparation of the 4*H*-tellurin-4-ones **29** employs the controlled Michael addition of one equivalent of ethanol across one triple bond to give **31** as the actual Michael acceptor as shown in Scheme 13. Both symmet-

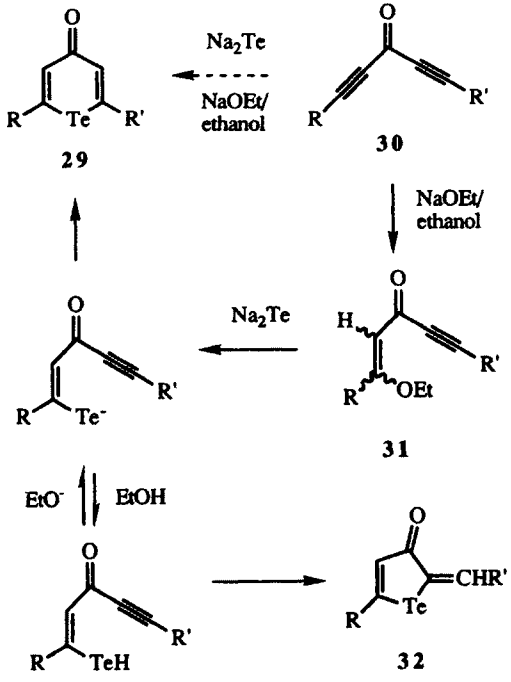

Scheme 13

rical[38-42,44] and unsymmetrical[42,43] 4*H*-tellurin-4-ones **29** have been prepared via this chemistry as compiled in Table 3. The formation of the five-membered-ring product **32** is competitive with the formation of the six-membered ring. The use of 0.25–1.0 *M* sodium ethoxide in ethanol maximizes the yield of tellurin-4-one presumably by promoting anionic cyclization to give the six-membered ring as opposed to tellurol cyclization which presumably leads to the five-membered ring.[38]

The tellurating species have been formed by reduction of tellurium metal with either lithium triethylborohydride in tetrahydrofuran[38] or with sodium borohydride in sodium ethoxide in ethanol.[39-43] In the lithium triethylborohydride reduction, sodium ethoxide in ethanol is added to the dilithium telluride prior to addition to the diynone. In the absence of the added base, the tellurin-4-ones **29** are not isolated from the reactions.

The addition of tetra-*n*-butylammonium fluoride to bis(*tert*-butyldimethylsilyl)telluride in the presence of diynone **30a** and *tert*-butanol as a proton source gives tellurin-4-one **29a** in 19% yield.[38] The major product of this reaction is the five-membered ring compound **32a** (R = R′ = Ph), which is isolated in 28% yield. This reaction illustrates the importance of proper "buffering" in these reactions to optimize the amount of six-membered ring product.

The preparation of tellurin-4-ones unsubstituted at the 2- and/or 6-positions requires protection of the terminal acetylides. The addition of disodium telluride to 1,4-pentadiyn-3-one gives only oligomeric products and none of the desired parent 4*H*-tellurin-4-one (**29d**).[42] The addition of disodium telluride to 1-phenyl-1,4-pentadiyn-3-one gives only a 12% yield of the desired 1-phenyl-4*H*-tellurin-4-one (**29e**).[43] However, the use of trimethylsilylacetylenes allows the preparation of the unsubstituted derivatives as shown in Scheme 14. The addition of disodium telluride to 1,5-bis(trimethylsilyl)-1,4-pentadiyn-3-one (**30d**) gives 4*H*-tellurin-4-one (**29d**) in 38% isolated yield, and the addition of

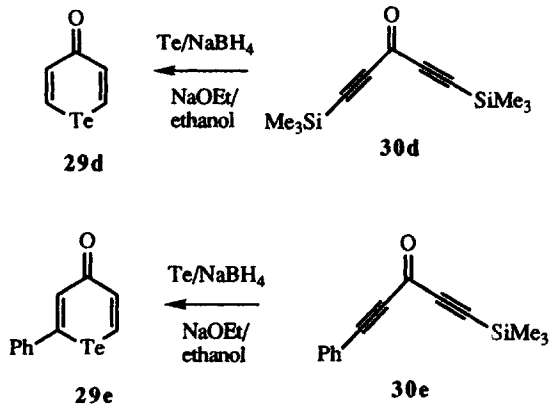

Scheme 14

disodium telluride to 1-trimethylsilyl-5-phenyl-1,4-pentadiyn-3-one (**30e**) gives 1-phenyl-4*H*-tellurin-4-one (**29e**) in 32% isolated yield.[42]

4*H*-Tellurin-4-one **29b** can be substituted at the 3-position by metallation of the symmetrical tellurin-4-one with lithium diisopropylamide followed by quenching with an appropriate electrophile.[49] As shown in Scheme 15, metallation of the ring generates the 3-lithio derivative **33**. Anion **33** either is in equilibrium with ring-opened anion **34** or irreversibly ring-opens to **34** since the addition of methyl triflate or methyl iodide to the anion generates the methyl telluroether **35** in 93% isolated yield. However, the use of either phenyl ditelluride or benzaldehyde as an electrophile gives carbon-functionalized tellurin-4-ones **36** in 18 and 80% isolated yields, respectively.

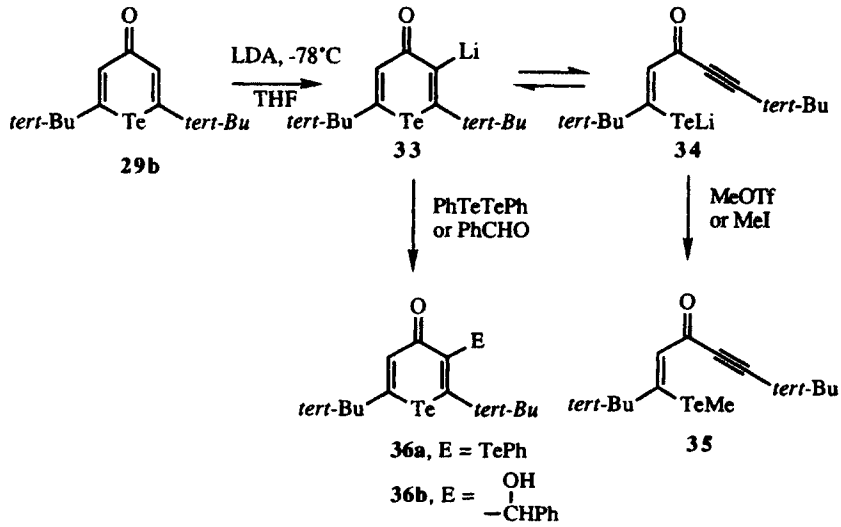

Scheme 15

The tellurin-4-ones **29** also have been prepared with tellurium in the tellurium(IV) oxidation state.[50] The oxidative addition of chlorine, bromine, or iodine to **29b** gives dihalides **37a** in 79% yield, **37b** in 71% yield, and **37c** in 46% yield, while the oxidation of **29b** with peracetic acid gives the acetate analog **37d** in 76% yield. Oxidative addition of bromine to **29a** has given tellurium(IV) dibromide **38a** in 79% yield, while peracetic acid oxidation gives the corresponding acetate **38b** in 72% yield.

4*H*-Tellurin-4-thiones **39** have been prepared from the corresponding tellurin-4-ones **29** by the use of the Lawessen reagent.[41] The conversions go in nearly quantitative yield for the preparation of **39a** and **39b** (96% for each) and in 63% yield for the preparation of **39c**.

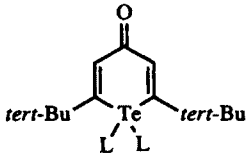

37a, L=Cl
37b, L=Br
37c, L=I
37d, L=OAc

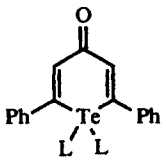

38a, L=Br
38b, L=OAc

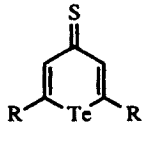

39a, R=Ph
39b, R=*tert*-Bu
39c, R=Me

3. *2H- and 4H-Tellurins and Derivatives*

The diisobutylaluminum hydride reduction of 4*H*-tellurin-4-ones **29** gives good yields of 4*H*-tellurins **40**.[51] Compound **40a** is isolated in 65% yield, and compound **40b** is isolated in 73% yield. In these reactions, the corresponding 2*H*-tellurins **41** are produced as minor components in 4% yield for **41a** and 5% yield for **41b**. As shown in Scheme 16, the initial reduction of the tellurin-4-one produces a 4-oxoaluminum compound that could solvolyze to the telluropyrylium species **42**. Hydride reduction of the telluropyrylium species via nucleophilic attack of hydride at the 4-position would give the 4*H*-tellurin products (as well as the 2*H*-tellurin minor component via nucleophilic attack of hydride at the 2-position).

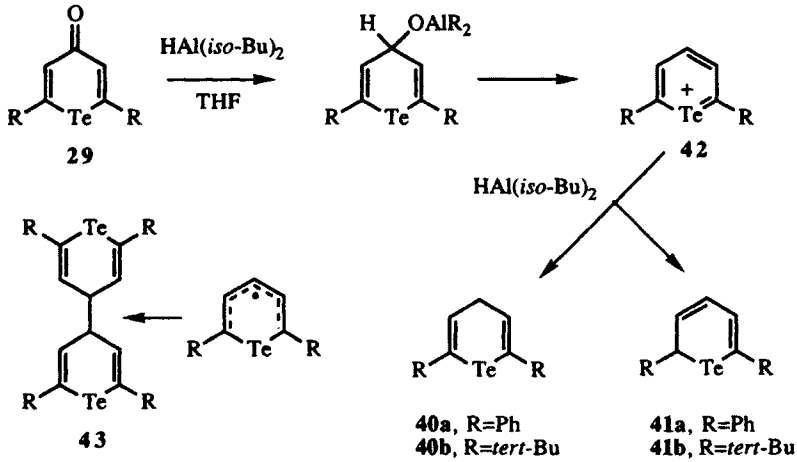

Scheme 16

The actual reaction mechanism may not be so simple, however. The tellurin dimer **43** (R = *tert*-Bu) is produced in 29% yield on diisobutylaluminum hydride reduction of **29b**.[51] The formation of the dimer is suggestive of radical

coupling from the telluropyranyl radical shown in Scheme 16. One-electron electrochemical reduction of **42** (R = *tert*-Bu) leads to formation of the dimer **43** (R = *tert*-Bu) in essentially quantitative yield. Electrochemical oxidation of the dimer **43** regenerates the telluropyrylium salt **42**. These data obfuscate a clear mechanistic picture since both one-electron and two-electron pathways appear to be operative in the diisobutylaluminum hydride reductions.

4*H*-Tellurins bearing alkylidene groups in the 4-position have been prepared via several routes. The condensation of malononitrile with the 1,1-diacetoxy-4*H*-tellurin-4-one **37d** gives 4-dicyanomethyliden-4*H*-tellurin **44** in 29% yield.[50] The condensation of malononitrile with 1,1-diacetoxy-4*H*-2,6-diphenyltellurin-4-one **38b** gives 4-dicyanomethyliden-4*H*-tellurin **45** in roughly 24% yield and the tellurium(IV) analog **46** in 11% yield.[50] The formation of compound **46** presumably arises from attack of malononitrile anion on tellurium followed by loss of a cyano group to generate the tellurium(IV) ylide.

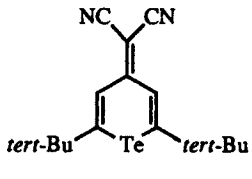

44

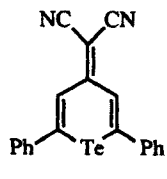

45

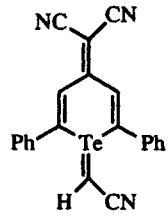

46

The condensation of malononitrile with tellurin-4-ones **29a** and **29b** in the presence of base did not give compounds **44** and **45**.[50] Unreacted tellurin-4-one was recovered in these reactions. This behavior is not observed with thiopyranones and selenopyranones where condensation reactions with malononitrile give dicyanomethylidene products.[52] Presumably, the tellurium(IV) center activates the carbonyl group at the 4-position to nucleophilic attack in **37** and **38**. Oxidation of the tellurium center utilizing the 5*p* orbital of tellurium would eliminate the possibility of an "aromatic" resonance form for the tellurin-4-one.

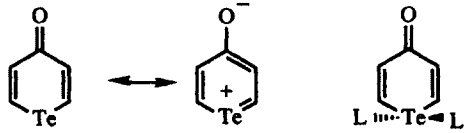

Tellurium(IV) analogs of **44** and **45** have been prepared.[50] Even though the dicyanomethylidene group is a strongly electron-withdrawing substituent, oxidative addition reactions occur readily to give tellurium(IV) derivatives **47** and **48**. Peracetic acid oxidation of **44** and **45** gives **47a** and **48a** in 48 and 65% yields, respectively, as crystalline solids. Oxidative addition of chlorine to **44** gives **47b** in 82% yield, while oxidative addition of bromine to **44** and **45** gives the corresponding dibromides **47c** and **48b** in 70 and 79% yields, respectively.

Oxidative addition of iodine to **44** is more sluggish than oxidative addition of chlorine or bromine, but diiodide **47d** is isolated in 50% yield.

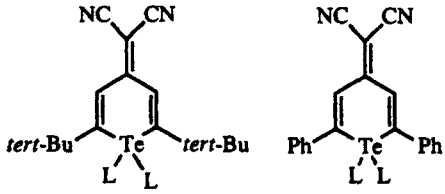

47a, L=OAc
47b, L=Cl
47c, L=Br
47d, L=I

48a, L=OAc
48b, L=Br

4*H*-Tellurins bearing a Meldrum acid residue at the 4-position have been prepared by the condensation of Meldrum's acid with 4-ethoxytellurapyrylium salts **49**[39] and **50**[52] as shown in Scheme 17. The Meldrum acid adducts **51** and **52** were isolated in 80 and 78% yields, respectively, as red crystalline solids. The 4-ethoxytellurapyrylium salts **49** and **50** are prepared by alkylation of tellurin-4-ones **29a** and **29b** with ethyl fluorosulfonate.[39,52]

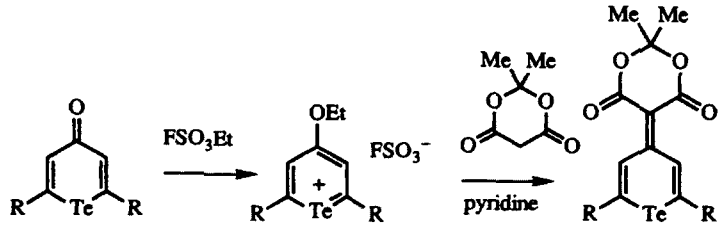

29a, R=Ph
29b, R=*tert*-Bu

49, R=Ph
50, R=*tert*-Bu

51, R=Ph
52, R=*tert*-Bu

Scheme 17

4-*H*-Tellurins bearing an acetaldehyde or substituted-acetaldehyde residue at the 4-position have been prepared via two different routes. As shown in Scheme 18, the condensation of a 4-methyltellurapyrylium salt **53** with *N*,*N*-dimethylthioformamide gives iminium salts **54** in roughly 90% yields.[39,53,54] Hydrolysis of the iminium salts **54** gives nearly quantitative yields of aldehydes **55**. Alternatively, 2,6-disubstituted tellurapyrylium compounds **56** react with enamines to generate iminium salts **54c–54e**[55] as shown in Scheme 18. Hydrolysis of the iminium salts generates the aldehydes **55c–55e** in 78%,[54] 74%,[55] and 6%[55] isolated yields, respectively.

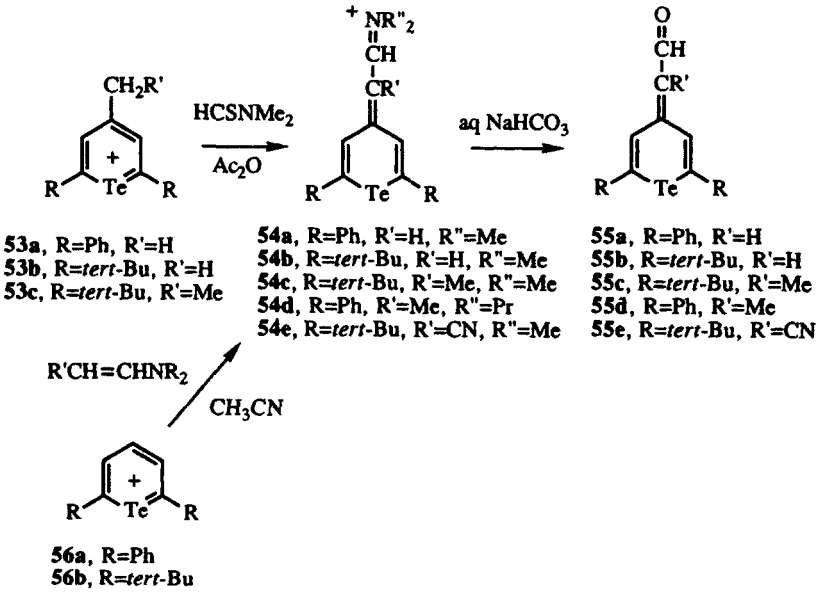

Scheme 18

C. Synthesis of the Benzotellurane Nucleus and Derivatives

1. The Benzotellurane Nucleus

The benzotellurane nucleus has been prepared by the addition of a tellurium atom to a 5-atom carbon unit to form the tellurane ring, and more highly oxidized materials have been prepared by cyclization of a six-atom unit to form the tellurane ring. The naphthotelluranes **57** and **58** are prepared as shown in Scheme 19.[56] Nucleophilic attack of tellurium of 1,8-di-(bromomethyl)naphthalene gives diiodotellurane **57** in 58% isolated yield. Hydrazine reduction of tellurium(IV) to tellurium(II) gives tellurane **58** in 46% isolated yield.

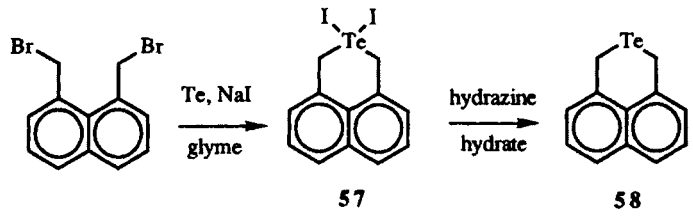

Scheme 19

2. *Benzotellurane-4-ones*

The syntheses of benzotellurane-4-one analogs have employed cyclization reactions of six-atom units[57–59] or the reduction of benzotellurin-4-one compounds.[60] The syntheses of benzotellurane-4-ones and the more highly oxidized benzotellurin-4-ones have not been trivial pursuits. Friedel–Crafts acylation reactions of aryltelluro-substituted molecules often give unexpected products due to the lability of the tellurium–carbon bond.

The first benzotellurane-4-one to be synthesized was the 2-phenyl derivative **59**, which has been prepared as shown in Scheme 20.[57] Condensation of benzaldehyde with *o*-methyltelluroacetophenone gives chalcone **60** in 50% isolated yield. The reaction of **60** with hydrobromic acid in acetic acid gives two products. The major product, isolated in 70% yield, is tellurenyl bromide **61**. The minor product is the desired benzotellurane-4-one **59**, isolated in 20% yield. Mechanistically, the cyclization of **60** to **59** involves cleavage of one tellurium–carbon bond with formation of a new tellurium–carbon bond. As shown in Scheme 20 for one scenario, the addition of hydrobromic acid to the double bond of chalcone **60** would lead to an intramolecular alkylating agent for tellurium (**62**). The resulting telluronium species **63** is demethylated by nucleophilic attack of bromide to give the benzotellurane-4-one **59**.

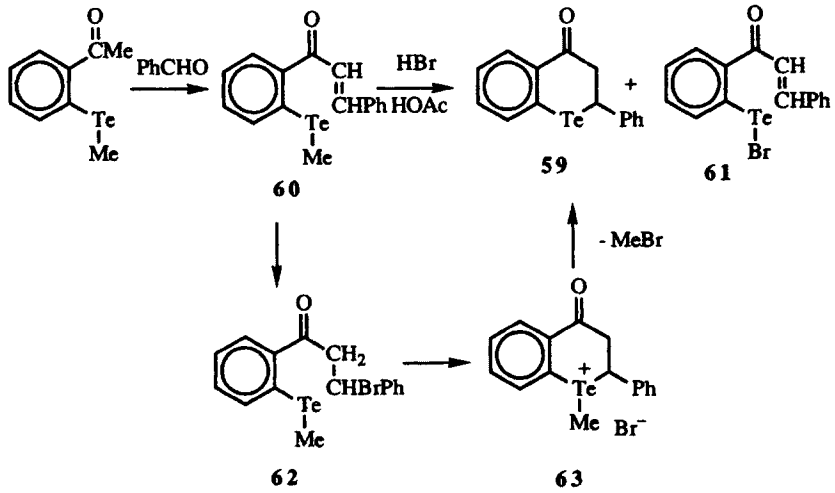

Scheme 20

Tellurenyl bromide **61** arises from nucleophilic attack of bromide at tellurium with electrophilic attack at carbon. (The electropositive character of tellurium relative to carbon leads to a reversal of polarization in the tellurium–carbon bond relative to oxygen–carbon and sulfur–carbon bonds.) Part of the driving force for the production of **61** is the formation of a three-center, four-electron

bond involving tellurium as the central electropositive element and bromine and the carbonyl oxygen as the electronegative ligands.[61-63] Tellurenyl bromide **61** is a nontraditional heterocycle in that a covalent interaction of tellurium and the carbonyl oxygen leads to the formation of a five-membered ring as shown below.

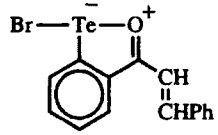

A more general approach to the benzotellurane-4-ones involves intramolecular cyclization of 3-aryltelluropropanoic acids **64** under mild conditions to give the benzotellurane-4-ones **65** as shown in Scheme 21.[58] The use of butyldichloromethyl ether with aluminum chloride gives Friedel–Crafts acylation

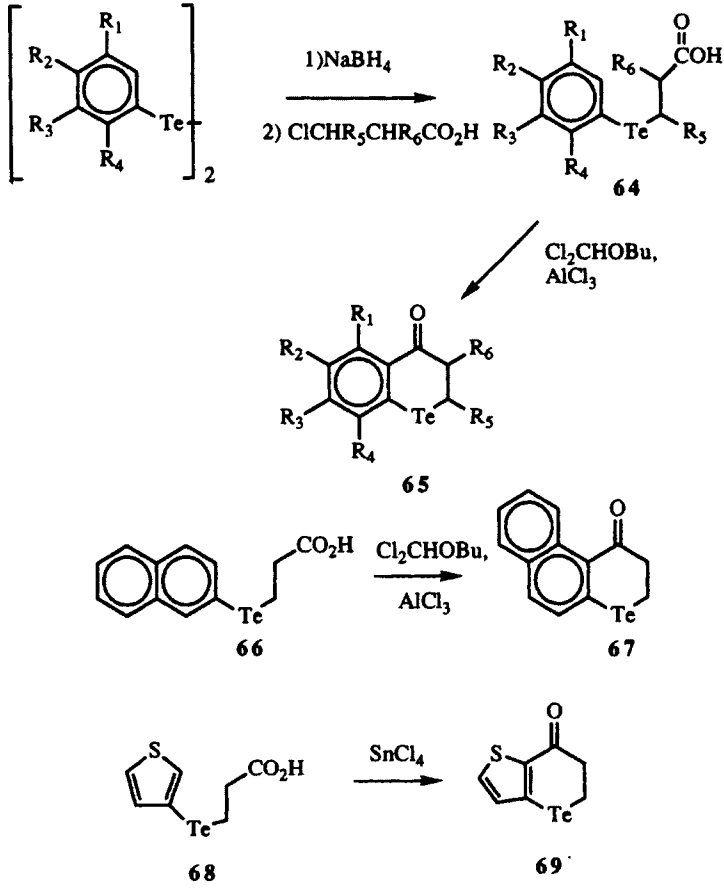

Scheme 21

without tellurium–carbon bond cleavage. The benzotellurane-4-ones prepared in this manner are listed in Table 5.

Other aromatic rings also undergo the cyclization. The β-naphthyl propanoic acid **66** gives **67** in 66% isolated yield via intramolecular acylation at the α carbon of the ring. Thiophene derivative **68** is cyclized under very mild conditions with tin tetrachloride as catalyst to give thiophenotellurane-4-one in 65% isolated yield.[59]

Reduction of benzotellurin-4-ones with hypophosphoric acid has also given benzotellurane-4-ones in good yield.[60] Reductions of 4*H*-benzotellurin-4-one (**70**) and 4*H*-2-methyltellurin-4-one (**71**) give benzotellurane-4-ones **65a** and **65g** in 60 and 65% yields, respectively. Similarly, reduction of thiophene derivatives **72** and **73** gives **69** and **74** in 60 and 10% isolated yields, respectively.

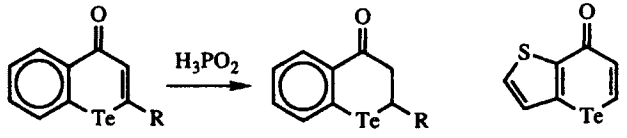

70, R=H
71, R=Me

65a, R=H
65g, R=Me

72

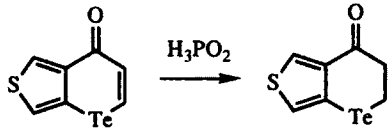

73 **74**

3. *Benzotellurane-2-ones and Benzo-2-tellurane-1-one*

One compound surprisingly absent from the literature is benzotellurane-2-one (**75**). Selenium, sulfur, and oxygen analogs of **75** have been prepared.[64–70]

Structural isomers of **75** have been prepared as shown in Scheme 22. Benzo-2-tellurane-1-one (**76**) is prepared in 52% yield by the addition of sodium hydrogen telluride to *o*-(2-bromoethyl)benzoyl chloride,[71] while benzo-2-tellurane-3-one (**76a**) is prepared in 60% yield by the addition of sodium hydrogen telluride to *o*-(bromomethyl)phenylacetyl chloride using tetra-*n*-butylammonium hydrosulfate as a phase-transfer catalyst.[71a]

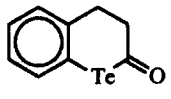

75

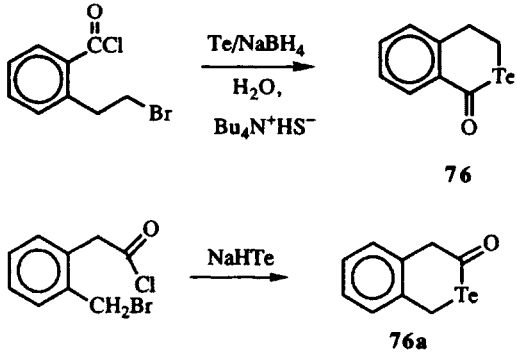

Scheme 22

D. Syntheses of the Benzotellurin Nuclei and Derivatives

1. 2H-Benzotellurins and Derivatives

2*H*-Benzotellurins **77** have been prepared by reduction of benzotellurane-4-ones followed by dehydration of the resulting alcohol as shown in Scheme 23.[58,59] Sodium borohydride reduction of benzotellurane-4-ones **65**, **67**, or **69** gives the corresponding 4-hydroxybenzotelluranes **78** as compiled in Table 6. Distillation of the 4-hydroxybenzotelluranes from potassium bisulfate under

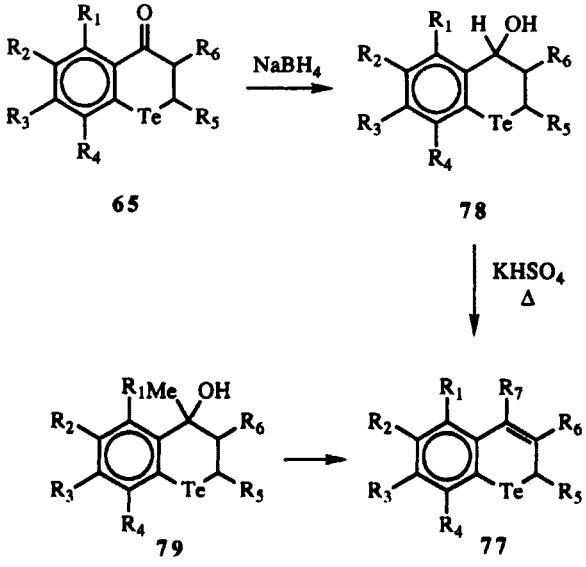

Scheme 23

reduced pressure gives the 2*H*-benzotellurins **77** as compiled in Table 7. The addition of methylmagnesium bromide to benzotellurane-4-one **65a** gives 4-hydroxy-4-methylbenzotellurane **79**, which is dehydrated via distillation under reduced pressure over potassium bisulfate to give 4-methyl-2*H*-benzotellurin **77** (see Table 7).

Attempts to oxidize 2*H*-benzotellurins **77** to the corresponding 2*H*-benzotellurin-2-ones **80** have been unsuccessful with oxidants such as selenium dioxide, chromium trioxide-pyridine, or thallium triacetate.[59] Selenium dioxide oxidations give benzotellurophenes from 2*H*-benzotellurins via ring contraction as shown below. Thallium triacetate oxidation gives *o*-cinnamoyl ditelluride derivatives.

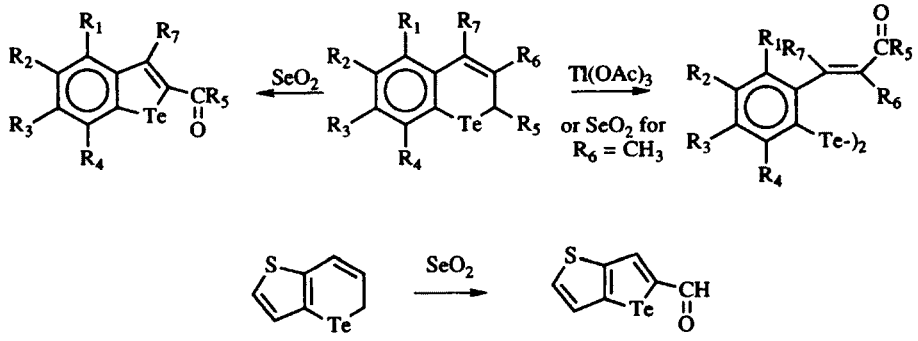

2*H*-Benzotellurin-2-one **80** has been successfully prepared from *o*-(methyltelluro)benzaldehyde **81** in two steps as shown in Scheme 24.[64] Condensation of malonic acid with aldehyde **81** gives cinnamic acid derivative **82** in 50% yield. Cyclization with zinc chloride in dichloromethyl methyl ether gives 2*H*-benzotellurin-2-one in 20% isolated yield.

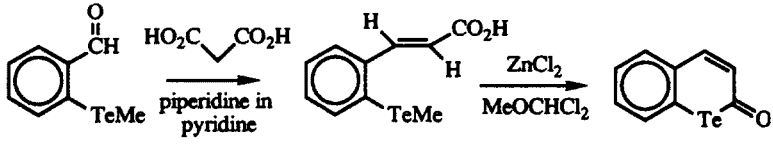

81 **82** **80**

Scheme 24

The isomeric 2-benzotellurin-1-one **83** has been prepared as outlined in Scheme 25.[72] The Michael addition of sodium methyltelluride to ester **84** followed by saponification with potassium hydroxide in aqueous ethanol gives benzoic acid derivative **85** in 82% isolated yield. The acid is converted to the acid chloride with anhydrous zinc chloride in dichloromethyl methyl ether, and the resulting compound is cyclized with aluminum chloride in dichloromethane to give isotellurocoumarin **83** in 30% yield.

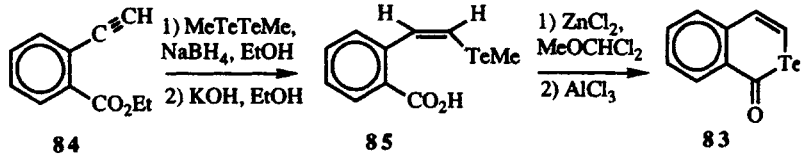

84 **85** **83**

Scheme 25

4*H*-Benzotellurin derivatives **86** have been prepared by the reduction of 4*H*-benzotellurin-4-ones with diisobutylaluminum hydride.[51] As shown in Scheme 16, this reaction most likely proceeds through a benzotelluropyrylium intermediate. In the reduction of the benzotellurin-4-ones, no 2*H*-benzotellurin derivatives were detected, and the 4*H*-benzotellurins were isolated in 85, 82, and 75% yields for **86a**, **86b**, and **86c**, respectively.

86a, R=Ph
86b, R=*tert*-Bu
86c, R=H

Tellurium(IV) analogs of the 4*H*-benzotellurins have been prepared. Oxidative addition of chlorine and bromine to **86b** gives tellurium(IV) dichlorides **87** and **88** in 80 and 92% isolated yields, respectively.[73]

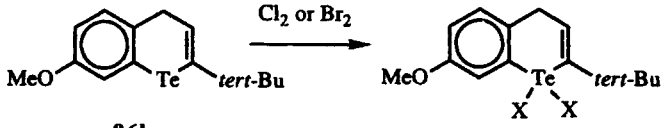

86b

87, X = Cl
88, X = Br

2. *4H-Benzotellurin-4-ones and Derivatives*

4*H*-Benzotellurin-4-ones **89** have been prepared by two different routes. The first preparation of 4*H*-benzotellurin-4-ones is outlined in Scheme 26.[60] In this particular route, the second tellurium–carbon bond is formed in the cyclization step. The condensation of the dimethyl acetal of either dimethylformamide or dimethylacetamide with an aryltellurenyl bromide bearing an *ortho*-acetyl group leads to the homologous amides **90a** and **90b** in 80 and 45% isolated

yields, respectively. The tellurenyl bromides **90** are cyclized with hypophosphoric acid to give the 4*H*-benzotellurin-4-ones **89** in 45% isolated yield for both **89a** and **89b**. If used in excess, the hypophosphoric acid acts as a reducing agent for the double bond of the 4*H*-benzotellurin-4-one to give the corresponding benzotellurane-4-ones.

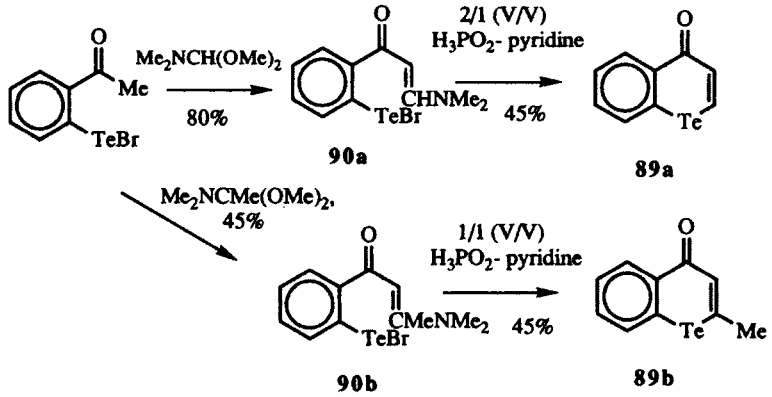

Scheme 26

The three possible fused-thiophene analogs of **89** have also been prepared by this route as shown in Scheme 27.[60] Even though the thiophene nucleus is highly reactive toward electrophiles, the tellurenyl bromide cyclization with hypophosphoric acid leads to the desired products **90–92**.

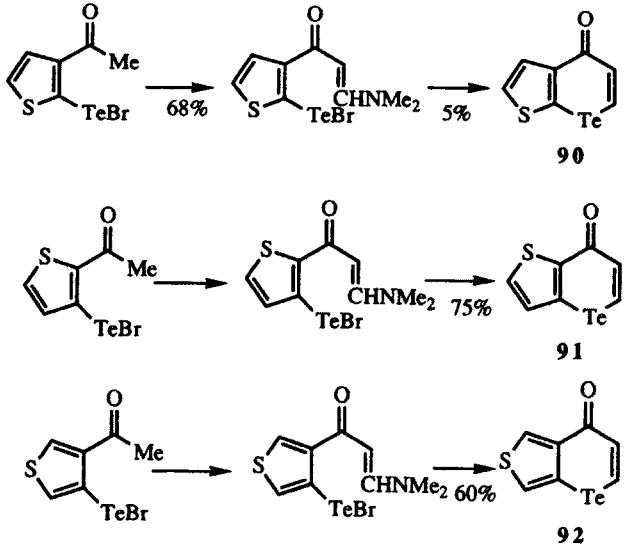

Scheme 27

The synthetic sequences outlined in Schemes 26 and 27 suffer from an inability to prepare 4*H*-2-phenylbenzotellurin-4-one. The parent "telluroflavone" remains unknown. More highly substituted derivatives of "telluroflavone" have been prepared by the second general route to 4*H*-benzotellurin-4-ones described below.[74,75]

The second route to 4*H*-benzotellurin-4-ones involves intramolecular acylation of the aryl ring to form the final carbon–carbon bond of the ring system.[74–76] The intramolecular acylation of 3-aryltelluropropenoic acid derivatives can proceed via two different paths. As shown in Scheme 28, one path involves *ipso* acylation of the aryl carbon atom bearing tellurium to give rearrangement products of the acid chloride. Thus, treating acid chlorides **93** with aluminum chloride at $-78°C$ in dichloromethane leads to *ipso* acylation followed by attack of chloride to give oxatellurolylium chlorides **94**.[74] Similar chemistry has been observed with *o*-(phenyltelluro)benzoyl chloride **95** where reaction with zinc chloride gives *o*-(chlorotellurenyl)benzophenone **96** instead of the desired telluroxanthone.[77,78] In rearrangements of this type, the driving force for reaction is the formation of three-center, four-electron bonds. Neither electron-donating nor electron-withdrawing substituents in the *ortho* or *para* positions of the tellurium-bearing ring lead to *ortho* acylation.

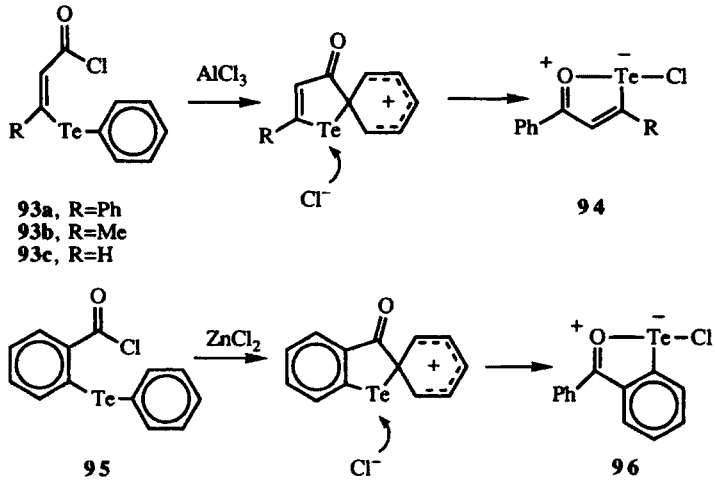

Scheme 28

As shown in Scheme 29, *ortho–para*-directing substituents that are *meta*-deactivating on the basis of σ^+ substituent constants[79] can be used to direct *ortho* acylation of the tellurium-bearing ring.[75,76] When such substituents are placed *meta* to the tellurium-bearing carbon as in acid chlorides **97**, benzotellurin-4-ones **98** can be isolated as products with varying amounts of the

oxatellurolylium chlorides **99**. The methoxy group ($\sigma_p^+ = -0.648$ and $\sigma_m^+ = 0.047$)[79] and the fluoro group ($\sigma_p^+ = -0.247$ and $\sigma_m^+ = 0.352$)[79] have been found to be useful as substituents in these reactions, and benzotellurin-4-ones **98** prepared in this manner are summarized in Table 8. These results are in direct contrast to the cyclization of acid chloride **97e** bearing a methyl substituent ($\sigma_p^+ = -0.256$ and $\sigma_m^+ = -0.065$).[79] The methyl substituent is weakly *meta*-activating in addition to being *ortho–para*-activating. The only observed reaction on treatment of acid chloride **97e** with aluminum chloride is oxatellurolylium chloride **99e**.

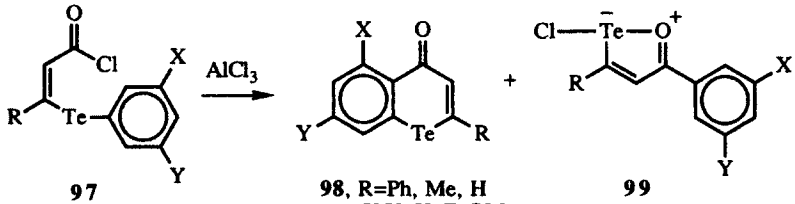

97 **98**, R=Ph, Me, H; X,Y=H, F, OMe **99**

Scheme 29

With the aryltellurogroups of acid chlorides **97**, *ortho* acylation is observed with one or more σ_p^+-activating, σ_m^+-deactivating substituents *meta* to the carbon bearing tellurium. Other *meta* substituents and both activating and deactivating *para* substituents give only *ipso* acylation. Of the two effects, *ortho–para* activation appears to be more important than *meta* deactivation if one compares the substituent constants of the methoxy ($\sigma_p^+ = -0.648$ and $\sigma_m^+ = 0.047$)[79] and fluoro ($\sigma_p^+ = -0.247$ and $\sigma_m^+ = 0.352$)[79] substituents. The selenium and sulfur analogs of **93** and **97** have quite different substituent effects. With (arylseleno)cinnamoyl chlorides **100**, *ortho–para*-activating substituents *para* to the carbon bearing selenium promote *ipso* acylation to give oxaselenolylium chlorides **101**, while the phenyl group promotes *ortho* acylation and the formation of 4*H*-2-phenylselenin-4-one (**102**) as shown in Scheme 30.[75] Other mildly activating substituents such as 1-naphthyl also give *ipso* acylation in the selenium series.

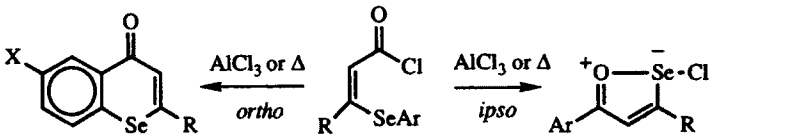

102a, R=Ph, X=H, 85%
102b, R=Me, X=F, 24%
102c, R=Me, X=OMe, 0%
102d, R=Ph, X=benzo, 0%
102e, R=Ph, X=OMe, 0%

100a, R=Ar=Ph
100b, R=Me, Ar=*p*-FPh
100c, R=Me, Ar=*p*-MeOPh
100d, R=Ph, Ar=1-naphthyl
100e, R=Ph, Ar=*p*MeOPh

101a, R=Ar=Ph, 0%
101b, R=Me, Ar=*p*-FPh, 36%
101c, R=Me, Ar=*p*-MeOPh, 96%
101d, R=Ph, Ar=1-naphthyl, 79%
101e, R=Ph, Ar=*p*-MeOPh, 95%

Scheme 30

(Arylthio)cinnamoyl chlorides **103** give only 4*H*-2-phenylbenzothiopyran-4-ones **104** on treatment with aluminum chloride as shown in Scheme 31. No oxathiolylium salts **105** were detected by ^{1}H NMR spectroscopy even with a strongly *ortho–para*-directing methoxy substituent in the *para* position of the arylthio ring.[75]

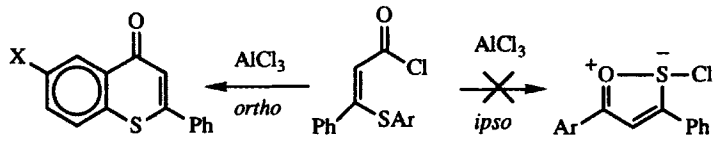

104a, X=H, 85%
104b, X=OMe, 74%

103a, Ar=Ph
103b, Ar=*p*-MeOPh

105

Scheme 31

The carboxylic acids **106** give 4*H*-benzotellurin-4-ones **98** on treatment with phosphorus pentoxide in methanesulfonic acid.[80] As shown in Table 9, a variety of 4*H*-benzotellurin-4-ones can be prepared in this manner.

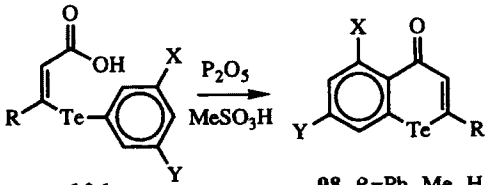

106

98, R=Ph, Me, H
X,Y=H, F, OMe

3. *5-Hydroxy-4H-benzotellurin-4-ones*

5-Methoxychromones **107** and 5-methoxyflavones **108** have been converted to the phenolic chromones and flavones with boron trichloride as shown in Scheme 32.[81] The intermediate dichloroboronates, which were not isolated, are rapidly hydrolyzed in water to give the corresponding 5-hydroxy compounds.

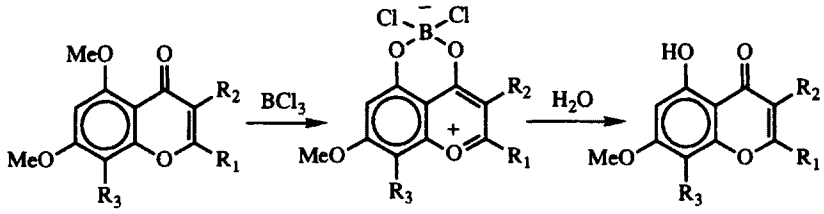

107, R_1 = Me, R_2 = H, R_3 = $CH_2CH{=}CMe_2$
108, R_1 = 3,4-$(MeO)_2C_6H_3$, R_2 = OMe, R_3 = H

Scheme 32

Similar chemistry has been used for the conversion of 5-methoxy-4-*H*-benzotellurin-4-ones of structure **98** to the corresponding difluoroboronate compounds **109**.[76] Hydrolysis of the difluoroboronates gives the corresponding phenolic benzotellurin-4-ones **110** as shown in Scheme 33. The various 5-hydroxy-4*H*-benzotellurin-4-ones produced via this route are compiled in Table 10.

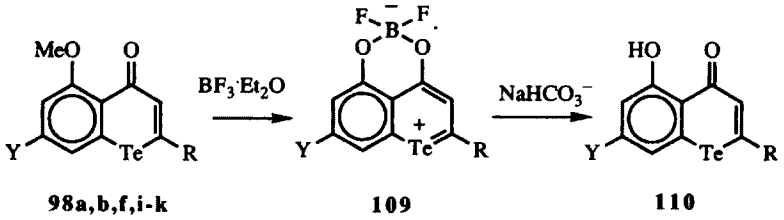

98a,b,f,i-k **109** **110**

Scheme 33

4. *2-Styryl-4H-benzotellurin-4-ones*

The condensation of 2-methyl-4*H*-benzotellurin-4-ones with various aldehydes and ketones gives various styryl-substituted derivatives. Typically, the 2-methyl substituent is activated by the addition of a Lewis acid to the carbonyl

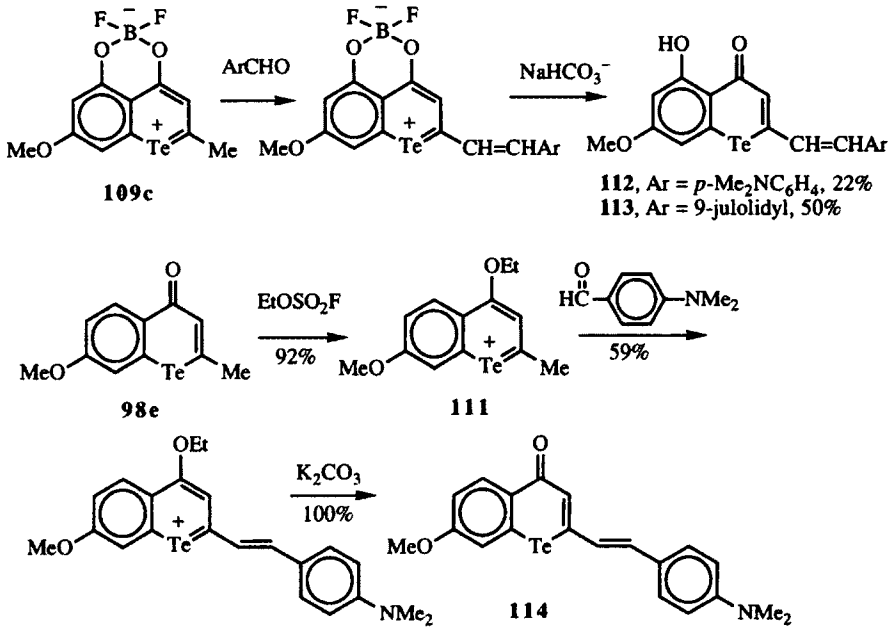

Scheme 34

such as borontrifluoride etherate to **98f** (to give **109c**) or ethyl fluorosulfonate to **98e** (to give **111**).[76] As shown in Scheme 34, hydrolysis of the intermediate condensation products gives the corresponding benzotellurin-4-ones **112–114**.

5. *4H-Benzotellurin-4-thiones and Derivatives*

4*H*-benzotellurin-4-thiones **115** have been prepared from the corresponding benzotellurin-4-ones **98** by the use of the Lawessen reagent.[82] The conversion of **98a** to **115** is nearly quantitative in yield. However, the use of excess Lawessen reagent and longer reaction times leads to oxidation of tellurium as well as thione formation to give the sulfur analog of a telluroxide **116**.

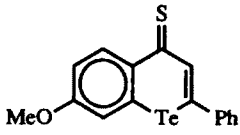

115

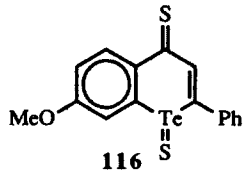

116

E. Syntheses of the Telluroxanthene and Telluroxanthone Nuclei and Derivatives

Constructions of the telluroxanthene and telluroxanthone nuclei have consisted of either a one-atom addition to a five-atom fragment or the cyclization of a six-atom array to construct the central ring of the system. Derivatives have been prepared via further functionalization of the parent nuclei.

1. *Telluroxanthene and Derivatives*

The first reported synthesis of telluroxanthene (**117**) is outlined in Scheme 35.[83,84] The cyclization step involves electrophilic attack of tellurium on a phenyl ring to form the central ring of the dibenzo-fused system. Lithiation of *o*-bromodiphenylmethane, tellurium insertion into the C–Li bond, and oxidation gives the ditelluride **118**. The addition of chlorine[83] or bromine[84] to ditelluride **118** gives the trihalotellurium(IV) species **119a** in 93% isolated yield and **119b** in 98% isolated yield. The addition of aluminum chloride to **119a** gives the dichlorotelluroxanthene **120** in 80% isolated yield. Potassium bisulfite reduction of tellurium(IV) to tellurium(II) gives telluroxanthene (**117**) in 93% isolated yield.

More direct routes to both **117** and **120** have been reported.[85] The addition of *n*-butyllithium to *o,o'*-dibromodiphenylmethane gives, via metal–halogen exchange, *o,o'*-dilithiodiphenylmethane (**121**) as shown in Scheme 36. The addition

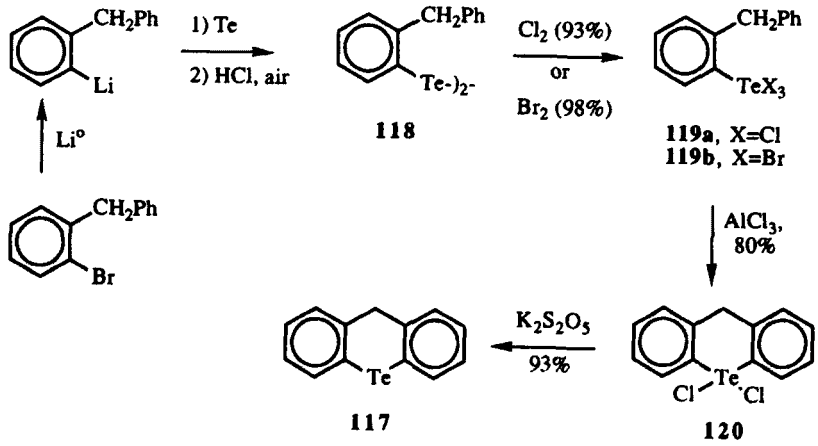

Scheme 35

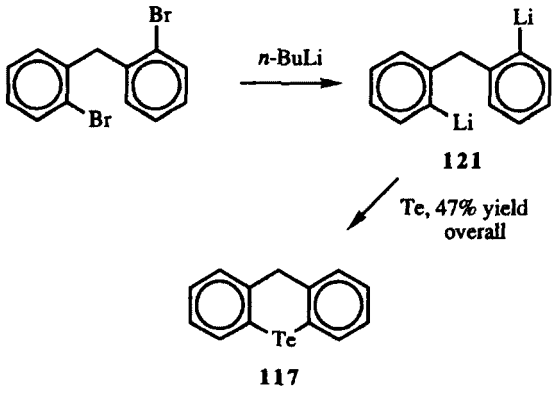

Scheme 36

of tellurium metal to **121** gives telluroxanthene (**117**) in 47% isolated yield. The addition of chlorine to **117** gives dichlorotelluroxanthene **120** in 81% isolated yield.

A carboxylic acid derivative of telluroxanthene (**117**) has been prepared as shown in Scheme 37.[84] Metallation of **117** with phenyllithium gives 9-lithiotelluroxanthene (**112**). The addition of carbon dioxide to **122** and an acidic workup give 9-carboxytelluroxanthene (**123**).

The addition of nucleophiles to various telluroxanthylium salts has given a variety of 9-substituted telluroxanthenes.[86,87] The additions of sodium methoxide and sodium isopropoxide to telluroxanthylium perchlorate (**124**) give 9-methoxytelluroxanthene (**125**) and 9-isopropoxytelluroxanthene (**126**), respectively, as shown in Scheme 38.[86] The addition of ammonium chloride to **124**

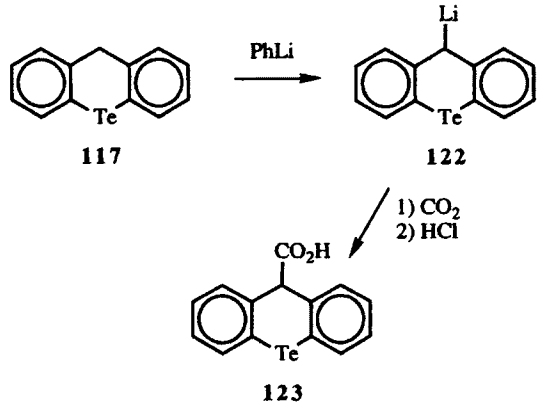

Scheme 37

gives the dimer **127**—not the expected 9-chlorotelluroxanthene.[86] The dimer **127** has also been prepared by the reduction of telluroxanthone (**128**) with zinc in glacial acetic acid.[88]

9-(*p*-Tolyl)telluroxanthylium perchlorate (**129**) adds a variety of nucleophiles to give 9,9-disubstituted telluroxanthenes **130**.[86,87,89] The addition of ammonium halides to **129** gives the 9-halo derivatives instead of dimeric products.[86,87] Sodium methoxide introduces a 9-methoxy substituent and potassium hydroxide introduces a 9-hydroxy substituent.[86] The additions of ammonium pseudohalides (thiocyanate, acetate)[87] and sodium azide[89] to **129** also give 9-substituted derivatives.

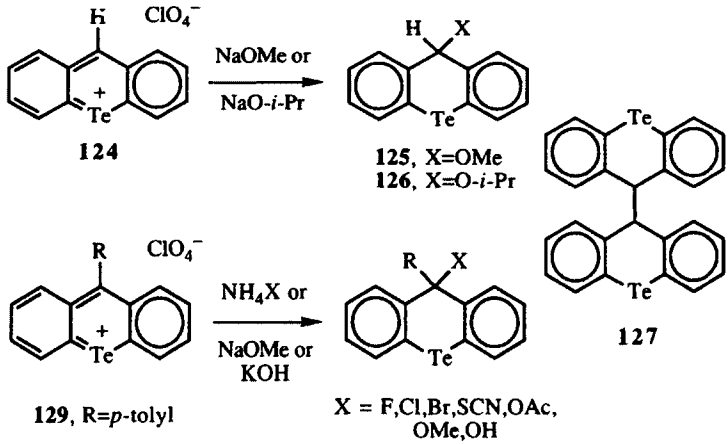

Scheme 38

Although nucleophilic additions to the carbonyl carbon of telluroxanthones are typically followed by elimination reactions to generate telluroxanthylium species, these additions can be stopped to give 9-hdyroxytelluroxanthone

derivatives. The addition of sodium borohydride[91] or lithium aluminum hydride[84] to telluroxanthone (**128**) gives 9-hydroxytelluroxanthene (**131**) as shown in Scheme 39. Similarly, the addition of Grignard reagents to the carbonyl carbon of **128** gives 9-alkyl-or 9-aryl-9-hydroxytelluroxanthenes **132**.[84,90-92]

The addition of lithium aluminum hydride to 9-(*p*-tolyl)-9-hydroxytelluroxanthene (**132a**) in the presence of aluminum trichloride gives 9-(*p*-tolyl)telluroxanthene (**133**).[91] Although a nucleophilic displacement via hydride is suggested, it would appear to be more reasonable to form telluroxanthylium **129** via an elimination reaction followed by hydride addition to the telluroxanthylium salt.

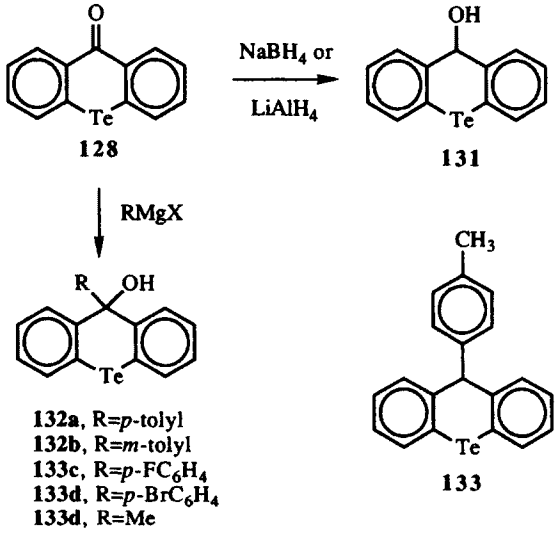

Scheme 39

2. *Tellurium(IV) Derivatives of Telluroxanthene*

Several tellurium(IV) derivatives of telluroxanthene (**117**) have been prepared. In addition to the dichloro derivative **120**,[83-85] the corresponding dibromo derivative **134** and diiodo derivative **135** have been prepared by oxidative addition of the corresponding halogen to telluroxanthene (**117**).[84] As with **120**, both **134** and **135** are reduced to telluroxanthene (**117**) in the presence of sulfite.

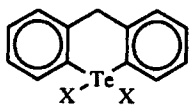

134, X=Br
135, X=I

The addition of Meldrum's acid (5,5-dimethyl-1,3-dioxocyclohexane) to **120** in the presence of triethylamine gives tellurium(IV) ylide **136** in quantitative yield as shown in Scheme 40.[84] Compound **136** reacts with ethanolic hydrogen fluoride to give difluorotelluroxanthene **137** and with trifluoroacetic acid to give the bistrifluoroacetate **138**.[84]

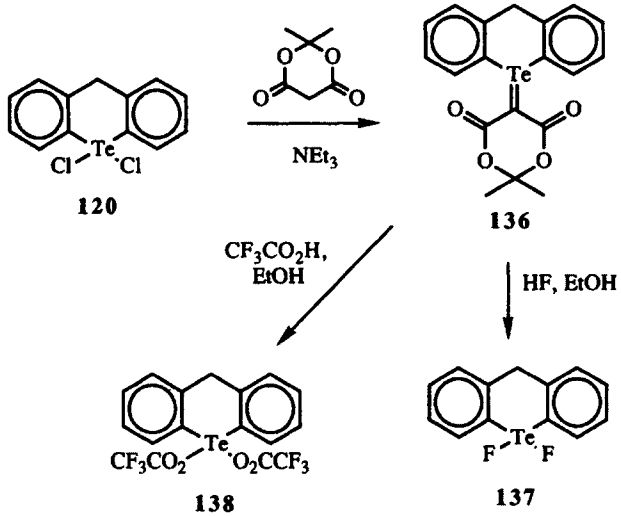

Scheme 40

The addition of iodine to dimer **127** gives tetraiodide **139**.[84,93] The tetraiodide is reduced by the lithium salt of tetracynaoquinodimethane (TCNQ) to give a one-to-one complex of **127** and TCNQ.

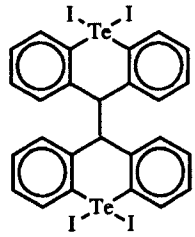

139

F. Syntheses of Telluroxanthones

1. Telluroxanthone and Tellurium(IV) Derivatives

Attempts to synthesize telluroxanthone (**128**) via intramolecular acylation of the acid chloride **95** were unsuccessful, as shown in Scheme 28.[77,78] *Ipso*

acylation at the carbon bearing tellurium was observed leading to intramolecular rearrangement to **96**. Since this route represents the most direct entry into the telluroxanthone system and is uniformly unsuccessful, other routes to telluroxanthone have been less direct and few in number.

The first reported synthesis of telluroxanthone gave **128** in only 2% yield in the cyclization step.[93] As shown in Scheme 41, the addition of disodium telluride to the bis(diazonium salt) **140** gives telluroxanthone (**128**) via sequential nucleophilic displacements.

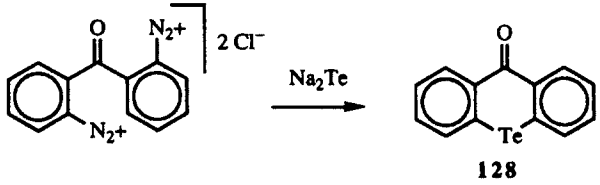

128

Scheme 41

Telluroxanthone (**128**) has been prepared from dichlorotelluroxanthene **120** via oxidation of the 9-position with either potassium dichromate[90] or chromium trioxide in acetic acid[85] as shown in Scheme 42. In both reactions, dichlorotelluroxanthone **141** is formed (use of the dichlorotelluroxanthene **120** "protects" the tellurium atom from chromic acid oxidation to various tellurium oxides) and is reduced to telluroxanthone (**128**) with either sulfite[85] or bisulfite.[90]

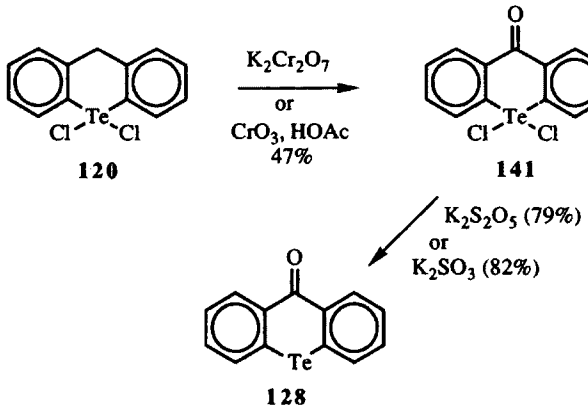

120 **141** **128**

Scheme 42

The oxidation of telluroxanthene with potassium dichromate in glacial acetic acid gives telluroxanthone bisacetate **142** in 63% isolated yield as shown in Scheme 43.[84] The initial reaction in this transformation is most likely oxidation

of telluroxanthene **117** to the telluroxide **143**. The intermediate telluroxide reacts with acetic acid to give the bisacetate **144**, which then reacts further with the dichromate to give oxidation of the methylene. Reduction of **142** with potassium bisulfite gives telluroxanthone **128** in 87% yield.

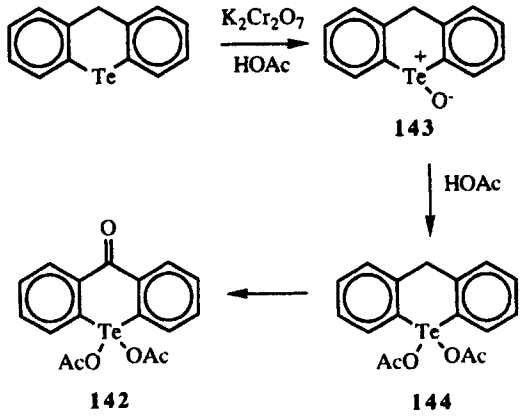

143

142 **144**

Scheme 43

The oxidative addition of chlorine to **128** gives dichloride **141** in 98% isolated yield and the oxidative addition of bromine to **128** gives dibromide **145** in 98% isolated yield.[84] The difluoro and diiodo analogs have also been described.

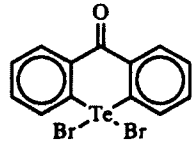

145

An arylimine of telluroxanthone has been prepared from 9-(*p*-tolyl)-telluroxanthylium perchlorate (**129**) as shown in Scheme 44.[89] The addition of sodium azide to **129** gives 9-azidotelluroxanthene **146**. When **146** is heated in refluxing xylenes, loss of nitrogen presumably generates nitrene **147**. A 1,2-shift of the aryl group generates telluroxanthone imine **148** in 32% isolated yield. A 1,2-shift of a ring carbon–carbon bond to the nitrene leads to ring expansion and the generation of dibenzotellurazepine **149** in 21% isolated yield. Imine **148** can be hydrolyzed to telluroxanthone **128**.

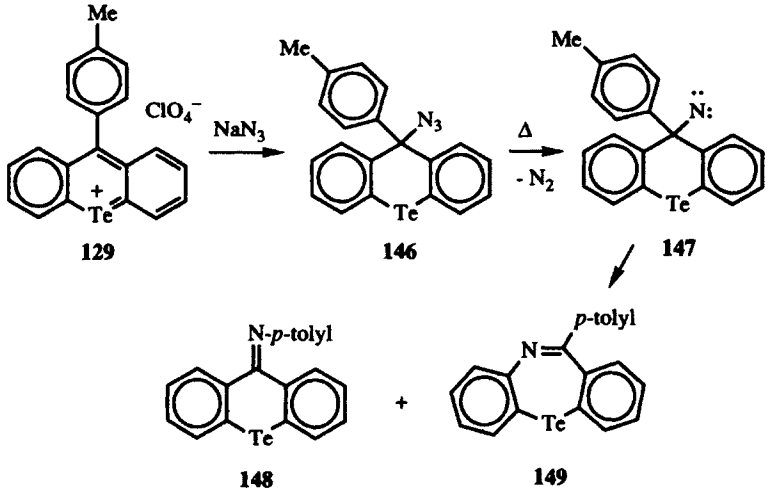

Scheme 44

III. PHYSICAL AND SPECTROSCOPIC PROPERTIES OF THE TELLURANE AND TELLURIN NUCLEI, THEIR DERIVATIVES, AND BENZO-FUSED ANALOGS

A. The Tellurane Nucleus and Related Compounds

1. The Tellurane Nucleus

The structure of tellurane **1** and related compounds has been elucidated by X-ray crystallographic analysis[95] and NMR studies.[96-100] The X-ray structure of 1-phenyltellurane bromide (**150**, Fig. 4) shows that the six-membered ring is in a chair conformation in the crystal.[95] The C1–Te–C5 bond angle of 91.6° and the long Te–C bond lengths of 2.15 Å distort the geometry of the six-membered ring. As a consequence, the dihedral angles of the planes defined by C2, C3, and

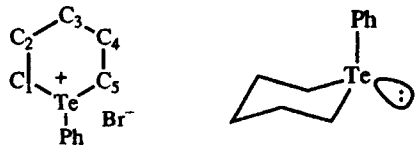

150

Figure 4. Numbering scheme for 1-phenyltellurane bromide (**150**).

C4 or by C1, Te, and C5 with the "base" atoms C1, C2, C4, and C5 are quite different with values of 119.9° and 140.5°, respectively. Values of bond lengths and angles are compiled in Table 11 for compound **150**.

In the structure of **150**, the phenyl ring was found to occupy an axial position.[95] The tellurium atom has three "short" contacts with neighboring bromines. The Te–Br bond lengths of 3.47, 3.54, and 3.67 Å are all less than the sum of van der Waals radii of 3.91 Å for tellurium and bromine.

In ^{1}H and ^{13}C NMR studies of **1** the tellurane ring was shown to have a chair conformation in solution.[96–100] Torsional angle analysis of the tellurane system relative to lighter chalcogen analogs of **1** suggests that the tellurane ring is somewhat flattened. The barrier to inversion in tellurane **1** has been calculated to be 7.3 kcal mol^{-1}, which can be compared to 8.2 kcal mol^{-1} for selenane (**151**).[98]

1, X = Te
151, X = Se
152, X = S
153, X = O
13b, X = $TeBr_2$
13c, X = TeI_2

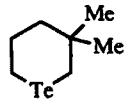

14

The ^{1}H and ^{13}C NMR spectra for the entire series of chalcogen analogs of tellurane **1** have been recorded. Although the ^{1}H NMR spectra are non-first-order, dihedral angles have been calculated from electronegativities and vicinal coupling constants.[96–98,100] In strong acid media, protonated tellurane **1** was found to have the proton on tellurium in an axial position.[97]

The ^{13}C NMR spectra of tellurane **1**, selenane **151**, thiane **152**, and oxane **153** were found to be quite sensitive to the heteroatom.[7,101] These data are compiled in Table 12. Not surprisingly, the most sensitive positions to heteroatom effects are the α carbons, which are some 10 times more sensitive to heteroatom changes than the γ carbon, which, in turn, is twice as sensitive to heteroatom changes as the β carbons. The same trends were observed in tellurane **14** (Table 12) and its lighter chalcogen analogs. Tellurium is the most electropositive of the chalcogen atoms and reverses the σ-bond polarity of the tellurium–carbon bond relative to the tellurium–oxygen bond. Thus, the carbon atoms bearing tellurium in **1** is shielded by 70 ppm relative to the carbon atoms bearing oxygen in **153**.

Tellurium(IV) analogs of **1**—dibromide **13b** and diiodide **13c**—display slightly different ^{13}C resonances. The α carbons are deshielded by roughly 35–40 ppm in the tellurium(IV) derivatives relative to the tellurium(II) derivative, the β carbons are shielded by roughly 8–10 ppm, and the γ carbon is shielded by roughly 5 ppm (Table 12).

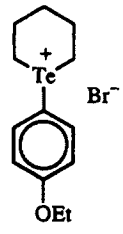

154

The ^{13}C NMR spectrum of telluronium salt **154**, a closely related analog of **150**, has been reported.[9] Values for the ring carbons are compiled in Table 12. These values are more similar to the ^{13}C NMR chemical shifts observed for the tellurium(IV) analogs **13b** and **13c** than to the ^{13}C NMR chemical shifts observed for telluranes **1** and **14**. The similarity of these data is consistent with the effective electronegativity of the heteroatom [tellurium(IV) is more electronegative than tellurium(II); tellurium in a telluronium salt is more electronegative than in a telluride] being an important determinant of chemical shift.

The alternating effects of heteroatoms on the chemical shifts of the ring carbons in these six-membered heterocycles have been explained in terms of Pople–Gordon alternation of charge[7] and in terms of linear electric-field effects.[102] The correlation of ^{13}C NMR chemical shift with heteroatom electronegativity gives excellent linearity.

The ^{125}Te NMR spectrum of tellurane **1** has been reported.[103] The chemical shift of δ 210 (δ Me_2Te = 0 ppm) for **1** is typical of other diorgano tellurium(II) compounds.

2. *Tellurane-3,5-diones*

The X-ray crystal structures of several tellurane-3,5-diones **19** have been reported[104–110] as well as one dichlorotellurane-3,5-dione, **18a**.[104] Values of bond lengths and angles are compiled in Table 11 according to the numbering scheme shown in Figure 4. As in tellurane **150**, the tellurane-3,5-diones **18a** and **19** adopt chair conformations in the crystal. The long Te–C bonds (2.14–2.20 Å) and small C—Te—C bond angles (88–96°) distort the geometry of the six-membered rings. The dihedral angles of the planes defined by C2, C3, and C4 or by C1, Te, and C5 with the "base" atoms C1, C2, C4, and C5 are 121° and 147°, respectively, for the tellurium(IV) derivative **18a** and are 122° and 125°, respectively, for **19a**.[104]

The tellurium(II) and tellurium(IV) compounds display some differences in structure. The tellurium(IV) derivative **18a** has a geometry about tellurium that is best described as trigonal bipyramidal. The two chlorine atoms occupy axial positions, while the tellurium–carbon bonds and a tellurium-atom lone pair of electrons occupy the equatorial positions. The geometry about the tellurium

atoms of the tellurium(II) derivatives **19** and **150** is best described as tetrahedral with two lone pairs of electrons occupying tetrahedral sites. Consequently, the C—Te—C bond angle is somewhat larger in **18a** (95–96°) than in **19** (88–91°). The distortion in dihedral angles in comparing **18a** and **19a** and differences in the Te–C–C bond angles are a consequence of the different geometric requirements of the bonding arrays at tellurium in these compounds.

The bonding in compounds **19** has been examined by ^{125}Te Mössbauer spectroscopy.[111] These studies suggest that bonding between tellurium and its attached carbons occurs mostly through the *p* -orbitals of tellurium. Qualitatively, such an argument is consistent with the roughly 90° bond angles observed in diorganotellurium compounds. It was also suggested that the low ^{125}Te Mössbauer chemical shifts [δ (0.39–0.47) $\pm$ 0.008 mm s^{-1}, Δ (9.81–11.25) $\pm$ 0.01 mm s^{-1}] in compounds **19** are indicative that the short Te–Te contacts observed by X-ray crystallography may be a consequence of tellurium $5s^2$ electrons populating conductance bands between tellurium atoms. The latter argument is perhaps somewhat speculative in view of the fact that phenoxtellurine (**155**) has similar chemical-shift values (δ 0.24 mm s^{-1}, Δ 11.2 mm s^{-1}) and no short intermolecular tellurium–tellurium contacts.[112,113] However, dibenzotellurophene (**156**) has even smaller chemical-shift values than the tellurane diones **19** (δ 0.14 mm s^{-1}, Δ 9.3 mm s^{-1}) and displays short intermolecular tellurium–tellurium contacts in X-ray structures.[112,114]

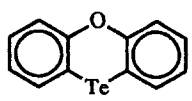

155

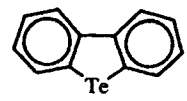

156

The structures of the tellurane-3,5-diones **19** appear to be similar both in solution and in the crystal.[107] ^{1}H and ^{13}C NMR spectra of compounds **19** confirm the bonding through the methylene groups via ^{125}Te coupling. The methylene groups do not appear to be enolized in solution.

3. *The 3,5-Dihydro-2H-tellurin Nucleus and Derivatives*

No X-ray crystal structures of the parent 3,5-dihydro-2*H*-tellurin nucleus have been reported. However, the crystal structure of the bicyclic dihydrotellurin system *exo*-**26** has been reported, and the effect of tungsten coordination on bond lengths and angles on the parent system can be inferred.[22] The Te—C bond lengths of 2.21 and 2.22 Å are somewhat longer than those observed in **18a**, **19**, and **150**.[95,104–110] The C—Te—C bond angle of 80.6° is also quite small. Coordination to the metal has created a distorted tetrahedral array about tellurium, which compresses the C—Te—C angle.

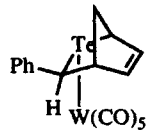

exo-**26**

The 3,5-dihydro-2*H*-tellurin **27a** is an unsaturated version of telluranes **1** and **14**. Selenium (**157**), sulfur (**158**), and oxygen (**159**) analogs of **27a** have been prepared, and their ^{1}H and ^{13}C NMR spectra have been compared to those of **27a** (Table 13).[21] The ^{13}C NMR chemical shifts of the carbon atoms attached to the heteroatom (Table 13) follow the same trends as those observed for **1** and **151–153** (Table 12). Decreasing electronegativity of the heteroatom leads to increased shielding at the α carbons. The ^{1}H NMR chemical shifts of the protons attached to the α carbons follow a somewhat different trend, however. Although decreasing electronegativity in the heteroatom leads to increased shielding of the protons attached to the α carbons for oxygen, sulfur, and selenium derivatives **157–159**, the protons attached to the α carbons in tellurium derivative **27a** (tellurium is the most electropositive of the chalcogen atoms) are found at lower field than those of **151–153**.

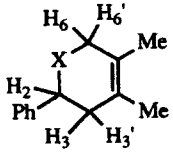

27a, X = Te
157, X = Se
158, X = S
159, X = O

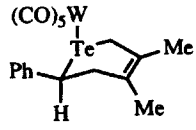

cis-**25**

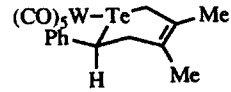

trans-**25**

Complexes **25** (the *cis* and *trans* complexes of **27a** with tungsten pentacarbonyl) have ^{1}H and ^{13}C NMR spectra (Table 13) that show small chemical-shift differences from those of **27a**. The ^{1}H NMR chemical shifts of the protons attached to the α carbons and the ^{13}C NMR chemical shifts of the α carbons are at lower field in complexes **25** relative to **27a**.[22]

4. 4H-Tellurin-4-ones and Derivatives

The single-crystal X-ray structures of 4*H*-tellurin-4-one (**29d**), the selenium analog **160**, and the sulfur analog **161** have been reported.[42] Selected bond lengths and bond angles for these compounds are compiled in Table 14 utilizing the numbering scheme shown in Figure 5. Unlike tellurane **1** and derivatives that have chair conformations in the solid state and in solution, tellurin-4-one

29d, selenin-4-one **160**, and thiapyran-4-one **161** are all planar in the solid state. As the heteroatom–carbon bond lengths increase, little change is observed in the X—C1—C2 and X—C5—C4 (where X is a chalcogen atom) bond angles (124.8–125.8°) in the three molecules even though the C1—X—C5 bond angle varies from 91.3–100.9° in these systems. A 5° variance is found in the C2—C3—C4 angles (from 117° in **161** to 122° in **29d**), and a 3° variance is found in the C1—C2—C3 and C3—C4—C5 bond angles (from 125.1° in **161** to 128° in **29d**). The carbon–carbon bond lengths are similar in the three molecules, although there are some minor differences.

The spectroscopic properties of the chalcogenapyranones **29d** and **160–162** are compiled in Table 15.[42,115–117] All four compounds display *AA'BB'* patterns in their ^{1}H NMR spectra, and **29d**, **160**, and **161** display three-line spectra in the proton-decoupled ^{13}C NMR spectra. The assignments of chemical shifts to H_A and H_B were made possible by ^{125}Te satellite coupling (J_{Te-H_A} = 107 Hz) in **29d** and ^{77}Se satellite coupling (J_{Se-H_A} = 51 Hz) in **160**. Although proton–proton couplings were not assigned in these systems, the *cis*-olefinic coupling constant in **29d** should be similar to $J_{H_A-H_B}$ of 11.4 Hz observed in **29e**. The value of $J_{H_A-H_B}$ is dependent on geometry since a value of 10.3 Hz is observed in thiopyranone **163**.

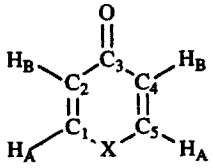

29d, X = Te
160, X = Se
161, X = S
162, X = O

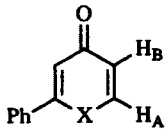

29e, X = Te
163, X = S

Figure 5. Numbering scheme for chalcogenapyranones **29d** and **160–162**.

The carbon chemical shifts are similar in **29d**, **160**, and **161** with the chemical shift of each carbon varying by only ± 2 ppm, while proton chemical shifts are more sensitive to the heteroatom.[42] In compounds **29d** and **160–162**, the chemical shifts of H_A vary by 1.24 ppm, while the chemical shifts of H_B vary by 1.01 ppm.[42,116] The changes in chemical shift observed in this set of four molecules cannot be correlated with either size or electronegativity. While the chemical-shift changes observed from **29d** to **160** to **161** are systematic, the chemical-shift values for pyranone **162** do not follow the trends.

The carbonyl stretching frequencies change systematically from tellurium-containing pyranone **29d** to the parent pyranone **162** increasing from 1560 to 1650 cm^{-1}. This trend correlates inversely with the size of the heteroatom and directly with the electronegativity of the heteroatom. The O—C3 bond lengths

are given for **29d**, **160**, and **161** in Table 14. Values are nearly identical in **160** and **161**. In 4*H*-tellurin-4-one **29d**, the O—C3 bond length is 0.03 Å longer than in **160** and **161**, which is consistent with a weaker C=O stretching frequency.

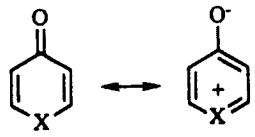

The chalcogenapyranones **29d** and **160–162** can be viewed in terms of the resonance forms shown above in which the MO descriptions of the molecules may have fractional double-bond character for the carbonyl group. The dipole moments listed in Table 15 for these compounds[115] are consistent with an MO picture with increased separation of charge as the heteroatoms become more electropositive. The increased separation of charge in these planar molecules should give rise to a larger dipole moment. Furthermore, the energies of the absorption maxima of **29d**, **160**, and **161** vary in nearly identical fashion to the absorption spectra of chalcogenopyrylium compounds (Chapter 4), which suggests a significant contribution from the charge-separated resonance form.

The introduction of substituents at the 2- and 6-positions has little effect on the carbonyl stretching frequencies (Table 16) of the tellurin-4-ones **29**, which vary from 1560 to 1595 cm^{-1}.[38,41-43] The chemical shift of H_B is sensitive to the type of substituent on the adjacent carbon.[38,41-43] Thus, tellurin-4-ones **29** with aryl substituents at the 2- and 6-positions have ^1H NMR chemical shifts for H_B in the range of δ 7.17–7.37, while tellurin-4-ones **29** with alkyl substituents at the 2- and 6-positions have ^1H NMR chemical shifts for H_B in the range δ 6.74–6.90 (Table 16).

The oxidative addition of halogens or peracetic acid to the tellurium atom of the tellurin-4-ones **29** gives the corresponding tellurium(IV) derivatives **37** and **38**. The spectroscopic properties of **37** and **38** are quite different from those of their tellurium(II) analogs (Table 16).[50] A charge-separated resonance form is not possible in the tellurium(IV) compounds since the 5*p* orbital is utilized in bonding to the ligands. Consequently, the carbonyl stretching frequency is at higher energies (1615–1635 cm^{-1}), which is indicative of more double-bond character in the carbonyl group.

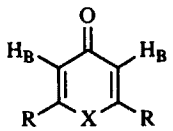

29a, X = Te, R = Ph
29b, X = Te, R = *tert*-Bu
37a, X = $TeCl_2$, R = *tert*-Bu
37b, X = $TeBr_2$, R = *tert*-Bu
38, X = $TeBr_2$, R = Ph

The range of chemical shifts in ^{125}Te NMR covers several parts per million with multiple factors such as the electronegativity of ligands attached to the tellurium center, the net charge on the molecule, and the oxidation state of the tellurium center contributing to the observed shifts.[118,119] In general, the chemical shift moves downfield as oxidation state increases and as the electronegativity of the ligands attached to tellurium increases. In comparing the tellurapyranones **29** with their tellurium(IV) analogs **37** and **38** (Table 16), very little difference in ^{125}Te chemical shifts is observed between the tellurium(II) and tellurium(IV) derivatives of the molecules.[73] Core binding energies as determined by X-ray photoelectron spectroscopy (XPS) of the Te($3d_{5/2}$) electrons are consistent with distinct tellurium(II) compounds **29** and tellurium(IV) compounds **37** and **38**. Increased charge separation in the tellurapyranones **29** relative to the tellurium(IV) analogs **37** and **38** might contribute to the similarities in chemical shifts observed in the ^{125}Te NMR spectra for these compounds. It should be noted that the ^{125}Te chemical shifts of 4*H*-tellurins **40a** and **43** (Table 17) are 257 and 296 ppm, respectively. This difference in chemical shift is consistent with increased separation of charge contributing to the roughly 200-ppm downfield shift in the tellurin-4-ones.[73]

5. *The 4H-Tellurin Nucleus and Derivatives*

The two 4*H*-tellurin derivatives that have been described in the literature (**40a** and **40b**) have been noncrystalline.[51] As a consequence, most structural information concerning this system has come from NMR spectroscopy (Table 17). The complete chalcogen series related to 2,6-di-*tert*-butyl-4*H*-tellurin (**40a**) has been prepared (**163–166**), and spectroscopic data related to these compounds are compiled in Table 17 with numbering according to the legend shown in Figure 6. Spectroscopic data for the dimeric product **43**, a substituted 4*H*-tellurin, are also included in Table 17. The chemical shifts of the olefinic protons H_A shift upfield as the chalcogen atom becomes more electronegative. Furthermore, the changing C1—X—C5 bond angle alters the geometry of the heterocyclic ring and,

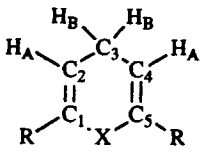

40a, X = Te, R = *tert*-Bu
40b, X = Te, R = Ph
164, X = Se, R = *tert*-Bu
165, X = S, R = *tert*-Bu
166, X = O, R = *tert*-Bu

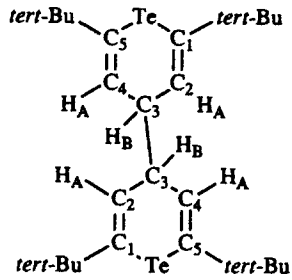

43

Figure 6. Numbering scheme for chalcogena pyrans **40**, **43**, and **164–166**.

consequently, the coupling constant between the olefinic protons H_A and the allylic protons H_B. The coupling constant decreases sequentially from 5.4 Hz for **40a** to 3.3 Hz for pyran **166**. The allylic methylene protons, H_B, are much less sensitive to changes in the heteroatom, varying by only 0.14 ppm.

B. The Benzotellurane Nucleus and Related Compounds

1. 2H-Benzotellurin-2-one and Derivatives

The ^1H and ^{13}C NMR spectral properties of 2*H*-benzotellurin-2-one (**80**)[64] and its selenium (**167**),[120] sulfur (**168**),[121,122] and oxygen analogs (coumarin, **169**)[123,124] have all been described.[125,126] These data are compiled in Table 18 according to the numbering scheme in Figure 7.

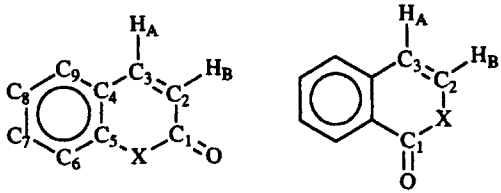

80, X = Te
167, X = Se
168, X = S
169, X = O

83, X = Te
170, X = Se
171, X = S
172, X = O

Figure 7. Numbering scheme for chalcogenocoumarins **80** and **167–169** and isocoumarins **83** and **170–172.**

The ^1H NMR spectra of **80** and **167–169** (Table 18) indicate that the chemical shifts of protons H_A and H_B are less sensitive to the heteroatom than protons H_A and H_B in pyranones **29d** and **160–162**.[64,120–123] In **80** and **167–169**, protons H_A vary by 0.33 ppm, while protons H_B vary by 0.87 ppm. No trend emerges for the dependence of heteroatom size or electronegativity for the chemical shift of H_A. The chemical shift of H_B moves to lower field as the electronegativity of the heteroatom increases. The effect of the different sizes of the chalcogen heteroatoms on the geometry of the heteroatom-containing ring is reflected in the magnitude of the coupling constant, $J_{H_A-H_B}$. The coupling constant decreases from 11.7 Hz for **80** to 9 Hz for coumarin (**169**) as the angle between the protons in the H_A—C—C—H_B array increases.

The ^{13}C NMR spectra of the four compounds differ from one another in systematic ways as the heteroatom changes (Table 19).[125] The chemical shift of the carbonyl carbon, C1, is most sensitive to heteroatom substitution and follows a trend that can be correlated with both size and electronegativity of the

heteroatom. The chemical shift of the carbonyl carbon increases from δ 160.5 ppm for coumarin (**169**) to 193.5 ppm for 2*H*-benzotellurin-2-one (**80**). The chemical shift of C3 is nearly independent of the heteroatom, with the chemical shift varying between 143.4 and 145.4 ppm. The chemical shift of C2 follows a trend similar to that of the carbonyl carbon, C1, although the chemical-shift range is much smaller (116.5–125.0 ppm).

The benzo carbon adjacent to the heteroatom (C5) follows a trend is opposite to that observed for the carbonyl carbon (which is also adjacent to the heteroatom).[125] The chemical shift of this carbon decreases from δ 153.9 ppm for **169** to 125.0 ppm for **80**. The other bridgehead carbon (C5) shows the opposite trend, with the chemical shift increasing from 118.8 ppm for **169** to 130.8 ppm for **80**. The chemical shift of C6 also increases incrementally with increasing heteroatom size, increasing from 116.5 ppm for **169** to 135.7 ppm for **80**. The remaining ^{13}C NMR chemical shifts are similar in all four of these systems.

The differing electronegativities of the heteroatoms serve to enhance or negate the separation of charges shown in the resonance forms below. On those carbon atoms bearing a positive charge, increasing electronegativity in the heteroatom leads to a downfield shift in the ^{13}C NMR chemical shift. On those carbon atoms bearing a negative charge, increasing electronegativity leads to an upfield shift.

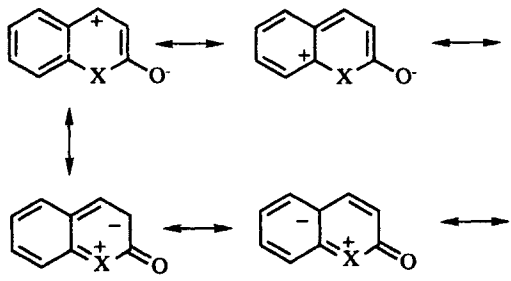

The carbonyl stretching frequency also is sensitive to the nature of the heteroatom and increases incrementally with decreasing heteroatom size from 1630 cm^{-1} for **80**[64] to 1698 cm^{-1} for **169**.[124] These changes are consistent with increased charge separation in the MO description of these coumarin analogs as the heteroatom becomes larger and more electropositive, as illustrated in the resonance forms shown below.

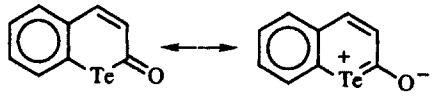

2. *2-Benzotellurin-1-one and Derivatives*

The ^1H NMR and IR spectral properties of 2-benzotellurin-1-one (**83**)[72] and its selenium (**170**),[72] sulfur (**171**),[126] and oxygen (**172**)[127] analogs have been described. The dipole moments for these compounds have also been measured.[128] These data are compiled in Table 19.

As the geometry of the six-membered ring (see Fig. 7 for numbering) changes with increasing heteroatom size, the coupling constant between H_A and H_B increases (Table 19). In these isocoumarin analogs, the coupling constant increases from 5.5 Hz for isocoumarin **172** to 10.7 Hz for **83**. The chemical shift of proton H_B on the carbon adjacent to the heteroatom shifts downfield as the heteroatom becomes more electropositive from δ 6.40 for **172** to δ 7.92 for **83**. Proton H_A follows a similar trend, but the chemical-shift range is from δ 7.17 for **172** to δ 7.61 for **83**. The chemical shifts of the protons on the carbocyclic ring are all similar in the four systems.

The assignment of chemical shifts to H_A and H_B in the series **83** and **170–172** was made "on the basis of broader and smaller peaks in the *AB* system for the (H_A) proton, due to long-range coupling with the aromatic protons."[72] The natural-abundance $^1H—^{125}Te$ and $^1H—^{77}Se$ coupling constants were not described. These satellites would permit unequivocal assignment of chemical shifts to H_A and H_B.

The carbonyl stretching frequency decreases in energy as the heteroatom becomes larger and more electropositive (Table 19). The magnitude of the change is substantial, decreasing from 1745 cm^{-1} for **172** to 1628 cm^{-1} for **83**. The changes in $\nu_{C=O}$ are consistent with increased separation of charge in the MO description of the molecules as the heteroatom becomes larger and more electropositive. This is illustrated in the resonance forms shown below.

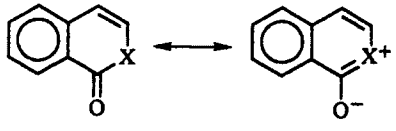

The dipole moments measured for these compounds follow a trend opposite to that observed for the pyranones **29d** and **160–162**, in which the dipole moment increased with heteroatom size. For **83** and **170** and **171**, the dipole moment decreases with increasing heteroatom size from 3.99 D for **171** to 3.25 D for **83**.[128] The arguments advanced for this trend suggest that the dipole moment created by the increased separation of charge would oppose the styrene dipole, which points in the opposite direction. Consequently, increased charge separation would lead to smaller net dipole moments.

3. 3,4-Dihydro-2-benzotellurin-1-one and Derivatives

The ^1H and ^{13}C NMR spectral properties and other properties of 3,4-dihydro-2-benzotellurin-1-one (**76**)[71,129] and its selenium (**173**),[71] sulfur (**174**),[71,130] and oxygen (**175**)[71] analogs have been described. Selected spectral data for this series of compounds are compiled in Table 20 according to the numbering scheme in Figure 8. The chemical shifts of the aliphatic carbons of the heterocyclic ring vary in a manner identical to those of tellurane **1** and its lighter chalcogen atoms. The ^{13}C chemical shift of C2, which is adjacent to the heteroatom, is most sensitive to heteroatom changes, decreasing from δ 67.3 ppm for **175** to δ 5.2 ppm for **76**. The ^{13}C NMR chemical shift of C1, which is β to the heteroatom, is roughly 10 times less sensitive to heteroatom changes, increasing from δ 27.7 for **175** to δ 34.3 for **76**. The carbonyl carbon C3, which is also adjacent to the heteroatom, is as sensitive to heteroatom changes as is C3, but the effect is opposite in sign. The chemical shift of C3 increases from δ 165 ppm for **175** to 193.6 ppm for **76**.

Other properties are little affected by heteroatom changes. The carbonyl stretching frequency $\nu_{C=O}$ is less sensitive to heteroatom changes in these systems (Table 20). The dipole moments of this series of compounds are not as sensitive to heteroatom changes as other heterocyclic systems. The dipole moment decreases from 4.56 D for lactone **175** to 4.32 D for selenolactone **173**.[128] These data suggest that the heteroatoms, although of different electronegativity and polarizability, contribute to separation of charge and lactone bonding in similar ways.

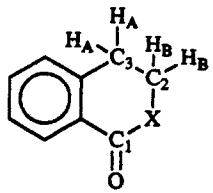

76, X = Te
173, X = Se
174, X = S
175, X = O

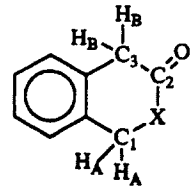

76a, X = Te
173a, X = Se
174a, X = S
175a, X = O

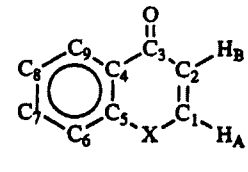

89a, X = Te
176, X = Se
177, X = S
178, X = O

Figure 8. Numbering scheme for 3,4-dihydro-2-benzotellurin-1-one (**76**) and lighter chalcogen analogs **173–175**, 1,4-dihydro-2-benzotellurin-3-one (**76a**), and lighter chalcogen analogs **173a–175a**, and 4-chalcogenochromones **89a** and **176–178**.

4. 3,4-Dihydro-2-benzotellurin-3-one and Derivatives

The ^1H and ^{13}C NMR spectral properties and other properties of 3,4-dihydro-2-benzotellurin-3-one (**76a**) and its selenium (**173a**), sulfur (**174a**), and

oxygen (**175a**) analogs have been described.[71a] Selected spectral data for this series of compounds are compiled in Table 20a. The chemical shifts of the aliphatic carbons of the heterocyclic ring vary in a manner identical to those of tellurane **1** and its lighter chalcogen atoms. The ^{13}C chemical shift of C1, which is adjacent to the heteroatom, is most sensitive to heteroatom and α to the carbonyl, is roughly 3-times less sensitive to heteroatom changes, decreasing from δ 69.9 ppm for **175a** to δ 8.5 ppm for **76a**. The ^{13}C NMR chemical shift of C3, which is β to the heteroatom and α to the carbonyl, is roughly 3 times less sensitive to heteroatom changes, increasing from δ 35.9 for **175a** to δ 58.1 for **76a**. The carbonyl carbon C2, which is also adjacent to the heteroatom, is between C1 and C3 with respect to sensitivity to heteroatom changes with the chemical shift of C2, increasing from δ 169.3 ppm for **175a** to 209.6 ppm for **76a**. The benzo carbons displayed surprisingly similar chemical shifts in all four compounds of this series.

The ^{1}H NMR spectra of **76a** and **173a–175a** show slight differences in chemical shift for protons H_A and H_B.[71a] Protons H_A, adjacent to the heteroatom, move downfield as the heteroatom becomes larger from δ 3.9 for **175a** to δ 4.3 for **76a**. Protons H_B show less than 0.1 ppm difference as the heteroatom changes. The assignment of chemical shift was aided by the ^{125}Te and ^{77}Se satellite coupling with H_A (31.5 and 15 Hz, respectively).

The carbonyl stretching frequency, $\nu_{C=O}$, is very similar for the three heavier chalcogen atoms in the range of 1625–1665 cm^{-1}. These values are much smaller than that observed for the oxygen analog **175a**, where the carbonyl stretching frequency is 1748 cm^{-1}.[71a]

5. *4 H-Benzotellurin-4-ones and Derivatives*

The ^{1}H and ^{13}C NMR spectral properties, IR spectra, UV absorption spectra, and dipole moments for the parent 4*H*-benzotellurin-4-one (**89a**) and its selenium (**176**), sulfur (**177**), and oxygen (**178**) analogs have been compared.[131] These data are compiled in Table 21 and, for the ^{13}C NMR data, Table 22.

The ^{1}H NMR spectra of **89a** and **176–178** vary significantly with respect to the chemical shifts of protons H_A and H_B as well as the coupling constants between these two protons (Table 21).[131] The chemical shifts of both H_A and H_B move upfield as the heteroatom increases in electronegativity. The chemical shift of H_A decreases from δ 8.61 for **89a** to δ 7.78 for **178**, while the chemical shift of H_B decreases from δ 7.38 for **89a** to δ 6.24 for **178**. The coupling constant decreases from 11.8 Hz for **89a** to 6.1 Hz for **178**.

The changes in the ^{13}C NMR spectra of **89a** and **176–178** (Table 22)[131] are similar to those observed for 2*H*-benzotellurin-2-one (**80**) and its selenium, sulfur, and oxygen analogs **167–169** (Table 18). The changes are also much more pronounced than those observed for **29d** and **160–162** (Table 15). In chalcogeno coumarins **80** and **167–169**, the chemical shift of the carbonyl carbon, which is adjacent to the heteroatom, varies by 30 ppm with respect to heteroatom

changes. In the chalcogeno chromones **89a** and **176–178**, the chemical shift of the carbonyl carbon (C3), which is γ to the heteroatom, varies by less than 8 ppm with respect to heteroatom changes. Carbon C1, which is adjacent to the heteroatom, varies by 21 ppm in **89a** and **176–178**, with the chemical shift moving downfield with increasing electronegativity. The chemical shift of C2 varies by 31 ppm with respect to heteroatom changes but moves upfield with increasing electronegativity.

As was described with the chalcogeno coumarins **80** and **167–169**, the alternation of charge depicted in the resonance forms shown below qualitatively describes the trends in chemical-shift changes for those carbon atoms in the heterocyclic ring as the heteroatoms vary. In the resonance forms depicted above for **80** and **167–169** and below for **89a** and **176–178**, the quaternary bridgehead carbons should follow similar trends. Thus, C5 for **89a** and **176–178** moves downfield with increasing electronegativity from δ 124.2 ppm for **89a** to 155.6 ppm for **178**, and C4 moves upfield with increasing electronegativity from δ 136.0 ppm for **89a** to 125.3 ppm for **178**.[131] (We have reversed the assignment of chemical shifts for C4 and C5 from those of the authors of reference 131. It seems plausible for C4 and C5 to follow the same trends in chemical shift as the heteroatoms vary for **80** and **167–169** and for **89a** and **176–178**. Consequently, it would appear that one set of assignments in references 64 and 131 is reversed for these to carbon atoms.) The chemical shift of C6 follows the same trend as C4 with an upfield shift with increasing electronegativity from δ 132.3 ppm for **89a** to 118.5 ppm for **178**.[131] The chemical shifts of C7–C9 show only minor changes with heteroatom substitution.

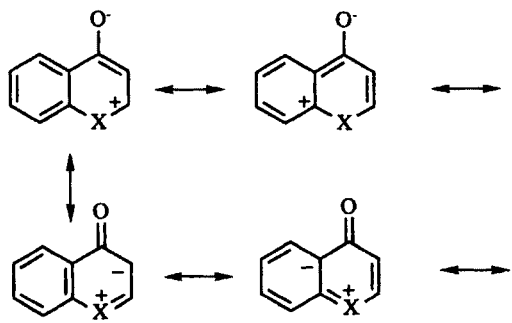

The carbonyl stretching frequency increases incrementally with increasing electronegativity from 1625.5 cm^{-1} for **89a**[131] to 1669 cm^{-1} for **178** (Table 21). These changes are consistent with increased charge separation in the MO description of these chromone analogs as the heteroatom becomes larger and more electropositive. However, the changes in carbonyl stretching frequency are much smaller than those observed for either the pyranone analogs **29d** and **160–162** or the coumarin analogs **80** and **167–169**. The dipole moments for **89a** and **176–178** are similar, varying by 0.19 D, which suggests that charge separation is similar in these four compounds (Table 21).

The absorption maxima in the absorption spectra of **89a** and **176–178** move to longer wavelengths as the heteroatoms become larger (Table 21). This trend is also observed in the chalcogenopyranones and in chalcogenopyrylium compounds (Chapter 4).

The ^{1}H NMR chemical shifts in 4*H*-2-methylbenzotellurin-4-one (**89b**) and its selenium (**179**), sulfur (**180**), and oxygen (**181**) analogs are similar to those observed for **89a** and **176–178**.[60] The chemical shifts of both the methyl group and H_B (with numbering as shown in Fig. 9) move upfield as the heteroatom increases in electronegativity (Table 23). The chemical shift of the methyl group decreases from δ 2.47 for **89b** to δ 2.25 for **181**, while the chemical shift of H_B decreases from δ 7.05 for **89b** to δ 6.03 for **818**. The coupling constant between the protons of the methyl group and H_B decreases from 1.3 Hz for **89b** to 0.65 Hz for **181**.

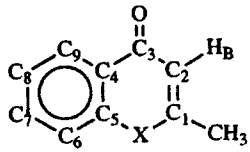

89b, X = Te
179, X = Se
180, X = S
181, X = O

Figure 9. Numbering scheme for 4*H*-2-methylbenzotellurin-4-one (**89d**) and its selenium (**179**), sulfur (**180**), and oxygen (**181**) analogs.

The ^{125}Te NMR spectra of 4*H*-benozotellurin-4-ones have been recorded only for substituted derivatives. 7-Methoxy-2-phenyl-4*H*-benzotellurin-4-ones (**98a1**) and 5-methoxy-2-*tert*-butyl-4*H*-benzotellurin-4-one (**182**) have ^{125}Te NMR chemical shifts of δ 519 and 465 ppm, respectively (δ $^{125}TeMe_2$ = 0.0 ppm).[73] These values are similar to the ^{125}Te chemical shift observed for the tellurium(IV) analog **183** of δ 541 ppm. Increased charge separation in the 4*H*-benzotellurin-4-ones **98a1** and **182** relative to the tellurium(IV) analog **183** might contribute to the similarities in chemical shifts observed in the ^{125}Te NMR spectra for these compounds. It should be noted that the ^{125}Te chemical shifts of 4*H*-benzotellurins **86a** and **86b** are δ 380 and 391 ppm, respectively.

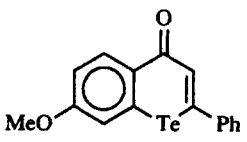

98a1

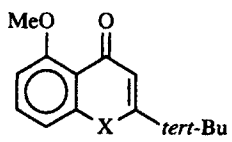

182, X = Te
183, X = $TeCl_2$

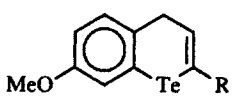

86a, R = Ph
86b, R = *tert*-Bu

This difference in chemical shift is consistent with increased separation of charge contributing to the roughly 100 ppm downfield shift in the benzotellurin-4-ones.[73] The benzo group attenuates the differences observed in these various systems relative to the monocyclic telluropyran systems.

The ^{1}H NMR chemical shifts of the protons H_B are somewhat sensitive to substituents attached to the 2-position but are much less affected by substituents in the benzo ring. For benzotellurin-4-ones **98a–98d**[75] and **98i–98o**,[76] where the 2-substituent is an aryl group, the proton on the heterocyclic ring, is a sharp singlet with a chemical-shift range of δ 7.31–7.45. For benzotellurin-4-ones **89b**,[60] **98e**,[75] and **98f**[75] where the 2-substituent is a methyl group, the proton on the heterocyclic ring is a quarter with a chemical-shift range of δ 6.91–7.05 (and a coupling constant with the methyl group of about 1 Hz). For benzotellurin-4-ones **89a**,[131] **90–92**,[60] **98g**, and **98h**[75] where proton H_A is the 2-substituent, the protons on the heterocyclic ring are doublets (J = 11.2–11.8 Hz) with H_A in the range δ 8.21–8.80 and with H_B in the range δ 7.27–7.47.

The UV absorption spectra of the benzotellurin-4-ones with a variety of substituents in the benzo ring and in the 2-position of the heterocyclic are surprisingly similar. For compounds **89** and **98**, the UV absorption spectra give λ_{max} in the rage 380–400 nm with molar extinction coefficients in the range of 5000–10,000.

6. *Benzotellurane-4-ones and Derivatives*

The benzotellurane-4-ones **59**, **65**, and **67** and condensed-thiophene derivatives **69** and **74** have been characterized primarily by their mass spectra.[57–59] The infrared spectrum and dipole moment of the parent benzotellurane **65a** have been compared to those of the corresponding selenium (**184**), sulfur (**185**), and oxygen (**186**) analogs (Table 24).[131]

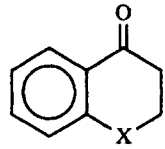

65a, X = Te
184, X = Se
185, X = S
186, X = O

The carbonyl stretching frequency $\nu_{C=O}$ varies by roughly 20 cm^{-1} with the heteroatom in both carbon tetrachloride solution (from 1679 cm^{-1} for **65a** to 1701 cm^{-1} for **186**) and in potassium bromide pellets (from 1668 cm^{-1} for **65a** to 1691 cm^{-1} for **186**).[131] The dipole moments μ vary by 0.26 D with respect to heteroatom substitution.[131]

7. *2H-Benzotellurin and Derivatives*

The ^{1}H NMR spectra of 2*H*-benzotellurins **77** have been reported and selected data are compiled in Table 25.[59] The chemical shifts of H_A, H_B, and H_C are little affected by substituent changes in the fused aromatic ring. Little other spectral information is available for these compounds.

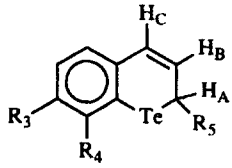

77a, $R_3 = R_4 = R_5 = H$
77b, $R_3 = Me$, $R_4 = R_5 = H$
77c, $R_4 = Me$, $R_3 = R_5 = H$
77f, $R_3 = R_4 = R_5 = H$, $H_B = Me$
77g, $R_3 = R_4 = H$, $R_5 = Me$
77j, $R_3 = R_4 = R_5 = H$, $H_C = Me$

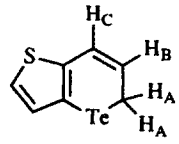

77i

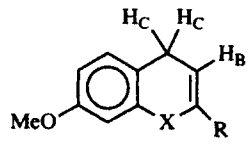

86a, R = Ph, X = Te
86b, R = *tert*-Bu, X = Te
86c, $R = H_A$, X = Te
87, R = *tert*-Bu, $X = TeCl_2$
88, R = *tert*-Bu, $X = TeBr_2$

8. *4H-Benzotellurins and Derivatives*

The ^{1}H NMR spectra of 4*H*-benzotellurins **86** and their tellurium(IV) analogs **87** and **88** have been reported.[51,73] Selected data for the heterocyclic rings are compiled in Table 26. The chemical shifts of the methylene protons and the vicinal coupling between the methylene protons and the olefinic proton in the tellurium(II) analogs **86** are quite similar to those of the 2*H*-benzotellurins **77**. The chemical shifts of the ring protons H_B and H_C move downfield on oxidation of the tellurium atom in tellurium(IV) analogs **87** and **88**. In these systems, where charge-separated resonance forms are not easily drawn, the ^{125}Te NMR chemical shifts of the tellurium(II) and tellurium(IV) analogs vary by more than 200 ppm. XPS binding energies for the Te($3d_{5/2}$) electrons in these systems show roughly a 2-eV difference between tellurium(II) and tellurium(IV).

C. Telluroxanthene and Telluroxanthone

The X-ray structure of telluroxanthene **117** has been described, and selected bond lengths and angles are compiled in Table 27 with numbering as shown in Figure 10.[88] The central ring is boat-shaped with the dihedral angle of 129.6° between the two planes defined by the fused benzo rings. The four carbons defining the base of the central heterocyclic ring (C1, C2, C3, and C4) form a dihedral angle of 151.9° with the plane defined by C1—Te—C5 and a dihedral angle of 132.7° with the plane defined by C2—C3—C4. The C1—Te—C5 angle

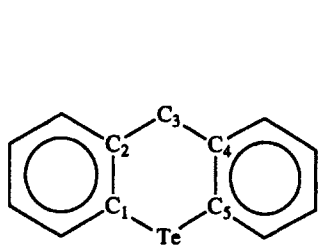

117

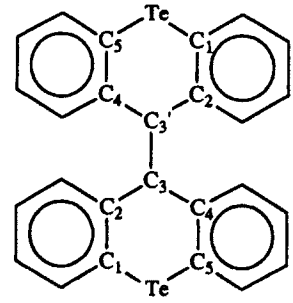

127

Figure 10. Numbering scheme for telluroxanthene (**177**), telluroxanthone (**128**), and telluraxanthenyl dimer **127**.

is 89.7°, while the C2—C3—C4 angle is 115°. The severe pucker of the central ring minimizes deviations from 120° angles at the sp^2 carbons and 109° angles at the sp^3 carbon.

The X-ray structure of telluoxanthenyl dimer **127** has also been reported, and selected bond lengths and bond angles are compiled in Table 27.[88] The bond lengths and bond angles are similar to those of **117**. The dihedral angles between the planes defined by the benzo-fused rings are larger in each half of **127** than in **117**. In compound **127**, these dihedrals are 138.8° and 140.5°. The four carbons defining the base of the central heterocyclic rings (C1, C2, C3, and C4) in **127** form an average dihedral angle of 156.1° with respect to the planes defined by C1—Te—C5 and an average dihedral angle of 139.8° with respect to the planes defined by C2—C3—C4. The C3—C3′ bond length of 1.574 Å in **127** is significantly longer than the standard single-bond length of 1.535 Å.

The ^{125}Te NMR spectra to telluroxanthene **117** and telluroxanthone **128** have been reported.[132] The chemical shifts of δ 729 ppm (vs. δ $^{125}TeMe_2 = 0.0$) for **128** and 764 ppm for **117** are both downfield of diphenyltelluride (688 ppm). However, the ^{125}Te chemical shift of the tellurin **117** is further downfield than the tellurin-4-one **128**, which indicates that there is little separation of charge in telluroxanthone **128** via the resonance forms shown below.

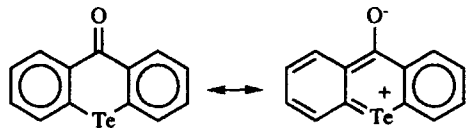

D. Electrochemical Reductions of 4*H*-Tellurins, Benzo Analogs, and Tellurium(IV) Derivatives

The electrochemical reduction of 4*H*-tellurin-4-one **29c** is an irreversible one-electron process with E_{red} of -1.60 V (vs. SCE).[50] The 4*H*-benzotellurin-4-one

98a1 undergoes a reversible one-electron reduction with E_{red} of -1.57 V. A second, irreversible reduction is also observed at -1.96 V in **98a1** (Table 28).

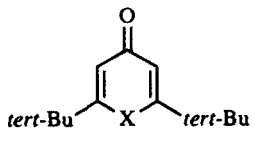

29c, X = Te
37a, X = $TeCl_2$
37b, X = $TeBr_2$
37c, X = TeI_2
37d, X = $Te(OAc)_2$

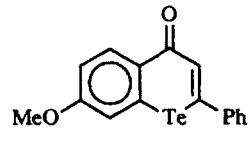

98a1

The tellurium(IV) analogs **37** undergo an initial two-electron reduction presumably to generate two equivalents of the halide or pseudohalide and tellurium(II) analog **29c** (Table 28).[50] A second, irreversible wave is observed in cyclic voltammograms of these compounds at -1.60 V [vs. SCE (standard calomel electrode)], which is presumably the reduction wave associated with **29c**. The tellurium(IV) analogs **37** are reduced at quite different potentials. Diacetate **37d** is reduced at -1.14 V, dichloride **37a** at -0.68 V, dibromide **37b** at -0.46 V, and diiodide **37c** at $+0.04$ V. Coulometric reduction of **37b** at -0.6 V (vs. SCE) required 2.1 faradays mol^{-1}. Following scans in the negative direction, scans in the positive direction show the oxidation of chloride to chlorine ($E_{ox} = 1.14$ V), bromide to bromine ($E_{ox} = 0.80$ V), and iodide to iodine ($E_{ox} = 0.67$ V).

The telluropyrans **44** and **45** bearing a dicyanomethylidene group are somewhat easier to reduce than the parent compounds (Table 28).[50] The one-electron reductions of **44** and **45** are reversible with E_{red} of 1.26 and -0.98 V, respectively. The dicyanomethylidene group serves to stabilize the anion radical. No EPR signals were observed either in solutions or in frozen glasses of the anion radicals, presumably because of spin–orbit-induced broadening from tellurium.

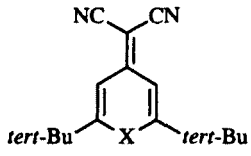

44, X = Te
47a, X = $Te(OAc)_2$
47b, X = $TeCl_2$
47c, X = $TeBr_2$
47d, X = TeI_2

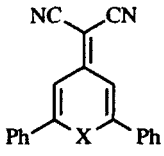

45, X = Te
48a, X = $Te(OAc)_2$
48b, X = $TeBr_2$

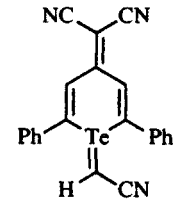

46

The reduction potentials of tellurium(IV) analogs of **44** and **45** followed the same trends as those observed for **29c** and **37** (Table 28). Initial two-electron reductions of tellurium(IV) analogs **47** regenerate the tellurium(II) analog **44**. The diacetate **47a** reduces at -0.58 V, and the dibromide **47c** reduces at 0.10 V.

Initial two-electron reductions of tellurium(IV) analogs **48** regenerate the tellurium(II) analogs **45**. The diacetate **48a** reduces at -0.30 V, and the dibromide **48b** reduces at 0.10 V.

The ylide **46** undergoes two reversible, one-electron reductions by cyclic voltammetry (Table 28).[50] The first wave is observed at 0.49 V (vs. SCE), and the second wave is observed at -0.96 V.

The reduction potentials of these telluropyranyl systems are made even more positive by incorporation of a Meldrum acid residue in the 4-position (Table 28).[50] The reduction potentials of **51** and **52** as measured by cyclic voltammetry are -0.79 and -1.09 V (vs. SCE), respectively, for two partially reversible waves. Similarly, the reduction potentials for benzo derivatives **187** and **188** are -0.80 and -0.63 V, respectively.

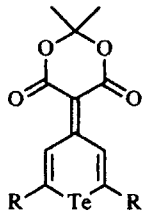

51, R = Ph
52, R = tert-Bu

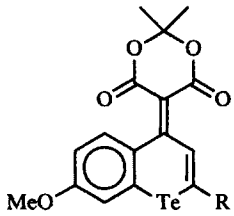

187, R = *tert*-Bu
188, R = Ph

Telluroxanthone (**128**) displays a partially reversible reduction wave at -1.62 V (vs. SCE).[133] The observations in the 4*H*-tellurin-4-one and 4*H*-benzotellurin-4-one derivatives might lead one to expect **127** to have a more positive reduction potential. In sulfone compounds **189**–**191**, the addition of each benzo-fused ring gives a more positive reduction potential from E_{red} of -0.74 V (vs. SCE) for **189** to -0.43 V for **191**.[52,134–138]

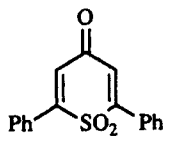

189

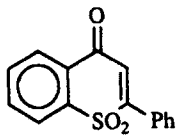

190

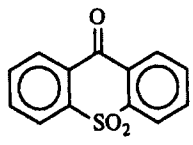

191

The dihalo tellurium(IV) analogs of **128** are easier to reduce than **128**.[133] The initial reduction is a two-electron process that is observed at -0.06 V (vs. SCE) for dichloride **141**, -0.05 V for dibromide **145**, 0.01 V for diiodide **192**, and -1.22 V for difluoride **193**. For each of these molecules, the initial two-electron reduction is followed by a partially reversible one-electron reduction at approximately -1.60 V, which is consistent with the regeneration of telluroxanthone (**128**) on two-electron reduction. The spread of reduction potentials for this

series is small relative to the dihalotellurin-4-ones **37a–c** (Table 28). From dichloride **141** to diiodide **193**, a range of 0.07 V is observed while from dichloride **37a** to diiodide **37c**, a range of 0.72 V is observed.

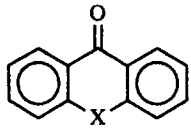

128, X = Te
141, X = $TeCl_2$
145, X = $TeBr_2$
192, X = TeI_2
193, X = F_2

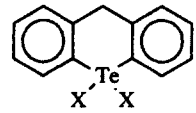

120, X = Cl
134, X = Br
135, X = I

Telluroxanthene tellurium(IV) derivatives **120**, **134**, and **135** display a much larger range of potentials for the two-electron reductions of the dihalides to telluroxanthene (**117**).[133] The dichloride **120** reduces at − 1.06 V (vs. SCE), dibromide **134** reduces at − 0.74 V, and diiodide **135** reduces at 0.01 V. The reduction potentials in this series cover a range of more than 1.0 V.

Telluroxanthone (**128**) is somewhat easier to reduce than selenoxanthone (**194**), which displays a partially reversible reduction wave at − 1.68 V (vs. SCE).[133] The chemistry of the chalcogen atom center is quite different in **128** and **194**. While telluroxanthone (**128**) readily forms the products of oxidative addition with the halogens, selenoxanthone **194** forms a selenium(IV) dichloride (**195**) with iodine but forms noncovalent complexes with iodine and bromide.[139,140] Thiaxanthone (**196**) forms noncovalent complexes only with the halogens.

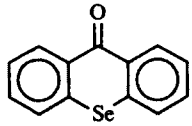

194

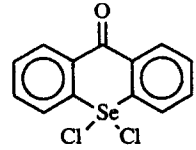

195

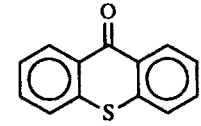

196

TABLES

TABLE 1. LIGAND EXCHANGE REACTIONS WITH SILVER SALTS AND 1,1-DICHLOROTELLURANE (**13a**[a])

Compd.	Conditions	Ligand	% Yield
13d	Ag_2O, H_2O, HF	F	85
13e	AgSCN	SCN	45
13f	AgCN	CN	65
13g	AgN_3	N_3	95
13h	AgNCO	NCO	85
13i	AgSeCN	SeCN	40
13j	AgO_2CCH_3	O_2CCH_3	65
13k	AgO_2CPh	O_2CPh	74
13l	AgO_2CCH_2Ph	O_2CCH_2PH	70
13m	AgO_2CCCl_3	O_2CCCl_3	82
13n	$AgO_2C(CH_2)_{13}CH_3$	$O_2C(CH_2)_{13}CH_3$	60

[a] Reference 8.

TABLE 2. REPRESENTATIVE EXAMPLES OF TELLURANE-3,5-DIONES **19** AND THEIR 1,1-DICHLORO ANALOGS **18** PREPARED BY TELLURIUM TETRACHLORIDE ADDITION TO 2,4-PENTANEDIONES FOLLOWED BY REDUCTION OF Te(IV) TO Te(II)

Compd.	R_1	R_2	R_3	R_4	% Yield	Compd.	% Yield	Ref.
18a	H	H	H	H	62	**19a**	70	1, 12
18b	H	Me	H	H	62	**19b**	76	12
18c	H	Et	H	H	80	**19c**	88	12, 13
18d	H	Et	Et	H	23	**19d**	100	12, 14
18e	Me	H	H	Me	71	**19e**	—	12, 14
18f	Me	Me	H	Me	68	**19f**	100	15
18g	Et	Et	H	H	63	**19g**	100	16
18h	Et	Et	H	Et	76	**19h**	—	12, 16
18i	Me	Me	H	H	—	**19i**	100	17
18j	H	Cl	H	H	—	**19j**	51	12
18k	H	*i*-Pr	H	H	—	**19k**	—	16
18l	Me	*n*-Pr	H	H	62	**19l**	—	18
18m	Me	H	H	Et	19	**19m**	—	14
18n	Me	Et	H	Me	—	**19n**	—	14
18o	*n*-Butyl	H	H	H	50	**19o**	70	18
18p	*n*-Decyl	H	H	H	—	**19p**	—	18
18q	Benzyl	H	H	H	—	**19q**	—	18
18r	H	Benzyl	H	H	60	**19r**	—	15
18s	H	Benzyl	Benzyl	H	23	**19s**	—	18
18t	Et	Me	H	H	80	**19t**	—	12
18u	*n*-Pr	H	H	*n*-Pr	—	**19u**	—	16

TABLE 3. PREPARATION OF 4*H*-TELLURIN-4-ONES **29** FROM 1,4-PENTADIYN-3-ONE PRECURSORS

Diynone	R	R′	Tellurating Agent	Compd.	R	R′	% Yield	Ref.
30a	Ph	Ph	Te, $LiEt_3BH$, THF NaOEt in EtOH	**29a**	Ph	Ph	51	38
30a	Ph	Ph	(*tert*-$BuMe_2$)$_2$Te, THF *tert*-BuOH, Bu_4NF	**29a**	Ph	Ph	19	38
30a	Ph	Ph	Te, $NaBH_4$, NaOEt in EtOH	**29a**	Ph	Ph	67	41
30b	*tert*-Bu	*tert*-Bu	Te, $NaBH_4$, NaOEt in EtOH	**29b**	*tert*-Bu	*tert*-Bu	66	41
30c	Me	Me	Te, $NaBH_4$, NaOEt in EtOH	**29c**	Me	Me	37	41
30d	Me_3SI	Me_3Si	Te, $NaBH_4$, NaOEt in EtOH	**29d**	H	H	38	42
30e	Ph	Me_3Si	Te, $NaBH_4$, NaOEt in EtOH	**29e**	Ph	H	32	42
30f	Ph	H	Te, $NaBH_4$, NaOEt in EtOH	**29f**	Ph	H	12	43
30g	Ph	4-$MeOC_6H_4$	Te, $NaBH_4$, NaOEt in EtOH	**29g**	Ph	4-$MeOC_6H_4$	38	43
30h	Ph	4-FC_6H_4	Te, $NaBH_4$, NaOEt in EtOH	**29h**	Ph	4-FC_6H_4	53	43
30i	Ph	2,5-$F_2C_6H_3$	Te, $NaBH_4$, NaOEt in EtOH	**29i**	Ph	2,5-$F_2C_6H_3$	58	43
30j	Ph	2-Thienyl	Te, $NaBH_4$, NaOEt in EtOH	**29j**	Ph	2-Thienyl	30	43
30g[a]	Ph	$(CH_2)_3OSiR_3$	Te, $NaBH_4$, NaOEt in EtOH	**29g**	Ph	$(CH_2)_3OSiR_3$	31	43

[a] SiR_3 = *tert*-$BuMe_2Si$.

TABLE 4. 2-SUBSTITUTED-3,4-DIMETHYL-3,5-DIHYDRO-2*H*-TELLURINS **27** AND **28** FROM CYCLOADDITION REACTIONS OF DIENES WITH *IN SITU*-GENERATED TELLUROALDEHYDES AND TELLUROKETONES

Compd.	Tellurating Agent	% Yield	Ref.
27a	Ph_3P/Te, Ph_3PCHPh	11	20
27a	$Me_2AlTeAlMe_2$	49	21
27b	$Me_2AlTeAlMe_2$	44	21
27c	$Me_2AlTeAlMe_2$	62	21
28a	$Me_2AlTeAlMe_2$	55	21
28b	$Me_2AlTeAlMe_2$	52	21

TABLE 5. CYCLIZATION OF 3-ARYLTELLUROPROPANOIC ACIDS **64** TO GIVE BENZOTELLURANE-4-ONES **65**

Compd.	R_1	R_2	R_3	R_4	R_5	R_6	% Yield	Ref.
65a	H	H	H	H	H	H	60	58
65b	H	H	Me	H	H	H	45	58
65c	H	H	H	Me	H	H	45	58
65d	Me	H	H	Me	H	H	13.5	58
65e	H	Me	Me	H	H	H	2	58
65f	H	H	H	H	H	Me	55	58
65g	H	H	H	H	Me	H	60	58
67	R_1,R_2 = benzo		H	H	—	—	66	58
69	5,6-[3,2]thiopheno			—	—	—	65	59

TABLE 6. PREPARATION OF 4-HYDROXYBENZOTELLURANES **78** VIA SODIUM BOROHYDRIDE REDUCTION OF BENZOTELLURANE-4-ONES **65**, **67**, AND **69**

Compd.	R_1	R_2	R_3	R_4	R_5	R_6	R_7	% Yield	Ref.
78a	H	H	H	H	H	H	H	66	58
78c	H	H	H	Me	H	H	H	55	58
78d	Me	H	H	Me	H	H	H	63	58
78f	H	H	H	H	H	Me	H	65	58
78g	H	H	H	H	Me	H	H	74	58
78h	R_1,R_2 = benzo		H	H	H	H	H	66	58
78i	5,6-[3,2]-thiopheno			—	H	H	H	64	59

TABLE 7. PREPARATION OF 2*H*-BENZOTELLURINS **77** VIA DEHYDRATION OF 4-HYDROXYBENZOTELLURANES **78**

Compd.	R_1	R_2	R_3	R_4	R_5	R_6	R_7	% Yield	Ref.
77a	H	H	H	H	H	H	H	87	58
77b	H	H	Me	H	H	H	H	78	59
77c	H	H	H	Me	H	H	H	80	59
77f	H	H	H	H	H	Me	H	85	59
77g	H	H	H	H	Me	H	H	75	59
77i	5,6-[3,2]-thiopheno			—	H	H	H	25	59
77j	H	H	H	H	H	H	Me	80	59

TABLE 8. SYNTHESIS OF 4*H*-2-PHENYLTELLURIN-4-ONES **98** ("TELLUROFLAVONES") AND OXATELLUROLYLIUM CHLORIDES **94** AND **99** FROM ACID CHLORIDES **93a** AND **97** VIA INTRAMOLECULAR ACYLATION WITH ALUMINUM CHLORIDE

Acid Chloride	X	Y	R	Product	% Yield	*ortho/ipso*	Ref.
93a	H	H	Ph	**94** (R = Ph)	81	0	74
97a	H	OMe	Ph	**98a1** (X = H, Y = OMe)	92	24	75
				98a2 (X = OMe, Y = H)	4		
				99a	4		
97b	OMe	OMe	Ph	**98b**	90	> 100	75
97c	H	F	Ph	**98c** (X = H, Y = F)	5	0.06	75
				99c	78		
97d	F	F	Ph	**98d**	18	0.20	76
				99d	72		
97e	H	Me	Ph	**99e**	92	0	74
97i	OMe	OMe	4-MeOPh	**98i**	58	> 100	76
97j	OMe	OMe	3,4-$(MeO)_2$Ph	**98j**	57	> 100	76
97k	OMe	OMe	2,5-$(MeO)_2$Ph	**98k**	72	> 100	76
97l	H	OMe	4-MeOPh	**98l**	44	20	76
97m	H	OMe	3,4-$(MeO)_2$Ph	**98m**	68	20	76
97n	H	OMe	2,5-$(MeO)_2$Ph	**98n** (X = H, Y = OMe)	13	20	76
	H	OMe	2,5-$(MeO)_2$Ph	**98o** (X = OMe, Y = H)	50		76

TABLE 9. CYCLIZATION OF (ARYLTELLURO)PROPENOIC ACIDS **106** WITH PHOSPHORUS PENTOXIDE IN METHANE SULFONIC ACID

Acid	X	Y	R	Product	% Yield	Ref.
106a	H	OMe	Ph	**98a**	90	75
106b	OMe	OMe	Ph	**98b**	85	75
106c	H	F	Ph	**98c**	6	76
106d	F	F	Ph	**98d**	18	76
106e	H	OMe	Me	**98e**	67	75
106f	OMe	OMe	Me	**98f**	62	75
106g	H	OMe	H	**98g**	67	75
106h	OMe	OMe	H	**98h**	74	75

TABLE 10. SYNTHESIS OF 5-HYDROXYTELLURIN-4-ONES **110** FROM 5-METHOXYTELLURIN-4-ONES **98** VIA HYDROLYSIS OF INTERMEDIATE DIFLUOROBORONATES **109**[a]

Starting Material	Y	R	Difluoroboronate	% Yield	Product Tellurinone	% Yield
98a	H	Ph	**109a**	72	**110a**	90
98b	OMe	Ph	**109b**	73	**110b**	84
98f	OMe	Me	**109c**	91	**110c**	90
98i	OMe	4-$MeOC_6H_4$	**109d**	66	**110d**	93
98j	OMe	3,4-$(MeO)_2C_6H_3$	**109e**	96	**110e**	91
98k	OMe	2,5-$(MeO)_2C_6H_3$	**109f**	83	**110f**	86

[a] Reference 76.

TABLE 11. BOND LENGTHS AND BOND ANGLES FOR TELLURANE DERIVATIVE **150**, DICHLOROTELLURANE-3,5-DIONE **18a**, AND TELLURANE-3,5-DIONES **19**

Bond Length (Å) or Angle (°)	Compound		
	150[a]	**18a**[b]	**19**[c]
Te—Cl	2.14	2.14–2.18	2.14–2.20
Te—C5	2.15	2.14–2.18	2.14–2.20
C1—C2	1.52	1.46–1.50	1.45–1.49
C2—C3	1.49	1.50–1.53	1.52–1.55
C3—C4	1.52	1.50–1.53	1.52–1.55
C4—C5	1.49	1.46–1.50	1.45–1.51
C1—Te–C5	91.6	95.2–95.7	88.4–90.8
Te—C1—C2	112.1	112	103.4–107.9
C1—C2—C3	114.7	117–119	115.9–118.4
C2—C3—C4	114.3	110–111	109.6–110.9
C3—C4—C5	114.7	117–119	115.9–118.4
C4—C5—Te	115.4	112	103.4–107.9

[a] Reference 95. [b] Reference 104. [c] References 104–110.

TABLE 12. ^{13}C NMR DATA FOR COMPOUNDS **1**, **13b**, **13c**, **14**, AND **151–154**

Compd.	Chemical Shift (δ, ppm)				
	C1	C2	C3	C4	C5
1[a]	− 2.1	29.9	30.9	29.9	− 2.1
151[a]	20.2	29.1	28.4	29.1	20.2
152[a]	29.3	28.2	26.9	28.2	29.3
153[a]	68.0	26.6	23.6	26.6	68.0
14[b]	11.35	28.96	42.09	25.06	− 4.03
13b[a]	36.9	20.3	25.9	20.3	36.9
13c[a]	33.2	21.4	25.5	21.4	33.2
154[c]	27.5	26.3	21.3	26.3	27.5

[a] Reference 101.
[b] Reference 7.
[c] Reference 9.

TABLE 13. SELECTED ^{1}H AND ^{13}C NMR CHEMICAL SHIFTS FOR **27a**, **157–159**, AND TUNGSTEN-COORDINATED COMPLEXES **25**

Compd.	X	Chemical Shift (δ, ppm)						
		H_2	H_3	$H_{3'}$	H_6	$H_{6'}$	C_2	C_6
27a[a]	Te	4.80	2.97	2.41	3.78	3.11	34.6	4.3
157[a]	Se	3.80	2.40	2.06	2.93	2.60	38.5	24.1
158[a]	S	3.90	2.59	2.41	3.46	2.90	43.4	32.8
159[a]	O	4.48	2.43	2.30	4.19	4.15	—	—
25a[b]	W–Te	4.93	3.31	2.29	4.25	3.76	—	—
25b[b]	W–Te	4.72	3.08	2.35	4.11	3.28	49.3	14.3

[a] Reference 21.
[b] Reference 22.

TABLE 14. SELECTED BOND LENGTHS AND BOND ANGLES FOR 4*H*-TELLURIN-4-ONE **29d**, 4*H*-SELENIN-4-ONE **160**, AND 4*H*-THIAPYRAN-4-ONES **161**

Bond Length (Å) or Angle (°)	Compound		
	29d[a]	**160**[a]	**161**[a]
X—Cl	2.05	1.853	1.698
X—C5	2.05	1.853	1.700
C1—C2	1.32	1.342	1.334
C2—C3	1.45	1.448	1.437
C3—C4	1.45	1.448	1.428
C4—C5	1.32	1.342	1.329
C3—O	1.27	1.242	1.244
C1—X—C5	91.3	97.8	100.9
X—C1—C2	125	124.8	125.7
C1—C2—C3	128	126.7	125.1
C2—C3—C4	122	119.2	117.0
C3—C4—C5	128	124.8	125.5
C4—C5—X	125	124.8	125.8

[a] Reference 42.

TABLE 15. ^{1}H AND ^{13}C NMR CHEMICAL SHIFTS, CARBONYL STRETCHING FREQUENCIES, UV ABSORPTION MAXIMA, AND DIPOLE MOMENTS FOR 4*H*-CHALCOGENAPYRAN-4-ONES **29d** AND **160–162**

		^{1}H NMR[a]		^{13}C NMR[a]					
		[δ, ppm ($CDCl_3$)]					$\nu_{C=O}$[a] (cm^{-1})	λ_{max} (log ε)[a] (nm)	μ[b] (D)
Compd.	X	H_A	H_B	C_1, C_5	C_2, C_4	C_3	(KBr)	(CH_2Cl_2)	($CH_3C_6H_5$)
29d	Te	8.71	7.31	136.8	129.3	184.7	1560	344 (4.30)	4.31
160	Se	8.20	7.17	138.8	132.6	181.0	1585	310 (4.22)	3.80
161	S	7.47	7.02	137.7	131.7	179.6	1610	297 (4.04)	3.75
162	O	8.10[c]	6.30[c]	—	—	—	1650[d]	—	3.48

[a] Reference 42.
[b] Reference 115.
[c] In DMSO-d_6
Reference 116.
[d] Reference 117.

TABLE 16. COMPARISON OF SPECTROSCOPIC PROPERTIES FOR TELLURIUM(II) AND TELLURIUM(IV) ANALOGS OF TELLURIN-4-ONES **29a** AND **29b**

Compd.	R	X	^{1}H NMR[a] (δ, ppm) H_B	$\nu_{C=O}$[a] (cm^{-1}) (KBr)	Binding Energy[b] Te($3d_{5/2}$) ($\pm$ 0.1 eV) (eV)	^{125}Te NMR[b] (δ, ppm) (CD_2Cl_2)
29a	Ph	Te	7.31	1570	574.3	553
29b	*tert*-Bu	Te	6.90	1595	574.1	445
37a	*tert*-Bu	$TeCl_2$	6.10	1635	576.4	434
37b	*tert*-Bu	$TeBr_2$	6.12	1615	576.0	363
38	Ph	$TeBr_2$	6.45	1615	—	424

[a] Reference 50.
[b] Reference 73.

TABLE 17. COMPARISON OF NMR SPECTROSCOPIC PROPERTIES OF TELLURINS **40a** AND **40b** WITH LIGHTER CHALCOGEN ANALOGS **164–166**

Compd.	^{1}H NMR[a] (δ, ppm) H_A	H_B ($CDCl_3$)	$J_{H_A-H_B}$ (Hz)	^{13}C NMR[a] (δ, ppm) C1, C5	C2, C4 ($CDCl_3$)	C3	^{125}Te NMR[b] (δ, ppm) ($CDCl_3$)
40a	6.02	2.66	5.4	146.2	123.6	39.8	257
40b	6.15	2.70	5.5	—	—	—	—
43	5.95	2.48	1.9	146.9	128.8	55.6	296
164	5.87	2.58	5.0	—	—	—	—
165	5.62	2.66	4.7	—	—	—	—
166	4.53	2.72	3.3	—	—	—	—

[a] Reference 51.
[b] Reference 73.

TABLE 18. SELECTED ^{1}H AND ^{13}C NMR CHEMICAL SHIFTS FOR 2*H*-BENZOTELLURIN-2-ONE (**80**) AND ITS SELENIUM, SULFUR, AND OXYGEN ANALOGS **167–169**

Compd.	X	H_A (δ, ppm)	H_B (δ, ppm)	$J_{H_A-H_B}$ (Hz)	C1 (δ, ppm)	C2 (δ, ppm)	C3 (δ, ppm)	C4 (δ, ppm)	C5 (δ, ppm)	C6 (δ, ppm)
80	Te	7.59[a]	5.61	11.7	193.5	125.0	145.4	130.8	125.0	135.7[e]
167	Se	7.45[b]	6.02	11.0	188.4	122.8	144.2	126.9	137.0	128.2[e]
168	S	7.76[c]	6.48	—	184.5	123.6	143.4	125.7	137.2	125.2[e]
169	O	7.78[d]	6.42	9.0	160.5	116.5	143.6	118.8	153.9	116.5[e]

[a] Reference 64.
[b] Reference 120.
[c] Reference 121.
[d] Reference 123.
[e] Reference 125.

TABLE 19. SELECTED SPECTRAL PROPERTIES FOR 2-BENZOTELLURIN-1-ONE (**83**) AND ITS SELENIUM, SULFUR, AND OXYGEN ANALOGS **170–172**

Compd.	X	H_A (δ, ppm)	H_B (δ, ppm)	$J_{H_A-H_B}$ (Hz)	$\nu_{C=O}$ (cm^{-1})	μ^d (D)
83	Te	7.61[a]	7.92	10.7	1628	3.25
170	Se	7.26[a]	7.46	9.8	1643	3.77
171	S	7.10[b]	6.98	9.5	1640	3.99
172	O	7.17[c]	6.40	5.5	1745	—

[a] Reference 72.
[b] Reference 126.
[c] Reference 127.
[d] Reference 128.

TABLE 20. SELECTED SPECTRAL PROPERTIES FOR 3,4-DIHYDRO-2-BENZOTELLURIN-1-ONE (**76**) AND ITS SELENIUM, SULFUR, AND OXYGEN ANALOGS **173–175**

Compd.	X	^{13}C NMR[a] (δ, ppm) C1	C2	C3	$\nu_{C=O}$ (cm^{-1})	μ^b (D)
76	Te	193.6	5.2	34.3	1720(w), 1635[c]	—
173	Se	192.5	20.7	32.0	1663[a]	4.32
174	S	190.3	28.6	30.2	1715(w), 1655[d]	4.49
175	O	165.0	67.3	27.7	—	4.56

[a] Reference 71.
[b] Reference 128.
[c] Reference 129.
[d] Reference 130.

TABLE 20a. SELECTED SPECTRAL PROPERTIES FOR 3,4-DIHYDRO-2-BENZOTELLURIN-3-ONE (**76a**) AND ITS SELENIUM, SULFUR, AND OXYGEN ANALOGS **173a–175a**[a]

Compd.	X	^1H NMR (δ, ppm) H_A	H_B ($CDCl_3$)	J_{X-H_A} (Hz)	^{13}C NMR (δ, ppm) C1	C2 ($CDCl_3$)	C3	$\nu_{C=O}$ (cm^{-1}) (KBr)
76a	Te	4.3	3.7	31.5[b]	8.5	209.6	58.1	1655
173a	Se	4.2	3.7	15[c]	27.7	206.4	52.5	1665
174a	S	4.1	3.7	—	34.1	202.4	49.2	1660
175a	O	3.9	3.6	—	69.9	169.3	35.9	1748

[a] Reference 71a.
[b] X = ^{125}Te.
[c] X = ^{77}Se.

TABLE 21. SELECTED SPECTRAL PROPERTIES FOR 4*H*-BENZOTELLURIN-4-ONE (**89a**) AND ITS SELENIUM, SULFUR, AND OXYGEN ANALOGS **176–178**[a]

Compd.	X	H_A (δ, ppm)	H_B (δ, ppm)	$J_{H_A-H_B}$ (Hz)	$\nu_{C=O}$ (cm^{-1})	λ_{max}(log ε)	μ (D)
89a	Te	8.61	7.38	11.8	1625.5	388 (4.029)	3.65
176	Se	8.14	7.10	10.7	1629	348 (4.020)	3.47
177	S	7.74	6.91	10.5	1636	334 (3.974)	3.48
178	O	7.78	6.24	6.1	1669	301 (3.842)	3.46

[a] Reference 131.

TABLE 22. ^{13}C NMR CHEMICAL SHIFTS FOR 4*H*-BENZOTELLURIN-4-ONE (**89a**) AND ITS SELENIUM, SULFUR, AND OXYGEN ANALOGS **176–178**[a]

		^{13}C NMR (δ, ppm)								
Compd.	X	C1	C2	C3	C4	C5	C6	C7	C8	C9
89a	Te	134.6	134.3	185.5	136.0	124.2	132.3	131.5	126.4	128.9
176	Se	137.6	128.4	181.2	136.5	133.3	130.1	131.3	127.8	128.7
177	S	138.2	127.1	180.0	132.8	137.9	126.3	131.8	128.2	129.1
178	O	155.8	113.3	177.9	125.3	155.6	118.5	134.1	125.6	126.1

[a] Reference 131.

TABLE 23. SELECTED ^1H NMR DATA FOR 4*H*-2-METHYLBENZOTELLURIN-4-ONE (**89b**) AND ITS SELENIUM, SULFUR, AND OXYGEN ANALOGS **181–183**[a]

Compd.	X	CH_3 (δ, ppm)	H_B (δ, ppm)	$J_{CH_3-H_B}$ (Hz)
89b	Te	2.47	7.05	1.3
181	Se	2.41	6.88	1.18
182	S	2.35	6.74	1.15
183	O	2.25	6.03	0.65

[a] Reference 60.

TABLE 24. CARBONYL STRETCHING FREQUENCIES $\nu_{C=O}$ AND DIPOLE MOMENTS μ FOR BENZOTELLURANE-2-ONE **65a** AND ITS SELENIUM, SULFUR, AND OXYGEN ANALOGS **184–186**[a]

Compd.	X	$\nu_{C=O}$ (cm^{-1})		μ (D)
		CCl_4	KBr	
65a	Te	1679	1668	2.23
184	Se	1685	1679	2.00
185	S	1688	1681	2.07
186	O	1701	1691	2.24

[a] Reference 131.

TABLE 25. SELECTED ^{1}H NMR DATA FOR 2*H*-BENZOTELLURINS **77**[a]

Compd.	H_A	H_B	H_C	$J_{H_A-H_B}$	$J_{H_B-H_C}$	$J_{H_A-H_C}$
	(δ, ppm)			(Hz)		
77a	3.26	5.31	6.10	5.9	10.8	1.5
77b	3.31	5.28	6.14	5.8	10.4	1.5
77c	3.21	5.23	6.14	5.8	10.4	1.4
77f	3.18	—	6.14	—	—	—
77g	3.82	5.23	6.16	5.6	10.2	—
77i	3.38	5.33	6.22	5.9	10.4	—
77j	3.00	5.50	—	6.9	—	—

[a] Reference 59.

TABLE 26. SELECTED ^{1}H[a,b] AND ^{125}Te NMR DATA AND Te ($3d_{5/2}$) XPS BINDING ENERGIES FOR 4*H*-BENZOTELLURINS **86** AND THEIR TELLURIUM(IV) ANALOGS **87** AND **88**[a]

Compd.	H_A	H_B	H_C	$J_{H_A-H_B}$	$J_{H_B-H_C}$	$J_{H_A-H_C}$	^{125}Te NMR (δ, ppm)	Te($3d_{5/2}$) (eV)
	(δ, ppm)			(Hz)				
86a	—	6.47	3.37	—	5.8	—	380	—
86b	—	6.19	3.25	—	5.6	—	391	573.9
86c	6.31	5.44	3.26	10.6	5.5	1.0	—	—
87	—	6.27	4.20	—	4.5	—	611	576.1
88	—	6.18	4.18	—	4.5	—	550	575.8

[a] Reference 73.
[b] Reference 51.

TABLE 27. SELECTED BOND LENGTHS AND BOND ANGLES FOR TELLUROXANTHENE **117** AND TELLUROXANTHENYL DIMER **127**[a]

Bond Length (Å) or Angle (°)	Compound	
	117	**127**[b]
Te—C1	2.14	2.10
Te—C5	2.13	2.10
C1—C2	1.38	1.39
C2—C3	1.52	1.51
C3—C4	1.52	1.52
C4—C5	1.38	1.39
C3—C3'	—	1.57
C1—Te—C5	89.7	91.5
Te—C1—C2	119	121
C1—C2—C3	120	122.6
C2—C3—C4	115	1115.3
C3—C4—C5	119	122.6
C4—C5—Te	121	121

[a] Reference 88. [b] Average of both rings.

TABLE 28. REDUCTION POTENTIALS FOR 4*H*-TELLURIN-4-ONES, DERIVATIVES, BENZO-FUSED ANALOGS, AND TELLURIUM(IV) ANALOGS AS DETERMINED BY CYCLIC VOLTAMMETRY[a]

Compd.	E_1 (V)		E_2 (V)	
	E_{pc}	E_{pa}	E_{pc}	E_{pa}
29c	− 1.60	—	—	
98l	− 1.61	− 1.52	− 1.96	—
37a	− 0.68	—	− 1.60	—
37b	− 0.46	—	− 1.60	—
37c	0.04	—	− 1.60	—
37d	− 1.14	—	− 1.60	—
44	− 1.30	− 1.21	—	
45	− 1.03	− 0.93	—	
46	0.45	0.52	− 0.99	− 0.93
47a	− 0.58	—	− 1.32	− 1.20
47c	0.10	—	− 1.31	− 1.21
48a	− 0.30	—	− 1.03	− 0.91
48b	0.10	—	− 1.01	− 0.92
51	− 0.85	− 0.73	− 1.48	—
52	− 1.16	− 1.02	− 1.95	—
187	− 0.85	− 0.75	− 1.78	—
188	− 0.70	− 0.55	− 1.38	—

[a] Reference 50. Potentials versus SCE in dichloromethane with 0.2 *M* tetra-*n*-butylammonium tetrafluoroborate as supporting electrolyte at a Pt disk electrode and a sweep rate of 0.1 $V s^{-1}$.

REFERENCES

1. Morgan, G. T.; Drew, H. D. K. *J. Chem. Soc.* **1920**, *117*, 1456.
2. Morgan, G. T.; Burgess, H. *J. Chem. Soc.* **1928**, *133*, 321.
3. Morgan, G. T.; Burstall, F. H. *J. Chem. Soc.* **1931**, *145*, 180.
4. Farrar, W. V.; Gulland, J. M. *J. Chem. Soc.* **1945**, 11.
5. Lambert, J. B.; Vagenas, A. R. *Org. Magn. Reson.* **1981**, *17*, 270.
6. Srivastava, T. N.; Srivastava, R. C.; Singh, H. B. *Ind. J. Chem.* **1979**, *18A*, 71.
7. Al-Rubaie, A. Z.; Al-Shirayda, H. A. *J. Iraqi Chem. Soc.* **1985**, *10*, 149.
8. Smith, M. R.; Thomas, J. W., Jr.; Meyers, E. A. *Cryst. Struct. Commun.* **1979**, *8*, 351.
9. Pathirana, H. M. K. K.; McWhinnie, W. R. *J. Chem. Soc., Dalton. Trans.* **1986**, 2003.
10. Ayoob, A. I.; Al-Allef, T. A. K.; Mohammed, S. A. *Asian J. Chem.* **1991**, *3*, 38.
11. Evers, M.; Christiaens, L.; Renson, M. *Tetrahedron Lett.* **1985**, *26*, 5441.
12. Morgan, G. T.; Drew, H. D. K. *J. Chem. Soc.* **1922**, *121*, 922.
13. Morgan, G. T.; Rawson, A. E. *J. Soc. Chem. Ind.* **1925**, *44*, 462.
14. Morgan, G. T.; Drew, H. D. K. *J. Chem. Soc.* **1924**, *125*, 731.
15. Morgan, G. T.; Taylor, C. J. A. *J. Chem. Soc.* **1925**, *127*, 797.
16. Morgan, G. T.; Thomason, R. W. *J. Chem. Soc.* **1924**, *125*, 754.
17. Morgan, G. T.; Drew, H. D. K. *J. Chem. Soc.* **1924**, *125*, 1601.
18. Morgan, G. T.; Corly, F. J.; Elvins, O. C.; Jones, E.; Kellett, R. E.; Taylor, C. J. A. *J. Chem. Soc.* **1925**, *127*, 2611.
19. Fischer, H.; Gerbing, U. *J. Organomet. Chem.* **1986**, *299*, C7.
20. Segi, M.; Koyama, T.; Takata, Y.; Nakajima, T.; Suga, S. *J. Am. Chem. Soc.* **1989**, *111*, 8749.
21. Erker, G.; Hock, R. *Angew. Chem.* **1989**, *101*, 181.
22. Fischer, H.; Fruh, A.; Troll, C. *J. Organomet. Chem.* **1991**, *415*, 211.
23. Barrett, A. G. M.; Barton, D. H. R.; Read, R. W. *J. Chem. Soc., Chem. Commun.* **1979**, 645.
24. Barrett, A. G. M.; Read, R. W.; Barton, D. H. R. *J. Chem. Soc., Perkin Trans. I* **1980**, 2191.
25. Severengiz, T.; du Mont, W. W. *J. Chem. Soc., Chem. Commun.* **1987**, 820.
26. Lerstrup, K. A.; Henrikson, L. *J. Chem. Soc., Chem. Commun.* **1979**, 1102.
27. Bender, S. L.; Haley, N. F.; Luss, H. R. *Tetrahedron Lett.* **1981**, *22*, 1495.
28. Lakshmikantham, M. V.; Cava, M. P.; Albeck, M.; Engman, L.; Bergman, J.; Wudl, F. *J. Chem. Soc., Chem. Commun.* **1981**, 828.
29. Lakshmikantham, M. V.; Cava, M. P.; Albeck, M.; Engman, L.; Carroll, P. *Tetrahedron Lett.* **1981**, *22*, 4199.
30. Lappert, M. F.; Martin, T. R.; MacLaughlin, G. M. *J. Chem. Soc., Chem. Commun.* **1980**, 635.
31. Fischer, H.; Zeuner, S. *J. Organomet. Chem.* **1983**, *252*, C63.
32. Fischer, H.; Pashalidis, I. *J. Organomet. Chem.* **1988**, *348*, C1.
33. Headford, C. E. L.; Roper, W. R. *J. Organomet. Chem.* **1983**, *244*, C53.
34. Hill, A. F.; Roper, W. R.; Waters, J. M.; Wright, A. H. *J. Am. Chem. Soc.* **1983**, *105*, 5939.
35. Herrman, W. A.; Weichmann, J.; Serrano, R.; Blechschmitt, K.; Pfisterer, H.; Ziegler, M. L. *Angew. Chem., Int. Ed. Engl.* **1983**, *22*, 314.
36. Paul, W.; Werner, H. *Angew. Chem., Int. Ed. Engl.* **1983**, *22*, 316.
37. Wolf, J.; Zolk, R.; Schubert, U.; Werner, H. *J. Organomet. Chem.* **1988**, *340*, 161.
38. Detty, M. R.; Murray, B. J.; Seidler, M. D. *J. Org. Chem.* **1982**, *47*, 1968.
39. Detty, M. R.; Murray, B. J. *J. Org. Chem.* **1982**, *47*, 5235.

40. Detty, M. R.; Murray, B. J.; Perlstein, J. H. U.S Patent 4,431,586 (1984).
41. Detty, M. R.; Hassett, J. W.; Murray, B. J.; Reynolds, G. A. *Tetrahedron* **1985**, *41*, 4853.
42. Detty, M. R.; Luss, H. R. *Organometallics* **1992**, *11*, 2157.
43. Wadsworth, D. H.; Geer, S. M.; Detty, M. R. *J. Org. Chem.* **1987**, *52*, 3662.
44. Regnault du Mottier, C.; Brutus, M.; Le Coustumer, G.; Sauve, J. P.; Ebel, M.; Mollier, Y. *Mol. Cryst. Liq. Cryst.* **1988**, *154*, 361.
45. Tolmachev, A. I.; Sribnaya, V. P. *Khim. Geterotsikl. Soedin.* **1966**, 183.
46. Gaudemar-Bardone, F. *Ann. Chim. (Paris)* **1958**, *3*, 52.
47. Tolmachev, A. I.; Kudinova, M. A. *Khim. Geterotskil. Soedin.* **1974**, 274.
48. Wadsworth, D. H.; Detty, M. R. *J. Org. Chem.* **1980**, *45*, 4611.
49. Detty, M. R.; McGarry, L. W. *J. Org. Chem.* **1988**, *53*, 1203.
50. Detty, M. R.; Murray, B. J. *J. Org. Chem.* **1987**, *52*, 2123.
51. Detty, M. R. *Organometallics* **1988**, *7*, 1122.
52. Scozzafava, M.; Chen, C. H.; Reynolds, G. A.; Perlstein, J. H. U.S. Patent 4,514,481 (1985).
53. Detty, M. R.; McKelvey, J. M.; Luss, H. R. *Organometallics* **1988**, *7*, 1131.
54. Detty, M. R.; Merkel, P. B.; Hilf, R.; Gibson, S. L., Powers, S. K. *J. Med. Chem.* **1990**, *33*, 1108.
55. Wadsworth, D. H.; Detty, M. R.; Murray, B. J.; Weidner, C. H.; Haley, N. F. *J. Org. Chem.* **1984**, *49*, 2676.
56. Singh, H. B.; Khanna, P. K.; Kumar, S. K. *J. Organomet. Chem.* **1988**, *338*, 1.
57. Piette, J.-L.; Renson, M. *Bull. Soc. Chim. Belges* **1971**, *80*, 669.
58. Dereu, N.; Piette, J.-L.; Van Coppenolle, J.; Renson, M. *J. Heterocycl. Chem.* **1975**, *12*, 423.
59. Dereu, N.; Renson, M. *J. Organomet. Chem.* **1983**, *258*, 163.
60. Dereu, N.; Renson, M. *J. Organomet. Chem.* **1981**, *208*, 11.
61. Gillespie, R. J. *J. Chem. Educ.* **1970**, *47*, 18.
62. Drago, R. S. *J. Chem. Educ.* **1973**, *50*, 244.
63. Rundle, R. E. *Rec. Chem. Prog.* **1962**, *50*, 3677.
64. Christiaens, L.; Piette, J.-L.; Luxen, A.; Renson, M. *J. Heterocycl. Chem.* **1984**, *21*, 1281.
65. Renson, M.; Collienne, R. *Bull. Soc. Chim. Belg.* **1964**, *73*, 491.
66. Gunther, W. H. H. *J. Org. Chem.* **1966**, *31*, 1202.
67. Gunther, W. H. H. *J. Org. Chem.* **1967**, *32*, 3929.
68. Christiaens, L.; Renson, M. *Tetrahedron* **1972**, *28*, 5405.
69. McMurray, W. J.; Lipsky, S. R.; Cashley, R. J.; Mautner, H. G. *J. Heterocycl. Chem.* **1972**, *9*, 1093.
70. Wallmark, I.; Krackov, M. H.; Shi-Hsi Chu; Mautner, H. G. *J. Am. Chem. Soc.* **1970**, *92*, 4447.
71. Loth-Compere, M.; Luxen, A.; Thibaut, P.; Christiaens, L.; Guillaume, M.; Renson, M. *J. Heterocycl. Chem.* **1981**, *18*, 343.
71a. Lemaire, Ch.; Luxen, A.; Christiaens, L.; Guillaume, M. *J. Heterocycl. Chem.* **1983**, *20*, 811.
72. Luxen, A.; Christiaens, L., Renson, M. *J. Org. Chem.* **1980**, *45*, 3535.
73. Detty, M. R.; Lenhart, W. C.; Gassman, P. G.; Callstrom, M. R. *Organometallics* **1989**, *8*, 861.
74. Detty, M. R.; Murray, B. J.; Smith, D. L.; Zumbulyadis, N. *J. Am. Chem. Soc.* **1983**, *105*, 875.
75. Detty, M. R.; Murray, B. J. *J. Am. Chem. Soc.* **1983**, *105*, 883.
76. Detty, M. R.; *Organometallics* **1988**, *7*, 2188.
77. Piette, J.-L.; Thibaur, P.; Renson, M. *Chem. Scr.* **1975**, *8*, 117.
78. Piette, J.-L.; Thibaur, P.; Renson, M. *Tetrahedron* **1978**, *34*, 655.
79. Swain, C. G.; Lupton, E. C., Jr. *J. Am. Chem. Soc.* **1968**, *90*, 4328.
80. Eaton, P. E.; Carlson, G. R.; Lee, J. T. *J. Org. Chem.* **1973**, *38*, 4071.

81. Dean, F. M.; Goodchild, J.; Houghton, L. E.; Martin, J. A.; Morton, R. B.; Parton, B.; Price, A. W.; Somvichien, N. *Tetrahedron Lett.* **1966**, 4153.
82. Detty, M. R.; Murray, B. J. *J. Org. Chem.* **1982**, *47*, 1147.
83. Sadekov, I. D.; Ladatko, A. A.; Minkin, V. I. *Khim. Geterotsikl. Soedin.* **1978**, 1567.
84. Sadekov, I. D.; Ladatko, A. A.; Sadekova, E. I.; Minkin, V. I. *Khim. Geterotsikl. Soedin.* **1980**, 1342.
85. Lohner, W.; Praefcke, K. *J. Organomet. Chem.* **1981**, *205*, 167.
86. Ladatko, A. A.; Sadekov, I. D.; Etmatchenko, L. N.; Minkin, V. I. *Khim. Geterotskil. Soedin.* **1989**, 691.
87. Sadekov, I. D.; Barchan, I. A.; Ladatko, A. A.; Abakarov, G. M.; Sadekova, E. I.; Simkina, Yu. N.; Minkin, V. I. *Khim.-Fhar. Zh.* **1982**, *16*, 1070.
88. Karaev, K. Sh.; Furmanova, N. G.; Belov, N. V.; Sadekov, I. D.; Ladatko, A. A.; Minkin, V. I. *Zh. Strukt. Khim.* **1981**, *22*, 106.
89. Ladatko, A. A.; Sadekov, I. D.; Minkin, V. I. *Khim. Geterotsikl. Soedin.* **1987**, 279.
90. Sadekov, I. D.; Ladatko, A. A.; Sadekova, E. I.; Minkin, V. I. *Khim. Geterotskil. Soedin.* **1980**, 274.
91. Sadekov, I. D.; Ladatko, A. A.; Sadekova, E. I.; Dorofeenko, G. N.; Minkin, V. I. *Khim. Geterotsikl. Soedin.* **1981**, 343.
92. Ladatko, A. A.; Nivorozhkin, V. L.; Sadekov, I. D. *Khim. Geterotsikl. Soedin.* **1986**, 1571.
93. Eremenko, O. N.; Ladatko, A. A.; Lynbovskaya, R. N.; Minkin, V. I.; Sadekov, I. D.; Khidekel, M. L. *Izv. Akad. Nauk SSSR, Ser. Khim.* **1983**, 690.
94. Lohner, W.; Praefcke, K. *Chem.-Zeit.* **1979**, *103*, 265.
95. Smith, M. R.; Thomas, J. W., Jr.; Meyers, E. A. *Cryst. Struct. Commun.* **1979**, *8*, 351.
96. Lambert, J. B.; Keske, R. G. *Tetrahedron Lett.* **1967**, 4755.
97. Lambert, J. B.; Keske, R. G.; Weary, D. K. *J. Am. Chem. Soc.* **1967**, *89*, 5921.
98. Lambert, J. B.; Mixan, C. E.; Johnson, D. H. *J. Am. Chem. Soc.* **1973**, *95*, 4634.
99. Lambert, J. B.; Sun, H.-N. *Org. Magn. Reson.* **1977**, *9*, 621.
100. Forest, T. P. *J. Am. Chem. Soc.* **1975**, *97*, 2628.
101. Lambert, J. B.; Netzel, D. A.; Sun, H.-N.; Lilianstrom, K. K. *J. Am. Chem. Soc.* **1976**, *98*, 3778.
102. Schneider, H.-J.; Hoppen, V. *J. Org. Chem.* **1978**, *43*, 3866.
103. Hope, E. G.; Kemmitt, T.; Levason, W. *Organometallics* **1988**, *7*, 78.
104. Raston, C. L.; Secomb, R. J.; White, A. H. *J. Chem. Soc., Dalton Trans.* **1976**, 2307.
105. Dewan, J. C.; Silver, J. *Acta Crystallogr., Sect. B* **1977**, *B33*, 2671.
106. Dewan, J. C.; Silver, J. *Acta Crystallogr., Sect. B* **1977**, *B33*, 1469.
107. Dewan, J. C.; Silver, J. *Inorg. Nucl. Chem. Lett.* **1976**, *12*, 647.
108. Dewan, J. C.; Silver, J. *J. Chem. Soc., Dalton Trans.* **1977**, 644.
109. Dewan J. C.; Silver, J. *Aust. J. Chem.* **1977**, *30*, 487.
110. Dewan, J. C.; Silver, J. *J. Organomet. Chem.* **1977**, *125*, 125.
111. Berry, F. J.; Silver, J. *J. Organomet. Chem.* **1980**, *188*, 255.
112. Dance, N. S.; Jones, C. H. W. *Can. J. Chem.* **1978**, *56*, 1746.
113. Smith, M. R.; Mangion, M. M.; Zingaro, R. A.; Mengers, E. A. *J. Heterocycl. Chem.* **1973**, *10*, 527.
114. McCullough, J. D. *Inorg. Chem.* **1975**, *14*, 2639.
115. Detty, M. R.; Fitzgerald, J.; McKelvey, J. M. *Organometallics*, manuscript submitted for publication.
116. Pouchert, C. J. *The Aldrich Library of NMR Spectra*, 2nd ed., Aldrich Chemical Co., 1983, Vol. 1, p. 416D.

117. Pouchert, C. J. *The Aldrich Library of Infrared Spectra*, Aldrich Chemical Co., 1975, Vol. 2, p. 216D.
118. McFarlane, H. C. E.; McFarlane, W. In *NMR of Newly Accessible Nuclei*; Laszlo, P. Ed.; Academic Press, Orlando, FL, 1983.
119. Lutz, O. In *The Multinuclear Approach to NMR Spectroscopy*, Lambert, J. B.; Riddell, F. G. eds.; D. Reidel, Boston, 1983.
120. Ruwet, A.; Renson, M. *Bull. Soc. Chim. Belg.* **1969**, *78*, 449.
121. Meth-Cohn, O.; Ternowski, B. *Synthesis* **1978**, 76.
122. Still, I.; Plavac, N.; McKinnon, D.; Chauhan, M. *Can. J. Chem.* **1976**, *54*, 280.
123. Pouchert, C. J. *The Aldrich Library of NMR Spectra*, 2nd ed. Aldrich Chemical Co., 1983, Vol. 2, p. 309A.
124. Pouchert, C. J. *The Aldrich Library of Infrared Spectra*, Aldrich Chemical Co., 1975, Vol. 2, p. 913B.
125. Baiwir, M.; Llabres, G.; Christiaens, L.; Luxen, A.; Piette, J. L. *Spectrochim. Acta Part A* **1983**, *39A*, 693.
126. Dijksman, D. J.; Newbold, G. T. *J. Chem. Soc.* **1951**, 1213.
127. Korte, D. E.; Hegedus, L. S.; Wirth, R. K. *J. Org. Chem.* **1977**, *42*, 1329.
128. Lumbroso, H.; Liegeois, Ch.; Dereu, N.; Christiaens, L.; Luxen, A. *J. Mol. Struct.* **1980**, *67*, 251.
129. Renson, M.; Piette, J.-L. *Spectrochim. Acta Part A* **1973**, *29A*, 285.
130. Lumma, W. C.; Dutra, G. A.; Voecker, C. A. *J. Org. Chem.* **1970**, *35*, 3442.
131. Dereu, N.; Renson, M.; Mollier, Y.; le Coustumer, G. *J. Organomet. Chem.* **1981**, *208*, 23.
132. Lohner, W.; Praefcke, K. *J. Organomet. Chem.* **1981**, *208*, 39.
133. Bumber, A. A.; Ladatko, A. A.; Sadekov, I. D. *Zh. Obshch. Khim.* **1990**, *60*, 847.
134. Aruga, T.; Ito, O.; Matsuda, M. *J. Am. Chem. Soc.* **1979**, *101*, 7585.
135. Arndt, F.; Nachtweg, P.; Pusch, *J. Chem. Ber.* **1925**, *58*, 1612.
136. Arndt, F.; Nachtweg, P.; Pusch, *J. Chem. Ber.* **1925**, *58*, 1633.
137. Shinriki, N. *Yakugaku Zasshi* **1968**, *88*, 1529.
138. Fehnel, E. A. *J. Am. Chem. Soc.* **1949**, *71*, 1063.
139. Nakanishi, W.; Hayashi, S.; Tukada, H.; Iwamura, H. *J. Phys. Org. Chem.* **1990**, *3*, 358.
140. Nakanishi, W.; Yamamoto, Y.; Hayashi, S.; Tukada, H.; Iwamura, H. *J. Phys. Org. Chem.* **1990**, *3*, 369.

Chemistry of Heterocyclic Compounds, Volume 53
Michael R. Detty, Marrie B. O'Regan

CHAPTER IV

Telluropyrylium Compounds

I. INTRODUCTION

Telluropyrylium compounds are emerging as important materials in various technologies. The development of diode lasers emitting in the near infrared has triggered research aimed at the syntheses of new classes of near-infrared-absorbing dyes for a variety of applications, including use in optical storage disks, in liquid-crystal displays, the photosemiconductor layer of laser printers, in laser filters, as photochemotherapeutic agents, and as fluorescence dyes in HPLC (high-pressure liquid chromatography) laser fluorimetry.[1,2] While chalcogenopyrylium dyes based on the lighter heteroatoms oxygen, sulfur, and selenium have been prepared that absorb at wavelengths longer than 700 nm, telluropyrylium dyes reach the near infrared with shorter hydrocarbon π-frameworks. Telluropyrylium dyes in particular have been useful in the near infrared where they have been utilized as electrophotographic sensitizers,[3,4] sensitizers for optical recording,[5,6] sensitizers for photodynamic therapy,[7–12] protective filter elements in eyeglasses,[13] sensitizers for laser-induced thermal dye transfer,[14] and catalysts for the photochemical conversion of water and oxygen to hydrogen peroxide.[15,16] The telluropyrylium nucleus has also been useful catalytically for two-electron oxidations with singlet oxygen or hydrogen peroxide.[15,16] Little of the work on telluropyrylium dyes has been included in other reviews of organotellurium chemistry.

This chapter is segmented into three main parts. The first part, Section III, is a compilation of synthetic methods for construction of the telluropyrylium ring system and some of the absorption properties of the telluropyrylium dyes. The second part, Section IV, is an analysis of the photophysical properties of

the telluropyrylium nucleus relative to the other chalcogenopyrylium nuclei. The third part, Sections V–VII, is a compilation of the reactions of the telluropyrylium nucleus. Many of the reactions of the telluropyrylium nucleus do not have analogy in the chemistry of the other chalcogenopyrylium nuclei—the pyrylium, thiopyrylium, and selenopyrylium systems.

Through an understanding of the changes in photophysical properties as one moves down the periodic table, one might approach the design of a dye for a particular purpose far more efficiently. In particular, control of wavelength of absorption (the S_0–S_1 gap), oxidation and reduction potentials, triplet energy levels, triplet lifetimes, rates of intersystem crossing, net singlet lifetimes, and rates of internal conversion is possible through dye design. The telluropyrylium dyes incorporate the heaviest chalcogen atom, and one might expect heavy-atom effects, redox properties, and reactivity to be different from those of the lighter chalcogens.

While this chapter is devoted to the telluropyrylium nucleus and comparison of its properties to the properties of corresponding lighter chalcogenopyrylium compounds, the conclusions concerning the effect of chalcogen atoms on physical and photophysical properties should be applicable to other dye classes as well. In particular, the photophysical properties of cationic cyanine-type dyes containing the heavier chalcogen atoms selenium and tellurium are less studied.

II. NOMENCLATURE

Chemical Abstracts names the tellurium analogs of pyrylium dyes **1** as *tellurinium species*—not as telluropyrylium species. However, the "colloquial" and IUPAC conventions of naming the selenium and tellurium analogs of pyrylium rings as selenopyrylium and telluropyrylium species, respectively, follows from the IUPAC- and *Chemical Abstracts*-accepted name of *thiopyrylium* for the sulfur analogs of the pyrylium nucleus. Collectively, all these species are referred to as *chalcogenopyrylium species* in this chapter and, for the sake of consistency and for ease of visualization, the tellurium analogs are referred to as *telluropyrylium species*. The numbering system for the ring starts with the tellurium atom at the 1-position and proceeds around the ring.

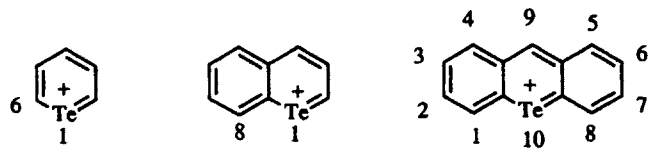

Tellurinium
Telluropyrylium

Benzo[b]tellurinium
Benzo[b]telluropyrylium

Telluroxanthylium

The benzo[*b*]telluropyrylium nuclues **2** as named by IUPAC convention is named as the benzotellurinium nucleus by *Chemical Abstracts*. The numbering system is as shown above.

The dibenzo[*b*]telluropyrylium system **3** is named as a telluroxanthylium system by both IUPAC and *Chemical Abstracts*. The numbering system is as shown above.

III. SYNTHESIS OF THE TELLUROPYRYLIUM NUCLEUS

A. Telluropyrylium Nuclei from Transformations of Telluropyranones

The monocyclic telluropyrylium (or tellurinium) nuclues **1**, the benzo[*b*]telluropyrylium (or benzo[*b*]tellurinium) nuclues **2**, and the dibenzo[*b*]telluropyrylium (or telluroxanthylium) nuclues **3**, as well as derivatives, have been prepared via synthetic techniques similar to those employed for the lighter chalcogenopyrylium species. Precursor materials for **1**–**3** have been the corresponding 2*H*- or 4*H*-tellurins, 4*H*-tellurin-4-ones, or their benzo-fused analogs.

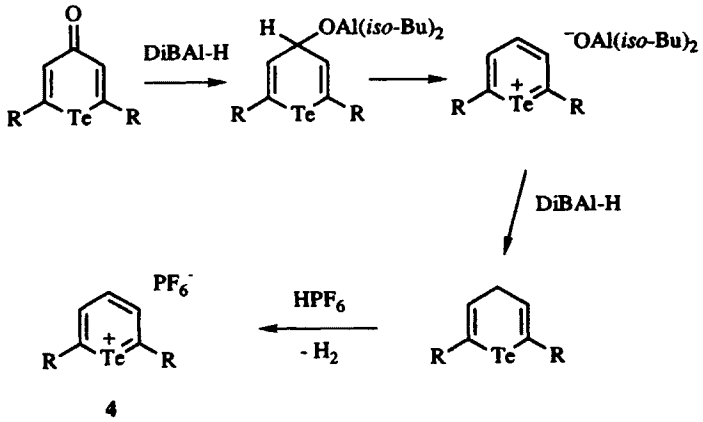

Scheme 1

Monocyclic telluropyrylium salts **4** and benzo[*b*]telluropyrylium salts **5** have been prepared from the corresponding 2,6-disubstituted tellurin-4-ones or 2-substituted benzotellurin-4-ones via diisobutylaluminum hydride reduction of the carbonyl followed by treatment with strong acid (Scheme 1).[17,18] Surprisingly, the intermediates prior to acid treatment are not the 4-hydroxy compounds, but the 4*H*-tellurins.[18] Strong acids oxidize the tellurin intermediates to the corresponding telluropyrylium salt with the evolution of hydrogen gas. This reaction appears to be a general reaction for all the chalcogenopyranones.[18] Examples of telluropyrylium salts **4** and **5** that have been prepared in this way are compiled in Table 1.

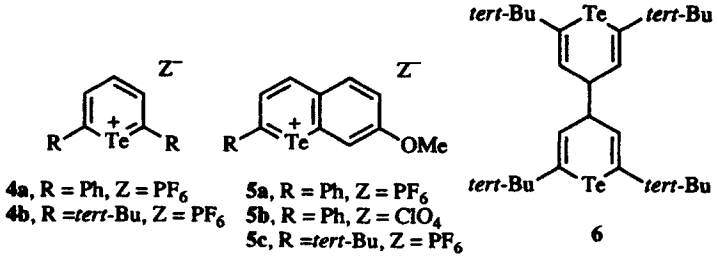

4a, R = Ph, Z = PF_6
4b, R = *tert*-Bu, Z = PF_6

5a, R = Ph, Z = PF_6
5b, R = Ph, Z = ClO_4
5c, R = *tert*-Bu, Z = PF_6

6

As shown in Scheme 1, the initial hydride transfer to the carbonyl is thought to give an aluminum alkoxide intermediate. Solvolysis of this intermediate would generate a telluropyrylium intermediate that would then be reduced to the tellurin with a second equivalent of diisobutylaluminum hydride. Evidence of single-electron-transfer reactions have been found in the preparation of **4** (R = *tert*-Bu). The isolation of bistellurin **6** suggested a radical coupling. Similar products have not been observed in diisobutylaluminum hydride reactions of the corresponding oxygen, sulfur, and selenium analogs.[18]

The parent benzo[*b*]telluropyrylium (**2**) and telluroxanthylium (**3**) nuclei have been prepared as shown in Scheme 2. 2*H*-Benzotellurin reacts with trityl perchlorate to give **2** as its perchlorate salt in 35% isolated yield.[19]

In contrast to the monocylic and benzo-fused tellurin-4-ones, the telluroxanthone is reduced by either lithium aluminum hydride[20] or sodium borohydride[21] to the corresponding alcohol (Scheme 2). Treating the alcohol with perchloric acid gives telluroxanthylium perchlorate **7**. Telluroxanthene **8** is a known compound,[21] and, in analogy to the behavior of the tellurins of Scheme

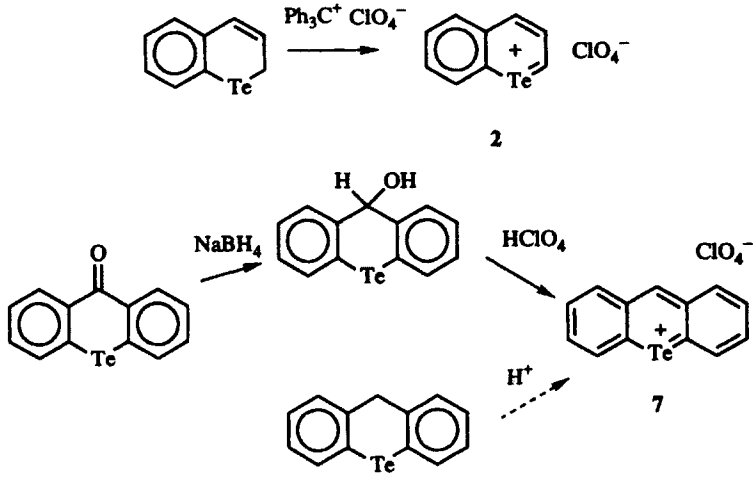

2

7

8

Scheme 2

1, one might expect strong acid treatment of **8** to give the telluroxanthylium nucleus and hydrogen gas, although this transformation has yet to be described.

The addition of strong Lewis acids to the carbonyl oxygen of tellurin-4-ones has given 4-alkoxy telluropyrylium salts. Electrophilic attack of ethylfluorosulfonate on the carbonyl oxygen of 4*H*-2,6-diphenyltellurin-4-one,[22] 4*H*-2-phenyl-7-methoxybenzotellurin-4-one,[17] or 4*H*-2-methyl-7-methoxybenzotellurin-4-one[23] gave 4-ethoxytelluropyrylium fluorosulfonate salts **9**–**11**, respectively, in greater than 87% isolated yields.

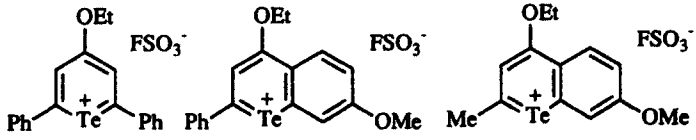

9 **10** **11**

Zwitterionic telluropyrylium species have been prepared via the formation of boronate complexes of 5-methoxybenzotellurin-4-one derivatives with boron trifluoride etherate as illustrated in Scheme 3. Demethylation of the 5-methoxy group is observed with formation of the difluoroboronates **12** in 66–91% isolated yield (Table 2).[23] A sulfur containing derivative **13** was prepared from the corresponding thione in 95% isolated yield.[23] Related compounds (**12g** and **12h**) have been prepared by the addition of phosphorus pentafluoride to glyme solutions of 4*H*-5-methoxybenzotellurin-4-one derivatives.[4] As shown in Table 2, the telluropyrylium boronates absorb in the visible spectrum and appear orange to magenta in solution with extinction coefficients in the visible of around 10^4 L mol^{-1} cm^{-1}.[23]

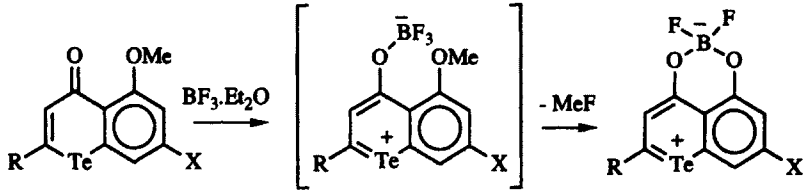

12a-f

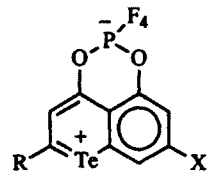

12g, R=Ph, X=H
12h, R=2,4-$(MeO)_2$Ph, X=OMe

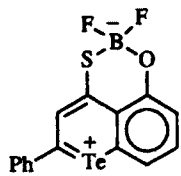

13

Scheme 3

Nucleophilic addition of Grignard reagents to the carbonyl carbon of tellurin-4-ones followed by acid-catalyzed dehydration has given good yields of 4-substituted telluropyrylium species as illustrated in Scheme 4.[17,19-29] The intermediate alcohols are typically not isolated. Reactions of this type have been observed for the monocyclic tellurin-4-ones,[22,24-28] benzotellurin-4-ones,[17] and telluroxanthones[19-21,29] as compiled in Table 3.

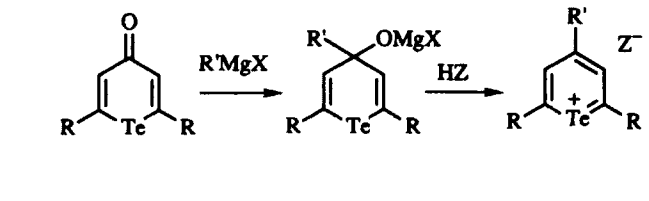

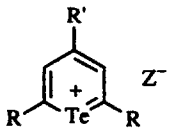

14, R= H, *tert*-Bu, Ph
R'= Me, Et,
4-$(Me_2N)C_6H_4$

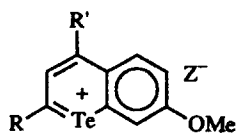

15, R=Ph, Me
R'=Ph, 4-$(Me_2N)C_6H_4$

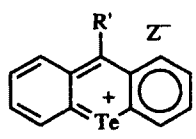

16, R'= Me, $PhCH_2$,
α-Naphthyl,
3-MeC_6H_4, 4-FC_6H_4,
4-BrC_6H_4, 4-$MeOC_6H_4$

Scheme 4

The compounds produced by addition of *p-N,N*-dimethylaminophenylmagnesium bromide to tellurin-4-ones followed by acid-induced dehydration are telluropyrylium dyes with absorption maxima at wavelengths longer than 600 nm. The absorption maxima in dichloromethane are 650 nm (log ε 4.83) for **14c**,[22,24] 610 nm (log ε 4.82) for **14f**,[27] 630 nm (log ε 4.83) for **14g**,[26] and 655 nm (log ε 4.80) for **14h**.[28] Similarly, the addition of *p-N,N*-dimethylaminophenylmagnesium bromide to 4*H*-2-phenyl-7-methoxybenzotellurin-4-one followed by perchloric acid treatment gave dye **15a** in 44% isolated yield with an absorption maximum in dichloromethane of 678 nm (log ε 4.46).[22]

The 4-methyltelluropyrylium nuclei **14a** and **14d** and the 4-methylbenzo[*b*]-telluropyrylium nucleus **17**[3] have been prepared via alternative syntheses as shown in Scheme 5 for the preparation of **14**.[22] Nucleophilic addition of the anion of Meldrum's acid to 4-ethoxytelluropyrylium salts in pyridine gives tellurinylidene compounds in greater than 80% yield.[22,24] Heating the tellurinylidene compounds with formic acid induces loss of carbon dioxide and formation of the formate salt of the 4-methyltelluropyrylium salts. The addition of fluoroboric acid (or other strong acids) gives the fluoroborate salts of the 4-methyltelluropyrylium compounds.

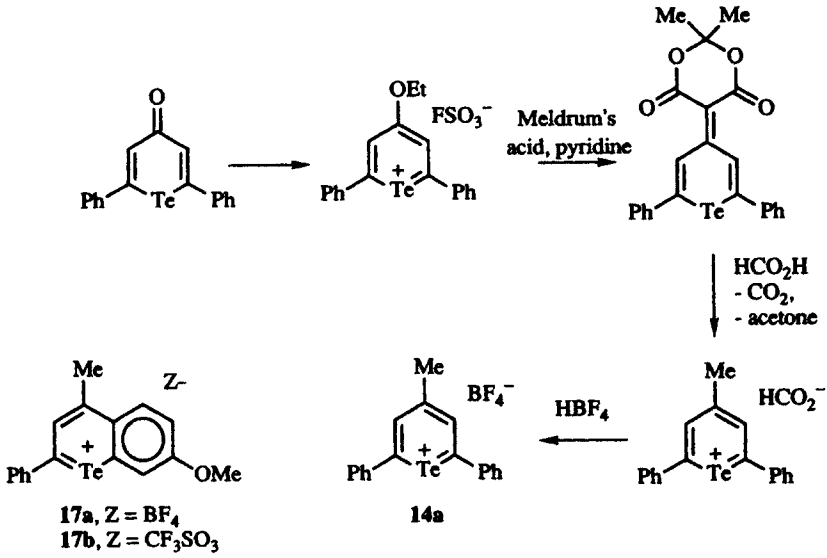

Scheme 5

B. Condensation Reactions of Alkyl-Substituted Chalcogenopyrylium Compounds to Give Telluropyrylium Nuclei

1. Condensation Reactions with 4-Alkyltelluropyrylium Nuclei

The majority of telluropyrylium dyes reported to date have been prepared by condensation reactions of a 2-alkyl- or 4-alkyl-substituted chalcogenopyrylium nucleus with a carbonyl-containing compound.[3,17,22–25,27] This general reaction is illustrated in Scheme 6 for the condensation of 2,6-diphenyl-4-methyltelluropyrylium salt **14a** with 4*H*-2,6-diphenyltellurin-4-one in acetic anhydride to give the corresponding monomethine dye **18a** in 91% isolated yield (Table 4).[22] Similarly, monomethine dyes **18b–c** were prepared from

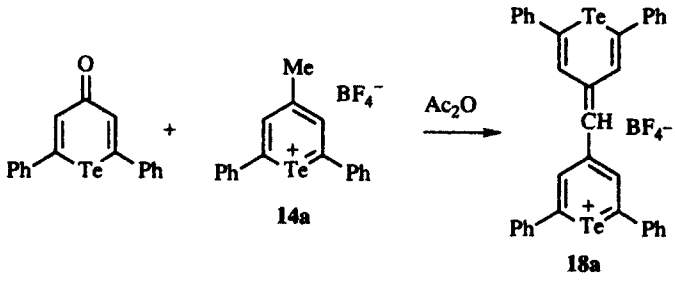

Scheme 6

4*H*-2,6-diphenyltellurin-4-one and the corresponding 4-methylchalcogenopyrylium salts (Table 4).[22]

2,6-Di-*tert*-butyl-4-methyltelluropyrylium salt **14d** undergoes similar condensation reactions with 4*H*-2,6-di-*tert*-butyltellurin-4-one and the corresponding selenapyranone, thiapyranone, and pyranone in acetic anhydride to give monomethine dyes **19a–d** (Table 4).[24] The conditions of reaction were nearly identical to those employed for the phenyl-substituted derivatives even though steric factors are increasing dramatically.

An unsymmetrical monomethine dye has been prepared by the condensation of **14d** with 4*H*-2,6-diphenyltellurin-4-one. The resulting dye **20** has absorption properties (λ_{max} 745 nm) in between those of **18a** (λ_{max} 759 nm) and **19a** (λ_{max} 715 nm).[24]

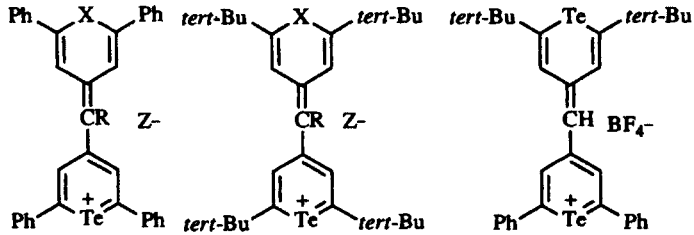

18, R = H
22, R = Me

19, R = H
23, R = Me

20

The condensation of **17a** with 4H-2-phenyl-7-methoxybenzotellurin-4-one gives **21a** in 79% isolated yield (Table 4).[3] Similar condensation reactions of 2-phenyl-4-methylbenzo[*b*]chalcogenopyrylium species give **21b–d** (Table 4)[30] and of **17a** with 2,6-diphenylchalcogenopyran-4-ones give **21e–g**.[3]

Dyes **18**, **19**, and **21** have absorption maxima at increasingly longer wavelengths as X becomes heavier. Thus, dyes **18** have absorption maxima at 759 (X = Te), 722, 690, and 650 nm (X = O) for **18a–d**, respectively, in dichloromethane.[22] Similarly, dyes **19a–d** have absorption maxima at 715 (X = Te), 674, 651, and 594 nm (X = O), respectively,[24] and dyes **21a–d** have absorption maxima at 810 (log ε 4.79), 744, and 698 nm, respectively.[3]

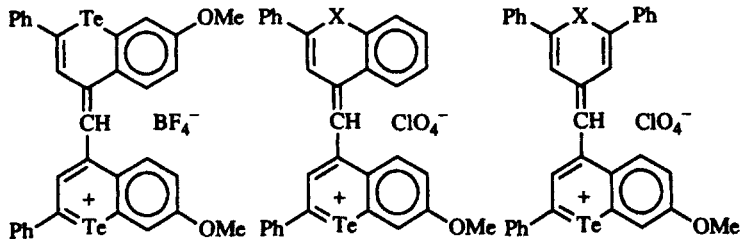

21a

21b, X = Se
21c, X = S
21d, X = O

21e, X = Se
21f, X = S
21g, X = O

The condensation of 2,6-diphenyl-4-ethyltelluropyrylium salt **14b** with 4*H*-2,6-diphenyltellurin-4-one gives the corresponding methylmethine dye **22a** (X = Te) in 55% isolated.[24] The condensation of other 4-ethylchalcogenopyrylium salts with 4*H*-2,6-diphenyltellurin-4-one or the condensation of **14b** with other 2,6-diphenylchalcogenopyranones gives **22b–d** (Table 4).[24] Similarly, the condensation of 2,6-di-*tert*-butyltelluropyrylium salt **14e** with 4*H*-2,6-di-*tert*-butyltellurin-4-one in acetic acid gives methylmethine dye **23** (X = Te) in 25% isolated yield (Table 4).[25]

The absorption maxima of the dyes **22** and **23** are at much longer wavelength than the corresponding dyes **18** and **19**. The absorption maxima in dichloromethane are 834, 795, 762, and 720 nm for **22a–d**,[24] respectively, and 772 nm for **23**.[25]

Related condensation reactions have given telluropyrylium dyes with more extended conjugation. As shown in Scheme 7, the condensation of **14a** with (2,6-diphenyltellurin-4-yl)acetaldehyde leads to trimethine dye **24a** (Table 5).[22] The condensation of **14a** with other (2,6-diphenylchalcogenopyran-4-yl)-acetaldehyde derivatives leads to trimethine dyes **24b–d** (Table 5).[22] Similarly, the condensation of **14d** with (2,6-di-*tert*-butylchalcogenopyran-4-yl)acetaldehydes gives the corresponding trimethine dyes **25**.[24] The condensation of **14a** with 1,3,3-trimethoxypropene gives pentamethine dye **26** and with 2-chlorocyclohexene-1,3-biscarboxaldehyde gives heptamethine dye **27** (Scheme 7).[24]

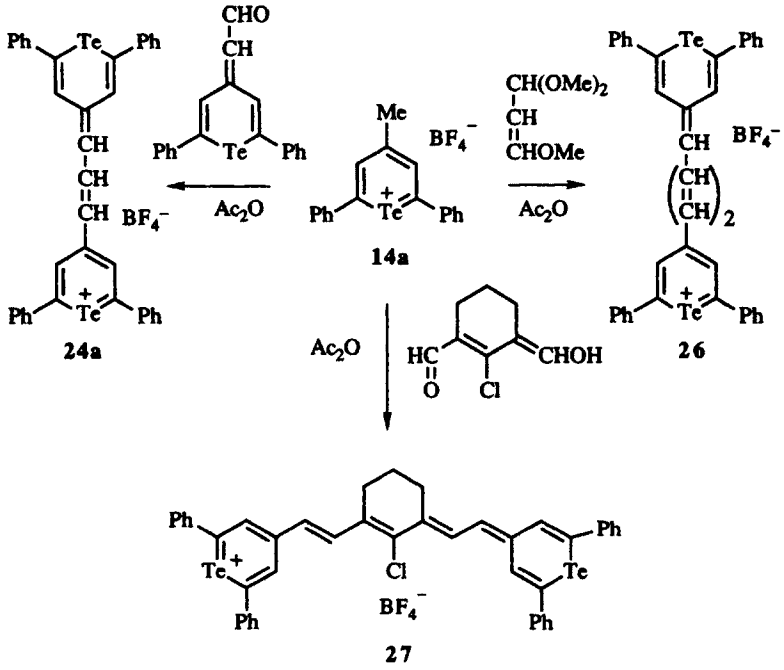

Scheme 7

Similarly, the condensation of **17a** with (2-phenyl-7-methoxybenzo[*b*]-tellurin-4-yl)acetaldehyde gives trimethine dye **28a** (Table 5).[3] The condensation of **17b** with 1,3,3-trimethoxypropene gives pentamethine dye **28b** and with 2-chlorocyclohexene-1,3-biscarboxaldehyde, gives heptamethine dye **28c** (Table 5).[3] As shown in Scheme 8, the condensation of **17b** with the anilino iminium salt gave heptamethine dye **28d**. Dye **28d** was thermally unstable with a half-life on the order of minutes in solution.[3]

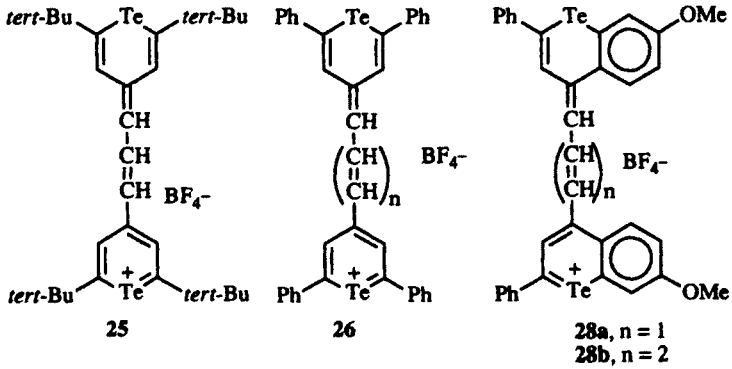

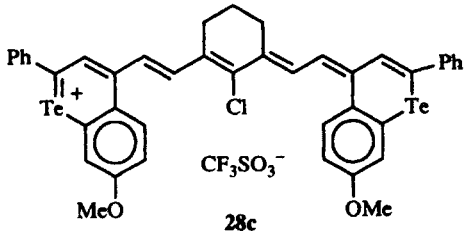

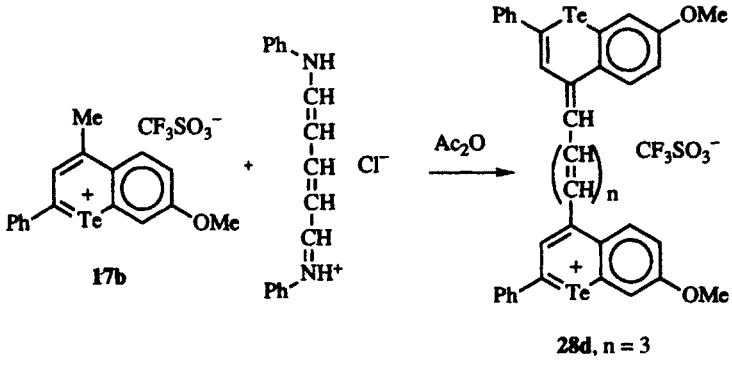

Scheme 8

The addition of each double bond into the chromophore of **24–27** adds approximately 110–120 nm to the absorption maxima relative to those of the monomethine dyes (Table 5).[22,24] The same trend is observed in the benzo[*b*]telluropyrylium dyes, as well (Table 5).[3]

Condensation reactions of **14d** with 2-(2,6-di-*tert*-butylchalcogenopyran-4-yl)propionaldehyde (**29**)[31] or with the cyanoacetaldehyde derivative **30**[31] gave trimethine dyes **31** and **32**, respectively, with substituents on the trimethine linkage.[6,24] Synthetic yields and spectral properties are compiled in Table 5. Alternatively, the condensation of 2,6-di-*tert*-butyl-4-ethylselenopyrylium hexafluorophosphate with 2-(2,6-di-*tert*-butyltellurin-4-yl)acetaldehyde gave trimethine dye **31b** (X = Se) in 50% yield as the hexafluorophosphate salt.[25]

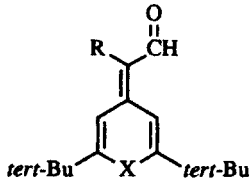

29, R = Me
30, R = CN

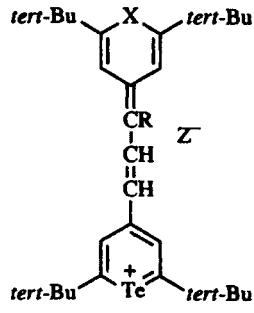

31, R = Me
32, R = CN

The substituents in the trimethine backbones of these systems are on "starred carbons" where electron-donating substituents give bathochromic shifts and electron-withdrawing substituents give hypsochromic shifts.[6] The addition of the electron-donating methyl substituent gives a bathochromic shift of approximately 15 nm, while the introduction of the electron-withdrawing cyano substituent gives an hypsochromic shift of approximately 15 nm.

The condensation of **14d** with squaric acid in ethanol in the presence of diisopropylethylamine as shown below gives the only example of a squarylium dye incorporating a telluropyrylium nucleus.[32] The resulting pentamethine dye **32a** is isolated in 33% yield and absorbs with λ_{max} of 910 nm (ε 350,000 L mol^{-1} cm^{-1}) in dichloromethane.

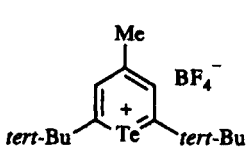

14a

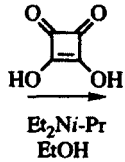

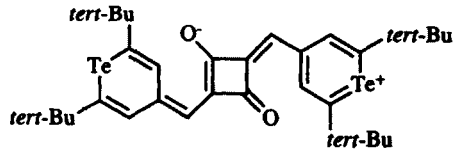

32a

Condensation reactions of 4-methyltelluropyrylium compounds with carbonyl groups conjugated with dialkylamino substituents lead to other classes of

dyes incorporating the dialkylamino group in the major chromophore.[3,22,24,27] The condensation of 4-methyltelluropyrylium compounds with *N,N*-dimethylthioformamide as shown in Scheme 8a in acetic anhydride gave imminium dyes **33** and **34** (Table 6). The dyes **33a** and **33b** absorb at 525 nm (log ε4.85)[22] and 508 nm (log ε4.94),[27] respectively, while dye **34** absorbs at 553 nm (log ε4.65).[3]

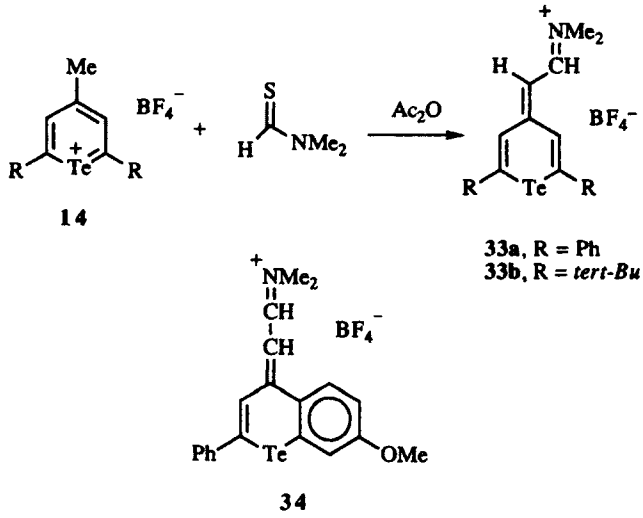

Scheme 8a

In analogy to the polymethine dyes described above, the dyes can be shifted to longer wavelength by increasing the number of conjugated double bonds between the telluropyrylium nucleus and the dialkylamino group. The next higher homologs of **33** and **34** would be the 4-(4-dialkylamino-1,3-butadienyl)telluropyrylium dyes. These dyes have not been described, but the benzene ring should be similar to the butadiene fragment in that the longest chromophore through the aromatic ring would include two conjugated double bonds. The absorption maxima of the *p-N,N*-dimethylaminophenyl-substituted dyes **14c**, **14f**, and **15a** are included in Table 6 to show the effect of an additional double bond in the chromophore, which is a red shift of 100–125 nm.

Telluropyrylium dyes with even longer conjugation have been prepared. The condensation of **14a** with *p-N,N*-dimethylaminobenzaldehyde gave styryl dye **35**, while the condensation of **14a** with *p-N,N*-dimethylaminocinnamaldehyde gave dye **36**.[22] Benzo[*b*]telluropyrylium analogs **37** and **38** were prepared in a similar fashion from **17b**.[3] As shown in Table 6, the insertion of the first double bond gave approximately a 100-nm bathochromic shift, and the addition of the second double bond gave an additional 80–90-nm bathochromic shift.

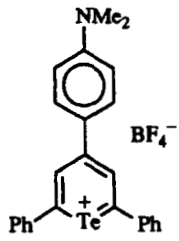

14c

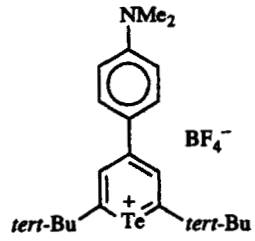

14f

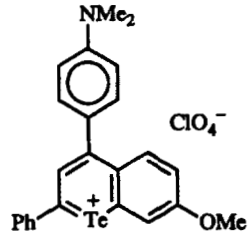

15a

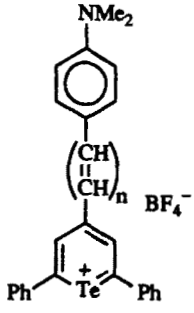

35, n = 1
36, n = 2

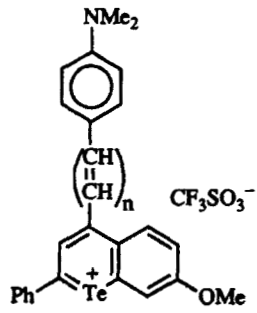

37a, n = 1
37b, n = 2

Constraining the alkyl groups of *N*,*N*-dialkylaminophenyl groups gives longer-wavelength absorption maxima in cationic dyes.[33–35] This effect has been attributed to enforced conjugation of the nitrogen lone pair of electrons with the aromatic ring[34] as well as steric shielding of the nitrogen lone pair of electrons.[35] If this effect were operative with analogues of telluropyrylium dyes, one would expect increasing bathochromic shifts with increasing constraint of the nitrogen lone pair of electrons. Condensation of **14a** with the aldehydes of Scheme 9 in acetic anhydride gives telluropyrylium dyes **39** and **40**.[22] The

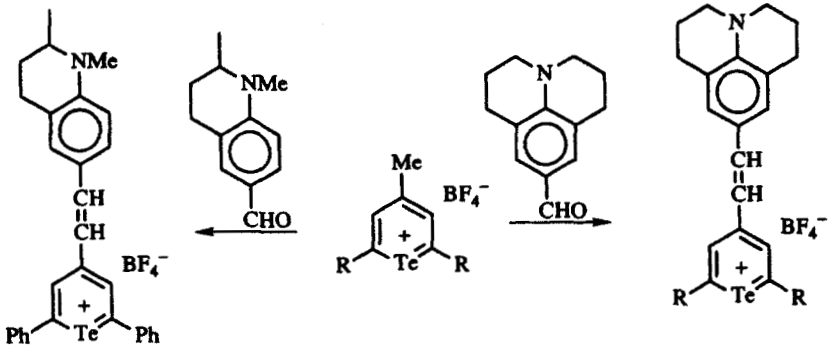

39

40, R = Ph
41a, R = *tert*-Bu

Scheme 9

introduction of one ring in **39** gives a 5-nm bathochromic shift while the introduction of two rings in julolyldyl dye **40** gives a 28-nm bathochromic shift relative to **35** (Table 6).[22]

Julolyldyl dye **41a** has been prepared by condensation of **14d** with 9-formyljulolyldine.[24] Again, constraint of the nitrogen lone pair of electrons by the two rings gives a dye with an absorption maximum of 775 nm (log ε 5.16).

2. *Condensation Reactions of 2-Alkyltelluropyrylium Nuclei*

2-Methyl-4-ethoxybenzo[*b*]telluropyrylium fluorosulfonate **11** undergoes condensation reactions with a variety of aldehydes and ketones to give the corresponding dyes **42–45** (Table 7).[23] These dyes undergo hydrolysis to the telluropyranones such as the basic hydrolysis of **42**, to give benzo[*b*]tellurin-4-one **46**.[15]

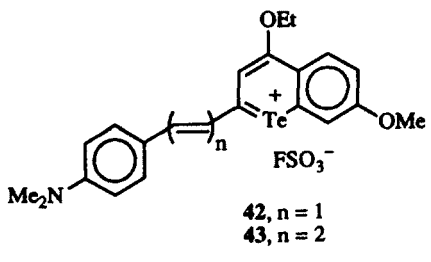

42, n = 1
43, n = 2

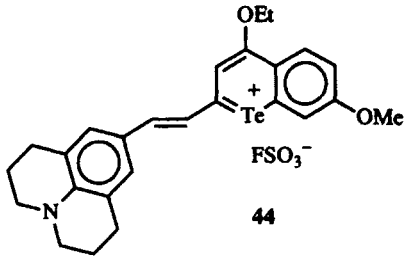

44

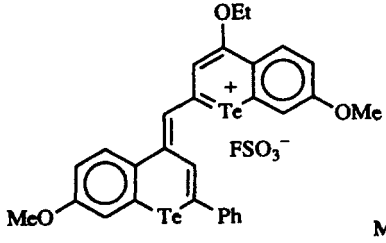

45

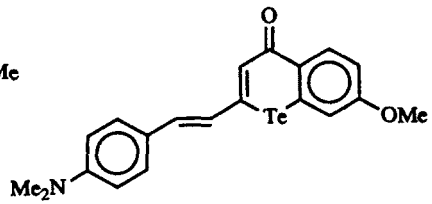

46

Difluoroboronate **12a** undergoes condensation reactions with a variety of aldehydes and ketones to give the dyes **47–50**. The resulting benzotellurinone-based dyes are more readily hydrolyzed than the 4-ethoxy-substituted dyes **42–45**. The hydrolysis products of **47** and **48** are the 5-hydroxy-substituted benzotellurin-4-ones **51** and **52**, respectively.[23]

The dyes with the difluoroboronate substituent absorb at longer wavelengths than the corresponding dyes with the 4-ethoxy substituent (Table 7). The difluoroboronate-containing dyes have an additional oxygen substituent on the benzo[*b*]-telluropyrylium nucleus at the 5-position relative to those dyes with the 4-ethoxy substituent. However, the additional oxygen substituent alone

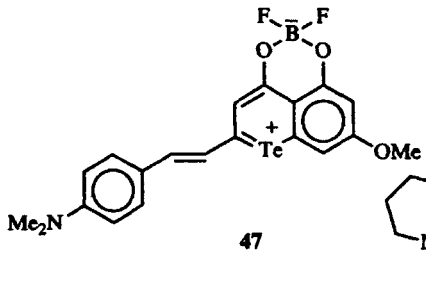

47

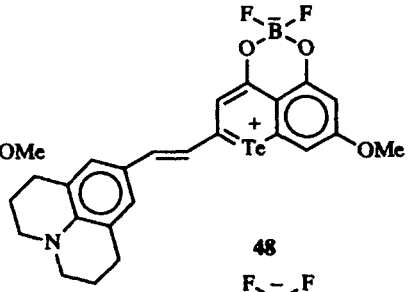

48

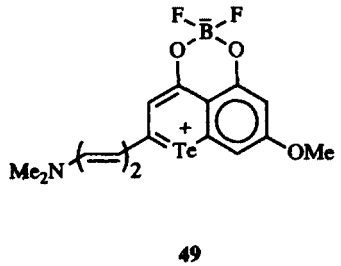

49

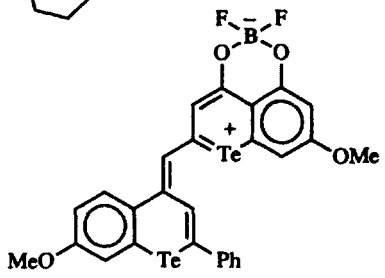

50

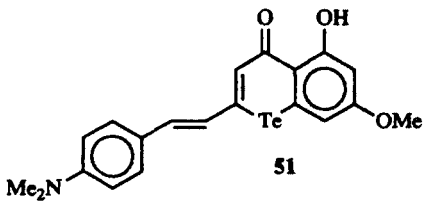

51

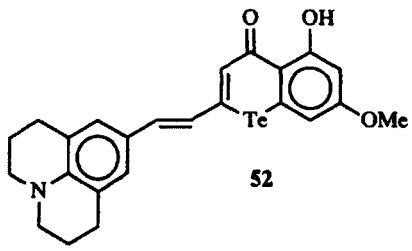

52

would not explain the 20–69-nm difference observed between corresponding members of the two classes of dyes.

C. Telluropyrylium Species via Two-Electron Oxidation of (Telluropyranyl)telluropyrans

The two-electron oxidations of (telluropyranyl)telluropyrans **53** gives bis-telluropyrylium species **54** as shown in Scheme 10.[36–38] Oxidation by either electrochemical[36,37] or chemical[38] means as shown in Scheme 10 produces the bistelluropyrylium species **54**. Controlled one-electron oxidation of the

(telluropyranyl)telluropyrans produces the radical cations **55** containing a telluropyranyl radical attached to a telluropyrylium ring.[36,39] (The radical-cation materials are discussed in Chapter VII concerning tellurium-containing donors.) Oxidation of (benzotelluropyranyl)benzotelluropyran **56** gives only the bistelluropyrylium salt **57**.[37] The radical cation of **56** has not been detected. The bistelluropyrylium salts **54** and **57** are isolable solids that appear yellow in solution.[38]

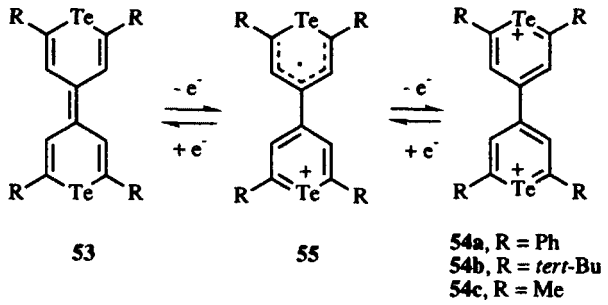

53 **55**

54a, R = Ph
54b, R = *tert*-Bu
54c, R = Me

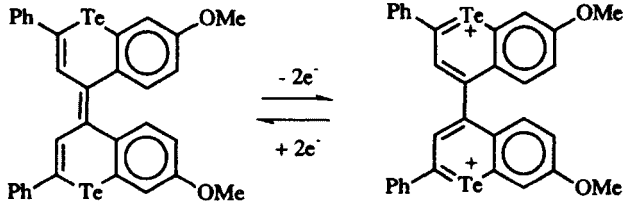

56 **57**

Scheme 10

D. Telluropyrylium Nuclei via Protonation of Carbon–Carbon Double Bonds

The addition of hexafluorophosphoric acid to telluropyrylium dye **18a** gives bistelluropyrylium salt **58** as shown in Scheme 11.[28] Compound **58** was isolated in 75% yield as a bright yellow, crystalline solid.

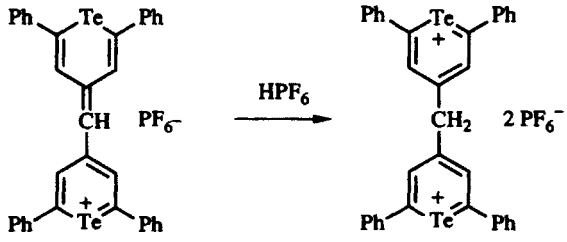

18a **58**

Scheme 11

IV. PHYSICAL AND PHOTOPHYSICAL PROPERTIES OF THE TELLUROPYRYLIUM NUCLEUS RELATIVE TO OTHER CHALCOGENOPYRYLIUM NUCLEI

A. Structure and Bonding in the Telluropyrylium Nucleus

The tellurium atom is the largest of the chalcogen atoms. The size of the chalcogen atoms increases from a covalent radius of 0.73 Å for oxygen to 1.36 Å for tellurium.[24] One would expect the geometries of six-membered rings containing one chalcogen atom to differ significantly as the chalcogen atom increases in size from oxygen to tellurium. This point is illustrated from the X-ray structure for telluropyrylium dye **18d** incorporating one pyrylium ring and one telluropyrylium ring.[24] Selected bond distances and angles for **18d** are compiled in Table 8 according to the numbering scheme of Figure 1.[24]

As shown in Figure 1, the pyrylium nucleus of **18d** resembles a regular hexagon. The telluropyrylium ring of **18d**, on the other hand, is severely distorted from a regular hexagon. While the pyrylium nucleus of Figure 1 contains six angles all close to 120°, the telluropyrylium nucleus is significantly distorted by the C1—Te—C5 angle of 94.3°. To accommodate the C1—Te—C5 angle, the C1—C2—C3 and the C3—C4—C5 angles are greater than 129°. The Te—C1—C2, C2—C3—C4, and the Te—C5—C4 angles are all approximately 122°.[24]

The pyrylium ring is bent 4.2° out of plane along the O—C8 axis while the telluropyrylium ring is bent 8.7° out of plane along the Te—C3 axis. The Te-C bond lengths of 2.068 Å are significantly longer than the 1.369-Å O—C bond lengths. The long Te—C bond lengths, as well as the C—Te—C angle, are responsible for the angle distortions observed in the telluropyrylium ring.

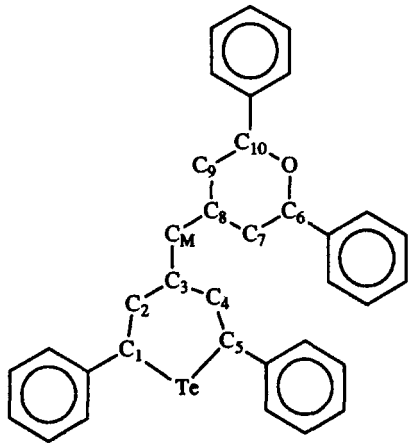

Figure 1. Numbering scheme for **18d**.

The telluropyrylium ring of **18d** can be compared to the tellurinyl ring of **59**.[27] Using the same numbering system for the tellurium-containing ring as shown in Figure 1, selected bond angles and distances for **59** are compiled in Table 9.[27] The oxidative addition of bromine across the tellurium atom of **59** has removed the *p* orbital of tellurium from conjugation with the carbon π framework. The Te—C bond lengths of **59** are 2.12 Å, which is 0.05 Å longer than the Te—C bond lengths of **18d**. The C1—C2 and C4—C5 bonds in **59** are 0.02 Å shorter than the same bonds in **18d**. The C2—C3 and C3—C4 bonds in **59** are 0.02 Å longer than the same bonds in **18d**. With the assumption that **59** has single Te—C bonds and well-defined C—C single and double bonds, the telluropyrylium nucleus in **18d** has a delocalized π framework with shortened single bonds and lengthened double bonds. In the pyrylium nucleus of **18d**, the C6—C7 and C9—C10 bond lengths (average = 1.344 Å) are near-normal double bonds, but the C7—C8 and C8—C9 bond lengths (average = 1.422 Å) are 0.05 Å shorter than normal single bonds. The O—C bond lengths (average = 1.369 Å) are shortened by 0.02 Å relative to the O—C bond lengths of 2,2′6,6′-tetraphenylpyranylpyran (average = 1.389 Å).[40] As one would expect, considering the differences in size of tellurium and oxygen relative to carbon, the pyrylium ring appears to have more π bonding from the heteroatom than does the telluropyrylium ring.

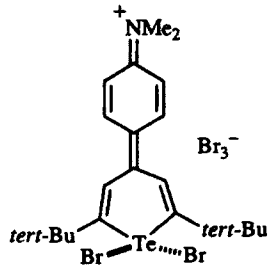

59

B. ^{1}H NMR Data for Telluropyrylium Compounds

The chalcogenopyrylium rings are Hückel 6π aromatic systems with the positive charge delocalized on the heteroatom and 2-, 4-, and 6-positions as shown in Scheme 12. The aromatic ring current and the positive charge would both contribute to the deshielding of the ring protons. As shown in Table 10, chemical shifts are similar for H_A, H_B, and H_C in both the monocyclic nucleus **1** and the benzo[*b*]chalcogenopyrylium nucleus **2**. Data for the selenopyrylium, thiopyrylium, and pyrylium nuclei were taken from **63–65**.

The delocalized positive charge in the parent chalcogenopyrylium nuclei is further delocalized in chalcogenopyrylium dyes containing a second heteroatom

Scheme 12

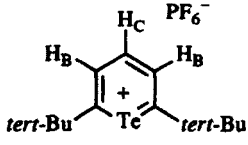

4a, X = Te, R = Ph
4b, X = Te, R = *tert*-Bu
63a, X = Se, R = *tert*-Bu
63b, X = S, R = *tert*-Bu
63c, X = O, R = *tert*-Bu

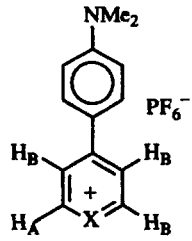

14g, X = Te
64, X = Se

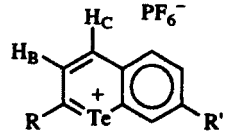

5a, X = Te, R = Ph, R '= OMe
5c, X = Te, R = *tert*-Bu, R '=O Me
65a, X = Se, R = Ph, R' = H
65b, X = S, R = Ph, R' = H
65c, X = O, R = Ph, R' = H

in addition to increased conjugation. This is reflected in an upfield shift in chemical shifts for the ring protons in the chalcogenopyrylium nuclei for dyes **19a**, **25a**, **66**, and **67** (Table 10).

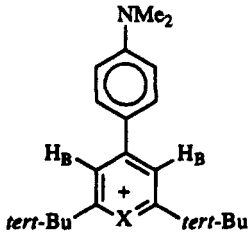

14f, X = Te
66a, X = Se
66b, X = S
66c, X = O

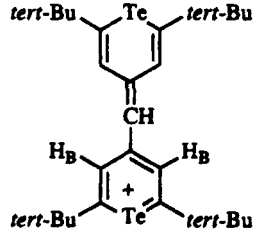

19a

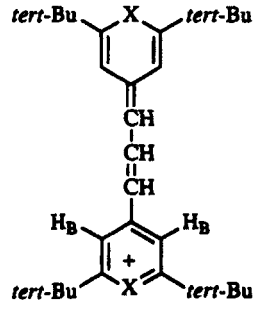

25a, X = Te
67a, X = Se
67b, X = S
67c, X = O

The distortion of the geometry of the chalcogenopyrylium ring from that of a regular hexagon and the change in electronegativity of the chalcogen atom as the size of the chalcogen atom increases appear to have little effect on the chemical shifts on the ring protons from the data in Table 10. However, coupling constants between the ring protons are affected by the geometry changes. The H_B—H_C coupling constant increases from 8.2 Hz in pyrylium compound **63c** to 8.5 Hz in thiopyrylium compound **63b** to 8.8 Hz in selenopyrylium compound **63a** to 9.6 Hz in telluropyrylium compound **4b**.[18] Similarly, the H_A—H_B coupling constant of 11.6 Hz in **14g** is larger than the 10.6 Hz coupling constant in **64**.[26]

C. ^{125}Te NMR Data for Telluropyrylium Compounds

Two trends that have emerged in the study of ^{125}Te NMR chemical shifts of organotellurium compounds are that the chemical shift moves downfield as the oxidation state increases form tellurium(II) to tellurium(IV) and as the electronegativity of the ligands attached to tellurium increases.[41] The range of ^{125}Te chemical shifts covers several thousand parts per million (ppm), and one would expect factors other than these two trends to be important contributors, although relatively few ^{125}Te chemical shifts have been determined.[42,43]

In the telluropyrylium nuclei, one might expect the positive charge on the ring system to contribute to chemical shift. As one example, the addition of methyl iodide to dimethyl telluride to give the telluronium salt $Me_3Te^+I^-$ gives a 443-ppm downfield shift in the ^{125}Te NMR spectrum of the telluronium salt relative to the telluride.[44] In contrast to this result, the increased formal positive charge per tellurium in comparing Te_6^{4+} with Te_4^{2+}, systems in which charge is delocalized, is not reflected in chemical shifts. The ^{125}Te NMR chemical shift of Te_6^{4+} is over 2500 ppm upfield of the ^{125}Te NMR chemical shift of Te_4^{2+}.[45]

As shown in Scheme 12, resonance forms place the positive charge of the telluropyrylium ring on tellurium as well as on the carbon atoms at the 2-, 4-, and 6-positions. The ^{125}Te NMR chemical shifts of the telluropyrylium compounds might be quite sensitive to substituents. The ^{125}Te NMR chemical shifts for a variety of compounds (**4b**, **5a**, **5c**, **14c**, **14d**, **14f**, **14h**, and **58**) have been measured and are compiled in Table 11.[20] ^{125}Te chemical shifts for neutral 2,6-diphenyl, 2,6-di-*tert*-butyl, and unsubstituted tellurin-4-ones (**60–62**, respectively)[28] are also included in Table 11 for the purpose of comparison.

As indicated in Table 10, the ^{125}Te NMR chemical shifts for the telluropyrylium compounds are hundreds of parts per million downfield from those of the uncharged tellurin-4-ones **60–62**. In the telluropyrylium systems, resonance forms which place a formal positive charge on tellurium are expected to make a greater contribution than in the telluropyranones.

The concept of resonance forms also helps explain differences in ^{125}Te chemical shifts in other comparisons as well. In comparing benzo[*b*]telluropyrylium salt **5c** with 2,6-di-*tert*-butyltelluropyrylium salt **4b**, one *tert*-butyl group in **4b** has been replaced with a fused benzo group, which should delocalize the positive charge away from tellurium. In fact, the ^{125}Te chemical shift of 1124 ppm for **5c** is 180 ppm upfield of the 1304 ppm ^{125}Te chemical shift of **4b**. Replacing the *tert*-butyl group of **5c** with a phenyl group in **5a** offers more sites for delocalization of the positive charge. Consequently, the ^{125}Te chemical shift of 1086 ppm for **5a** is 38 ppm upfield of that of **5c**.

Telluropyrylium dyes **14c**, **14f**, and **14h** incorporate a second heteroatom in addition to the tellurium atom in the dye chromophore in the form of an *N,N*-dimethylaniline substituent in the 4-position. The effects of increased conjugation and the additional heteroatom are apparent in these systems. Adding the dimethylaniline substituent gives a 370-ppm upfield shift for **14f** (δ 934) relative

to **4b** (δ 1304). Replacing the *tert*-butyl groups of **14f** with phenyl groups in **14c** gives a ^{125}Te NMR chemical shift of 875 ppm (59 ppm upfield). The introduction of a second heteroatom in addition to tellurium in **14h** with the *p*-anisyl substituent gives a ^{125}Te NMR chemical shift of 784 ppm—an additional 91 ppm upfield.

The sequential changes observed in the ^{125}Te NMR chemical shifts in **14c**, **14f**, and **14h** suggest that in addition to the resonance forms shown in Scheme 10, contributions from the resonance form **71a** in Scheme 13 are important in all three dyes. Increased delocalization into the aromatic rings as in **71b–d** is important in **14c** and **14h**, while the contribution from **71e** is important with the additional heteroatom in **14h**.

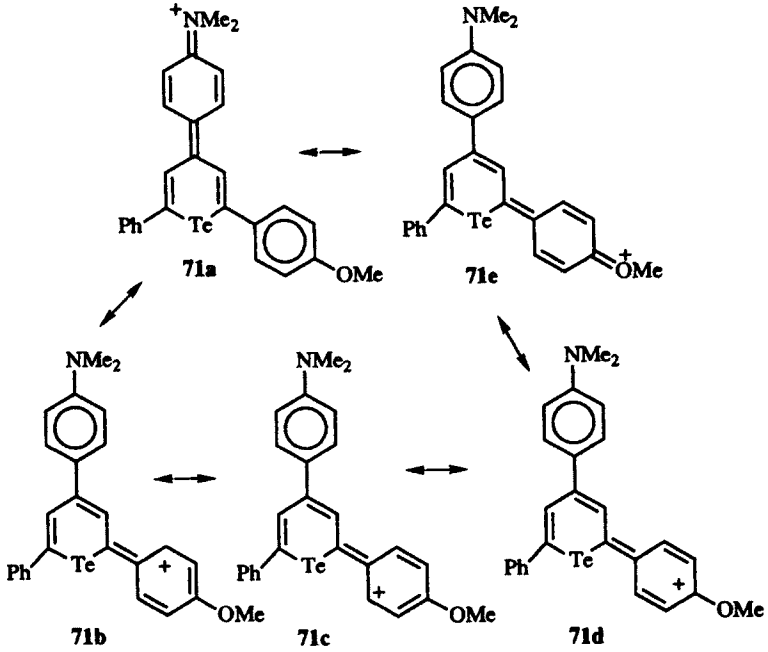

Scheme 13

Simple inductive effects appear to be important as well in determining ^{125}Te NMR chemical shifts. The introduction of an electron-donating 4-methyl substituent gives a 119-ppm upfield shift from **4b** to **14d**.

D. Tellurium XPS Data for Telluropyrylium Compounds

The electronic factors that contribute to the binding-energy shifts observed in X-ray photoelectron spectroscopy [XPS or ESCA (electron spectroscopy for

chemical analysis)] are primarily inductive in nature, while NMR chemical shifts are sensitive to both the diamagnetic screening and paramagnetic screening of the nucleus.[46,47] However, in some closely related organometallic systems,[48,49] including tellurium heterocycles,[28,50] linear correlations between XPS binding energies and NMR chemical shifts have been observed. A comparison of Te($3d_{5/2}$) XPS binding energies and ^{125}Te NMR chemical shifts as shown in Table 11 for **4b**, **5c**, **14c**, **14d**, **14f**, **14h**, and **58** shows similar trends for the two techniques.[28]

For the Te($3d_{5/2}$) XPS binding energies in Table 11, the range of 574.5–575 eV in the telluropyrylium compounds is a minimum of 0.4 eV higher than those of the analogous telluropyranone compounds **60–62**. Again, as in the ^{125}Te NMR chemical shifts, resonance forms that place a positive charge on tellurium are more important in the telluropyrylium compounds than in the tellurin-4-ones. In benzo[*b*]telluropyrylium salt **5c**, the addition of the benzo-fused ring leads to a full 0.7-eV lowering of the Te($3d_{5/2}$) XPS binding energy relative to **4b** [Te($3d_{5/2}$), 572.2 eV for **4b** vs 574.5 eV for **5c**]. This is consistent with the positive charge in **5c** being delocalized over more of the π framework, resulting in less charge at tellurium.

The Te($3d_{5/2}$) XPS binding energies observed of 573.7, 574.1, and 573.1 eV for **14c**, **14f**, and **14h**, respectively, vary by 1.0 eV on the addition of more conjugation and an additional heteroatom into the π framework. The binding energies of these compounds suggest that resonance forms **71** (Scheme 11) contribute heavily to the electronic structure of the dyes. Furthermore, the binding energies of **14c**, **14f**, and **14h** are closer to those observed for the neutral tellurin-4-ones **60** and **61** than those of the other telluropyrylium compounds (Table 11).

A plot of Te($3d_{5/2}$) XPS binding energies versus ^{125}Te NMR chemical shifts for the compounds **4b**, **5c**, **14c**, **14d**, **14f**, **14h**, and **58** is linear.[20] The least-squares correlation coefficient for these data is 0.98, which suggest that similar factors influence Te($3d_{5/2}$) XPS binding energies and ^{125}Te NMR chemical shifts for these compounds.[28]

E. Absorption Properties of Telluropyrylium Dyes in Comparison with Those of the Other Chalcogenopyrylium Dyes

1. Theoretical Background of Absorption Properties

The donor and acceptor properties of dye molecules as well as their electronic excitations are linked to the energy of the highest occupied (HOMO) and lowest unoccupied (LUMO) molecular orbitals. According to Koopmans' theorem, the energy of the HOMO and LUMO are defined by

$$IP = -\varepsilon_{HOMO} \quad (1)$$

$$EA = \varepsilon_{LUMO} \quad (2)$$

where IP and EA are experimental ionization potentials and electron affinities, respectively.[51,52] While values of IP and EA are not trivial to obtain, experimental information about the HOMO and LUMO can be gained by spectroscopic and electrochemical techniques. The cyclic voltammetry (CV) time scale is much slower[53] than the time scale for the absorption of a photon.[54] While the CV time scale allows equilibrium conditions to be observed for both oxidation and reduction, the absorption of a photon involves an adiabatic promotion of an electron. In closely related series of compounds, such as related chalcogenopyrylium dyes, it can be assumed that nonadiabatic changes are comparable such that differences reflect the adiabatic processes.[24]

Reversible polarographic half-wave potentials (E°_{ox} and E°_{red}) of the chalcogenopyrylium dye have been related to ε_{HOMO} and ε_{LUMO} by the Equations[55-58]

$$E^{\circ}_{ox} = -\varepsilon_{HOMO}(\text{solvent}) + C \tag{3}$$

$$\varepsilon_{HOMO}(\text{solvent}) = -\text{IP} + \Delta E^{R^-}_{sol} \tag{4}$$

$$E^{\circ}_{red} = \varepsilon_{LUMO}(\text{solvent}) + C \tag{5}$$

$$\varepsilon_{LUMO}(\text{solvent}) = \text{EA} + \Delta E^{R^+}_{sol} \tag{6}$$

where the term C is a constant that includes the potential of the reference electrode on an absolute scale,[56,57] the solvation terms $\Delta E^{R^-}_{sol}$ and $\Delta E^{R^+}_{sol}$ are the differences in real solvation energies between the reduced and oxidized forms of the chalcogenopyrylium nuclei and the nuclei in the gas phase, and EA and IP are the gas-phase molecular electron affinity and ionization potential, respectively. The potential of the reference electrode will cancel out when the chalcogenopyrylium nuclei are compared to one another. Furthermore, within a series of dyes where structurally only the heteroatom is changing, the solvation terms should be quite similar such that solution values should give the same relative ordering of energy levels as one would expect in the gas phase.

Although, to a first approximation, the difference in energy between the HOMO and LUMO should give the energy necessary to reach the first excited state (the S_0–S_1 transition), a more accurate representation of this energy is given by the self-consistent-field (SCF) model, in which an orbital energy corresponds to the energy of an electron that "feels" the field of the nuclei as well as the time-averaged fields of the other electrons.[52] The energy of the S_0–S_1 transition, E_{S1}, can be related in the gas phase to the HOMO and LUMO levels by the equation[52]

$$E_{S1} = \varepsilon_{HOMO} - \varepsilon_{LUMO} - J_{12} + 2K_{12} \tag{7}$$

where J_{12} is the Coulomb repulsion integral and K_{12} is the exchange integral. The "$-J_{12} + 2K_{12}$" term represents the difference in energy of the LUMO in the ground state with occupancy by one electron after excitation.

The energy of the first electronic transition for the chalcogenopyrylium nucleus (the absorption maximum) is added to ε_{HOMO} to give the absolute level of E_{S1}. As shown in Equations (3) and (4), ε_{HOMO} can be approximated by E°_{ox} and

the absolute level of ε_{HOMO} can be approximated by incorporating the Fermi level of the reference electrode (for SCE in acetonitrile, -4.38 eV).[58] The difference in energy between E_{S1} and E°_{red} represents the "$-J_{12}+2K_{12}$" term plus relaxation energies (including solvation) between the adiabatic and non-adiabatic HOMO and LUMO levels.

2. *Experimental Redox Potentials and Absorption Maxima in Chalcogenopyrylium Dyes*

The absorption maxima of a chalcogenopyrylium dye series increase in wavelength as the chalcogen atom becomes heavier. This is illustrated in Table 12 for two different series of 2,6-substituted-4-(*p*-*N*,*N*-dimethylaminophenyl) chalcogenopyrylium dyes **72(X)** and **73(X)**. (For purposes of ease of reference, the π frameworks will be renumbered for this discussion with the chalcogen atoms listed in parentheses.) The telluropyrylium dyes absorb at approximately 100-nm longer wavelengths than the corresponding pyrylium dyes.[24] The increase in the wavelength of the maxima of absorption as the chalcogen atom increases in size is a consequence of a lower-energy S_0–S_1 transition as illustrated in Table 12 with values of $E_{\lambda_{max}}$ [in electronvolts (eV)]. In the ground state, the changes in the S_0–S_1 transition are mirrored in the narrowing of the HOMO–LUMO gap in the chalcogenopyrylium dyes.[55] The HOMO–LUMO gap in solution is in turn approximated by the absolute difference between the oxidation and reduction potentials of the dyes (ΔE°).[55–58] The oxidation and reduction potentials of the chalcogenopyrylium dyes are also compiled in Table 12.[24]

As shown in Table 12, $E_{\lambda_{max}}$ and ΔE° follow identical trends as the chalcogen atom of the dye increases in size. Plots of $E_{\lambda_{max}}$ versus ΔE° for chalcogenopyrylium dyes in either acetonitrile or dichloromethane are linear with values of the "$-J_{12}+2K_{12}$" term of approximately 0.53 eV in both solvents.[24] Because the "$-J_{12}+2K_{12}$" term remains constant in the telluropyrylium dyes, this term will be ignored in further discussion in this section.

Values of E°_{ox} become more negative, and values of E°_{red} become more positive as the chalcogen atoms increase in size. Thus, the telluropyrylium dyes both oxidize and reduce more readily than the other chalcogenopyrylium dyes. In terms of the HOMO and LUMO energy levels, the HOMO levels are higher in energy in the order Te > Se > S > O, while the LUMO levels are higher in the order O > S > Se > Te. As a consequence, the energy of the S_0–S_1 transition is lower (which is reflected in longer wavelengths of absorption) in the order Te < Se < S < O.[24]

Similar trends are observed in the monomethine dyes **74(X,Y)** and **75(X,Y)** of Table 13, the trimethine dyes [**76(X,Y)** and **77(X,Y)**] and pentamethine dyes [**78(X,Y)**] of Table 14, and squarylium dye **32a** and lighter chalcogen analogs.[32] Dyes in this series that incorporate two tellurium atoms absorb at wavelengths more than 200 nm longer than the corresponding dyes containing two oxygen

atoms. The trends observed with changes in one chalcogen atom are doubled with changes in two. Again, values of E°_{ox} become more negative, and values of E°_{red} become more positive as the chalcogen atoms increase in size. Thus the tellurium-containing dyes both oxidize and reduce more readily than do the other chalcogenopyrylium dyes.

The heptamethine dyes **79**, **80**, and **81** absorb in the near infrared with absorption maxima at 1190 nm (log ε 5.43),[22] 1050 nm,[59] and 1017 nm,[59] respectively. The heptamethine dyes have limited stability both in the dark and in the light.

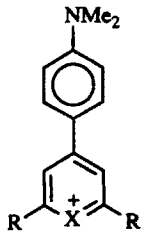

72(X), R=Ph
73(X), R=*tert*-Bu

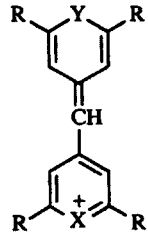

74(X,Y), R=Ph
75(X,Y), R=*tert*-Bu

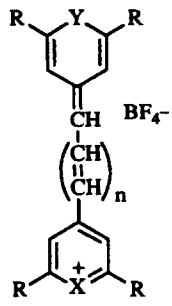

76(X,Y), R = Ph, n = 1
77(X,Y), R = *tert*-Bu, n = 1
78(X,Y), R = Ph, n = 2

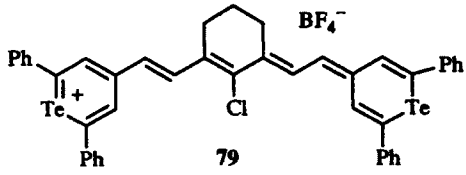

79

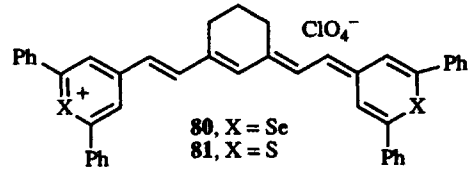

80, X = Se
81, X = S

As can be seen from the redox data of Tables 12–14, the values of E°_{ox} and E°_{red} are sensitive to the substituents in the 2- and 6-positions. Reduction potentials are much more sensitive to substituent changes than are oxidation potentials. The same observation can be made for the effect of chalcogen atom changes as well. Reduction potentials are more affected by chalcogen atom changes than are oxidation potentials. These observations can be explained in terms of substituent effects on the HOMO and LUMO of the dyes of Tables 12–14.

Several theoretical treatments of the pyrylium and thiopyrylium ring systems have given similar results for coefficients on the ring and for the relative ordering of energy levels. CNDO calculations[60] and Hückel MO calculations[61] of 2,4,6-triphenylpyrylium and 2,4,6-triphenylthiopyrylium have shown that the π or-

bitals are benzene-like. The HOMO and LUMO in these systems are located in the heterocyclic π framework and are not localized on the heteroatom lone pair of electrons, because of the nodal properties of the e_2 benzene-like molecular orbitals.[60,61] Similar results were obtained from MNDO calculations on the unsubstituted pyrylium and thiopyrylium rings.[24]

MNDO[62,63] calculations on pyrylium and thiopyrylium dye models **82** and **83** offer an insight to the heteroatom and substituent effects observed in the dyes of Tables 12–14.[24] The HOMO coefficients for the aniline-substituted pyrylium and thiopyrylium systems indicate that the HOMO is predominantly on the aniline fragment ($\approx$ 65%) with much less contribution from the chalcogen atom (3–6%).[24] The LUMO coefficients for these systems indicate that the LUMO is predominantly on the chalcogenopyrylium ring ($\approx$ 75%) with approximately a 9% contribution from the chalcogen atom.[24] These results are consistent with the experimental observations that both chalcogen atom and substituent effects in the 2- and 6-positions are most pronounced with respect to reduction potentials relative to oxidation potentials.

The MNDO calculations on the model monomethine dyes **83** indicate that the contribution from each chalcogenopyrylium ring to the HOMO is comparable to that calculated for the chalcogenopyrylium ring in the aniline-substituted dyes **82**.[24] However, the large coefficient for the central methine carbon indicates that 30–40% of the HOMO lies here. In the LUMOs of these systems, there is no contribution from the central methine (a nodal position), with the entire LUMO distributed over the two chalcogenopyrylium rings.[24] The MNDO calculations predict similar heteroatom contributions in both the HOMO and LUMO of the monomethine dyes **83**.[24] This prediction is not reflected in the oxidation and reduction potentials of Table 13, where reduction potentials are shown to be more sensitive to the chalcogen atom.

82(X), X = O,S

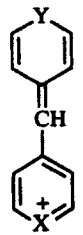

83(X,Y), X,Y = O,S

Although theoretical treatment of telluropyrylium and selenopyrylium species at the CNDO or MNDO level has not been reported, one would expect similar trends to be observed. Certainly, those trends predicted theoretically and observed experimentally from pyrylium to thiopyrylium are continued experimentally with selenopyrylium and telluropyrylium systems (ordering of redox potentials, absorption properties).

An electron-donating substituent attached to the central methine carbon of systems related to **83** should raise the energy of the HOMO, leading to bathochromic shifts as well as more negative oxidation potentials. A number of telluropyrylium dyes and a few other chalcogenopyrylium dyes with a methyl substituent on the central methine [**84(X,Y)** and **85(X,Y)**] have been prepared.[24,25] Spectral properties and oxidation and reduction potentials for these dyes are compiled in Table 15. The chalcogenopyrylium dyes with a methyl substituent on the methine bridge show a large bathochromic shift in absorption maxima relative to the unsubstituted methine dyes of Table 13. If one compares reduction potentials for corresponding dyes in Tables 13 and 15, one finds them to be essentially identical. However, as predicted by theory, oxidation potentials of the methyl-substituted compounds are more negative.

The magnitude of the bathochromic shift observed on methyl substitution is quite large for a strictly electronic effect. The extinction coefficients for the methyl-substituted derivatives are 33.3–50% smaller than for the unbsubstituted systems, suggesting a weaker oscillator, perhaps from increased steric interactions. Steric interactions of the methine methyl group with the two chalcogenopyranyl rings leads to increased dihedral angles via AM1 calculations on the parent pyrylium systems.[24] Again, the effect of increasing the dihedral angle appears to raise only the HOMO and has little effect on the LUMO. The steric interactions appear to be identical in both the pyrylium and telluropyrylium systems. In each case, methyl substitution at the methine carbon leads to a 0.25 eV lowering of the energy of the S_0–S_1 transition.[24]

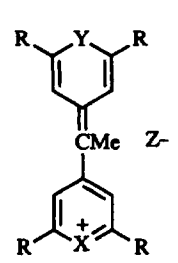

84(X,Y), R = Ph
85(X,Y), R = *tert*-Bu

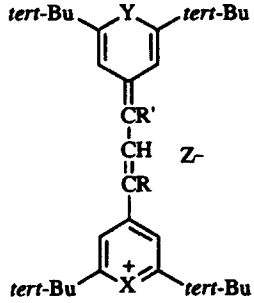

86(X,Y)(R,R')

The effect of methyl substitution is much less pronounced in methyl-substituted trimethine dyes **86(X,Y)(R,R')** as shown in Table 16.[25] In these materials, each methyl substituent increases the maximum of absorption by approximately 15 nm. The addition of the first methyl group has little effect on the extinction coefficient. However, with the addition of a second methyl group, steric interactions increase and the magnitude of the extinction coefficient drops by a factor of 3.[25]

OMEGA[64,65] calculations on model trimethine dye **87(O,O)** show large coefficients on the allyl termini of the bridging three-carbon unit in the HOMO

(± 0.44) consistent with 0.61 for the methine carbon of **83(O,O)** and negligible coefficients for the LUMO [0.05 compared with 0.02 for the bridging methine in **83(O,O)**]. These facts suggest that purely electronic contributions from the methyl group might be expected to be significantly less in **84(X,Y)** and **85(X,Y)** than is actually observed in the large bathochromic shifts for **84(X,Y)** and **85(X,Y)**.

In the aniline-substituted dyes, structural rigidity can lower the energy of the S_0–S_1 transition leading to bathochromic shifts. In a series of styryl dyes **35**, **39**, and **40**, each additional ring decreases the rotational degrees of freedom of the nitrogen lone pair of electrons, which leads to sequentially greater bathochromic shifts in the series as shown in Table 6.[22]

In styryl dyes of this type, modified OMEGA calculations were employed to determine coefficients for model compounds **88(X)**.[24] The weight of the aniline moiety predominates in the HOMO (75–80%) with little contribution from the bridging carbons or the chalcogenopyrylium ring. The chalcogenopyrylium ring predominates in the LUMO (≈ 70%) with little contribution from the bridging carbons or the aniline ring.

In support of this analysis as shown in Table 17, the julolyldyl dyes **89(X)** show nearly identical oxidation potentials, but show reduction potentials that differ by more than 0.27 V and absorbed-photon energies that differ by 0.31 eV at λ_{max}.[24] Thus, the 121-nm difference in absorption maxima observed from the pyrylium nucleus to the telluropyrylium nucleus is strictly a function of the chalcogen-atom effect on the LUMO.

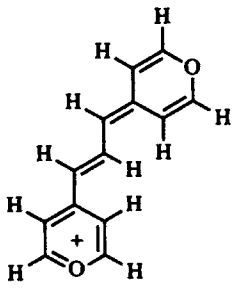

87(O,O)

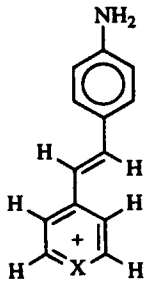

88(X)

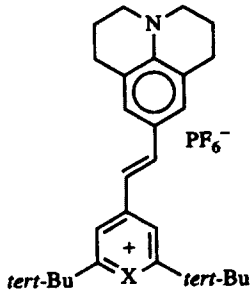

89(X)

In summary, the absorption properties of the chalcogenopyrylium dyes are driven primarily by changes in the LUMO as a function of the chalcogenopyranyl ring. The chalcogen atom has a smaller influence on the HOMO. The effect of the chalcogen atom on the HOMO indicates that the HOMO level is higher in energy in the order Te > Se > S > O while the effect of the chalcogen atom on the LUMO indicates that the LUMO level is higher in energy in the order O > S > Se > Te. The S_0–S_1 transition of chalcogenopyrylium dyes decreases in energy in the order Te < Se < S < O such that telluropyrylium dyes absorb

at the longest wavelengths and pyrylium dyes absorb at the shortest wavelengths.

F. Photophysical Properties of Telluropyrylium Dyes and Related Chalcogenopyrylium Dyes

In the excited state, the chalcogenopyrylium dyes can undergo single-electron-transfer (SET) reaction, can undergo internal conversion back to the ground state, can fluoresce back to the ground state, can undergo *cis–trans* isomerizations, and can undergo intersystem crossing to the triplet state. The chalcogen-atom effects dominate the photochemistry of the chalcogenopyrylium dyes.

In this class of compounds, the heteroatom effects show opposite trends with respect to SET and triplet yield. Typically, SET reactions of the chalcogenopyrylium dyes are driven by the fact that the excited state is both a more powerful oxidant and a more powerful reducing agent by roughly the energy of the absorbed photon. Because the S_0–S_1 splitting narrows as the heteroatoms become heavier, the excited-state pyrylium dyes will be the most powerful oxidizing and reducing agents while excited-state telluropyrylium dyes will be the least powerful. Intersystem crossing from the S_1 state to the T_1 state can be promoted by increased spin–orbit coupling between an attached heavy atom and the molecular orbitals of the dye.[54,56] As the chalcogen atoms increase in atomic number, spin–orbit coupling should increase such that telluropyrylium dyes should produce higher triplet yields than do pyrylium dyes.

The heavy-atom effects on spin–orbit coupling should be a function of Z^4 (where Z is the atomic number of the heavy atom).[66] The heavy-atom effects on spin–orbit coupling can be demonstrated in the yields of singlet oxygen shown below for the xanthene dyes. As the attached halogen atoms increase in atomic number, the singlet oxygen yields (and, presumably, the triplet yields) increase for a variety of halogen-substituted xanthene dyes.[44] Even more pronounced heavy-atom effects are observed in the chalcogenopyrylium dyes of Tables 12–14, where the heavy atoms are intimate parts of the dye chromophore.

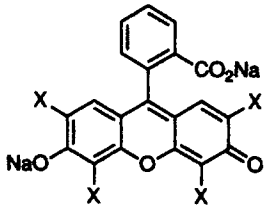

X=H; $\Phi(^1O_2) = 0.03$
X=Cl; $\Phi(^1O_2) = 0.05$
X=Br; $\Phi(^1O_2) = 0.32$
X=I; $\Phi(^1O_2) = 0.69$

1. *Oxygen Concentration Effects and Triplet Yields and Lifetimes*

From measurements of singlet-oxygen-generation efficiencies as a function of oxygen concentration, quantum yields for formation of dye triplets (Φ_T) and estimates of triplet lifetimes (τ_T) for chalcogenopyrylium dyes have been determined.[25] These data are compiled in Table 18. For telluropyrylium dye **77(Te,Te)**, a Φ_T value of 0.18 is calculated in methanol and τ_T is estimated to be approximately 0.3 μs.[25] In water, a triplet lifetime of 0.3 μs is calculated.

In a similar manner, a triplet yield of 0.11 is estimated in methanol for telluropyrylium dye **77(Te,Se)**.[25] In water, an estimated triplet lifetime of 0.9 μs has been determined.

For dye **77(Se,Se)**, a triplet lifetime of $\geq 10\,\mu$s has been determined. For this dye, the triplet yield is essentially the same as the singlet oxygen yield since the triplet lifetime is long enough for complete scavenging of triplets by oxygen.[25] For the dyes **77(O,O)** through **77(Se,S)**, the singlet oxygen yield is assumed to be identical to the triplet yield since triplet lifetimes would be expected to be longer with smaller heavy-atom effects.[25]

2. *Emission Studies of Chalcogenopyrylium Dyes* **74(X,Y)**

Additional photophysical properties of the chalcogenopyrylium dyes may be derived from their emission spectra. The fluorescence emission spectra of many of the dyes **74(X,Y)**[25] and the tellurium-containing dyes **77(X,Y)**[67] have been measured, and data for these emissions are compiled in Table 18. The excitation or absorption maxima of these dyes are also compiled in Table 18. The excitation and emission spectra are characterized by small Stokes shifts. In the excitation spectra of dyes **77(X,Y)**, the H-aggregate contribution is quite pronounced and may be nearly as intense as the excitation maximum.

The quantum efficiencies of fluorescence Φ_F are quite sensitive to the chalcogen atoms in the dye chromophore and vary in an inverse manner to the triplet yields. For example, Φ_F decreases from 0.048 for **77(O,O)** to 0.0004 for **77(Te,Te)** while Φ_T increases from 0.0004 for **77(O,O)** to 0.18 for **77(Te,Te)**. This behavior might be expected if variations in the rate of intersystem crossing (k_{isc}) from S_1 to T_1 were controlling both processes.

The estimated values for the net lifetime of the S_1 state τ_S and for the intersystem crossing rate constant k_{isc} in Table 18 help clarify the effects of heavy atoms on the photophysics of chalcogenopyrylium dyes. Attempts to measure τ_S experimentally for the dyes **74(X,Y)** and **77(X,Y)** containing selenium and tellurium were unsuccessful since lifetimes were shorter than 80 ps.[25] The radiative lifetime τ_{rad} can be approximated from the absorption spectra of the dyes by the equation[54]

$$\tau_{rad} = \frac{3.5 \times 10^8}{(E_{SO})^2 \varepsilon_m \Delta\nu_{1/2}} \tag{8}$$

where E_{S0} is the energy of the absorption maximum in cm^{-1} (reciprocal centimeters), ε_m is the molar extinction coefficient, and $\Delta\nu_{1/2}$ is the bandwidth at half height in cm^{-1}. The product of τ_{rad} and Φ_F yields an approximate τ_S and the rate of intersystem crossing k_{isc} can be approximated by the following equations

$$\tau_S = \tau_{rad}\Phi_F \tag{9}$$

$$k_{isc} = \frac{\Phi_T}{\tau_S} \tag{10}$$

where Φ_T is the triplet yield. As shown in Table 18, radiationless decay increases dramatically as the chalcogen atoms become heavier, with τ_S decreasing from approximately 230 ps for **77(O,O)** to about 5 ps for **77(Te,Te)** and **74(Te,Te)**.

It is evident that the heavy-atom effect on k_{isc} values is even more pronounced than the heavy-atom effect on τ_S. The former increases by four orders of magnitude for **77(Te,Te)** relative to **77(O,O)**. It is also evident from the values of k_{isc}, τ_{rad}, and τ_S that the radiationless decay of the S_1 state is dominated by internal conversion rather than intersystem crossing. This follows from the relationship

$$k_s = k_{ic} + k_{rad} + k_{isc} \tag{11}$$

where k_s is $1/\tau_S$, k_{rad} is $1/\tau_{rad}$, and k_{ic} is the rate of internal conversion. For example, the net decay constants for the S_1 states (i.e., $1/\tau_S$ or k_s) of **77(Te,Te)** and **74(Te,Te)** are approximately $2 \times 10^{11}\,s^{-1}$, which makes k_{isc} approximately 20% of S_1 decay for **77(Te,Te)** and 10% of S_1 decay for **74(Te,Te)**, assuming that $\Phi(^1O_2)$ approximates Φ_T for **74(Te,Te)**. The contributions of k_{isc} to S_1 decay decrease with decreasing chalcogen atomic number, reducing to 0.05% for **77(O,O)**. Thus, while increases in S_1 internal-conversion rates with increasing chalcogen weight tend to decrease triplet yields, this is more than offset by large increases in k_{isc}.

Graphically, a plot of $\log k_s$ as a function of $\log k_{isc}$ is linear as shown in Figure 2. This is indicative that the heteroatom contributions to heavy-atom effects are similar in a relative sense with respect to both rates, but rates of intersystem crossing are more sensitive to spin–orbit effects than rates of internal conversion.

Luminescence studies have been directed at obtaining triplet energy levels. The luminescence of **77(Te,O)** was measured in ethanol–methanol glass at 77 K. The major emission band at 77 K has a maximum at about 770 nm, a shoulder at approximately 800 nm, and, at higher amplification, a very weak emission in the vicinity of 885 nm, due to phosphorescence (or perhaps an additional vibronic fluorescence band).[25] If the weak emission at 885 nm were due to phosphorescence from **77(Te,O)**, S_1–T_1 splitting in this molecule would be $2700\,cm^{-1}$, which is on the order of 8 kcal mol^{-1}. Other cationic dyes have given S_1–T_1 splittings of this magnitude, typically $1500–4500\,cm^{-1}$.[68] Data of Gilman indicate an S_1–T_1 splitting of $2900\,cm^{-1}$ for 1,1′-diethyl-2,2′-cyanine.[69]

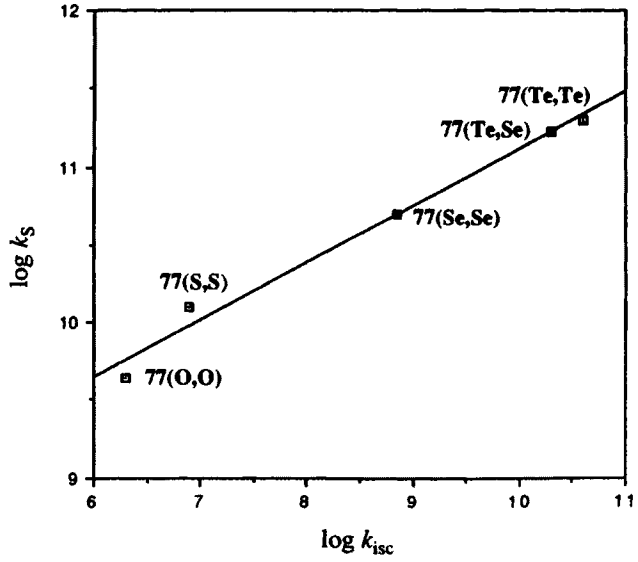

Figure 2. A log–log plot of the rate of excited singlet decay (k_s) as a function of k_{isc} for chalcogenopyrylium dyes **77(X,Y)**.

3. *Effect of Steric Interactions on Photophysical Properties of Telluropyrylium and Related Chalcogenopyrylium Dyes*

The methine carbon of monomethine dyes **74(X,Y)** and the noncentral methine carbons of trimethine dyes **76(X,Y)** and **77(X,Y)** are "nonstarred" positions. Methyl substituents at these positions should give bathochromic shifts since a methyl group is electron-donating as a substituent. Furthermore, steric interactions resulting in twisting of the molecule should raise the HOMO relative to the LUMO and also give a bathochromic shift. Such has been observed with chalcogenopyrylium dyes **84(X,Y)**, where methyl substitution on the methine carbon leads to large bathochromic shifts of 60–75 nm.[24]

The introduction of substituents that can disrupt the planarity of the molecule might promote nonradiative, internal conversion back to ground state, which could lower the triplet yield. The methyl-substituted dyes **84(X,Y)**, **85(X,Y)**, and **86(Se,Se) (Me,Me)** have much broader spectral bandwidths ($\approx$ 100 nm) when compared to those of the unsubstituted dyes **74(X,Y)**, **75(X,Y)**, and **77(X,Y)** ($\approx$ 40–60 nm), which is consistent with a less rigid structure in the methyl-substituted molecules.[25] Values of Φ_T for the methyl-substituted dyes **85(Te,Te)**, **86(Se,Se) (Me,H)**, and **86(Se,Se) (Me,Me)** can be compared to those for their unsubstituted analogs **75(Te,Te)** and **77(Se,Se)**. These data are also compiled in Table 18.

For the monomethine dyes **75(Te,Te)** and **85(Te,Te)**, Φ_T values are 0.07 and 0.006, respectively. From the emission data compiled in Table 18 and the triplet

yield, nearly identical rates of intersystem crossing (10^9–$10^{10}\,s^{-1}$) can be calculated. The net decay constants for these two molecules are estimated to be $8 \times 10^{10}\,s^{-1}$ for **75(Te,Te)** and $5 \times 10^{11}\,s^{-1}$ for **85(Te,Te)** (from $1/\tau_S$). These data suggest that decreased triplet yields are a result of an increase in the rate of radiationless decay back to ground state on methyl substitution, presumably from increased steric interactions.

Similar trends are observed for trimethine dyes **86(Se,Se) (Me,H)** and **86(Se,Se) (Me,Me)** when compared to **77(Se,Se)**. If one assumes that $\Phi(^1O_2)$ is identical to the triplet yield in these molecules,[25] then identical rates of intersystem crossing are calculated for all three [Eq. (3), $10^9\,s^{-1}$]. The rate of radiationless decay increases dramatically, though, in this series from $5 \times 10^{10}\,s^{-1}$ for **8** (Se,Se) to $3 \times 10^{11}\,s^{-1}$ for the addition of one methyl group [**86(Se,Se) (Me,H)**] to $1 \times 10^{12}\,s^{-1}$ for the addition of a second methyl group [**86(Se,Se) (Me,Me)**]. The yield of singlet oxygen decreases by a factor of 3–4, as well, for each methyl group.

V. REACTIONS OF TELLUROPYRYLIUM COMPOUNDS

The reactions of telluropyrylium compounds to be discussed in these sections fall into four categories. The first category consists of reactions to give reactive oxygen species. The T_1 state of a telluropyrylium dye can react with ground-state ($^3\Sigma_-$) oxygen via a spin-allowed process to produce the S_0 state of the dye and the first excited state ($^1\Delta_g$) of oxygen, singlet oxygen ($^1O_2$). A second category is the reaction of the tellurium atom of telluropyrylium species with various oxidants such as ground-state and singlet oxygen, hydrogen peroxide, or the halogens. A third category consists of the reactions of various electron-rich or nucleophilic reagents with the positively charged carbon π framework. The fourth category consists of nucleophilic addition reactions of the deprotonation products of alkyl-substituted telluropyrylium dyes. This category includes the dye-forming condensation reactions discussed in the first part of this chapter.

The chemistry of tellurium(IV) analogs of telluropyrylium compounds is also discussed in these sections. These reactions include reductive elimination reactions to regenerate the telluropyrylium compounds, rearrangement reactions to generate tellurophenes, and reaction sequences involving tellurium(II)–tellurium(IV)–tellurium(II) shuttles.

A. Reaction of Triplet States of Telluropyrylium and Other Chalcogenopyrylium Dyes with Oxygen to Produce Singlet Oxygen

Singlet oxygen lies approximately 22.6 kcal mol^{-1} higher in energy than ground-state oxygen. This energy corresponds to a wavelength of absorption of approximately 1270 nm (7874 cm^{-1}) for a chalcogenopyrylium dye to have

sufficient energy to produce singlet oxygen. The energy of the T_1 state of the dye should lie close to or higher than this energy relative to the energy of the S_0 state for efficient production of singlet oxygen.[70] In porphyrin and phthalocyanine systems, where molecular orbitals are benzene-like, the S_1-T_1 splittings (Δ_E) are quite large, on the order of approximately 15 kcal mol^{-1}. To produce singlet oxygen in systems of this type, the energy of the absorbed photon must be at least 38 kcal mol^{-1}, which corresponds in energy to a wavelength of 750 nm or shorter. Cationic dyes have S_1-T_1 splittings that are much smaller, typically 8–12 kcal mol^{-1} (3000–4000 cm^{-1}).[68,69] Thus the energy of the absorbed photon need be on the order of only 31–35 kcal mol^{-1} to produce singlet oxygen, which corresponds to a wavelength of approximately 900 nm or shorter. As shown in Table 18, values of Δ_E are on the order of 8 kcal mol^{-1} for the telluropyrylium dyes **77(Te,Y)**. The factors that affect self-sensitized, singlet oxygen generation and dye stability can be defined as the quantum yield for triplet generation, the energy of the T_1 state, the lifetime of the T_1 state, and the rate of reaction of the dye with singlet oxygen. The quantum efficiency for the production of singlet oxygen [$\Phi(^1O_2)$] will be, to some extent, proportional to the triplet yield of the excited dye.

The quantum yield for self-sensitized generation of singlet oxygen from chalcogenopyrylium dyes **77(X,Y)** increases as the chalcogen atoms become heavier (Table 19).[7,10,25] This is a direct consequence of increased spin–orbit coupling allowing faster intersystem crossing to the triplet state. Telluropyrylium dyes **74(Te,Te)** and **75(Te,Te)** show quantum yields for singlet oxygen generation of 0.09 and 0.07, respectively (Table 19).[25]

The triplet lifetimes of the telluropyrylium dyes are significantly shorter than the triplet lifetimes of the other chalcogenopyrylium compounds (Table 18). Consequently, the conversion of dye triplets and ground-state oxygen to singlet oxygen and singlet dye is not unity. Thus the quantum yield for singlet oxygen generation [$\Phi(^1O_2)$] is 0.12 for **77(Te,Te)**, 0.09 for **77(Te,Se)**, and 0.09 for **75(Te,Te)**, while triplet yields (Φ_T) are 0.18, 0.11, and 0.12, respectively, in these compounds.[25]

Not all telluropyrylium species produce singlet oxygen on irradiation. The dimethylaniline-substituted dyes **14c**, and **14f–14h** have quantum yields for singlet oxygen generation of ≤ 0.0005 and suggest that dyes whose chromophores are charge transfer in nature will not produce significant yields of singlet oxygen.

B. Reactions of Telluropyrylium Dyes with Oxidants

1. Rate Constants for Reaction of Dyes 77(X,Y) *with Singlet Oxygen*

In dyes of structure **77(X,Y)**, singlet oxygen might attack either the heteroatoms incorporated in the dye chromophore or the hydrocarbon backbone of

the dye. The pyrylium dye **77(O,O)** should be a good model for the rate of reaction of singlet oxygen with the π framework. The sulfur atoms of the thiopyrylium dyes, selenium atoms of the selenopyrylium dyes, and tellurium atoms of the telluropyrylium dyes can all be oxidized by singlet oxygen to give higher oxidation states not available to oxygen. Rates of reaction of the dyes **77(X,Y)** with singlet oxygen [$k(^1O_2)$] in 50% aqueous methanol are compiled in Table 19.[7,10,25] These values were determined by the rate of reaction of the dye with singlet oxygen generated by irradiation of methylene blue and/or rose bengal in aqueous methanol solution. Where comparative measurements were carried out, rate constants determined were similar whether methylene blue or rose bengal was employed to generate singlet oxygen.

As shown in Table 19, the telluropyrylium dyes are one to two orders of magnitude more reactive toward singlet oxygen than the other chalcogenopyrylium dyes. The pyrylium and selenopyrylium dyes appear to have very similar values of $k(^1O_2)$, while the thiopyrylium compounds appear to be about four times more reactive than the pyrylium and selenopyrylium compounds.

The higher reactivity of the telluropyrylium compounds appears to reflect reaction at the tellurium atom. On sensitized photooxidation with singlet oxygen in water or aqueous methanol, the telluropyrylium dyes yield products that absorb in the vicinity of 500 nm. The same products can be produced by self-sensitized dye photooxidation,[15,25] by reaction with hydrogen peroxide,[15,16,71] or by reaction with ozone.[71a]

The products of oxidation are derived by the formal oxidative addition of hydrogen peroxide across the tellurium atom of a telluropyrylium dye as shown below for compounds **90**. Similar products have not been characterized for thiopyrylium and selenopyrylium species.

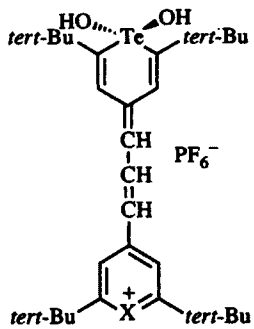

90a, X = Te
90b, X = Se
90c, X = S
90d, X = O

In water, the rate constant for reaction of **77(Te,Te)** with singlet oxygen is $8 \times 10^8 M^{-1} s^{-1}$. This is 4.5-fold larger than the value in 50% aqueous methanol ($1.8 \times 10^8 M^{-1} s^{-1}$) and 100-fold larger than the value in 99% methanol

($9 \times 10^6 M^{-1}s^{-1}$).[25] Under identical photooxidation conditions, the efficiency of methylene blue–sensitized oxidation increases by a factor of 10 in deuterium oxide relative to water. This is consistent with the roughly 10-fold longer singlet oxygen lifetime in deuterated water.[72,73] The effect of deuteration on aqueous photooxidation efficiencies together with the similarities of $k(^1O_2)$ values obtained with rose bengal and methylene blue were taken as evidence to support the involvement of singlet oxygen in the chalcogenopyrylium dye photobleach process.[25]

2. *Rates of Reaction of Chalcogenopyrylium Dyes* 77(X,Y) *with Hydrogen Peroxide*

The telluropyrylium dyes have been found to be much more reactive toward oxidants such as hydrogen peroxide than are the other chalcogenopyrylium dyes.[71,74] Of the dyes **77(X,Y)**, the pyrylium dye **77(O,O)** is much less reactive toward hydrogen peroxide than are the other chalcogenopyrylium dyes. The second-order rate constant for reaction of the dyes **77(X,Y)** with hydrogen peroxide increases from $9.88 \times 10^{-5} M^{-1}s^{-1}$ for **77(O,O)** to $4.68 \times 10^{-4} M^{-1}s^{-1}$ for **77(Se,Se)** to $1.81 \times 10^{-3} M^{-1}s^{-1}$ for **77(S,S)**. Rate constants for the telluropyrylium dyes are some 1000-fold larger still at $1.04 M^{-1}s^{-1}$ for **77(Te,O)**, $2.32 M^{-1}s^{-1}$ for **77(Te,S)**, $1.53 M^{-1}s^{-1}$ for

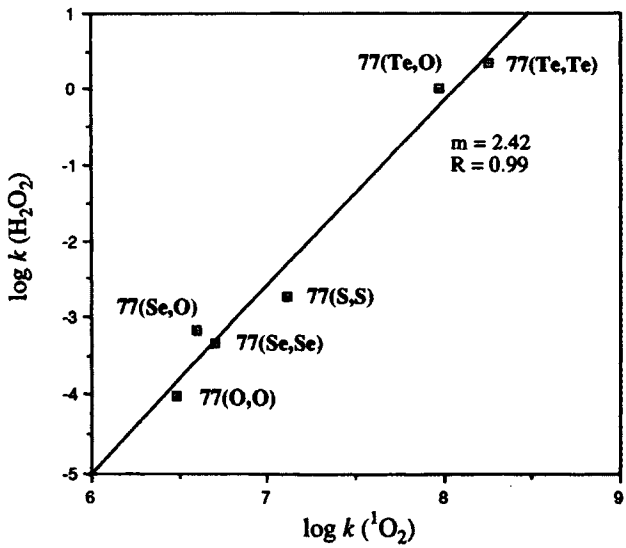

Figure 3. A plot of the log of the rate constant for reaction with hydrogen peroxide against the log of the rate constant for reaction with singlet oxygen for chalcogenopyrylium dyes **77(X,Y)**. (Reprinted with permission from *Organometallics* **1992**, *11*, 2310. Copyright 1992 American Chemical Society.)

77(Te,Se), and $2.26\,M^{-1}s^{-1}$ for **77(Te,Te)**.[71] The reaction products of the hydrogen peroxide oxidation are the dihydroxy telluranes **90**.

It should be noted that the chalcogenopyrylium dyes follow the same reactivity patterns for rate constants of reaction for both singlet oxygen and hydrogen peroxide. A plot of $\log k(H_2O_2)$ versus $\log k(^1O_2)$ is linear for compounds **77(X,Y)** with a slope of 2.42 as shown in Figure 3.[74] The slope of this plot is indicative of a roughly 250-fold difference in selectivity of the two reagents, although the linearity indicates that the "oxophilicity" of the heteroatoms is similar toward the two reagents. Similar selectivity is also observed with the reactions of **77(X,Y)** with ozone.[71a]

3. *Reaction of Chalcogenopyrylium Dyes* 77(X,Y) *with Halogens*

Halogens add across the tellurium atom of organotellurium compounds to give tellurium(IV) species. The addition of bromine to **73(Te)** ($Z = ClO_4$) gives **59** (whose X-ray structure is described earlier in this chapter) in 90% isolated yield.[27] In this reaction, the perchlorate salt of the telluropyrylium dye is replaced by a tribromide salt in the isolated product. The oxidative addition of bromine to phenyl-substituted derivative **72(Te)** gives **91** in 97% isolated yield.[27]

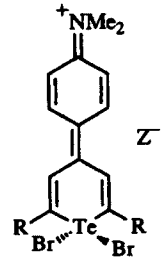

59, R = *tert*-Bu, Z=Br_3
91, R = Ph, Z=BF_4

The halogen oxidation occurs in other variations of telluropyrylium dyes as well.[27,75,76] The oxidative addition of chlorine, bromine, and iodine across the tellurium atom of telluropyrylium dye **74(Te,Te)** has given tellurium(IV) derivatives **92a** in 79% yield, **92b** in 75% yield, and **92c** in 75% yields (as a 1 : 1 mixture of BF_4^- and I_3^- salts). The oxidative additions of bromine and chlorine to monomethine dye **75(Te,Te)** give **93a** and **93b**, respectively.[75] Similarly, the oxidative addition reactions of bromine and iodine to **33b** have given tellurium(IV) derivatives **94a** and **94b** in 91 and 67% yields, respectively.[27] Oxidative additions of bromine to **77(Te,Te)** as the tetrafluoroborate salt, **77(Te,Se)** as the hexafluorophosphate salt, and **77(Te,S)** as the hexafluoro-

phosphate salt give **95a–c** in 81, 63, and 92% yields, respectively. The oxidative additions of chlorine to **77(Te,Te)** and **77(Te,Se)** as both the hexafluorophosphate and chloride salts give **96a–d** in 89, 80, 89, and 89% yields, respectively.[76] Finally, the addition of chlorine to **97** gives **98** in 90% yield.[76] Rate constants associated with the oxidative addition of chlorine or bromine are $\geq 10^8\ M^{-1}\,s^{-1}$.[71a]

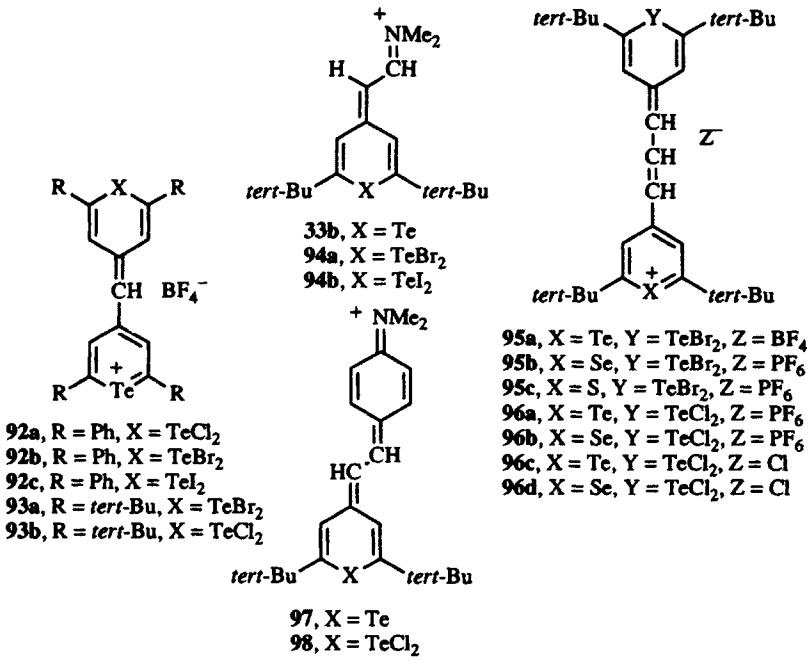

4. *Reaction of Chalcogenopyrylium Dyes* 77(X,Y) *with Ground-State Oxygen in the Presence of Pyridine and Triphenylphosphine*

Attempts to dimerize salts **4a**, **4b**, and **5b** with pyridine and triphenylphosphine do not give (telluropyranyl)telluropyrans.[77] As shown in Scheme 14, the (telluropyranyl)telluropyran carbon framework is formed with **4a** and **4b** under these reaction conditions, but one tellurium atom is in the tellurone oxidation state in the isolated product **99** (20–25% isolated yield). With benzo[*b*]telluropyrylium salt **5b**, a similar reaction occurs, but both tellurium atoms are in the telluroxide oxidation state in the isolated product **100** (25% isolated yield, Scheme 14). Sulfone analogs of **99** are known,[78] and spectral comparisons between the tellurium and sulfur analogs facilitated structural assignment of **99** and **100**.[77]

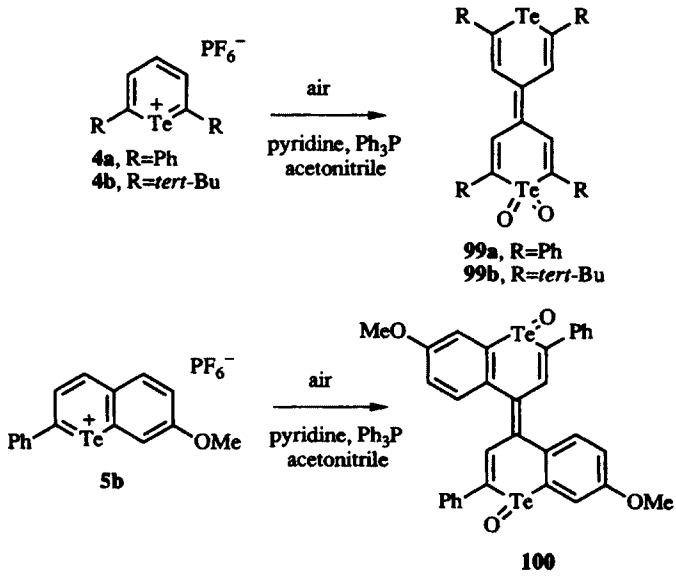

Scheme 14

C. Reactions of Telluropyrylium Species with Nucleophiles

1. Hydrolysis Reactions

Hydrolysis reactions with telluropyrylium dyes have been observed in both the telluropyrylium ring and the hydrocarbon backbone of polymethine telluropyrylium dyes. In the former reactions, the tellurium atom of the ring is replaced by oxygen and the overall transformation is the conversion of a telluropyrylium ring to a pyrylium ring as shown in Scheme 15. Telluropyrylium dye **77(Te,O)** is most susceptible to this reaction, giving **77(O,O)**.[67] The order of ease of hydrolysis is Te > Se ≫ S. Carboxylate anions have also initiated tellurium–oxygen exchange in dyes based on **72(Te)** with various alkyl carboxylate anions.[6]

Scheme 15

The condensation reactions used to synthesize the dyes **77(X,Y)** produce a molecule of water for every dye molecule that is formed. As shown in Scheme 16,

the molecule of water can lead to a reverse aldol reaction to give the 4-methylchalcogenopyrylium salt and a (chalcogenopyranyl)acetaldehyde **101(X)**. In the unsymmetrical dyes **77(X ≠ Y)**, the reverse aldol can follow two routes as shown in Scheme 16. The resulting component parts can recombine to give a statistical scrambling of the heteroatoms.[10]

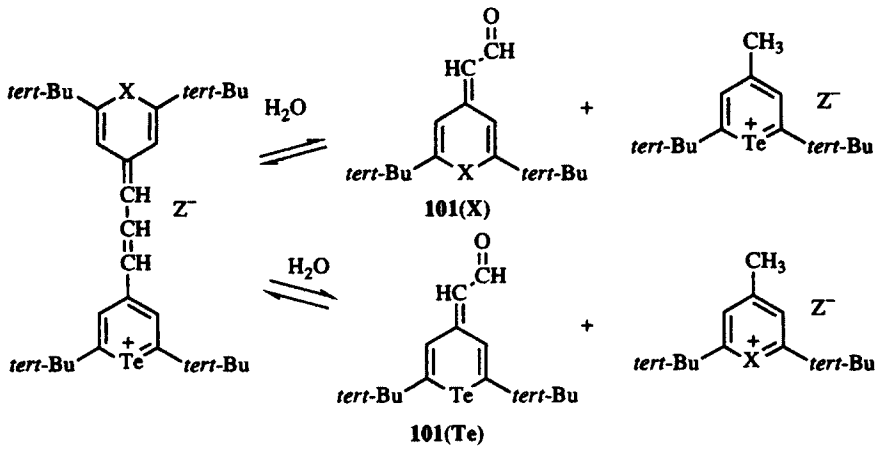

Scheme 16

The counterion involved in the preparation of dyes **77(X,Y)** appears to play a significant role in the amount of scrambling observed.[10] The condensation of 2,6-di-*tert*-butyl-4-methylselenopyrylium hexafluorophosphate with aldehyde **101(Te)** gives a 7/91/2 mixture of **77(Se,Se)/77(Te,Se)/77(Te,Te)**, all as the hexaflurophosphate salts. In contrast to this result, the condensation of 2,6-di-*tert*-butyl-4-methylselenopyrylium chloride with aldehyde **101(Te)** gives a statistical 1/2/1 mixture of **77(Se,Se)/77(Te,Se)/77(Te,Te)** as the chloride salts.[10] The condensation of **14d** with **101(S)** gave an 88/12 mixture of **77(Te,S)/77(S,S)**, both as the hexafluorophosphate salts.

The addition of bromine to the hexafluorophosphate mixtures described above gave either **95b** or **95c** in > 98% purity. The tellurium(IV) dibromides could be further purified and then reduced to give **77(Te,Se)** and **77(Te,S)** in > 99% purity.[10,79]

A ^{14}C-labeled dye was employed to confirm that heteroatom scrambling involved carbon–carbon bond cleavage in the trimethine linkage.[10] As shown in Scheme 17, the radiolabel is found only in the selenium-containing dyes, and the dye containing two selenium atoms has twice the relative activity of the dye containing one selenium atom.[10] These data eliminate a mechanism involving heteroatom scrambling via ring opening of the chalcogenopyrylium rings.

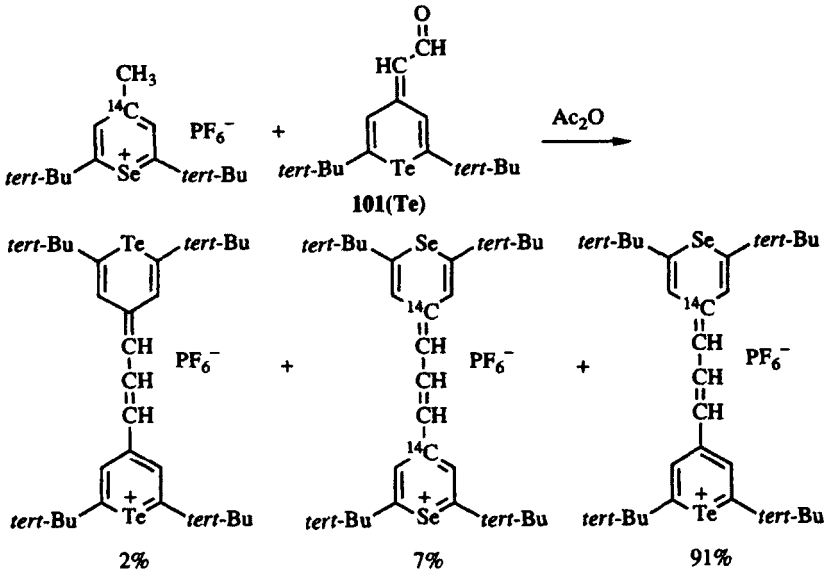

Scheme 17

2. *Other Nucleophiles*

The telluroxanthylium perchlorates are susceptible to nucleophilic attack at the 9-position.[80,81] As shown in Scheme 18, ammonium bromide, ammonium thiocyanate, and ammonium acetate give the corresponding telluroxanthenes **102** in 32–77% yields.[80] Ammonium chloride gives the telluroxanthene dimers **103**, while sodium methoxide and sodium isopropoxide give mixtures of nucleophilic addition and dimer formation.[81]

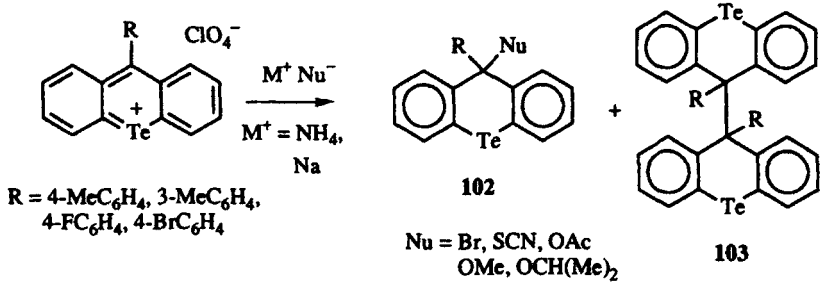

Scheme 18

VI. SPECTRAL PROPERTIES AND REACTIONS OF TELLURIUM(IV) ANALOGS OF TELLUROPYRYLIUM COMPOUNDS

A. Changes in Spectral and Redox Properties on Oxidation

The oxidative addition of singlet oxygen and water, hydrogen peroxide, or halogens across a tellurium atom in a telluropyrylium compound removes a tellurium–atom *p* orbital from conjugation with the carbon π framework via formation of a trigonal bipyramid with the halo ligands in the axial positions (Scheme 19).[27] As is discussed earlier in this chapter, the X-ray structure of compound **59** shows alternating single and double bonds in the carbon π framework and is consistent with loss of delocalization through the tellurium(IV) center. While many of the telluropyrylium dyes absorb in the near infrared, the tellurium(IV) species may absorb at wavelengths more than 200 nm shorter. Spectral properties for the tellurium(IV) analogs of telluropyrylium species are compiled in Table 20.

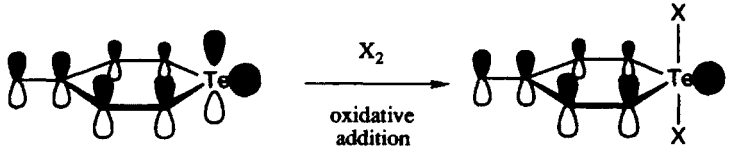

Scheme 19

The tellurium(IV) species are easier to reduce than the corresponding telluropyrylium dyes, allowing selective reduction of the tellurium(IV) center while leaving the telluropyrylium nucleus intact as shown in Scheme 20. Chemical reductions with sodium bisulfite[10,79] or sodium ascorbate[79] have reduced the

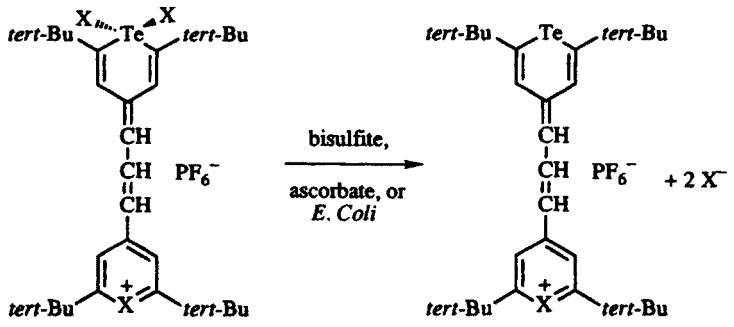

Scheme 20

tellurium(IV) dyes to the corresponding telluropyrylium dyes. The huge spectral shifts on reduction have been used as detection systems for reducing microorganisms such as *Escherichia coli*. The tellurium(IV) compounds **90** are reduced to the telluropyrylium dyes **77(Te,Y)** in the presence of *E. coli*.[82]

Electrochemically, the tellurium(IV) compounds undergo facile, irreversible two-electron reductions (as determined by bulk electrolysis)[71,75] to give the telluropyrylium dyes as compiled in Table 20. The two-electron reduction E_1 is several hundred millivolts more positive than the reversible one-electron reduction of the telluropyrylium nucleus E_1, which is formed as consequence of the initial two-electron reduction (Table 20).

B. Changes in Physical Properties on Oxidation

1. *Acid–Base Behavior and Intramolecular Reactions*

The dihydroxy tellurium(IV) compounds **90** are dibasic, and the initial acid is quite strong as shown in Scheme 21.[71] Spectrophotometric pK_a measurements for these dyes have give values of -2.1 and -1.9 for **90a** and **90b**, respectively, for the first proton. Titration has given values of 7.7 and 7.8 for pK_a^2 of **90a** and **90b**, respectively.

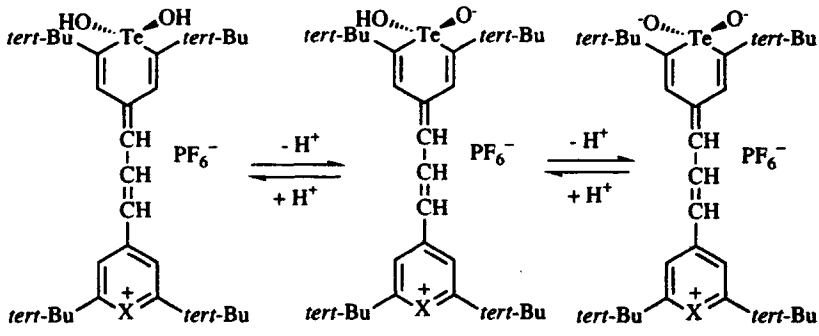

X=Te, $pK_a^1 = -2.1$, $pK_a^2 = 7.7$
X=Se, $pK_a^1 = -1.9$, $pK_a^2 = 7.8$

Scheme 21

The zwitterionic and/or dibasic forms of these compounds undergo a structural rearrangement on heating to give tellurophenes **104** in 25–59% isolated yield.[71] This rearrangement requires the reduction of a tellurium(IV) center to a tellurium(II) center, contraction of a six-membered ring to a five-membered ring, and oxidation of a carbon center. As shown in Scheme 22, intermediate **105** would lead to the ring-contraction step and oxidation of carbon. Intermediate

105 might arise from two different routes. Reductive elimination of hydrogen peroxide from the tellurium(IV) center followed by addition of hydroxyperoxy anion to the 2-position of the reduced dye is one approach to intermediate **105**. Alternatively, intermediate **105** could form via intramolecular oxidation of the carbon center adjacent to tellurium. Ring contraction and ketone formation might be a concerted process from the telluroxirane, or hydroxide addition might lead to intermediate **105**.

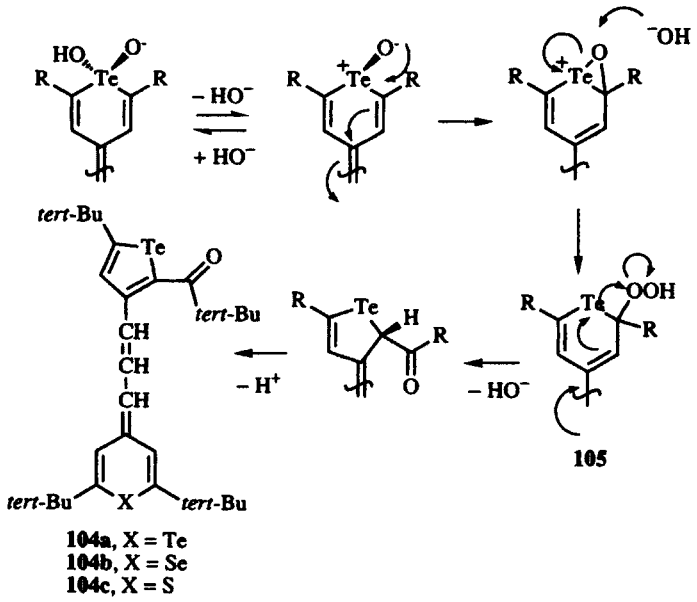

Scheme 22

2. *Ligand Exchange Reactions from Tellurium(IV) Compounds to Telluropyrylium Dyes*

The first reported examples of exchange of ligands from a tellurium(IV) center to a tellurium(I) center were halogen exchange reactions between diphenyltellurium dihalides and diphenyltelluride as shown in Scheme 23.[83,84] Similar examples have been observed for the exchange of hydroxide ligands between **90b** and **77(Te,Se)**[71] and for the self-exchange of ligands between the two tellurium centers of **95a**.[27]

The exchange reactions involving diphenyltellurium dichloride, dibromide, and diiodide are second-order reactions, first-order with respect to both dihalide and diphenyltelluride. A change in mechanism is observed for the halogen exchange between diphenyltellurium difluoride and diphenyltelluride in which the exchange process is first-order with respect to difluoride.[83]

$$Ph_2TeX_2 + Ph_2Te^* \rightleftharpoons Ph_2Te + Ph_2Te^*X_2$$

X = F, Cl, Br, I

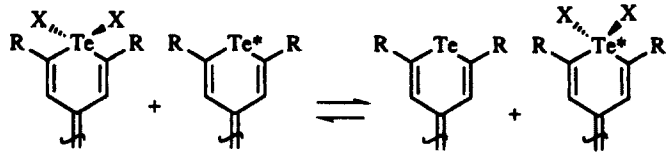

X = OH, Br

Scheme 23

The self-exchange process for the bromide ligands in **95a** follows first-order kinetics in acetonitrile and second-order kinetics in tetrechloroethane.[27] In chloroform, the kinetics of exchange are not clearly first-order or second-order. In acetonitrile, the relevant activation parameters are calculated to be E_a = 5.62 kcal mol^{-1}, $\Delta H^{\ddagger}$ = 5.06 kcal mol^{-1}, $\Delta S^{\ddagger}$ = − 26 cal K^{-1} mol^{-1}, and $\Delta G^{\ddagger}_{298}$ = 12.8 kcal mol^{-1}.[27] In tetrachloroethane, the relevant activation parameters are calculated to be E_a = 12.5 kcal mol^{-1}, $\Delta H^{\ddagger}$ = 11.8 kcal mol^{-1}, $\Delta S^{\ddagger}$ = − 22 cal K^{-1} mol^{-1}, and $\Delta G^{\ddagger}_{298}$ = 18.3 kcal mol^{-1}.[27] In chloroform, $\Delta G^{\ddagger}_{316}$ was estimated to be 14.9 kcal mol^{-1}.[27]

The first-order behavior observed in polar acetonitrile argues for a rate-determining heterolytic dissociation of one Te—Br bond which then generates bromine following loss of the second bromide ligand.[27] This argument is similar to the one put forth for the first-order exchange of fluoride ligands in diphenyltellurium difluoride.[83] In less polar solvents, the rate of dissociation of the Te—Br bond to give charged intermediates should be lowered allowing a competing second-order process to be observed.

C. Thermal Reductive Elimination Reactions of Tellurium(IV) Analogs of Telluropyrylium Dyes

Reactions similar to the exchange of ligands between tellurium(IV) and tellurium(II) species are the thermal reductive elimination of hydrogen peroxide from tellurium(IV) dyes **90**[15,71] and the thermal reductive elimination of chlorine from tellurium(IV) dyes **96** and **98**.[76] Both of these reactions follow first-order behavior with respect to the tellurium(IV) compound. The first-order rate constants for these reactions are compiled in Table 21 as well as the calculated values of E_a, $\Delta H^{\ddagger}$, $\Delta S^{\ddagger}$, and ln A. As can be seen in Table 21, values of E_a, $\Delta H^{\ddagger}$, $\Delta S^{\ddagger}$, and ln A are quite similar in these systems independent of the leaving group and solvent.

Although few mechanistic studies of oxidative-addition and reductive-elimination reactions of organotellurium compounds have been described, analogous chemistry in oxidative additions of halogens to platinum(II) and reductive

eliminations from platinum(IV) has been described and is applicable to oxidative-addition and reductive-elimination reactions of organotellurium compounds.[85-93] Among the mechanistic possibilities explored in this chemistry have the potential for synchronous oxidative addition of halogen across platinum,[85-87] or the possibility of stepwise formation of an η^1 complex of halogen with platinum followed sequentially by oxidative addition and formation of the second platinum–halogen bond.[85,88-93]

Analogs of these two mechanistic possibilities are shown in Scheme 24 for oxidative-addition and reductive-elimination reactions of chlorine with organotellurium compounds. A unimolecular reductive elimination of chlorine would presumably involve simultaneous formation of the chlorine–chlorine bond and breaking of the tellurium–chlorine bonds (Scheme 24, path A). Little charge generation should be observed along the reaction coordinate of this path and entropy requirements should be large and negative. If path B (Scheme 24) were followed, heterolytic cleavage of one tellurium–chlorine bond would lead to a charged intermediate. Subsequent attack of chloride at the chloro ligand would lead to cleavage of the second tellurium–chlorine bond as well as reduce the tellurium center from tellurium(IV) to tellurium(II). Again, the formation of two species from one would lead to a more positive entropy of activation.

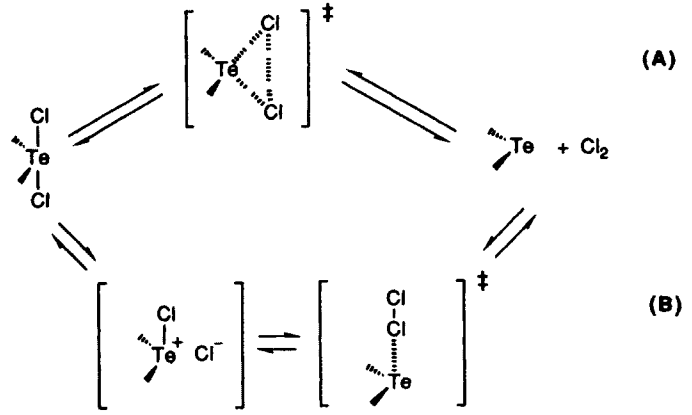

Scheme 24

The principal of microscopic reversibility suggests that the reverse of paths A and B should be valid for oxidative addition. Thus, path A represents a concerted oxidative addition of chlorine across tellurium with synchronous cleavage of the chlorine–chlorine bond, oxidation of tellurium(II) to tellurium(IV), and formation of the tellurium–chlorine bonds, while path B suggests the formation of an η^1 complex of chlorine and tellurium(II) followed

by stepwise formation of one tellurium–chlorine bond with oxidation and then formation of the second tellurium–chlorine bond.

If polar intermediates were involved in rate-determining steps, then one would expect changes in solvent polarity to have a large impact on the kinetics of reaction. Rate constants in acetonitrile for the reductive elimination were only slightly larger than those observed in tetrachloroethane, suggesting that the rate-determining step does not involve intermediates with large separation of charge.[76] However, more recent studies suggest ionic intermediates are involved in both oxidative addition and reductive elimination.[93a]

Chloride appears to function as a catalyst in the reductive-elimination reactions observed for **96** when one compares identical heterocycles with chloride and hexafluorophosphate counterions. From the apparent first-order rate constants at 348 K (Table 21), k_{cat} for chloride is calculated to be 7.60×10^{1} mol^{-1} s^{-1} for **96c** relative to **96a** and is calculated to be 2.26×10^{2} mol^{-1} s^{-1} for **96d** relative to **96b** when measured for at 5×10^{-6} *M* dye (identical chloride concentration for **96c** and **96d**) in tetrachloroethane.[76] Added chloride to solutions of both **96a** and **96b** accelerate the rate of reaction for both compounds. In the presence of added chloride (10^{-3} *M*), **96a** and **96b** display nearly identical rates of reaction. A threefold increase in the rate of catalysis in acetonitrile relative to tetrachloroethane is consistent with more polar intermediates or transition states in the catalyzed reaction versus the noncatalyzed reaction.[76]

One possible mechanistic path for chloride catalysis is illustrated in Scheme 25 as path C. This pathway resembles path A of Scheme 24 in that a synchronous—albeit via a second-order reaction—cleavage of both tellurium–chlorine bonds might be accompanied by reduction of tellurium(IV) to tellurium(II) and resembles path B in that either an η^1 complex of chlorine and tellurium(II) or a linear alignment of reacting atoms is involved in tellurium–chlorine bond cleavage. The negative charge added by the approach of chloride would be stabilized in acetonitrile relative to tetrachloroethane. This is reflected in a threefold increase in rate of catalysis in acetonitrile. Conversely, a chloride-catalyzed oxidative addition would follow the reverse of Scheme 25.[76]

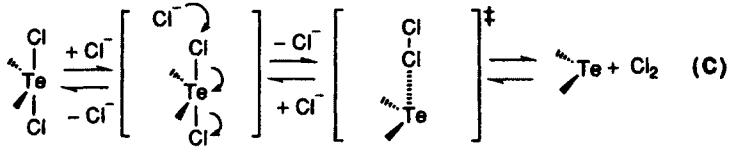

Scheme 25

Reductive-elimination reactions of **90** accelerate at either low or high pH.[71] The increased rate at high pH may be a consequence of hydroxide acting as a catalyst similar to the role of chloride in Scheme 25. At low pH, protonation and dehydration of the tellurium(IV) intermediate might lead to reductive elimination via a different route as shown in Scheme 26.

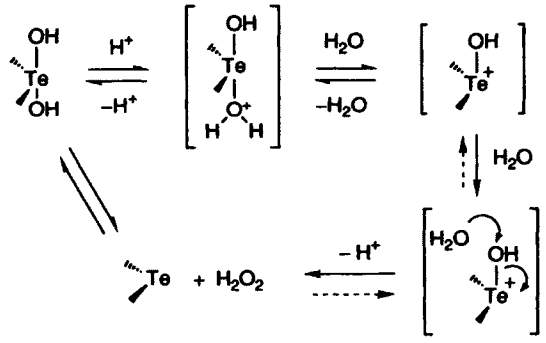

Scheme 26

The reductive-elimination reactions are thought to be driven by the regeneration of the aromaticity of the telluropyrylium ring on reduction of the tellurium(IV) center. The equilibrium between tellurium(II) and oxidant on one side and tellurium(IV) on the other is driven toward tellurium(IV) at higher concentrations, giving kinetic stability to the isolated tellurium(IV) salts. The regeneration of aromaticity in the reduction of **98** to **97** regenerates a benzene ring as opposed to a telluropyrylium ring. This is reflected in values of $\Delta H^{\ddagger}$ that are 5–7 kcal mol^{-1} lower for **98** relative to telluropyrylium dyes **96**.[76]

The reductive elimination of halogens from tellurium(IV) dihalides has been observed only in cationic systems derived from telluropyrylium dyes. The neutral tellurin-4-one dihalide derivatives **106** and **107** have been prepared.[77] However, heating tetrachloroethane solutions of these materials at 400 K gives no detectable reductive elimination after 4 h.[76] While other thermal reductive elimination reactions of halogens from tellurium(IV) compounds may one day be described, these reactions in tellurium(IV) analogs of telluropyrylium dyes offer interesting systems for study.

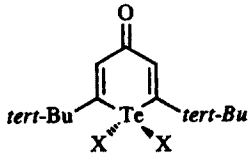

106, X = Br
107, X = Cl

VII. CATALYTIC REACTIONS EMPLOYING A TELLURIUM(II)–TELLURIUM(IV) SHUTTLE OF ELECTRONS

The use of a tellurium(IV)–tellurium(II) shuttle in organic redox reactions is becoming more common in organic and organometallic chemistry. Arene

tellurinic anhydrides have been employed as mild oxidants for a variety of organic substrates, including thiols, phosphines, and hydroquinones.[94-96] Both telluroxides[97-101,101a] and dihalotellurium(IV) derivatives[102,103] have been employed as two-electron oxidants in similar reactions. A catalytic scheme using 1,2-dibromotetrachloroethane as a brominating agent of tellurium(II) has been devised in which telluroxides produced *in situ* are the working oxidants.[104] Tribromotellurium(IV) species (with an odd number of ligands to tellurium) have functioned as mild oxidants for thiols and selenols.[103,105]

Of interest to this chapter are catalytic reactions of telluropyrylium dyes in which dihydroxytellurium(IV) intermediates are the working oxidants.[15,16] These intermediates have been produced by oxidation either with singlet oxygen and water or with hydrogen peroxide. With either mode of oxidation, a tellurium(II)–tellurium(IV)–tellurium(II) cycle avoids the use of a sacrificial electron donor in these reactions. The catalytic behavior described in these references has not been observed with either seleno- or thiopyrylium dyes.

A. Oxidation of Leucodyes with Dihydroxytellurium(IV) Analogs of Telluropyrylium Dyes

The oxidation of leucodyes **108** to dyes **109** with hydrogen peroxide as shown in Scheme 27 is a slow process in the absence of a catalyst with second-order rate constants of $< 10^{-6}\ M^{-1}s^{-1}$ for **108a** and $1.57 \times 10^{-5}\ M^{-1}s^{-1}$ for **108b**.[16] Dihydroxytellurium(IV) analogs of telluropyrylium dyes are kinetically much faster as oxidants for these substrates. The second-order rate constants for oxidation of either **108a** or **108b** with **90a** are $> 10^{3}\ M^{-1}s^{-1}$.[16]

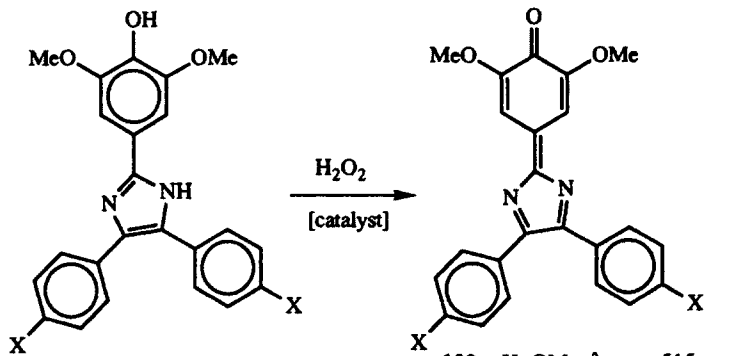

108a, X=OMe
108b, X=NMe_2

109a, X=OMe, λ_{max} = 515 nm
109b, X=NMe_2, λ_{max} = 660 nm

Scheme 27

Telluropyrylium compounds function as effective catalysts for the oxidation of leucodyes **108** to dyes **109** with hydrogen peroxide in aqueous solution

(pH 6.8).[15,16] Values of the pseudo-first-order rate constants k_{app} for oxidation of leucodyes **108** (10^{-4} *M*) with hydrogen peroxide (10^{-2} *M*) for a variety of telluropyrylium nuclei are compiled in Table 22. Rate constants for catalysis k_{cat} are also included in Table 22. The k_{cat} values are derived from

$$\frac{-\,d[\mathbf{108}]}{dt} = \{k_{cat}[cat]\}[\mathbf{108}][H_2O_2] + k_{H_2O_2}[\mathbf{108}][H_2O_2] \qquad (12)$$

where the product of k_{cat} and catalyst concentration $k\{k_{cat}[cat]\}$ constitutes the effective second-order rate constant for the oxidation. Where catalysis is significant, the $kH_2O_2[\mathbf{108}][H_2O_2]$ term is small and can be omitted such that

$$k_{cat} = \frac{k_{app}}{[cat][H_2O_2]} \qquad (13)$$

As shown in Table 22, a variety of telluropyrylium nuclei catalyze the oxidation of leucodyes **108**.[16] The most efficient are telluropyrylium dye structures that contain a second heteroatom for charge delocalization. Dyes **77(Te,Te)**, **77(Te,Se)**, and **77(Te,S)** are the most efficient with values of k_{cat} of approximately $10^4\ M^{-2}s^{-1}$. Monomethine dyes **74(Te,Te)** and **75(Te,Te)** and dimethylaniline-containing dye **14f** are an order of magnitude less efficient ($k_{cat} \approx 10^3\ M^{-2}s^{-1}$) while benzo[*b*]telluropyrylium dyes **110** and **111** are another order of magnitude less efficient still ($k_{cat} \approx 10^2\ M^{-2}s^{-1}$). The simple telluropyrylium salts **5c** and **14b** show little catalytic activity, and the $k_{H_2O_2}[\mathbf{108}][H_2O_2]$ term is significant and cannot be ignored.

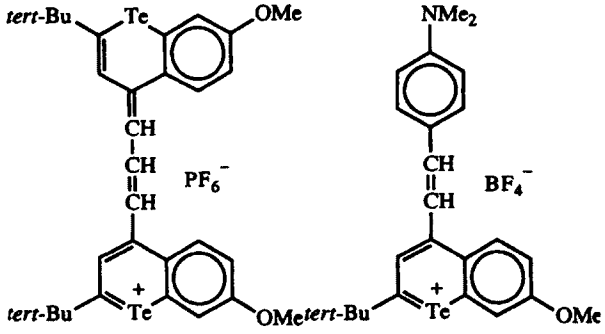

110 **111**

Turnover numbers are high with telluropyrylium catalysts in these reactions.[16] Turnover numbers of > 330 have been observed, suggesting that competing reactions of hydrogen peroxide with the carbon π framework are slow as are other reactions of the tellurium(IV) intermediates relative to the catalytic cycle.

Thiopyrylium and selenopyrylium dyes do not function as catalysts in these reactions.[16] The "catalyzed" oxidations of **108** with **77(Se,S)** and **77(Se,Se)** gave

rates of reaction essentially identical to the "uncatalyzed" rate of oxidation. The telluropyrylium nucleus appears to be unique among the chalcogenopyrylium nuclei in its ability to promote catalytic tellurium(II)–tellurium(IV)–tellurium(II) two-electron shuttles.

The neutral tellurium(II) compounds telluropyranone **112**, (phenyltelluro)cinnamic acid **113**, and diaryltelluride **114** show less catalytic activity (Table 22).

Simple telluropyrylium salts (**5c** and **14b**) and the neutral organotellurium compounds behave poorly as catalysts and suggest that the second heteroatom in the telluropyrylium dyes is necessary to stabilize the positive charge. Furthermore, regeneration of aromaticity appears to be the thermodynamic and kinetic driving force to return the tellurium(IV) state to the tellurium(II) state.

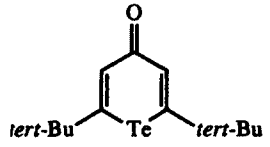

112

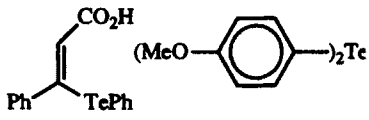

113 **114**

B. Oxidation of Thiols with Dihydroxytellurium(IV) Analogs of Telluropyrylium Dyes

The oxidation of thiophenol to phenyl disulfide with hydrogen peroxide in 75% methanol is a relatively slow process at 296 K with a half-life of approximately one day.[16] The addition of 0.1 mol% of **77(Te,Te)** or 0.3 mol% of **14f** gives complete oxidation (> 5 half-lives) within 5 min. On a preparative scale, the addition of 0.15 mol% of these two catalysts to 0.1 *M* solutions of thiophenol, *p*-methoxybenzenethiol, and *p*-fluorobenzenethiol gave the corresponding disulfides in > 96.9% isolated yield with turnover numbers of > 600, based on thiol.

The addition of 1.0 mol% of simple telluropyrylium salts **5c** and **14d**, telluropyranone **112**, and dyes **77(Se,Se)** and **77(Se,Se)** to solutions of thiol and hydrogen peroxide gives rates of oxidation identical to those of the uncatalyzed reaction.[16] Thus, structural requirements for catalysts appear to be identical in the leucodye and thiol reactions. Compound **114** shows some catalytic activity although less than for **77(Te,Te)**.[101a]

C. Catalytic Oxidations with Dihydroxytellurium(IV) Analogs of Telluropyrylium Dyes Generated Photochemically

The singlet oxygen produced by irradiation of telluropyrylium dyes in the presence of oxygen and water is scavenged by the tellurium atom of the dyes to

produce dihydroxytellurium(IV) analogs of the telluropyrylium dyes. The stoichiometry of this reaction is shown in Scheme 28.[15,16] For each molecule of singlet oxygen that is consumed, two tellurium dye molecules are oxidized with the consumption of two molecules of water. Thermally, the dihydroxytellurium(IV) species can produce hydrogen peroxide and the hydrolysis of either the telluropyrylium dye or the tellurium(IV) compound can remove the dye from the system. An efficient use of the dihydroxytellurium(IV) compounds produced in this reaction would be to use them as oxidants as they are formed. As shown above for oxidation of leucodyes **108**, the reaction of dihydroxytellurium(IV) compounds with leucodyes **108** is much faster than the first-order reductive elimination of hydrogen peroxide from these compounds (Table 21).

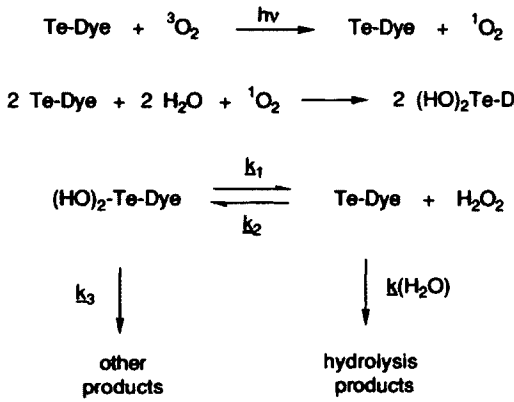

Scheme 28

At 10^{-4} *M* leucodye **108** and 1 mol% of **77(Te,Te)**, **77(Te,Se)**, or **77(Te,S)** in water, 150–300 s of irradiation with 630–850-nm light gives essentially complete conversion to dyes **109** with turnover numbers of ≥ 75. Similar behavior is observed in 99% methanol but turnover numbers are somewhat smaller at ≥ 50.[16]

D. Catalytic Generation of Hydrogen Peroxide from Irradiation of Telluropyrylium Dyes in Air-Saturated Solutions

The photochemical generation of dihydroxytellurium(IV) derivatives of telluropyrylium dyes and the use of these compounds as oxidants could drive a variety of light-to-chemical energy conversions. This technology is important for solar-energy storage. While the major emphasis in research dedicated to solar-energy storage has been splitting of water for the production of hydrogen, the photoproduction of other energy-rich compounds such as hydrogen peroxide has also received attention.[106–113]

As shown in Scheme 28, the use of telluropyrylium dyes to generate hydrogen peroxide requires no sacrificial electron donor. In metal-based and in other dye-based chemistries, the sacrificial electron donor is necessary to minimize electron back-transfer from the electron relay.[106-113]

In Scheme 28, the photochemical process determines the maximum efficiency of the system while the thermal reactions determine the effective rate of hydrogen peroxide production. The quantum yields for hydrogen peroxide production, $\Phi(H_2O_2)$, in 99% methanol are given in Table 23 as well as the turnover number for telluropyrylium dyes **77(Te,Te)**, **77(Te,Se)**, **77(Te,S)**, **74(Te,Te)**, and **75(Te,Te)**.[16] The quantum yields vary between 3.1×10^{-5} and 9.5×10^{-5} for these compounds, while the turnover numbers vary between 1.5 and 11.1, all in 99% methanol.[16] The effective quantum yield for **77(Te,Te)** increases in 50% methanol and in water since the rate of scavenging of singlet oxygen is higher in these solvents. Thus, $\Phi(H_2O_2)$ increases to 1.2×10^{-3} in 50% methanol and 5.5×10^{-3} in water. The turnover number also increases in these solvents to 33.4 in 50% methanol and 89.0 in water.

TABLES

TABLE 1. PREPARATION OF TELLUROPYRYLIUM SALTS **4** AND **5** FROM TELLURIN-4-ONES VIA DIISOBUTYLALUMINUM HYDRIDE REDUCTION

Compd.	R	Z	% Yield[a]	Ref.
4a	Ph	PF_6	47	18
4b	*tert*-Bu	PF_6	53	18
5a	Ph	PF_6	51	18
5b	Ph	ClO_4	50	17
5c	*tert*-Bu	PF_6	53	18

[a] Isolated yield from telluropyranone.

TABLE 2. FORMATION OF TELLUROPYRYLIUM BORONATE COMPLEXES **12a–f** AND RELATED COMPOUNDS **12g**, **12h**, AND **13** FROM TELLURIN-4-ONES AND BORONTRIFLUORIDE ETHERATE

Compd.	R	X	% Yield[a]	λ_{max} (log ε) (nm)[b]	Ref.
12a	Me	OMe	91	480 (3.93)	23
12b	Ph	H	73	505 (3.85)	23
12c	Ph	OMe	72	488 (3.84)	23
12d	4-Methoxyphenyl	OMe	66	492 (3.96)	23
12e	3,4-Dimethoxyphenyl	OMe	96	490 (3.95)	23
12f	2,5-Dimethoxyphenyl	OMe	83	491 (4.03)	23
12g	Ph	H	48	515 (3.86)	4
12h	2,5-Dimethoxyphenyl	OMe	—	—	4
13	Ph	H	95	518 (3.96)	23

[a] Isolated yield from telluropyranone.
[b] In dichloromethane.

TABLE 3. ADDITION OF GRIGNARD REAGENTS (R'MgBr) TO TELLURIN-4-ONES FOLLOWED BY ACID HZ TO GIVE TELLUROPYRYLIUM COMPOUNDS **14–16**

Compd.	R	R'	Z	% Yield[a]	Ref.
14a	Ph	Me	PF_6	61	24
14b	Ph	Et	PF_6	18	24
14c	Ph	4-$(Me_2N)C_6H_4$	ClO_4	81	22
14d	*tert*-Bu	Me	PF_6	61	24
14e	*tert*-Bu	Et	PF_6	82	25
14f	*tert*-Bu	4-$(Me_2N)C_6H_4$	ClO_4	72	27
14g	H	4-$(Me_2N)C_6H_4$	PF_6	68	26
14h	4-$MeOC_6H_4$	4-$(Me_2N)C_6H_4$	PF_6	25	28
15a	Ph	4-$(Me_2N)C_6H_4$	ClO_4	44	17
15b	Me	Ph	ClO_4	72	17
16a	—	4-MeC_6H_4	ClO_4	44	19
16b	—	Me	ClO_4	—	19
16c	—	3-MeC_6H_4	ClO_4	—	29
16d	—	4-MeC_6H_4	ClO_4	—	29
16e	—	4-FC_6H_4	ClO_4	—	29
16f	—	4-BrC_6H_4	ClO_4	—	29
16g	—	α-naphthyl	ClO_4	—	29
16h	—	$PhCH_2$	ClO_4	—	29

[a] Isolated yield from telluropyranone.
[b] Unsymmetrical compound with Ph as second R group.

TABLE 4. TELLUROPYRYLIUM MONOMETHINE DYES **18**, **19**, AND **21–23** FROM CONDENSATION REACTIONS OF CHALCOGENOPYRYLIUM SALTS WITH CHALCOGENOPYRANONES

Compd.	X	Y	Z	R	R′	% Yield[a]	λ_{max} (log ε) (nm)[b]	Ref.
18a	Te	Te	BF_4	Ph	H	91	759 (5.20)	22
18b	Te	Se	ClO_4	Ph	H	62	722 (5.00)	22
18c	Te	S	ClO_4	Ph	H	77	690 (5.11)	22
18d	Te	O	BF_4	Ph	H	37	650 (5.14)	22
19a	Te	Te	BF_4	*tert*-Bu	H	71	715 (5.11)	24
19b	Te	Se	BF_4	*tert*-Bu	H	39	674 (4.98)	24
19c	Te	S	BF_4	*tert*-Bu	H	43	651 (5.01)	24
19d	Te	O	BF_4	*tert*-Bu	H	27	594 (5.00)	24
21a	Te	—	CF_3SO_3	MeO	—	54	810 (4.79)	3
21e	Se	—	ClO_4	—	—	40	743 (4.84)	3
21f	S	—	ClO_4	—	—	38	720 (4.85)	3
21g	O	—	BF_4	—	—	14	678 (4.83)	3
22a	Te	Te	PF_6	Ph	Me	55	834 (4.85)	24
22b	Te	Se	PF_6	Ph	Me	33	795 (4.85)	24
22c	Te	S	PF_6	Ph	Me	74	762 (4.74)	24
22d	Te	O	PF_6	Ph	Me	47	720 (4.75)	24
23	Te	Te	PF_6	*tert*-Bu	Me	25	772 (4.85)	25

[a] Isolated Yield.
[b] In dichloromethane.

TABLE 5. TELLUROPYRYLIUM POLYMETHINE DYES **24–28**, **31**, AND **32** FROM CONDENSATION REACTIONS

Compd.	X	Y	Z	R	R′	*n*	% Yield[a]	λ_{max} (log ε) (nm)[b]	Ref.
24a	Te	Te	BF_4	Ph	H	1	61	885 (5.45)	22
24b	Te	Se	ClO_4	Ph	H	1	74	843 (5.26)	22
24c	Te	S	ClO_4	Ph	H	1	25	820 (5.30)	22
24d	Te	O	BF_4	Ph	H	1	30	780 (5.35)	22
25a	Te	Te	PF_6	*tert*-Bu	H	1	88	828 (5.52)	25
25b	Te	Se	PF_6	*tert*-Bu	H	1	82	786 (5.45)	25
25c	Te	S	PF_6	*tert*-Bu	H	1	81	760 (5.44)	25
25d	Te	O	PF_6	*tert*-Bu	H	1	44	715 (5.40)	25
26a	Te	Te	BF_4	Ph	H	2	17	1010 (5.18)	22
28a	Te	Te	BF_4	—	—	1	41	898 (5.18)	3
28b	Te	Te	BF_4	—	—	2	49	1007 (5.18)	3
28d	Te	Te	CF_3SO_3	—	—	3	—	1120 (—)	3
31a	Te	Te	BF_4	*tert*-Bu	Me	1	34	843 (5.42)	24
31b	Se	Te	PF_6	*tert*-Bu	Me	1	50	801 (5.44)	25
31c	Te	Se	ClO_4	*tert*-Bu	Me	1	41	803 (5.44)	24
32	Te	Te	BF_4	*tert*-Bu	CN	1	71	792 (5.41)	6

[a] Isolated Yield.
[b] In dichloromethane.

TABLE 6. DIALKYLAMINO-SUBSTITUTED TELLUROPYRYLIUM DYES **14c**, **14f**, **15a**, AND **33–41a**

Compd.	% Yield[a]	Z	λ_{max} (log ε) (nm)[b]	Ref.
33a	95	BF_4	525 (4.85)	22
33b	91	PF_6	508 (4.94)	27
34	79	CF_3SO_3	535 (4.61)	3
14c	—[c]	BF_4	653 (4.83)	22
14f	—[c]	ClO_4	611 (4.82)	27
15a	—[c]	ClO_4	678 (4.48)	17
35	72	BF_4	790 (4.97)	22
36	22	BF_4	870 (5.19)	22
37a	36	CF_3SO_3	770 (5.00)	3
37b	49	CF_3SO_3	865 (5.18)	3
39	90		795 (5.08)	22
40	86		818 (5.02)	22
41a	79	PF_6	775 (5.16)	24

[a] Isolated Yield.
[b] In dichloromethane.
[c] See Table 3.

TABLE 7. TELLUROPYRYLIUM DYES **42–44** AND **47–50** FROM CONDENSATION OF 2-METHYLTELLUROPYRYLIUM SALTS

Compd.	% Yield[a]	λ_{max} (log ε) (nm)[b]	Ref.
42	20	715 (4.93)	23
43	53	822 (4.57)	23
		744 (4.80)	23
44	46	588 (4.81)	23
45	25	742 (4.33)	23
47	59	695 (4.98)	23
48	17	780 (4.95)	23
49	67	753 (4.97)	23
50	16	720 (4.60)	23

[a] Isolated Yield.
[b] In dichloromethane.

TABLE 8. SELECTED BOND DISTANCES AND ANGLES IN **18d**[a]

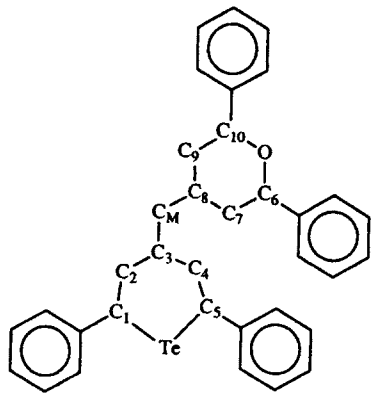

Atom 1	Atom 2	Distance (Å)[b]	Atom 1	Atom 2	Atom 3	Angle (°)[c]
Te	C1	2.067(5)	C1	Te	C5	94.3(2)
Te	C5	2.069(5)	Te	C1	C2	122.0(3)
C1	C2	1.358(6)	Te	C5	C4	121.6(3)
C2	C3	1.441(6)	C1	C2	C3	129.3(4)
C3	C4	1.434(6)	C2	C3	C4	122.3(4)
C4	C5	1.370(6)	C3	C4	C5	129.4(4)
O	C6	1.378(5)	C6	O	C10	119.7(4)
O	C10	1.359(5)	O	C6	C7	120.1(4)
C6	C7	1.340(6)	O	C10	C9	121.0(4)
C7	C8	1.416(6)	C6	C7	C8	122.8(4)
C8	C9	1.428(6)	C7	C8	C9	114.3(4)
C9	C10	1.348(6)	C8	C9	C10	121.6(4)

[a] Reference 24.
[b] Numbers in parentheses are estimated standard deviations in the least significant digits.
[c] Numbers in parentheses are estimated standard deviations in the least significant digits.

TABLE 9. SELECTED BOND DISTANCES AND ANGLES IN **59**[a]

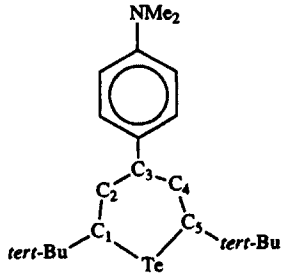

Atom 1	Atom 2	Distance (Å)[b]	Atom 1	Atom 2	Atom 3	Angle (°)[c]
Te	C1	2.12(1)	C1	Te	C5	95.6(4)
Te	C5	2.11(1)	Te	C1	C2	120.4(9)
C1	C2	1.33(2)	Te	C5	C4	120.1(9)
C2	C3	1.47(2)	C1	C2	C3	130.(1)
C3	C4	1.45(2)	C2	C3	C4	124.(1)
C4	C5	1.35(2)	C3	C4	C5	130.(1)
Te	Br1	2.681(2)	Br1	Te	Br2	173.2(2)
Te	Br2	2.684(2)				

[a] Reference 27.
[b] Numbers in parentheses are estimated standard deviations in the least significant digits.
[c] Numbers in parentheses are estimated standard deviations in the least significant digits.

TABLE 10. ^{1}H NMR CHEMICAL SHIFTS FOR RING PROTONS OF CHALCOGENOPYRYLIUM NUCLEI

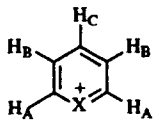

I

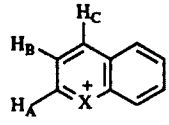

II

Parent Nucleus	Compd.	X	H_A (δ, ppm)	H_B (δ, ppp)	H_C (δ, ppm)	Ref.
I	**4a**	Te	—	8.50	8.97	18
I	**4b**	Te	—	8.47	9.03	18
I	**14g**	Te	10.60	8.80	—	28
I	**63a**	Se	—	8.55	8.93	18
I	**63b**	S	—	8.69	8.94	18
I	**63c**	O	—	8.10	9.09	18
I	**64**	Se	9.48	8.61	—	28
I	**14f**	Te	—	8.40	—	22
I	**19a**	Te	—	7.70	—	24
I	**25a**	Te	—	7.71	—	25
I	**66a**	Se	—	8.35	—	24
I	**66b**	S	—	8.37	—	24
I	**66c**	O	—	7.57	—	24
I	**67a**	Se	—	7.75	—	25
I	**67b**	S	—	7.70	—	25
I	**67c**	O	—	7.40	—	25
II	**5a**	Te	—	8.47	9.12	18
II	**5c**	Te	—	8.57	9.03	18

TABLE 11. ^{125}Te NMR CHEMICAL SHIFTS AND XPS Te($3d_{5/2}$) BINDING ENERGIES FOR TELLUROPYRYLIUM NUCLEI **4b**, **5a**, **5c**, **14c**, **14d**, **14f**, **14h**, AND **58** AND MODEL TELLURINS **60–62**

Compd.	Chem Shift ^{125}Te (δ, ppm)	Binding Energy Te($3d_{5/2}$) ($\pm$ 0.1 eV) (eV)	Ref.
4b	1304	575.2	28
5a	1086	—	28
5c	1124	574.5	28
14c	875	573.7	28
14d	1185	574.9	28
14f	934	574.1	28
14h	784	573.1	28
58	1150	574.6	28
60	553	574.3	28
61	445	574.1	28
62	519	—	28

TABLE 12. ABSORPTION MAXIMA, PHOTON ENERGIES, AND REDOX POTENTIALS (BY CYCLIC VOLTAMMETRY) FOR CHALCOGENOPYRYLIUM DYES **72(X)** AND **73(X)**

Compd.	R	Z	λ_{max} (log ε)[a] (nm)	$E_{\lambda_{max}}$ (eV)	E_{ox}[a] (V vs. SCE)	E_{red}[a] (V vs. SCE)	ΔE (V)	Ref.
72(Te)	Ph	BF_4	636 (4.76)	1.95	1.09	− 0.32	1.41	24
72(Se)	Ph	BF_4	603 (4.80)	2.06	1.16	− 0.41	1.57	24
72(S)	Ph	BF_4	583 (4.82)	2.13	1.19	− 0.50	1.69	24
72(O)	Ph	BF_4	542 (4.89)	2.29	1.26	− 0.59	1.85	24
73(Te)	*tert*-Bu	BF_4	591 (4.84)	2.10	1.06	− 0.54	1.60	24
73(Se)	*tert*-Bu	ClO_4	555 (4.81)	2.23	1.12	− 0.61	1.73	24
73(S)	*tert*-Bu	ClO_4	524 (4.80)	2.37	1.13	− 0.72	1.85	24
73(O)	*tert*-Bu	BF_4	487 (4.75)	2.54	1.22	− 0.81	2.03	24

[a] In acetonitrile.

TABLE 13. ABSORPTION MAXIMA, PHOTON ENERGIES, AND REDOX POTENTIALS (BY CYCLIC VOLTAMMETRY) FOR CHALCOGENOPYRYLIUM DYES 74(X,Y) AND 75(X,Y)

Compd. (X,Y)	R	Z	λ_{max} (log ε)[a] (nm)	$E_{\lambda_{max}}$ (eV)	E_{ox}[a] (V vs. SCE)	E_{red}[a] (V vs. SCE)	ΔE (V)	Ref.
74(Te,Te)	Ph	BF_4	759 (5.20)	1.64	1.19	− 0.08	1.12	24
74(Te,Se)	Ph	ClO_4	722 (5.00)	1.72	1.25	− 0.13	1.38	24
74(Te,S)	Ph	ClO_4	690 (5.11)	1.80	1.26	− 0.18	1.44	24
74(Te,O)	Ph	BF_4	650 (5.14)	1.91	1.31	− 0.24	1.55	24
74(Se,Se)	Ph	ClO_4	667 (5.15)	1.85	—	—	—	67
74(Se,S)	Ph	ClO_4	643 (5.11)	1.92	—	—	—	67
74(Se,O)	Ph	ClO_4	605 (5.13)	2.04	—	—	—	67
74(S,S)	Ph	ClO_4	622 (5.05)	1.99	—	—	—	67
74(S,O)	Ph	ClO_4	585 (4.90)	2.11	—	—	—	67
74(O,O)	Ph	ClO_4	545 (5.10)	2.27	—	—	—	67
75(Te,Te)	*tert*-Bu	BF_4	715 (5.11)	1.74	1.01	− 0.40	1.41	24
75(Te,Se)	*tert*-Bu	BF_4	674 (4.98)	1.84	1.05	− 0.45	1.50	24
75(Te,S)	*tert*-Bu	BF_4	651 (5.01)	1.91	1.04	− 0.52	1.56	24
75(Te,O)	*tert*-Bu	BF_4	594 (5.00)	2.09	1.08	− 0.59	1.67	24
75(Se,Se)	*tert*-Bu	ClO_4	623 (5.15)	1.99	1.16	− 0.51	1.67	24
75(Se,S)	*tert*-Bu	ClO_4	599 (5.01)	2.07	—	—	—	24
75(Se,O)	*tert*-Bu	ClO_4	549 (5.00)	2.26	—	—	—	24
75(S,S)	*tert*-Bu	ClO_4	577 (5.10)	2.15	—	—	—	24
75(S,O)	*tert*-Bu	ClO_4	526 (5.10)	2.36	—	—	—	24
75(O,O)	*tert*-Bu	ClO_4	480 (5.10)	2.59	—	—	—	24

[a] In dichloromethane.

TABLE 14. ABSORPTION MAXIMA, PHOTON ENERGIES, AND REDOX POTENTIALS (BY CYCLIC VOLTAMMETRY) FOR CHALCOGENOPYRYLIUM DYES **76(X,Y)**, **77(X,Y)**, AND **78(X,Y)**

Compd. (X,Y)	R	Z	*n*	λ_{max} (log ε)[a] (nm)	$E_{\lambda_{max}}$ (eV)	E_{ox}[a] (V vs. SCE)	E_{red}[a] (V vs. SCE)	ΔE (V)	Ref.
76(Te,Te)	Ph	BF_4	1	885 (5.45)	1.40	0.85	− 0.06	0.91	24
76(Te,Se)	Ph	ClO_4	1	843 (5.26)	1.47	0.87	− 0.09	0.96	24
76(Te,S)	Ph	ClO_4	1	820 (5.30)	1.51	—	—	—	24
76(Te,O)	Ph	BF_4	1	780 (5.35)	1.59	—	—	—	24
76(Se,Se)	Ph	ClO_4	1	795 (—)	1.56	—	—	—	59
76(Se,S)	Ph	ClO_4	1	782 (—)	1.58	—	—	—	22
76(Se,O)	Ph	ClO_4	1	743 (—)	1.66	—	—	—	22
76(S,S)	Ph	ClO_4	1	751 (—)	1.65	—	—	—	59
76(S,O)	Ph	ClO_4	1	725 (—)	1.71	—	—	—	22
76(O,O)	Ph	ClO_4	1	686 (—)	1.80	—	—	—	22
77(Te,Te)	*tert*-Bu	PF_6	1	810 (5.22)	1.53	0.86	− 0.32	1.18	25
77(Te,Se)	*tert*-Bu	PF_6	1	770 (5.10)	1.61	0.94	− 0.42	1.36	25
77(Te,S)	*tert*-Bu	PF_6	1	755 (5.02)	1.64	0.73	− 0.50	1.23	25
77(Te,O)	*tert*-Bu	PF_6	1	700 (5.27)	1.77	0.78	− 0.56	1.34	25
77(Se,Se)	*tert*-Bu	PF_6	1	730 (5.48)	1.69	0.75	− 0.50	1.25	25
77(Se,S)	*tert*-Bu	PF_6	1	708 (5.40)	1.75	0.82	− 0.54	1.36	25
77(Se,O)	*tert*-Bu	PF_6	1	665 (5.38)	1.86	0.71	− 0.61	1.32	25
77(S,S)	*tert*-Bu	PF_6	1	685 (5.42)	1.81	0.72	− 0.62	1.34	25
77(S,O)	*tert*-Bu	ClO_4	1	640 (5.32)	1.93	0.84	− 0.68	1.52	25
77(O,O)	*tert*-Bu	ClO_4	1	593 (5.31)	2.09	0.92	− 0.75	1.67	25
78(Te,Te)	Ph	BF_4	2	1010 (5.18)	1.22	—	—	—	22
78(Se,Se)	Ph	ClO_4	2	910 (—)	1.36	—	—	—	59
78(S,S)	Ph	ClO_4	2	879 (—)	1.41	—	—	—	59

[a] In dichloromethane.

TABLE 15. ABSORPTION MAXIMA, PHOTON ENERGIES, AND REDOX POTENTIALS (BY CYCLIC VOLTAMMETRY) FOR CHALCOGENOPYRYLIUM DYES **84(X,Y)** AND **85(Te,Te)**

Compd. (X,Y)	R	Z	λ_{max} (log ε)[a] (nm)	$E_{\lambda_{max}}$ (eV)	E_{ox}[a] (V vs. SCE)	E_{red}[a] (V vs. SCE)	ΔE (V)	Ref.
84(Te,Te)	Ph	PF_6	834 (4.85)	1.49	0.75	− 0.03	0.78	24
84(Te,Se)	Ph	PF_6	795 (4.85)	1.56	0.80	− 0.06	0.86	24
84(Te,S)	Ph	PF_6	762 (4.74)	1.63	0.84	− 0.11	0.95	24
84(Te,O)	Ph	PF_6	720 (4.75)	1.72	0.85	− 0.17	1.02	24
84(Se,Se)	Ph	PF_6	746 (4.93)	1.66	0.88	− 0.10	0.98	24
84(Se,S)	Ph	PF_6	721 (4.69)	1.72	—	—	—	24
84(Se,O)	Ph	PF_6	678 (4.82)	1.83	—	—	—	24
84(S,S)	Ph	PF_6	691 (4.72)	1.79	—	—	—	[b]
84(S,O)	Ph	PF_6	655 (4.89)	1.89	—	—	—	[b]
84(O,O)	Ph	PF_6	614 (4.93)	2.02	—	—	—	24
85(Te,Te)	*tert*-Bu	PF_6	772 (4.61)	1.61	0.75	− 0.40	1.15	24

[a] In dichloromethane.

[b] C. H. Chen, unpublished results.

TABLE 16. ABSORPTION MAXIMA, PHOTON ENERGIES, AND REDOX POTENTIALS (BY CYCLIC VOLTAMMETRY) FOR CHALCOGENOPYRYLIUM DYES **86(X,Y)(R,R')**

Compd. (X,Y)	R	R'	Z	λ_{max} (log ε)[a] (nm)	$E_{\lambda_{max}}$ (eV)	E_{ox}[a] (V vs. SCE)	E_{red}[a] (V vs. SCE)	ΔE (V)	Ref.
86(Te,Te)	H	Me	BF_4	843 (5.42)	1.93	0.82	− 0.35	1.17	67
86(Te,Se)	Me	H	BF_4	801 (5.46)	1.54	0.87	− 0.40	1.27	67
86(Te,Se)	H	Me	ClO_4	803 (5.44)	1.54	0.87	− 0.39	1.26	67
86(Se,Se)	Me	H	PF_6	760 (5.38)	1.64	0.69[b]	− 0.52[b]	1.21	25
86(Se,Se)	Me	Me	PF_6	782 (4.86)	1.59	0.65[b]	− 0.51[b]	1.16	25
86(Te,Te)	CN	H	BF_4	792 (5.41)	1.56	0.95	− 0.41	1.36	67

[a] In dichloromethane.
[b] In acetonitrile.

TABLE 17. ABSORPTION MAXIMA, PHOTON ENERGIES, AND REDOX POTENTIALS (BY CYCLIC VOLTAMMETRY) FOR CHALCOGENOPYRYLIUM DYES **89(X)**

Compd. (X,Y)	Z	λ_{max} (log ε)[a] (nm)	$E_{\lambda_{max}}$ (eV)	E_{ox}[a] (V vs. SCE)	E_{red}[a] (V vs. SCE)	ΔE (V)	Ref.
89(Te)	PF_6	758 (5.15)	1.64	0.67	− 0.475	1.145	24
89(Se)	PF_6	717 (5.12)	1.73	0.69	− 0.53	1.22	24
89(S)	PF_6	660 (5.10)	1.88	0.69	− 0.62	1.31	24
89(O)	PF_6	637 (5.11)	1.95	0.68	− 0.74	1.42	24

[a] In dichloromethane.

TABLE 18. PHOTOPHYSICAL PROPERTIES OF CHALCOGENOPYRYLIUM DYES[a,b]

Compd. (X,Y)	λ_{EX} (nm)	λ_{EM} (nm)	τ_{rad} (ns)	τ_S (ps)	Φ_F	τ_T (μs)	Φ_T	k_{isc} (s^{-1})
77(O,O)	(552), 593	604	4.8	230	0.048	≥ 10	0.0004[e]	2×10^6
77(S,S)	(647), 686	698	7.3	80	0.011	≥ 10	0.0006[e]	8×10^6
77(Se,Se)	(652), 725	740	8.1	20	0.0024	≥ 10	0.013[b,e]	7×10^8
77(Te,O)	(650), 696	713	10.1	50	0.0050	—	—	—
77(Te,S)	(653), 730	762	12.0	20	0.0014	—	—	—
77(Te,Se)	(655), 758	783	15.0	6	0.0004	0.8	0.11[b]	2×10^{10}
77(Te,Te)	(660), 802	818	13.2	5	0.0004	0.3	0.18[b]	4×10^{10}
74(Te,O)	645	686[c]	7.5	61	0.0080	—	—	—
74(Te,S)	706	722[c]	10.1	16	0.0016	—	—	—
74(Te,Se)	703	725[c]	15.8	25	0.0016	—	—	—
74(Te,Te)	749	778[c]	12.2	5	0.0004	—	0.09[d,e]	2×10^{10}
75(Te,Te)	705	720	20.2	12	0.0006	—	0.07[d,e]	6×10^9
85(Te,Te)	765	790	16.3	2	0.0001	—	0.006[d,e]	4×10^9
86(Se,Se) (Me,H)	(646), 730	752	11.1	3	0.0003	—	0.004[d,e] —	1×10^9
86(Se,Se) (Me,Me)	(668), 752	775	16.3	1	0.00006	—	0.001[d,e]	1×10^9

[a] Reference 25.
[b] In water. Values in parentheses represent excitation maximum of the H aggregate.
[c] $\Delta_E = 8$ kcal mol^{-1}.
[d] In acetonitrile.
[e] Assumes singlet oxygen yield is identical to triplet yield; value given is $\Phi(^1O_2)$.

TABLE 19. QUANTUM YIELDS FOR SINGLET OXYGEN GENERATION IN METHANOL AND ABSOLUTE AND RELATIVE RATES OF REACTION OF CHALCOGENOPYRYLIUM DYES 77(X,Y) WITH SINGLET OXYGEN IN 50% AQUEOUS METHANOL

Compd.	$\Phi(^1O_2)$, in MeOH[a]	$10^{-7}\,k(^1O_2)\,(M^{-1}\,s^{-1})$		k_{rel}
		Methylene Blue[b]	Rose Bengal[b]	
77(O,O)	0.0004		0.3 ± 0.1	1
77(S,O)	0.0006			
77(S,S)	0.0006		1.3 ± 0.1	4.2
77(Se,O)	0.004	0.3 ± 0.1	0.4 ± 0.1	1.3
77(Se,S)	0.007			
77(Se,Se)	0.014		0.5 ± 0.1	1.7
77(Te,O)	0.05	8.5 ± 0.9	9.4 ± 0.9	31
77(Te,S)	0.07			
77(Te,Se)	0.09			
77(Te,Te)	0.12	17.6 ± 1.0	17.8 ± 1.0	59

[a] Reference 10.
[b] Reference 25.

TABLE 20. SPECTRAL AND ELECTROCHEMICAL PROPERTIES OF TELLURIUM(IV) ANALOGS **59**, **90–96**, AND **98** OF TELLUROPYRYLIUM DYES

Compd.	λ_{max} (nm)[a]	log ε	E_1 (V vs. SCE)[b]	N (Faradays mol^{-1})[c]	E_2 (V vs. SCE)[b]	Ref.
59	496	4.48	+ 0.48	1.90[b]	− 0.45	16,27
90a	510[d]	4.75	− 0.10[c]	2.06	− 0.42	71,75
90b	502[d]	4.74	− 0.22[c]	1.84	− 0.45	71,75
90c	480[d]	4.72	− 0.10[c]	1.91	− 0.48	71,75
90d	452[d]	4.69	—	—	—	71
91	522	4.26	—	—	—	27
92a	497	4.41	+ 0.28	—	− 0.12	27
92b	525	4.45	+ 0.35	—	− 0.12	27
92c	—	—	+ 0.58	—	− 0.12	27
93a	488	4.45	+ 0.18	—	− 0.55	75
93b	475	4.44	+ 0.28	—	− 0.42	16
94a	388	4.88	—	—	—	27
95a	565	4.81	+ 0.24[c]	1.95	− 0.45	16,27
95b	543	4.74	+ 0.10[c]	—	− 0.44	16
95c	524	4.73	− 0.05[c]	1.84	− 0.48	16
96a	548	4.74	—	—	—	76
96b	532	4.78	—	—	—	76
96c	548	4.75	—	—	—	76
96d	535	4.77	—	—	—	76
98	530	4.68	—	—	—	76

[a] In dichloromethane.
[b] In dichloromethane with 0.2 *M* tetra-*n*-butylammonium fluoroborate as supporting electrolyte.
[c] In 10% aqueous acetonitrile with 0.2 *M* tetra-*n*-butylammonium fluoroborate as supporting electrolyte.
[d] In water.

TABLE 21. RATE CONSTANTS AND ARRHENIUS AND EYRING ACTIVATION PARAMETERS FOR REDUCTIVE ELIMINATION OF HYDROGEN PEROXIDE FROM **90** IN METHANOL AND PHOSPHATE BUFFERED SALINE AND CHLORINE FROM TELLUROPYRYLIUM DICHLORIDE DYES **96** AND **98** IN TETRACHLOROETHANE

Compd.	T (K)	k (s^{-1})	$\Delta H^{\ddagger}$ (kcal mol^{-1})	$\Delta S^{\ddagger}$ (cal $mol^{-1} K^{-1}$)	E_a (kcal mol^{-1})	ln A	Ref.
90a	296.0	$(2.38 \pm 0.06) \times 10^{-3}$	18.5 ± 0.5	-7 ± 1	19.1 ± 0.5	24.4	71
	303.0	$(5.38 \pm 0.25) \times 10^{-3}$		in MeOH			
	310.0	$(1.10 \pm 0.005) \times 10^{-2}$					
	317.0	$(2.03 \pm 0.02) \times 10^{-2}$					
90a	310.0	$(2.24 \pm 0.03) \times 10^{-5}$	20.9 ± 0.1	-12 ± 1	21.4 ± 0.1	24.3	71
	323.0	$(9.15 \pm 0.02) \times 10^{-5}$		in PBS			
	333.0	$(2.51 \pm 0.04) \times 10^{-4}$					
90b	310.0	$(4.42 \pm 0.16) \times 10^{-5}$	20.5 ± 0.9	-12 ± 3	21.2 ± 0.9	24.4	71
	323.0	$(2.05 \pm 0.03) \times 10^{-4}$		in PBS			
	333.0	$(4.66 \pm 0.11) \times 10^{-4}$					
90c	310.0	$(1.79 \pm 0.01) \times 10^{-5}$	21.3 ± 0.6	-11 ± 2	21.9 ± 0.6	24.7	71
	323.0	$(8.29 \pm 0.05) \times 10^{-5}$		in PBS			
	333.0	$(2.07 \pm 0.03) \times 10^{-4}$					

96a	323.0	$(4.92 \pm 0.01) \times 10^{-6}$	21.7 ± 0.3	-16 ± 2	22.3 ± 0.3	22.3	76
	348.0	$(5.20 \pm 0.01) \times 10^{-5}$		in tetrachloroethane			
	373.0	$(4.99 \pm 0.08) \times 10^{-4}$					
96b	348.0	$(7.17 \pm 0.00) \times 10^{-5}$	23.4 ± 0.2	-10 ± 4	24.1 ± 0.2	25.4	76
	363.0	$(3.20 \pm 0.02) \times 10^{-4}$		in tetrachloroethane			
	378.0	$(1.17 \pm 0.04) \times 10^{-3}$					
96c	333.0	$(9.76 \pm 0.01) \times 10^{-5}$	20.6 ± 0.5	-15 ± 8	21.3 ± 0.5	23.0	76
	348.0	$(4.44 \pm 0.01) \times 10^{-4}$					
	363.0	$(1.41 \pm 0.03) \times 10^{-3}$					
96d	323.0	$(8.54 \pm 0.02) \times 10^{-5}$	22.6 ± 0.2	-7 ± 6	23.3 ± 0.2	26.9	76
	338.0	$(4.45 \pm 0.02) \times 10^{-4}$		in tetrachloroethane			
	348.0	$(1.20 \pm 0.02) \times 10^{-3}$					
	363.0	$(4.61 \pm 0.02) \times 10^{-3}$					
98	340.5	$(5.31 \pm 0.10) \times 10^{-4}$	16.8 ± 0.5	-24 ± 3	17.5 ± 0.5	18.5	76
	348.0	$(1.15 \pm 0.02) \times 10^{-3}$		in tetrachloroethane			
	353.0	$(1.42 \pm 0.03) \times 10^{-3}$					
	358.0	$(1.94 \pm 0.04) \times 10^{-3}$					
	363.0	$(2.78 \pm 0.08) \times 10^{-3}$					
	368.0	$(3.75 \pm 0.10) \times 10^{-3}$					
	370.5	$(5.01 \pm 0.12) \times 10^{-3}$					

TABLE 22. PSEUDO-FIRST-ORDER RATE CONSTANTS (k_{app}) AND CONVERSION RATES (k_{cat}) FOR CHALCOGENOPYRYLIUM DYES AND NEUTRAL TELLURIUM (II) SPECIES AS CATALYSTS FOR OXIDATION OF LEUCODYES **108** (1.0×10^{-4} *M*) IN WATER (pH 6.8) WITH 0.01 *M* HYDROGEN PEROXIDE AT 298.0 ± 0.1 K[a]

Catalyst	Concentration (*M*)	Substrate	k_{app} (s^{-1})	k_{cat} ($M^{-2}s^{-1}$)
77(Te,S)	1.0×10^{-5}	**108a**	$(9.11 \pm 0.02) \times 10^{-4}$	9.11×10^{3}
	1.0×10^{-5}	**108b**	$(1.62 \pm 0.03) \times 10^{-3}$	1.62×10^{4}
77(Te,Se)	1.0×10^{-5}	**108a**	$(1.19 \pm 0.05) \times 10^{-3}$	1.19×10^{4}
	1.0×10^{-5}	**108b**	$(1.33 \pm 0.04) \times 10^{-3}$	1.33×10^{4}
77(Te,Te)	1.0×10^{-5}	**108a**	$(2.25 \pm 0.03) \times 10^{-3}$	2.25×10^{4}
	1.0×10^{-5}	**108b**	$(1.98 \pm 0.05) \times 10^{-3}$	1.98×10^{4}
	1.0×10^{-6}	**108a**	$(1.86 \pm 0.04) \times 10^{-4}$	1.86×10^{4}
75(Te,Te)	1.0×10^{-5}	**108a**	$(1.65 \pm 0.09) \times 10^{-4}$	1.65×10^{3}
74(Te,Te)	1.0×10^{-5}	**108a**	$(1.18 \pm 0.06) \times 10^{-4}$	1.18×10^{3}
	1.0×10^{-5}	**108b**	$(2.05 \pm 0.08) \times 10^{-5}$	2.03×10^{2}
110	3.0×10^{-5}	**108a**	$(4.25 \pm 0.02) \times 10^{-5}$	1.42×10^{2}
	1.0×10^{-5}	**108b**	$(3.82 \pm 0.06) \times 10^{-5}$	3.80×10^{2}
14f	1.0×10^{-6}	**108a**	$(1.24 \pm 0.02) \times 10^{-5}$	1.24×10^{3}
	1.0×10^{-6}	**108b**	$(1.02 \pm 0.01) \times 10^{-5}$	1.01×10^{3}
111	1.0×10^{-5}	**108a**	$(5.52 \pm 0.08) \times 10^{-6}$	5.52×10^{1}
14b	2.0×10^{-5}	**108a**	$(1.08 \pm 0.01) \times 10^{-6}$	5.40
	2.0×10^{-5}	**108b**	$(1.82 \pm 0.03) \times 10^{-6}$	8.33
5c	2.0×10^{-5}	**108a**	$(8.10 \pm 0.10) \times 10^{-8}$	4.05×10^{-1}
112	1.0×10^{-4}	**108b**	$(1.71 \pm 0.03) \times 10^{-6}$	1.55
113	1.0×10^{-5}	**108b**	$(8.70 \pm 0.15) \times 10^{-8}$	8.7×10^{-1}
114	1.0×10^{-5}	**108a**	$< 1 \times 10^{-8}$	$< 10^{-1}$
77(Se,S)	1.0×10^{-5}	**108a**	$(8.12 \pm 0.13) \times 10^{-8}$	8.12×10^{-1}
77(Se,Se)	1.0×10^{-4}	**108a**	$(7.57 \pm 0.06) \times 10^{-7}$	7.57×10^{-1}
	1.0×10^{-5}	**108b**	$(2.75 \pm 0.15) \times 10^{-8}$	2.75×10^{-1}

[a] Reference 16.

TABLE 23. QUANTUM EFFICIENCIES OF AND TURNOVER NUMBERS FOR HYDROGEN PEROXIDE GENERATION AT 10^{-5} *M* CATALYST IN WATER AND AQUEOUS METHANOL AT 298 K[a]

Compd.	Solvent	Turnover Number	$\Phi(H_2O_2)$
7a	99% MeOH	11.1 ± 2.9	3.1×10^{-5}
7b	99% MeOH	5.1 ± 0.5	3.4×10^{-5}
7c	H_2O	89.0 ± 2.6	5.5×10^{-3}
	50% MeOH	33.4 ± 2.2	1.2×10^{-3}
	99% MeOH	8.7 ± 1.4	9.5×10^{-5}
8	99% MeOH	1.5 ± 0.4	3.8×10^{-5}
11	99% MeOH	1.7 ± 0.4	5.0×10^{-5}

[a] Reference 16.

REFERENCES

1. Fabian, J.; Zahradnik, R. *Angew. Chem. Int. Ed. Engl.* **1989**, *28*, 677.
2. Matsuoka, M., ed., *Infrared Absorbing Dyes*, Plenum: New York, 1991.
3. Detty, M. R.; Murray, B. J.; Perlstein, J. H. U.S. Patent 4,365,017 (1982).
4. Detty, M. R.; Murray, B. J.; Perlstein, J. H. U.S. Patent 4,365,016 (1982).
5. TDK Corp., Jpn. Patent 73,892 (1985); *Chem. Abs.* **1985**, *103*: 79586x.
6. Detty, M. R.; Thomas, H. T. U.S. Patent 4,584,258 (1986).
7. Detty, M. R.; Merkel, P. B.; Powers, S. K. *J. Am. Chem. Soc.* **1988**, *110*, 5920.
8. Powers, S. K.; Walstad, D. L.; Brown, J. T.; Detty, M. R.; Watkins, P. J. *J. Neuro-Oncol.* **1989**, *7*, 179.
9. Powers, S. K. *Proceedings SPIE* **1987**, *847*, 74.
10. Detty, M. R.; Merkel, P. B.; Hilf, R.; Gibson, S. L.; Powers, S. K. *J. Med. Chem.* **1990**, *33*, 1108.
11. Walstad, D. L.; Brown, J. T.; Powers, S. K. *Photochem. Photobiol.* **1989**, *49*, 285.
12. Kessel, T. *Photochem. Photobiol.* **1991**, *53*, 73.
13. Eastman Kodak Co., Jpn. Patent 63 68,161 (1988); *Chem. Abs.* **1989**, *110*, 121466e.
14. DeBoer, C.; Evans, S. U.S. Patent 4,948,777 (1990).
15. Detty, M. R.; Gibson, S. L. *J. Am. Chem. Soc.* **1990**, *112*, 4086.
16. Detty, M. R.; Gibson, S. L. *Organometallics* **1992**, *11*, 2147.
17. Detty, M. R.; Murray, B. J. *J. Am. Chem. Soc.* **1983**, *105*, 883.
18. Detty, M. R. *Organometallics* **1988**, *7*, 1122.
19. Ladatko, A. A.; Nivorozhkin, V. L.; Sadekov, I. D. *Khim. Geterotsikl. Soedin.* **1986**, 1571.
20. Sadekov, I. D.; Ladatko, A. A.; Sadekova, G. I.; Minkin, V. I. *Khim. Geterotsikl. Soedin.* **1980**, 274.
21. Sadekov, E. I.; Ladatko, A. A.; Sadekova, E. I.; Minkin, V. I. *Khim. Geterotsikl. Soedin.* **1980**, 1342.
22. Detty, M. R.; Murray, B. J. *J. Org. Chem.* **1982**, *47*, 5235.
23. Detty, M. R. *Organometallics* **1988**, *7*, 2188.
24. Detty, M. R.; McKelvey, J. M.; Luss, H. R. *Organometallics* **1988**, *7*, 1131.
25. Detty, M. R.; Merkel, P. B. *J. Am. Chem. Soc.* **1990**, *112*, 3845.
26. Detty, M. R.; Luss, H. R. *Organometallics* **1992**, *11*, 2157.
27. Detty, M. R.; Luss, H. R. *Organometallics* **1986**, *5*, 2250.
28. Detty, M. R.; Lenhart, W. C.; Gassman, P. G.; Callstrom, M. R. *Organometallics* **1989**, *8*, 861.
29. Sadekov, I. D.; Ladatko, A. A.; Sadekova, E. I.; Dorofeenko, G. N.; Minkin, V. I. *Khim. Geterotsikl. Soedin.* **1981**, 343.
30. Tolmachev, A. E.; Kudinova, M. A. *Khim. Geterotsikl. Soedin.* **1971**, 1924.
31. Wadsworth, D. H.; Detty, M. R.; Murray, B. J.; Weidner, C. H.; Haley, N. F. *J. Org. Chem.* **1984**, *49*, 2676.
32. Detty, M. R.; Henne, B. *Heterocycles* **1993**, *35*, 1149.
33. Barker, C.; Hallas, G. *J. Chem. Soc. B* **1969**, 1068.

33a. Smith, P.; Yu, T.-Y. *J. Org. Chem.* **1952**, *17*, 1281.

34. Castelino, R.; Hallas, G. *J. Chem. Soc. B* **1971**, 793.
35. Reynolds, G. A.; Van Allan, J. A. *J. Heterocycl. Chem.* **1975**, *12*, 367.
36. Detty, M. R.; Hassett, J. W.; Murray, B. J.; Reynolds, G. A. *Tetrahedron* **1985**, *41*, 4853.
37. Detty, M. R. *J. Org. Chem.* **1982**, *47*, 1146.
38. Detty, M. R.; Murray, B. J.; Perlstein, J. H. *Tetrahedron Lett.* **1983**, *24*, 539.

39. Regnault du Mottier, C.; Brutus, M.; Le Coustumer, G.; Sauve, J. P.; Ebel, M.; Mollier, Y. *Mol. Cryst. Liq. Cryst.* **1988**, *154*, 361.
40. Chasseau, D.; Gaultier, J.; Hauw, C.; Fugnitto, R.; Gionis, V.; Strzelecka, H. *Acta Crystallogr., Sect. B: Struct. Crystallogr. Cryst. Chem.* **1980**, *B38*, 1629.
41. Zumbulyadis, N.; Gysling, H. J. *J. Organomet. Chem.* **1980**, *192*, 183.
42. McFarlane, H. C. E.; McFarlane, W. In *NMR of Newly Accessible Nuclei*; Laszlo, P., ed., Academic Press, New York, 1983.
43. Lutz, O. In *The Multinuclear Approach to NMR Spectroscopy*, Lambert, J. B.; Riddell, F. G., eds., D. Reidel, Boston, 1983.
44. McFarlane, H. C. E.; McFarlane, W. *J. Chem. Soc., Dalton Trans.* **1973**, 2416.
45. Schrobilgen, G. J.; Burns, R. C.; Granger, P. *J. Chem. Soc., Chem. Commun.* **1978**, 957.
46. Mason, J. *Chem. Rev.* **1987**, *87*, 1299.
47. Gelius, U.; Johansson, G.; Siegbahn, H.; Allan, C. J.; Allison, D. A.; Allison, J.; Siegbahn, K. *J. Electron Spectrosc. Related Phenom.* **1973**, *1*, 285.
48. Gassman, P. G.; Campbell, W. H.; Macomber, D. W. *Organometallics* **1984**, *3*, 385.
49. Gassman, P. G.; Macomber, D. W.; Hershberger, J. W. *Organometallics* **1983**, *2*, 1470.
50. Detty, M. R.; Lenhart, W. C.; Gassman, P. G.; Callstrom, M. R. *Organometallics* **1989**, *8*, 566.
51. Koopmans, T. *Physica* **1933**, *1*, 1453.
52. Michl, J.; Thulstrup, E. W. *Tetrahedron* **1976**, *32*, 205.
53. Bard, A. J.; Faulkner, L. R. *Electrochemical Methods*, Wiley, New York, 1980.
54. Turro, N. J. In *Modern Molecular Photochemistry*, Benjamin Cummings, Menlo Park, CA, 1978.
55. Saeva, F. D.; Olin, G. R. *J. Am. Chem. Soc.* **1980**, *102*, 299.
56. Maccoll, A. *Nature* (London) **1949**, *163*, 178.
57. Hoijtink, G. H. *Recl. Trav. Chim. Pays-Bas* **1958**, *77*, 555.
58. Loutfy, R. O.; Sharp, J. H. *Photogr. Sci. Eng.* **1976**, *20*, 165.
59. Tolmachev, A. I.; Kudinova, M. A. *Khim. Geterotsikl. Soedin.* **1974**, 49.
60. Bigelow, R. W. *J. Chem. Phys.* **1977**, *67*, 4498.
61. Pragst, F.; Janda, M.; Stibor, I. *Electrochim. Acta* **1980**, *25*, 779.
62. Dewar, M. J. S.; Thiel, W. J. *J. Am. Chem. Soc.* **1977**, *99*, 4899.
63. Dewar, M. J. S.; Thiel, W. *J. Am. Chem. Soc.* **1977**, *99*, 4907.
64. Streitweiser, A., Jr. *Molecular Orbital Theory for Organic Chemists*, Wiley, New York, 1962.
65. McKelvey, J. M., work to be published. The α term is a function of the Slater exponent; the β term is a linear function of bond order; the π term is atom-type-dependent.
66. Devanthan, S.; Dahl, T. A.; Neckers, D. C. *SPIE* **1988**, *997*, 113–117.
67. Detty, M. R. *Proceedings SPIE* **1987**, *847*, 68.
68. McGlynn, S. P.; Azumi, T.; Kinoshita, M. In *Molecular Spectroscopy of the Triplet State*; Prentice-Hall, Englewood Cliffs, NJ, 1969; pp. 172–174.
69. Gilman, P. B. *Photo. Sci. Eng.* **1967**, *11*, 222.
70. Firey, P. A.; Ford, W. E.; Sounik, J. R.; Kenney, M. E.; Rodgers, M. A. G. *J. Am. Chem. Soc.* **1988**, *110*, 7626.
71. Detty, M. R. *Organometallics* **1991**, *10*, 702.

71a. Detty, M. R.; Friedman, A. E. *Organometallics* **1994**, *13*, 533.

72. Merkel, P. B.; Kearns, D. R. *J. Am. Chem. Soc.* **1972**, *94*, 7244.
73. Rodgers, M. A. J. *J. Am. Chem. Soc.* **1983**, *105*, 6201.
74. Detty, M. R. *Organometallics* **1992**, *11*, 2310.
75. Detty, M. R. *Phosphorus, Sulfur, and Silicon* **1992**, *67*, 383.
76. Detty, M. R.; Frade, T. M. *Organometallics* **1993**, *12*, 2496.
77. Detty, M. R.; Murray, B. J. *J. Org. Chem.* **1987**, *52*, 2123.

78. Scozzafava, M.; Chen, C. H.; Reynolds, G. A.; Perlstein, J. H. U.S. Patent 4,514,481 (1985).
79. Detty, M. R. U.S. Patent 4,963,669 (1990).
80. Sadekov, I. D.; Barchan, I. A.; Ladatko, A. A.; Abakarov, G. M.; Sadekova, E. I.; Simkina, Yu. N.; Minkin, V. I. *Khim.-Farm. Zh.* **1982**, *16*, 1070.
81. Ladatko, A. A.; Sadekov, I. D.; Etmetchenko, L. N.; Minkin, V. I. *Khim. Geterotsikl. Soedin.* **1989**, 691.
82. Detty, M. R. U.S. Patent 5,082,771 (1992).
83. Nefedov, V. D.; Sinotova, E. N.; Sarbash, A. N.; Kolobov, E. A.; Kapustin, V. K. *Radiokhimiya* **1971**, *13*, 435.
84. Nefedov, V. D.; Sinotova, E. N.; Sarbash, A. N.; Timofev, S. A. *Radiokhimiya* **1969**, *11*, 154.
85. van Koten, G.; Terheijden, J.; van Beek, J. A. M.; Wehman-Ooyevaar, I. C. M.; Muller, F.; Stam, C. H. *Organometallics* **1990**, *9*, 903–912.
86. Braterman, P. S.; Cross, R. J. *Chem. Soc. Rev.* **1973**, *2*, 271.
87. Pearson, R. G. *Pure Appl. Chem.* **1971**, *27*, 145.
88. Skinner, C. E.; Jones, M. M. *J. Am. Chem. Soc.* **1969**, *91*, 4405–4408.
89. Jones, M. M.; Morgan, K. A. *J. Inorg. Nucl. Chem.* **1972**, *34*, 259–274.
90. Morgan, K. A.; Jones, M. M. *J. Inorg. Nucl. Chem.* **1972**, *34*, 275–296.
91. Hopgood, D.; Jenkins, R. A. *J. Am. Chem. Soc.* **1973**, *95*, 4461–4463.
92. Elding, L. I.; Gustafson, L. *Inorg. Chim. Acta* **1976**, *19*, 165–171.
93. van Beek, J. A. M.; van Koten, G.; Smeets, W. J. J.; Spek, A. L. *J. Am. Chem. Soc.* **1986**, *108*, 5010–5011.
93a. Detty, M. R.; Friedman, A. E. *Organometallics* **1994**, *13*.
94. Hu, A. X.; Aso, Y.; Otsubo, T.; Ogura, F. *Phosphorus and Sulfur* **1988**, *38*, 177–189.
95. Hu, N. X.; Aso, Y.; Otsubo, T.; Ogura, F. *Tetrahedron Lett.* **1986**, *27*, 6099–7102.
96. Barton, D. H. R.; Finet, J.; Thomas, M. *Tetrahedron* **1986**, *42*, 2319.
97. Hu, A. X.; Aso, Y.; Otsubo, T.; Ogura, F. *Bull Chem. Soc. Jpn.* **1986**, *59*, 879–884.
98. Ogura, F.; Yamaguchi, H.; Otsubo, T.; Tanaka, T. *Bull. Chem. Soc. Jpn.* **1982**, *55*, 641.
99. Ogura, F.; Otsubo, T.; Ariyoshi, K.; Yamaguchi, H. *Chem. Lett.* **1983**, 1833.
100. Ariyoshi, K.; Aso, Y.; Otsubo, T.; Ogura, F. *Chem. Lett*, **1984**, 891.
101. Barton, D. H. R.; Ley, S. V.; Meerholz, C. A. *J. Chem. Soc., Chem. Commun.* **1979**, 755.
101a. Engman, L.; Stern, D.; Pelcman, M.; Andersson, C. M. *J. Org. Chem.* **1994**, *59*, 1973.
102. Barton, D. H. R.; Finet, J.-P.; Giannotti, C.; Thomas, M. *Tetrahedron Lett.* **1988**, *29*, 2671.
103. Detty, M. R.; Luss, H. R. *J. Org. Chem.* **1983**, *48*, 5149.
104. Ley, S. V.; Meerholz, C. A.; Barton, D. H. R. *Tetrahedron* **1981**, *37*, Supplement No. 1, 213.
105. Detty, M. R.; Luss, H. R.; McKelvey, J. M.; Geer, S. M. *J. Org. Chem.* **1986**, *51*, 1692.
106. Gratzel, M., ed., *Energy Resources through Photochemistry and Catalysis*, Academic Press, New York, 1983.
107. Connolly, J. S., ed., *Photochemical Conversion and Storage of Solar Energy*, Academic Press, New York, 1981.
108. Hall, D. O.; Palz, W.; Pirrwitz, D., eds., *Photochemical, Photoelectrochemical and Photobiological Processes*, Reidel Publishing Co., Dordrecht, The Netherlands, 1983, Series D, Vol. 2.
109. Martin, J. P.; Logsdon, N. *Arch. Biochem. Biophys.* **1987**, *256*, 39.
110. Albery, W. J.; Foulds, A. W.; Daruent, J. R. *J. Photochem.* **1982**, *19*, 37.
111. Navarro, J. A.; Roncel, M.; De la Rosa, F. F.; De la Rosa, M. A. *Photochem. Photobiol.* **1987**, *40*, 279.
112. Kurimura, Y.; Nagashima, M.; Takato, K.; Tsuchida, E.; Kaneko, M.; Yamada, A. *J. Phys. Chem.* **1982**, *86*, 2432.
113. Kurimura, Y.; Katsumata, K. *Bull. Chem. Soc. Jpn.* **1982**, *55*, 2560.

Chemistry of Heterocyclic Compounds, Volume 53
Michael R. Detty, Marrie B. O'Regan

CHAPTER V

Tellurium-Containing Heterocycles with at Least One Group Va Element (Nitrogen, Phosphorus, or Arsenic)

A variety of tellurium-containing heterocyles with at least one nitrogen, phosphorus, or arsenic atom have been prepared and are described in this chapter. The ring sizes in these molecules vary between three and nine atoms.

I. THREE-MEMBERED TELLURIUM-CONTAINING HETEROCYCLES

Of the tellurium-containing heterocycles, the three-membered rings have the fewest representative examples in ring sizes of eight or smaller. Telluraziridines

and telluradiaziridines remain as unknown molecules. However, several three-membered tellurium-containing rings have been prepared, which incorporate at least one phosphorus or arsenic atom. The addition of disodium telluride to *tert*-butyldichlorophosphine or to di-*tert*-butyldichlorodiphosphine gives telluradiphosphidine **1** as shown in Scheme 1.[1,2] The telluradiphosphidine **1** was characterized by its mass spectrum with a strong parent ion of m/z 306 (for $C_8H_{18}{}^{31}P_2{}^{130}Te$) and its ^{31}P NMR spectrum with a singlet at δ − 69 and strong tellurium–phosphorus coupling (J_{Te-P} = 229.3 Hz).

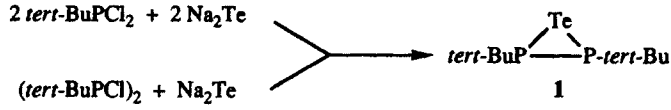

Scheme 1

Several examples of three-membered rings containing tellurium, silicon, and phosphorus atoms have been prepared as shown in Scheme 2.[3–5] In each case, tellurium metal is allowed to react with a phosphasilene **2** to generate the heterocyclic rings **3** in 40–55% isolated yields. These products tend to be unstable thermally and photochemically, depositing tellurium metal.

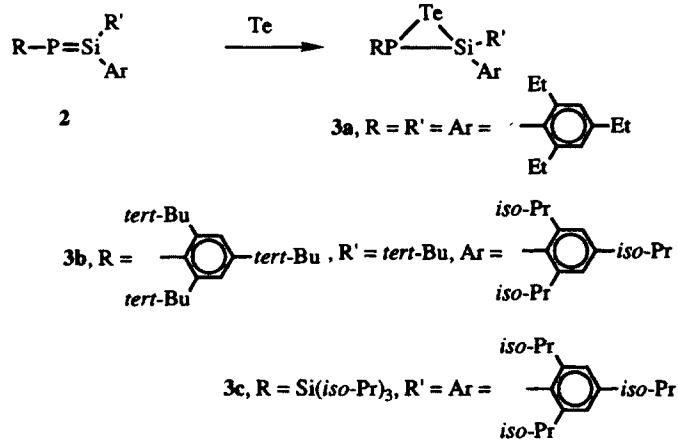

Scheme 2

The ^{31}P NMR spectra of **3a** and **3b** reveal singlets at δ − 126 and − 116, respectively, which are shielded significantly from the δ − 69 signal observed for **1**.[3,4] The tellurium–phosphorus coupling of 222 Hz, which was observed in the ^{31}P NMR spectrum of **3a**, is quite similar to J_{Te-C} of 229 Hz observed in **1**. The ^{125}Te NMR spectrum of **3c** displays the tellurium signal at δ − 1125 (vs. Me_2Te) and the INEPT-determined ^{29}Si NMR signal is observed at δ − 66.5.

A related arsenic-containing heterocycle has been prepared via the addition of tellurium metal to arsasilene **4** as shown in Scheme 3.[5] The heterocycle **5** is isolated as a yellow, crystalline solid in 40% yield. The heterocycle **5** was characterized through its mass spectrum. which displayed both a strong parent ion (*m/z* 796) and a strong ion corresponding to loss of tellurium from the complex (*m/z* 666). The ^{125}Te NMR signal at δ − 1157 is similar to the δ − 1125 signal observed for **3c** and the INEPT-determined ^{29}Si NMR signal is observed at δ − 44.5, which is similar to the chemical shift of silicon in **3c** observed at δ − 66.5.

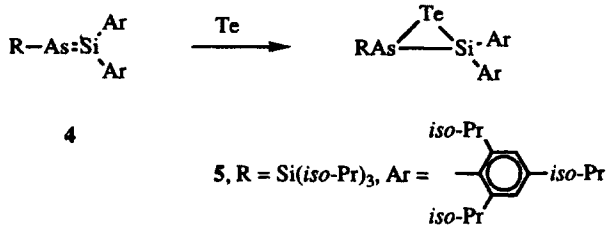

Scheme 3

One example of a metal complex telluradiarsadine has been described.[6] As shown in Scheme 4, the reaction of cobalt(II) with As_2Te_3 for 8 days in the presence of the triphos ligand in a solvent mixture of ethanol, THF, and benzene gives a 15–20% yield of **6**. A single-crystal X-ray structure of **6** reveals 60° internal angles in the ring, Te—As bond lengths of 2.497 and 2.539 Å, and an As—As bond length of 2.408 Å.

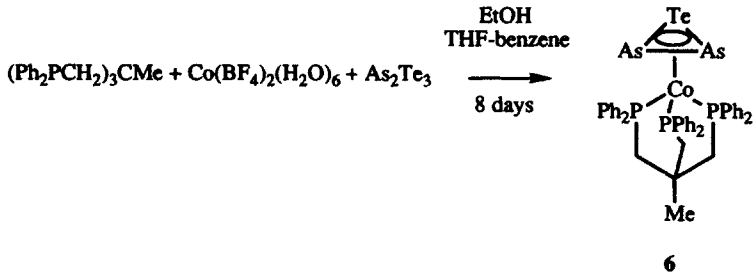

Scheme 4

II. FOUR-MEMBERED TELLURIUM-CONTAINING HETEROCYCLES

One example of a tellura-2,4-diazacyclobutan-3-one has been prepared as shown in Scheme 5.[7] The heterocycle **7** is isolated in 34% yield and is

characterized by a strong parent ion (m/z 488) in its mass spectrum, a carbonyl stretching frequency of 1638 cm^{-1}, and trifluoromethyl-associated bands at 1365 and 1117 cm^{-1}. The ^{19}F NMR spectrum of 7 displays the fluorine signal at δ − 62.1.

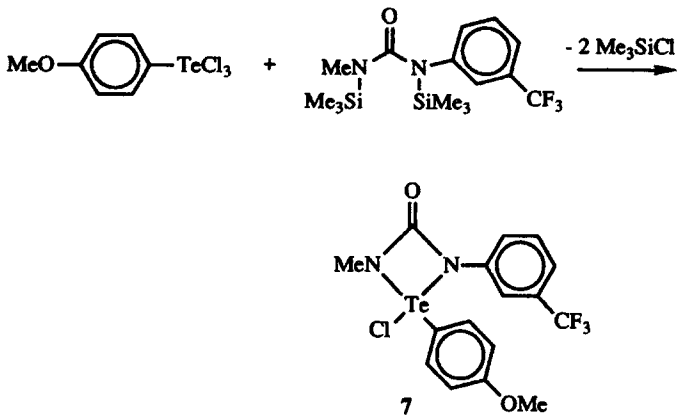

Scheme 5

The four-membered telluratriphosphetane **8** has been prepared as shown in Scheme 6.[1,2] The reaction of excess tellurium metal with bis(trimethylsilyl)-*tert*-butylphosphine in toluene produces **8** in addition to bis(trimethylsilyl)telluride. Compound **8** gives a strong parent-ion signal (m/z 394) in its mass spectrum. The ^{31}P NMR spectrum of **8** displays an AM_2 pattern with signals at δ − 4 and − 60 with J_{P-P} coupling of 173 Hz.

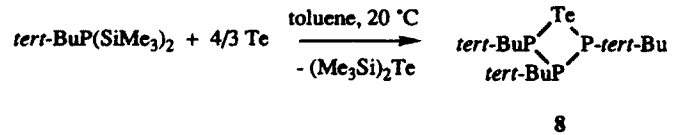

Scheme 6

III. FIVE-MEMBERED TELLURIUM-CONTAINING HETEROCYCLES

Several different classes of nitrogen- and tellurium-containing five-membered rings have been prepared. Among them are the isotellurazoles, benzoisotellurazoles, benzotellurazoles, telluradiazoles, benzotelluradiazoles, and various heteroatom-alkylated derivatives.

A. 1,2-Isotellurazoles and Their Benzo Analogs

1. Synthesis and Reactions

The 1,2-isotellurazoles **9** are prepared in low yields by the addition of hydroxylamine-*O*-sulfonic acid to acetylenic ketones **10** in buffered aqueous sodium acetate in the presence of potassium telluride as shown in Scheme 7.[8,9] Yields for this reaction vary between 3 and 10%. The 1,2-isotellurazoles **9** are isolated from a mixture that also contains low yields of the diketones **11**, which have strong interactions between the carbonyl oxygens and the central tellurium atom (ν_{CO} 1640–1653 cm^{-1}). The 1,2-isotellurazoles **9** are crystalline compounds, unlike the corresponding 1,2-isoselenazoles and 1,2-isothiazoles, which are oils.

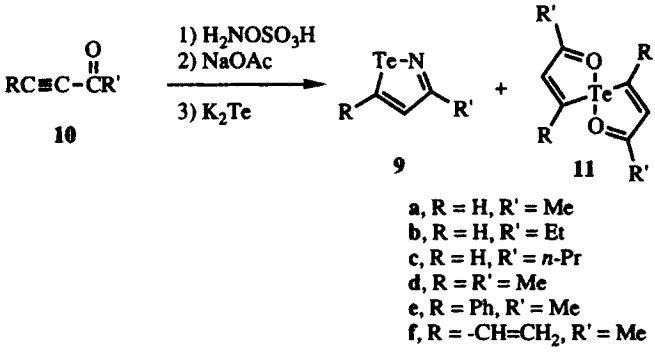

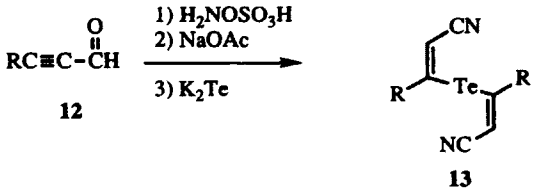

Scheme 7

Attempts to prepare 1,2-isotellurazoles from the propargyl aldehydes **12** have failed to give detectable yields of the isotellurazoles.[8] Instead, the dinitrile compounds **13** are isolated in 10–14% yield.

The 1,2-benzoisoltellurazole nucleus (**14**) has been prepared via two different routes as shown in Scheme 8.[10] The addition of ammonia to a benzene solution of 2-bromotellurenyl benzaldehyde (**15a**) gives 1,2-benzoisotellurazole (**14**) in 74% isolated yield. If 2-bromotellurenyl acetophenone is employed as starting material, the product of reaction is not the expected 3-methyl-1,2-benzoisotellurazole but is the telluraindanone **16**. 1,2-Benzoisotellurazole (**14**) is

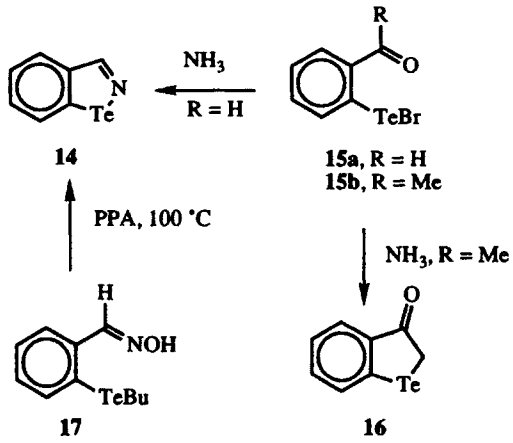

Scheme 8

also prepared in 40% isolated yield from the reaction of hydroxylamine derivative **17** with polyphosphoric acid (PPA) at 100°C.

The nitrogen atom of **14** is alkylated with iodomethane in ethanol to give the 2-methyl-1,2-benzoisotellurazolium salt **18** as shown in Scheme 9.[10] *N*-Arylated derivatives of **18** have been prepared from the corresponding 4-methylaniline-condensation product of 2-chlorotellurenyl benzaldehyde (compound **19**).[11-13] The addition of silver perchlorate or silver tetrafluoroborate to acetone solutions of **19** leads to precipitation of silver chloride and formation of the 2-(4-tolyl)-1,2-benzoisotellurazolium salts **20** in > 80% yield.

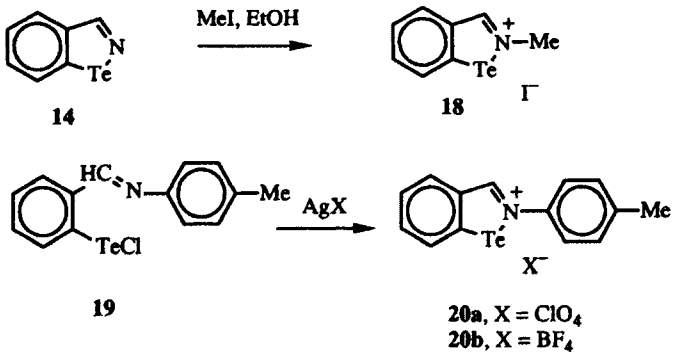

Scheme 9

2. *Structure and Properties*

The X-ray structure of 3,5-dimethyl-1,2-isotellurazole (**9d**) has been described.[14] The numbering scheme for **9d** is shown in Figure 1, and selected bond

lengths and angles are compiled in Table 1. The molecule is planar with an N—Te—C5 angle of 82.1°, which is similar to values found for similar angles (tellurium as central element) in other five-membered, tellurium-containing heterocycles. In this particular crystal, the unit cell is composed of six different **9d** molecules. The values given in Table 1 are the range of values for each bond length and the average of the six bond angles.

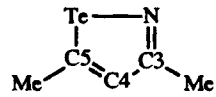

Figure 1. Numbering scheme for the X-ray structural data for **9d**.

The crystal packing in **9d** is characterized by extremely short intermolecular tellurium–nitrogen contacts.[14] The tellurium–nitrogen bond lengths of 2.028–2.071 Å can be compared with the intermolecular contacts of 2.640–2.774 Å. Physically, the short intermolecular contacts are manifested in high melting points relative to the lighter chalcogen analogs and diminished solubility.

The ^{1}H NMR spectra and the maxima of absorption in the UV spectra of the derivatives **9** are compiled in Table 2. The ring protons are found at extremely low field in the 1,2-isotellurazoles **9**. The chemical-shift values for the methyl group and the H4 proton of 3-methyl-5-vinyl derivative **9e** can be compared to those of the lighter chalcogen analogs **21**. While the chemical shift of the methyl group is little affected by heteroatom changes in the ring, the ring proton H4 moves upfield by 1 ppm from the sulfur analogs **21b** to the tellurium analog **9e**.

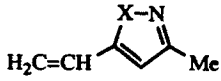

9e, X = Te
21a, X = Se
21b, X = S

In the mass spectra of the 1,2-isotellurazoles **9**, fragmentation patterns are similar to those observed for isothiazoles.[8] Fragments corresponding to loss of RC_2H and to loss of R'CN from parent ion are observed.

The X-ray crystal structure of 1,2-benzoisotellurazole (**14**) has been described.[15] Selected bond lengths and angles are compiled in Table 3 according to the numbering scheme in Figure 2. Bond lengths and angles are similar to those observed in 3,5-dimethyl-1,2-isotellurazole (**9d**). 1,2-Benzoisotellurazole (**14**) is a planar molecule with extremely short intermolecular tellurium–nitrogen contacts. The 2.46–2.48-Å contacts are even shorter than those observed in 3,5-dimethyl-1,2-isotellurazole (**9d**). Compound **14** shows decreased solubility

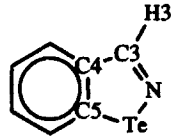

Figure 2. Numbering scheme for the X-ray crystal structure of 1,2-benzoisotellurazole (**14**).

due to the close intermolecular contacts. The melting point of 173°C for **14** is much higher than the 57°C melting point observed for the selenium analog and the 39°C melting point for the sulfur analog.

The ring proton H3 moves upfield as the heteroatom is changed from tellurium in **9d** to selenium in **22a** to sulfur in **22b** as shown in Table 4.[10] The absorption maxima in the UV spectra of these same molecules move to shorter wavelengths with the same heteroatom changes. The ^{125}Te NMR spectrum of **14** displays a signal at δ 1589 (vs. Me_2Te), which is quite downfield for tellurium(II) derivatives.[16] The mass spectrum of **14** displays a strong parent ion (m/z 233) and significant ions for Te^+ (m/z 130), loss of HCN from the parent ion, and loss of tellurium from the parent ion.

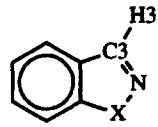

14, X = Te
22a, X = Se
22b, X = S

The ^{15}N NMR spectrum of **14** has also been measured.[15] The nitrogen signal is observed at δ 0.107 (vs. $NaNO_3$). The N—H3 coupling is 13.37 Hz, and the N—Te coupling is 157 Hz.

The ^{1}H NMR spectra of the 1,2-benzoisotellurazolium salts **18** and **20** show a small upfield shift in the chemical shift of H3 relative to that observed in **14**[10–13] In the ^{1}H NMR spectrum of **18**, H3 is observed at δ 9.65 while the methyl group is observed as a singlet at δ 4.10. These values can be compared to similar values for the corresponding 1,2-benzoisoselenazolium salt **23**, in which the ring proton is observed at δ 9.50, which is a small downfield shift from **21a** (Table 4), and the methyl group is observed at δ 3.67. The chemical shift of H3 in *N*-aryl-substituted 1,2-isobenzotellurazolium salts **20** is observed to be δ 9.82.

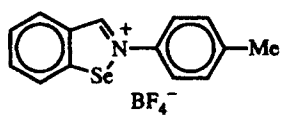

23

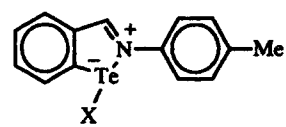

24, X = F, Cl, Br, I

The strength of the tellurium–nitrogen interactions in **14** and **20b** has been evaluated via the Raman spectra of the two compounds.[13] The Te–N band is observed at 249 cm^{-1} in **14** and at 206 cm^{-1} in **20b**, which is indicative of a stronger bonding interaction in **14** relative to **20b**. The Te—N frequency observed in **20b** is similar to the Te—N interaction observed in 1,2-benzotelluradiazolium halides **24**, which have three-center, four-electron bonding to tellurium. In the **24** series, the Te—N Raman frequency is observed at 219 cm^{-1} in the fluoride, 214 cm^{-1} in the chloride and bromide, and 206 cm^{-1} in the iodide.[13] The molecules **24** have a fractional covalent bond between tellurium and nitrogen.

B. Tellurazoles and Benzotellurazoles

1. Synthesis

The 1,3-tellurazole nucleus (**25**) remains an unknown system, although synthetic routes to this system would be a valuable addition to heterocyclic synthesis. In pharmaceutical chemistry, the synthesis and testing of chalcogenazole derivatives has given new leads for anticancer and antiviral agents. Tiazofurin[17] and selenazofurin[18] have been shown to be effective antitumor agents in animals while selenazofurin has been shown to possess broad spectrum antiviral activity in cell cultures.[19] The oxazole derivative does not display such biological activity. Synthetic entry to tellurazoles might allow the synthesis of "tellurazofurin."

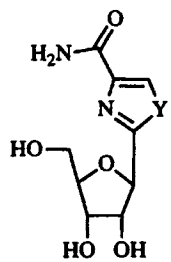

Tiazofurin, Y = S
Selenazofurin, Y = Se
Tellurazofurin, Y = Te

The 1,3-benzotellurazole nucleus **26** has been prepared via a number of different routes. The first synthesis of the benzotellurazole nucleus cyclized *ortho*-ethyltelluroanilides **27** with phosphorus oxychloride as shown in Scheme 10.[20] The yields of the benzotellurazoles are low (2–15% isolated yield), but a variety of substituents can be introduced at the 4-position via this procedure.

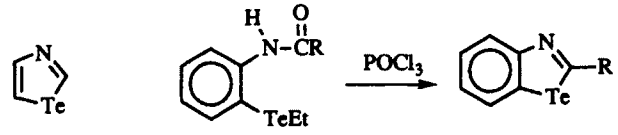

25 **27**

26a, R = H
26b, R = Me
26c, R = Ph
26d, R = CO_2Et
26e, R = COPh

Scheme 10

The methyltelluro group has also been utilized in this reaction with slightly improved yields.[21] Utilizing the methyltelluro group, **26b** and **26c** are isolated in 35 and 65% yields, respectively, while the 2-*p*-tolyl-(**26f**) and 2-*p*-anisyl-substituted (**26g**) derivatives are isolated in 55 and 58% yields, respectively.

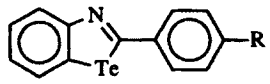

26f, R = Me
26g, R = OMe

Azobenzene derivatives have also been used as precursors to 1,3-benzotellurazoles **26** as shown in Scheme 11.[22] The addition of tellurium tetrachloride to **28** in the presence of aluminum chloride gives a 63% yield of the *ortho*-tellurated product **29**, which is reduced with sodium borohydride to give 2-aminophenyltellurol (**30**). The condensation of **30** with acetic anhydride followed by workup with aqueous hydrochloric acid gives **26b** in 41% yield.

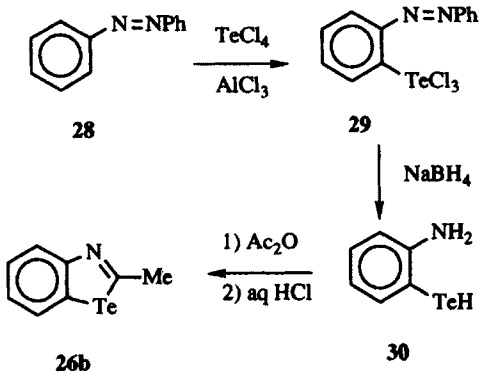

28 **29** **30** **26b**

Scheme 11

The 2-aminoaryltellurols have also been prepared from diaryl tellurides as shown in Scheme 12.[22] Nitration and cyclization lead to the hypervalent tellurium-containing heterocycle **31**, which is then reduced with sodium borohydride in THF to give the 2-aminoaryltellurol **32**. Condensation with acetic anhydride gives benzotellurazole **33**.

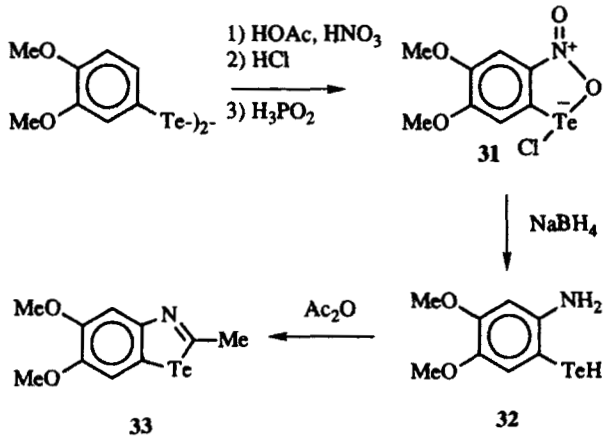

Scheme 12

The reaction of 2-hydrotelluroacetanilides **34** with acetic anhydride also gives benzotellurazole derivatives.[22] As shown in Scheme 13, both mono- and disubstituted derivatives **35** have been prepared via this route.

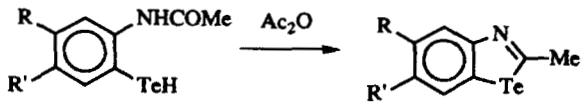

35a, R = Me, R' = H
35b, R = OMe, R' = H
35c, R = SMe, R' = H
35d, R = OH, R' = H
35e, R = R' = Me

Scheme 13

The 2-hydrotelluroacetanilides **34** can be prepared via the routes shown in Schemes 11 and 12.[23] Alternatively, organomercurials can be utilized as precursors to compounds **34** as shown in Scheme 14. The synthetic routes in Scheme 14 are complementary to the route shown in Scheme 12 for the preparation of monosubstituted derivatives **35**. Scheme 12 leads to 5-substituted-1,3-benzotellurazoles **35a–35d**, while the process in Scheme 14 leads to 6-substituted-1,3-benzotellurazoles **35f–35h**. The cyclizations of 2-hydrotelluroacetanilides **34** with phosphorus trichloride give 1,3-benzotellurazoles **35** in

30–60% isolated yields. 2-Hydrotelluroacetanilide **34f** was also converted to the methyltelluro derivative **36**, which cyclized with phosphorus trichloride to give **35f** in 46% yield.

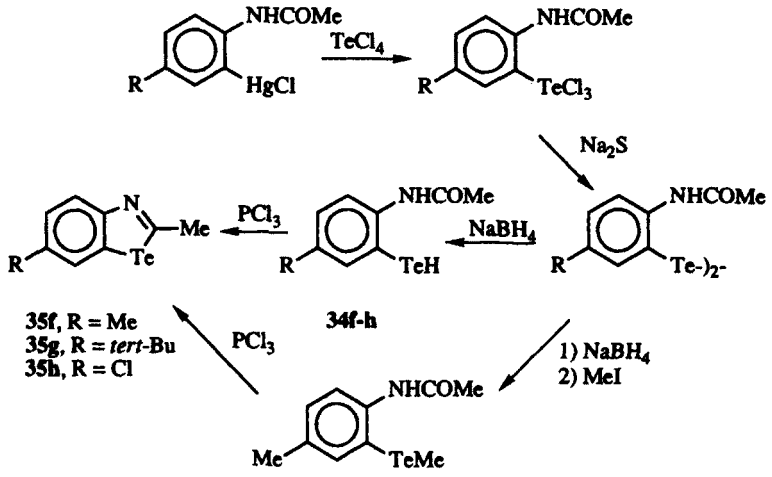

Scheme 14

Using the organomercurial approach of Scheme 14, the naptho[*a*]tellurazole **37** is produced.[23] The naphtho[*c*]tellurazoles **38** are synthesized via the procedure shown in Scheme 15, which utilizes the 1-aminonaphthalene-2-tellurol as the penultimate intermediate.[22]

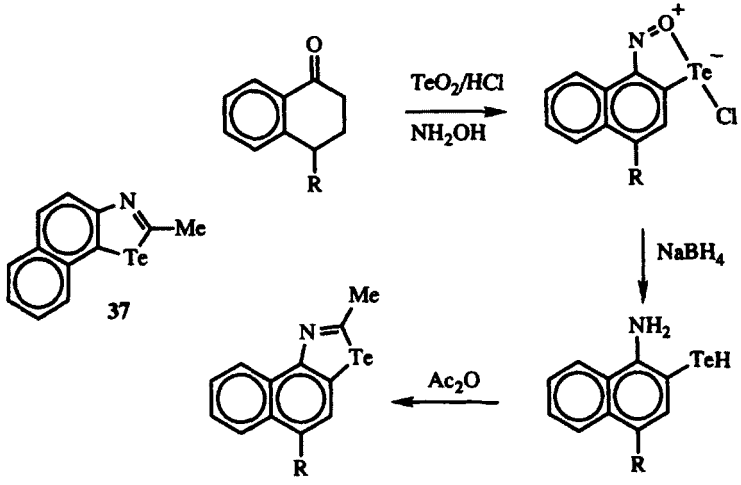

Scheme 15

The 2-aryltellurazoles **26c**, **26h**, and **26i** have been prepared from 2-methyltelluroacetanilides **39** as shown in Scheme 16.[21] Addition of thionyl chloride to **39** gives the imminium chloride **40** (with oxidation of tellurium). Reduction of tellurium(IV) to tellurium(II) with sodium bisulfite gives **41**, which on heating cyclizes to the corresponding 2-substituted-1,3-benzotellurazoles **26**.

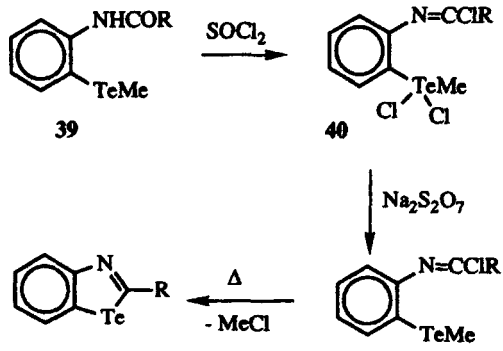

26c, R = Ph
26h, R = *p*-BrPh
26i, R = *p*-ClPh

Scheme 16

The 1,3-benzotellurazole nucleus undergoes a variety of transformations at both the tellurium and nitrogen atoms as outlined in Scheme 17.[24,25] The tellurium atom of 2-phenyl-1,3-benzotellurazole (**26c**) is methylated with a mixture of iodomethane and silver perchlorate to give **42**. In contrast, the sequential addition of iodomethane followed by silver perchlorate gives the

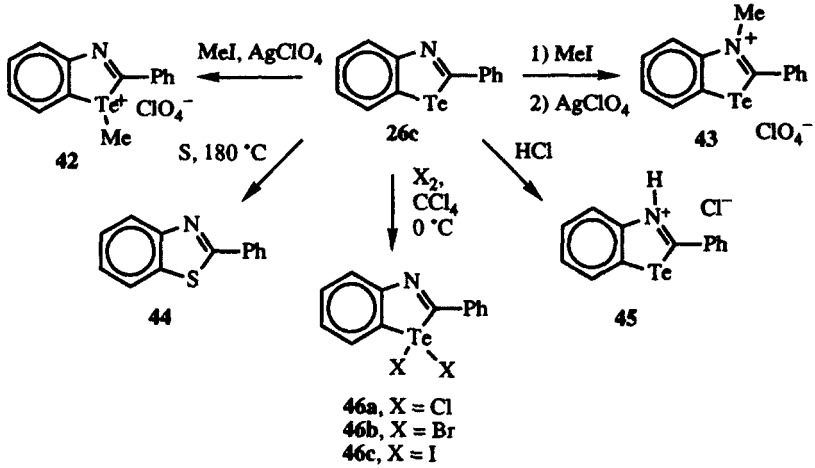

Scheme 17

N-methyl derivative **43**. Heating **26c** at 180°C with elemental sulfur leads to tellurium–sulfur exchange and a 42% isolated yield of 2-phenyl-1,3-benzothiazole (**44**). The addition of hydrochloric acid to **26c** gives protonation of the nitrogen with the production of benzotellurazolium chloride **45**. The oxidative addition of chlorine, bromine, and iodine to **26c** gives the corresponding tellurium(IV) dihalides **46** in nearly quantitative yield.

The benzotellurazoles also function as two-electron donor ligands with mercury(II) halides and palladium(II) halides.[24,25] The tellurium atom is presumably the donor atom in these complexes.

The condensation products of aldehydes and 2-methyl-1,3-benzotellurazole (**26b**) are the styryl derivatives **47** as shown in Scheme 18.[25] The reaction is catalyzed with zinc chloride, and the products are isolated in 61–65% yields.

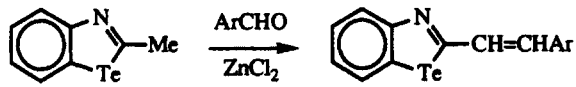

26b

47a, Ar = Ph
47b, Ar = *p*-NO_2Ph
47c, Ar = *p*-MeOPh
47d, Ar = *p*-EtOPh

Scheme 18

The benzotellurazolium dyes **48** have been prepared from 2-methyl-1,3-benzotellurazole (**26b**) as shown in Scheme 19.[25] The addition of iodomethane to **26b** gives 2-methyl-1,3-benzotellurazolium iodide (**49**). The condensation of **49** with triethyl orthoformate gives the symmetrical trimethine dye **48a** in 81% isolated yield (λ_{max} 610 nm, log ε = 3.78). The unsymmetrical 1,3-benzotellurazolium trimethine dyes **48b** and **48c** have also been prepared with λ_{max} of 574 nm (log ε 3.99) and 546 nm (log ε 3.89), respectively.

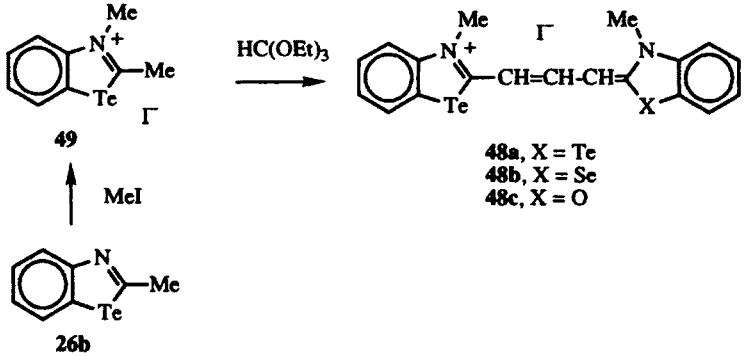

49

48a, X = Te
48b, X = Se
48c, X = O

26b

Scheme 19

2. *Structure and Properties*

The X-ray crystal structure of 2-phenyl-1,3-benzotellurazole (**26c**) has been reported.[26] Selected bond lengths and angles are compiled in Table 5 according to the numbering scheme in Figure 3. The molecule is planar. The Te—C5 bond length of 2.080 Å in **26c** is comparable to those determined for 3,5-dimethyl-1,2-isotellurazole (**9d**, 2.05–2.08 Å) and 1,2-benzoisotellurazole (**14**, 2.080 Å). The angle about tellurium is 78.6°, which is also similar to comparable angles of 82.1° and 82.0° for **9d** and **14**, respectively.

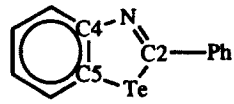

Figure 3. Numbering scheme for the X-ray crystal structure of 2-phenyl-1,3-benzotellurazole (**26c**).

The crystal structure of **26c** reveals short intermolecular Te···N contacts of 3.43 Å.[26] However, these contacts are longer than the 2.640–2.774-Å contacts observed in **9d**,[14] the 2.46–2.48-Å contacts observed in **14**,[15] or the 2.76 Å contacts observed in 1,2,5-telluradiazoles (vide infra).[27] Consequently, the physical properties of the 1,3-benzotellurazoles, such as melting points and solubility, are not altered significantly relative to their lighter chalcogen analogs.

Selected NMR parameters for some of the benzotellurazoles **26**, **35**, and **37** are compiled in Table 6.[20,23] The proton at the 2-position of **26a** appears as a singlet at δ 11.3 in the ^{1}H NMR spectrum of this molecule. This is more than 1.6 ppm downfield from the chemical shift of the 2-proton in 1,3-diselenazole (**50**).[20] Interestingly, the chemical shifts of the methyl protons in 2-methyl-1,3-benzotellurazole (**26a**) and 2-methyl-1,3-benzoselenazole (**51**) are nearly identical at δ 2.76 and δ 2.66, respectively.[20]

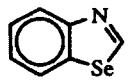

50

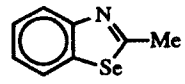

51

In the 2-methyl derivatives in Table 6, the chemical shifts of the protons of the 2-methyl groups are little affected by substituents in the benzo ring. The observed range for the methyl singlets is δ 2.48–2.82.[20,23] The ^{13}C NMR chemical shifts of the methyl carbons may be more sensitive to substituent changes, with the methyl signal of **35f** observed at δ 20.9 and the methyl signal of **35h** observed at δ 38.9.[23] The chemical shifts of the C2 carbons also appear to be quite sensitive to substituent changes with a chemical shift of δ 168.4 in **35g** and a chemical shift of δ 142.7 in **35h**.[23] The ^{125}Te chemical shifts in **35g**, **35h**, and **37**

are all similar (δ 891–945)[23] and are in the range typically observed for diaryltellurium(II) compounds.[16]

The ^{1}H NMR chemical shifts of the methyl groups in telluronium salt **42** and telluradiazolium salt **43** are quite different.[25] The observed chemical shift of δ 2.28 for the telluronium methyl is 1.6 ppm upfield of the chemical shift of δ 3.88 for the telluradiazolium methyl.

The mass spectra of 1,3-benzotellurazoles are characterized by strong parent ion clusters.[20,23] In the parent 1,3-benzotellurazole (**26a**), the parent ion (*m/z* 233 for ^{130}Te) is the base peak. Other strong ions include Te^+ (*m/z* 130, 30%) and M—HCN (*m/z* 206, 79%). In 2-substituted derivatives, the M—RCN ion is significant.

The basicities of the series of 2-methyl-1,3-benzochalcogenazoles (**26b**, **52**) and the series of 2-phenyl-1,3-benzochalcogenazoles (**26c**, **53**) have been measured and are compiled in Table 7.[28] In both series, the basicity of the nitrogen increases as the heteroatom decreases in electronegativity from oxygen to tellurium. It has been suggested that inductive effects outweigh π contributions to increased electron density at nitrogen, since π overlap decreases from oxygen to tellurium. Also consistent with this evaluation is the observation that the 2-methyl derivatives (electron-donating substituent) are more basic than the corresponding 2-phenyl derivatives (slightly electron-withdrawing substituent).

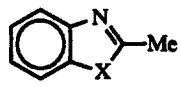

26b, X = Te
52a, X = Se
52b, X = S
52c, X = O

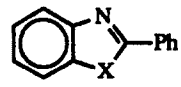

26c, X = Te
53a, X = Se
53b, X = S
53c, X = O

C. Telluradiazoles and Their Benzo Analogs

1. Synthesis

The 1,2,5-telluradiazole nucleus (**54**) has been prepared from either the corresponding 1,2,5-thiadiazole or 1,2,5-selenadiazole as shown in Scheme 20.[29] Sulfur or selenium is lost on the addition of two equivalents of ethyl magnesium bromide to give a dimetallated species, which reacts with tellurium tetrachloride to give the telluradiazole **54**. Yields for this reaction are compiled in Table 8. In general, the use of selenazoles as precursors to tellurazoles gives higher yields than the use of thiadiazoles.

The tellurazoles **54** are easily hydrolyzed as shown in Scheme 21. The products of acidic hydrolysis are the α-diketones **55**, ammonia, tellurium metal,

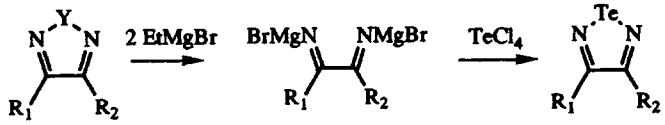

Y = S, Se

54a, $R_1 = R_2 = H$
54b, $R_1 = H$, $R_2 = Me$
54c, $R_1 = H$, $R_2 = Ph$
54d, $R_1 = R_2 = Me$
54e, $R_1 = R_2 = Ph$

Scheme 20

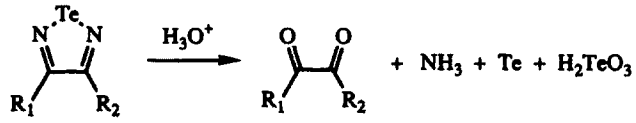

54 **55**

Scheme 21

and H_2TeO_3.[29] The chalcogenazoles are essentially α-diimines, which are joined via a tellurium atom.

A similar approach has been utilized for the synthesis of a quinone-fused 1,2,5-telluradiazole **56** as shown in Scheme 22. The addition of tellurium tetrachloride to diamine **57** gives **56** in unspecified yield.[30] The quinone **56** could not be condensed with malononitrile in pyridine in the presence of titanium tetrachloride as catalyst. Ring opening of the tellurazole ring was observed.

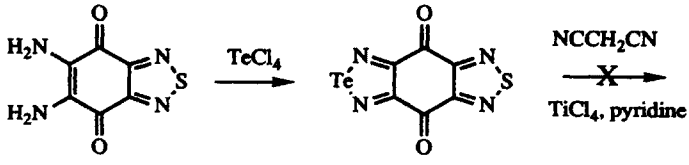

57 **56**

Scheme 22

1,2,3-Benzotelluradiazolium salts **58** have been prepared from diazo compounds as shown in Scheme 23.[11-13] The addition of silver salts to the tellurenyl chloride **59** leads to formation of the benzotelluradiazolium salt from the tellurenyl cation in roughly 65% yield. Both the perchlorate and tetrafluoroborate salts have been prepared via this route.

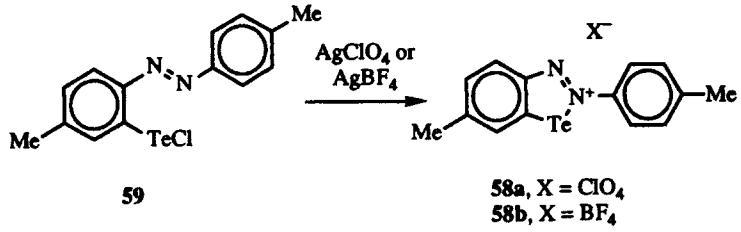

59

58a, X = ClO_4
58b, X = BF_4

Scheme 23

2. *Structure and Properties*

The X-ray crystal structure of 1,2,5-telluradiazole (**54a**) has been reported.[27] Selected bond lengths and angles are compiled in Table 9 according to the numbering scheme in Figure 4. The molecule is planar. The ring angle around tellurium is 82.5°, which is similar to values of the atom–tellurium–atom ring angles found in other five-membered heterocyclic systems containing tellurium. The most unusual feature of the crystal structure is found in the very short tellurium–nitrogen intermolecular contacts (2.764 Å), which lead to low solubility and high melting point relative to the other chalcogenadiazoles (Table 10).

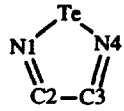

Figure 4. Numbering scheme for the X-ray crystal structure of 1,2,5-telluradiazole (**54a**).

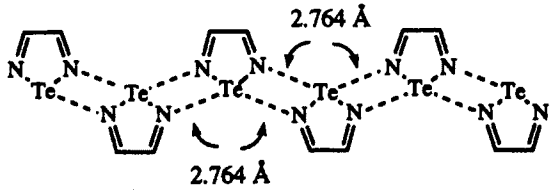

Figure 5. Secondary structure in crystals of 1,2,5-telluradiazole (**54a**).

The short intermolecular tellurium–nitrogen contacts create a polymeric array of telluradiazole molecules as shown in Figure 5. The secondary structure is ribbon-like. Such ordering might be advantageous in the design of materials based on the properties of tellurium in these molecules.

Selected physical parameters are compiled in Table 10 for the chalcogenadiazoles **54a** and **60**. As with other heterocyclic systems, the absorption max-

imum moves to longer wavelengths as the size of the heteroatom increases. The absorption maximum moves from 253 nm for thiadiazole (**60b**) to 336 nm for telluradiazole (**54a**). The mass spectral fragmentation patterns of the telluradiazoles show intense peaks corresponding to the parent ion, loss of R—CN, and tellurium metal (*m/z* 130). As with other five-membered tellurium-containing heterocycles discussed in this chapter, the chemical shift of the ring protons in the ^{1}H NMR spectrum of **54a** is significantly downfield of those of the chalcogenadiazoles **60**.

54a, X = Te
60a, X = Se
60b, X = Se
60c, X = O

The vibrational analyses of telluradiazole **54a** and selenadiazole **60a** have been compared.[31] Infrared and Raman analysis of the 4000–50-cm^{-1} region allows the assignment of the fundamental frequencies in the vibrational spectra of **54a** and **60a**. Zeroth-order calculations and comparison of **54a** with selenadiazole **60a** have been made. Group assignments in **54a** and **60a** are compiled in Table 11.

D. Tellurazolines

1. Synthesis and Properties

Thiaazetidine **61** is in equilibrium with its ring-opened iminothione **62**. The ring-opened form reacts with antimony telluride over a period of many days to give a 15% yield of tellurathiazoline **63** as shown in Scheme 24.[32]

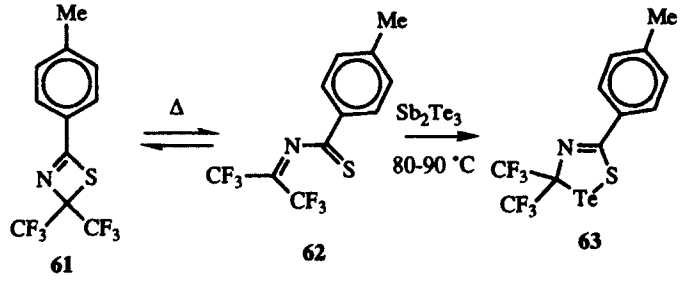

Scheme 24

The addition of mesityl cyanate to tetramethyl indane tellurone **64** gives a 70% yield of the telluraoxazoline **65** as shown in Scheme 25.[33] This product is thermally unstable and decomposes to give tellurium metal, indanone **66**, and mesityl isocyanide. The regiochemical assignment of telluraoxazoline was based on the mass spectrum of the reaction mixture, which gave indanone **66** and mesityl telluroisocyanate.

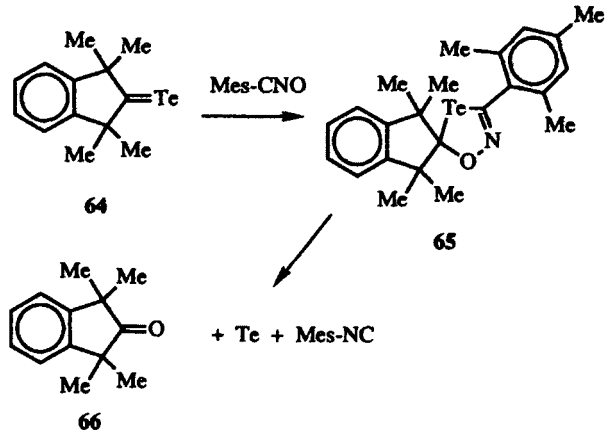

64 65 66

Scheme 25

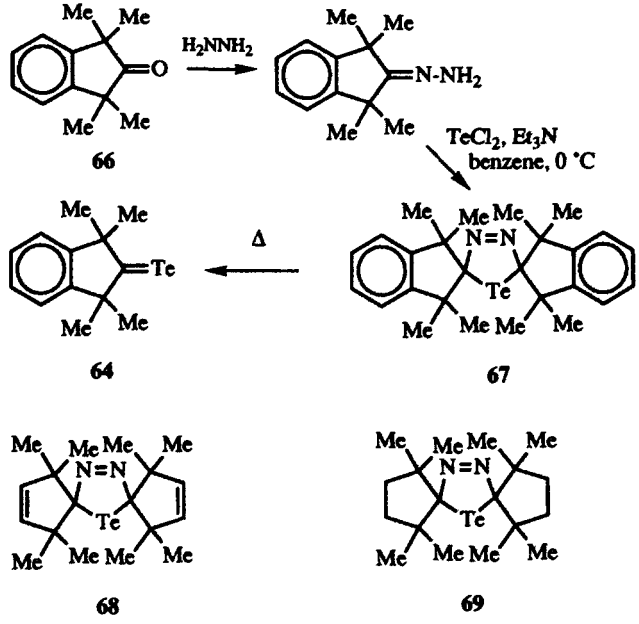

64 67 68 69

Scheme 26

1,3,4-Telluradiazolines have been prepared from hydrazones as shown in Scheme 26.[34] The addition of tellurium dichloride to the hydrazone of indanone **66** gives telluradiazoline **67** in 26% yield. 1,3,4-Telluradiazolines **68** and **69** have been prepared via similar routes in 10 and 11% isolated yields, respectively. The telluradiazolines **67–69** are characterized by weak absorption in the UV spectrum with λ_{max} of 340 nm ($\varepsilon = 640$). In the ^{13}CNMR spectra of **67–69**, the spirocarbon is found at low-field chemical shifts (δ 133.2 for **67**, δ 128.7 for **68**, and δ 130.0 for **69**). All three of these molecules give strong parent ions via field desorption mass spectrometry. On heating, the 1,3,4-telluradiazoline **67** loses nitrogen to form the telluroketone **64**.[34]

IV. SIX-MEMBERED TELLURIUM-CONTAINING HETEROCYCLES

A. Phenotellurazines

1. Synthesis

The first synthesis of a phenotellurazine-like molecule utilized the addition of tellurium tetrachloride to a quinoline phenyl amine **71** as shown in Scheme 27.[35] The intermediate tellurium(IV) derivative **72** is deprotonated with base and reduced with bisulfite to give the quinoline analog **73**.

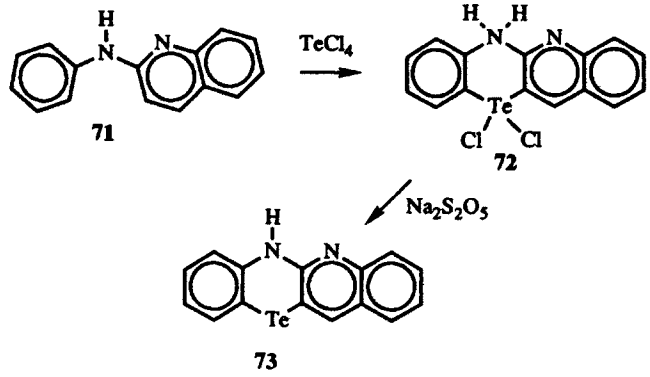

Scheme 27

More general approaches to phenotellurazines utilize metallated diarylamine intermediates. Lithiation of α,α'-dibromodiphenyl methyl amine two equivalents of *n*-butyllithium gives dilithio diarylamine **74** as shown in Scheme 28.[36] The

addition of tellurium tetrachloride gives an 18% yield of 10,10-dichloro-5-methylphenotellurazine (**75**), which is reduced to 5-methylphenotellurazine (**76**) in nearly quantitative yield with hydrazine hydrate.

Dibromodiphenyl ethyl amine and dibromoditolyl ethyl amine can be metallated as well.[37,38] The addition of tellurium diiodide gives 5-ethylphenotellurazine (**77**) and 5-ethyl-2,8-dimethylphenotellurazine (**78**) as shown in Scheme 28. The latter compound is isolated in 48% yield via this procedure.

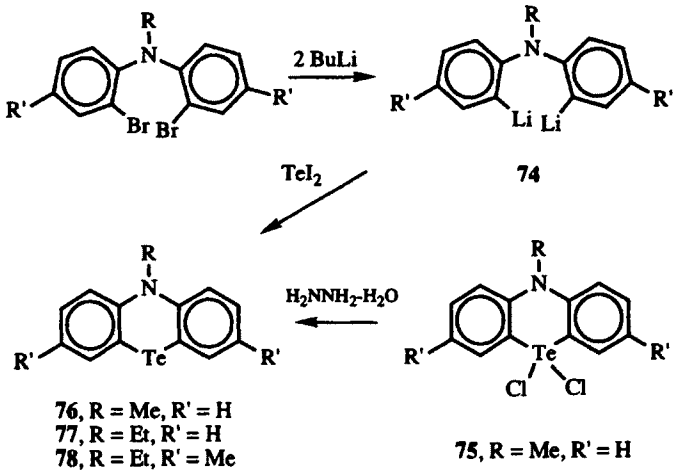

Scheme 28

Organomercurials can also be used as precursors to phenotellurazines as shown in Scheme 29.[39] The addition of mercuric acetate to a methanol solution of diphenylamine followed by lithium chloride and tellurium tetrachloride gives a 7% yield of 10,10-dichlorophenotellurazine (**79**), which can be reduced with aqueous disodium sulfide in quantitative yield to give the parent phenotellurazine (**80**). Although the yield via this route is low, it is easily reproduced and product isolation is facile.

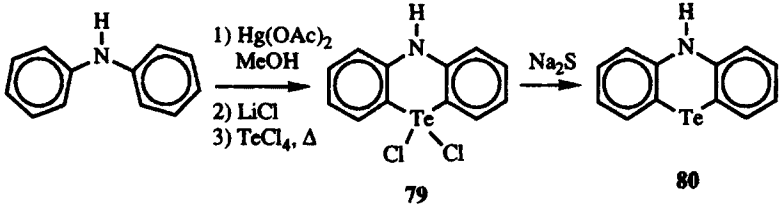

Scheme 29

Mercuration of naphthyl phenyl amine gives organomercurial **81**.[39] As shown in Scheme 30, the addition of tellurium tetrachloride presumably generates the

trichlorotellurium derivative, which cyclizes on heating to give the dichloro tellurazine **82** in 53% yield. Reduction with aqueous disodium sulfide gives tellurazine **83** in nearly quantitative yield.

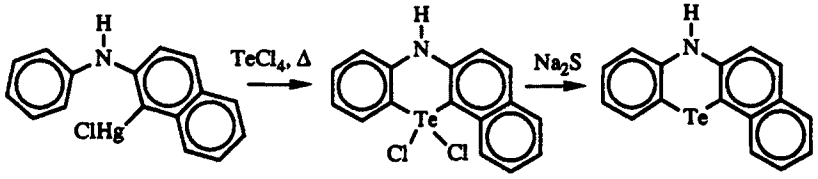

Scheme 30

The tellurium atom of phenotellurazine **78** undergoes reactions typical of the tellurium atom in other heterocyclic systems as shown in Scheme 31. Oxidation with thionyl chloride or bromine converts phenotellurazine **78** to 10,10-dihalo-5-ethylphenotellurazines **84** and **85**, respectively.[37] Alkylation of **78** with iodomethane followed by ion exchange with silver perchlorate gives telluronium salt **86** in 90% yield.[40] Dibromide **85** reacts with dimedone in benzene in the presence of triethylamine to give the telluronium ylide **87** in 80% yield.[40] The ylide reacts with ethanolic hydrofluoric acid to give 10,10-difluorophenotellurazine (**88**). Phenotellurazine **78** also forms complexes with various mercuric and rhodium salts, although the complexes have been poorly characterized.[40]

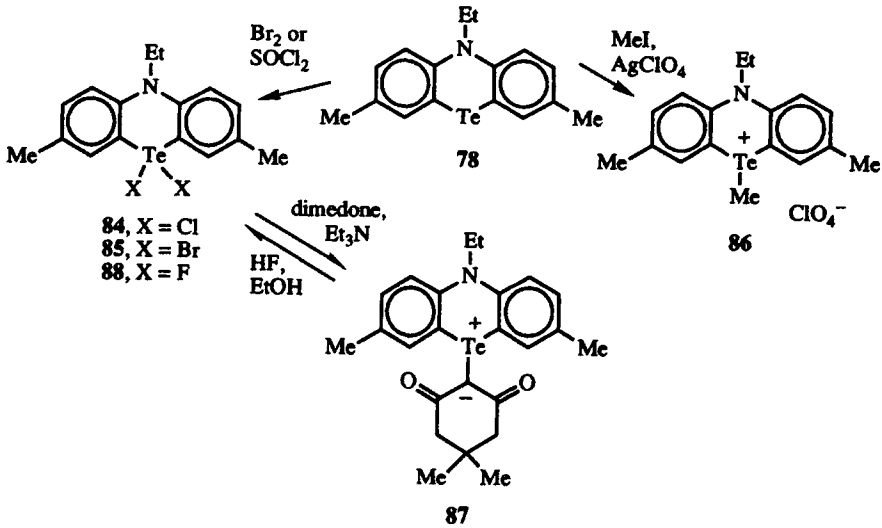

Scheme 31

2. *Physical and Spectral Properties*

The ^{1}H, ^{13}C, and ^{125}Te NMR spectra of phenotellurazine (**80**) have been recorded. Chemical-shift values are recorded in Table 12 according to the numbering scheme shown in Figure 6.[39] In the ^{1}H NMR spectrum of **80**, the protons located 1,3 relative to the tellurium atom are found at lower field than the other protons. The carbon atom bearing tellurium in phenotellurazine (**80**) and related compounds is shielded significantly relative to the other carbon atoms in the molecule (δ 97.7). The ^{125}Te NMR chemical shift of δ 409 is typical of other organotellurium(II) compounds. For **83**, the ^{125}Te NMR signal is observed at δ 294. In 5-methylphenotellurazine (**76**), the ^{1}H NMR chemical shift of the methyl group attached to nitrogen is δ 3.50.

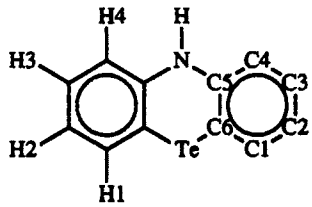

Figure 6. Numbering scheme for phenotellurazine **80**.

The mass spectra of the phenotellurazines show strong parent-ion clusters. However, the base peak corresponds to loss of tellurium ($M^{+} - {}^{130}Te$). Naphthophenotellurazine (**83**) shows similar behavior with strong ions for the parent ion and loss of tellurium from the parent ion.

B. Phosphatelluranes

The addition of sodium telluride to dialkynylphosphine oxides gives good yields of the 4-substituted-4-oxo-phosphatelluranes **89** as shown in Scheme 32.[41] Steric bulk at the termini of the acetylenes appears to be important as the yield of the addition reaction decreases from 65–70% for R_2 equal to H to 58–71% for R_2 equal to methyl to 25–45% for R_2 equal to *tert*-butyl. Yields are comparable with R_1 equal to either phenyl or cyclohexyl.

By ^{1}H NMR spectroscopy, the phosphatelluranes **89** are quite similar to the corresponding telluropyran-4-one with respect to chemical shift.[41] For **89d**, the olefinic protons on the carbons adjacent to tellurium appear as a doublet-of-doublets pattern at δ 8.19 with $^{3}J_{H-H}$ equal to 14.0 Hz and $^{3}J_{P-C=CH}$ equal to 32 Hz. The protons on the carbon atoms adjacent to phosphorus also appear as a doublet-of-doublets pattern at δ 6.80 with 14.0 Hz coupling between the adjacent protons and 10.8 Hz coupling for $^{2}J_{PCH}$.

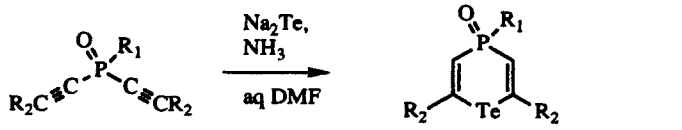

89a, R_1 = Ph, R_2 = H
89b, R_1 = Ph, R_2 = Me
89c, R_1 = Ph, R_2 = *tert*-Bu
89d, R_1 = cyclohexyl, R_2 = H
89e, R_1 = cyclohexyl, R_2 = Me
89f, R_1 = cyclohexyl, R_2 = *tert*-Bu

Scheme 32

V. SEVEN-MEMBERED TELLURIUM-CONTAINING HETEROCYCLES

Seven-membered tellurium-containing heterocycles with at least one group Va element are rather rare in the heterocyclic literature. A dibenzotellurazepine has been prepared as shown in Scheme 33.[42] The addition of sodium azide to telluroxanthylium perchlorate **90** gives azidotelluroxanthene **91**. When **91** is heated in refluxing xylenes, loss of nitrogen is observed, which is presumably indicative of formation of nitrene **92**. A 1,2-shift of the *p*-tolyl group generates imine **93** in 32% isolated yield while a 1,2-shift of a ring carbon–carbon bond leads to ring expansion and the generation of dibenzotellurazepine **94** in 21% isolated yield.

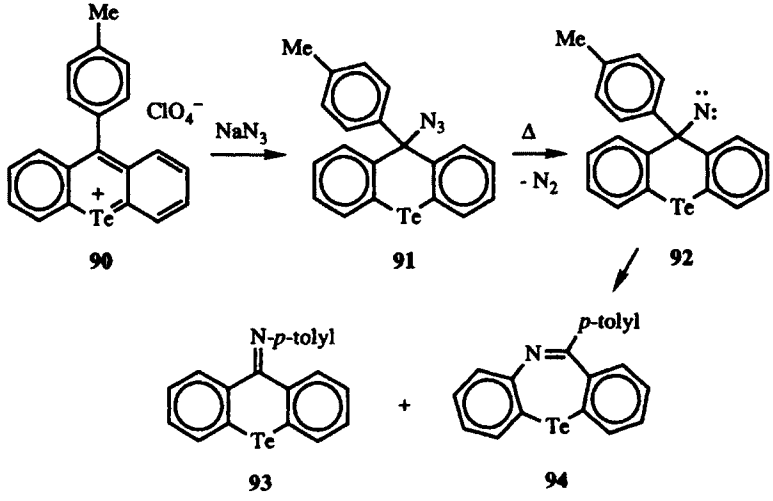

90 **91** **92** **93** **94**

Scheme 33

The condensation of telluroanhydride **95** and its diiodo tellurium(IV) analog **96** with ethylene diamine or *o*-phenylene diamine gives seven-membered tellurium-containing heterocycles with two nitrogen atoms as shown in Scheme 34.[43] The products of these reactions (**97**–**100**) are isolated in 40–60% yields.

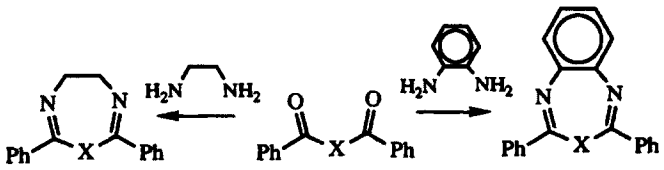

97, X = Te
98, X = TeI_2

95, X = Te
96, X = TeI_2

99, X = Te
100, X = TeI_2

Scheme 34

VI. EIGHT-MEMBERED TELLURIUM-CONTAINING HETEROCYCLES

A similar approach as described in Scheme 34 has been utilized for the construction of an eight-membered heterocyclic ring containing a tellurium atom and two nitrogen atoms.[43] The condensation of 1,3-diaminopropane with **95** gives **101**.

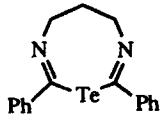

101

VII. NINE-MEMBERED TELLURIUM-CONTAINING HETEROCYCLES

Two examples of nine-membered heterocyclic rings containing one tellurium atom and two nitrogen atoms have been reported utilizing chemistry similar to that described in Scheme 33.[44] The addition of ethylene diamine or *o*-phenylene diamine to the tellurium(IV) derivative **102** in refluxing methanol gives **103** and **104**, respectively, as shown in Scheme 35. Under the conditions of reaction, tellurium(IV) is reduced to tellurium(II).

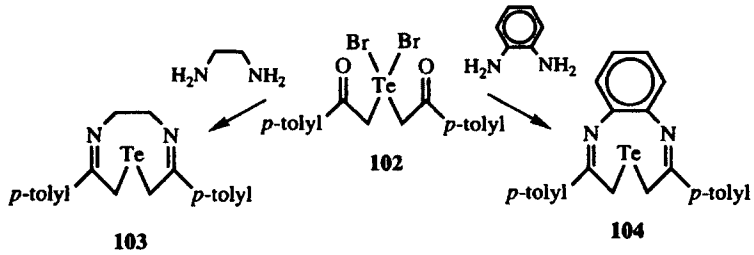

Scheme 35

TABLES

TABLE 1. BOND LENGTHS (Å) AND BOND ANGLES (°) IN 3,5-DIMETHYL-1,2-ISOTELLURAZOLE (**9d**) AS DETERMINED BY X-RAY CRYSTALLOGRAPHY[a]

Bond	(Å)	Angle	(°)
Te—N	2.028–2.071	N—Te—C5	82.1
Te—C5	2.047–2.079	Te—N—C3	110.8
N—C3	1.245–1.322	N—C3—C4	119.7
C3—C4	1.409–1.465	C3—C4—C5	118.2
C4—C5	1.294–1.365	C4—C5—Te	109.2

[a] Reference 14.

TABLE 2. ^{1}H NMR PARAMETERS AND UV ABSORPTION MAXIMA FOR 1,2-ISOTELLURAZOLES **9** AND THEIR LIGHTER CHALCOGEN ANALOGS **21**[a]

Compd.	R	R′	H4	λ_{max} (ε) (nm)
	(δ, ppm)			
9a	H (10.22)[b]	Me (2.42)	8.09[b]	306 (5200)
9b	H (10.23)[c]	Et (2.81,1.26)	8.14[c]	305 (5400)
9c	H (10.24)[d]	Pr	8.13[d]	305 (5400)
9d	Me (2.28)	Me (2.59)	7.55	304 (5400)
9e	Ph	Me (2.50)	8.01	306 (8400), 331 (3600)
9f	—CH=CH_2	Me (2.45)	7.72	—
21a	—CH=CH_2	Me (2.43)	7.06	—
21b	—CH=CH_2	Me (2.46)	6.80	—

[a] References 8 and 9.
[b] $^3J_{HC=CH}$ = 6.6 Hz.
[c] $^3J_{HC=CH}$ = 6.5 Hz.
[d] $^3J_{HC=CH}$ = 6.5 Hz.

TABLE 3. BOND LENGTHS (Å) AND BOND ANGLES (°) IN 1,2-BENZOISOTELLURAZOLE (**14**) AS DETERMINED BY X-RAY CRYSTALLOGRAPHY[a]

Bond	(Å)	Angle	(°)
Te—N	2.11	N—Te—C5	80.0
Te—C5	2.08	Te—N—C3	113.4
N—C3	1.27	N—C3—C4	119.5
C3—C4	1.46	C3—C4—C5	115.5
C4—C5	1.40	C4—C5—Te	111.6

[a] Reference 15.

TABLE 4. SELECTED ^{1}H AND ^{13}C NMR SIGNALS AND UV ABSORPTION MAXIMA FOR 1,2-BENZOISOTELLURAZOLE (**14**) AND LIGHTER CHALCOGEN ANALOGS **22**[a]

Compd.	H3 (δ, ppm)	C3 (δ, ppm)	^{125}Te (vs. Me_2Te)	λ_{max} (log ε) (nm)
14	10.16[b]	168.3	1589[c]	344 (3.65)
22a	9.15[d]	160.7	—	318 (3.67)
22b	8.73	—	—	303 (3.57)

[a] Reference 10.
[b] $J_{Te-H} = 35$ Hz.
[c] Reference 13.
[d] $J_{Se-H} = 24$ Hz.

TABLE 5. BOND LENGTHS (Å) AND BOND ANGLES (°) IN 2-PHENYL-1,3-BENZOTELLURAZOLE (**26c**) AS DETERMINED BY X-RAY CRYSTALLOGRAPHY[a]

Bond	(Å)	Angle	(°)
Te—C2	2.123	C2—Te—C5	78.6
Te—C5	2.080	Te—C2—N	114.4
N—C2	1.297	C2—N—C4	116.9
N—C4	1.385	N—C4—C5	119.8
C4—C5	1.396	C4—C5—Te	110.3

[a] Reference 26.

TABLE 6. SELECTED NMR DATA FOR 1,3-BENZOTELLURAZOLES **26a, 26b, 35f–h,** AND **37**

Compd.	H, Me	C2, Me (δ, ppm)	^{125}Te (vs. Me_2Te)
26a	H (11.3)[a]	—	—
26b	Me (2.76)[a]	—	—
35f	Me (2.82)[b]	168.4, 20.9	891
35g	Me (2.82)[b]	—	—
35h	Me (2.81)[b]	142.7, 38.9	945
37	Me (2.48)[b]	—	900

[a] Reference 20.
[b] Reference 23.

TABLE 7. BASICITIES OF 2-SUBSTITUTED-1,3-BENZOCHALCOGENAZOLES[a]

Compd.	X	R	pK_{BH^+}
26b	Te	Me	10.10
52a	Se	Me	8.87
52b	S	Me	8.63
52c	O	Me	7.30
26c	Te	Ph	8.67
53a	Se	Ph	7.46
53b	S	Ph	7.24
53c	O	Ph	6.03

[a] Reference 28.

TABLE 8. SYNTHESIS OF 1,2,5-TELLURADIAZOLES **54** FROM THIA- AND SELENADIAZOLE PRECURSORS[a]

Compd.	Y	R_1	R_2	% Yield
54a	Se	H	H	20
54b	Se	H	Me	26
54c	Se	H	Ph	60
54d	Se	Me	Me	12
	S	Me	Me	6
54e	Se	Ph	Ph	79
	S	Ph	Ph	39

[a] Reference 29.

TABLE 9. BOND LENGTHS (Å) AND BOND ANGLES (°) IN 1,2,5-TELLURADIAZOLE (**54a**) AS DETERMINED BY X-RAY CRYSTALLOGRAPHY[a]

Bond	(Å)	Angle	(°)
Te—N1	2.023	N1—Te—N4	82.5
Te—N4	2.023	Te—N1—C2	109.4
N1—C2	1.274	N1—C2—C3	119.3
C2—C3	1.421	C2—C3—C4	119.3
C3—N4	1.274	C3—N4—Te	109.4

[a] Reference 27.

TABLE 10. COMPARISON OF SELECTED PHYSICAL AND SPECTRAL PROPERTIES FOR 1,2,5-CHALCOGENADIAZOLES **54a** AND **60**[a]

Compd.	Y	mp (°C)	UV (ε) (nm)	^{1}H NMR (δ)	J_{Y-H} (Hz)
54a	Te	185–188	336 (3900)	10.81	46.5 (^{125}Te)
60a	Se	21	285 (6500)	9.47	28.8 (^{77}Se)
60b	S	− 50	253 (10,100)	8.89	—
60c	O	− 28	—	8.66	—

[a] Reference 29.

TABLE 11. VIBRATIONAL ANALYSIS OF 1,2,5-TELLURADIAZOLE (**54a**) AND 1,2,5-SELENADIAZOLE (**60a**) BASED ON RAMAN AND IR SPECTRA[a]

Symmetry Group	Selenadiazole **60a** (cm^{-1})		Telluradiazole **54a** (cm^{-1})	
	Obs.	Calc.	Obs.	Calc.
	In-Plane Vibrational Frequencies			
A_1	3067	3047	2998	3034
	1360	1364	1358	1371
	1290	1288	1290	1280
	1008	1011	974	979
	726	725	660	661
	488	488	388	372
B_1	3028	308	2975	3038
	1385	1389	1377	1376
	1234	1229	1252	1238
	880	876	870	879
	589	589	492	475
	Out-of-Plane Vibrational Frequencies			
A_2	868	868	860	855
	672	671	511	512
B_2	833	827	828	829
	438	438	359	356

[a] Reference 31.

TABLE 12. ^{1}H, ^{13}C, AND ^{125}Te NMR DATA FOR PHENOTELLURAZINE (80)[a]

Proton	δ (ppm)	Carbon	δ (ppm)	^{125}Te (δ)
H1	7.39	C1	135.0	409
H2	6.85	C2	123.7	
H3	7.09	C3	128.5	
H4	6.75	C4	116.2	
		C5	144.5	
		C6	97.7	

[a] Reference 39.

REFERENCES

1. DuMont, W.-W.; Hensel, R.; Severengiz, T. *Phosphorus Sulfur* **1983**, *18*, 73.
2. Dumont, W.-W.; Severengiz, T.; Meyer, B. *Angew. Chem. Int. Ed. Engl.* **1983**, *22*, 983.
3. Smit, C. N.; Bickelhaupt, F. *Organometallics* **1987**, *6*, 1156.
4. Van den Winkel, Y.; Bastiaans, H. M. M.; Bickelhaupt, F. *J. Organoment. Chem.* **1991**, *405*, 183.
5. Driess, M.; Pritzkow, H. *Angew. Chem. Int. Ed. Engl.* **1992**, *31*, 316.
6. Di Vaira, M.; Peruzzini, M.; Stoppioni, P. *Polyhedron* **1986**, *5*, 983.
7. Roesky, H. W.; Münzenberg, J.; Bohra, R.; Noltemeyer, M. *J. Organomet. Chem.* **1991**, *418*, 339.
8. Lucchesini, F.; Bertini, V. *Synthesis* **1983**, 824.
9. Lucchesini, F.; Bertini, V.; De Munno, A.; Pocci, M.; Picci, N.; Ligouri, M. *Heterocycles* **1987**, *26*, 1587.
10. Weber, R.; Piette, J.-L.; Renson, M. *J. Heterocycl. Chem.* **1978**, *15*, 865.
11. Sadekov, I. D.; Maksimenko, A. A.; Abakarov, G. M.; Maslakov, A. G.; Minkin, V. I. *Khim. Geterotsikl. Soedin.* **1988**, 1426.
12. Sadekov, I. D.; Maksimenko, A. A.; Maslakov, A. G.; Minkin, V. I. *J. Organomet. Chem.* **1990**, *391*, 179.
13. Maslakov, A. G.; McWhinnie, W. R.; Perry, M. C.; Shaikh, N.; McWhinnie, S. L. W.; Hamor, T. A. *J. Chem. Soc., Dalton Trans.* **1993**, 619.
14. De Munno, G.; Lucchesini, F. *Acta Crystallogr., Sect. C: Cryst. Struct. Commun.* **1992**, *C48*, 1437.
15. Campsteyn, H.; Dupont, L.; Lamotte-Brasseur, J.; Vermeire, M. *J. Heterocycl. Chem.* **1978**, *15*, 745.
16. McFarlane, H. C. E.; McFarlane, W. In *NMR of Newly Accessible Nuclei*, Academic Press, New York, 1983, Vol. 2, Ch. 10.
17. Robins, R. K.; Srivastiva, P. C.; Narayanan, V. L.; Plowman, J; Paull, K. D. *J. Med. Chem.* **1982**, *25*, 107.
18. Srivastava, P. C.; Robins, R. K. *J. Med. Chem.* **1983**, *26*, 445.
19. Kirsi, J. J.; North, J. A.; McKernan, P. A.; Murry, B. K.; Canonico, P. G.; Huggins, J. W.; Srivastava, P. C.; Robins, R. K. *Antimicrob. Agents Chemother.* **1983**, *24*, 353.
20. Mbuyi, M.; Evers, M.; Tihange, G.; Luxen, A.; Christiaens, L. *Tetrahedron Lett.* **1983**, *24*, 5873.
21. Sadekov, I. D.; Abakarov, G. M.; Shneider, A. A.; Kuren', S. G.; Starikov, A. G.; Garnovskii, A. D; Minkin, V. I. *Khim. Geterotsikl. Soedin.* **1989**, 120.
22. Günther, W. H. H.; Przyklek-Elling, R. U.S. Patent 4,661,438 (1987).

23. Junk, T.; Irgolic, K. J. *Phosphorus Sulfur* **1988**, *38*, 121.
24. Sadekov, I. D.; Abakarov, G. M.; Shneider, A. A.; Minkin, V. I. *Khim. Geterotsikl. Soedin.* **1988**, 136.
25. Sadekov, I. D.; Abakarov, G. M.; Shneider, A. A.; Minkin, V. I. *Khim. Geterotsikl. Soedin.* **1989**, 989.
26. Mistryukov, A. E.; Sadekov, I. D.; Sergienko, V. S.; Abakarov, G. M.; Porai-Koshits, M. A.; Shneider, A. A.; Garnovskii, A. D. *Khim. Geterotsikl. Soedin.* **1989**, 1690.
27. Bertini, V.; Dapporto, P.; Lucchesini, F.; Sega, A.; DeMunno, A. *Acta Crystallogr. Sect. C.: Cryst. Struct. Commun.* **1984**, *40*, 653.
28. Abakarov, G. M.; Shneider, A. A.; Kuren', S. G. *Khim. Geterotsikl. Soedin.* **1991**, 836.
29. Bertini, V.; Lucchesini, F. *Synthesis* **1982**, 681.
30. Suzuki, T.; Fujii, H.; Yamashita, Y.; Kabuto, C.; Tanaka, S.; Harasawa, M.; Mukai, T.; Miyashi, T. *J. Am. Chem. Soc.* **1992**, *114*, 3034.
31. Muniz-Miranda, M.; Sbrana, G.; Bertini, V.; Lucchesini, F.; Benedetti, E.; DeMunno, A. *Spectrochim. Acta* **1984**, *40A*, 847.
32. Burger, K.; Ottlinger, R.; Provoksch, A.; Firl, J. *J. Chem. Soc. Chem. Commun.* **1979**, 80.
33. Minoura, M.; Kawashima, T.; Okazaki, R. *J. Am. Chem. Soc.* **1993**, *115*, 7019.
34. Okazaki, R.; Minoura, M.; Kawashima, T. *Chem. Lett.* **1993**, 1047.
35. Zankowska-Jasinska, W.; Burgiel, M. M. *Zeszyty Naukowe Uniw. Jagiellonskiego, Prace Chem.* **1977**, *22*, 50.
36. Bergman, J.; Engman, L. *J. Organomet. Chem.* **1983**, *251*, 223.
37. Sadekov, I. D.; Abakarov, G. M.; Garnovskii, A. D.; Minkin, V. I. *Khim. Geterotsikl. Soedin.* **1982**, 707.
38. Sadekov, I. D.; Abakarov, G. M.; Panov, V. B.; Ukhin, L. Yu; Garnovskii, A. D.; Minkin, V. I. *Khim. Geterotsikl. Soedin.* **1985**, 757.
39. Junk, T.; Irgolic, K. J. *Heterocycles* **1989**, *28*, 1007.
40. Sadekov, I. D.; Abakarov, G. M.; Garnovskii, A. D.; Varshavskii, Yu. S.; Cherkasova, T. G.; Minkin, V. I. *Dokl. Akad. Nauk SSSR. Ser. Khim.* **1982**, *271*, 1164.
41. Naaktgeboreu, A.; Meijer, J.; Vermeer, P.; Brandsma, L. *Recl. Trav. Chim. Pays-Bas* **1975**, *94*, 92.
42. Ladatko, A. A.; Sadevov, I. D.; Minkin, V. I. *Khim. Geterotsikl. Soedin.* **1987**, 279.
43. Kulkarni, Y. D.; Srivastava, S.; Athar, M. *Inf. J. Chem.* **1986**, *25A*, 57.
44. Kulkarni, Y. D.; Saxena, N.; Srivastava, O. P. *Ind. J. Chem.* **1990**, *29A*, 77.

Chemistry of Heterocyclic Compounds, Volume 53
Michael R. Detty, Marrie B. O'Regan

CHAPTER VI

Tellurium-Containing Heterocycles Composed of Group IVa (Carbon, Silicon, Germanium, and Tin) and Group VIa Elements (Tellurium, Selenium, Sulfur, and Oxygen)

This chapter is devoted to the syntheses and spectroscopic properties of tellurium-containing heterocycles in which the ring is composed of one or more group VIa atoms (oxygen, sulfur, selenium, and tellurium) and two or more group IVa atoms (carbon, silicon, germanium, and tin). A variety of different heterocyclic systems have been prepared within these limitations. Tellurium-containing heterocycles, which have been prepared as donor molecules for charge-transfer complexes and that also contain more than one group VIa atom, are considered in Chapter VII.

I. THREE-MEMBERED TELLURIUM-CONTAINING HETEROCYCLES

A. Simple Epitellurides

Epitellurides or telluriranes are relatively short-lived species, which were first detected in the gas phase.[1,2] UV flash photolysis of a mixture of dimethyltelluride and either ethylene or propylene gave epitellurides **1** and **2** as shown in Scheme 1.[1] The parent epitelluride **1** has maxima at 247.2, 241, and 235.6 nm in its absorption spectrum and has a lifetime of several milliseconds. 2-Methyl epitelluride **2** has maxima at 248 and 245.8 nm in its absorption spectrum and gives a parent ion of m/z 172 ($C_3H_6{}^{130}Te$) in its mass spectrum.

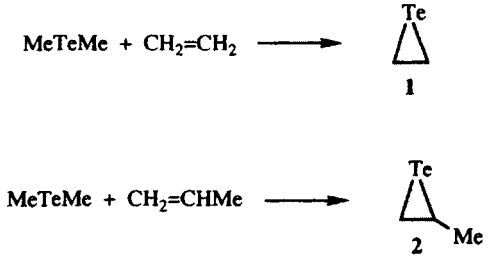

Scheme 1

The electron-impact mass spectrum of benzotellurophene (**3**) displays a very weak ion (0.2%) for loss of acetylene (C_2H_2).[2] As shown in Scheme 2, the observed isotope pattern is consistent with benzoepitelluride cation **4** (m/z 206 for $C_6H_4{}^{130}Te$). However, there is no other supporting evidence for this structure.

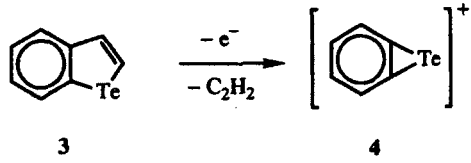

3 4

Scheme 2

Epitellurides have found synthetic utility in transposition reactions of hydroxymethyl epoxides to allylic alcohols.[3-8] The simplest conversion is illustrated in Scheme 3, in which the epoxy tosylate **5** is converted with disodium telluride to the epitelluride **6**, which then loses tellurium to generate the allylic alcohol **7**. From deuterium labeling studies,[8] the epitelluride ring is formed from the two carbon atoms of the starting epoxide and the epoxide oxygen atom has displaced the tosylate oxygen.

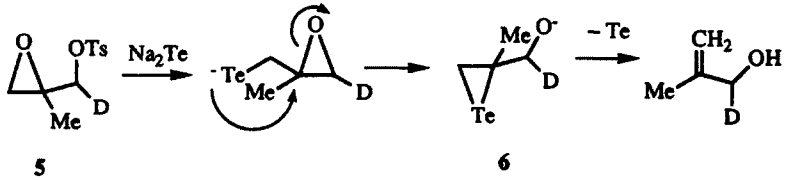

5 6

Scheme 3

With di-, tri-, and tetrasubstituted oxiranes, the epitelluride is formed with a different regiochemical outcome.[8] As shown in Scheme 4, disodium telluride initially displaces the tosylate group in these systems. Intramolecular ring opening of the epoxide generates the epitelluride **8** or **9** with 1,3-transposition of the alcohol functionality. Loss of tellurium generates the corresponding allylic alcohols.

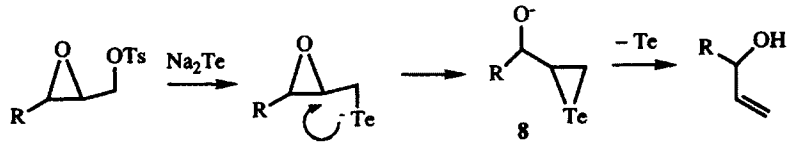

8

R = $PhCH_2CH_2$, *n*-pentyl, *n*-hexyl, Ph, *tert*-Bu, $PhCH_2OCH_2$

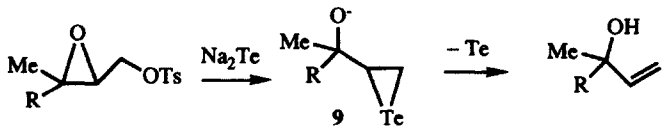

9

R = $Me_2C{=}CHCH_2CH_2$-, $Me_2C{=}CHCH_2CH_2CMe{=}CHCH_2CH_2$-

Scheme 4

B. Epitellurides Containing Silicon, Germanium, and Tin

With the larger group IVa elements silicon, germanium, and tin, stable three-membered-ring compounds containing tellurium can be prepared. The addition of tellurium metal to a benzene solution of silylene **10** at 25°C gives disilatellurirane **11** as shown in Scheme 5.[9] This synthetic approach is also useful for the preparation of disilaselenirane **12a**. The corresponding disilathiirane (**12b**)[10] and disilaoxirane (**12c**)[11] analogs are also known.

The X-ray crystal structures of disilatellurirane **11** and its lighter chalcogen analogs **12** have been determined.[9-11] Values of bond lengths and angles for these compounds are compiled in Table 1. The Si—X bond length decreases

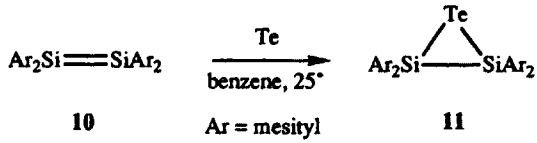

10 Ar = mesityl **11**

Scheme 5

from 2.523 Å in disilatellurirane **11** to 1.732 Å in disilaoxirane **12c**. The Si—X—Si bond angle increases from 55.2° in **11** to 80.0° in **12c**.

The ^{29}Si NMR chemical shifts of the silicon atoms in **11** and **12** also vary monotonically with the heteroatom as shown in Table 1.[9] From a value of − 90.3 ppm for **11**, the chemical shift increases sequentially to − 27.2 ppm for **12c**. The ^{125}Te NMR chemical shift for **11** is highly shielded at δ − 783.8 (vs. Me_2Te), which is consistent with a three-membered ring, and $^1J_{Si-Te}$ is 166 Hz.

Heating cyclotrigermanes **13** at 80°C in benzene leads to digermenes **14** as shown in Scheme 6.[12] In the presence of tellurium metal, addition of tellurium across the germanium–germanium double bonds gives digermanatelluriranes **15** as isolable crystalline solids (mp 158–159°C for **15a** and mp 171–173°C for **15b**).

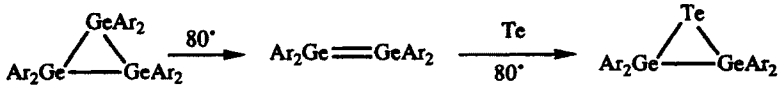

13 **14** **15a**, Ar = mesityl
15b, Ar = 2,6-Et_2Ph

Scheme 6

The digermanatelluriranes **15** are characterized by strong parent ions in their mass spectra with ion clusters from *m/z* 740–755 for **15a** and *m/z* 796–811 for **15b**.[12] The single-crystal X-ray structure of **15b** confirms the structural assignment. In **15b**, the tellurium–germanium bond lengths are 2.597 Å and the germanium–germanium bond length is 2.435 Å. The Ge—Te—Ge angle is 55.9° and the Te—Ge—Ge angles are 62.05°.

Similar chemistry has been utilized to prepare the corresponding tin analogs as shown in Scheme 7.[13] Thermolysis or photolysis of cyclotristannane **16** leads

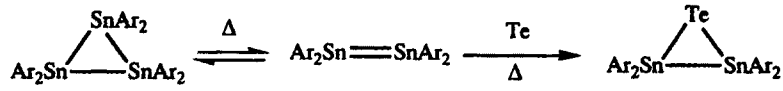

16 **17** **18**

Ar = 2,4,6-(*iso*-Pr)$_3$Ph

Scheme 7

to distannene **17**.[14] The careful addition of a stoichiometric amount of tellurium leads to distannatellurirane **18**.

The single-crystal X-ray structure of **18** is indicative of a nearly equilateral triangle.[13] The tellurium–tin bond lengths of 2.779 and 2.800 Å are nearly identical to the tin–tin bond length of 2.827 Å. Consequently, the three angles are nearly identical with the Sn—Te—Sn angle of 60.9°, one Te—Sn—Sn angle of 59.2°, and the other Te—Sn—Sn angle of 59.9°.

The ^{125}Te and ^{119}Sn NMR spectra of **18** are also consistent with a three-membered ring with δ − 903 (vs. Me_2Te) for tellurium and δ − 594 (vs. Me_4Sn) for tin.[13] The ^{125}Te—^{119}Sn and ^{125}Te—^{117}Sn coupling constants are 844 and 806 Hz, respectively, and the ^{119}Sn—^{117}Sn coupling constant is 3382 Hz.

II. FOUR-MEMBERED TELLURIUM-CONTAINING HETEROCYCLES

A. Telluracyclobutanes

Telluracyclobutane (**19**) was first prepared in 1945 by Farrar and Gulland[15] as shown in Scheme 8. The reaction of 1,3-dibromopropane with disodium telluride in aqueous solution gives **19** as a "foul-smelling oil," which continually precipitates a white solid on standing. The white solid has been described as a polymeric material based on **19**.

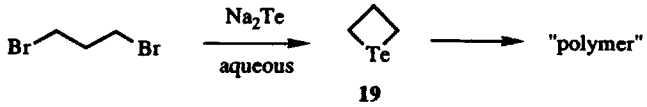

19

Scheme 8

The reaction of *p*-anisyltelluride anion with 1,3-dibromopropane also gives telluracyclobutane products as shown in Scheme 9.[16] In this example, the reaction product is the telluronium salt **20**, which is isolable as a high melting (mp 260–262°C) crystalline solid.

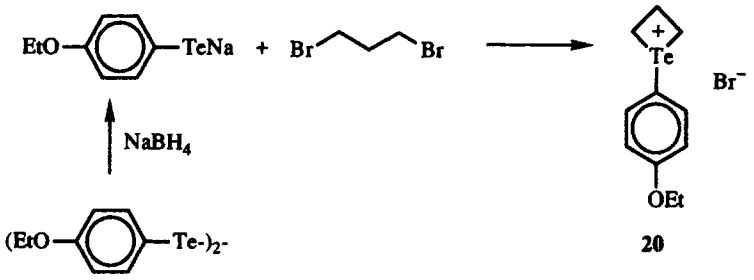

20

Scheme 9

B. Ditelluracyclobutanes

The product isolated from the first synthesis of a ditelluracyclobutane was assigned an incorrect structure in the literature.[17] The reaction shown in Scheme 10 was thought to give ditellurole products and not the two ditelluracyclobutanes **21** and **22**, which are the actual products isolated. The structures of **21** and **22** were assigned unequivocally by single-crystal X-ray crystallographic analysis.[18] The major component of the product mixture is a high-melting solid (mp 270–275°C), which was shown to have the *trans* stereochemistry. The minor component is lower melting (mp 175–177°C) and is assigned the *cis* stereochemistry.

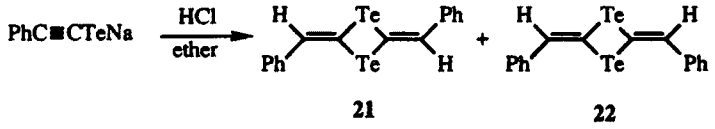

21 **22**

Scheme 10

Both **21** and **22** display strong parent ions in their mass spectra (*m/z* 464 for $C_{16}H_{12}{}^{130}Te_2$).[18] The chemical shifts of the two olefinic protons are nearly identical at δ 8.60 for **21** and δ 8.51 for **22**. The stereochemistry of these two molecules as well as their heterocyclic structure was assigned only following the X-ray structural analysis of **21**. Bond lengths and angles for **21** are compiled in Table 2 according to the numbering scheme shown in Figure 1. The *trans* stereochemistry is present in a nearly planar molecule (except for the phenyl groups). The C—Te—C angles are quite small at 79.8°, although tellurium–carbon and carbon–carbon bond lengths associated with the ring are normal at 2.11–2.12 Å and 1.34 Å, respectively. There are short, intermolecular tellurium interactions at 3.63 Å, which are less than the sum of van der Waals radii (4.40 Å).

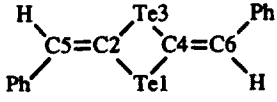

Figure 1. Numbering scheme for ditelluracyclobutane **21**.

The dimerization of telluroketones has also given ditelluracyclobutane products as shown in Scheme 11.[19] Adamantanone is converted to the telluroketone **23** with bis(dimethylaluminum)telluride in dioxane at 100°C. In the absence of other reactive substrates (such as dienes or 1,3-dipolarophiles), telluroketone **23** dimerizes to give ditelluracyclobutane **24** in 28% isolated yield. The mass spectrum of **24** displays a parent ion cluster, which includes *m/z* 528 ($C_{20}H_{28}{}^{130}Te_2$).

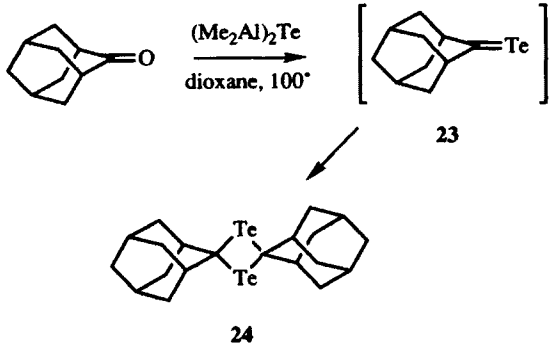

23

24

Scheme 11

C. Four-Membered Tellurium-Containing Heterocycles with Germanium and Tin

Cyclotrigermane **25** reacts with tellurium metal at 20°C as shown in Scheme 12 to give trigermanatelluracyclobutane **26** in 46% isolated yield.[20] The material is a stable crystalline solid.

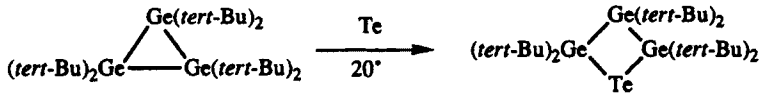

25 26

Scheme 12

The structure of **26** was assigned unambiguously through single-crystal X-ray crystallographic analysis.[20] Bond lengths and angles are compiled in Table 3 according to the numbering scheme in Figure 2. The heterocyclic ring is planar and is nearly a square with bond lengths of 2.583–2.591 Å and four nearly right angles of 88.1–91.8°. The molecule gives a parent ion at m/z 691 in its mass spectrum. The ^{1}H and ^{13}C NMR spectra of **26** are indicative of two different *tert*-butyl groups (δ 1.428 (36 H) and 1.424 (18 H); δ 32.45 and 33.61 for the quaternary carbons and δ 35.60 for the methyl carbons).

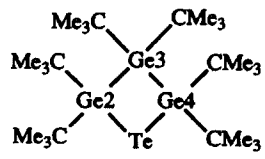

Figure 2. Numbering scheme for trigermantelluracyclobutane **26**.

A 2,4-distanna-1,3-ditelluracyclobutane has been prepared as shown in Scheme 13.[13] The addition of excess tellurium to distannene **17** or to distannatellurirane **18** gives distannaditelluracyclobutane **27** as a high-melting crystalline solid (mp 229–231°C). In solution, **27** is yellow with λ_{max} 460 nm (ε 320). The ^{125}Te NMR spectrum of **27** displays a signal at δ171 (vs. Me_2Te) with $^1J(^{125}Te—^{119}Sn)$ and $^1J(^{125}Te—^{117}Sn)$ couplings of 1975 and 1894 Hz, respectively. The ^{119}Sn NMR spectrum gives a signal at δ −752 (vs. Me_4Sn) with $^2J(^{119}Sn—^{117}Sn)$ of 417 Hz.

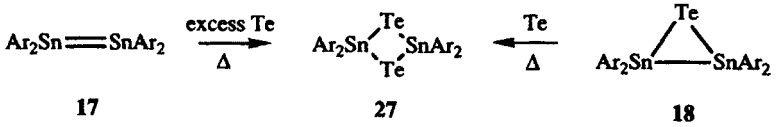

17 **27** **18**

Ar = 2,4,6-(*iso*-Pr)$_3$Ph

Scheme 13

III. FIVE-MEMBERED TELLURIUM-CONTAINING HETEROCYCLES

A. 1,3-Diheteroles

The addition of disodium telluride to chloromethyl acetylenic sulfides **28** gives 5-substituted 1,3-thiatelluroles **29** in excellent yield as shown in Scheme 14.[21] The products are isolated as oils, except for **29d**, which is isolated as a crystalline solid, in 85–90% yields.

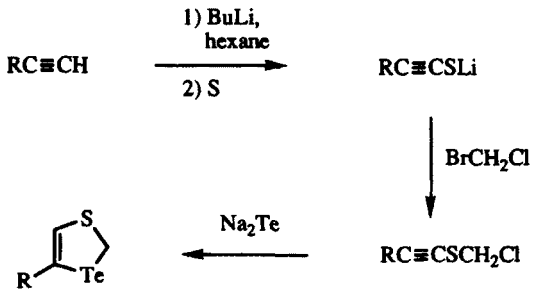

28

29a, R = Me
29b, R = Et
29c, R = *tert*-Bu
29d, R = Ph

Scheme 14

The spectroscopic properties of the thiatelluroles **29** can be compared to those of the thiaheteroles **30** as compiled in Table 4.[21] The mass spectra of diheteroles **29** and **30** show strong parent ions.[22] In the ^{1}H NMR spectra of compounds **29a** and **30**, the protons attached to C2 appear at similar chemical shifts in all three compounds (δ 4.43–4.73), while the olefinic proton attached to C4 appears at higher field from the thiatellurole (**29a**, δ 6.16) to the thiaselenole (**30a**, δ 5.80) to the dithiole (**30b**, δ 5.53). Much larger differences appear in the ^{13}C NMR spectra of these compounds. The chemical shift of C2 is quite sensitive to the nature of the heteroatom with a chemical shift of δ 3.94 for **29a**, δ 27.1 for **30a**, and δ 37.0 for **30b**. The chemical shifts of C4 and C5 vary by up to 14 ppm as the heteroatom changes in the molecule.

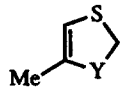

30a, Y = Se
30b, Y = S

Within the series of molecules **29**, substituent changes have minimal effect on the protons attached to C2 and C4 with respect to their ^{1}H NMR chemical shifts. In the ^{13}C NMR spectra of compounds **29**, only C4 appears to be sensitive to substituent effects, varying by nearly 23 ppm within the series of molecules **29**.

Similar chemistry to that employed in Scheme 14 can be utilized in the preparation of 1,3-ditelluroles.[23] As shown in Scheme 15, the addition of an ethanolic solution of dilithium telluride to chloromethyl acetylenic tellurides **31** gives isolable amounts of the ditelluroles **29**. In this particular reaction, disodium telluride did not add to give heterocyclic compounds and required dilithium telluride, which is prepared by the addition of lithium triethylborohydride to a THF slurry of tellurium metal. Following reduction, the THF

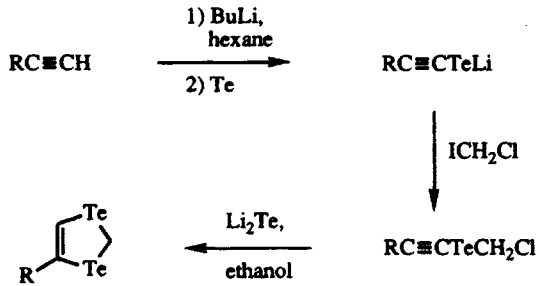

32a, R = H
32b, R = Me
32c, R = *n*-Bu
32d, R = Ph

Scheme 15

solution is diluted with an equal volume of 1 *M* sodium ethoxide in ethanol. With dilithium telluride, **32a** is isolated in 65% yield, **32b** is isolated in 4% yield, **32c** is isolated in 11% yield, and **32d** is isolated in 40% yield.

More highly substituted derivatives of **32** have been prepared by lithiation of the ring with lithium diisopropyl amide (LDA) as shown in Scheme 16.[24] The regiochemistry of lithiation is quite sensitive to substituents. Lithiation of **32d** gives 2-lithio-1,3-ditellurole **33**, which then reacts with a variety of electrophiles to give 2-substituted ditelluroles **34** in 68–91% isolated yields. In contrast, unsubstituted ditellurole **32a** is lithiated with LDA to give 4-lithio-1,3-ditellurole (**35**), which then reacts with electrophiles to give 4-substituted ditelluroles **36** in 40 to 95% yields.

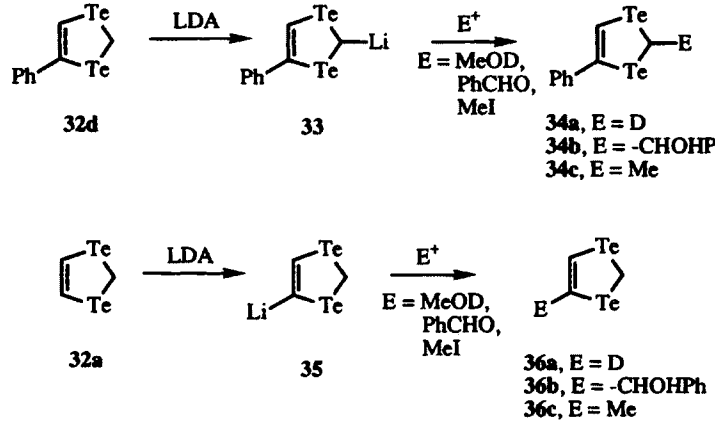

Scheme 16

The ditelluroles **32**, **34**, and **36** are characterized by strong parent-ion clusters in their field desorption mass spectra.[23] Selected ^{1}H and ^{13}C NMR chemical shifts for ditelluroles **32** are compiled in Table 5. With two tellurium atoms in the ring, the protons attached to C4 appear at much lower field (δ 8.07–8.06) than in thiatelluroles **29**, while the protons attached to C2 have chemical shifts (δ 4.65–4.73) quite similar to those of thiatelluroles **29** and thiaheteroles **30** (Table 4). In the ^{13}C NMR spectra of ditelluroles **32**, the chemical shifts of C2 are significantly more shielded (δ -20.7 to -41.9) than the corresponding carbons in thiatelluroles **29**. In the ditelluroles **32**, the chemical shifts of both C4 and C5 are sensitive to substituents with a chemical-shift range of δ 110.7 to 143.7 ppm.

All of the one-, two-, and three-bond coupling constants for the ^{125}Te nucleus with ^{1}H, ^{13}C, and ^{125}Te nuclei in 1,3-ditellurole (**32a**) have been determined and are compiled in Table 6.[25] The ^{125}Te couplings were measured through the use of ^{125}Te-enriched samples of **32a**. The one-bond tellurium–carbon (—CH_2—) coupling is 178.7 Hz while the one-bond tellurium–carbon (=CH—) coupling

is 288.3 Hz, while the two-bond coupling to the latter carbon is 12.3 Hz. The two-bond couplings between tellurium and the methylene protons, and the olefinic protons are 25.9 and 126.5 Hz, respectively, and the three-bond couplings between tellurium and the olefinic protons are 33.5 Hz. The two-bond tellurium–tellurium coupling constant is 260.3 Hz. The chemical shift of ^{125}Te in **32a** is δ − 53.5 from bis(diethyldithiocarbamato)tellurium(II).

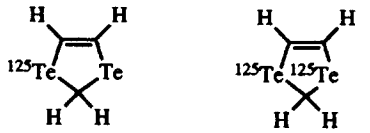

32a-^{125}Te **32a**-$^{125}Te,^{125}Te$

The structure of **32a** has been confirmed by single-crystal X-ray crystallographic analysis according to the numbering scheme in Figure 3.[26] Selected bond lengths and angles are compiled in Table 7. The C—Te—C angles are near 90°, which is typical of organotellurium (II) compounds. To accommodate these angles, the Te—C bond lengths are appropriately long at 2.17 Å to C2 and 2.094 Å to C4 and C5. The Te—C—Te angle is tetrahedral (109.8°), while the Te—C=C angles are near-trigonal (122.9°). The —C=C— bond length of 1.34 A° is a normal double bond.

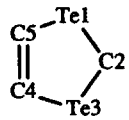

Figure 3. Numbering scheme for 1,3-ditellurole (**32a**).

B. Oxidations of 1,3-Diheteroles: 1,3- and 1,2-Ditellurolylium Salts

Ditellurole **32a** undergoes a one-electron oxidation at + 0.64 V (vs. SCE) to give cation radical **37** (λ_{max} 560 nm) at − 10°C as shown in Scheme 17.[26] At lower temperatures, the cation radical dimerizes to give dimer dication **38** (λ_{max} 610 nm at − 70°C). Warming the solution regenerates the spectrum of the cation radical. Radical cation **37** is oxidized at + 1.12 V (vs. SCE) to give a new species, which is presumably a dication of unknown structure. The cation radical **37** can also lose a proton to generate a neutral radical, which is oxidized at potentials more negative than + 0.64 V to give ditellurolylium cation **40**. Cation **40** undergoes a slow, thermal rearrangement to give 1,2-ditellurolylium cation **41**.

The EPR spectrum of cation radical **37** has been examined in a 1,1,2-trichloro-1,2,2-trifluoroethane (Freon 113) matrix.[26] Irradiation of frozen beads

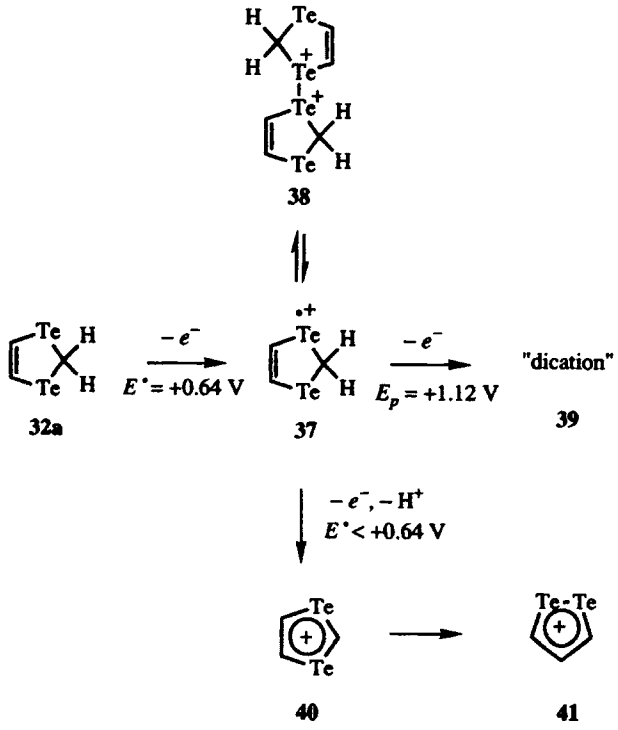

Scheme 17

of **32a** in Freon 113 with X-rays gives rise to a well-resolved 1 : 2 : 1 triplet absorption at 2882 G with g 2.2571 ± 0.0005. The triplet splitting is 21.0 ± 0.1 G. When **32a**-^{125}Te,^{125}Te is irradiated with X-rays, the triplet feature is split to a doublet of triplets feature where the doublet splitting is 260.0 ± 0.5 G, which corresponds to $a_{||}(^{125}\text{Te})$. The doublet feature suggests the unpaired spin is localized on one tellurium atom in cation radical **37**.

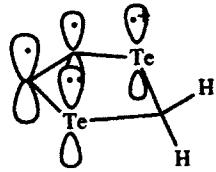

Ditellurolylium cation **40** can be prepared directly by hydride abstraction with trityl fluoroborate as shown in Scheme 18. The cation **40** displays a one-proton triplet at δ15.0 and a two-proton doublet at δ11.81 with a coupling constant of 1.2 Hz in its ^{1}H NMR spectrum. Hydride abstraction from 4-substituted 1,3-ditelluroles **32** may initially give the corresponding 1,3-ditellurolylium cations **42**, but the cations observed by ^{1}H NMR are the rearranged cations **43**.

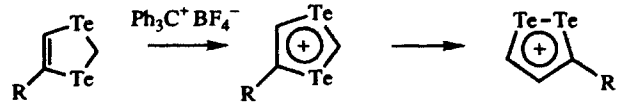

32 40 or 42 41, R = H
43a, R = Me
43b, R = *n*-Bu
43c, R = Ph

Scheme 18

The structures of **41** and **43** are suggested by the ^{1}H NMR spectra of the cations. Chemical shifts and coupling constants are compiled in Table 8.[23] The ring protons appear as doublets with a coupling constant of 6.6–6.9 Hz. The protons on carbons adjacent to tellurium (δ 13.25–13.83) are assigned from the presence of ^{125}Te satellites, while the magnitude of the proton–proton coupling suggests three-bond coupling in the ring. These coupling constants are similar to the approximately 5 Hz coupling constants observed in 1,2-dithiolium cations.[27]

The rearrangement of **40** to **41** can be followed kinetically by ^{1}H NMR.[23] The rearrangement proceeds with Arrhenius parameters of $E_a = 8.56$ kcal mol^{-1} and $\ln A = 2.75$ and Eyring parameters of $\Delta H^{\ddagger} = 8.00$ kcal mol^{-1}, $\Delta S^{\ddagger} = -24$ cal mol^{-1} K^{-1}, and $\Delta G^{\ddagger}_{298} = 15.1$ kcal mol^{-1}. A possible mechanism for this rearrangement is shown in Scheme 19. Deformation of the five-membered

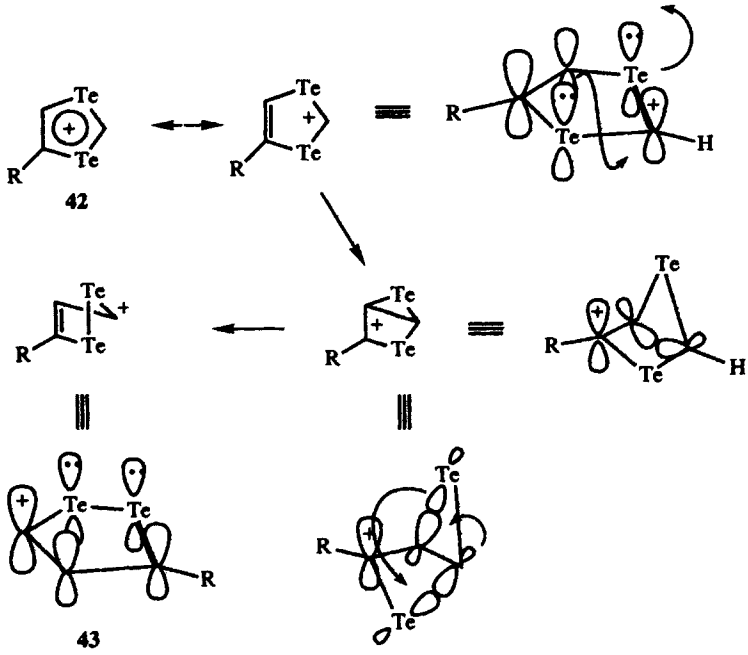

Scheme 19

ring would allow overlap of nonadjacent orbitals. Substituents at the 4-position accelerate the rearrangement (at 0°C, only rearranged cations are observed on hydride abstraction from **32b–d**), which is consistent with cationic character at this position.

In 1,3-thiatellurolylium cations **44**, which do not rearrange at a rapid rate if at all, two-bond $^{125}Te—^{1}H$ coupling constants of 67.5–69 Hz have been observed.[22] The 1,3-diselenolylium cation **45a** has been prepared, and the proton attached to C2 is observed at δ 13.4 in its ^{1}H NMR spectrum.[28] Similarly, 1,3-dithiolylium cation **45b** has been prepared and the proton attached to C2 is observed at δ 11.3 in its ^{1}H NMR spectrum.[28]

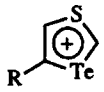

44a, R = Ph
44b, R = Me

45a, Y = Se
45b, Y = S

C. 1,3-Tellurafulvenes

The addition of tellurium to sodium acetylide gives phenylacetylenic telluride **46** as shown in Scheme 20.[29] Protonation of **46** with trifluoroacetic acid gives a mixture of tellurafulvenes **47** and **48**, which can be separated and isolated in 7 and 5% yields, respectively. Treating the pure isomers with acids reestablishes the equilibrium mixture of the two isomers.

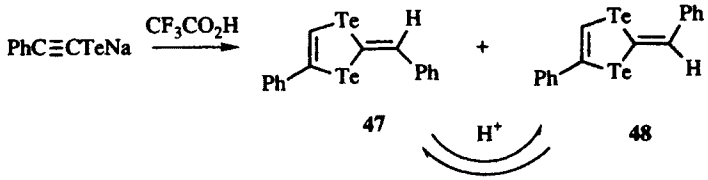

Scheme 20

The tellurafulvenes **47** and **48** are characterized by strong parent-ion clusters in their mass spectra with *m/z* 464 for $C_{16}H_{12}{}^{130}Te_2$.[29] These compounds undergo an irreversible electrochemical oxidation with $E_p^a = +0.724$ V (vs. SCE). The ^{1}H NMR spectra of **47** and **48** show two different one-proton singlets for each molecule in addition to the phenyl protons. For **47**, the two singlets appear at δ 8.85 and 7.86, respectively, while for **48**, the two singlets appear at δ 8.77 and 7.91, respectively.

The mixture of isomers **47** and **48** reacts with phenyldiazonium tetrafluoroborate to give azo compound **49** as shown in Scheme 21.[29] The mixture of isomers **47** and **48** also reacts with isoamyl nitrite to give nitrosyl compound

50.[29] Both **49** and **50** are characterized by strong parent ions in their mass spectra (*m/z* of 568 and 493, respectively, for ^{130}Te as the nominal mass). In addition to the ten aromatic protons, the ^1H NMR spectra of both **49** and **50** display one-proton singlets at δ 9.36 and 10.08, respectively.

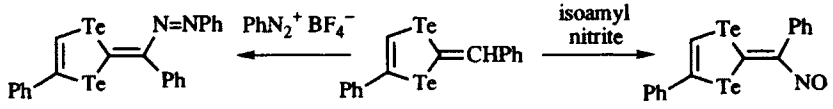

49 **47 and 48** **50**

Scheme 21

The literature contains one report of the reaction of tellurium metal and phenyl acetylene in a mixture of potassium hydroxide, HMPTA, $SnCl_2$, and water to give 1,2-tellurafulvene **51** as shown in Scheme 22.[30] This reaction was reinvestigated by Singh and Wudl, who found that the products of reaction were tellurafulvenes **47** and **48**.[31]

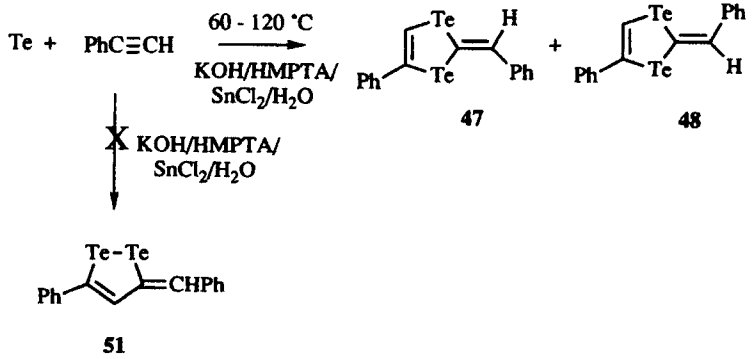

51

Scheme 22

D. 1,2-Ditelluracyclopentanes

The first synthesis of 1,2-ditelluracyclopentane (**52**) may have been realized with the addition of polytelluride dianion to 1,3-dibromopropane as shown in Scheme 23.[32] A blue species is formed in solution and a red, polymeric precipitate falls out of solution.

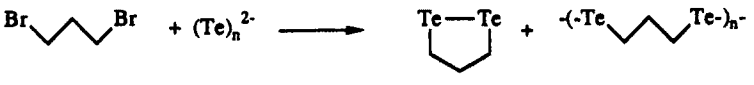

52

Scheme 23

Several 1,2-ditelluracyclopentanes have been prepared by the addition of potassium tellurocyanate to dimethyl sulfoxide solutions of 1,3-dihalides as shown in Scheme 24.[33] Reaction with 1,3-dibromopropane gives 1,2-ditelluracyclopentane (**52**). With 3,3-bis(chloromethyl)oxetane (**53**), spiro 1,2-ditelluracyclopentane **54** is isolated in 65% yield as a crystalline solid, mp 170°C. With 1,1-bis(tosyloxymethyl)cyclobutane (**55**), spiro 1,2-telluracyclopentane **56** is isolated in 21% yield as a crystalline solid, mp 98°C.

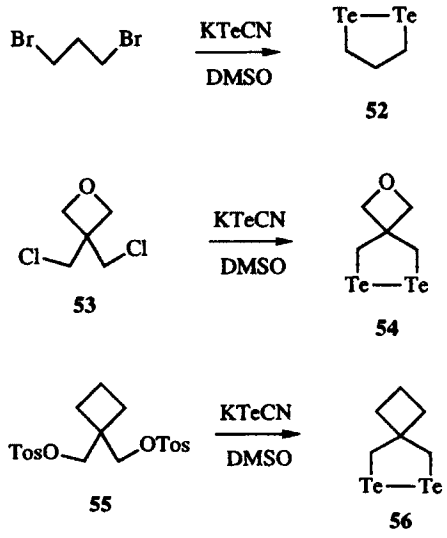

Scheme 24

Selected ^{1}H, ^{13}C, and ^{125}Te NMR spectral data are compiled in Table 9 for **52**, **54**, and **56**, respectively.[33] The ring protons appear between δ 3.42 and 3.843. In **52**, the coupling constant between adjacent methylene protons is 6.2 Hz. In the ^{13}C NMR spectra, the carbon atoms attached to tellurium are shielded (δ 18.0 for **54** and δ 12.8 for **56**). The spiro carbons are further downfield at δ 57.6 for **54** and at δ 56.4 for **56**. The ^{125}Te chemical shifts are δ 57.1 for **54** and δ 50.0 for **56**, which are typical for tellurium(II). The $^{2}J_{Te-H}$ coupling constants are 27.5 Hz for **54** and 29 Hz for **56**.

Compounds **54** and **56** are characterized by strong parent-ion clusters in their mass spectra (*m/z* 344 for $C_5H_8O\,^{130}Te_2$ in **54** and *m/z* 342 for $C_6H_{10}\,^{130}Te_2$ in **56**).[33] In solution, the molecules **52**, **54**, and **56** appear blue with weak absorption maxima around 690 and 600 nm (Table 9). The blue color may arise from Te—Te overlap, which is indicated by a dihedral angle of 8.5° in the single-crystal X-ray structure of **54**.[33]

E. Germanium- and Tin-Containing Tellurium Heterocycles

The addition of sodium hydrogentelluride to octaphenyl tetragermane diiodide **57** gives octaphenyl tetragermanatelluracyclopentane **58** as shown in Scheme 25.[34] Compound **58** is air-sensitive and is thermally labile at 50°C or above.

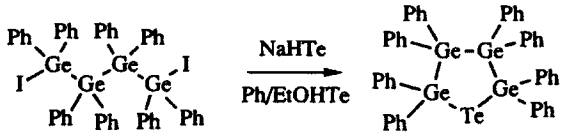

57 **58**

Scheme 25

Similar chemistry has been utilized for the preparation of a tin derivative.[35] As shown in Scheme 26, the reaction of tellurium metal with diiodide **59** gives octa-*tert*-butyl tetrastannatelluracyclopentane **60** as a crystalline solid. The structure of **60** has been unequivocally assigned through single-crystal, X-ray crystallographic analysis.

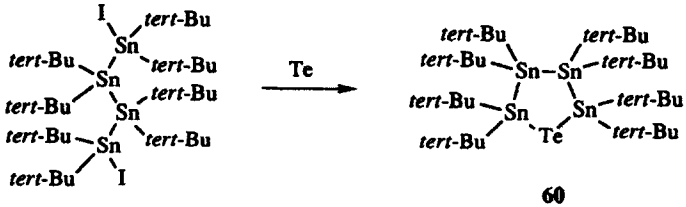

59 **60**

Scheme 26

Selected bond lengths and angles for **60** are compiled in Table 10 according to the numbering scheme shown in Figure 4.[35] The Te—Sn and Sn—Sn bond lengths are similar, and, as a consequence, the angles of the heterocyclic ring are near those of the 108° ideal angle for a five-membered ring. However, the molecule is nonplanar and the 273.2° phase angle is near that for an ideal twist form of 270°.

2,2,3,3,4,4,5,5-Octamethyl-2,3,4,5-tetrastannatelluracyclopentane (**61**) has been prepared by a somewhat different procedure as shown in Scheme 27.[36] The addition of sodium hydrogen telluride to tetramethyl distannane dichloride gives 2,3,5,6-tetramethyl-1,4-ditelluracyclohexane **62**. Photolysis of **62** leads to

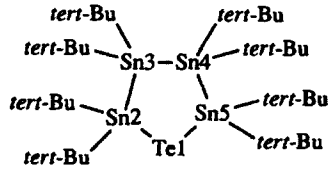

Figure 4. Numbering scheme for 2,2,3,3,4,4,5,5-octa-*tert*-butyl-2,3,4,5-tetrastannatelluracyclopentane (**60**).

loss of either a tellurium atom or a dimethyltin unit from the ring to give a mixture of **61** and 2,4,5-tristanna-1,3-ditellurole **63**. By ^{1}H NMR, two distinct methyl groups are observed in both **61** and **63**. In **61**, the two signals are observed at δ 0.76 for the methyls at the 2- and 5-positions and at δ 0.40 for the methyls at the 3- and 4-positions. In **63**, the methyl groups attached to the 2-position of the ring are observed at δ 0.93 and the methyl groups attached to the 4- and 5-positions are observed at δ 0.64.

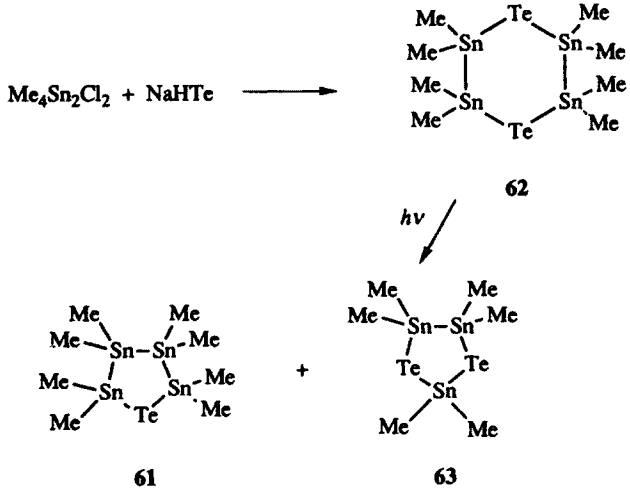

Scheme 27

IV. SIX-MEMBERED TELLURIUM-CONTAINING HETEROCYCLES

A. Tetrahydrotelluropyrans with One Other Group VIa Element

The addition of disodium telluride to 2,2′-dichlorodiethyl ether gives 4-oxatetrahydrotelluropyran **64** as shown in Scheme 28.[15] The addition of the

halogens to **64** gives crystalline tellurium(IV) derivatives **65–67** from oxidative addition of chlorine, bromine, and iodine, respectively. Alternatively, diiodide **67** can be prepared directly from 2-2′-dichlordiethyl ether, tellurium metal, and sodium iodide.[37] The tellurium derivatives are reduced to **64** with either sodium bisulfite[15] or hydrazine hydrate.[37]

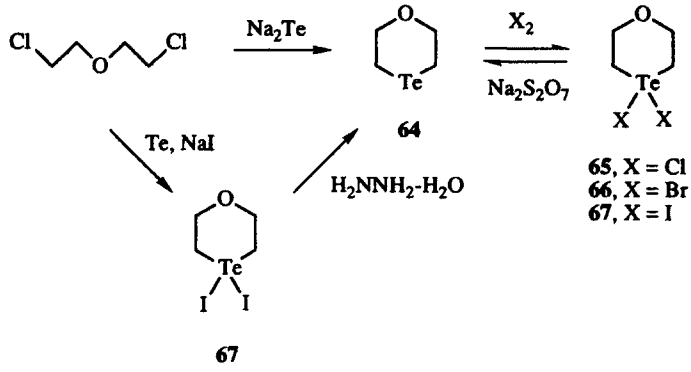

Scheme 28

The structure of 1,1-diiodo derivative **67** has been determined unequivocally by single-crystal X-ray crystallographic analysis.[38] The heterocyclic ring is in a chair conformation. The tellurium atom is displaced 0.682 Å from the carbon plane, while the oxygen atom is displaced −0.725 Å. These deformations describe dihedral angles of 27.5 and 70°, respectively. Selected bond lengths and angles are compiled in Table 11 according to the numbering scheme shown in Figure 5. The C—Te—C angle of 94.1° is typical of unconstrained C—Te—C angles. The I—Te—I angle is nearly linear at 177.1°, consistent with a three-center, four-electron bond.

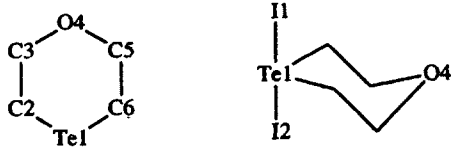

Figure 5. Numbering scheme for 1,1-diiodo-4-oxatetrahydrotelluropyran **67**.

Little spectroscopic information is available for these compounds. The ^{1}H NMR spectrum of **67** is characterized by a four-proton multiplet at δ 3.24 for the protons on carbons adjacent to tellurium and a four-proton multiplet at δ 4.42 for the protons on carbons adjacent to oxygen.

Similar chemistry has been employed to prepare 4-thiatetrahydrotelluropyran (**68**) as shown in Scheme 29.[39] The addition of disodium telluride to 2,2′-dichlorodiethylsulfide gives a 6.6% yield of **68**. The addition of halogens to **68**

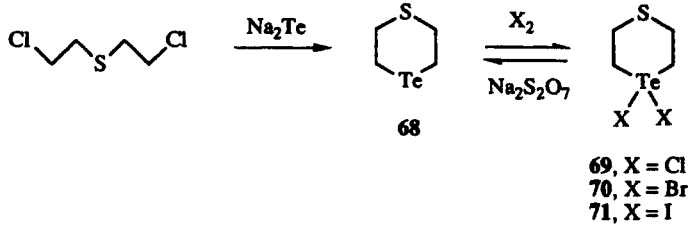

Scheme 29

gives the corresponding tellurium(IV) dihalides **69–71** from oxidative addition of chlorine, bromine, and iodine, respectively.

The structure of 1,1-diodo derivative **71** has been assigned unequivocally through single-crystal X-ray crystallographic analysis.[40] Selected bond lengths and angles are compiled in Table 12 according to the numbering scheme in Figure 6. Like **67**, the conformation of **71** is chair-like. The C—Te—C and C—S—C angles are both 100° in this molecule. The tellurium atom is displaced 0.63 Å from the carbon plane, while the sulfur atom is displaced − 0.57 Å. The dihedral angles described by these deformations are 26 and 64°, respectively. An interesting consequence of these angles is the observation that the sulfur atom lies in the C2—Te1—C6 plane. Again, the I—Te—I angle is nearly linear at 178.1°.

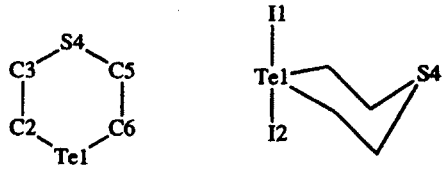

Figure 6. Numbering scheme for 1,1-diiodo-4-thiatetrahydrotelluropyran (**71**).

The reactions of **64** and **68** with iodine are quite different than the reactions of diselenane and dithiane with iodine.[41,42] With both of these molecules, crystalline complexes with iodine are formed whose single-crystal X-ray structures reveal structures **72** and **73** for the charge-transfer complexes of diselenane and dithiane with iodine, respectively. Interestingly, approach of iodine is equatorial

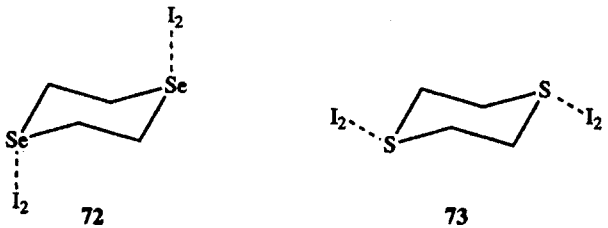

with dithiane but axial with diselenane. The X-ray crystal structures of **67** and **71** suggest that the initial approach of iodine to the tellurium heterocycles is most likely from the axial direction, which would suggest an initial charge-transfer complex resembling **72** with respect to tellurium–iodine bonding. A second reaction must break the iodine–iodine bond to form covalent tellurium–iodine bonds.

Both **64** and **68** react with various alkyl halides to give telluronium heterocycles as shown in Scheme 30.[37,39] The addition of iodomethane to **68** in acetone gives **74** in 82% isolated yield. A variety of alkyl and allyl halides react with **64** to give telluronium salts **75**.

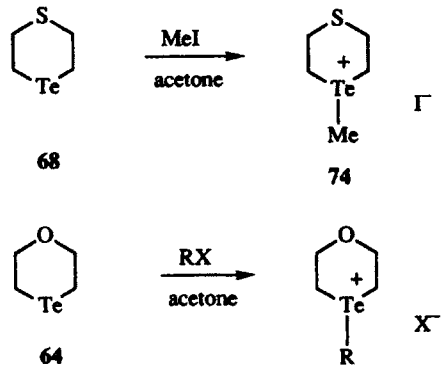

68 **74** **64**

75a, R = Me, X = I
75b, R = Me, X = ClO_4
75c, R = Et, X = BPh_4
75d, R = allyl, X = I
75e, R = allyl, X = Br
75f, R = *n*-Bu, X = I

Scheme 30

B. Six-Membered Tellurium Heterocycles Containing Silicon

The addition of dipotassium telluride to ethanolic solutions of dihalo tetraalkylsilanes **76** and **77** gives 3-silatetrahydrotelluropyrans **78** and **79** as shown in Scheme 31.[43] By ^1H NMR, the chemical shifts of 3-silatetrahydrotelluropyrans **78** and **79** are very similar to those of the tetrahydrotelluropyrans (Chapter 3), with the exception of silicon shielding of the protons attached to carbon atoms adjacent to silicon. For **78a**, the protons attached to C6 appear at δ 2.58 and, for **79**, these protons appear at δ 2.50 and 2.45. The protons attached to the carbon between the silicon and tellurium atoms (C2) are shielded by the silicon atom. In **78a**, these protons appear at δ 1.52 and, in **79**, these protons appear at δ 1.90 and 1.05. The protons attached to C4 are also shielded by silicon appearing at δ 0.62

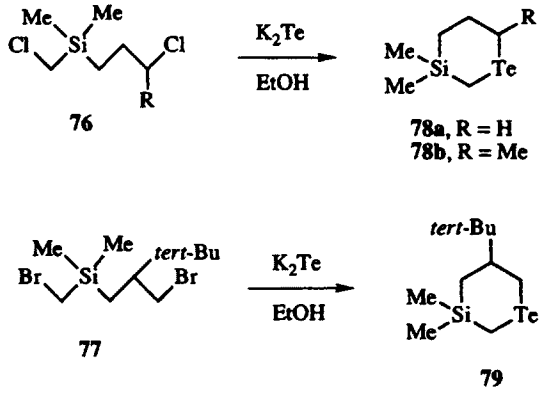

Scheme 31

in **78a** and at δ 0.79 and 0.20 in **79**. The protons attached to C5 appear at δ 2.36 in **78a** and at δ 1.90 in **79**.

The reduction of tellurium with sodium borohydride in the presence of dichloro disiloxane gives **80** as shown in Scheme 32.[44] Oxidative addition of chlorine, bromine, and iodine gives tellurium(IV) derivatives **81**–**83**, respectively, in nearly quantitative yield. The tellurium(IV) derivatives are reduced back to **80** with hydrazine hydrate. Alternatively, the reaction of sodium iodide and tellurium metal with dichlorodisiloxane in glyme gives **83** in one pot.

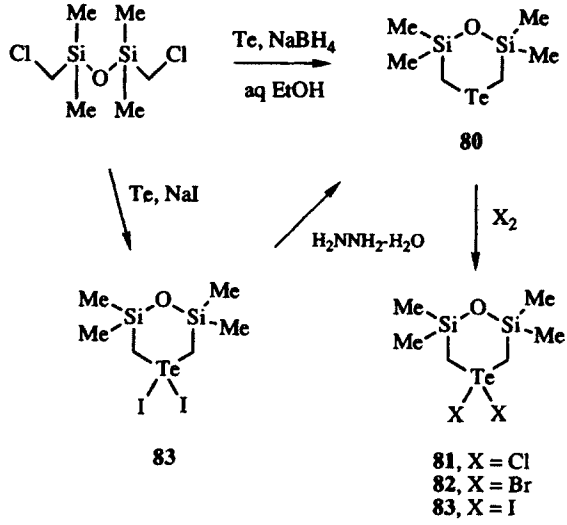

Scheme 32

The structure of **83** has been assigned unequivocally via single-crystal X-ray crystallographic analysis.[44] Selected bond lengths and angles are compiled in

Table 13 according to the numbering scheme in Figure 7. The conformation of **83** is an abnormal boat with C2 and Si5 out of the plane of the other four ring atoms. This may be a consequence of the large Si—O—Si angle of 144.3°. The C—Te—C angle is also large at 105.2°. The tellurium–carbon bond lengths are approximately 2.14 Å, while the silicon–oxygen bond lengths are approximately 1.61 Å. The I—Te—I angle is nearly linear at 178.3°.

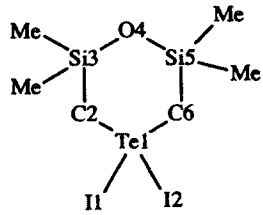

Figure 7. Numbering scheme for 1,1-diiodo-3,5-disila-4-oxatetrahydrotelluropyran **83**.

Disilaoxatetrahydrotelluropyran **80** is alkylated by both iodomethane and benzylbromide to give telluronium salts **84** and **85** as shown in Scheme 33.[44] The telluronium salts show a conformational preference on the ^{1}H NMR time scale. In both **84** and **85**, the ring methylene protons are split into an *AB*-quartet pattern.

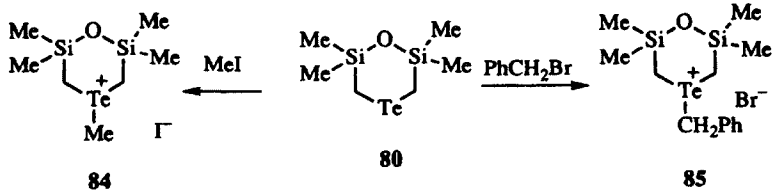

Scheme 33

Selected ^{1}H and ^{13}C NMR chemical shifts are compiled in Table 14 for compounds **80–85**.[44] The chemical shift of the ring methylene protons moves to lower field with a tellurium(IV) oxidation state. The alkylation of the tellurium atom in the ring also moves the chemical shift of these protons to lower field. The chemical shifts of the protons on the silyl methyl groups are little affected by changes at the tellurium atom. Interestingly, the magnitude of the ^{125}Te—C^{1}H$_2$ coupling constant increases as the tellurium atom is oxidized from tellurium(II) to tellurium(IV). In the mass spectra of **80** and **83**, strong parent-ion clusters are observed.

C. Six-Membered Tellurium Heterocycles Containing Tin

The preparation of 2,3,5,6-tetrastannaditelluracyclohexane **62** is described in Scheme 27.[36] Compound **62** exhibits a strong parent-ion cluster with a nominal mass of m/z 852 for $C_8H_{24}Sn_4{}^{130}Te_2$. The methyl protons are observed at δ 0.75 in the ^{1}H NMR spectrum of **62**, while the methyl carbons are observed at δ − 4.45 in the ^{13}C NMR spectrum of **62**.

V. SEVEN-MEMBERED TELLURIUM-CONTAINING HETEROCYCLES

A few examples of seven-membered tellurium-containing heterocycles have been described in the literature. As shown in Scheme 34, lithium–halogen exchange in diarylethane **85** gives dilithio derivative **86**.[45] The addition of tellurium diiodide to **86** gives a 32% yield of dibenzotelluracycloheptadiene **87**. The addition of bromine to **87** gives oxidative addition to tellurium(IV) derivative **88**. Sodium borohydride reduction of **88** regenerates **87**.

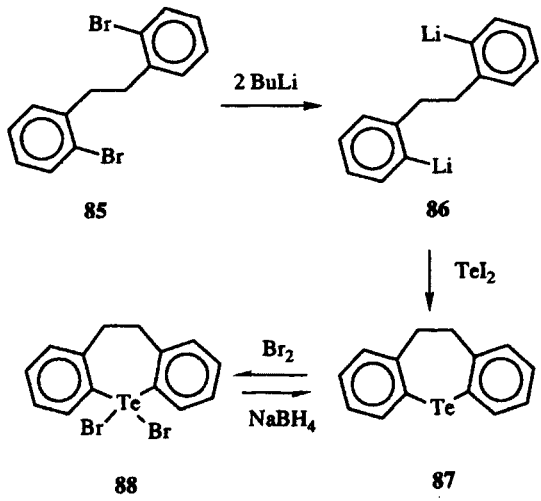

Scheme 34

The addition of disodium telluride to diacetylene **89** at room temperature in aqueous benzene in the presence of a phase-transfer catalyst and hydrazine hydrate gives 7-tellurabenzocycloheptatriene **90** in 60 to 70% yield as shown in Scheme 35.[46] Compound **90** reacts with thionyl chloride to give tellurium(IV) derivative **91** in nearly quantitative yield and reacts with bromine to give dibromide **92**. Compound **90** is thermally labile at ambient temperature or above. Tellurium extrusion is observed with the formation of naphthalene.

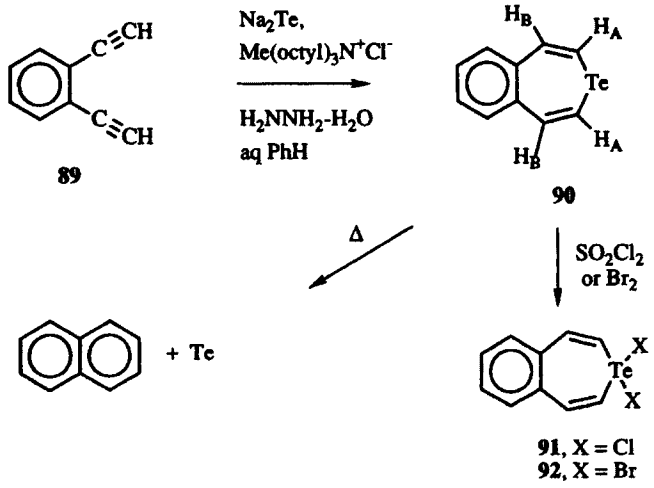

Scheme 35

Selected ^{1}H and ^{13}C NMR chemical shifts for compounds **90–92** are compiled in Table 15.[46] The tellurium oxidation state has very little effect on the chemical shifts of the ring protons. The proton–proton coupling constant of 10.3–10.5 Hz is consistent with a *cis*-olefinic coupling constant. The carbon bearing tellurium appears to be shielded relative to the β-carbon from tellurium.

VI. EIGHT-MEMBERED RINGS CONTAINING TELLURIUM

The addition of two equivalents of disodium telluride to 1,3-dibromopropane gives disodium ditelluride **93**.[47] The addition of a second equivalent of 1,3-dibromopropane under high dilution conditions gives 1,5-ditelluracyclooctane (**94**) as shown in Scheme 36. Compound **94** undergoes oxidation with iodine not to give the product of oxidative addition, but to give the product of transannular oxidation, **95**.[48] The addition of chlorine to **94** gives bicyclo product **96**. In a similar transannular reaction, oxidation of **94** with two equivalents of either nitrosyl tetrafluoroborate or nitrosyl hexafluorophosphate leads to dications **97**, which have formed a transannular bond.[47] Dications **97** are reduced with sodium borohydride to regenerate **94**, presumably via an electron transfer reaction with the borohydride reducing agent.

The ^{1}H, ^{13}C, and ^{125}Te NMR spectra of **94–97** display some interesting similarities and differences as compiled in Table 16. The dication **97** and neutral "parent" **94** both have tellurium atoms in the + 2 oxidation state. The chemical shifts of the ring protons fall in similar regions in both compounds. In tellurium(IV) derivatives **95** and **96**, the ring protons are at roughly 0.5 ppm to lower field. Chemical shifts of the ring carbons vary by approximately 30 ppm at the carbons adjacent to tellurium and by nearly 20 ppm at the internal

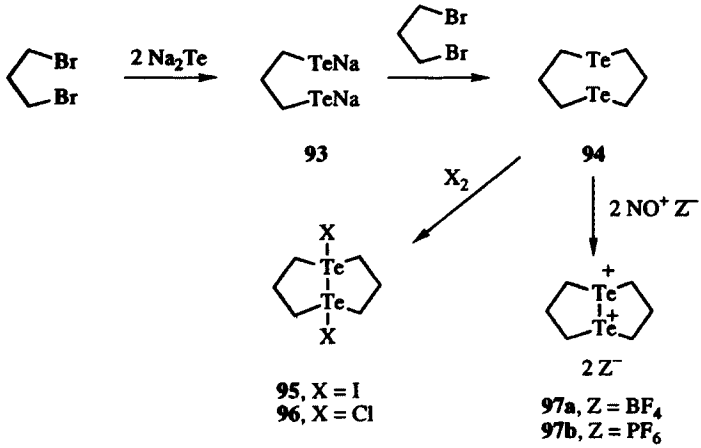

Scheme 36

methylene carbons. The ^{125}Te NMR chemical shifts vary by more than 1100 ppm in this series of compounds. The tellurium(II) derivatives show the extremes at δ 164 for **94** and δ 1304 for **97**. The latter value reflects the doubly cationic nature of the molecule. The ^{125}Te NMR chemical shifts of the tellurium(IV) derivatives **95** and **96** are more typical of values observed for other tellurium(IV) compounds at δ 706 for **95** and δ 1008 for **96**.

Dibenzo analogs of **94–97** have been prepared as shown in Scheme 37.[49–51] *o*-Tolyl telluride serves as the starting material for these materials. Oxidation with bromine gives the dibromo aryltelluride, which is converted to the dibenzylicbromide **98** with *N*-bromosuccinimide with photochemical initiation. The addition of disodium chalcogenides to **98** gives chalcogenatelluradibenzocyclooctadienes **99** with reduction of tellurium(IV) to tellurium(II).

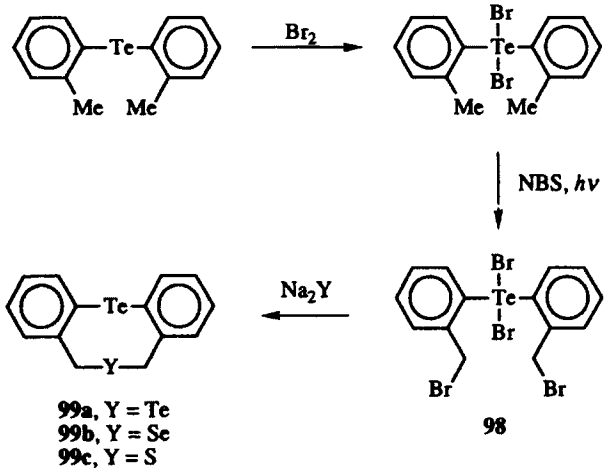

Scheme 37

Selected ^{1}H, ^{13}C, and ^{125}Te NMR chemical shifts for the compounds **99** are compiled in Table 17.[49-51] These molecules exist in both "chair" and "boat" forms, which can be observed on the NMR time scale. The methylene protons are split into an *AB* quartet in both conformations and discrete carbon and tellurium resonances are observed for each conformation. The boat form appears to predominate in solution.

The heteroatoms of compounds **99** undergo a variety of oxidation reactions, which can involve transannular participation of both heteroatoms. Exceptions to this are shown in Scheme 38, where addition of bromine to **99c** appears to give oxidative addition across the tellurium atom to give tellurium(IV) derivative **100**.[50] Hydrolysis of **100** with aqueous sodium hydroxide gives telluroxide **101**, which reacts with acetic anhydride or trifluroacetic anhydride to give **102** or **103**, respectively. Selected NMR chemical shifts for these compounds are compiled in Table 17. The NMR data suggest a single (boat?) conformation for these molecules.

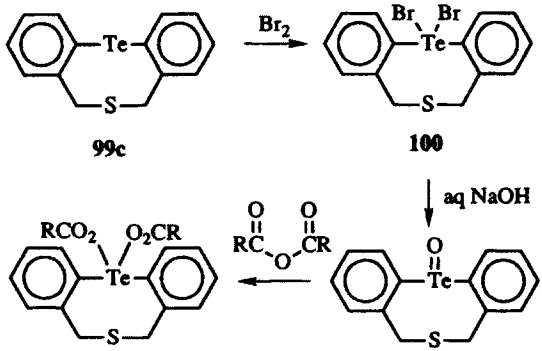

Scheme 38

The oxidation of **99c** with either two equivalents of nitrosyl hexafluorophosphate or with deterosulfuric acid generates bicyclo dications **104** as shown in Scheme 39.[49] Selected NMR chemical shifts for these cations are compiled in Table 17. The cations **104** appear to be in a boat conformation, which is distorted in the case of the hexafluorophosphate salts. The most striking feature of the NMR spectra is the nearly 1000 ppm downfield shift of the ^{125}Te resonance on oxidation, which is similar to the large shift observed on oxidation of **94** to **97**. The magnitude of the shift is most likely related to the doubly positive charge on the molecule since the tellurium atoms are formally in the tellurium(II) oxidation state.

The addition of iodine to **99a** presumably generates the transannular-oxidized tellurium(IV) derivative **105** as shown in Scheme 40.[51] The ^{125}Te NMR spectrum of **105** (Table 17) indicates that both tellurium atoms are downfield (δ 602

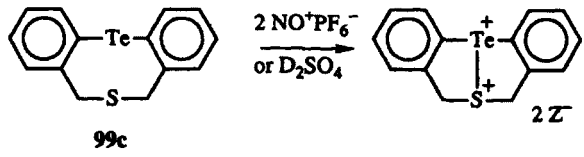

99c

104a, Z = PF_6
104b, Z = $DOSO_3$

Scheme 39

and 946) relative to the starting **99a** (δ 533–565 and 677–703), which is consistent with oxidation of both tellurium atoms. However, it should be noted that the oxidation of **94** with iodine gives a much more pronounced effect on ^{125}Te NMR chemical shifts (δ 164 in **94** to δ 706 in **95** for both tellurium atoms). Proton and carbon chemical shifts are consistent with those expected from oxidation of tellurium.

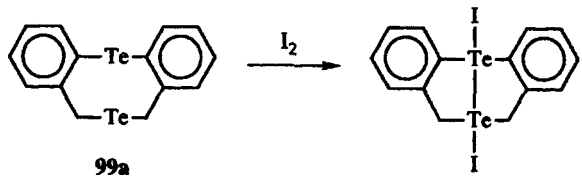

99a **105**

Scheme 40

The oxidation state of tellurium in **95**, **96**, and **105** is not easily described in terms of tellurium(IV) and tellurium(II) states. In one view of bonding in these molecules, oxidation by iodine would generate one tellurium(IV) center that is stabilized by iodide and the transannular tellurium atom as two-electron donor ligands. The resulting "bond" is a three-center, four-electron bond to

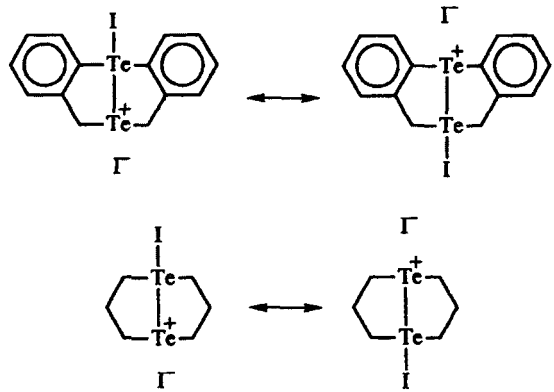

tellurium(IV), which is stabilized transannularly by tellurium(II). Assuming that either tellurium atom can be oxidized in **94** or **99a**, the net tellurium oxidation state at each tellurium atom is going to be between tellurium(II) and tellurium(IV) and the covalent iodine–tellurium bonds should be exceptionally long. Heterocycles containing this bonding array are discussed extensively in Chapter VIII.

The oxidation of **99b** with bromine gives a new product **106** in which the ^{125}Te chemical shift of the tellurium atom is dramatically downfield relative to the starting **99b** (δ 1239 for **106** and 570 for **99b**). The ^{77}Se chemical shift is relatively unaffected by this oxidation (δ 412 in **99b** and δ 361 in **106**). The proton and carbon NMR spectra are little affected by the oxidation. The two most likely structures for **106** are shown in Scheme 41 as resonance forms since the "onium" oxidized form should be stabilized by transannular donation of an electron pair and the "ate" form could also be stabilized by a "short" intramolecular Te···Se interaction. This type of interaction is discussed more extensively in Chapter 8.

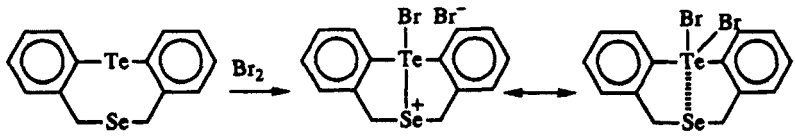

99b **106**

Scheme 41

VII. TELLURIUM-CONTAINING MACROCYCLES

The preparation of a 10-tellurabenzo-15-crown-5 ether **107** has been described.[52] The platinum complex of this molecule has been utilized as a catalyst for the hydrosilylation of olefins with triethoxysilane.

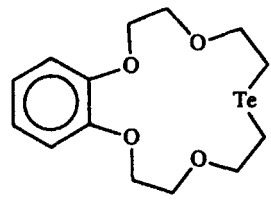

107

TABLES

TABLE 1. COMPARISON OF BOND LENGTHS (Å), BOND ANGLES (°), AND ^{29}Si NMR CHEMICAL SHIFTS IN DISILACHALCOGENIRANES **11** AND **12**

Compd.	Si—X	Si—Si	Si—X—Si	Si—Si—X	δ ^{29}Si (vs. TMS)	Ref.
11	2.523	2.337	55.2	62.4	− 90.3	9
12a	2.303	2.303	59.9	60.05	− 64.8	9
12b	2.161	2.289	64.0	58.0	− 59.0	10
12c	1.732	2.227	80.0	50.0	− 27.2	11

TABLE 2. BOND LENGTHS (Å) AND ANGLES (°) IN DITELLURACYCLOBUTANE **21**[a]

Bond Length	(Å)	Angle	(°)
Te1—C2	2.118	Te1—C2—Te3	100.3
C2—Te3	2.112	C2—Te3—C4	79.8
Te3—C4	2.118	Te1—C4—Te3	100.3
C4—Te1	2.112	C2—Te1—C4	79.8
C2—C5	1.34		
C4—C6	1.34		
Te1···Te1′	3.63		

[a] Reference 18.

TABLE 3. BOND LENGTHS (Å) AND ANGLES (°) FOR TRIGERMANATELLURACYCLOBUTANE **26**[a]

Bond Length	(Å)	Angle	(°)
Te1—Ge2	2.589	Te1—Ge2—Ge3	91.8
Ge2—Ge3	2.583	Ge2—Ge3—Ge4	88.4
Ge3—Ge4	2.585	Ge3—Ge4—Te1	91.7
Ge4—Te1	2.591	Ge2—Te1—Ge4	88.1

[a] Reference 20.

TABLE 4. ^1H AND ^{13}C NMR CHEMICAL SHIFTS FOR 5-SUBSTITUTED 1,3-THIATELLUROLES **29** AND 1,3-HETEROLES **30**[a]

Compd.	R	H5 (δ, ppm)	H2 (δ, ppm)	$^2J_{Te-H2}$ (Hz)	C2 (δ, ppm)	C4 (δ, ppm)	C5 (δ, ppm)
29a	Me	6.16	4.73	21.0	3.94	117.8	125.4
29b	Et	6.23	4.70	—	2.20	127.5	122.9
29c	*tert*-Bu	6.16	4.60	—	1.41	140.1	121.0
29d	Ph	6.70	4.66	19.3	2.79	128.3	122.9
30a	Me (Y = Se)	5.80	4.43	—	27.1	129.2	115.5
30b	Me (Y = S)	5.53	4.43	—	37.0	130.7	111.4

[a] Reference 21.

TABLE 5. ^1H AND ^{13}C NMR CHEMICAL SHIFTS FOR 1,3-DITELLUROLES **32**[a]

Compd.	R	H5 (δ, ppm)	H2 (δ, ppm)	$^2J_{Te-H2}$ (Hz)	C2 (δ, ppm)	C4 (δ, ppm)	C5 (δ, ppm)
32a	H	8.86	4.73	25.9	− 39.0	120.0	120.0
32b	Me	8.87	4.73	—	− 40.6	136.1	112.4
32c	*n*-Bu	8.10	4.65	—	− 41.9	143.7	110.7
32d	Ph	8.57	4.73	—	− 20.7	143.1	141.6

[a] Reference.

TABLE 6. ONE-, TWO-, AND THREE-BOND COUPLING CONSTANTS FOR ^1H, ^{13}C, AND ^{125}Te NUCLEI IN 1,3-DITELLUROLE (**32a**)

Coupling Constant	J (Hz)
^1J (^{125}Te—$^{13}CH_2$)	178.7
^1J (^{125}Te—^{13}CH)	288.3
^2J (^{125}Te—^{13}CH)	12.3
^2J (^{125}Te—C^1H_2)	25.9
^2J (^{125}Te—C^1H)	126.5
^3J (^{125}Te—C^1H)	33.5
^2J (^{125}Te—^{125}Te)	260.3
^3J (^1H—^1H)	8.12

TABLE 7. SELECTED BOND LENGTHS (Å) AND ANGLES (°) FOR 1,3-DITELLUROLE (**32a**)

Bond Length	(Å)	Angle	(°)
Te1—C2	2.17	Te1—C2—Te3	109.8
Te1—C5	2.094	C2—Te3—C4	92.2
Te3—C2	2.17	Te3—C4—C5	122.9
Te3—C4	2.094	C4—C5—Te1	122.9
C4—C5	1.34	C5—Te1—C2	92.2
Te1 ··· Te1′	3.864		
Te1 ··· Te1″	3.895		

TABLE 8. ^{1}H NMR CHEMICAL SHIFTS AND COUPLING CONSTANTS IN RING PROTONS OF 1,2-DITELLUROLYLIUM CATIONS **41** AND **43**[a]

		H4	H5	
Compd.	R	(δ, ppm)		$^3J_{H4-H5}$ (Hz)
41	H	10.31	13.83	6.9
43a	Me	10.20	13.40	6.6
43b	*n*-Bu	10.15	13.25	6.6
43c	Ph	10.61	13.30	6.9

[a] Reference 23.

TABLE 9. ^{1}H, ^{13}C, AND ^{125}Te NMR CHEMICAL SHIFTS AND ABSORPTION MAXIMA FOR 1,2-DITELLURACYCLOPENTANES **52**, **54**, AND **56**[a]

			C3	C4	C5		
Compd.	H3,5 (δ) (vs. TMS)	H4	(δ) (vs. TMS)			^{125}Te (δ) (vs. Me_2Te)	λ_{max} (ε) (nm) (in CS_2)
52	3.42	3.843	—	—	—	—	690.5, 601
54	3.65	—	18.0	57.6	18.0	57.1	697 (308), 602 (279), 381 (2347)
56	3.46	—	12.8	56.4	12.8	50.0	696 (308), 603 (270)

[a] Reference 33.

TABLE 10. SELECTED BOND LENGTHS (Å) AND ANGLES (°) FOR 2,2,3,3,4,4,5,5-OCTA-*tert*-BUTYL-2,3,4,5-TETRASTANNATELLURACYCLOPENTANE (60)[a]

Bond Length	(Å)	Angle	(°)
Te1—Sn2	2.748	Te1—Sn2—Sn3	109.0
Sn2—Sn3	2.879	Sn2—Sn3—Sn4	104.5
Sn3—Sn4	2.889	Sn3—Sn4—Sn5	103.3
Sn4—Sn5	2.869	Sn4—Sn5—Te1	109.9
Te1—Sn5	2.743	Sn2—Te—Sn5	107.4

[a] Reference 35.

TABLE 11. SELECTED BOND LENGTHS (Å) AND ANGLES (°) FOR 1,1-DIIODO-4-OXATETRAHYDROTELLURAPYRAN (67)[a]

Bond Length	(Å)	Angle	(°)
Te1—C2	2.15	Te1—C2—C3	112.8
Te—I1	2.86	C2—C3—O4	113.5
Te—I2	2.938	C3—O4—C5	114.2
Te—C6	2.17	O4—C5—C6	114.0
		C5—C6—Te1	113.5
		C2—Te1—C6	94.1
		I1—Te1—I2	177.1

[a] Reference 37.

TABLE 12. SELECTED BOND LENGTHS (Å) AND ANGLES (°) FOR 1,1-DIIODO-4-THIATETRAHYDROTELLUROPYRAN (71)[a]

Bond Length	(Å)	Angle	(°)
Te1—C2	2.16	Te1—C2—C3	116
Te—I1	2.895	C2—C3—S4	114
Te—I2	2.945	C3—S4—C5	100
Te—C6	2.16	S4—C5—C6	114
C2—C3	1.52	C5—C6—Te1	116
C3—S4	1.83	C2—Te1—C6	100
S4—C5	1.83	I1—Te1—I2	178.1
C5—C6	1.52		

[a] Reference 40.

TABLE 13. SELECTED BOND LENGTHS (Å) AND ANGLES (°) FOR 1,1-DIIODO-3,5-DISILA-4-OXATETRAHYDROTELLUROPYRAN (**83**)[a]

Bond Length	(Å)	Angle	(°)
Te1—C2	2.137	C2—Si3—O4	110.5
Te1—C6	2.156	Si3—O4—Si5	144.3
C2—Si3	1.869	Te1—C2—Si3	120.6
Si5—C6	1.868	Te1—C6—Si5	120.2
Si3—O4	1.608	O4—Si5—C6	109.2
O4—Si5	1.608	C2—Te1—C6	105.2
Te1—I1	2.909	I1—Te1—I2	178.32
Te1—I2	2.913		

[a] Reference 44.

TABLE 14. ^{1}H AND ^{13}C NMR CHEMICAL SHIFTS FOR 3,5-DISILA-4-OXATETRAHYDROTELLUROPYRANS **80–85**[a]

		$^{1}H2,6$	$^{13}C2,6$	$^{2}J_{Te-H}$	$^{1}H(Me)$	$^{13}C(Me)$	$^{1}H(Te^{+}R)$
Compd.	X or R	(δ, ppm)		(Hz)	(δ, ppm)		
80	—	1.49	—	33.6	0.33	—	—
81	Cl	2.65	17.8	56.2	0.45	3.8	—
82	Br	2.41	—	56.0	0.41	—	—
83	I	2.75	14.7	56.0	0.44	4.0	—
84	Me	2.34	—	27.8	0.31	—	2.74
85	CH_2Ph	1.17, 2.08	—	—	0.34	—	4.92

[a] Reference 44.

TABLE 15. ^{1}H AND ^{13}C NMR CHEMICAL SHIFTS FOR TELLURABENZOCYCLOHEPTATRIENES **90–92**[a]

		$^{1}H2,7$	$^{1}H3,6$	$^{3}J_{H-H}$	$^{13}C2,7$	$^{13}C3,6$
Compd.	X	(δ) (vs. TMS)		(Hz)	(δ) (vs. TMS)	
90	—	6.75	7.58	10.3	106.3	142.0
91	Cl	6.64	7.79	10.5	—	—
92	Br	6.77	7.75	10.4	—	—

[a] Reference 46.

TABLE 16. ^{1}H, ^{13}C, AND ^{125}Te NMR CHEMICAL SHIFTS FOR DITELLURACYCLOOCTANE **94**, BICYCLODITELLURAOCTANES **95** AND **96**, AND BICYCLO DICATION **97**[a]

Compd.	$^{1}H_{2,4,6,8}$ (δ) (vs. TMS)	$^{1}H_{3,7}$ (δ) (vs. TMS)	^{125}Te (δ) (vs. Me_2Te)	$^{13}C_{2,4,6,8}$ (δ) (vs. TMS)	$^{13}C_{3,7}$ (δ) (vs. TMS)	$^{1}J_{Te-C}$ (Hz)
94	2.74	2.13	164	4.9	34.1	158
95	—	—	706	35.1	28.3	—
96	3.28	2.52	1008	38.7	22.9	208
97	2.56	1.92	1304	17.8	16.1	—

[a] References 47 and 48.

TABLE 17. ^{1}H, ^{13}C, AND ^{125}Te NMR CHEMICAL SHIFTS FOR DIBENZO-5-CHALCOGENA-1-TELLURACYCLOOCTADIENES **99** AND OXIDIZED FORMS **101–106**[a]

Compd.	Confor-mation	$^{1}H_{A}$ (δ) (vs. TMS)	$^{1}H_{B}$ (δ) (vs. TMS)	$^{2}J_{AB}$ (Hz)	$^{13}CH_2$ (δ) (vs. TMS)	^{125}Te (^{77}Se) (δ) (vs. Me_2Y)
99a	Boat	4.08	4.08	br s	12.1	553,677
	Chair	4.22	5.48	12	14.1	565,703
99b	Boat	3.74	3.92	13	27.8	559(398)
	Chair	4.24	5.18	13	36.0	581(425)
99c	Boat	3.49	3.81	14	34.1	494
	Chair	4.13	4.95	14	44.5	528
101	Boat	3.90	4.24	14	29.7	1159(233)
102	—	3.49	4.03	br	31.1	—
103	—	4.09	4.48	14.9	—	—
104a	Distorted boat	4.54	4.87	16.7	41.9	—
		4.55	4.88	16.7	41.9	—
104b	Boat	4.32	4.70	16	41.9	1381
105	Boat	4.99	4.99	br s	45.9	602,946
106	Boat	4.64	5.13	15	39.7	1239(361)

[a] References 49–51.

REFERENCES

1. Connor, J.; Greig, G.; Strausz, O. P. *J. Am. Chem. Soc.* **1969**, *91*, 5695.
2. Buu-Hoi, N. P.; Mangane, M.; Renson, M.; Piette, J. L. *J. Heterocycl. Chem.* **1970**, *7*, 219.
3. Polson, G.; Dittmer, D. C. *Tetrahedron Lett.* **1986**, *27*, 5579.
4. Discordia, R. P.; Dittmer, D. C. *J. Org. Chem.* **1990**, *55*, 1414.
5. Discordia, R. P.; Murphy, C. K.; Dittmer, D. C. *Tetrahedron Lett.* **1990**, *31*, 5603.
6. Discordia, R. P.; Dittmer, D. C. U.S. Patent 4,935,451 (1990).

7. Dittmer, D. C.; Murphy, C. K.; Discordia, R. P. U.S. Patent 5,087,773 (1992).
8. Dittmer, D. C.; Discordia, R. P.; Zhang, Y.; Murphy, C. K.; Kumar, A.; Pepito, A. S.; Wang, Y. *J. Org. Chem.* **1993**, *58*, 718.
9. Tan, R. P. G.; Gillette, G.; Powell, D. R.; West, R. *Organometallics* **1991**, *10*, 546.
10. West, R.; De Young, D. J.; Haller, K. J. *J. Am. Chem. Soc.* **1985**, *107*, 4942.
11. Yokelson, H. B.; Millevolte, A. J.; Gillette, G. R. *J. Am. Chem. Soc.* **1987**, *109*, 6865
12. Tsumuraya, T.; Kabe, Y.; Ando, W. *J. Chem. Soc., Chem. Commun.* **1990**, 1159.
13. Schäfer, A.; Weidenbruch, M.; Saak, W.; Pohl, S.; Marsmann, H. *Angew. Chem. Int. Ed. Engl.* **1991**, *30*, 834.
14. Masamune, S.; Sita, L. R. *J. Am. Chem. Soc.* **1985**, *107*, 6390.
15. Farrar, W. V.; Gulland, J. M. *J. Chem. Soc.* **1945**, 11.
16. De Silva, K. G. K.; Monsef-Mirzai, Z.; McWhinnie, W. R. *J. Chem. Soc. Dalton Trans.* **1983**, 2143.
17. Petrov, M. L.; Laishev, V. Z.; Petrov, A. A. Zh. *Org. Khim.* **1979**, *15*, 2596.
18. Bender, S. L.; Haley, N. F.; Luss, H. R. *Tetrahedron Lett.* **1981**, *22*, 1495.
19. Segi, M.; Koyama, T.; Takata, Y.; Nakajima, T.; Suga, S. *J. Am. Chem. Soc.* **1989**, *111*, 8749.
20. Weidenbruch, M.; Ritschl, A.; Peters, K.; von Schnering, H. G. *J. Organomet. Chem.* **1992**, *437*, C25.
21. Sukhai, R. S.; Verboom, W.; Meijer, J.; Schoufs, M. J. M.; Brandsma, L. *Recl. Trav. Pays-Bas* **1981**, *100*, 10.
22. Haley, N. F.; Bender, S. L., unpublished results.
23. Bender, S. L.; Detty, M. R.; Haley, N. F. *Tetrahedron Lett.* **1982**, *23*, 1531.
24. Bender, S. L.; Detty, M. R.; Fichtner, M. W.; Haley, N. F. *Tetrahedron Lett.* **1983**, *24*, 237.
25. Detty, M. R.; Henrichs, P. M.; Whitefield, J. A. *Organometallics* **1986**, *5*, 1544.
26. Detty, M. R.; Haley, N. F.; Eachus, R. S.; Hassett, J. W.; Luss, H. R.; Mason, G. M; McKelvey, J. M.; Wernberg, A. A. *J. Am. Chem. Soc.* **1985**, *107*, 6298.
27. Prinzbach, H.; Futterer, E. In *Advances in Heterocyclic Chemistry*, Katritzky, A. R.; Boulton, A. J., eds.; Academic Press, New York, 1966, Vol. 7, p. 39.
28. Engler, E. M.; Patel, V. V. *Tetrahedron Lett.* **1975**, 1255.
29. Lakshmikanthan, M. V.; Cava, M. P.; Albeck, M.; Engman, L. *J. Chem. Soc., Chem. Commun.* **1981**, 829.
30. Potapov, V. A.; Gusarova, N. K.; Amosova, S. V.; Kashik, A. S.; Trofimov, B. A. *Sulfur Lett.* **1985**, *4*, 13.
31. Singh, H. B.; Wudl, F. *Tetrahedron Lett.* **1989**, *30*, 441.
32. Merkel, G.; Berge, H.; Jeroschewski, P. *J. Prakt. Chem.* **1984**, *326*, 467.
33. Lakshmikantham, M. V.; Cava, M. P.; Günther, W. H. H.; Nugara, P. N.; Belmore, K. A.; Atwood, J. L.; Craig, P. *J. Am. Chem. Soc.* **1993**, *115*, 885.
34. Ross, L.; Dräger, M. *J. Organomet. Chem.* **1980**, *194*, 23.
35. Puff, H.; Bongartz, A.; Schuh, W.; Zimmer, R. *J. Organomet. Chem.* **1983**, *248*, 61.
36. Mathiasch, B. *J. Organomet. Chem.* **1980**, *194*, 37.
37. Al-Rubaie, A. Z.; Al-Shirayda, H. H.; Auoob, A. I. *Inorg. Chim. Acta* **1987**, *134*, 139.
38. Hope, H.; Knobler, C.; McCullough, J. D. *Inorg. Chem.* **1973**, *12*, 2665.
39. McCullough, J. D. *Inorg. Chem.* **1965**, *4*, 862.
40. Knobler, C.; McCullough, J. D.; Hope, H. *Inorg. Chem.* **1970**, *9*, 797.
41. Chao, G. Y.; McCullough, J. D. *Acta Crystallogr.* **1961**, *14*, 490.
42. Chao, G. Y.; McCullough, J. D. *Acta Crystallogr.* **1962**, *15*, 887.
43. Dedeyne, R.; Anteunis, M. J. O. *Bull. Soc. Chim. Belg.* **1976**, *85*, 319.

44. Al-Rubaie, A. Z.; Uemura, S.; Masuda, H. *J. Organomet. Chem.* **1991**, *410*, 309.
45. Ladatko, A. A.; Zakharov, A. V.; Sadekov, I. D.; Minkin, V. I. *Khim. Geterotsikl. Soedin.* **1992**, 133.
46. Sashida, H.; Kurahashi, H.; Tsuchiya, T. *J. Chem. Soc., Chem. Commun.* **1991**, 802.
47. Fujihara, H.; Ninoi, T.; Akaishi, R.; Erata, T.; Furukawa, N. *Tetrahedron Lett.* **1991**, *32*, 4537.
48. Fujihara, H.; Takaguchi, Y.; Ninoi, T.; Erata, T.; Furukawa, N. *J. Chem. Soc. Perkin Trans. I* **1992**, 2583.
49. Fujihara, H.; Takaguchi, Y.; Chiu, J.-J.; Erata, T.; Furukawa, N. *Chem. Lett.* **1992**, 151.
50. Fujihara, H.; Takaguchi, Y.; Furukawa, N. *Chem. Lett.* **1992**, 501.
51. Fujihara, H.; Uehara, T.; Erata, T.; Furukawa, N. *Chem. Lett.* **1993**, 263.
52. Liu, X.; Li, W.; Lu, X.; Xu, H. *Chin. Chem. Lett.* **1992**, *3*, 589.

Note Added in Proof. Two manuscripts describing four-membered ring compounds with two telluriums (ditelluretane **108** and selenatelluretane **109**)[53,54] were not included in the initial writing of this chapter. The dimerization of difluorotelluroketone gave **108** in quantitative yield while the reaction of difluorotelluroketone with an excess of difluoroselenoketone gave **109**. Both compounds are air and light sensitive. The X-ray crystal structure of **108** gave Te—C—Te angles of 101.2(4)° and C—Te—C angles of 78.9(2)° with C—Te bond lengths of 2.191(11)Å in the planar molecule.[53] For **108**, the ^{125}Te NMR chemical shift is δ 2321.7 (vs Me_2Te).[53]

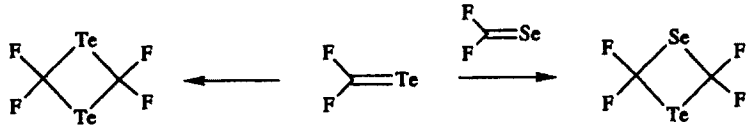

108 **109**

REFERENCES

53. Boese, R.; Haas, A.; Limberg, C. *J. Chem. Soc., Chem. Commun.* **1991**, 1378.
54. Haas, A.; Limberg, C. *Chimia* **1992**, *46*, 78.

Chemistry of Heterocyclic Compounds, Volume 53
Michael R. Detty, Marrie B. O'Regan

CHAPTER VII

Tellurium-Containing Heterocycles as Donor Molecules

Since the discovery of the high conductivity of the chloride salt of tetrathiafulvalene (TTF, **1**) in the early 1970s,[1] chemists and solid-state physicists have pursued organic conductors and semiconductors based on a variety of heterocyclic donor compounds.[2-15] Heterocyclic organotellurium compounds have been included in this quest.

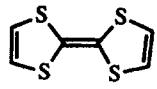

TTF, 1

Many organic metals are pseudo-one-dimensional conductors. Their one-dimensional character is a consequence of stacking in the crystal lattice where conductivity is highest along the stacking axis and much lower in the remaining two crystal-lattice directions. The anisotropy in electrical conductivity can be as high as a factor of 10^{13} in the three axis directions. Superconductivity has been observed at very low temperatures in salts of both tetrathiafulvalene[16-21] and tetraselenafulvalene.[16,22-24]

In the tetraselenafulvalenes, the intermolecular stacks are dominated by selenium–selenium contacts that are less than the sum of van der Waals radii. Furthermore, increased dimensionality has been strongly linked to the chalcogen network in these materials. Similarly, the chalcogen network has also been linked to bulk superconductivity. The tellurium-based analogs of donor molecules should offer increased polarizability and stronger intermolecular contacts. These hopes have fueled the synthetic efforts to generate new tellurium-containing donor molecules.

Organic metals fall structurally into two categories. In one, the organic metal consists of segregated stacks of planar (D_{2h}) donors and planar (D_{2h}) acceptors (Fig. 1). In the other, radical-ion stacks of either the donor (D) or acceptor (A) are accompanied by closed-shell counterions (D_mX_n and A_mM_n, Fig. 2). Electronically, mixed valency must be supported by individual molecules in the stacks for conduction to occur. In the case of neutral-donor molecules, this condition is met by either the neutral-donor/radical-cation pair or the radical-cation/dication pair. In the case of the acceptor molecules, the neutral-acceptor/radical-anion pair or radical-anion/dianion pair satisfy this condition.

As illustrated in Fig. 1, the stack structures may have a variety of orientations. In the segregated-stack structures the stacks may be either coplanar perpendicular to the *c* axis (Fig. 1*a*) or tilted in the same direction relative to the *c* axis (Fig. 1*b*). Alternatively, the segregated stacks may be tilted in opposite directions relative to the *c* axis (Fig. 1*c*). In donor stacks with closed-shell counterions, the stacks align with the counterions in between (Fig. 2*a*). In these systems with closed-shell counterions, the stacks may be tilted as well. In both the segregated-stack structure and in stacks with closed-shell counterions, the planar donor molecules may twist around the *c* axis (Fig. 2*b*). In the stacking arrangements

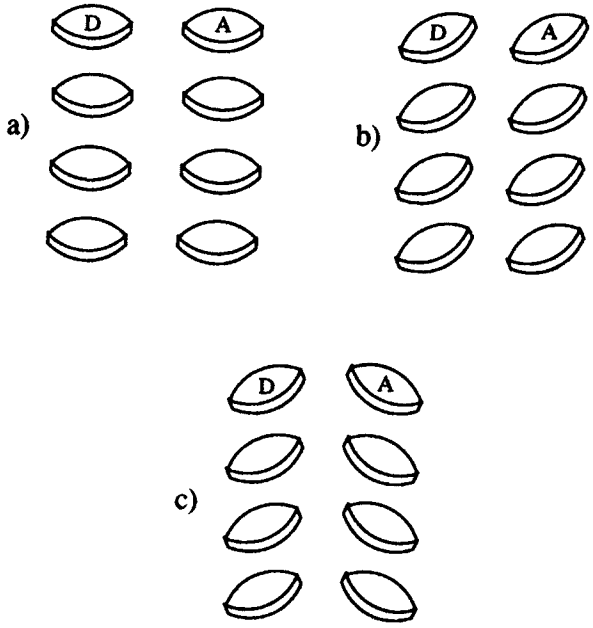

Figure 1. Some possible stacking modes in segregated-stack organic conductors: (*a*) parallel donor (D) and Acceptor (A) stacks perpendicular to the *c* axis; (*b*) a tilt of both stacks in the same direction relative to the *c* axis; (*c*) a tilt of the donor and acceptor stacks in opposite directions relative to the *c* axis.

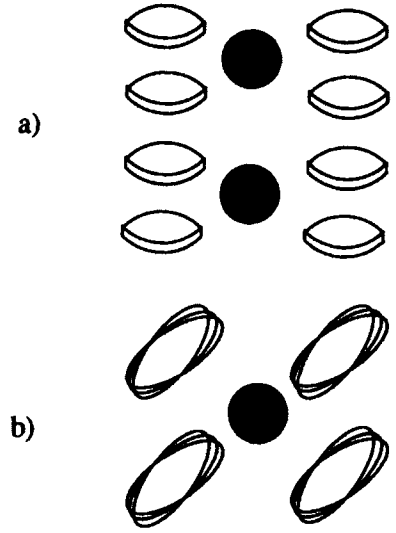

Figure 2. Stacking for donor stacks with closed-shell anions: (*a*) alignment along the *c* axis; (*b*) viewed down the *c* axis showing twisting within the stack.

of Figures 1 and 2, the closest intermolecular contacts will often involve chalcogen–chalcogen contacts. In segregated-stack structures, the donor stacks may be separated from other donor stacks by the acceptor stacks, which enforces one-dimensionality on the conductor. If donor stacks form adjacent columns, then increased dimensionality is possible.

In this chapter, a variety of tellurium heterocycles are considered as donor molecules. Typically, the radical-cation states of these molecules (if not the neutral donors themselves) are planar. Heterocyclic tellurium-containing systems considered in this chapter are the phenochalcogenatellurines from phenoxtellurine (**2**) through telluranthrene (**5**), the tetratellurafulvalenes **6**, naphtho[1,8-*c*,*d*]ditellurole **7** and related compounds, and the (telluropyranyl)telluropyrans **8**. The different synthetic routes to these systems are compiled; appropriate physical, structural, and spectral properties are compared to those of their lighter chalcogen analogs; and the synthesis and properties of conducting salts are compared to those of the lighter chalcogen analogs. All these compounds form reasonably stable radical cations on oxidation and form charge-transfer complexes with a variety of electron acceptors.

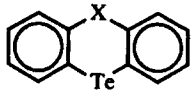

2, X = O
3, X = S
4, X = Se
5, X = Te

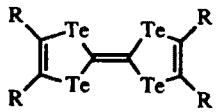

6

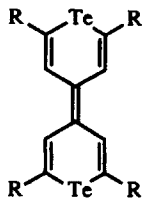

8

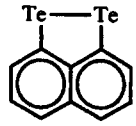

7

I. PHENOXTELLURINES AND HEAVIER CHALCOGEN ANALOGS

A. Synthesis of Phenoxtellurines

Of the heterocyclic, tellurium-containing donor molecules, phenoxtellurine (**2**) is the oldest.[25] The molecule was first prepared by Drew as shown in Scheme 1. The electrophilic attack of tellurium tetrachloride on diphenyl ether gives the tellurium(IV) phenoxtellurine dichloride **9** in 48% isolated yield, which is reduced to **2** in essentially quantitative yield with potassium bisulfite. This approach to phenoxtellurine (**2**), although more than 67 years old, is still the best synthetic procedure for the preparation of **2** on either a small or large scale.

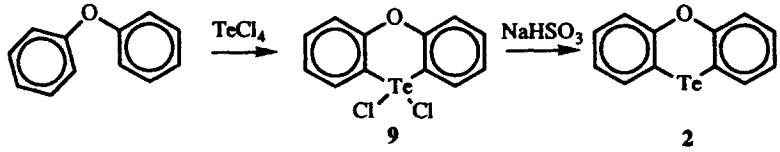

Scheme 1

A slightly different approach, as shown in Scheme 2, has been utilized to produce 2-methylphenoxtellurine (**10**) and 2-carboxyphenoxtellurine (**11**).[26] The 2-aminophenyl aryl ether **12** can be diazotized and converted into the organomercurial **13**. Compound **13** reacts with tellurium tetrachloride to give the phenoxtellurine dichlorides **15** via tellurium trichloride **14**. Sodium bisulfite reduction of the dichloride **15** gives **10** and **11**.

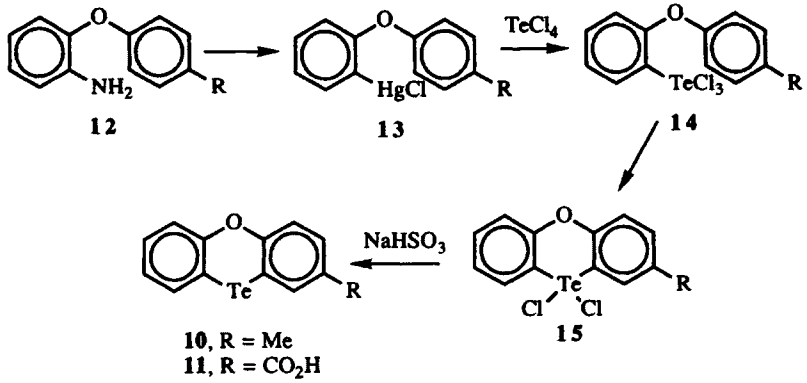

Scheme 2

Attempted condensation of 2-nitrodiphenyl ether with tellurium tetrachloride does not give the desired phenoxtellurine products but instead gives products of decomposition.[27] The direct nitration of phenoxtellurine **2** with nitric acid circumvents this problem. Initial oxidation gives the 10,10-dinitrate tellurium(IV) analog **16** of phenoxtellurine **2** as shown in Scheme 3. The use of concentrated nitric acid gives predominantly 2-nitrophenoxtellurine (**17**) with smaller amounts of 4-nitrophenoxtellurine (**18**), following reduction of the dinitrates with sodium bisulfite. The use of boiling, fuming nitric acid leads to formation of 2,7-dinitrophenoxtellurine (**19**) as the major product and smaller amounts of 4,7-dinitrophenoxtellurine (**20**), following reduction of tellurium(IV) to tellurium(II) with sodium bisulfite.

Phenoxtellurine (**2**) undergoes oxidative addition with chlorine, bromine, or iodine to give the 10,10-dihalophenoxtellurines **9**, **21**, and **22**, respectively. The chloride **9** reacts with bromide or iodide in methanol to give **21** and **22**, respectively, presumably from nucleophilic attack at tellurium. All three of these

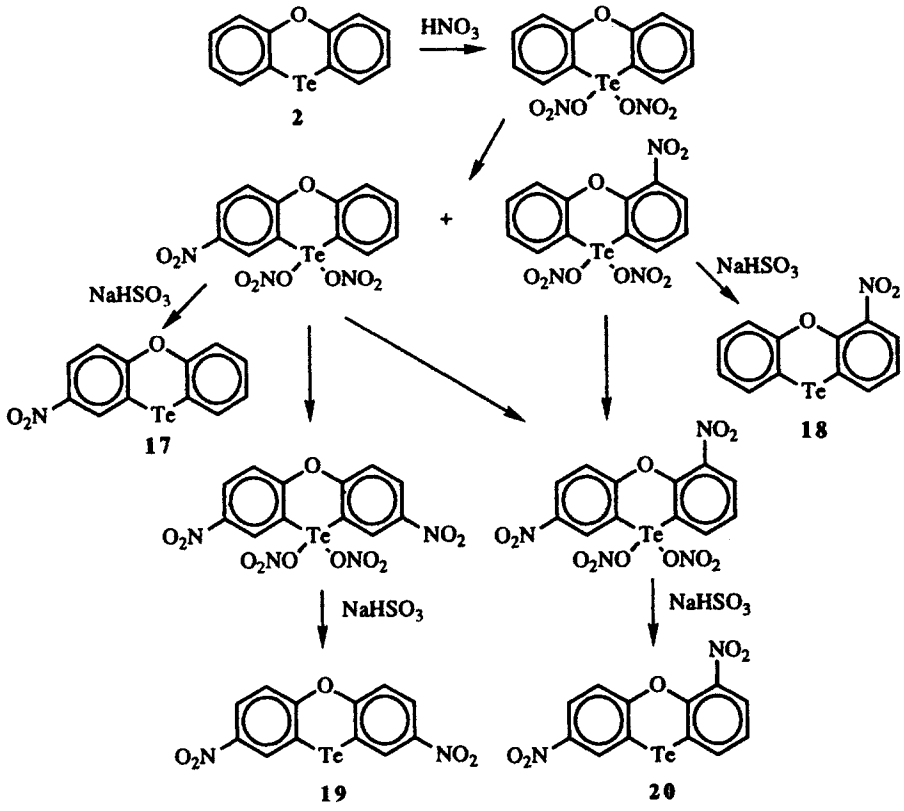

Scheme 3

tellurium(IV) analogs of phenoxtellurine, when treated with chlorine, give the tetrahalide **23** as shown in Scheme 4.[28] Bromination of **2** or **9** with bromine, employing either iodine or iron as a catalyst, gives the tetrabromide **24**.[29]

The reaction of fluorine- and chlorine-substituted diphenyl ethers with tellurium tetrachloride gives the expected halogen-substituted phenoxtellurines as well as products that are chlorinated at the 8-position as shown in Scheme 5.[30] 4-Fluorodiphenyl ether (**25**) gives a mixture of 10,10-dichloro-2-fluorophenoxtellurine (**26**) and 7,10,10-trichloro-2-fluorophenoxtellurine (**27**) in a combined yield of 28%, while 4-chlorodiphenyl ether (**28**) gives a mixture of 2,10,10-trichlorophenoxtellurine (**29**) and 2,7,10,10-tetrachlorophenoxtellurine (**23**) in a combined yield of 54%. 4-Bromodiphenyl ether and 4,4′-dibromophenyl ether react with tellurium tetrachloride to give phenoxtellurines in low yield that cannot be isolated in pure form.[30] 4-Iododiphenyl ether liberates iodine on reaction with tellurium tetrachloride, although phenoxtellurine products are not isolated from the product mixture.[29]

4,4′-Disubstituted-diphenyl ethers **30** react with tellurium tetrachloride to give the appropriate 10,10-dichlorophenoxtellurines **31** as shown in Scheme 6.

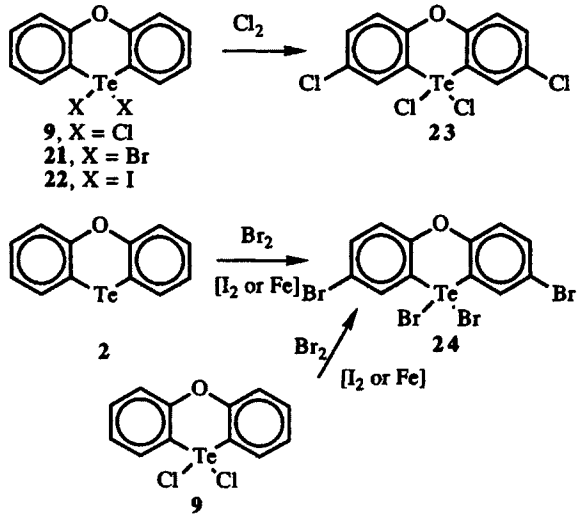

Scheme 4

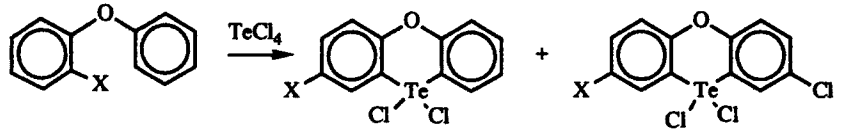

Scheme 5

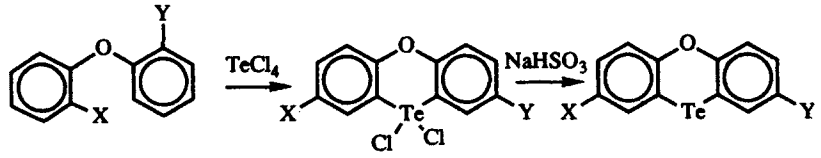

Scheme 6

4,4'-Dimethyldiphenyl ether (**30a**) gives **31a** in 38% isolated yield;[31] 4-chloro-4'-methyldiphenyl ether (**30b**) gives **31b** in 15% isolated yield;[26] 4-fluoro-4'-methyldiphenyl ether gives **31c** in 30% isolated yield;[32] 4,4'-difluorodiphenyl ether gives **31d** in 37% isolated yield;[33] and 4,4'-dichlorodiphenyl ether

gives **31e** in 42% isolated yield.[34] These molecules are reduced with bisulfite to give the corresponding 2,7-disubstituted phenoxtellurines **32** in greater than 90% yield.

The oxidation of the tellurium atom in phenoxtellurines is a facile process. As with other diorganotellurides, oxidation does not lead to well-defined telluroxide and tellurone states. Typically, an intermediate telluroxide reacts with two equivalents of some nucleophile to give a diorganotellurium(IV) intermediate with two additional ligands to tellurium.[35–39] Hydrogen peroxide can give oxidation products derived from the formal oxidative addition of hydrogen peroxide across tellurium.[36–39] Oxidation of phenoxtellurines with air or hydrogen peroxide in the presence of water produces tellurium oxides of phenoxtellurines. While these oxidation products have been described as telluroxides or tellurones, the actual species may be "hydrated" forms.[26,40,41] Phenoxtellurine (**2**) is oxidized with hydrogen peroxide in glacial acetic acid to give the tellurium(IV) analog 10,10-diacetoxyphenoxtellurine (**33**) in greater than 90% yield.[40,41] The air oxidation of phenoxtellurine (**2**) in trifluoroacetic acid gives 10,10-ditrifluoroacetoxyphenoxtellurine (**34**)[42] (Scheme 7).

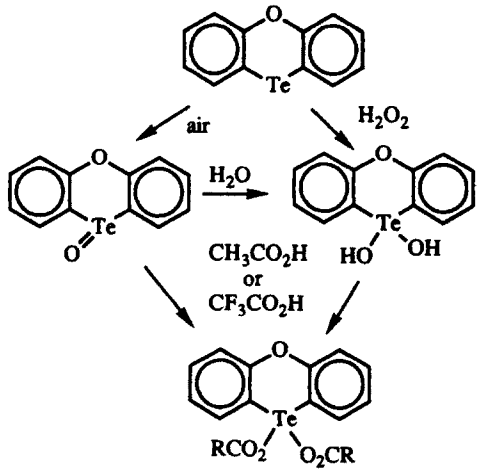

33, R = CH_3
34, R = CF_3

Scheme 7

Phenoxide and alkoxide analogs of **33** and **34** have been prepared from dichloride **9** by reaction with sodium phenoxides or alkoxides.[43] The reaction of **9** with silver oxide gives oxide products of phenoxtellurine (**2**).[25,41]

One reaction pathway of the phenoxtellurine ring system that is shared by other organotellurium compounds is loss of the tellurium atom as shown in Scheme 8. In the presence of potassium hydroxide or potassium carbonate

at reflux, various phenoxtellurines lose tellurium to give diaryl ethers.[27,29] Copper-induced detelluration converts phenoxtellurines to dibenzofurans.[44] Tellurium–sulfur exchange on heating phenoxtellurines with elemental sulfur at elevated temperatures gives phenoxthiins.[31,32,34]

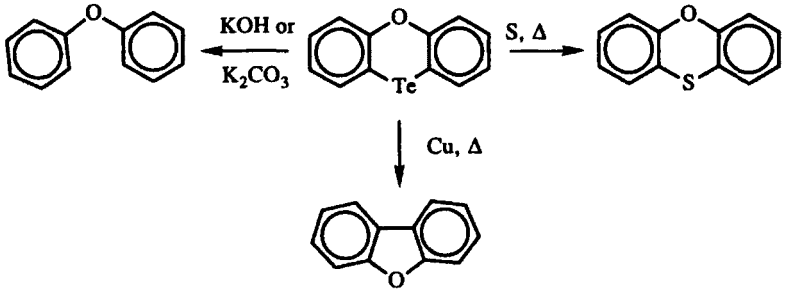

Scheme 8

The tellurium atom of phenoxtellurine (**2**) has been alkylated with methyl iodide.[45] As shown in Scheme 9, the dichloride **9** was reduced with disodium sulfide nonahydrate to give phenoxtellurine (**2**) which was then alkylated with methyl iodide. The telluronium iodide **35** was isolated in 95% yield as a yellow crystalline solid.

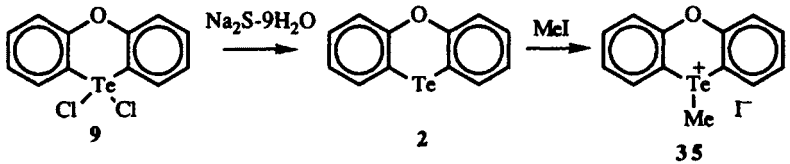

9 **2** **35**

Scheme 9

The lighter chalcogen analogs of phenoxtellurine (**2**) are known compounds Both phenoxselenine (**36**) and phenoxthiine (**37**) have been prepared and their structures examined by X-ray crystallography.[46] Dibenzo-1,4-dioxane (**38**) has been prepared by the coupling of 2-bromophenol with potassium carbonate and copper metal.[47] Analogs of phenoxtellurine (**2**) incorporating the heavier chalcogen atoms in place of oxygen are also known.

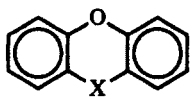

36, X = Se
37, X = S
38, X = O

B. Synthesis of Phenothiatellurine Derivatives

Very few phenothiatellurine derivatives have been described. The parent system **3** has been prepared as shown in Scheme 10. The addition of tellurium tetrachloride to diphenyl sulfide gives 10,10-dichlorophenothiatellurine (**39**).[48] The tellurium(IV) derivative **39** is reduced to phenothiatellurine (**3**) with either disodium sulfide nonahydrate[49] or potassium bisulfite.[48] The 10,10-dibromophenothiatellurine (**40**) is also a known compound.[48]

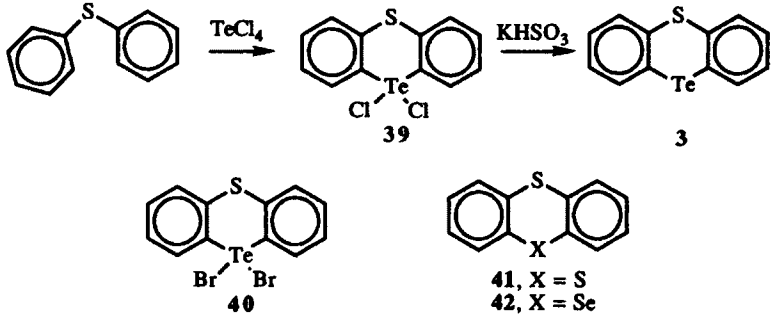

Scheme 10

Tellurium–sulfur exchange has been observed with **3**. Thianthrene **41** is produced on heating phenothiatellurine (**3**) with elemental sulfur.[48] Phenothiaselenine (**42**) has been described as well.

Phenothiatellurine (**3**) has also been prepared via the tellurium trichloride **43**.[49] Compound **43** is prepared from 2-nitrodiphenyl sulfide as shown in Scheme 11. The nitro compound is reduced to the aniline, which is diazotized with sodium nitrite. On treatment with mercury chloride, the diazonium salt–mercury chloride complex is formed. This complex is treated with copper to

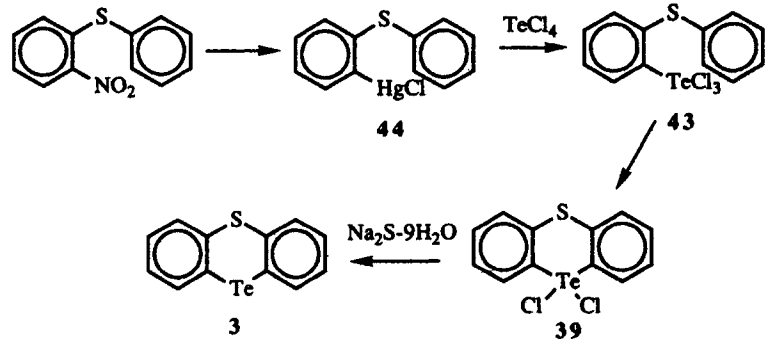

Scheme 11

give organomercurial **44**, which is converted to **43** in 38% overall yield on reaction with tellurium tetrachloride. Trichloro tellurium compound **43** is heated in a glass tube at 240–250°C to give 10,10-dichlorophenothiatellurine (**39**) in 42% yield. The tellurium(IV) compound **39** is reduced to phenothiatellurine (**3**) with disodium sulfide nonahydrate.

C. Synthesis of Phenoselenatellurine

The synthesis of phenoselenatellurine (**4**) has only recently been described and is analogous to the synthesis of 10,10-dichlorophenothiatellurine (**39**) described in Scheme 11.[50] 2-Nitrodiphenylselenide is converted to organomercurial **45** in 22% yield via reduction, diazotization, formation of the diazonium–mercury chloride complex, and decomposition to **45**. As shown in Scheme 12, the reaction of **45** with tellurium tetrachloride gives a nearly quantitative yield of trichlorotellurium derivative **46**. Heating **46** with aluminum chloride gives 10,10-dichlorophenoselenatellurine (**47**) in 33% yield. Reduction of the tellurium(IV) derivative with disodium sulfide nonahydrate gives **4** in quantitative yield.

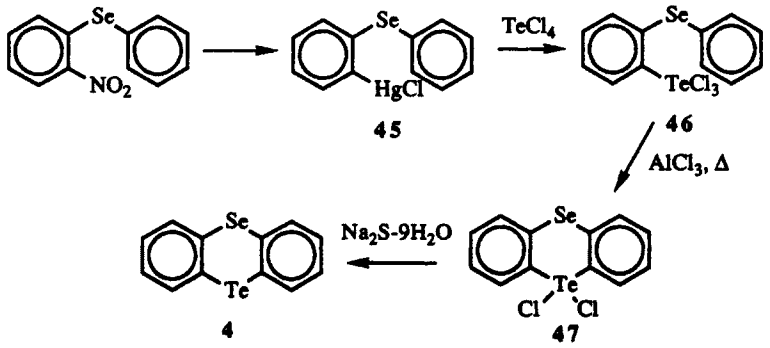

Scheme 12

Selenanthrene (**48**) is also a known analog of **4**.[51–53] As shown in Scheme 13, the oxidation of thianthrene (**41**) with chromic acid gives the disulfone **49**. Heating **49** with selenium metal gives selenanthrene **48**.

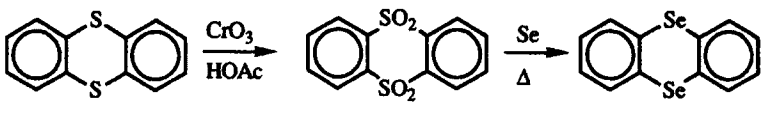

Scheme 13

D. Synthesis of Telluranthrenes

An attempted synthesis of telluranthrene (**5**) consisted of heating disulfone **49** with tellurium metal at 430°C.[54] Telluranthrene is not isolated. Instead, dibenzotellurophene (**50**) is produced.

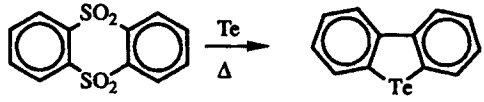

49 **50**

The first reported synthesis of **5** involves the thermal reaction of tetraphenyl tin with tellurium metal,[55] although others have reported this reaction to be capricious, at best.[56] The first practical synthesis of telluranthrene (**5**) is shown in Scheme 14 and involves the reaction of *o*-phenylene mercury with finely powdered tellurium metal at temperatures not exceeding 250°C.[56]

An alternative synthesis of **5** has been reported using inexpensive starting materials.[57] In this procedure, the reaction of disodium telluride with *o*-dichlorobenzene gives **5** in about 5% overall yield (Scheme 15).

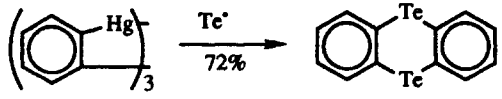

5

Scheme 14

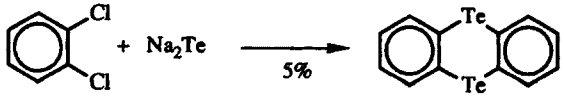

5

Scheme 15

A third synthesis of **5** is claimed as shown in Scheme 16 from the known poly(*o*-phenyleneditelluride) **51**.[58] The poly(ditelluride) is reduced with sodium borohydride to give the disodium ditelluride **52**.[59] The addition of *o*-diiodobenzene to **52** in dimethylformamide gives telluranthrene (**5**) in greater than 60% yield.

Halogen-substituted derivatives of telluranthrene have been prepared as shown in Scheme 17. Heating tellurium metal with 1,2-diiodotetrafluorobenzene gives octafluorotelluranthrene **53** in 6% overall yield.[60] The telluranthrene **53** is first isolated as the tetrabromide **54** via the addition of

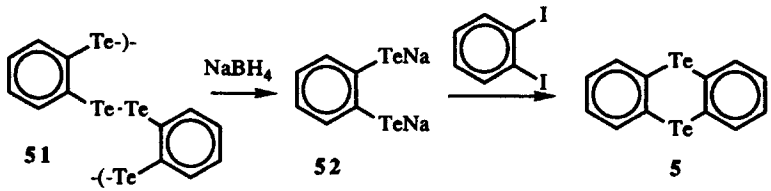

Scheme 16

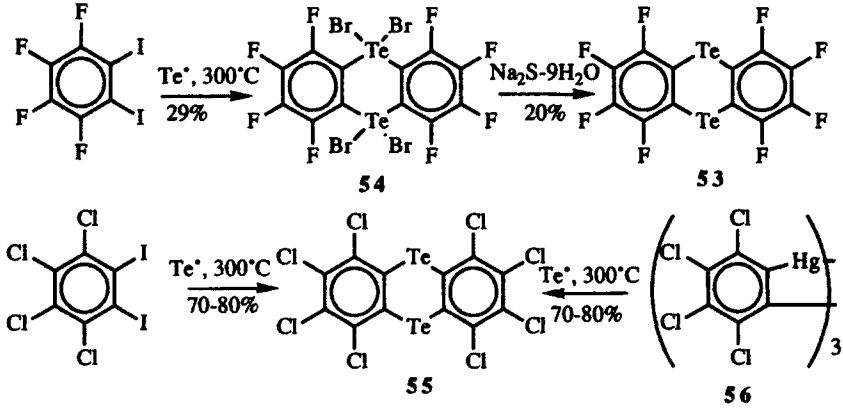

Scheme 17

bromine, and **54** is then reduced with disodium sulfide nonahydrate to **53**. Similarly, heating tellurium metal with 1,2-diiodotetrachlorobenzene gives octachlorotelluranthrene **55** in 70–80% isolated yields.[61] Octachlorotelluranthrene **55** is also produced in 70–80% isolated yield by the reaction of tetrachloro-*o*-phenylene mercury (**56**) with tellurium metal.[61]

E. Second-Generation Phenoxtellurines and Derivatives

The quest for better donor molecules has prompted recent interest in preparing alkoxy derivatives of phenoxtellurines and related compounds.[62,63] Alkoxy substitution would aid the formation of chalcogen channels in donor stacks and might increase the dimensionality of conducting complexes based on these donors. The chalcogen series **57** and **58** were prepared. Within these series, the telluranthrene analogs (X = Y = Te) were not prepared.

Phenoxtellurine analogs **57a** and **58a** are prepared via the classical route as shown in Scheme 18. The addition of tellurium tetrachloride to diaryl ethers **59** and **60** in refluxing chloroform in the presence of a catalytic amount of tin tetrachloride gives the 10,10-dichlorophenoxtellurines **61** and **62**, which are then reduced to **57a** and **58a** in 28 and 27% isolated yields, respectively.[63]

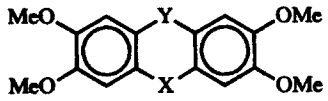

57a, X = Te, Y = O
57b, X = Te, Y = S
57c, X = Te, Y = Se
57d, X = Se, Y = O
57e, X = Se, Y = S
57f, X = Y = Se
57g, X = S, Y = O
57h, X = Y = S

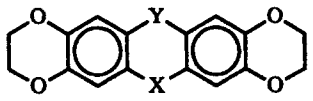

58a, X = Te, Y = O
58b, X = Te, Y = S
58c, X = Te, Y = Se
58d, X = Se, Y = O
58e, X = Se, Y = S
58f, X = Y = Se
58g, X = S, Y = O
58h, X = Y = S

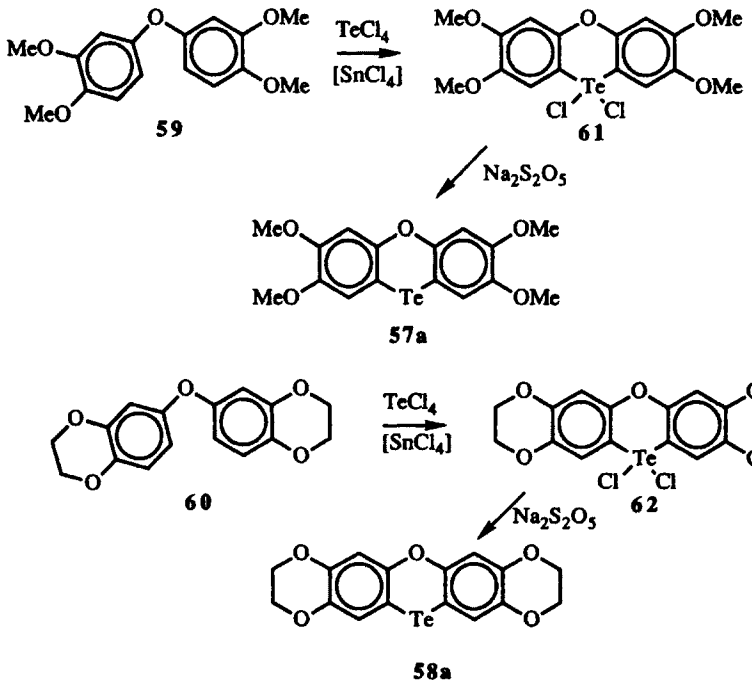

Scheme 18

The addition of tellurium tetrachloride to diaryl–sulfide analogs of **59** and **60** does not give the corresponding phenothiatellurines **57b** and **58b**. Routes to **57b** and **58b** utilize *o,o'*-dimetallated species as shown in Scheme 19. Compound **57b** has been prepared via two different routes.[62,63] The mercuration of diaryl sulfide **63** gives organomercury compound **64** in 90% yield. The addition of tellurium tetrachloride gives 10,10-dichlorophenothiatellurine **65** in 93% isolated yield. Reduction of the dichloride gives **57b** in 68% yield.[62]

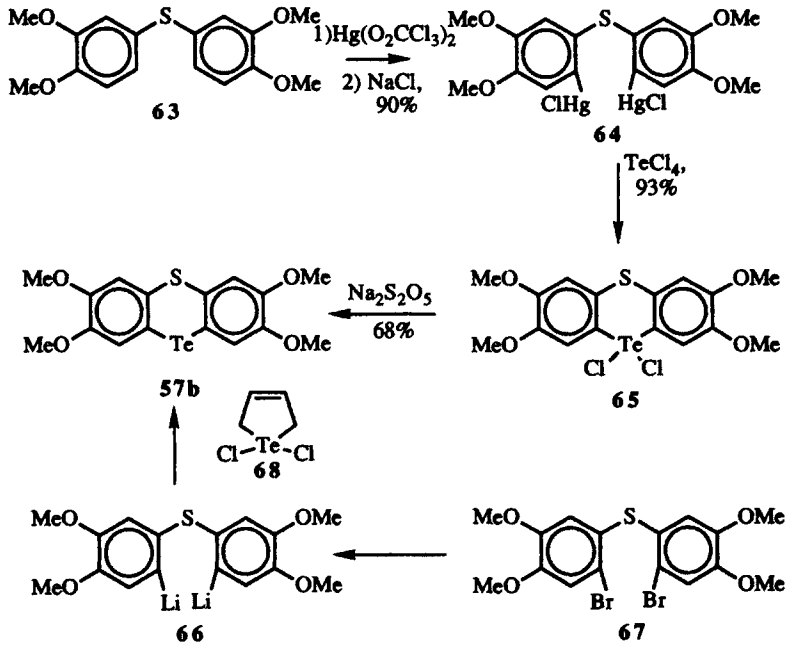

Scheme 19

The second route utilizes the *o,o'*-dilithio sulfide **66**, which is prepared via metal–halogen exchange from the dibromosulfide **67**.[63] The addition of 1,1-dichlorotelluracyclopent-3-ene (**68**) as the tellurating agent gives **57b** in 40% isolated yield.

A similar reaction sequence to the second route is utilized to prepare **58b** in 11% isolated yield from diaryl sulfide **69** as shown in Scheme 20.[63] Diaryl selenides **70** and **71** give phenoselenatellurines **57c** and **58c** in 18 and 7% isolated yields, respectively, utilizing similar chemistry to that depicted for the **67** to **66** to **57b** transformations.[63]

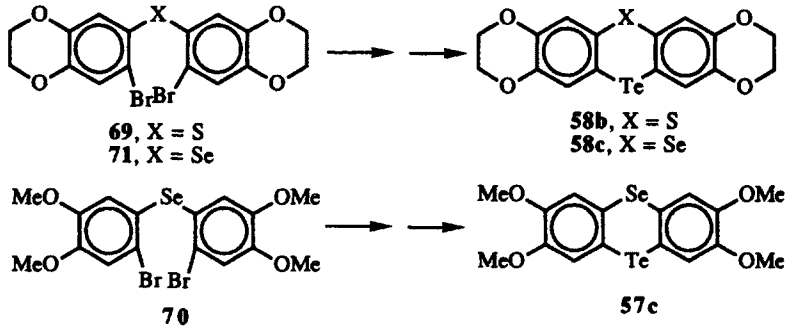

Scheme 20

F. Structures Related to Phenoxtellurines

The 4-chalcogenatellurin nucleus has appeared in other phenoxtellurine-like compounds as shown in Scheme 21.[64,65] The addition of tellurium tetrachloride to dilithiosulfide **72** gives 4-thiatellurin **73** via chemistry analogous to that described in Schemes 19 and 20.[64] The addition of tellurium tetrachloride to dilithiothiophene **74** gives 1,4-ditellurin **75**.[64] The addition of disodium telluride to a dimethylformamide solution of 1,2-diiodoacenaphthalene (**76**) gives 1,4-ditellurin **77** in 35% isolated yield.[65]

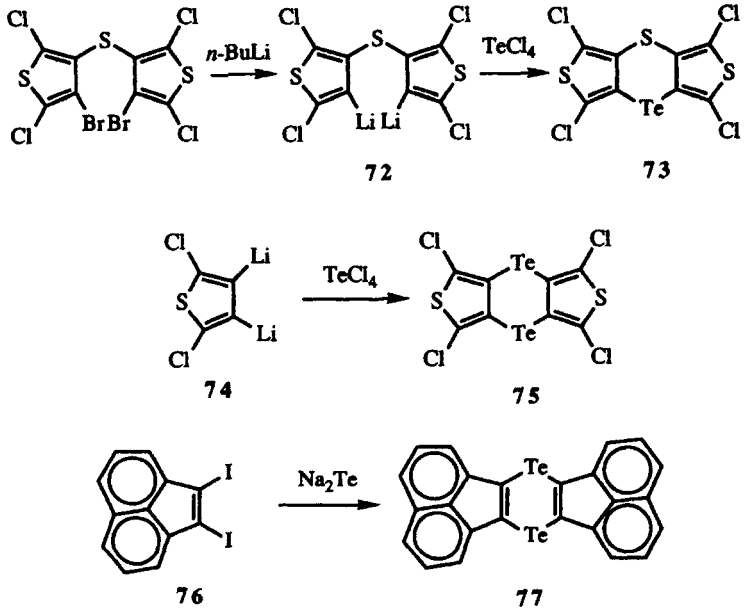

72 **73** **74** **75** **76** **77**

Scheme 21

G. Physical Properties of the Phenoxtellurines and Related Heavier Chalcogen Analogs

The structure and bonding of phenoxtellurine (**2**), telluranthrene (**5**), and all the various chalcogen combinations have been examined by X-ray crystallography in the solid state and, in solution, by photoelectron spectroscopy in combination with dipole moment and/or molecular orbital calculations. Not surprisingly, the solid state and solution conformations of these molecules can be quite different.[46,56,60,66-75]

Molecules structurally similar to phenoxtellurine (**2**) are boat-shaped, with the exception of the dioxin derivative **38**, which is approximately planar in the solid

state.[73,74] In the phenoxtellurines and derivatives, the two heteroatoms are out of plane with the four carbon atoms of the central ring. The fold in the boat shape of these molecules can be defined by two angles, Θ and Φ. The angle Θ is defined by the relationship of the two out-of-plane heteroatoms with the four carbons of the central ring. The angle Φ is defined by the angle of the planes of the two fused benzene rings with one another. Values of Θ in both the solid state and in solution and values of Φ in the solid state are compiled in Table 1 for phenoxtellurine (**2**), phenothiatellurine (**3**), phenoselenatellurine (**4**), and telluranthrene (**5**) as well as for related structures incorporating the lighter chalcogen atoms.

In comparisons of structure in solution and in the solid state, the angles of fold Θ for the central ring are 5–34 degrees larger in solution than the corresponding angle in the solid state with the exception of dioxin **38**, which is planar in the solid state and folded in solution. Crystal packing forces might explain the smaller angles (more folded) in the solid state in these compounds. Within the homoatomic series [**38** (O,O), **41** (S,S), **48** (Se,Se), **5** (Te,Te)], the amount of fold increases with increasing chalcogen size in both solution and the solid state. It is also interesting to note that phenoxtellurine (**2**) is nearly planar in solution. Gas-phase ionization energies as determined by photoelectron spectroscopy suggest that these molecules are folded in the gas phase as well.[66,68,75]

The tellurium–carbon bond lengths in phenochalcogenatellurines **2**–**5** are typical of those of tellurium–carbon single bonds. These bond lengths vary from 2.093 Å in **2**[67] to 2.111 Å in **5**.[60] The crystal structures of **3** and **4** suffer from disorder in the crystals, which render the bond lengths as average values with the bond lengths of the lighter chalcogen–carbon bonds.[69] The carbon–chalcogen–carbon angles are typical of those found in other six-membered rings containing the heteroatoms (Table 2). The molecular folding observed in these molecules serves to accommodate the chalcogen–carbon bond lengths and carbon–chalcogen–carbon angles.

Tellurium(IV) derivatives of phenoxtellurine adopt a slightly different geometry in the solid state. The tellurium(IV) dinitrate of phenoxtellurine is nearly planar with a value of Φ of 175°,[76] while values of Θ and Φ for ditrifluoroacetoxy tellurium(IV) derivative **34** are 152 and 156°, respectively.[42] The tellurium–carbon bonds in **34** are somewhat shorter than those observed in phenoxtellurine **2** (2.062 and 2.070 Å), while the carbon–tellurium–carbon angle is slightly larger at 91.5°.[42]

H. Oxidation of Phenoxtellurines and Related Compounds

The phenoxtellurines and related chalcogen analogs are characterized by (often reversible) one-electron oxidations to cation radicals. In many of the systems whose ionization or redox behavior has been observed, distinct cation-radical and dication states can be described.

The first ionization energies measured by photoelectron spectroscopy are adiabatic gas-phase oxidation potentials to the cation radicals. The analysis of the photoelectron spectra of phenoxtellurine (**2**) and related compounds has described the first two ionizations as being π bands with significant chalcogen character in each, on the basis of π-only semiempirical calculations (SCF-PPP).[66,68,70] The ionization energy of the first π band is the oxidation potential, while the ionization energy of the second π band is indicative of the mixing of the chalcogen atoms with the π framework.

Values of the first and second ionization energies (IE) and the difference between the energies of the first and second π bands (Δ_{IE}) are compiled in Table 3.[66,68,70] Two trends emerge from these data. As one examines values of IE_1 with increasing chalcogen mass, the value of IE_1 decreases. The ionization energies of the chalcogen atoms themselves decrease with increasing mass. This trend is observed with respect to phenoxtellurine (**2**), phenothiatellurine (**3**), phenoselenatellurine (**4**), and telluranthrene (**5**) as well as with other series of related chalcogen analogs. The second trend to emerge is that the energy of the second π band decreases with increasing heteroatom size. If, in fact, this π band is indicative of mixing of the chalcogen atoms with the carbon π framework, increased mixing should lower the energy of the MO and raise the observed value of IE_2. As the chalcogen atom increases in size, mixing of orbitals of different size becomes less efficient, the MO is higher in energy, and the value of IE_2 for the second π band decreases (Δ_{IE} is smaller). Mixing of the smaller heteroatom with the π framework appears to dominate in the second π band when one compares the fairly consistent values for compounds with at least one oxygen or compounds with at least one sulfur.

The oxidation potentials of **57** and **58** have been measured by cyclic voltammetry and are compiled in Table 4. The trends for chalcogen atom substitution correlated with the adiabatic ionization energies compiled in Table 3 are inverted in the nonadiabatic electrochemical oxidation potentials in Table 4. Oxidation is more positive (or more difficult) as the chalcogen atom becomes larger. If the chalcogen atoms were not mixed extensively with the π framework in the MO picture of the molecule, the π framework would not "assist" heteroatom-centered ionization of the molecule. In the nonadiabatic time frame, both molecular relaxation and solvation can lower the energy of ionization. If one were to assume that solvation energies were similar for formation of the cation radicals of **57** and **58**, then differences in chalcogen-atom ionization potentials and π framework participation should predict trends in oxidation potentials.

In **57** and **58**, the oxidation potential increases with increasing heteroatom size from phenoxtellurine **57a** or **58a** to phenothiatellurine **57b** or **58b** to phenoselenatellurine **57c** or **58c** in dichloromethane or acetonitrile (Table 4). Similar trends are observed from phenoxselenine **57d** or **58d** to selenanthrene **57f** or **58f** and in the comparison of phenoxthiine **57g** or **58g** and thianthrene **57h** or **58h**. This trend is consistent with lower energy oxidation potentials with increased chalcogen–π framework overlap. However, other factors are import-

ant since no trend is observed for changes in oxidation potentials from thianthrenes **57h** or **58h** to selenanthrenes **57f** or **58f** to phenoselenatellurines **57c** or **58c**.

The second oxidations of **57** and **58** to the dication do not follow obvious trends with respect to the heteroatoms (Table 4). However, the separation of first and second oxidation potentials (Δ_E) becomes smaller as the heteroatoms become larger.

I. ^{13}C NMR and ^{1}H NMR Spectra of Phenoxtellurines and Related Compounds

The ^{13}C NMR spectra of phenoxtellurine (**2**) and related chalcogen analogs have been reported.[56,77,78] The total charge densities on the carbon atoms (both σ and π) as calculated by CNDO/2 have been correlated with the observed experimental shifts.[78] The ^{13}C NMR chemical shifts are also consistent with the results of semiempirical PM3 calculations at the optimized minimum energy conformation for both canonical (CMO) and localized (LMO) molecular orbitals.[77]

The assignments of both proton and carbon chemical shifts in an unambiguous manner has been accomplished for phenoxtellurine (**2**) and related compounds through the application of two-dimensional NMR techniques and an analysis of one-, two-, and three-bond ^{13}C—^{125}Te and ^{13}C—^{77}Se couplings.[76] These assignments are compiled in Table 5 for ^{13}C NMR chemical shifts and in Table 6 for ^{1}H NMR chemical shifts.

From the data in Table 5, the ^{13}C NMR chemical shifts of the carbon atoms directly attached to the heteroatoms are most sensitive to changes in the heteroatom. The observed trend is that the ^{13}C NMR chemical shift moves upfield as the heteroatom increases in size. This is also the trend expected from electronegativity differences in the heteroatoms that would polarize σ-electron densities toward carbon with increasing electropositive character. Carbon atoms that are two or more bonds removed from the heteroatoms show the opposite trend with downfield ^{13}C NMR chemical shifts with increasing electropositive character.

The ^{1}H NMR chemical shifts in Table 6 all show the same trend. As the heteroatoms increase in size, the ^{1}H NMR chemical shifts move downfield. The largest change in ^{1}H NMR chemical shift occurs for the proton two-bonds removed from the heteroatom change.

J. Photophysical Properties of Phenoxtellurines and Related Compounds

Some aspects of the photophysics of the first excited singlet state and the relaxation processes of the first triplet state for phenoxtellurine (**2**), its lighter chalcogen analogs **36–38**, thianthrene (**41**), and selenanthrene (**48**) have been

described.[79] Values of triplet quantum yields (Φ_T) at 293 K, phosphorescence quantum yields (Φ_P) at 77 K, triplet lifetimes (τ_T), rates of intersystem crossing (k_{isc}), and rates of phosphorescence (k_p) are compiled in Table 7. In these systems, rates of intersystem crossing are all large ($> 10^{11}\ s^{-1}$, with the exception of thianthrene, where k_{isc} is $3 \times 10^7\ s^{-1}$) and, as a consequence, triplet yields are large. Triplet lifetimes are relatively long in these systems: on the order of milliseconds. However, triplet lifetimes decrease with increasing chalcogen weight. Rates of phosphorescence increase with increasing chalcogen weight.

Heavy-atom effects appear to dominate in the chalcogen-atom effects on rates of radiative transitions from singlet to triplet. The larger component of these transitions are nonradiative, and chalcogen-atom effects are less pronounced. Since values of k_{isc} are large, the conformational folding of phenoxtellurine and related compounds is thought to facilitate the intersystem crossing from singlet to triplet.[79]

K. Cation-Radical Salts of Phenoxtellurines and Related Compounds

Oxidation and reduction reactions of phenoxtellurine (**2**) have been observed to proceed with the formation of red- or violet-colored intermediates.[40,80] These colors have been reproduced by both chemical[81] and electrochemical[82] oxidations of phenoxtellurine (**2**) and the species responsible for the color formation have been identified as aggregates of two equivalents of the cation radical with one equivalent of the neutral donor molecule.[82]

Solution studies of phenoxtellurine (**2**) and various acceptor molecules have been consistent with the formation of 1 : 1 complexes. In dichloroethane, 1 : 1 charge-transfer complexes of phenoxtellurine (**2**) with 1,3,5-trinitrobenzene, picric acid, or picryl chloride are formed.[83] These complexes give broad absorption maxima with λ_{max} of approximately 420 nm and extinction coefficients on the order of $1000\ L\ mol^{-1}\ cm^{-1}$.[83] Values of the equilibrium constant for formation were in the range 8.0–13.2. Similar 1 : 1 complexes are formed between phenoxtellurine (**2**) and tetracyanoethylene (TCNE) or chloranil (tetrachloroquinone).[81] In dichloromethane, the **2**-TCNE complex has an absorption maximum at 710–720 nm with an extinction coefficient on the order of $1000\ L\ mol^{-1}\ cm^{-1}$. The equilibrium constant for complex formation is on the order of $1\ L\ mol^{-1}$. In dichloromethane, the **2**-chloranil complex has an absorption maximum at 590–610 nm with an extinction coefficient on the order of $180\ L\ mol^{-1}\ cm^{-1}$. The equilibrium constant for formation of the complex is approximately $4\ L\ mol^{-1}$.

In solution studies of this type, varying the heteroatom from tellurium (**2**) to selenium (**36**) to sulfur (**37**) to oxygen (**38**) has little effect on the thermodynamics of complex formation with TCNE.[81] For the four complexes studied, the range in equilibrium constants for complex formation is $1.4 \pm 0.5\ L\ mol^{-1}$, the range in ΔG is $0.2 \pm 0.2\ kcal\ mol^{-1}$, the range in ΔH is $-2.0 \pm 0.1\ kcal\ mol^{-1}$, and the range in ΔS is $-7.0 \pm 0.3\ cal\ K^{-1}$. The similarity of all the thermodynamic

values suggests that similar interactions are involved in the formation of charge complexes of all four phenoxchalcogines. All four complexes are probably of the π–π type.

Solid complexes have been isolated from solutions of **2** and **36–38** with TCNQ.[84] The stoichiometry of the complexes is one to one in all four cases. In solution, the thermodynamic parameters for formation of all four charge-transfer complexes are similar. The equilibrium constants vary over the range of 4–16, while the range in ΔH is -3.0 ± 2.0 kcal mol^{-1} and the range in ΔS is -4.4 ± 3.0 cal K^{-1}. The range in ΔG is quite narrow at 1.2 ± 0.2 kcal mol^{-1}.

The wavelength of the absorption maxima of the charge-transfer complexes of **2** and **36–38** with TCNQ varies somewhat with heteroatom.[84] For phenoxtellurine (**2**), λ_{max} is between 735 and 755 nm. For phenoselenine (**36**), λ_{max} is between 670 and 690 nm. For phenoxthiine (**37**), λ_{max} is between 695 and 715 nm. The lightest chalcogen gives the shortest wavelength with the complex of **38** and TCNQ absorbing with λ_{max} between 650 and 670 nm. The extinction coefficient is on the order of 100–200 L mol^{-1} cm^{-1} in these complexes.

Cyclic voltammetry has shown that the oxidation potentials of **2**, **36**, and **37** are $+0.76$, $+1.10$, and $+1.18$ V (vs. SCE in acetonitrile).[84] The first reduction potential of TCNQ is much higher at $+0.14$ V (vs. SCE) and suggests that the charge-transfer complexes will possess a nonionic ground state and should be insulating. Four probe dc conductivities of single crystals of **36**-TCNQ and **37**-TCNQ and 4×10^{-8} and 3×10^{-7} Ω^{-1} cm^{-1}, respectively. The use of a stronger acceptor ($TCNQF_4$) gives a semiconductive complex with phenoxtellurine (**2**) with a single-crystal conductivity of $< 6 \times 10^{-7}$ Ω^{-1} cm^{-1} at 300 K.

Charge-transfer complexes of phenoxtellurine **57a** and phenothiatellurine **57b** have been prepared. Phenoxtellurine **57a** forms a 4 : 3 complex with the octahedral anion AsF_6^- on electrochemical oxidation in dichloromethane.[63]

Phenothiatellurine **57b** forms a 1 : 1 complex with TCNQ. The X-ray structure of **57b**-TCNQ has been determined and shows a mixed stack ordering of the two molecules.[85] In the single crystals of **57b**-TCNQ, the phenothiatellu-

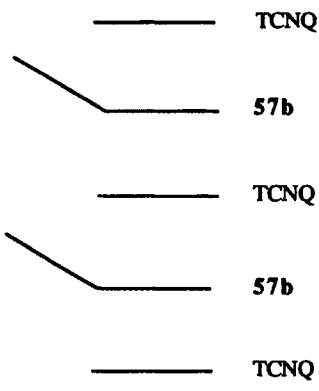

Figure 3. Side view of the stacking of phenothiatellurine **57b** with TCNQ.

rine ring is butterfly-shaped with a dihedral angle of approximately 137°.[85,86] The crystal structure indicates that the phenoxthiatellurine **57b** and TCNQ molecules form stacks in which the components alternate as shown in Figure 3. In these stacks, the folded phenothiatellurine molecule is arranged in such a way that one of the fused benzo groups is coplanar with the TCNQ molecules. The TCNQ molecules are nearly equidistant from the next phenothiatellurine molecule both above and below. The TCNQ molecules are stacked in such a way that a benzo group of one phenothiatellurine is aligned with the six-membered ring of TCNQ and the benzo group of the other phenothiatellurine in the "sandwich" is aligned with C4 of the TCNQ and the methylidene carbon.

Compressed pellet conductivities of TCNQ complexes of **57** at 10^8 bar of pressure indicate that these complexes are insulators at room temperature. For **57e**, **57f**, and **57h**, compressed-pellet conductivities at 293 K vary between 6.2×10^{-10} and $8.2 \times 10^{-9}\ \Omega^{-1}\,cm^{-1}$.[85] EPR studies on **57e**, **57f**, and **57h** indicate that spin concentrations are only on the order of 10^{15}–$10^{17}\ cm^{-3}$, which is consistent with insulator properties.

II. TELLUROPYRANYL(TELLUROPYRANS)

The discovery that (pyranyl)pyrans **78** form electrically conductive complexes with electron acceptors[86] prompted numerous investigations into the synthesis and physical properties of new members of this class[87] as well as other chalcogen analogs including (thiopyranyl)thiopyrans **79**[87–93] and (selenopyranyl)selenopyrans **80**.[94,95] (Telluropyranyl)telluropyrans **8**[95–97] and conducting salts incorporating them[95,98] have been more recently described.

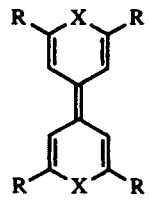

79, X = O
80, X = S
81, X = Se

A. Synthesis of Telluropyranyl(telluropyrans)

The reported syntheses of (telluropyranyl)telluropyrans **8** have all followed the same synthetic route as shown in Scheme 22.[95–97] A 4*H*-tellurin-4-one is converted to the corresponding thione **82** with the Lawessen reagent.[99] Copper-induced coupling of the thiones gives the (telluropyranyl)telluropyrans **8**. Some

care must be taken in the coupling step since prolonged reaction conditions or elevated temperature lead to the formation of (thiopyranyl)thiopyrans via tellurium–sulfur exchange.[96,97]

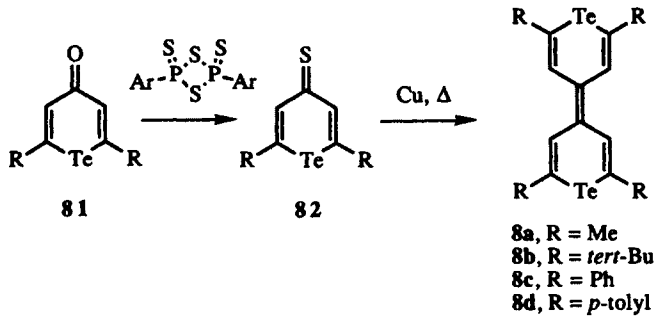

Scheme 22

The formation (thiopyranyl)thiopyrans **79** or (thiopyranyl)telluropyrans **83** is a consequence of tellurium–sulfur exchange as shown in Scheme 23. Such exchanges have been known since the beginning of the twentieth century with diaryltellurides.[100] Tellurium–sulfur exchange has been observed with dibenzotellurophenes,[101] phenoxtellurines,[31,33] and bis(trialkylsilyl)tellurides.[102] Products from sulfur exchange for one tellurium atom, **83**, are also produced.[96]

The (benzotelluropyranyl)benzotelluropyran **84** is prepared from the corresponding 4*H*-benzotellurin-4-one via the thione.[96] On heating with sulfur, **84**

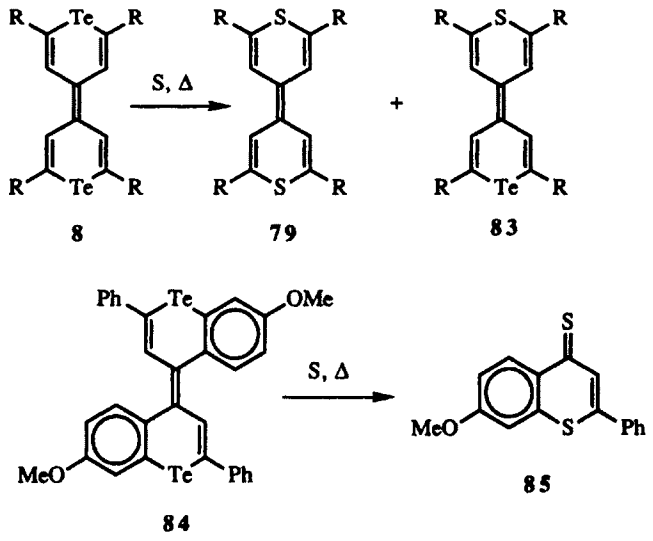

Scheme 23

gives both tellurium sulfur exchange as well as oxidative cleavage of the central double bond to give thione **85**.

If benzotellurin-4-one **86** is stirred with the Lawessen reagent at ambient temperature, a thione is isolated in which the tellurium atom is oxidized by sulfur to give tellurosulfide **87** as shown in Scheme 24. Heating a toluene solution of **87** at reflux produces **85** in 20% isolated yield.

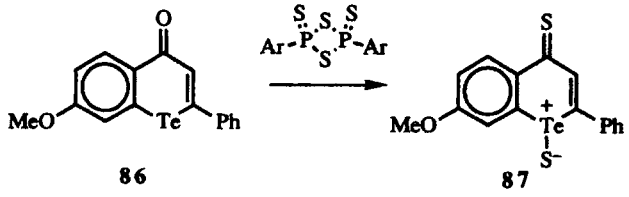

86 **87**

Scheme 24

Mechanistically, little is known about the tellurium–sulfur exchange. It is conceivable that elemental sulfur might act as an oxidant under appropriate conditions as shown in Scheme 25. Electron transfer from tellurium to sulfur might give a cation-radical/anion-radical pair, which could then collapse to give a tellurosulfide such as **87**. Intramolecular nucleophilic attack of sulfur at carbon could then lead to carbon–sulfur bond formation and elimination of tellurium.

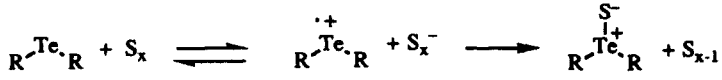

Scheme 25

B. X-Ray Structures of (Telluropyranyl)telluropyrans and Related Compounds

No X-ray structural data are available for the (telluropyranyl)telluropyrans. However, an X-ray structure of (selenopyranyl)selenopyran **81c** (R = Ph) shows that the heterocyclic rings are slightly boat-shaped at the heteroatom and C4.[95]

C. Oxidations of (Telluropyranyl)telluropyrans and Related Compounds

The (chalcogenopyranyl)chalcogenopyrans are characterized by two reversible one-electron oxidations. As shown in Scheme 26, these oxidations produce the cation-radical and dication states. Values for the electrochemical oxidation potentials of several series of (chalcogenopyranyl)chalcogenopyrans are compiled in Table 8.[98]

The (benzochalcogenopyranyl)benzochalcogenopyrans are characterized by a reversible two-electron oxidation.[96] Presumably, steric interactions between the 3 and 5′ and 5 and 3′ hydrogens are relieved by twisting around the central bond in the dication.

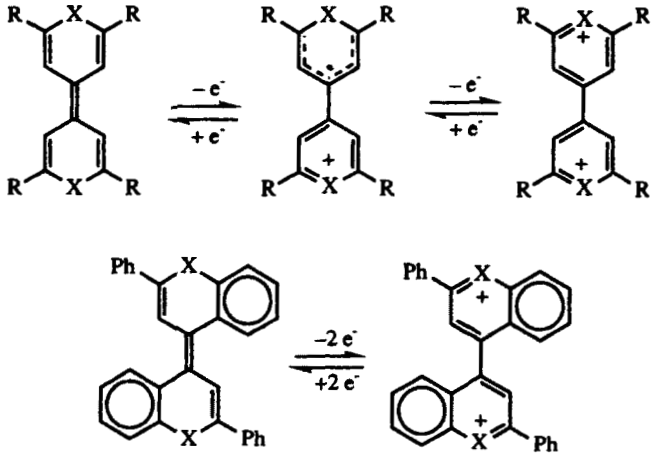

Scheme 26

One trend that emerges from the oxidation potentials of Table 8 is the narrowing of the gap between the first and second oxidations in these systems. While the ionization potentials of the chalcogen atoms become smaller with increasing size, which would indicate a lower oxidation potential, the observed trend is that oxidation becomes more difficult as the size of the chalcogen atom increases. Since π overlap of the chalcogen atom with the carbon π framework becomes less efficient with increasing size, this factor must predominate with respect to the first oxidation of (chalcogenopyranyl)chalcogenopyrans. With respect to the second oxidation, the oxidations potentials are fairly independent of heteroatom. Both the electronegativity of the chalcogen atoms and the size differences among the chalcogen atoms influence the ease of this oxidation. As the chalcogen atom increases in size down the series it becomes more electropositive. This helps overcome the Coulombic attraction for the second electron. However, less efficient overlap of the π framework leads to a more difficult oxidation. The net effect of these trends is to narrow the gap between E_1 and E_2.

D. EPR Spectra of (Telluropyranyl)telluropyrans and Related Compounds

The EPR spectra of cation radicals of **8b**, **8c**, **79–81** (R = *tert*-Bu), and **83** (R = *tert*-Bu) have been described.[97] The delocalization of the unpaired spin in the cation radicals of these species should be reflected in their EPR spectra and

in particular by the magnitude of the splitting of the unpaired spin with the ring protons (a_H). Values of the isotropic g value and a_H are compiled in Table 9 for these systems. It is interesting to note that a_H is larger for the (thiopyranyl)thiopyran **80** than for the (pyranyl)pyran **79**. The EPR spectra for the cation radicals of **81** and **8b** are featureless single lines with line widths of 1.26 and 4.06 G, respectively.

The increasing line widths and increasing g values are related to the spin–orbit coupling constant (λ) as the heteroatoms become larger.[103] The spin–orbit coupling constants for positively charged selenium and tellurium are available,[104] and for sulfur and oxygen they are assumed to be close to their neutral atom values.[103,104] A plot of g value versus the spin–orbit coupling constant (λ) is linear with $g = 2.0073 + 0.0571\,\lambda$ (where λ is in eV) with a correlation coefficient of 0.999.[97] The linearity of the data suggests that the spin populations on the heteroatoms are similar in the cation radicals of the (chalcogenopyranyl)chalcogenopyrans.[103] When the data for the (chalcogenapyranyl)chalcogenapyrans are plotted using the neutral-atom values of λ (values in Table 9, used for consistency with data presented later in the chapter), the relationship $g = 2.0072 + 0.0706\,\lambda$ is derived.

E. Cation-Radical Salts of (Telluropyranyl)telluropyrans and Related Compounds

(Telluropyranyl)telluropyran **8c**[98] forms a 1 : 1 complex and **8d**[95] forms a 1 : 0.9 complex when heated in solution with TCNQ. (Telluropyranyl)-telluropyran **8a** forms a 2 : 3 complex with TCNQ when one and a half equivalents of TCNQ are employed and forms a 1 : 2 complex with TCNQ when two equivalents of TCNQ are employed.[98] (Telluropyranyl)telluropyran **8b** forms emerald-green solutions with TCNQ, although no complexes have been isolated.

Typically, 1 : 1 complexes of (chalcogenopyranyl)chalcogenopyrans with closed-shell anions have been prepared by mixing one equivalent of the neutral (chalcogenopyranyl)chalcogenopyrans with one equivalent of the dication. However, under these conditions the (telluropyranyl)telluropyrans **8a–c** give 2 : 3 complexes of cation-radical/dication with the closed-shell anions. The dications of (telluropyranyl)telluropyrans are prepared by oxidation with copper perchlorate or copper tetrafluoroborate.[98]

Compressed-pellet conductivities of the various complexes of (telluropyranyl)telluropyrans and of some comparable lighter (chalcogenapyranyl) chalcogenopyrans are compiled in Table 10. The conductivities of the (telluropyranyl)telluropyran complexes are higher than those observed for phenoxtellurine (**2**) and related compounds at ambient temperature. There is an absence of X-ray structral data for conducting complexes of (telluropyranyl)telluropyrans. The conductivities of the 1 : 2 **8a**–TCNQ and the 1 : 0.9 **8d**–TCNQ complexes are high enough to require a segregated-stack

structure, while the relatively low conductivities of the 2 : 3 complexes of **8a–c** with closed-shell anions suggest a mixed stack behavior.

Quasi-one-dimensional metallic behavior has been suggested for the **81d**–TCNQ complex (R = *p*-tolyl) based on optical conductivities ($480\ \Omega^{-1}\,cm^{-1}$) from reflectance values in the 0.12–0.31 eV range and the temperature dependence of the static magnetic susceptibility down to 120 K.[95] This conclusion may be extrapolated to the **8d**–TCNQ complex with an optical conductivity of $193\ \Omega^{-1}\,cm^{-1}$.

III. NAPHTHO[1,8-*c*,*d*]-1,2-DITELLUROLES AND RELATED COMPOUNDS

The conducting properties of charge-transfer complexes of naphtho[1,8-*c*,*d*]-1,2-dithiole (**88**)[105] stimulated the search for heavier chalcogen analogs of **88** and the design of improved donor molecules for charge-transfer complexes of this type. The corresponding naphto[1,8-*c*,*d*]-1,2-diselenole (**89**) has been prepared, and its charge-transfer complex with TCNQ exhibits semiconductor properties at room temperature.[106] A plot of the logarithm of resistance versus $T^{-1/2}$ is linear with a positive slope over a large temperature range, which is again consistent with semiconductor properties.

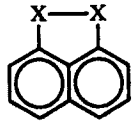

88, X = S
89, X = Se

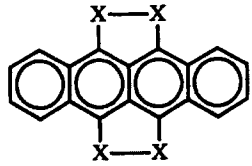

90, X = S
91, X = Se

The first improvements in conductivities in compounds of this type were realized with tetrathiatetracene (**90**). The room-temperature conductivity of the 2 : 3 complex of **90** with iodide is approximately $10^3\ \Omega^{-1}\,cm^{-1}$, but a conductivity increases with lower temperatures, which is indicative of metallic behavior. Below the temperature for maximum conductivity, a phase transition occurs and the conductivity follows an activation process below this temperature.[107] Conducting complexes of tetraselenatetracene (**91**) show a high conductivity at room temperature ($\approx 10^3\ \Omega^{-1}\,cm^{-1}$) and retain their metallic conductivity down to 26 K.[108–110] The solid-state properties of these complexes[111,112] and their band structure have been studied in some detail.[113]

In both series of compounds, the substitution of tellurium for selenium was expected to enhance certain features in conducting complexes of these molecules. The molecular polarizability of the donor molecule should increase on substitution of tellurium for selenium,[114] and the strength of intermolecular

chalcogen–chalcogen contacts should increase on tellurium substitution for selenium.

A. Synthesis of Naphtho[1,8-*c*,*d*]-1,2-ditelluroles and Related Compounds

The addition of tellurium metal to 1,8-dilithionaphthalene gives rise to naphtho[1,8-*c*,*d*]-1,2-ditellurole (**7**) in 8–12% isolated yield as shown in Scheme 27.[106] The addition of methyllithium to **7** gives loss of tellurium metal and the formation of 1,8-dimethylnaphthalene with just a trace of perylene.

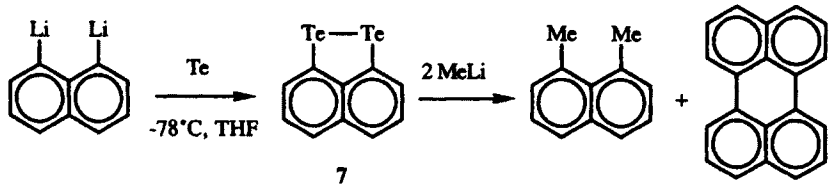

7

Scheme 27

Unsymmetrical naphtho[1,8-*c*,*d*]-1-chalcogena-2-telluroles have been prepared by similar chemistry as shown in Schemes 28 and 29.[115] Sequential lithiations of 1,8-dibromonaphthalene followed by sulfur and then tellurium insertion reactions give rise to naphtho[1,8-*c*,*d*]-1,2-thiatellurole (**92**) in about 2% isolated yield. Similar chemistry is employed in the preparation of naphtho[1,8-*c*,*d*]-1-selena-2-tellurole (**93**). Monolithiation of 1,8-dibromonaphthalene with one equivalent of *n*-butyllithium followed by selenium metal, lithiaton with a second equivalent of *n*-butyllithium, and tellurium metal gives naphtho[1,8-*c*,*d*]-1,2-selenatellurole (**93**) in 4% isolated yield.

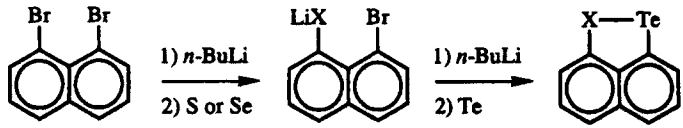

92, X = S
93, X = Se

Scheme 28

The yield of naphtho[1,8-*c*,*d*]-1-thia-2-tellurole (**92**) is improved on using 8-chloro-1-naphthalenethiol as a starting material.[115] As shown in Scheme 29, treatment of 8-chloro-1-naphthalenethiol with two equivalents of *n*-butyllithium followed by tellurium metal gives naphtho[1,8-*c*,*d*]-1-thia-2-tellurole (**92**) in 44% isolated yield.

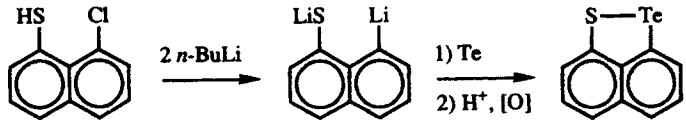

92

Scheme 29

Derivatives of **7** have been prepared that incorporate more rings in the carbon π framework as shown in Scheme 30. An acenaphthalene derivative of naphtho[1,8-*c*,*d*]-1,2-ditellurole (**7**) has been prepared via chemistry very similar to that for the preparation of **7**.[116] Treating 5,6-dibromoacenaphthalene with two equivalents of *n*-butyllithium in THF at − 78°C gives 5,6-dilithioacenaphthalene. The addition of fresh, finely divided tellurium metal to the 5,6-dilithioacenaphthalene at − 30°C gives **94** in 14% yield as brownish-black needles following sublimation. The fluoranthrene derivative **95** has been prepared in 18% yield from dichlorofluoranthrene and disodium ditelluride in DMF.[117,118] A 5,6-dihydroacenaphthalene derivative **96** has been prepared in 5% isolated yield by the addition of disodium telluride to 1,10-dichloro-5,6-dihydroacenaphthalene in HMPA.[119]

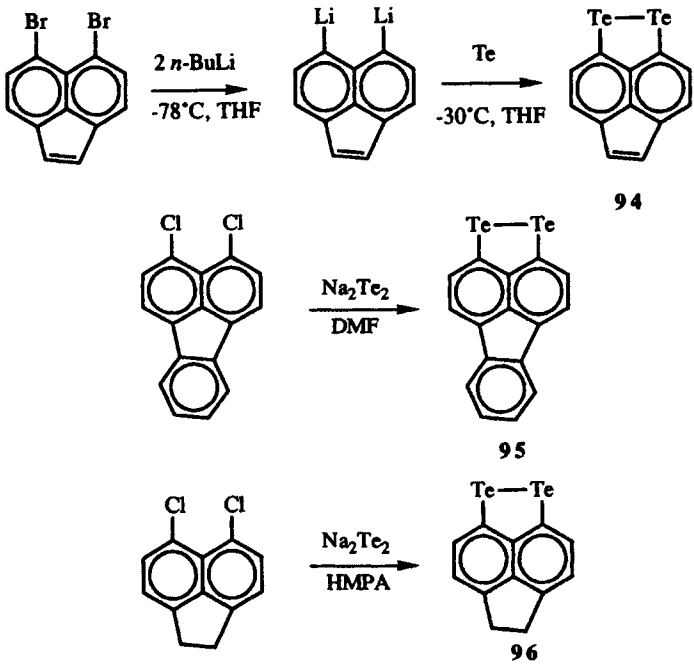

94

95

96

Scheme 30

A tetramethyl derivative of tetratelluranaphthalene (the parent compound remains unknown) has been prepared as shown in Scheme 31.[120] The reaction of 2,3,6,7-tetramethylnaphthalene with thionyl chloride gives 1,4,5,8-tetrachloro-2,3,6,7-tetramethylnaphthalene. The addition of disodium ditelluride (prepared from sodium and tellurium metals in HMPA) gives rise to **97** in about 6% isolated yield. The major product in this reaction, isolated in 31% yield, is naphtho[1,8-*c*,*d*]-1,2-ditellurole **98**.

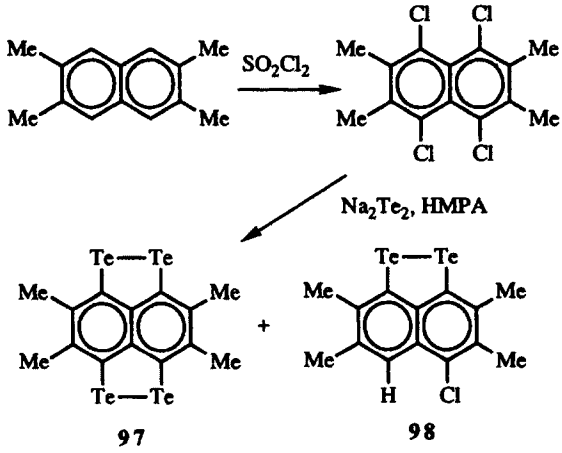

Scheme 31

Tetratellurotetracene **99** and diselenoditellurotetracene **100** have been prepared from chlorinated intermediates with chemistry similar to that used for the preparation of **97** as shown in Scheme 32. The addition of disodium ditelluride

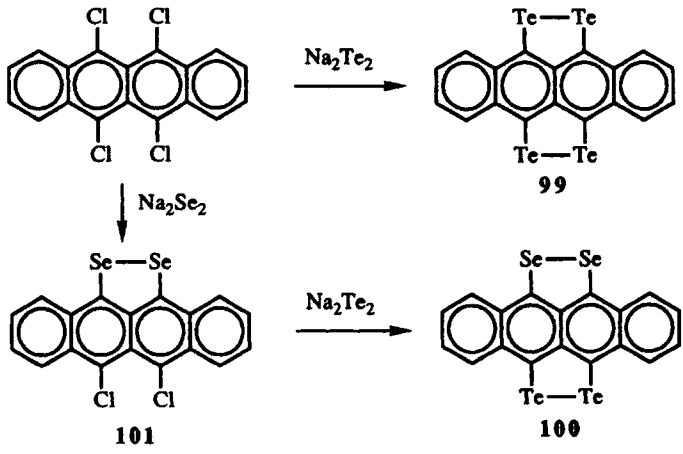

Scheme 32

to 5,6,11,12-tetrachlorotetracene in dimethylformamide gives **99** in 13% isolated yield.[121] The addition of one equivalent of disodium selenide to 5,6,11,12-tetrachlorotetracene gives diselenole **101** in 32% isolated yield. The addition of disodium telluride to **101** gives diselenoditellurotetracene **100** in 22% isolated yield.[122]

B. X-Ray Structural Data for Tetratellurotetracene

Two X-ray studies have been reported for tetratelluortetracene **99**.[121,123] Selected bond lengths and angles are compiled in Table 11.[121] Tetratellurotetracene **99** is a planar molecule and stacks with an intrastack distance of 3.732 Å and short interstack Te—Te contacts of 3.701 Å. The stacks are interconnected via infinite ···Te1—Te2···Te1′—Te2′··· chains with a Te1—Te2···Te1′ angle of 77.1° and a Te2···Te1′—Te2′ angle of 116.9°. In addition, there are infinite, equal ···Te1—Te1′—Te1″··· contacts of 4.055 Å. The Te—Te and Te—C bond lengths in **99** of 2.673 and 2.113 Å, respectively, are very close to the values observed for diphenyl ditelluride (2.712 and 2.115 Å, respectively).[124]

Although no X-ray structures have been reported for naphtho[1,8-*c*,*d*]-1,2-ditelluroles, some information can be inferred from the structure of naphtho-[1,8-*c*,*d*]-1,2-thiaselenole (**102**).[115] The molecule is planar with 4.244-Å stacking along the *b* axis (with a 25° tilt) in such a way that the chalcogen atoms form linear chains along the stacking direction.

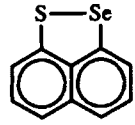

102

C. Oxidations of Naphtho[1,8-*c*,*d*]-1,2-ditelluroles and Related Compounds

The naphtho[1,8-*c*,*d*]-1,2-dichalcogenoles **7**, **88**, **89**, **92**, and **93** all exhibit low first vertical ionization potentials by He(I) photoelectron spectroscopy as compiled in Table 12.[103] Distinguishable bands are observed only in their low-energy region, and first ionization energies are found within a narrow range (7.03–7.14 eV). From parametrized HMO calculations, inductive perturbations and conjugative interactions follow opposite trends from sulfur to selenium to tellurium. Thus, the inductive shift to lower π-ionization energies (more electropositive element) in tellurium-containing derivatives is counteracted by the reduced second-order perturbation (or poorer overlap of tellurium with the carbon π framework). As a consequence, vertical ionization potentials are fortuitously similar throughout the series.

Electrochemical oxidation potentials of tetrachalcogenanaphthalenes **97**, **103**, and **104** follow trends that are similar to those found for vertical ionizations.[120] As shown in Table 13, a 0.15-V range in oxidation potentials is found from tetrathia derivative **103** to tetratellura derivative **97**. The difference between the first and second oxidation potentials (Δ_E) varies by only 0.06 V from **103** to **97**.

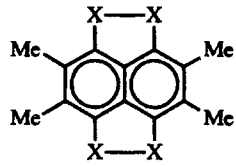

103, X = S
104, X = Se

The tetrachalcogenatetracenes **90**, **91**, and **99** show even smaller differences in oxidation potentials in solution than **97**, **103**, and **104**.[125] As shown in Table 13, first oxidation potentials vary by 0.08 V, while the difference between the first and second oxidation potentials varies by only 0.02 V.

In both systems, the tetratellura compounds undergo a more facile oxidation than either the tetrathia or tetraselena compounds. Presumably, the inductive component of the tellurium atom substitution is dominant. Similarly, the second oxidation is also more facile in the tetratellura compounds than in the sulfur and selenium analogs and ensures that the difference between first and second oxidation potentials (Δ_E) will always be smallest for the tellurium-containing derivatives. Interestingly, the difference between first and second oxidation potentials is smaller in the (chalcogenopyranyl)chalcogenopyrans (Table 8) than in the tetrachalcogenanaphthalenes or tetrachalcogenatetracenes.

D. EPR Spectra of Cation Radicals of Naphtho[1,8-*c*,*d*]-1,8-dichalcogenoles and Tetrachalcogenotetracenes

The naphtho[1,8-*c*,*d*]-1,8-dichalcogenoles are oxidized by aluminum trichloride in dichloromethane to give the corresponding cation radicals.[103] The EPR spectra of these cation radicals have been measured and values of the isotropic g value and a_H are compiled in Table 14.[103] While the cation radicals of **88**, **89**, **92**, **93**, and **102** give discernible EPR spectra, no discernible spectrum is observed from oxidized **7** down to 200 K. The isotropic g value can be plotted as a linear function of λ, the spin–orbit coupling constant, where $g = 2.0049 + 0.1116\,\lambda$. (The authors of reference 103 report $g = 2.00126 + 0.16421\,\lambda$. However, it is unclear which data are included in the linear regression to give these parameters. We include only the data for the acenaphthalene anion radical and data for cation radicals of the naphtho[1,8-*c*,*d*]-1,8-dichalcogenoles.)

The chalcogenatetracenes **90**, **91**, and **99** are oxidized by trifluoroacetic acid in dichloromethane to give the corresponding cation radicals. The EPR spectra of

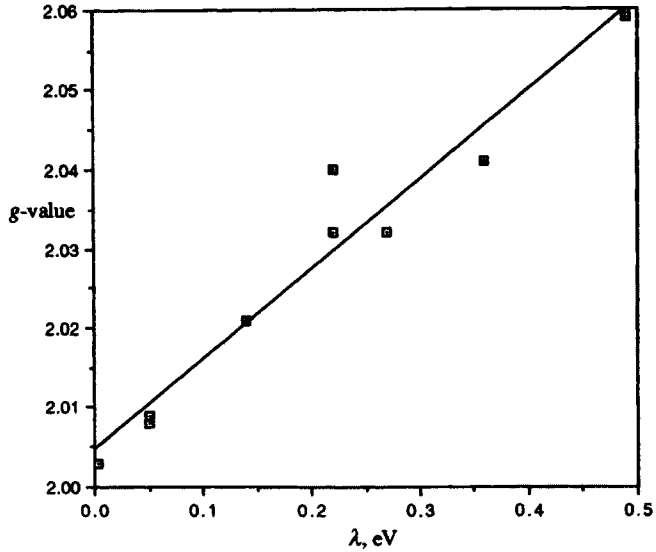

Figure 4. A plot of g value as a function of the neutral-atom spin–orbit coupling constant, λ (in eV).

these cation radicals have been measured, and values of the isotropic g value and a_H (or line width) are compiled in Table 15.[125]

The g values for the tetracenes and the naphtho[1,8-*c*,*d*]-1,8-dichalcogenoles can be plotted together as a function of λ as shown in Figure 4. The relationship is linear with $g = 2.0046 + 0.1128\,\lambda$ ($R^2 = 0.942$) and suggests that the chalcogen atoms bear similar spin densities in cation radicals of both the naphtho[1,8-*c*,*d*]-1,8-dichalcogenoles and the tetrachalcogenatetracenes.

In comparing the EPR spectra of the cation radicals of the naphtho[1,8-*c*,*d*]-1,8-dichalcogenoles, the tetrachalcogenatetracenes, and the (chalcogenopyranyl)-chalcogenopyrans, two characteristics appear to correlate with heteroatom changes. These characteristics are line widths and g values. Both characteristics are correlated with spin–orbit coupling, which increases as the chalcogen atoms increase in atomic weight. With increasing spin–orbit coupling, the longitudinal relaxation time decreases and the line width increases. With increasing spin–orbit interactions, one expects a shift in g values. From McLachlan spin density calculations,[103,125,126] the spin density on the heteroatoms is essentially independent of the heteroatom. Consequently, the g value is determined by the value of the chalcogen spin–orbit coupling constants.

E. Cation-Radical Salts of the Naphtho[1,8-*c*,*d*]-1,8-dichalcogenoles, Tetrachalcogenatetracenes, and Related Compounds

Complexes of the naphtho[1,8-*c*,*d*]-1,8-dichalcogenoles with TCNQ have been described.[127] In these 1 : 1 complexes, values of the room-temperature

conductivity (σ) increase by 10^9 from the dithiole **89** to the ditellurole **7** (Table 16). In the related series of acenaphthalene dichalcogenoles, an approximately 10^4 increase in σ is observed from the dithiole analog **105** to the ditellurole analog **94**.[116]

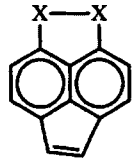

105, X = S
106, X = Se
94, X = Te

Plots of resistivity versus temperature for the 1 : 1 complexes of TCNQ with diselenole **89** and ditellurole **7** show two different types of behavior.[106] A plot of the logarithm of resistance for compressed pellets of the complexes versus $T^{-1/2}$ is linear with a positive slope over a large temperature range for the **89**–TCNQ complex. However, a similar plot for the **7**–TCNQ complex suggests metallic behavior over a narrow range around room temperature. At room temperature, the compressed-pellet conductivities of the **89**–TCNQ and **7**–TCNQ complexes are 5×10^{-8} and $2 \times 10^{-2}\ \Omega^{-1}\ \text{cm}^{-1}$, respectively.

Studies of salts of tetratelluratetracene **99** are hindered in part by the insolubility of the materials. Bromide salts of **99** and the mixed selenium–tellurium tetracene **100** are obtained as fine black needles by the electrochemical oxidations of solutions containing the corresponding donor and supporting electrolyte in benzonitrile.[128]

The low-temperature phases of the tetraselenatetracene **91**–chloride and tetraselenatetracene **91**–bromide complexes are considered to be semimetallic.[111,112] The tetraselenatetracene **91**–bromide salt exhibits metallic conductivity down to 38 K in that conductivity increases as temperature decreases. At 38 K, a phase transition occurs and conductivity follows an activation process in that the resistivity increases with decreasing temperature.[128]

The diselenaditelluratetracene **100**–bromide complex is a reasonably good conductor although resistivity increases with increasing temperature.[128] The X-ray crystal structure of the complex shows that the chalcogen atoms are disordered. Consequently, the disorder localizes electrons over a finite length in the chalcogen-containing stacks such that they cannot contribute to the conductivity. Even with this disorder, room-temperature conductivity of the compressed pellet is approximately $30\ \Omega\,\text{cm}^{-1}$.

As shown in Figure 5, the molecules of **100** in the **100**–Br complex form a uniform column along the *c* axis.[128] The molecular plane is tilted 48.2° from the perpendicular to the *c* axis. The interplanar spacing is 3.47 Å and the Se(Te)···Te(Se) contacts are short (3.554 Å). The **100**–Br crystals are isostructural with those of the $(\mathbf{91})_2$–Cl complex.[111,112]

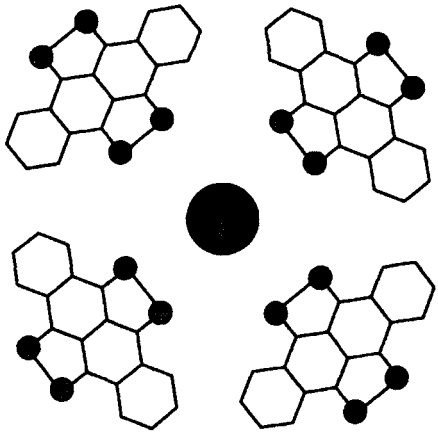

Figure 5. A view along the *c* axis of single crystals of the **100**–bromide complex.

A variety of conducting complexes have been formed between tetramethyltetratelluranaphthalene **97** and various π-acceptors.[117] For the most part, these are 1 : 1 complexes and stoichiometry, and conductivity data are compiled in Table 17. For comparison purposes, complexes with tetrathia derivative **103** and tetraselena derivative **104** are included as well. Complexes of **97**, **103**, and **104** are semiconductors at room temperature.

Attempted formation of conducting salts of **97** with the closed-shell anions chloride and bromide fails because **97** decomposes under the electrolysis conditions.[117] The iodide salt of **97** can be prepared by mixing **97** with tetrabutylammonium triiodide in benzonitrile. Data for the **97**-iodide complex are also compiled in Table 17.

IV. TETRATELLURAFULVALENES

An entire field has developed around the observations of high conductivity in TTF–Cl^1 and TTF–TCNQ[129] complexes. This field of organic conductors covers semiconducting to superconducting ground states, and contributions in this field are fundamental to current understanding of various physical phenomena including charge and spin density waves, Mott–Hubbard insulators, and Peierls transitions.[16–24,130]

Superconductivity in these systems has been achieved in tetramethyltetraselenafulvalenes (TMTSF, **107**) complexes and bis(ethylenedithio)tetrathiafulvalene (BEDT–TTF, **108**) complexes.[16] Achieving the superconducting ground state has been correlated with increased dimensionality in the intra- and interstack chalcogen contacts. These increased contacts produce a two-dimensional conducting network similar to those exhibited in the superconducting

ceramic complexes, which remain superconducting to much higher temperatures. The substitution of tellurium for the lighter chalcogens in these systems should provide stronger chalcogen–chalcogen contacts due to the larger size of tellurium.

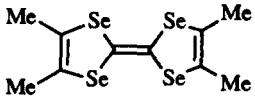

TMTSF, 107

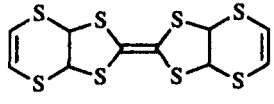

BEDT-TTF, 108

A. Synthesis of Tetratellurafulvalenes

The syntheses of the various tetratellurafulvalenes (TTeFs) that have been prepared to date all form a similar intermediate in the penultimate step. The addition of a tetrahaloethylene to a dilithium ethyleneditellurate is the final step for all the syntheses. This is illustrated in the first reported synthesis of a tetratellurafulvalene—the synthesis of hexamethylenetetratellurafulvalene (HMTTeF, **109**).[131] As shown in Scheme 33, the formation of dilithio-1,2-penteneditellurate (**110**) is the key to the synthesis. The addition of tetrachloroethylene gives **109** in 32% yield.

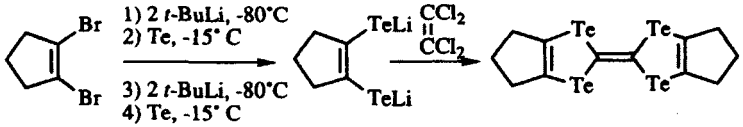

110 **109**

Scheme 33

Variations of this route have been utilized to prepare other derivatives of TTeF. As shown in Scheme 34, the addition of tellurium metal to 1,2-dilithiobenzene gives the dilithium salt of benzene-1,2-ditellurate (**111**).[132] The addition of tetrachloroethylene to **111** followed by stirring at ambient temperature for 3 days gives dibenzotetratellurafulvalene (**112**) in 10% isolated yield.

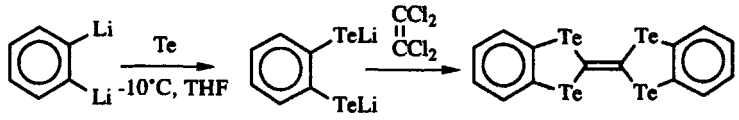

111 DBTTeF, 112

Scheme 34

Bis(dimethylthieno)tetratellurafulvalene (BDMT–TTeF, **113**) has been prepared by a similar route as shown in Scheme 35.[133] Metal–halogen exchange followed by tellurium insertion into the carbon–lithium bond and repetition of the sequence gives the dilithio ditellurate **114**. The addition of tetrachloroethylene gives **113** in 75% yield.

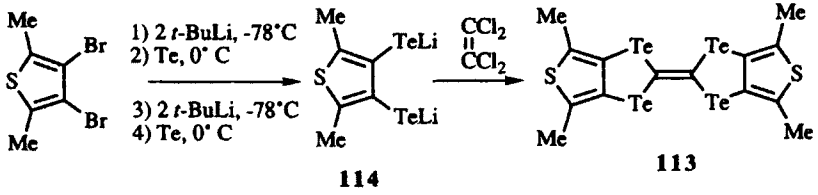

114 **113**

Scheme 35

The preparation of the parent TTeF (**115**) follows a slightly different procedure to arrive at the same penultimate intermediate as shown in Scheme 36.[134] Tin–lithium exchange followed by tellurium insertion into the carbon–lithium bond and repetition of the sequence gives **116**. The addition of tetrachloroethylene to **116** gives TTeF (**115**) in 36% isolated yield. Following rigorous purification to remove the six-membered ring compound **117**, TTeF is obtained in about 5% yield. The yield of TTeF as well as its purity have been improved by the use of tetrabromoethylene in place of tetrachloroethylene and by maintenance of the reaction temperature at $-78°C$ for the tellurium insertion reactions.[135]

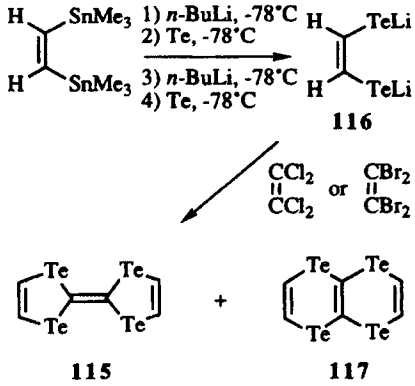

116

115 **117**

Scheme 36

Similar approaches have been utilized to prepare more soluble analogs of hexamethylenetetratellurafulvalene. Starting with the appropriate, 1,2-dibromocyclopentene, TTeFs **118–120** are prepared in 9–35% isolated yields via metal–halogen exchange and tellurium insertion reactions.[136,137]

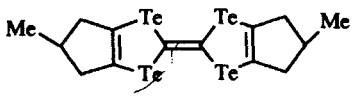

118

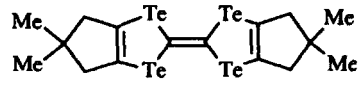

119

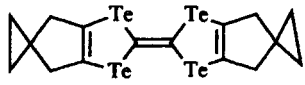

120

B. Physical Properties of Tetratellurafulvalenes

The X-ray crystal structures for HMTTeF (**109**)[138] and BDMT–TTeF (**113**)[133] have been described. Selected bond lengths and angles are compiled in Table 18 for HMTTeF (**109**). In the crystal, the HMTTeF molecules are nearly planar. The HMTTeF molecules display no tendency to form uniform stacks and display two intermolecular tellurium contacts that are significantly shorter than van der Waals radii at 3.743 and 3.583 Å. The Te3···Te3′ distance of 3.583 Å is the shortest intermolecular tellurium contact observed to date.

Unlike HMTTeF (**109**), BDMT–TTeF (**113**) is nonplanar in the crystalline state, exhibiting an asymmetric boat conformation as shown in Figure 6.[133] The dihedral angles in BDMT–TTeF for the exterior dimethylthienoditellural planes are quite different at 47.1° and 16.0°. In the crystal, the molecules of BDMT–TTeF are coupled together as dimers with short intermolecular Te···Te contacts of 3.666 and 3.758 Å (the van der Waals radius of tellurium is 2.20 Å).

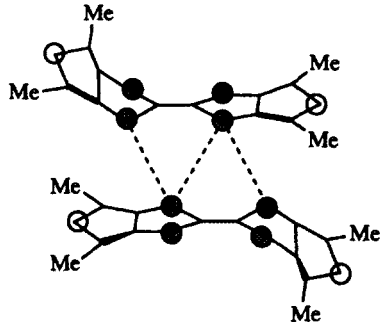

Figure 6. Molecular structure of BDMT–TTeF (**113**) and its association into dimers through short tellurium–tellurium contacts.

In both the crystal structures of both **109** and **113**, the intermolecular Te···Te contacts appear to be dominant forces in determining the strength of intermolecular interactions of TTeFs. As is discussed below, these contacts carry over to cation-radical salts of these molecules.

C. Electrochemical Oxidation Potentials for Tetratellurafulvalenes

Oxidation potentials for the various tetratellurafulvalenes are compiled in Table 19.[131,132,134,137] Oxidation potentials for the corresponding lighter chalcogen analogs are also compiled in Table 19. Dibenzotetratellurafulvalene (**112**) is the most difficult system to oxidize while hexamethylenetetratellurafulvalene derivatives (**109** and **118–120**) are the most facile to oxidize. A trend that has emerged in other chalcogen-containing donors reappears in the series of tetrachalcogenafulvalene donors. The gap between the first and second oxidation potentials (Δ_E) decreases as the chalcogen atoms increase in size.

As described before, increasing electropositive character in the heteroatom as the chalcogens increase in size should make oxidation more facile. Poorer overlap with the carbon π framework as the chalcogen atoms increase in size should work in the opposite sense and make oxidation more difficult. In general, in the series compiled in Table 19, the tetraselenafulvalene analogs are more difficult to oxidize than either the tetratellurafulvalenes or the tetrathiafulvalenes. The tetrathiafulvalenes appear to be somewhat easier to oxidize than the tetratellurafulvalenes. Both electronegativity differences and size differences appear to influence the oxidation potentials of these molecules.

D. EPR Spectra of Tetratellurafulvalenes Cation Radicals

The EPR spectrum of a microcrystalline salt of HMTTeF (**109**)–TCNQ has been recorded.[131] A g value of 2.0039 with a line width of 4 G is observed and suggests that the spins are observable on only the TCNQ molecules. EPR studies of the TTeF (**115**)–TCNQ salt down to 8 K have been performed but give no measurable resonances.[139,140] The absence of an EPR signal in the latter system could be due to either increased spin–orbit coupling in the tellurium atoms or increased dimensionality of the TTeF–TCNQ.

E. Conducting Salts of Radical-Cation Complexes of Tetratellurafulvalenes

Complexes of tetratellurafulvalenes with TCNQ have been reported. Single crystals of TTeF (**115**)–TCNQ have been obtained as shiny black needles by carefully layering a carbon disulfide/TTeF solution with an acetonitrile/TCNQ solution under an inert atmosphere.[139–141] Single-crystal conductivities for the TTeF–TCNQ complex as well as the corresponding selenium (TSF–TCNQ)[142] and sulfur (TTF–TCNQ)[129] analogs are compiled in Table 20.

The room-temperature conductivity of the TTeF–TCNQ salt is substantially larger than those of the TSF–TCNQ and TTF–TCNQ salts. In part, this is presumably due to the larger size of the tellurium atom, which should increase both inter- and intrastack contacts. Furthermore, the larger chalcogen should increase the bandwidth and reduce the on-site Coulombic repulsions.[141]

Magnetic susceptibility measurements of TTeF–TCNQ crystals are nearly independent of temperature and the magnetic susceptibility decreases below the core susceptibility around 200 K.[139] This Pauli-like paramagnetic behavior of the magnetic susceptibility is consistent with the metallic properties of TTeF–TCNQ.

The dc conductivity of single crystals decreases as the temperature is lowered from 300 to 100 K, reaching a value that is approximately two times the room-temperature conductivity.[140] Using a microwave perturbation technique to measure conductivity, the room temperature conductivity of approximately $1300\ \Omega^{-1}\,cm^{-1}$ increases by about a factor of 3 down to 100 K. Below 90 K a gradual decrease in conductivity, approaching the room-temperature conductivity, is observed. The conductivity response down to 100 K as a function of temperature is consistent with metallic behavior.

Two trends that are observed as the chalcogen varies from sulfur to selenium to tellurium are an increase in the stacking axis length (from 3.819 Å for TTF–TCNQ[143] to 3.876 Å for TSF–TCNQ[142] to 3.947 Å for TTeF–TCNQ[141]) and an increase in the amount of charge transfer from the donor to the acceptor (from $z = 0.59$ for TTF–TCNQ[144] to $z = 0.63$ for TSF–TCNQ[142] to $z = 0.71$ for TTeF–TCNQ[140]). The increase in the stacking direction from sulfur or selenium to tellurium (0.13 or 0.07 Å, respectively) is less than the increase in van der Waals radii from sulfur or selenium to tellurium (0.32 or 0.12 Å, respectively). This suggests that inter- and intrastack chalcogen–chalcogen contacts should be stronger in TTeF–TCNQ.

The Fermi level associated with $z = 0.71$ for charge transfer is not closed such that each donor layer of TTeF–TCNQ is a one-dimensional metal.[141] Tight-binding band electronic structure calculations on isolated donor and acceptor stacks of the tetrachalcogenafulvalene–TCNQ complexes show that all three salts are quasi-one-dimensional metals.[141] These calculations show that the acceptor bandwidth remains nearly constant in all three complexes but the donor bandwidth increases as the chalcogen atom varies from sulfur to selenium to tellurium. In this series, the experimental conductivity ratio is well reproduced by the relationship

$$\sigma(\mathrm{X}) \propto W_{\mathrm{D}}^2 + W_{\mathrm{A}}^2$$

where X is the chalcogen atom, W_{D} is the donor bandwidth, and W_{A} is the acceptor bandwidth. Since W_{A} is approximately constant, the increased conductivity in TTeF–TCNQ is due primarily to enhancement of conductivity along the donor stacks.[141]

The crystal structure of the TTeF–TCNQ complex is a segregated stack structure.[141] As shown in Figures 7 and 8, the layers of donor molecules have both intrastack (Fig. 7, 3.95 Å[139–141]) and interstack (Fig. 8) short Te···Te contacts. This mode of packing is quite different from the packing found for TSF–TCNQ and TTF–TCNQ complexes, in which donor stacks are separated by acceptor stacks such that there are no short interstack chalcogen–chalcogen

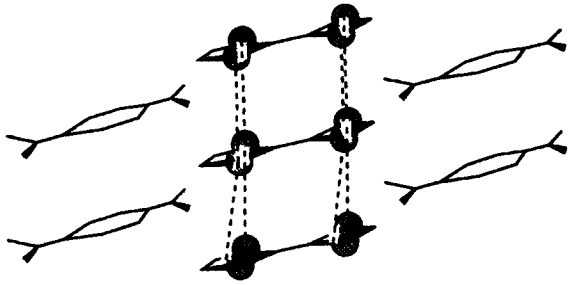

Figure 7. Projection along the *a* axis showing intrastack Te···Te contacts.

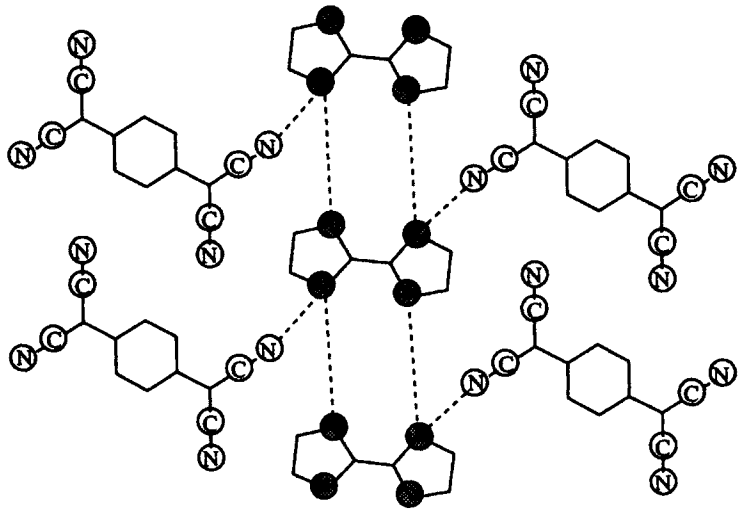

Figure 8. Projection along the *b* axis showing interstack Te···Te contacts.

contacts. Furthermore, the adjacent donor and acceptor molecules are locked in an "X"-type arrangement in the TSF–TCNQ and TTF–TCNQ complexes.

Selected bond lengths and angles for the TTeF–TCNQ complex are compiled in Table 21.[141] Both molecules are planar in the crystalline state. The carbon–carbon bond joining the two five-membered rings is quite long at 1.40 Å, which is consistent with diminished double-bond character in the cation-radical state.

The TTeF–ClO_4 complex can be grown electrolytically from a THF solution saturated in TTeF and containing tetrabutylammonium perchlorate as supporting electrolyte.[139] The conductivity response of this complex as a function of temperature is quite different from that of the TTeF–TCNQ complex. From an initial room-temperature conductivity of $3.6\,\Omega^{-1}\,cm^{-1}$ the conductivity decreases as the temperature decreases, which represents nonmetallic behavior.

Single crystals of the HMTTeF (**109**)–TCNQ complex have been grown by diffusion in H cells with HMTTeF in carbon disulfide and TCNQ in chlorobenzene, and conductivities have been measured.[145–147] Values of the room-temperature conductivity are compiled in Table 20. While the values are not as large as the room-temperature conductivity of the TTeF–TCNQ complex, at least one group reports metallic conductivity to 77 K, with the maximum conductivity being approximately twice ($910\ \Omega^{-1}\,cm^{-1}$) the room temperature conductivity.[147] Similar conductivities and thermal responses are observed for the HMTTeF-(2,5-*dim*ethyl–TCNQ) complex ($\sigma_{295}K = 460\ \Omega^{-1}\,cm^{-1}$, $\sigma_{83}K = 1000\ \Omega^{-1}\,cm^{-1}$).[147]

Oscillation photographs (Cr K_α radiation) about the needle axis for highly conducting salts of both the HMTTeF–TCNQ and HMTTeF–DMTCNQ complexes show only poorly developed zeroth- and first-order layer lines.[147] The repeat distance along the needle axis is 4.10 Å, which is indicative of a segregated stack.

A second phase of the HMTTeF–DMTCNQ complex crystallizes in a mixed stack.[147] In this structure, the HMTTeF molecules are planar with a 3.61-Å separation from the planar DMTCNQ molecules above and below. In this crystal form with carbon disulfides of crystallization, there are no short intermolecular Te···Te contacts. However, the N···Te contacts in plane are short at 3.16 and 3.26 Å.

The single-crystal conductivities of the complexes of substituted hexamethylenetetratellurafulvalenes **118–120** with TCNQ are at least eight orders of magnitude lower than the conductivity of the HMTTeF–TCNQ complex (Table 20).[137] The dramatic decrease in conductivity with substitution at the central methylenes of the hexamethylene units may be a direct consequence of steric interactions increasing the distance of the intrastack tellurium–tellurium contacts. Similar decreases in conductivity are also observed in comparisons of HMTTeF complexes with closed-shell anions and similar complexes of **118–120** with closed-shell anions.[136]

Conducting salts of HMTTeF (**109**) with closed-shell anions can be grown electrochemically with tetrabutylammonium salts of the closed-shell anion.[148–151] Single-crystal conductivities at ambient temperature for these materials are compiled in Table 20. These materials follow metallic behavior to 100 K for the HMTTeF–Br complex, to 170 K for the HMTTeF–Cl complex, and to 120 K for the HMTTeF–I complex.[148] The other radical salts of HMTTeF (**109**) behave as semiconductors with respect to their conductivity–temperature response with small activation energies.[148]

X-ray structures have been reported for two different forms of the $(HMTTeF)_4(PF_6)_2$ complex.[150,151] The most interesting feature of these two structural studies are the four HMTTeF molecules in the unit cell. Three of the HMTTeF molecules are stacked along the *a* axis to form a trimeric molecular column of HMTTeF molecules as shown in Figure 9. The fourth HMTTeF molecule is located in the space between the columns with its molecular plane almost parallel to the direction of the column. Standard deviations are large in

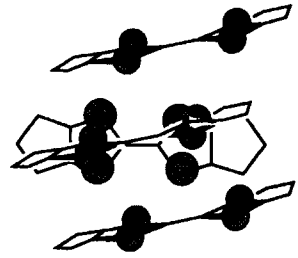

Figure 9. A side view of the stacking of the HMTTeF molecules in the $(HMTTeF)_4(PF_6)_2$ crystals with the PF_6 counterions not shown for clarity.

these studies, but the bond distances suggest the HMTTeF molecules in the columns are partially ionized while the intercalated molecules are neutral. Selected bond lengths are compiled in Table 22 for these salts. Short intrastack Te···Te contacts are observed at 4.02 and 4.12 Å in the α-crystal form[151] and somewhat shorter at 3.85 and 3.94 Å in the β-crystal form.[150] Much shorter Te···Te contacts are observed between columns and the intercalated HMTTeF.[150,151]

Highly conducting salts of BDMT–TTeF (**113**) can be electrochemically grown.[152,153] Single-crystal conductivities of these salts at ambient temperature are compiled in Table 20. These materials display semiconductor behavior with decreasing conductivity with lower temperatures. The activation energies for conduction are small—on the order of 0.07–0.18 eV.[152]

The X-ray crystal structure of the perchlorate salt of BDMT–TTeF reveals a planar BDMT–TTeF molecule.[152] This is in marked contrast to the boat-shaped neutral BDMT–TTeF (**113**) molecule.[133] The stoichiometry of the crystal is 3 : 2 : 4 with respect to BDMT–TTeF, perchlorate, and trichloroethane solvent, respectively. The three-molecule stack in the unit cell is twisted by approximately 45° such that overlapping is not in a zigzag fashion but in a twisted fashion. The donor stacks are separated from one another by the solvent and perchlorate units. In the unit cell, there are 14 short Te···Te intermolecular contacts (3.93–4.12 Å) that are less than the sum of van der Waals radii.

A stable fullerene charge-transfer complex with HMTTeF has been described recently.[154] The complex with C_{60} is a one-to-one complex, black, weakly magnetic, insoluble in most solvents, and stable in air. The room-temperature, two-probe resistance is $> 20\ M\Omega$.

V. OTHER CHARGE-TRANSFER COMPLEXES WITH TELLURIUM-CONTAINING DONOR MOLECULES

The TCNQ complex of dibenzotellurophene (**50**) has been prepared. Single-crystal conductivities of the 1 : 1 complex have been measured by two different groups and found to be $8 \times 10^{-5}\ \Omega^{-1}\,cm^{-1}$ and $10^{-7}\ \Omega^{-1}\,cm^{-1}$,

respectively.[155,156] The crystal structure of this complex shows a mixed stack with the interplanar spacing between donors and acceptors of 3.45 Å.[155]

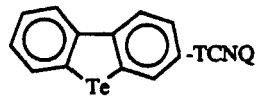

50

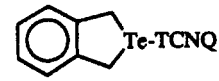

121

The TCNQ complex of 1,3-dihydro-2-telluraindane has also been described.[156] The conductivities of compressed pellets of this material are on the order of $10^{-14}\ \Omega^{-1}\,cm^{-1}$, which suggests that this complex is insulating.

TABLES

TABLE 1. VALUES OF Θ AND Φ FOR PHENOXTELLURINES AND RELATED COMPOUNDS

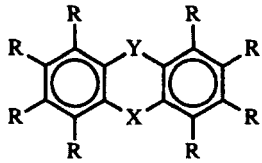

Compd.	X	Y	R	Θ (°) (Solution)	Ref.	Θ (°) (Solid)	Φ (°) (Solid)	Ref.
2	Te	O	H	172.2	66	138	145	67
3	Te	S	H	133.3	68	120.2	126.8	69
4	Te	Se	H	134.0	68	119.9	122.8	69
5	Te	Te	H	124.6	70	120.0	112.0	56
53	Te	Te	F	—	—	118.4	111.5	60
36	Se	O	H	162.6	66	139.7	147.0	69
42	Se	S	H	135.0	68	123.7	128.3	69
48	Se	Se	H	139.0	70	123.4	126.8	69
—	Se	Se	F	—	—	123	126	71
37	S	O	H	163.4	66	141	151	46
41	S	S	H	142.4	69	128	—	72
38	O	O	H	163.8	66	180	180	73,74

TABLE 2. CARBON–CHALCOGEN–CARBON ANGLES AND CARBON–CHALCOGEN BOND LENGTHS IN PHENOXTELLURINES AND RELATED COMPOUNDS

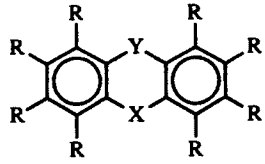

Compd.	X	Y	R	C—X—C	C—Y—X	C—X	C—Y	Ref.
				(°)		(Å)		
2	Te	O	H	89.4	121.2	2.10	1.40	67
3[a]	Te	S	H	92.8	93.5	2.05	1.94	69
4[a]	Te	Se	H	94.7	96.4	2.03	2.01	69
5	Te	Te	H	95.6	95.6	2.11	2.11	56
53	Te	Te	F	92.9	92.9	2.11	2.11	60
36	Se	O	H	93.5	119.4	1.90	1.39	69
42[a]	Se	S	H	97.5	97.5	1.87	1.84	69
48	Se	Se	H	97.8	98.3	1.90	1.90	69
—	Se	Se	F	96.5	96.5	1.90	1.90	71
37	S	O	H	97	118	1.74	1.38	46
41	S	S	H	100.2	100.2	1.74	1.74	72
38	O	O	H	118.8	118.8	1.39	1.39	73,74

[a] Disorder in crystal leads to average values.

TABLE 3. AVERAGE IONIZATION ENERGIES (IE) AND SPLITTINGS OF THE FIRST TWO π IEs FOR PHENOXTELLURINES AND RELATED COMPOUNDS

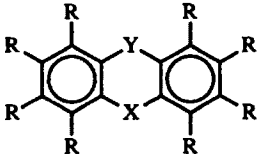

Compd.	X	Y	R	IE_1	IE_2	Δ_{IE}	Ref.
				(eV)			
2	Te	O	H	8.13	9.28	1.05	66
3	Te	S	H	7.97	8.52	0.55	68
4	Te	Se	H	7.87	8.27	0.40	68
5	Te	Te	H	7.62	7.82	0.20	70
36	Se	O	H	8.21	9.14	0.93	66
42	Se	S	H	8.12	8.51	0.39	68
48	Se	Se	H	8.05	8.30	0.25	70
37	S	O	H	8.22	9.21	0.99	66
41	S	S	H	8.19	8.68	0.49	70
38	O	O	H	8.27	9.25	0.98	70

TABLE 4. ELECTROCHEMICAL OXIDATION POTENTIALS FOR PHENOXTELLURINES **57a** AND **58a** AND RELATED COMPOUNDS IN DICHLOROMETHANE AND ACETONITRILE[a]

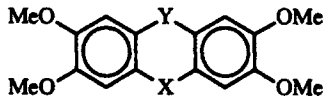

57

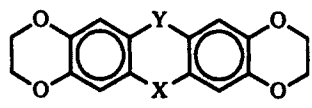

58

			In CH_2Cl_2			In CH_3CN		
			E^1	E^2	Δ_E	E^1	E^2	Δ_E
Compd.	X	Y	[V (vs. SCE)]		(V)	[V (vs. SCE)]		(V)
57a	Te	O	0.65	(1.45)	0.80	(0.70)	(1.65)	0.95
57b	Te	S	0.79	(1.21)	0.42	(0.86)	1.50	0.64
57c	Te	Se	(0.98)	(1.10)	0.12	(0.90)	(1.46)	0.56
57d	Se	O	0.89	1.42	0.53	0.79	1.21	0.42
57e	Se	S	1.02	1.37	0.35	0.90	1.21	0.31
57f	Se	Se	1.06	(1.43)	0.37	0.87	1.19	0.32
57g	S	O	0.87	1.44	0.57	0.77	1.24	0.47
57h	S	S	0.98	1.37	0.39	0.86	1.21	0.35
58a	Te	O	(0.92)	—	—	0.62	1.30	0.68
58b	Te	S	(1.05)	(1.80)	0.75	(0.94)	(1.58)	0.64
58c	Te	Se	(1.08)	(1.55)	0.47	(0.95)	(1.42)	0.47
58d	Se	O	1.02	1.42	0.40	0.92	(1.30)	0.38
58e	Se	S	1.15	(1.52)	0.37	1.04	1.32	0.28
58f	Se	Se	1.18	(1.55)	0.37	1.06	(1.34)	0.28
58g	S	O	1.01	1.52	0.51	0.92	1.39	0.47
58h	S	S	1.10	1.51	0.41	1.01	1.33	0.32

[a] Reference 63. Numbers in brackets are E_p for irreversible waves. Data taken from a Pt disk electrode with 0.002 *M* sample and 0.15 *M* tetra-*n*-butylammonium tetrafluoroborate as supporting electrolyte with a scan rate of 0.1 $V\,s^{-1}$.

TABLE 5. ^{13}C NMR CHEMICAL SHIFTS FOR PHENOXTELLURINE (2) AND RELATED COMPOUNDS[a]

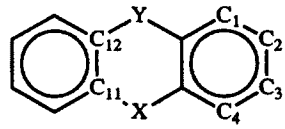

			C1	C2	C3	C4	C11	C12
Compd.	X	Y	(δ, ppm in $CDCl_3$)					
2	Te	O	119.71	129.21	125.61	135.05	102.11	155.91
3	Te	S	130.42	128.45	127.97	136.10	123.22	139.71
4	Te	Se	131.70	128.54	128.07	136.36	124.79	138.71
5	Te	Te	136.56	128.44	128.44	136.56	130.62	130.62
36	Se	O	118.71	128.24	125.00	116.29	116.29	153.02
42	Se	S	129.49	127.92	127.91	130.75	133.66	136.20
48	Se	Se	131.20	128.05	128.05	131.20	134.55	134.55
37	S	O	117.77	127.58	124.49	126.75	120.10	152.13
41	S	S	128.71	127.66	127.66	128.71	135.52	135.52
38	O	O	116.20	123.60	123.60	116.20	142.10	142.10

[a] Reference 77.

TABLE 6. ^{1}H NMR CHEMICAL SHIFTS FOR PHENOXTELLURINE (2) AND RELATED COMPOUNDS

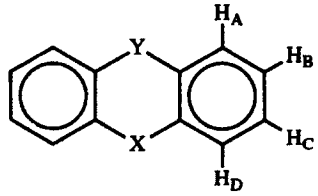

			H_A	H_B	H_C	H_D
Compd.	X	Y	(δ, pppm in $CDCl_3$)			
2	Te	O	7.244	7.236	7.03	7.51
3	Te	S	7.73	7.28	7.16	7.84
4	Te	Se	7.85	7.25	7.17	7.90
5	Te	Te	8.03	7.17	7.17	8.03
36	Se	O	7.11	7.19	7.03	7.29
42	Se	S	7.59	7.28	7.23	7.64
48	Se	Se	7.71	7.24	7.24	7.71
37	S	O	6.70	7.12	7.00	7.09
41	S	S	7.48	7.23	7.23	7.48
38	O	O	6.81	6.85	6.85	6.81

[a] Reference 77.

TABLE 7. VALUES OF TRIPLET QUANTUM YIELDS (Φ_T) AT 293 K, PHOSPHORESCENCE QUANTUM YIELDS (Φ_P) AT 77 K, TRIPLET LIFETIMES (τ_T), RATES OF INTERSYSTEM CROSSING (K_{isc}), AND RATES OF PHOSPHORESCENCE (k_P) FOR PHENOXTELLURINE (2) AND RELATED COMPOUNDS[a]

Compd.	X	Y	Φ_T	Φ_P	τ_T (ms)	k_{isc} (s^{-1})	k_P (s^{-1})
2	Te	O	—	1.00	< 0.3	> 10^{11}	> 3300
36	Se	O	0.63	1.00	0.7	> 10^{11}	1400
37	S	O	0.69	0.64	72	> 10^{11}	13
38	O	O	—	0.73	800	> 10^{11}	0.9
48	Se	Se	—	0.91	0.9	> 10^{11}	1100
41	S	S	0.94	0.95	35	3×10^7	29

[a] Reference 79.

TABLE 8. ELECTROCHEMICAL OXIDATION POTENTIALS FOR (TELLUROPYRANYL)TELLUROPYRANS **8a–c** AND RELATED CHALCOGEN ANALOGS

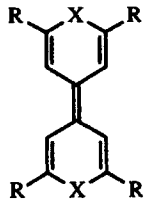

Compd.	X	R	E^1 [V (vs. SCE)]	E^2 [V (vs. SCE)]	Δ_E (V)
8a	Te	Me	0.22	0.36	0.14
81a	Se	Me	0.12	0.29	0.17
80a	S	Me	0.09	0.34	0.25
79a	O	Me	0.04	0.42	0.38
8b	Te	*tert*-Bu	0.24	0.39	0.15
81b	Se	*tert*-Bu	0.20	0.44	0.24
80b	S	*tert*-Bu	0.11	0.37	0.26
79b	O	*tert*-Bu	0.10	0.53	0.43
8c	Te	Ph	0.33	0.48	0.15
81c	Se	Ph	0.33	0.48	0.15
80c	S	Ph	0.22	0.41	0.19
79c	O	Ph	0.15	0.47	0.32
8d	Te	*p*-tolyl	0.20[c]	0.27[c]	0.07
81d	Se	*p*-tolyl	0.23[c]	0.39[c]	0.16

[a] Reference 97.

[b] Sample concentration of 5×10^{-4} *M* 0.2 *M* tetrabutylammonium tetrafluoroborate as supporting electrolyte in dichloromethane.

[c] Reference 95. In 1,1,2-trichloroethane with tetraethylammonium *p*-toluene sulfonate as supporting electrolyte.

TABLE 9. EPR DATA FOR CATION RADICALS OF (TELLUROPYRANYL)TELLUROPYRANS **8b** AND **8c** AND RELATED COMPOUNDS AS WELL AS VALUES OF SPIN–ORBIT COUPLING CONSTANT (λ)[a]

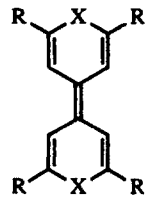

Compd.	X	R	g	a_H (or Line Width) (G)	λ (eV)
8b	Te	*tert*-Bu	2.041	(4.06)	0.49
83b	Te,S	*tert*-Bu	2.027	(2.02)	0.27
81b	Se	*tert*-Bu	2.024	(1.25)	0.22
80b	S	*tert*-Bu	2.009	0.532	0.05
79b	O	*tert*-Bu	2.008	0.438	0.004
8c	Te	Ph	2.029	(4.10)	0.49

[a] Reference 97. [b] References 103 and 104.

TABLE 10. ELECTRICAL CONDUCTIVITY OF COMPRESSED PELLETS OF COMPLEXES OF (TELLUROPYRANYL)TELLUROPYRANS AND RELATED COMPOUNDS[a]

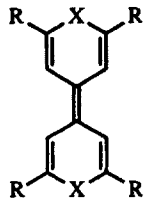

Compd.	X	R	Anion	Stoichiometry	σ^b (Ω^{-1} cm^{-1})	Ref.
8a	Te	Me	TCNQ	1 : 2	4	98
8a	Te	Me	TCNQ	2 : 3	0.4	98
8a	Te	Me	BF_4	2 : 3	10^{-4}	98
80a	S	Me	TCNQ	1 : 2	0.5	91
80a	S	Me	TCNQ	1 : 1	10^{-4} (10^{-3})	5
79a	O	Me	TCNQ	1 : 1	10^{-6}	86
8b	Te	*tert*-Bu	ClO_4	2 : 3	4×10^{-4}	98
8c	Te	Ph	TCNQ	1 : 1	0.5	98
8c	Te	Ph	ClO_4	2 : 3	10^{-4}	98
81c	Se	Ph	TCNQ	1 : 1	0.5	95
80c	S	Ph	TCNQ	1 : 1	10 (250)	90,92
79c	O	Ph	TCNQ	1 : 1	1.7 (40)	88,90
8d	Te	*p*-tolyl	TCNQ	1 : 0.9	1	95
81d	Se	*p*-tolyl	TCNQ	1 : 1	0.3	95

[a] Single-crystal values are in parentheses. [b] At ambient temperature.

TABLE 11. SELECTED BOND LENGTHS AND ANGLES FOR TETRATELLUROTETRACENE **99**[a]

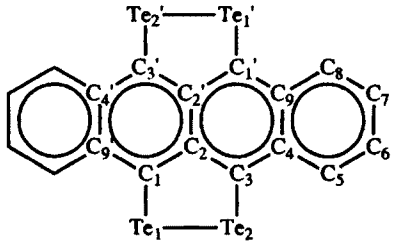

Bond	Length (Å)	Angle	(°)
Te1—Te2	2.673	Te1—Te2—C3	87.54
Te1—C1	2.114	C1—Te1—Te2	87.71
Te2—C3	2.111	C1—C2—C3	122.7
C2—C2'	1.452	Te1—C1—C2	120.8
C1—C2	1.428	C2—C3—Te2	121.3
C2—C3	1.418	C2—C3—C4	121.5
C1—C9'	1.396	C2—C1—C9'	121.8
C3—C4	1.397	C1—C9'—C4'	119.7
C4—C9	1.434	C3—C4—C9	118.0
		C1—C2—C2'	118.0
		C3—C2—C2'	119.3

[a] Reference 121.

TABLE 12. THE FIRST SIX VERTICAL IONIZATION ENERGIES (IE) FOR NAPHTHO[1,8-*c*,*d*]-1,2-DICHALCOGENOLES AS DETERMINED BY He(I) PHOTOELECTRON SPECTROSCOPY[a]

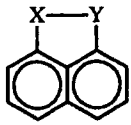

			IE_1	IE_2	IE_3	IE_4	IE_5	IE_6
Compd.	X	Y	(eV)					
7	Te	Te	7.10	8.80	(9.0)	(9.1)	(10.6)	(11.0)
93	Te	Se	7.05	(8.7)	(8.9)	(9.0)	(10.6)	(10.9)
92	Te	S	7.03	8.70	8.91	9.32	(10.6)	(10.9)
89	Se	Se	7.06	8.90	9.10	9.21	(10.9)	(11.6)
102	Se	S	7.14	8.91	(9.1)	(9.3)	(11.0)	(11.7)
88	S	S	7.14	(8.9)	(9.1)	(9.4)	(11.1)	(12.0)

[a] Reference 103. Numbers in parentheses are approximated from overlapping bands.

TABLE 13. ELECTROCHEMICAL OXIDATION POTENTIALS FOR TETRACHALCOGENANAPHTHALENES AND TETRACHALCOGENATETRACENES

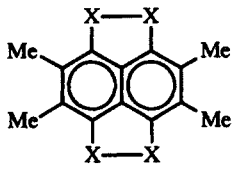

97, 103, 104

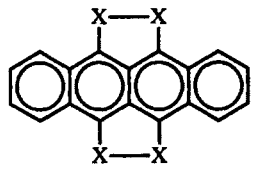

90, 91, 99

Compd.	X	E^1 [V (vs. SCE)]	E^2 [V (vs. SCE)]	Δ_E (V)	Ref.
97	Te	0.31	0.73	0.42	120
104	Se	0.45	0.90	0.45	120
103	S	0.46	0.94	0.48	120
99	Te	−0.17	0.19	0.36	125
91	Se	−0.09	0.28	0.37	125
90	S	−0.10	0.28	0.38	125

[a] In benzonitrile with 0.1 *M* tetra-*n*-butylammonium perchlorate as supporting electrolyte.

TABLE 14. EPR DATA FOR CATION RADICALS OF NAPHTHO[1,8-*c*,*d*]-1,8-DICHALCOGENOLES AND VALUES OF SPIN–ORBIT COUPLING CONSTANT (λ)[a]

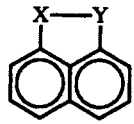

Compd.	X	Y	g	a_H (or Line Width) (G)[b]	λ (eV)
93	Te	Se	2.041	(2.0)	0.36
92	Te	S	2.032	—	0.27
89	Se	Se	2.040	0.37, 0.06, 0.43	0.22
102	Se	S	2.021	0.44, 0.08, 0.48	0.14
88	S	S	2.009	0.432, 0.092 0.525, 0.733 (^{33}S)	0.05

[a] Reference 103.

[b] Each value of a_H is for two protons.

TABLE 15. EPR DATA FOR CATION RADICALS OF TETRACHALCOGENATETRACENES **90**, **91**, AND **99** AND VALUES OF SPIN-ORBIT COUPLING CONSTANT (λ)[a]

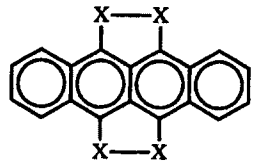

Compd.	X	g	a_H (or Line Width) G	λ (eV)
99	Te	2.059	(20)	0.49
91	Se	2.032	(2.5)	0.22
90	S	2.0079	0.553 (0.25)	0.05

[a] Reference 125.

TABLE 16. ROOM-TEMPERATURE CONDUCTIVITIES (σ) OF COMPLEXES OF **7**, **88**, **89**, **94**, **105**, AND **106**

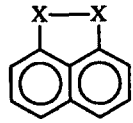

7, **88**, **89**

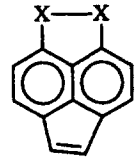

94, **105**, **106**

Compd.	X	Anion	Stoichiometry	σ[a] (Ω^{-1} cm^{-1})	Ref.
7	Te	TCNQ	1 : 1	2×10^{-2}	127
89	Se	TCNQ	1 : 1	5×10^{-8}	127
88	S	TCNQ	1 : 1	10^{-11}	127
94	Te	TCNQ	1 : 1	5×10^{-5}	116
106	Se	TCNQ	1 : 1	10^{-7}	116
105	S	TCNQ	1 : 1	10^{-8}	116

[a] At ambient temperature.

TABLE 17. COMPRESSED-PELLET CONDUCTIVITIES AT AMBIENT TEMPERATURE OF TETRAMETHYLTETRACHALCOGENANAPHTHALENES **97**, **103**, AND **104**[a]

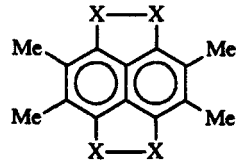

Compd.	X	Anion	Stoichiometry[b]	σ (Ω^{-1} cm^{-1})
97	Te	TCNQ	1 : 1.1 : 0.5	3.5×10^{-3}
104	Se	TCNQ	1.3 : 1	2.4×10^{-3}
103	S	TCNQ	1 : 1	5.8×10^{-3}
97	Te	$TCNQF_4$	1 : 1 : 0.5	2.6×10^{-5}
104	Se	$TCNQF_4$	1 : 1	2.2×10^{-6}
103	S	$TCNQF_4$	1 : 1	2.6×10^{-8}
97	Te	HCBD	1.1 : 1	5.0×10^{-7}
104	Se	HCBD	1 : 1 : 0.8	2.4×10^{-6}
103	S	HCBD	1 : 1	4.5×10^{-3}
97	Te	TCNE	1 : 0.9 : 0.1	1.6×10^{-6}
104	Se	TCNE	1 : 1	7.6×10^{-6}
103	S	TCNE	1 : 1	4.8×10^{-6}
97	Te	DDQ	1 : 1	1.9×10^{-4}
104	Se	DDQ	1 : 1	3.4×10^{-8}
103	S	DDQ	1 : 1	6.8×10^{-8}
97	Te	I	2 : 1	2.1×10^{-4}
104	Se	I	2 : 1	(8.2×10^{-2})
103	S	I ·	2 : 1	(11.8)

[a] Reference 120. Values in parentheses are single-crystal conductivities.
[b] Third numbers are solvent (benzonitrile) of crystallization.

TABLE 18. SELECTED BOND LENGTHS AND ANGLES FOR HEXAMETHYLENETETRATELLURAFULVALENE (HMTTeF, **109**)[a]

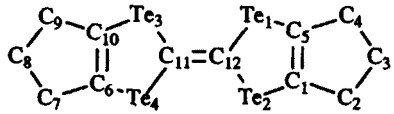

Bond	Length (Å)	Angle	(°)
Te1—C5	2.090	C5—Te1—C12	90.2
Te1—C12	2.098	Te1—C5—C1	122.1
C11—C12	1.356	Te1—C12—Te2	115.2

[a] Reference 138.

TABLE 19. ELECTROCHEMICAL OXIDATION POTENTIALS FOR TETRATELLURAFULVALENES AND THEIR LIGHTER CHALCOGEN ANALOGS

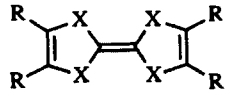

Compd.	X	R	E^1	E^2	Δ_E	Ref.
				(V)		
109, HMTTeF	Te	$-(CH_2)_3-$	0.12	0.34	0.22	137[a]
HMTSF	Se	$-(CH_2)_3-$	0.18	0.45	0.27	137[a]
109, HMTTeF	Te	$-(CH_2)_3-$	0.40	0.69	0.29	131[b]
TMTSF	Se	Me	0.42	0.81	0.39	131[b]
TMTTF	S	Me	0.24	0.73	0.49	131[b]
112, DBTTeF	Te	benzo	0.71	1.05	0.34	132[c]
DBTSF	Se	benzo	0.78	1.17	0.39	132[c]
DBTTF	S	benzo	0.71	1.14	0.43	132[c]
115, TTeF	Te	H	0.59	0.84	0.25	134[c]
TSF	Se	H	0.62	0.90	0.28	134[c]
TTF	S	H	0.47	0.81	0.34	134[c]
113, BDMT–TTeF			0.40	0.80	0.40	137[a]
118, DMHM–TTeF			0.08	0.34	0.26	137[a]
119, TMHM–TTeF			0.10	0.31	0.21	137[a]
120, CpHM–TTeF			0.11	0.34	0.23	137[a]

[a] Volts versus $Ag/AgNO_3$ at Pt button with 0.1 *M* tetrabutylammonium fluoroborate in butyronitrile.

[b] Volts versus SCE with 0.1 *M* tetrabutylammonium hexafluoroarsenate in benzonitrile.

[c] Volts versus SCE at Pt button with 0.2 tetrabutylammonium tetrafluoroborate in dichloromethane.

TABLE 20. SINGLE-CRYSTAL CONDUCTIVITIES OF TETRATELLURAFULVALENE CATION-RADICAL COMPLEXES AT AMBIENT TEMPERATURE

Compd.	X	Anion	Stoichiometry	σ^a ($\Omega^{-1}\,cm^{-1}$)	Ref.
115, TTeF	Te	TCNQ	1 : 1	2200	141
TSF	Se	TCNQ	1 : 1	800	142
TTF	S	TCNQ	1 : 1	500	129
109, HMTTeF	Te	TCNQ	1 : 1	550 (1400)	147 (146)
118, DMHM–TTeF	Te	TCNQ	1 : 1	10^{-6}	137
119, TMHM–TTeF	Te	TCNQ	1 : 1	10^{-6}	137
TMHM–TSF	Se	TCNQ	1 : 1	10^{-7}	137
120, CpHM–TTeF	Te	TCNQ	1 : 1	10^{-6}	137
CpHM–TSF	Se	TCNQ	1 : 1	10^{-7}	137
115, TTeF	Te	ClO_4	–	3.6	139
109, HMTTeF	Te	Cl	2 : 1	360 (1.6)	148
109, HMTTeF	Te	Br	2 : 1	350 (18)	148
109, HMTTeF	Te	I	2 : 1	390 (3.9)	148
109, HMTTeF	Te	I	5 : 3	87	148
109, HMTTeF	Te	I	5 : 2	2.6	148
109, HMTTeF	Te	PF_6	2 : 1	23	148
109, HMTTeF	Te	AsF_6 (plate)	2 : 1	15	148
109, HMTTeF	Te	AsF_6 (needle)	2 : 1	8.3	148
109, HMTTeF	Te	ClO_4 (needle)	2 : 1	470	148
109, HMTTeF	Te	ClO_4 (rod)	2 : 1	10^{-3}	148
113, BDMT–TTeF	Te	ClO_4	3 : 2	2.6	152
113, BDMT–TTeF	Te	AsF_6	3 : 2	76 (50)	152 (153)
113, BDMT–TTeF	Te	PF_6	3 : 2	25	152
113, BDMT–TTeF	Te	ReO_4	—	0.92	152
113, BDMT–TTeF	Te	SbF_6	—	0.17	152

[a] Numbers in parentheses are measured at 5 K.
[b] Compressed pellet.

TABLE 21. SELECTED BOND LENGTHS AND ANGLES FOR TTeF–TCNQ COMPLEX

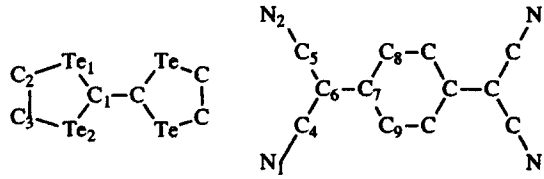

Bond	Length (Å)	Angle	(°)
Te1—C2	2.05	C2—Te1—C1	90.4
Te2—C1	2.091	C1′—C1—Te2	120.3
Te1—C1	2.08	C2—C3—Te2	119.6
C1—C1′	1.40	C3—Te2—C1	90.8
Te2—C3	2.08	Te1—C1—Te2	115.6
C2—C3	1.38	C1′—C1—Te1	123.8
C4—N1	1.11	C3—C2—Te1	123.0
C5—C6	1.40	C5—C6—C4	116.7
C7—C9	1.44	C8—C7—C9	118.9
C4—C6	1.45	C9—C8′—C7′	120.9
C6—C7	1.46	N1—C4—C6	175.2
C8—C9′	1.32	N2—C5—C6	174.7
C5—N2	1.15	C5—C6—C7	120.0
C7—C8	1.43	C7—C9—C8′	120.2
		C4—C6—C7	123.0
		C9—C7—C6	120.4

[a] Reference 141.

TABLE 22. SELECTED BOND LENGTHS (Å) FOR THE HMTTe MOLECULES IN $(HMTTeF)_4(PF_6)_2$ CRYSTALS

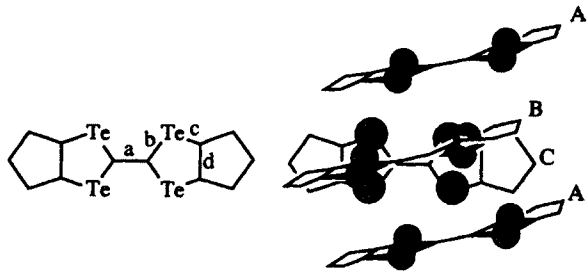

Molecule	*a*	*b*	*c*	*d*	Ref.
A	1.59	2.05	2.07	1.40	151
B	1.44	2.09	2.07	1.46	151
C	1.23	2.15	2.10	1.28	151
A	1.38	2.08	2.07	1.35	150
B	1.28	2.11	2.11	1.34	150
C	1.22	2.145	2.07	1.30	150
109	1.356	2.098	2.090	—	131

REFERENCES

1. Wudl, F.; Wobschall, D.; Hufnagel, E. J. *J. Am. Chem. Soc.* **1972**, *94*, 670.
2. Perlstein, J. H. *Angew. Chem., Int. Ed. Engl.* **1977**, 16, 519.
3. Keller, J. H., ed., *Chemistry and Physics of One-Dimensional Metals*, Plenum Press, New York, 1977.
4. Soos, Z. G. *J. Chem. Educ.* **1978**, *55*, 121.
5. Torrance, J. B. *Acc. Chem. Res.* **1979**, *12*, 79.
6. Devresse, J. T., Evrad, P. R.; van Doren, V. E., eds., *Highly Conducting One-Dimensional Solids*, Plenum Press, New York, 1979.
7. Alcacer, L., ed., *The Physics and Chemistry of Low-Dimensional Solids*, Reidel; Dordrecht, The Netherlands, 1980.
8. Wegner, G. *Angew. Chem., Int. Ed. Engl.* **1981**, *20*, 361.
9. Miller, J. S., ed., *Extended Linear Chain Compounds*, Plenum Press, New York, 1982, 1983; Vols. 1-3.
10. Bryce, M. R.; Murphy, L. C. *Nature* **1984**, *309*, 119.
11. Wudl, F. *Acc. Chem. Res.* **1984**, *17*, 227.
12. Bryce, M. R. *Aldrichimica Acta* **1985**, *18*, 73.
13. Schukat, G.; Richter, A. M.; Fanghaenel, E. *Sulfur Rep.* **1987**, *7*, 155.
14. Aitkin, R. A. *Prog. Heterocycl. Chem.* **1991**, *3*, 156.
15. Sadekov, I. D.; Rivkin, B. B. *Khim. Geterotsikl. Soedin.* **1991**, 291.
16. Williams, J. M.; Wang, H. H.; Emge, T. J.; Geiser, U.; Beno, M. A.; Leung, P. C. W.; Carlson, K. D.; Thorn, R. J.; Schultz, A. J.; Whangbo, M.-H. *Prog. Inorg. Chem.* **1987**, *35*, 51.
17. Yagubskii, E. B.; Shchegolev, I. F.; Laukhin, V. N.; Kononovich, P. A.; Kartzovnik, M. V.; Zvarikina, A. V.; Buravov, L. I. *Pis'ma Zh. Eksp. Teor. Fiz.* **1984**, *39*, 12.
18. Kaminskii, V. F.; Prokhorova, T. G.; Shibaeva, R. P.; Yagubskii, E. B. *Pis'ma Zh. Eksp. Teor. Fiz.* **1984**, *39*, 15.
19. Williams, J. M.; Emge, T. J; Wang, H. H.; Beno, M. A.; Copps, P. T.; Hall, L. N.; Carlson, K. D.; Crabtree, G. W. *Inorg. Chem.* **1984**, *23*, 2558.
20. Crabtree, G. W.; Carlson, K. D.; Hall, L. N.; Copps, P. T.; Wang, H. H.; Emge, T. J.; Beno, M. A.; Williams, J. M. *Phys. Rev. B: Condens. Matter* **1984**, *B30*, 2958.
21. Parkin, S. S. P.; Engler, E. M.; Schumaker, R. R.; Lagier, R.; Lee, V. Y.; Scott, J. C.; Greene, R. L. *Phys. Rev. Lett.* **1983**, *50*, 270.
22. Bechgaard, K. *Mol. Cryst. Liq. Cryst.* **1982**, *79*, 1.
23. Friedel, J.; Jerome, D. *Contemp. Phys.* **1982**, *23*, 583.
24. Jerome, D.; Schultz, H. *J. Adv. Phys.* **1982**, *31*, 299.
25. Drew, H. D. K. *J. Chem. Soc.* **1926**, 223.
26. Campbell, I. G. M.; Turner, E. E. *J. Chem. Soc.* **1938**, 37.
27. Drew, H. D. K.; Thomason, R. W. *J. Chem. Soc.* **1927**, 116.
28. Gioaba, A.; Maior, O. *Rev. Chim.* (Bucharest) **1970**, *21*, 613.
29. Gioaba, A.; Maior, O. *An. Univ. Bucuresti, Chim.* **1973**, *22*, 111.
30. Gioaba, A.; Nedea, M.; Maior, O. *Rev. Roum. Chim.* **1976**, *21*, 739.
31. Gioaba, A.; Vasiliu, G. *An. Univ. Bucuresti, Ser. Stiint, Nat. Chim.* **1966**, *15*, 89.
32. Gioaba, A.; Maior, O.; Mitran, M. *Rev. Roum.* **1976**, *21*, 733.
33. Vasiliu, G.; Gioaba, A. *Rev. Chim.* (Bucharest) **1969**, *20*, 357.
34. Vasiliu, G.; Gioaba, A. *Rev. Chim* (Bucharest) **1968**, *19*, 253.

35. Detty, M. R. *J. Org. Chem.* **1980**, *45*, 274.
36. Detty, M. R.; Merkel, P. B. *J. Am. Chem. Soc.* **1990**, *112*, 3845.
37. Detty, M. R. *Organometallics* **1991**, *10*, 702.
38. Detty, M. R.; Gibson, S. L. *Organometallics* **1992**, *11*, 2147.
39. Detty, M. R. *Organometallics* **1992**, *11*, 2310.
40. Drew, H. D. K. *J. Chem. Soc.* **1926**, 3054.
41. Drew, H. D. K. *J. Chem. Soc.* **1934**, 1790.
42. Mangion, M. M.; Meyers, E. A. *Cryst. Struct. Commun.* **1973**, *2*, 629.
43. Garad, M. V.; Gopinathan, S.; Gopinathan, C. *Ind. J. Chem. Sect. A* **1979**, *18*, 267.
44. Bergman, J. *Chem. Scr.* **1975**, *8A*, 116.
45. Rainville, D. P.; Zingaro, R. A. *Inorg. Chim. Acta* **1984**, *86*, L33.
46. Hosoya, S. *Acta Cryst.* **1966**, *20*, 429.
47. Gilman, H.; Dietrich, J. J. *J. Am. Chem. Soc.* **1952**, *79*, 1439.
48. Gioaba, A.; Maior, O. *Rev. Roum. Chim.* **1970**, *15*, 1967.
49. Petragnani, N. *Tetrahedron* **1960**, *11*, 15.
50. Junk, T.; Irgolic, K. J., unpublished results reported in Houben-Weyl Methoden der Organischen Chemie: Organotellurium Chemistry, Klamann, D., ed, George Thieme, New York, 1990.
51. Krafft, B.; Kashaw, A. *Ber.* **1896**, *29*, 443.
52. Cullinane, N. M.; Morgan, N. M. E.; Plummer, C. A. J. *Rec. Trav. Chim. Pays-Bas* **1937**, *56*, 627.
53. Cullinane, N. M.; Rees, A. G.; Plummer, C.A. J. *J. Chem. Soc.* **1939**, 151.
54. Passerini, R.; Purrello, G. *Ann. Chim.* (Rome) **1958**, *48*, 738.
55. Schmidt, M.; Shumann, H. *Z. Naturforsch. B* **1964**, *19*, 74.
56. Dereu, N. L. M.; Zingaro, R. A. *J. Organomet. Chem.* **1981**, *212*, 141.
57. Junk, T.; Irgolic, K. J. *Organomet. Synth* **1988**, *4*, 582.
58. Rivkin, B. B.; Sadekov, I. D.; Minkin, V. I. *Khim. Geterotsikl. Soedin.* **1988**, 1144.
59. Sadekov, I. D.; Rivkin, B. B.; Gadzhieva, P. I.; Minkin, V. I. *Khim. Geterotsikl. Soedin.* **1990**, 137.
60. Rainville, D. P.; Zingaro, R. A.; Meyers, E. A. *J. Fluorine Chem.* **1980**, *16*, 245.
61. Humphries, R. E.; Al-Jabar, N. A. A.; Bowen, D.; Massey, A. G.; Deacon, G. B. *J. Organomet. Chem.* **1987**, *319*, 59.
62. Schulz, P.; Klar, G. *Phosphorus Sulfur* **1987**, *29*, 377.
63. Engman, L.; Hellberg, J.; Ishag, C. *J. Chem. Soc. Perkin Trans. 1* **1988**, 2095.
64. Al-Soudani, A. R.; Massey, A. G. *Appl. Organomet. Chem.* **1988**, *2*, 553.
65. Suzuki, H.; Padmanabban, S.; Inouye, M.; Ogawa, T. *Synthesis* **1989**, 468.
66. Colonna, F. P.; Distefano, G.; Galasso, V.; Irgolic, K. J.; King, C. E.; Pappalardo, G. C. *J. Organomet. Chem.* **1978**, *146*, 235.
67. Smith, M. R.; Mangion, M. M.; Zingaro, R. A.; Meyers, E. A. *J. Heterocycl. Chem.* **1973**, *10*, 527.
68. Distefano, G.; Galasso, V.; Junk, T.; Irgolic, K. J.; Pappalardo, G. C. *Phosphorus Sulfur* **1988**, *38*, 281.
69. Meyers, E. A,; Irgolic, K. J.; Zingaro, R. A.; Junk, T.; Chakravorty, R.; Dereu, N. L. M.; French, K. *Phosphorus Sulfur* **1988**, *38*, 257.
70. Distefano, G.; Galasso, V.; Irogolic, K. J.; Pappalardo, G. C. *J. Chem. Soc. Perkin Trans. II* **1983**, 1109.
71. Rainville, D. P.; Zingaro, R. A.; Meyers, E. A. *Cryst. Struct. Commun.* **1980**, *9*, 291.
72. Lynton, H.; Cox, E. G. *J. Chem. Soc.* **1956**, 4887.
73. Cordes, A. W.; Fain, G. K. *Acta Cryst.* **1974**, *B30*, 164.
74. Senma, N.; Taira, Z.; Taga, T.; Osaki, K. *Cryst. Struct. Commun.* **1973**, *2*, 311.

75. Rodin, O. G.; Traven, V. F.; Redchenko, V. V.; Eismont, M. Yu.; Stepanov, B. I. *Zh. Obshch. Khim.* **1983**, *53*, 2537.
76. Mangion, M. M.; Smith, M. R.; Meyers, E. A. *J. Heterocycl. Chem.* **1973**, *10*, 533.
77. Amato, M. E.; Grassi, A.; Irgolic, K. J.; Pappalardo, G. C.; Radics, L. *Organometallics* **1993**, *12*, 775.
78. Galasso, V.; Irgolic, K. J.; Pappalardo, G. C. *J. Organomet. Chem.* **1979**, *181*, 329.
79. Jardon, P. *J. Chim. Phys Phys.-Chim. Biol.* **1977**, *74*, 1177.
80. Drew, H. D. K. *J. Chem Soc.* **1928**, 506.
81. Heller, C. A.; Zingaro, R. A.; Meyers, E. A. *Can. J. Chem.* **1974**, *52*, 3814.
82. Cauquis, G.; Maurey-Mey, M. *Bull. Soc. Chim. Fr.* **1973**, 2870.
83. Hetnarski, B.; Hofman, W. *Bull. Acad. Pol. Sci. Ser. Sci. Chim.* **1969**, *17*, 1.
84. Rainville, D. P.; Zingaro, R. A.; Ferraris, J. P. *Can. J. Chem.* **1980**, *58*, 1133.
85. Sanchez Martinez, E.; Diaz Calleja, R.; Gunsser, W.; Berges, P.; Klar, G. *Synth. Met.* **1989**, *30*, 67.
86. Syper, L.; Sucharda-Sobczyk, A. *Bull. Acad. Pol. Sci.* **1975**, *13*, 563.
87. Hunig, S.; Garner, B. J.; Ruider, G.; Schenk, W. *Justus Liebigs Ann. Chem.* **1973**, 1036.
88. Alizon, J.; Gallice, J.; Robert, H.; Delplanque, G.; Weyl, C.; Fabre, C.; Strzelecka, H. *Mol. Cryst. Liq. Cryst.* **1976**, *33*, 91.
89. Fabre, C.; Fugnitto, R.; Strzelecka, H. *C. R. Acad. Sci. Paris, Series C* **1976**, *282*, 175.
90. Alizon, J.; Blanc, J.; Gallice, J.; Robert, H.; Fabre, C.; Strzelecka, H.; Rivory, J.; Weyl, C. *Lecture Notes in Physics* **1977**, *65*, 563.
91. Sandman, D. J.; Epstein, A. J.; Holmes, T. J.; Fisher, A. R., III *J. Chem. Soc., Chem. Commun.* **1977**, 177.
92. Perlstein, J. H.; Van Allan, J. A.; Isett, L. C.; Reynolds, G. A. *Ann. N. Y. Acad. Sci.* **1978**, *313*, 61.
93. Sandman, D. J.; Epstein, A. J.; Holmes, T. J.; Lee, J. S.; Titus, D. D. *J. Chem. Soc., Perkin Trans. 2* **1980**, 1578.
94. Es-Seddiki, S.; Coustumer, G. L.; Mollier, Y. *Tetrahedron Lett.* **1981**, *22*, 2771.
95. Regnault du Mottier, C.; Brutus, M.; Le Coustumer, G.; Sauve, J. P.; Ebel, M.; Mollier, Y. *Mol. Cryst. Liq. Cryst.* **1988**, *154*, 361.
96. Detty, M. R.; Murray, B. J. *J. Org. Chem.* **1982**, *47*, 1146.
97. Detty, M. R.; Hassett, J. W.; Murray, B. J.; Reynolds, G. A. *Tetrahedron* **1985**, *41*, 4853.
98. Detty, M. R.; Murray, B. J.; Perlstein, J. H. *Tetrahedron Lett*, **1983**, *24*, 539.
99. Pedersen, B. S.; Schiebye, S.; Nilsson, N. H.; Lawesson. S. O. *Bull. Soc. Chim. Belg.* **1978**, *97*, 223.
100. Krafft, K.; Steiner, O. *Chem. Ber.* **1901**, *34*, 560.
101. Courtot, C.; Bastani, M. G. *C. R. Acad. Sci.* **1936**, *203*, 197.
102. Bochkarev, M. N.; Sanina, L. P.; Vyazankin, N. S. *Zh. Obschch. Khim.* **1969**, *39*, 135.
103. Bock, H.; Brahler, G.; Dauplaise, D.; Meinwald, *J. Chem. Ber.* **1981**, *114*, 2622.
104. Wittel, K.; Manne, R. *Theor. Chim. Acta* **1974**, *33*, 347.
105. Sandman, D. J.; Ceasar, G. P.; Nielsen, P.; Epstein, A. J.; Holmes, T. J. *J. Am. Chem. Soc.* **1978**, *100*, 202.
106. Meinwald, J.; Dauplaise, D.; Wudl, F.; Hauser, J. J. *J. Am. Chem. Soc.* **1977**, *99*, 255.
107. Kaminskii, V. F.; Khidekel, M. L.; Lyubovskii, R. B.; Shchegolev, I. F.; Shibaeva, R. P.; Yagubskii, E. B.; Zvarykina, A. V.; Zvereva, G. L. *Phys. Status Solidi A* **1977**, *44*, 77.
108. Zolotukhin, S. P.; Kaminskii, V. F.; Kotov, A. I.; Lyubovskii, R. B.; Khidekel, M. L.; Shibaeva, R. P.; Shchegolev, I. F.; Yagubskii, E. B. *Pis'ma Zh. Eksp. Teor. Fiz.* **1977**, 25, 480.
109. Delhaes, P.; Coulon, C.; Flandrois, S.; Hilti, B.; Mayer, C. W.; Rihs, G.; Rivory, J. *J. Chem. Phys.* **1980**, *73*, 1452.
110. Khidekel, M. L.; Zhilyaeva, E. I. *Synth. Met.* **1981**, *4*, 1.

111. Shchegolev, I. F.; Yagubskii, E. B. in reference 9 (above), Vol. 2, p 385.
112. Shibaeva, R. P. in reference 9, Vol. 2, p 435.
113. Mori, T.; Kobayashi, A.; Sasaki, Y.; Kobayashi, H. *Bull. Chem. Soc. Jpn.* **1983**, *56*, 3376.
114. Garito, A. F.; Heeger, A. J. *Acc. Chem. Res.* **1974**, *7*, 232.
115. Meinwald, J.; Dauplaise, D.; Clardy, J. *J. Am. Chem. Soc.* **1977**, *99*, 7743.
116. Chiang, L.-Y.; Meinwald, J. *Tetrahedron Lett.* **1980**, *21*, 4565.
117. Miyamoto, H.; Yui, K.; Aso, Y.; Otsubo, T.; Ogura, F. *Tetrahedron Lett.* **1986**, *27*, 2011.
118. Otsubo, T.; Miyamoto, H.; Aso, Y.; Ogura, F. *Synth. Met.* **1987**, *19*, 595.
119. Aso, Y.; Yui, K.; Miyoshi, T.; Ogura, F.; Tanaka, J. *Bull. Chem. Soc. Jpn.* **1988**, *61*, 2013.
120. Otsubo, T.; Sukenobe, N.; Aso, Y.; Ogura, F. *Synth. Met.* **1988**, *27*, 509.
121. Sandman, D. J.; Stark, J. C.; Foxman, B. M. *Organometallics* **1982**, *1*, 739.
122. Balodis, K. A.; Medne, R. S.; Neiland, O. Ya. *Zh. Org. Chim.* **1984**, *20*, 891.
123. Shibaeva, R. P.; Kaminskii, V. F. *Cryst. Struc. Commun.* **1981**, *10*, 663.
124. Liabres, G.; Dideberg, O.; Dupont, L. *Acta Crystallogr., Sect. B*, **1972**, *B28*, 2438.
125. Jones, M. T.; Jansen, S.; Acampora, L. A.; Sandman, D. J. *J. de Phys.* **1983**, *44*, C-1159.
126. McLachlan, A. D. *Mol. Phys.* **1960**, *3*, 233.
127. Dauplaise, D.; Meinwald, J.; Scott, J. C.; Tamkin, H.; Clardy, J. *Ann. N. Y. Acad. Sci.* **1978**, *313*, 382.
128. Kato, R.; Kobayashi, H.; Kobayashi, A. *Physica* **1986**, *143B*, 304.
129. Ferraris, J. P.; Cowan, D. O.; Walatka, V., Jr.; Perlstein, J. H. *J. Am. Chem. Soc.* **1973**, *95*, 948.
130. Cowan, D. O.; Wiygul, F. M. *Chem. Eng. News* **1986**, *14*, 28.
131. Wudl, F.; Aharon-Shalom, E. *J. Am. Chem. Soc.* **1982**, *104*, 1154.
132. Lerstrup, K.; Talham, D.; Bloch, A.; Poehler, T.; Cowan, D. *J. Chem. Soc., Chem. Commun.* **1982**, 336.
133. Lerstrup, K.; Cowan, D. O.; Kistenmacher, T. J. *J. Am. Chem. Soc.* **1984**, *106*, 8303.
134. McCullough, R. D.; Kok, G. B.; Lerstrup, K. A.; Cowan, D. O. *J. Am. Chem. Soc.* **1987**, *109*, 4115.
135. McCullough, R. D.; Mays, M. D.; Bailey, A. B.; Cowan, D. O. *Synth. Met.* **1988**, *27*, B487.
136. Lerstrup, K.; Bailey, A.; McCullough, R.; Mays, M.; Cowan, D.; Kistenmacher, T. *Synth. Met.* **1987**, *19*, 647.
137. Bailey, A. B.; McCullough, R. D.; Mays, M. D.; Cowan, D.O.; Lerstrup, K. A. *Synth. Met.* **1988**, *27*, B425.
138. Carroll, P. J.; Lakshmikantham, M. V.; Cava, M. P.; Wudl, F.; Aharon-Shalom, E.; Cox, S. D. *J. Chem. Soc., Chem. Commun.* **1982**, 1316.
139. Mays, M. D.; McCullough, R. D.; Bailey, A. B.; Cowan, D. O.; Bryden, W. A.; Poehler, T. O.; Kistemmacher, T. J. *Synth. Met.* **1988**, *27*, B493.
140. Mays, M. D.; McCullough, R. D.; Cowan, D. O.; Poehler, T. O.; Bryden, W. A.; Kistenmacher, T. J. *Solid State Commun.* **1988**, *65*, 1089.
141. Cowan, D. O.; Mays, M. D.; Kistenmacher, T. J.; Poehler, T. O.; Beno. M. A.; Kini, A. M.; Williams, J. M.; Kwok, Y. K.; Carlson, K. D.; Xiao, L.; Novoa, J. J.; Whangbo, M.-H. *Mol. Cryst. Liq. Cryst.* **1990**, *181*, 43.
142. Etemad, S.; Penney, T.; Engler, E. M.; Scott, B. A.; Seiden, P. E. *Phys. Rev. Lett.* **1975**, *30*, 741.
143. Kistenmacher, T. J.; Philips, T. E.; Cowan, D. O. *Acta Crystallogr., Sect. B* **1973**, *30*, 763.
144. Chappel, J. S.; Bloch, A. N.; Bryden, W. A.; Maxfield, M.; Poehler, T. O.; Cowan, D. O. *J. Am. Chem. Soc.* **1981**, *103*, 2442.
145. Saito, G.; Enoki, T.; Inokuchi, H.; Kumagai, H.; Tanaka, J. *Chem. Lett.* **1983**, 503.
146. Saito, G.; Kumagai, H.; Tanaka, Enoki, T.; Inokuchi, H. *Mol. Cryst. Liq. Cryst.* **1985**, *120*, 337.

147. Cowan, D. O.; Mays, M.; Lee, M.; McCullough, R.; Bailey, A.; Lerstrup, K.; Wiygul. F.; Kistenmacher, T.; Poehler, T.; Chiang, L.-Y. *Mol. Cryst. Liq. Cryst.* **1985**, *125*, 191.

148. Matsuzaki, S.; Li, Z. S.; Sano, M. *Chem. Lett.* **1986**, 1343.

149. Matsuzaki, S.; Li, Z. S.; Sano, M. *Synth. Met.* **1987**, *19*, 399.

150. Li, Z. S.; Matsuzaki, S.; Kato, R.; Kobayahi, H.; Kobayashi, A.; Sano, M. *Chem. Lett.* **1986**, 1105.

151. Kikuchi, K.; Yakushi, K.; Kuroda, H.; Ikemoto, I.; Kobayashi, K.; Honda, M.; Katayama, C.; Tanaka, J. *Chem. Lett.* **1985**, 419.

152. Kobayashi, K.; Kikuchi, K.; Koide, A.; Ishikawa, Y.; Saito, K.; Ikemoto, I. *J. Chem. Soc., Chem. Commun.* **1992**, 1198.

153. Lerstrup, K.; Lee, M.; Cowan, D. O.; Kistenmacher, T. *Mol. Cryst. Liq. Cryst.* **1985**, *120*, 1985.

154. Pradeep, T.; Singh, K. K.; Sinha, A. P. B.; Morris, D. E. *J. Chem. Soc., Chem. Commun.* **1992**, 1747.

155. Engler, E. M. In *Proceedings of Third International Symposium on Organic Selenium and Tellurium Compounds*, Cagniant, D.; Kirsch, A., eds.; University of Metz, France, 1979, p. 357.

156. Singh, H. B.; McWhinnie, W. R.; Ziolo, R. F.; Jones, C. H. W. *J. Chem. Soc. Dalton Trans.* **1984**, 1267.

Chemistry of Heterocyclic Compounds, Volume 53
Michael R. Detty, Marrie B. O'Regan

CHAPTER VIII

Tellurium-Containing Heterocycles with Hypervalent or Coordination Bonds to Tellurium

I. NOMENCLATURE

Compounds containing hypervalent tellurium are most often named using the *N–X–L* scheme suggested by Perkins et al.[1] In this system, *N* is the number of valence-shell electrons associated with the central atom, *X* in these cases is tellurium, and *L* is the number of ligands bound to the central atom. Illustrative cases are shown in Figure 1. Derivatives of Te(IV) are typically called *pertelluranes.*

10-Te-3 **12-Te-5**

Figure 1. *N–X–L* nomenclature for tellurapentalenes.

II. ORGANIZATION

The existence of compounds that contain tellurium in a hypervalent state has been inferred from spectroscopic data for some time. Moieties through which a Lewis basic atom coordinates to tellurium to form heterocyclic compounds include azo, azomethine, CH_2NR_2, NO_2, C═O, and OR. The 10-Te-3 dioxatellurapentalenes represent an earlier class of such complexes. This class of compounds is described first simply because they form a group of compounds that have been thoroughly characterized and thus, will suitably lay the groundwork for consideration of other systems, some of which are not as well defined because of the lack of complete spectroscopic and structural characterization. Also included in this chapter are some compounds in which the intramolecular contacts are weaker than a single bond, but are still within the limits of van der Waals interactions.

III. TELLURAPENTALENES

A. Preparation of Dioxatellurapentalenes

Perrier et al.[2] described the preparation of the first 2,5-diaza-1,6-dioxa-6a-tellurapentalene derivatives in a 1971 communication, via the route shown in Scheme 1. Subsequent papers described the properties[3] of these compounds as well as the synthesis of further derivatives.[4]

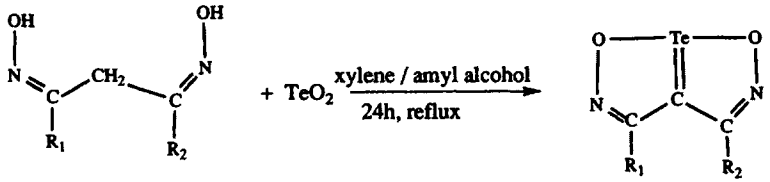

$R_1 = R_2 = H$, **1a**
$R_1 = R_2 = Me$, **1b**
$R_1 = R_2 = (CH_2)_3$, **1c**
$R_1 = R_2 = -CH_2C(Me)_2CH_2-$, **1d**
$R_1 = R_2 =$ **1e**

$R_1 = R_2 = -(CH_2)_4-$, **1f**
$R_1 = CO_2Et$, $R_2 = Me$, **1g**
$R_1 = R_2 =$ **1h**

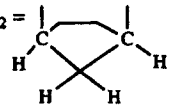

Scheme 1

The structure of the products as drawn in Scheme 1 was inferred by comparison with the X-ray crystal structure of the selenium analog of **1d**,[5] which had been determined shortly before, although the synthesis of the compound was first reported in 1949.[6] The bonding about selenium was found to be symmetrical, with Se—O distances of 2.02 and 2.03 Å, indicating that the compound is bicyclic.

A related compound, 1,2,5,6-tetraaza-6a-tellurapentalene, **2** was prepared[7] in 2% yield via the reaction shown in Scheme 2.

Detty subsequently prepared 10-Te-3 and 12-Te-5 dioxatellurapentalenes with a five-carbon framework, related to the diazatellurapentalenes (**2**), and two members of the series have been structurally characterized.[8] The starting material used in the synthesis of these compounds, 3-methyl-5-phenyl-1,2-oxatellurol-1-ium chloride (**3**) (Scheme 3), is itself a 10-Te-3 complex whose synthesis and properties are described in a later section of this chapter.

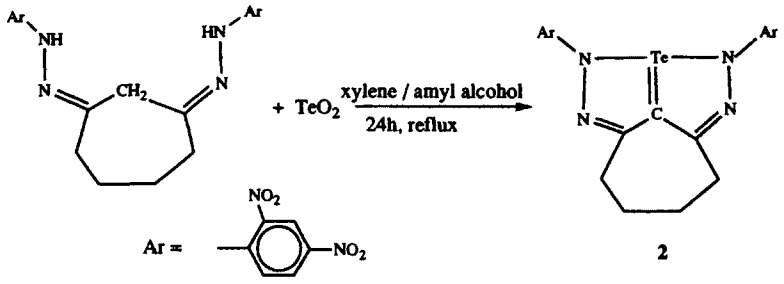

Scheme 2

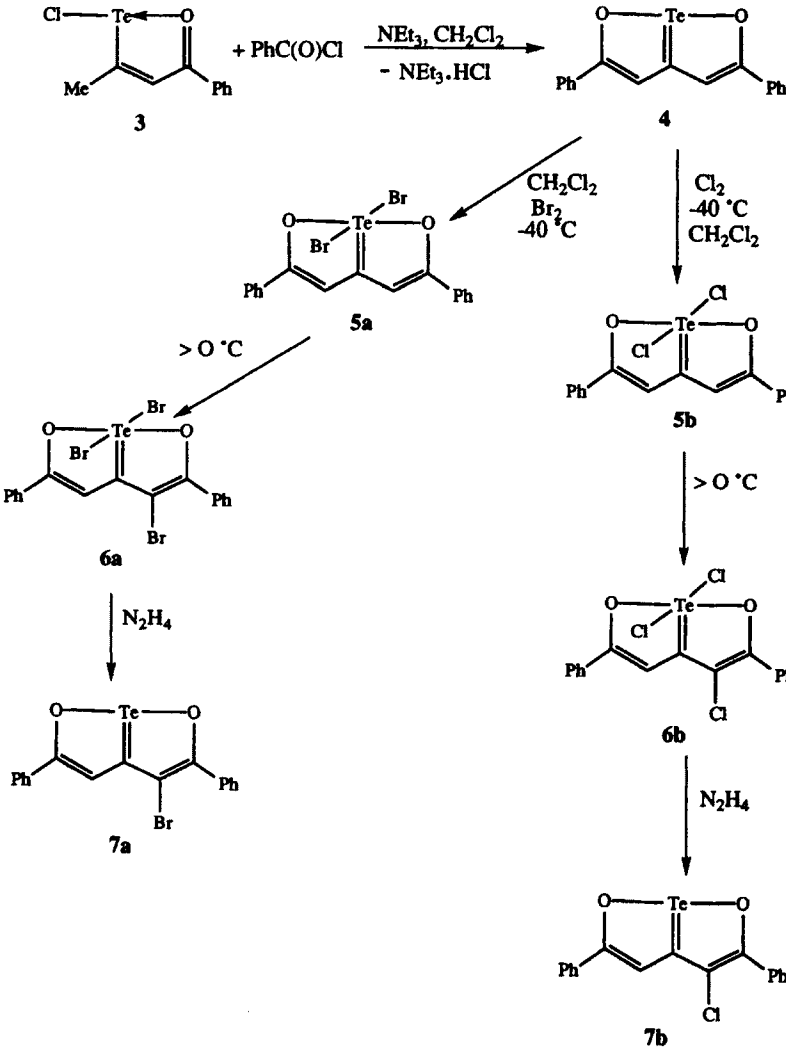

Scheme 3

Compound **4**, a yellow crystalline solid, was isolated in 39% yield and its crystal structure determined. Compound **5a**, prepared in quantitative yield, showed negligible specific conductances, suggesting that it is covalent in nature, and not ionic as could be supposed.

A further series of dioxatellurapentalenes was prepared[9] by analogous methods via the reactions of various substituted 1,2-oxatellurolyl-1-ium chlorides with the appropriate acid chlorides. These compounds incorporated a series of electron-donating and electron-withdrawing groups substituted on the phenyl rings. The substitution patterns and compound numbers of this series are shown in Figure 2.

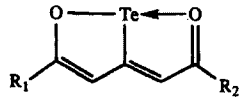

R_1 = Me; R_2 = Ph, **8a**.
R_1 = 4-$MeOC_6H_4$; R_2 = Ph, **8b**.
R_1 = 4-$ON_2C_6H_4$; R_2 = Ph, **8c**.
R_1 = 4-$ON_2C_6H_4$; R_2 = 4-$Me_2NC_6H_4$, **8d**.
R_1 = 4-NCC_6H_4; R_2 = 4-$Me_2NC_6H_4$, **8e**.
R_1 = 4-$ON_2C_6H_4$; R_2 = 4-$MeOC_6H_4$, **8f**.
R_1 = 4-$MeOC_6H_4$; R_2 = 4-$MeOC_6H_4$, **8g**.
R_1 = Me; R_2 = 4-$MeOC_6H_4$, **8h**.
R_1 = Ph; R_2 = 4-FC_6H_4, **8i**.
R_1 = 4-$ON_2C_6H_4$; R_2 =4-FC_6H_4, **8j**.
R_1 = 4-NCC_6H_4; R_2 =4-FC_6H_4, **8k**.
R_1 = 4-FC_6H_4; R_2 =4-FC_6H_4, **8l**.
R_1 = 4-$MeOC_6H_4$; R_2 =4-FC_6H_4, **8m**.
R_1 = 2,4-$(O_2N)_2C_6H_3$; R_2 =4-FC_6H_4, **8n**.
R_1 = 3,5-$(O_2N)_2C_6H_3$; R_2 =4-FC_6H_4, **8o**.
R_1 = Me; R_2 = 4-FC_6H_4, **8p**.
R_1 = 4-$MeOC_6H_4$(CH=CH); R_2 = 4-$MeOC_6H_4$, **8q**.

R_1 = 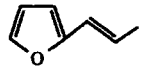 R_2 = 4-FC_6H_4, **8r**.

R_1 = 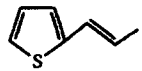 R_2 = 4-FC_6H_4, **8s**.

Figure 2. Structure and numbering of various 10-Te-3 tellurapentalenes.

An unusual derivative where one of the oxygen atoms of a dioxatellurapentalene has been replaced by a nitrogen was also reported,[9] prepared by the reaction of **3** with an imidoyl chloride, as shown in Scheme 4.

The reaction of chlorine or bromine with the 10-Te-3 tellurapentalenes to yield 12-Te-5 pertelluranes as shown in Scheme 3 (syntheses of **5a**, **5b**, **6a**, and **6b**) proved to be a general reaction. The structures and numbering of the other 12-Te-5 pertelluranes prepared[9] by reactions analogous to those in Scheme 3 are shown in Figure 3.

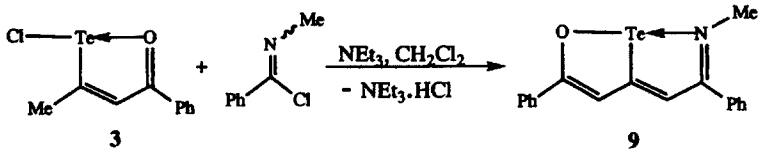

Scheme 4

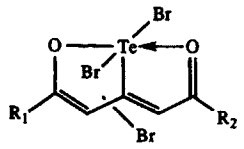

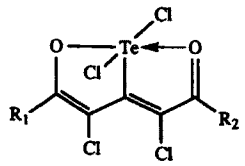

11

$R_1 = R_2 = 4\text{-}FC_6H_4$, **10a**.
$R_1 = Me$; $R_2 = Ph$; **10b**.
$R_1 = Me$; $R_2 = 4\text{-}MeOC_6H_4$, **10c**.
$R_1 = 4\text{-}O_2NC_6H_4$; $R_2 = 4\text{-}FC_6H_4$, **10d**.
$R_1 = 4\text{-}O_2NC_6H_4$; $R_2 = 4\text{-}MeOC_6H_4$, **10e**.
$R_1 = 4\text{-}O_2NC_6H_4$; $R_2 = 4\text{-}Me_2NC_6H_4$, **10f**.
$R_1 = 4\text{-}NCC_6H_4$; $R_2 = 4\text{-}Me_2NC_6H_4$, **10g**.

Figure 3. Structure and compound numbers of various 12-Te-5 pertelluranes.

B. Physical Studies of Tellurapentalenes

The structure of the tellurapentalenes shown in Scheme 1 could only be deduced initially from variable temperature ^{1}H NMR spectroscopy[4] of the selenium analog of **1a** and by analogy with the crystal structure of the selenium derivative of **1d**. Only one signal for the two protons of **1a** (Se) was observed, when spectra were collected from -60 to $+40$°C. Only one ^{1}H NMR signal was observed for the methyl groups in **1b**, again indicating a symmetrical structure about tellurium. The IR spectra are also very informative, since the shift in the carbonyl band on coordination to tellurium may be monitored. The C=O stretching frequency for **4** is at 1500 cm^{-1}, while the corresponding band for **6a** appears at 1550 cm^{-1}; the C=O stretching frequencies for these compounds are shifted to lower wavenumbers because of the strong interaction between the oxygen atom of the carbonyl group and tellurium.

The first X-ray crystal structure determinations[8] on tellurapentalenes were carried out in 1983, when the structures of 2,5-diphenyl-1,6-dioxa-6a-tellurapentalene, **4** and the 12-Te-5 pertellurane, **6a** were elucidated. Representative drawings of the two molecules are shown in Figure 4 with the numbering scheme for the atoms of interest. Relevant bond distances are assembled in Table 1.

The bicyclic rings in both structures are planar. The C—C distances in the bicyclic rings of **4** are aromatic in nature, being close to 1.39 Å. The C—O

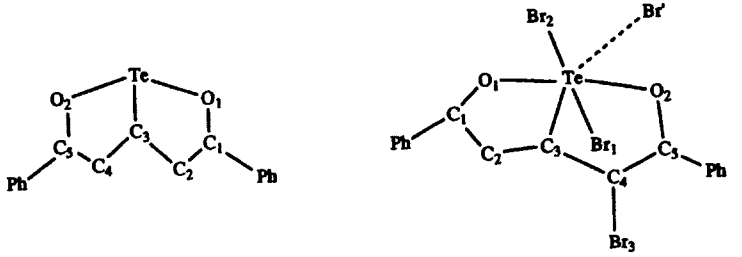

4 6a

Figure 4. Drawing of **4** and **6a** with non-hydrogen atom labeling.

distances of 1.312 (6) and 1.316 (4) Å in **4** are intermediate between C—O (1.36 Å) and C=O (1.22 Å). The Te—C bond in **4** is shorter than that found in **6a** and is close to the value for a Te—C single bond (2.08 Å).[10] The Te—O bond distances in both molecules are longer than the expected single bond value of 2.00 Å. The Te—Br distances in **6a** of 2.668 (2) and 2.620 (2) Å are similar to other Te—Br_{axial} bond lengths. For example, in $RTeX_3$ (R = 2-$C_6H_5C_6H_4$), the average Te—Br_{axial} bond length is 2.661 Å.[11]

The oxidation state of tellurium in **4** should be considered as + 2, but the molecule has very different geometry and bonding relative to conventional divalent Te(II) compounds. The ligand coordination about Te in **4** is T-shaped with O—Te—C_3 angles of 78.6 (2) and 78.5 (2)°. The geometry about Te may also be considered as trigonal bipyramidal (tbp) of AB_3E_2 structure,[12] with the two oxygen atoms occupying the axial sites and the carbon and two lone pairs taking up the equatorial sites The O2—Te—O1 angle of 156.9° is distorted from the ideal 180° of a trigonal bipyramidal structure due to the bending away of the bond pairs from the equatorial lone pairs. For the same reason, the O—Te—C3 angles are less than 90°.

The scheme used to account for the placement of more than eight electrons about tellurium must include *d* orbitals as in the hybridization model, or three-center, four-electron bonds.[13] Both models are extreme approximations, with the full inclusion of *d* orbitals in the former model and their total exclusion in the latter. Foss[14] was the first to suggest multicenter bonding to explain the linear three-center coordination found in Te(II) complexes, in his case of the complex of tellurium with thiourea. Both models have value in the rationalization of structures, but may fail in the prediction of geometry. The long axial O—Te linkages are best considered as a three-center, four-electron bond, although the exclusion of *d* orbitals implied by use of this terminology is probably not correct.

The oxidation state of Te in **6a** should be considered as Te(IV) with the structure of AB_5E molecules.[12] The coordination sphere about Te in **6a** is that of a distorted octahedron, with the axial positions occupied by the bromide ligands and the position trans to the Te—C bond occupied by the Te lone pair and exhibiting a long intermolecular contact to the bromide ligand of another molecule in the unit cell. The bonding in this compound may best be considered as having two linear three-center, four electron bonds involving Br—Te—Br

and O—Te—O, with a covalent (two-center, two-electron) Te—C bond. The pseudoequatorial ligands (O1, O2, and C) are bent away, due to repulsion from the lone pair of electrons occupying the fourth equatorial site.

The results of XPS studies[15] on the dioxatellurapentalenes **4**, **8a**, and **8j** are shown in Table 2. The binding energies of these compounds correspond well to the values obtained for the model Te(II) compounds, 2,6-di-*tert*-butyltellurapyranone[16] (574.1 eV) and (*Z*)-3-(phenyltelluro)but-2-enoate ethyl ester[17] (574.0 eV) to which they were compared, a strong indication that the formulation of the dioxatellurapentalenes as having tellurium in oxidation state + 2 is correct. The Te($3d_{5/2}$) binding energies for **4**, **8a**, and **8j** vary over a 0.6-eV range. The difference in binding energies among the three molecules is attributed to the perturbation of the symmetry of the molecule about Te by varying the substituents on the five-carbon chain.

^{125}Te data for some of the derivatives are tabulated in Table 3. Ph_2Te was used as an external standard, and the spectra were collected in CD_2Cl_2. H_2TeCl_6[18] was chosen for comparison with **6b** and **11** because of the octahedral coordination about Te(IV). As may be seen from the NMR shifts, the formulation of the pertelluranes as Te(IV) appears to have been correct. However, the ^{125}Te NMR shifts of the trigonal bipyramidal Te(II) dioxatellurapentalenes are vastly different from the shifts reported for divalent Te(II) compounds such as Ph_2Te and Me_2Te. The downfield shifts in **4**, **8a**, and **8j** relative to other Te(II) compounds are attributed to the three-center, four-electron bonds present in the dioxatellurapentalenes, which lead to an increase in the paramagnetic shielding about Te.

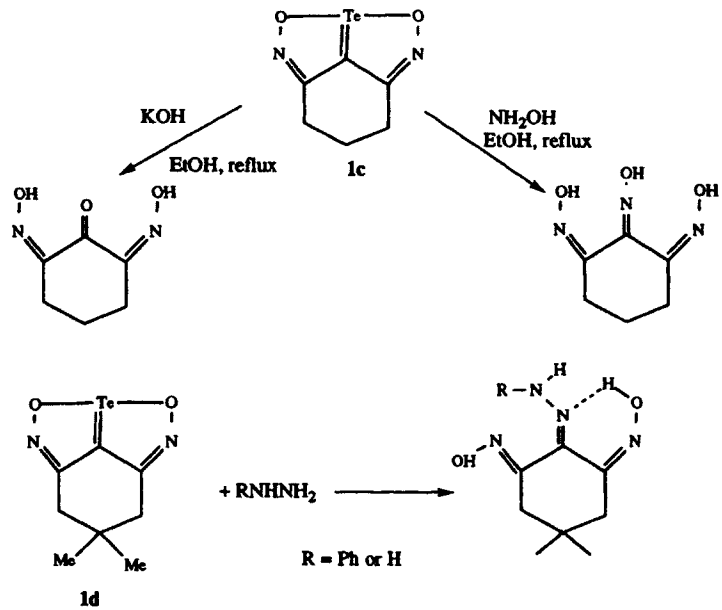

Scheme 5

C. Reactivity of Tellurapentalenes

There is not a great deal of reaction chemistry reported for the tellurapentalenes. The reactivity of the 10-Te-3 dioxatellurapentalenes toward halogens has been described in the previous section. Tellurium may be eliminated from tellurapentalenes by a variety of methods,[4] as shown in Scheme 5.

IV. OXATELLUROLYLIUM HALIDES

Research that began as a study on the reactions of β-(aryltelluro)acryloyl and cinnamoyl chlorides with Lewis acids resulted in the isolation of a well-characterized series of complexes in which the interaction between the carbonyl oxygen and Te is very strong. In fact, these compounds are best regarded as heterocycles of Te.

A. Synthesis of 10-Te-3 and 12-Te-5 Oxatellurolylium Halides

A general method of preparation of 10-Te-3 oxatellurolylium halides is shown in Scheme 6. Reaction of β-(aryltelluro)cinnamoyl chlorides[17] with aluminum trichloride in methylene chloride yields compounds of type **12**. The carbonyl stretching frequencies in the IR spectra of these compounds are in the range of 1520–1530 cm^{-1}, indicating significant interaction between Te and the carbonyl oxygen.

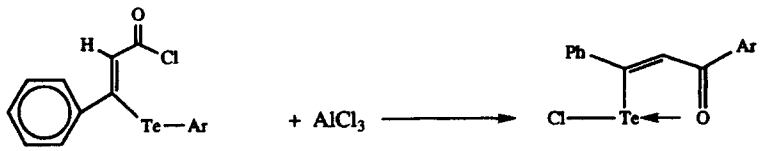

Ar = Ph, **12a**
Ar = 4-$OMeC_6H_4$, **12b**
Ar = 4-MeC_6H_4, **12c**
Ar = 4-$C(O)MeC_6H_4$, **12d**
Ar = *m*-FC_6H_4, **12e**
Ar = *m*-MeC_6H_4, **12f**
Ar = *o,m*-$(OMe)_2C_6H_4$, **12g**
Ar = *m*-$F_2C_6H_4$, **12h**
Ar = 1-naphthyl, **12i**
Ar = *o*-MeC_6H_4, **12j**

Scheme 6

Analogous reactions were observed when β-(phenyltelluro)acryloyl chlorides were reacted with $AlCl_3$, as shown in Scheme 7.

The aryl migration from tellurium could occur via two different mechanisms, *ortho* or *ipso* acylation. *Ortho* acylation would yield tellurochromones, an original aim of the research.[19] By varying substituents on the aryl ring bound to

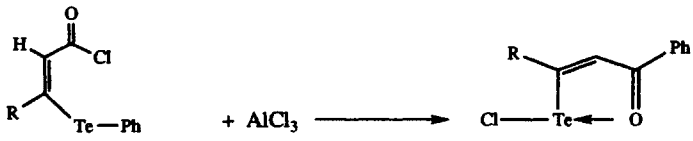

R = H, **13a**
R = Me, **13b**
R = *o,m*-$(OMe)_2C_6H_3$, **13c**
R = *o,m*-$(OMe)_2C_6H_3$, X = OSO_2Me, **13d**

Scheme 7

tellurium, it was possible[19,20] to facilitate *ortho* or *ipso* acylation (or a mixture of products) depending on the substituents. The *ortho* acylation reaction has been described elsewhere in this book (Chapter 3) and thus will not be dealt with here, other than to say that when Ar (Scheme 6) is *m*-$(MeO)_2C_6H_3$ telluroflavone is the only product isolated. When Ar is *m*-$MeOC_6H_4$, the telluroflavone is isolated in 92% yield, with 4% of the oxatellurolylium chloride also being isolated. Conversely, **12e** and **12f**, oxatellurolylium chlorides, are the only products isolated from the corresponding acid chlorides.

Compound **12b** is not isolated from the reaction of the corresponding acid chloride with $AlCl_3$, but thermally from the acid precursor of the acid chloride in the presence of oxalyl chloride. In many cases, it was found that heating of the acid chloride solution is sufficient to yield the oxatellurolylium chloride. This is not the case in the preparation of **12d** where $AlCl_3$ must be added.

Oxatellurolylium chlorides undergo substitution reactions[17] at the halide to yield further examples of 10-Te-3 compounds, as shown in Scheme 8.

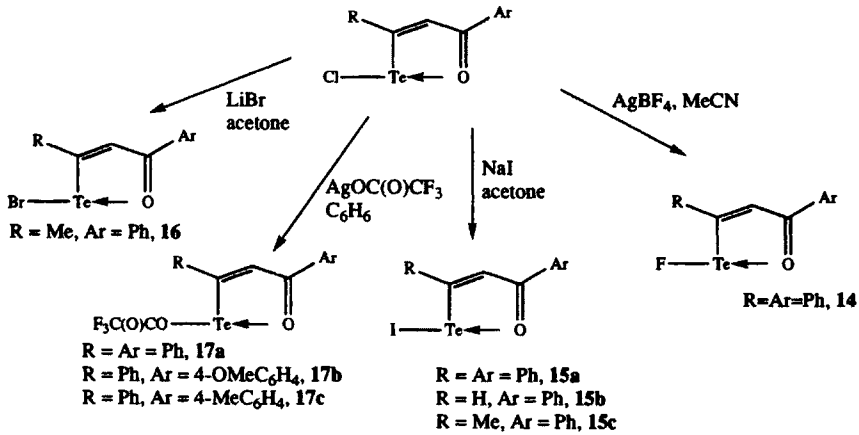

Scheme 8

Addition[21] of Cl_2 or Br_2 to the corresponding oxatellurolylium halide resulted in the isolation of 12-Te-5 pertelluranes, as shown in Scheme 9.

X = Br, R = Ph, **18a**
X = Cl, R = Ph, **18b**
X = Br, R = H, **18c**
X = Cl, R = H, **18d**
X = Cl, R = Me, **18e**
X = Br, R = Me, **18f**

Scheme 9

These reactions were reversible, with mild heat or hypophosphorus acid giving back the starting material. Interestingly, attempts to prepare mixed halide derivatives of **18** resulted only in the isolation of mixtures of the homohalogenated pertelluranes.

B. Physical Studies of Oxatellurolylium Halides

X-ray crystal structures have been determined for two members of this class of compounds, 3-phenyl-5-(4-methoxyphenyl)-1,2-oxatellurolyl-1-ium chloride,[17] **12b**, a 10-Te-3 compound and the 12-Te-5 pertellurane,[21] **18a**.

Drawings of the molecules with atom labels are shown in Figure 5 with relevant bond lengths and angles listed in Table 4.

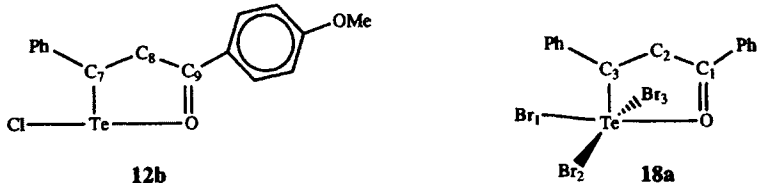

12b **18a**

Figure 5. Drawings of **12b** and **18a** with non-hydrogen-atom labeling.

The structure of **12b** shows trigonal bipyramidal coordination about tellurium, if the two lone pairs on Te occupy two of the equatorial sites, with the carbon ligand occupying the third. The chloride ligand and the carbonyl oxygen occupy the axial sites. Compound **12b** can be classified as AB_3E_2, to explain the T-shaped coordination about Te, similar to the structure[8] observed in **4**. Both **4** and **12b** have Te—O bonds that are longer than single bonds, indicating their fractional nature (three-center, four-electron bonds) and strong equatorial

Te—C single bonds. The Cl—Te—O bond angles in the two independent molecules that occupy the unit cell in the crystal structure of **12b** are close to linear, deviating from 180° perhaps as a result of the equatorial lone pair effect. The C=O distances in both **12b** and **18a** are longer than one would expect for normal C=O bonds. The bond lengths of the C—C bonds in the ring of **12b** indicate less than double-bond character for C7—C8 and greater than single bond character for C8—C9, implying that there is significant electron delocalization in the ring.

Conversely, in **18a** the electron density in the ring appears to be more localized, with C1—C2 at 1.47 Å and C2—C3 at 1.33 Å, values very close to ideal single and double bonds, respectively. The coordination about Te in **18a** is octahedral with the axial positions occupied by two bromide ligands and the equatorial positions occupied by O with Br *trans* to it and the carbon ligand *trans* to the lone pair on tellurium. The Te—C bond here is significantly longer than that found in **12b**. The Te—$Br_{equatorial}$ bond distance of 2.513 Å is close to the sum of the covalent radii (2.50 Å).[10] The Te—O bond that is *cis* to the Te—C bond is much longer than that seen in **12b** or **4**. Therefore, in the case of **18a**, the long bonds are *cis* to each other, as opposed to being *trans* in the case of **12b**. The Te—Br_{axial} distances are similar to those obtained for **6a** and examples seen in the literature.[11] There is a long intermolecular contact between Te and a bromide ligand of another molecule in the unit cell, of 3.757 Å.

The carbonyl stretching frequencies in the IR spectra[21] of these compounds are collected in Table 5. The carbonyl stretching frequencies for these molecules are significantly lower than one would expect were Te not interacting strongly with the carbonyl oxygen. The frequencies observed indicate significant Te—O bond order, as is borne out by the X-ray crystal data, with the Te—O bond distance in **12b** corresponding with a carbonyl band at 1530 cm^{-1} and the longer bond in **18a** having the carbonyl band at 1595 cm^{-1}. Thus, the position of the carbonyl band appears to correlate well with the strength of the Te—O interaction.

XPS (X-ray photoelectron spectroscopy) was used[15] to probe the oxidation states of Te in these compounds. Data are shown in Table 6. The binding energies of **13b**, **12a**, **12i**, **16**, **12i** (Br) and **15a** correspond well to those obtained for the model Te(II) compounds mentioned previously, 2,6-di-*tert*-butyltelluropyranone[16] (574.1 eV) and *Z*-(phenyltellurobut-2-enoate) ethyl ester[17] (574.0 eV). These data indicate that the oxatellurolylium halides are best considered as having Te in the + 2 oxidation state. Correspondingly, the XPS data for the 12-Te-5 pertelluranes (**18b–f**) are similar to the binding energies obtained for the model Te(IV) compounds, 2,6-di-*tert*-butyldichlorotellura-(IV)pyranone (576.4 eV) and the dibromo analog (576.0 eV), verifying the oxidation state of Te in these compounds as Te(IV). The ^{125}Te NMR shifts for these compounds are shown in Table 7. NMR shifts are referenced to Ph_2Te (external) and run in CD_2Cl_2. The NMR shifts of the 10-Te-3 compounds with one exception fall in the range of 1650–1726 ppm. The shift of the iodo derivative, **15a** is more upfield at + 1501 ppm. The 12-Te-5 pertelluranes studied fall in the range of 1359–1386 ppm.

C. Reactivity of Oxatellurolylium Halides

The reactions[21] of oxatellurolylium halides and 12-Te-5 pertelluranes with a variety of nucleophiles are shown in Scheme 10. Some reactions of these compounds yield further oxatellurolylium derivatives and were described in Section IV.B (above).

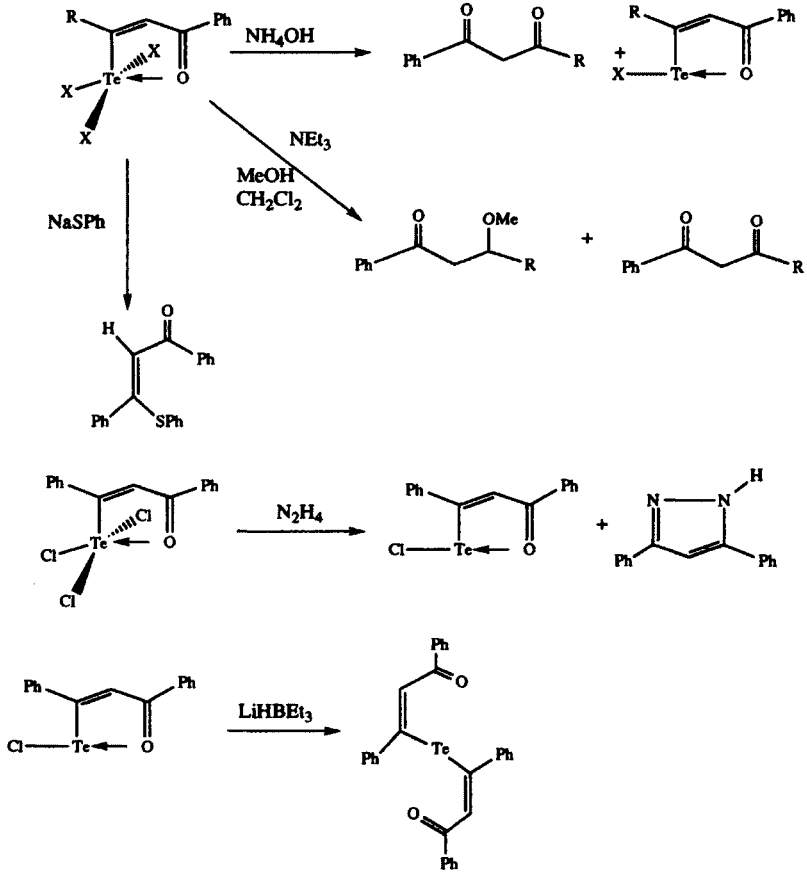

Scheme 10

V. INTRAMOLECULAR COORDINATION THROUGH AN ALKOXY GROUP

A. Synthesis of Compounds

Among the earlier examples of intramolecular coordination to Te are the ethoxycycloalkyltellurium tribromides, two of which have been prepared and characterized by different research groups.

Bergman and Engman[22] reported the synthesis of 8-ethoxy-4-cyclooctenyltellurium trichloride as shown in Scheme 11.

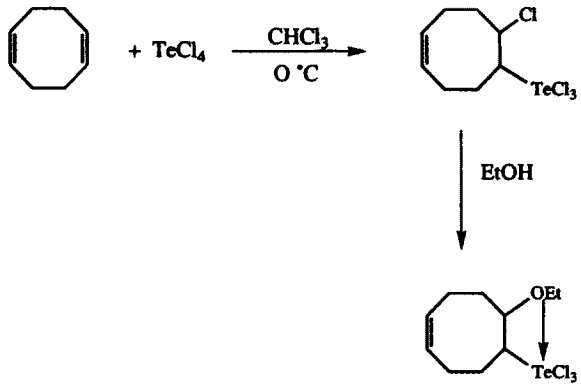

19

Scheme 11

The reaction of the β-chloroalkyltellurium trichloride precursor to **19** with ethylene glycol resulted in the loss of HCl and the isolation of 8-(2-hydroxyethoxy)-4-cyclooctenyltellurium trichloride. COD and elemental tellurium are recovered if **19** is reacted with a reducing agent, $Na_2S_2O_4$. Cameron and coworkers[23] prepared *cis*-2-ethoxycycloheptyltellurium tribromide, **20** by the reaction of $TeBr_2$ with cycloheptene in ethanol as shown in Scheme 12.

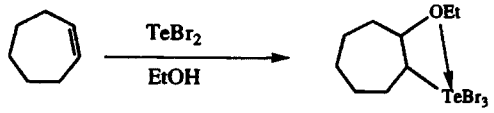

20

Scheme 12

B. X-Ray Structural Data

Both **19**[22] and **20**[23] have been characterized by X-ray crystallography. Drawings with numbering schemes are shown in Figure 6, while bond lengths and angles are listed in Table 8.

In both cases, the coordination environment about Te is that of a distorted octahedron, with the fourth equatorial coordination site occupied by a lone pair of electrons on Te. Two halide ligands occupy the axial positions.

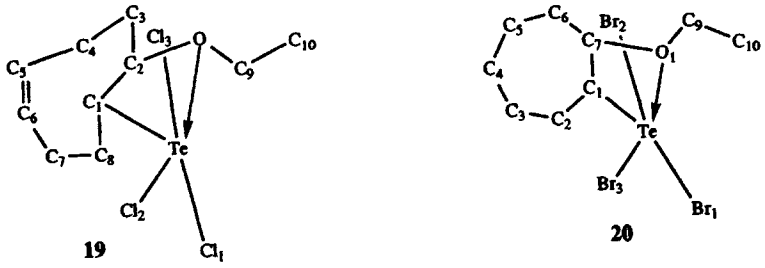

Figure 6. Drawings of **19** and **20** with non-hydrogen-atom labeling.

The Te—C bond in **19** is similar in length to that seen in **18a** (2.175 Å), while the corresponding bond distance in **20** is slightly longer. The Te—O distances of 2.49 Å in **20** and 2.419 Å in **19** are much longer than those observed in **12b** (2.206 Å and 2.175 Å), and only a little longer than the value obtained in **18a** (2.362 Å). As in **18a**, the two long (Te—O and Te—C) bonds are *cis* to each other, while in **12b** the two long bonds are *trans* to each other. The Te—$X_{equatorial}$ distances in **19** and **20** are both of single-bond length. The Te—X_{axial} bonds are longer than the equatorial bonds, as is normally observed. There is a long Te—Cl′ intermolecular interaction of 3.558 Å in **19**. A similar interaction is not present in **20**.

VI. LONGER Te—O INTRAMOLECULAR INTERACTIONS

A number of other crystallographically characterized compounds display much longer Te—O intramolecular contacts, and should be mentioned here for the sake of completeness. Drawings of the X-ray crystal structures have not been included because the Te—O contact is too long to be defined as a bond. The structure[24] of dichloro[4,4-dimethyl-5-oxo-2,3,4,5-tetrahydro-2-furyl methyl]-(4-methoxyphenyl)tellurium, **21**, has a Te—O interaction of 3.194 Å, much too long to be considered a bond, but shorter than the sum of the van der Waals radii (3.60 Å).[10] The structure[25] of *p-N*-ethylanilino(*trans*-2-ethoxy-1-cycloalkyl)tellurium dibromide, **22**, has a Te—O distance of 3.058 Å, again longer than a single bond but shorter than the sum of the van der Waals radii. This product is made by the addition of the aniline derivative to the product of the *trans* addition of $TeBr_4$ to cyclohexene,[26] as shown in Scheme 13.

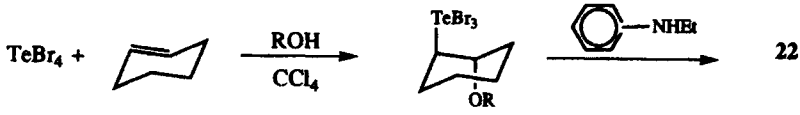

Scheme 13

It is interesting to note that the reaction of Te(IV) halides with cyclohexene gives *trans* addition products, while the same reaction with larger cycloalkenes gave[23] *cis* addition products. This effect is presumably due to the smaller ring size of cyclohexene, resulting in the increased steric crowding on substitution. The structure[27] of (*p*-methoxyphenyl)(8-oxo-7-oxabicyclo[4.3.0]non-5-yl)tellurium dichloride, **23** has an even longer Te—O interaction of 3.273 Å.

IR evidence has been used[28] to verify the postulated coordination of the carbonyl oxygen to Te in the cases of two other compounds for which structural data are not available. The compounds are shown below together with IR stretching frequencies.

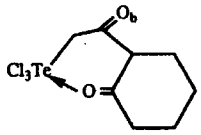

$\nu(C{=}O_b)$: 1570 cm^{-1}
$\nu(C{=}O_b)$: 1540 cm^{-1}

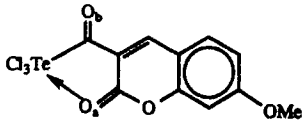

$\nu(C{=}O_b)$: 1669 cm^{-1}
$\nu(C{=}O_b)$: 1635 cm^{-1}

Frequency $\nu_{C=O}$ of free 2-acetylcyclohexane is 1650 cm^{-1}, while those of 3-acetyl-7-methoxycoumarin are 1672 and 1735 cm^{-1}. The shift of 60 and 100 cm^{-1} from the free values indicates strong Te—O interaction.

VII. ORTHOTELLURATED BENZALDEHYDES

Organotellurium compounds containing one C=O to Te intramolecular bond form a large class of compounds stabilized by such interactions. Among the earliest examples of such compounds are those of Piette, with the first structurally characterized compound published in 1974. Without X-ray structural data, the IR stretching frequency of the carbonyl group becomes the leading indicator of intramolecular coordination to Te.

A. Synthesis of Orthotellurated Benzaldehydes

Orthosubstituted alkyl, aryl, or halotellurabenzaldehydes may be prepared[29–32] by the general routes shown in Scheme 14.

More than seventy derivatives of the general classes shown above have been prepared. Substitution patterns and compound numbering scheme are shown in Figure 7.

Further derivatives of the same general type as those above have been prepared by a slightly different route,[33] as shown in Scheme 15.

The rearrangement reaction that compound **33** undergoes to yield ortho(chlorotellurenyl)benzophenone, **35a** or derivatives (**35b**, **35c**) is an ex-

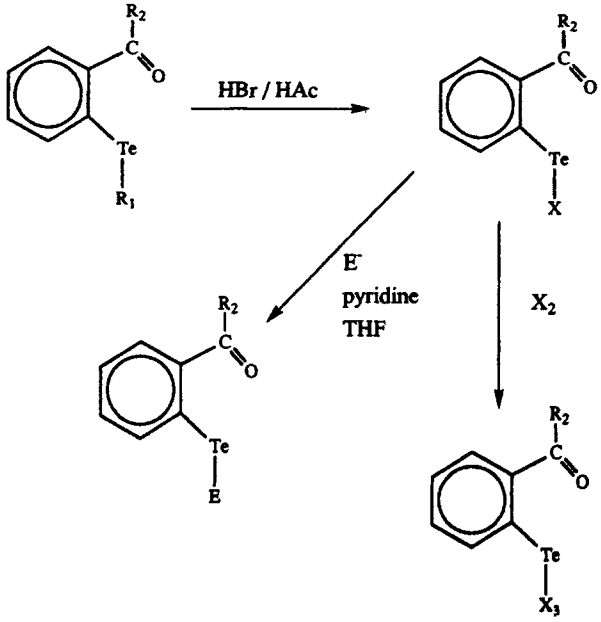

Scheme 14

ample of intramolecular attack on a Te–aryl group, and presumably proceeds via an *ipso*-acylated intermediate.

The preparation of orthocarbonyl aryl or bromotellurothiophenes is effected as shown in Scheme 16.[34]

An orthotellurated benzaldehyde with Te formally in the + 4 oxidation state has been prepared and structurally characterized.[35] The synthesis is shown in Scheme 17.

B. Physical Studies of Orthotellurated Benzaldehyde Derivatives

The X-ray crystal structures of compounds **24b**[36], **30a**[37] and **29b**[37] have been determined. In all cases the molecules adopt the planar *cis* configuration with the carbonyl oxygen pointing toward Te and the R group pointing away, confirming the conclusions drawn from IR data. Pertinent bond distances and angles are tabulated in Table 9, with the numbering scheme as shown in Figure 8.

The Te—C2 distances are in the correct range for a tellurium to sp^2-hybridized carbon single bond (2.11 Å),[10] with the distance in the formyl derivative being the shortest at 2.081 Å. The Te—X bond distances in the three molecules are similar, with the Te—Br distances longer, as would be expected. The C—O distances are longer than in complexes where intramolecular co-

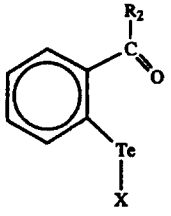
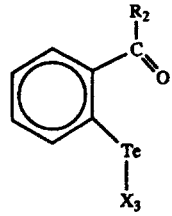
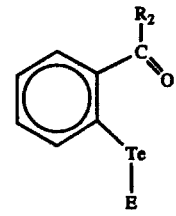

R_2 = H; X = Cl, **24a**
R_2 = H; X = Br,**24b**
R_2 = H; X = I, **24c**
R_2 = Me; X = Cl, **25a**
R_2 = Me; X = Br, **25b**
R_2 = Me; X = I **25c**
R_2 = OH; X = Br, **26a**
R_2 = OEt; X = Cl, **27a**
R_2 = OEt; X = Br, **27b**
R_2 = OEt; X = I, **27c**
R_2 = Cl; X = Cl, **28a**
R_2 = Cl; X = Br, **28b**
R_2 = NH_2; X = Cl, **29a**
R_2 = NH_2; X = Br, **29b**
R_2 = NH_2; X = I, **29c**
R_2 =NHMe; X=Cl, **30a**
R_2=NHMe; X =Br, **30b**
R_2 = NHMe; X = I, **30c**
R_2 = NMe_2; X =Cl, **31a**
R_2 = NMe_2; =Br, **31b**
R_2 = NMe_2; X = I, **31c**

R_2 = H; X = Cl, **24d**
R_2=Me; X=$MeCl_2$, **25d**
R_2 = Me; X = Cl, **25e**
R_2 = NH_2; X = Br, **29d**
R_2 =NHMe; X=Br, **29d**

R_2 = H; E = CN, **24e**
R_2 = H; E = Me, **24f**
R_2 = H; E = SePh, **24g**
R_2 =Me; E = SePh, **25f**
R_2 =OH; E = SPh, **26b**
R_2 =OH; E =SePh, **26c**
R_2 = OH; E = Me, **26d**
R_2 = OH; E = Ph, **26e**
R_2 = Me; E = SPh, **25g**
R_2 =Me; E = SCN, **25h**
R_2 = Me; E=SeCN,**25i**
R_2 = Me; E = CN, **25j**
R_2=OMe; E=SCN, **32a**
R_2=OMe; E=SeCN, **32b**
R_2 = OEt; E = CN, **27d**
R_2 = OMe; E=SPh, **32c**
R_2=OMe; E=SePh, **32d**
R_2 = Cl; E = Me, **28c**
R_2 = Cl; E = Ph, **28d**
R_2=NH_2; E=SCN, **29e**
R_2=NH_2; E=SeCN, **29f**
R_2 = NH_2; E =CN, **29g**
R_2=NH_2; E =SPh, **29h**
R_2 =NH_2; E=SePh, **29i**
R_2 = NH_2; E = Me, **29j**
R_2 = NH_2; E = Ph, **29k**
R_2=NHMe; E=SCN, **30e**
R_2=NHMe; E=SeCN, **30f**
R_2=NHMe; E=CN, **30g**
R_2=NHMe; E=SPh, **30h**
R_2=NHMe; E=SePh, **30i**
R_2 = NHMe; E = Me, **30j**
R_2 =NHMe; E = Ph, **30k**
R_2 = NMe_2; E = Ph, **31d**

Figure 7. Compound numbering scheme for orthotellurated benzaldehyde derivatives.

ordination is not present. The lengthening of the bond may be attributed to the partial polarization caused by the intramolecular bond between oxygen and tellurium. The Te—O distances in the three molecules fall in the range 2.237–2.31 Å. The sum of the covalent radii of Te and O is 2.03 Å[10] while the sum of the van der Waals radii is 3.60 Å. Clearly these intramolecular contacts, while longer than single bonds are more significant than van der Waals interactions. A consequence of the presence of the phenyl ring is that there is a lower limit on the distance between Te and O due to the rigid geometry imposed by the ring. Therefore, maximum overlap of orbitals for bonding is not possible.

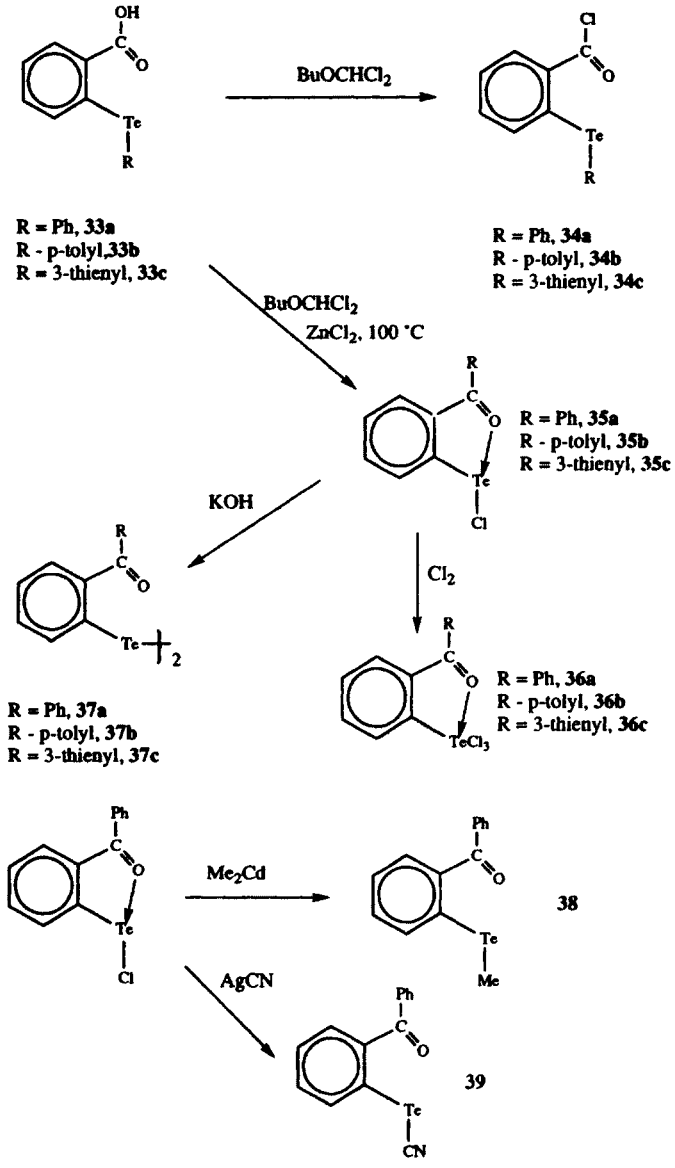

Scheme 15

One could consider these compounds as having T-shaped or trigonal bipyramidal (AB_3E_2) coordination about tellurium, with the axial sites occupied by X and O in a three-center, four-electron bond with tellurium. The equatorial sites are taken up by C2 and two lone pairs. The C2—Te—O angles vary in the range of 74.4° to 78.5°, while the C2—Te—Br angles are in the range of 92.7° to 95.1°.

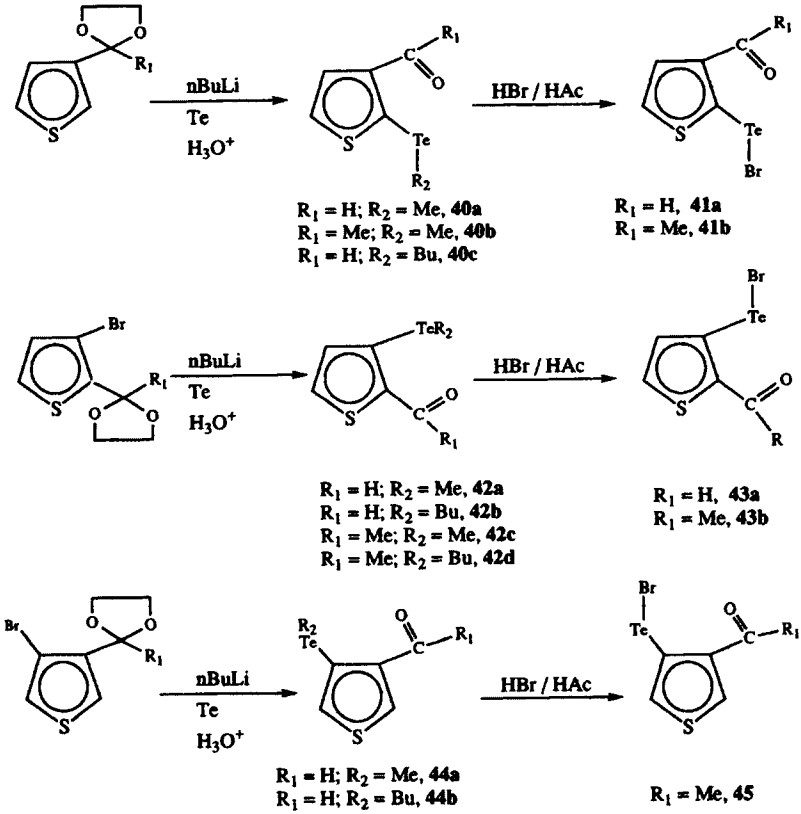

Scheme 16

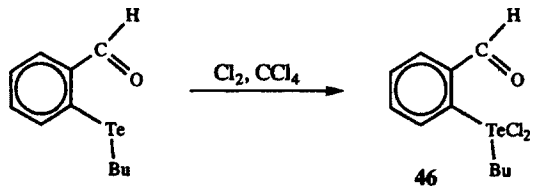

Scheme 17

There are examples in the literature of orthotellurated benzaldehyde derivatives where the intramolecular interaction between tellurium and oxygen is much weaker than in the compounds described heretofore. Some of these compounds have been structurally characterized and are described here for the sake of completeness. These compounds show tellurium–oxygen interactions that are much longer than Te—O single bonds, but still within the limits of a van der Waals interaction. For example, 2-(butyldichlorotelluro)benzaldehyde,

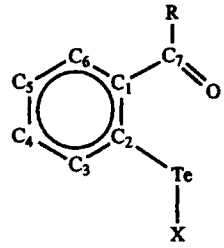

Figure 8. Numbering scheme for orthotellurated benzaldehyde derivatives.

46, has a Te—O distance of 2.83 Å, while 9-telluro-1-formyl-3,4,5,6,7,8-hexahydro-2*H*-anthracene[38] has Te---O interactions of 2.577 (15) Å and 2.574 (14) Å in the two molecules of the unit cell. A slightly shorter Te---O distance of 2.438 (5) Å is found in the X-ray crystal structure of the aliphatic carbonyl compound, 4-oxo-2-methylpent-2-en-1-yl tellurium trichloride.[39] The longest intramolecular interaction found for a carbonyl oxygen to tellurium interaction is at 2.935 (2) Å [average value from the two molecules in the unit cell], in dichloro(*p*-methoxyphenyl)(2-oxocyclohexyl)tellurium.[40]

It is not always practical to carry out X-ray crystallographic studies on all compounds of interest, to determine the nature of the Te—O intramolecular interactions. IR spectroscopy is a valuable routine tool, in that the shift of the carbonyl band on coordination to Te may be monitored and the strength of the intramolecular interaction may be ascertained by the number of wavenumbers by which the appropriate band shifts. The carbonyl shifts for a selection of compounds may be found in Table 10. Immediately obvious is the shift of the carbonyl band to lower wavenumber on replacement of an alkyl or aryl substituent by the more electronegative halide group. For example, in 2-chlorotelluro benzaldehyde, **24a**, the IR stretch for the carbonyl group is at 1585 cm^{-1}, while in the methyltelluro analog, **24f**, the IR stretch is found at 1698 cm^{-1}, a downward shift of 113 cm^{-1} on replacement of a methyl group with the chloride ligand. This trend is as one would expect, since the more electron-deficient tellurium in the halide compound should bond more strongly to the adjacent carbonyl oxygen than an alkyl or aryl-substituted tellurium would be expected to, thus shifting the IR stretching band for the carbonyl group to a higher energy. Also of interest is the resonance at 1700 cm^{-1} for **28c**, when the carbonyl carbon bears an electron-withdrawing group and the tellurium an alkyl group. The position of the IR stretch indicates that there is little or no interaction between Te and oxygen in this case.

C. Reactions of Orthotellurated Benzaldehyde Derivatives

The reactions of tellurenyl halide orthobenzaldehyde derivatives with chlorine or bromine to yield the organotellurium(IV) trichloride compounds have

been described in the previous section on the synthesis of the compounds of interest. Suffice it to say that the reaction is a general one. Also documented in the same section was the fact that the *ortho*-carbonyl-substituted phenyl tellurenyl monohalide derivatives readily undergo substitution reactions in which the halide ligand is replaced with, amongst others, alkyl, aryl, thio, seleno, and cyano groups.

Ortho-tellurenyl alkyl benzaldehydes are useful starting materials in the preparation of some tellurium heterocycles as shown in Scheme 18.[22]

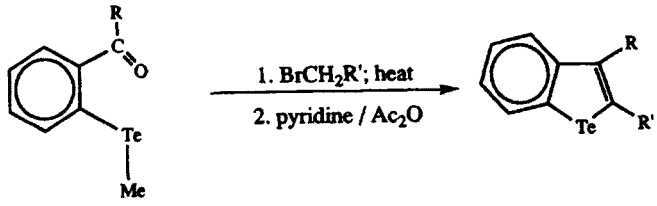

Scheme 18

The formation of another heterocycle, telluroindoxyl, in 80% yield is observed[41] in the reaction with KOH shown in Scheme 19. The same product may be made by reaction with ammonia.[42]

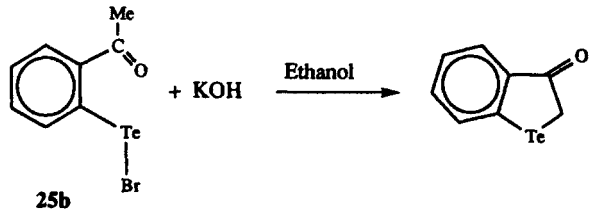

25b

Scheme 19

The reverse, ring-opening reaction is observed on addition of acid to the telluriondoxyl compound. The chloro, bromo, and iodo derivatives of **25b** may be obtained by this method. This reaction provides the only, somewhat circuitous, route to the iodo derivative of **25b**.

VIII. INTRAMOLECULAR COORDINATION THROUGH NO_2

There is a report[43] in the literature of the isolation and use of (*o*-nitrophenyl) tellurenyl bromide. The compound is reported to be very stable, unlike unsubstituted aryl tellurenyl halide compounds. This compound is presumably

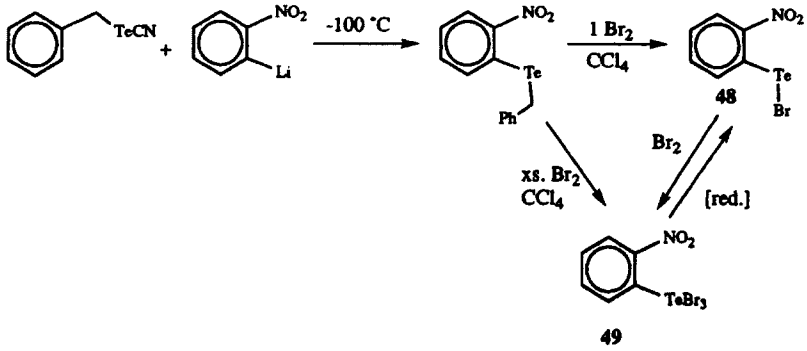

Scheme 20

stabilized by intramolecular coordination between Te and the NO_2 group. It was prepared as shown in Scheme 20.

The compounds were postulated[43] to have an intramolecular Te—NO_2 contact by analogy with *o*-nitroaryl sulfenyl chlorides, but unfortunately no physical data are available to confirm this supposition.

IX. INTRAMOLECULAR COORDINATION VIA NO

Examples of intramolecular Te—O coordination from an N—O group may be found in the patent literature. The synthesis[44,45] of a number of these compounds is shown in Scheme 21.

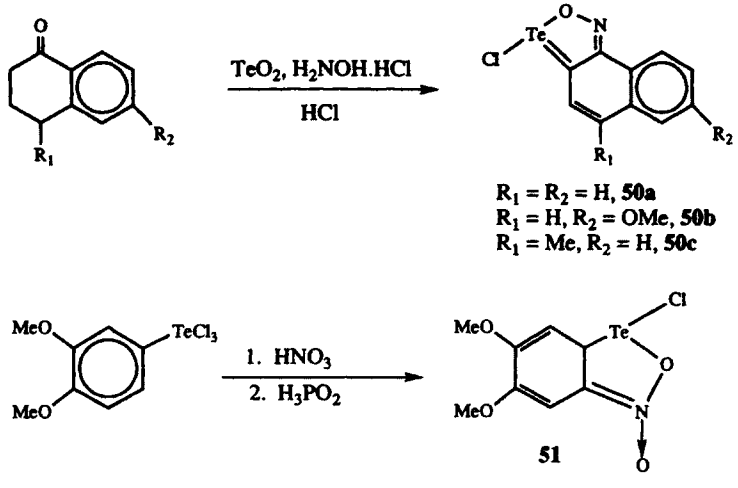

Scheme 21

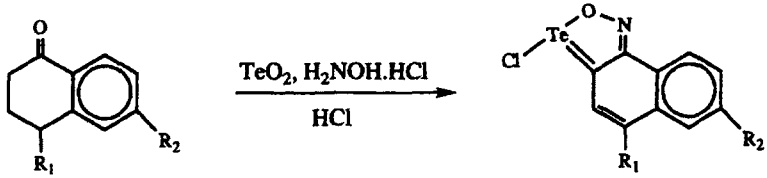

$R_1 = R_2 = H$, **50a**
$R_1 = H, R_2 = OMe$, **50b**
$R_1 = Me, R_2 = H$, **50c**

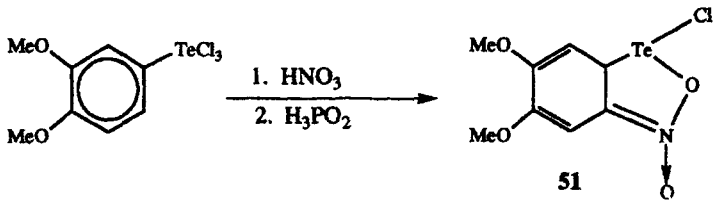

51

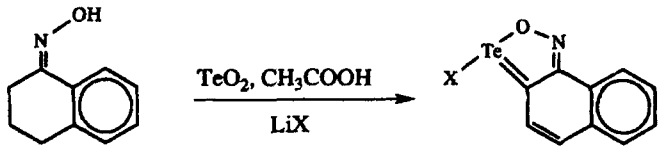

X = Br, **52a**
X= Cl, **52b**

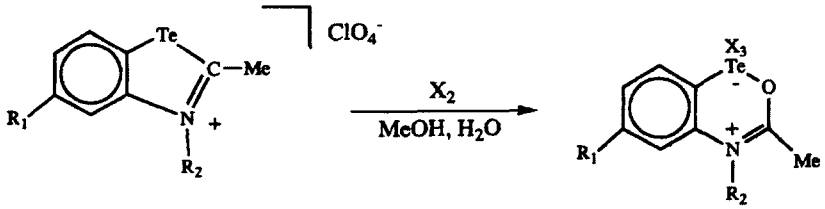

X = Cl, R_1 = H, R_2 = Me, **53a**
X = Cl, R_1 = Me, R_2 = Me, **53b**
X = Cl, R_1 = H, R_2 = Et, **53c**
X = Br, R_1 = H, R_2 = Me, **53d**
X = Br, R_1 = Me, R_2 = Me, **53e**
X = Br, R_1 = H, R_2 = Et, **53f**

Scheme 22

1-Chloro-5,6-dimethoxy-2,1,3-benzoxatellurazole-*N*-oxide, **51**, can also be prepared by the analogous reaction with the phenyl ditelluride derivative, but only in 32% yield, as opposed to the 69% yield obtained if the reaction is carried out as shown in Scheme 21. The reaction shown in Scheme 21, which results in

the preparation of 3-chloronaphtho[2,1-*c*]-1,2,5-oxatellurazole, **50**, gives elemental tellurium as a side product. The desired product may be separated from the metal by Soxhlet extraction with dichloromethane. The 1,1,1-trihalo-(substituted)2,1,4-benzotellurazinium inner salts, **53**, are prepared by the reaction of Cl_2 or Br_2 with the corresponding *N*-alkylated benzotellurazolium salts.

Compound **52b** undergoes substitution reactions[46] at the ring carbon *meta* to Te. A number of these reactions are illustrated in Scheme 22.

X. INTRAMOLECULAR COORDINATION THROUGH PYRIDYL LIGANDS

A. Synthesis of Pyridyl Compounds

Intramolecular coordination to Te in organotellurium compounds can occur from a nitrogen atom in an aromatic ring, such as pyridine and 2,2′-bipyridine. The first example of such a compound was prepared and structurally characterized in 1980.[28] The reaction of $TeCl_4$ with 2,6-diacetylpyridine yielded **54** as shown in Scheme 23.

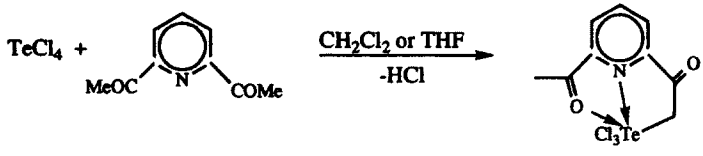

54

Scheme 23

A series[47,48] of 2-pyridyl and 2-quinolinyl organotellurium compounds have been prepared, and four of these compounds have been structurally characterized. The routes to the 2-pyridyl derivatives are shown in Scheme 24. In each case the 2-quinolinyl compound may be prepared by an analogous method.

The preparation of **57**, **58**, and **55** and their subsequent X-ray structure determinations enabled examination of the effect of different *trans* substituents on the length of the Te—N bond.

A series of 2-(3-thienyl) tellurenyl mono- and trihalides have been prepared[49] and their syntheses are shown in Scheme 25.

B. Physical Data on Pyridyl Derivatives

The X-ray crystal structure of **54** has been determined.[28] A drawing with atom labeling is shown in Figure 9 and bond lengths are tabulated in Table 11.

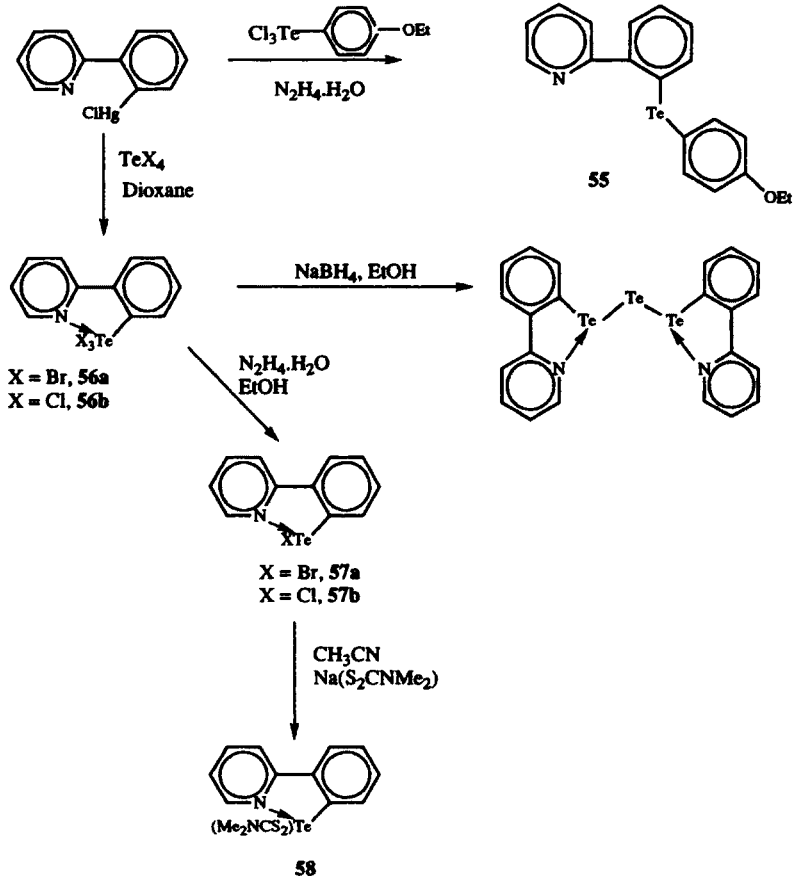

Scheme 24

The coordination about Te is that of a distorted pentagonal bipyramid with the axial sites occupied by chlorides and the equatorial sites by the N, C1, C13 groups, a long Te—O bond from the carbonyl oxygen and a lone pair on tellurium. The structure is distorted because of the lone pair on Te, situated between O2 and C13 that causes distortions in the bond angles between ligands near the lone pair and Te. For example, O2—Te—C13 is 135.56° and N—Te—C13 is 163.37°, rather than the expected 144° in each case. These facts are explained by the observation that lone-pair–bond-pair repulsions are greater than bond-pair–bond-pair repulsions.[13] The Te—C1 distance of 2.129 Å is standard for a Te—C single bond. The sum of the covalent radii for a Te—N single bond is 2.07 Å,[10] while the Te—N distance observed in **54** is considerably longer at 2.402 Å. The Te—O bond length is very long, but is still less than the sum of the van der Waals radii, at 2.878 Å. As is normally observed, the $Te—Br_{equatorial}$ distance is shorter than the $Te—Br_{axial}$ bond lengths.

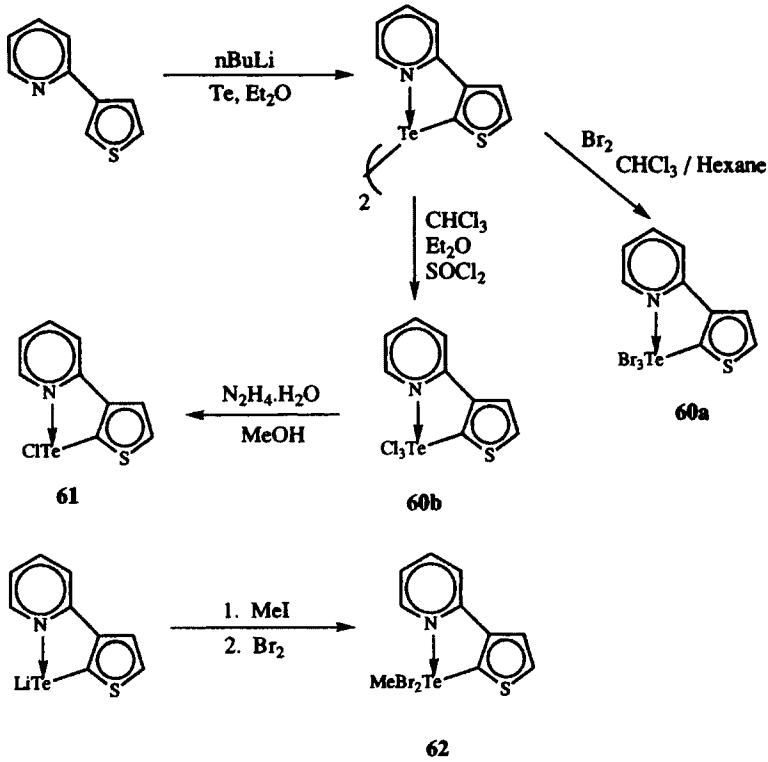

Scheme 25

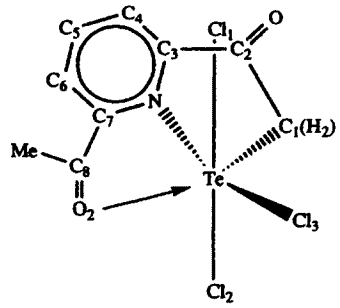

Figure 9. Drawing of **54** with non-hydrogen-atom labeling.

Figure 10 shows the drawings with atom labeling for four 2-pyridyl derivatives, **55**[48], **56a**[48], **57a**[50], and **58**[48] with bond lengths shown in Tables 12 and 13.

Three of the structures illustrated in Figure 10 show quite strong Te—N interactions, of 2.244 (**56a**), 2.236 (**57a**) and 2.354 (**58**), but they are still longer than the sum of the covalent radii. The same three compounds show strong

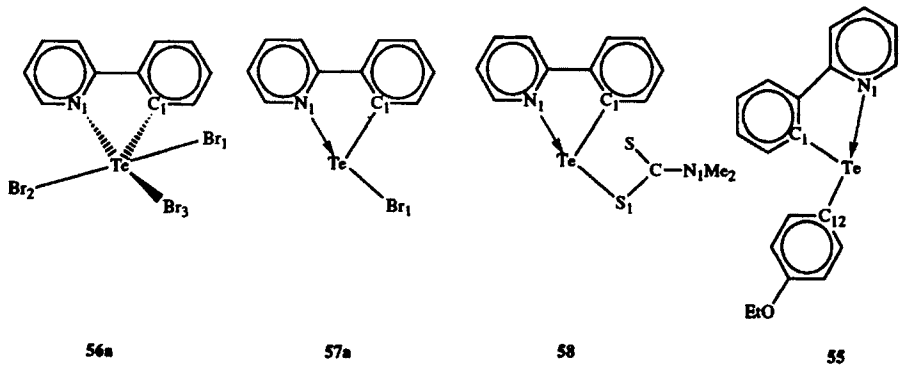

56a 57a 58 55

Figure 10. Drawings of **56a**, **57a**, **58**, and **55** with non-hydrogen-atom labeling.

Te—C single bonds, with the fourth somewhat weaker. The Te—N interaction in **55** is much weaker, at 2.695 Å. The structure[48] of **56a** is that of a distorted octahedron, with two bromide ligands occupying the axial sites and a N, C, Br, and lone pair occupying the equatorial sites. As seen previously, the Te—Br_{axial} bond distances are longer than the Te—$Br_{equatorial}$ bonds. There is a weak intermolecular interaction (3.596 Å) between Te and a bromide ligand of another molecule. Also, as has been observed in other structures discussed in this chapter, there is distortion of the bond angles due to the presence of the lone pair of electrons in the equatorial plane. The C1—Te—N1 angle of 78.2° is short of the ideal angle, in part due to the constraints placed on the geometry by the rigid ligand.

Compound **57a** has[50] a trigonal bipyramidal coordination about Te, with the axial positions occupied by N and Br1 and two equatorial sites filled by lone pairs on Te. The coordination about Te may also be referred to as T-shaped of AB_3E_2-type structure. A strong Te—N bond (2.236 Å) is accompanied by a weaker Te—Br1 bond (2.707 Å) *trans* to it. Once again, there is a small C1—Te—N1 angle (75.9°) due to the chelate of the ring.

The coordination[48] about **58** is analogous to that in **57a**, the axial ligands in this case are the nitrogen moiety and the dithiocarbamate group. The Te—N distance is longer than in **57a** and **56a**, but is still a strong link. The Te—S1 distance is that of a strong single bond (sum of the covalent radii is 2.58 Å).[10] The structure of **55** shows[48] a much weaker Te—N interaction of 2.695 Å, probably due to the strong Te—C bond of 2.144 Å *trans* to it. This is the only molecule of the four where the organic 2-pyridyl ligand is not planar, undoubtedly because the Te—N bond is not sufficiently strong to form a strong chelate. The Te—S1 bond is close to the sum of the covalent radii (2.58 Å).[10] There is only a weak interaction of 3.667 Å between Te and the other sulfur of the dimethyldithiocarbamate ligand.

An X-ray crystal structure[51] of dimethyldithiocarbamato 2-(2-quinolinyl)-phenyl tellurium, the quinolinyl analog of **58** has also been published and is shown below in Figure 11 with bond distances and angles in Table 14.

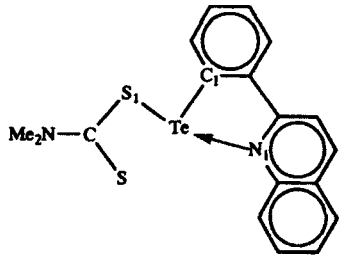

58 (quin)

Figure 11. Drawings of **58** (quin.) with non-hydrogen-atom labeling.

As may be seen by comparison with the data for **58**, the important features are almost identical, just as one would expect. The secondary Te—S interaction in this case is somewhat stronger than in the structure of **58**.

Raman spectroscopy has been used[52] to examine the molecular vibrations of these compounds, but the number and position of bands due to the 2-phenylpyridyl ligand made assignment of ν(Te—N) impossible.

XI. INTRAMOLECULAR COORDINATION VIA AZOMETHINE LINKAGES

A. Preparation of Compounds

Complexes where tellurium is stabilized intramolecularly via coordination to an *ortho*-situated azomethine fragment have been prepared by two general methods. The first examples were reported by McWhinnie and Singh[53] via the reaction of mercurated azomethines with $TeBr_4$. The general synthetic methodology used is shown in Scheme 26.

The reaction to form **63** was only successful if tellurium tetrabromide was employed as the source of tellurium. $TeCl_4$ yielded ionic products, while use of TeI_4 resulted in intractable products. A more general method of preparing analogous compounds has been described by Sadekov,[54,55] as shown in Scheme 27.

A disadvantage of this route from *o*-butyltellurobenzalanines to compounds **67** is that about 20% of the corresponding trihalide, **68**, is a side product of the reaction. The trihalides precipitate out of the reaction mixture and may be filtered away from the desired product, but the reduction in the yield of product is not desirable.

A convenient reaction that avoids formation of the side product has been reported[55] by the same authors, as shown in Scheme 28.

Orthotellurated azomethines of type **67** and **68** are crystalline compounds which are very stable to reduction. It is necessary to heat the compounds in the

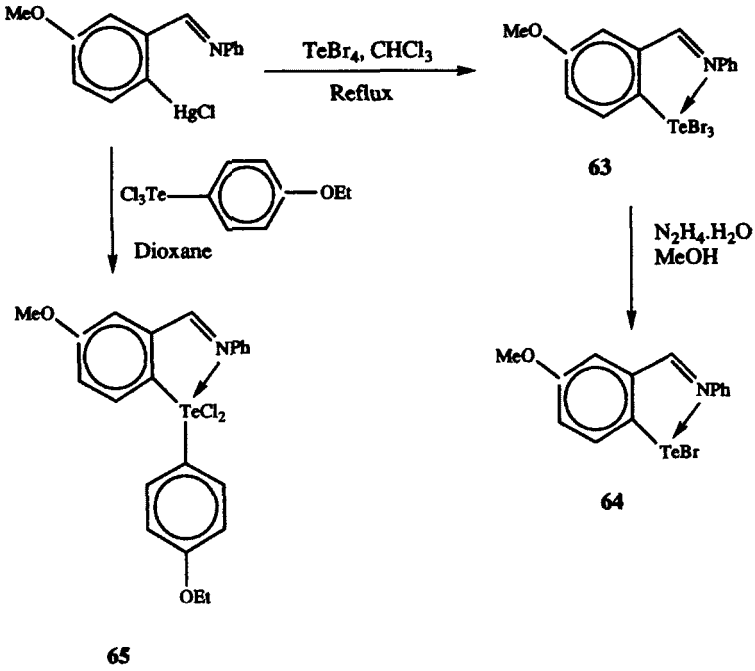

Scheme 26

presence of an excess of reducing agent to effect the formation of the ditellurides, **69**, as shown in Scheme 29.[55]

Alkylation occurs at tellurium on reaction of **66a** with methyl iodide, in the presence of silver perchlorate, to yield **70**, a telluronium salt.

The reaction[56] of the telluride, di(2-formylphenyl)telluride with aniline derivatives yielded 12-Te-4 pertelluranes, which reacted further with sulfuryl chloride to give the 14-Te-6 pertellurane as shown in Scheme 30.

X-ray crystal structures of **71j** and **71k** have been determined and will be discussed in Section XI.C.

1,6-Bis-2-butyltellurophenyl-2,5-diazahexa-1,5-diene, **73**, was prepared[57] by the reaction of ethylenediamine with the orthotellurated benzaldehyde as shown in Scheme 31.

14-Te-6 compounds, dimethylbis(2-arylmethylenaminophenyloxy)telluranes were prepared[58,59] as shown in Scheme 32 by the reaction of benzylidene-*o*-aminophenols with $R_2Te(OMe)_2$.

Twenty-four derivatives of type **74** have been prepared, where R is either a methyl or an aryl group; R_1 is H, 4-NO_2, 4-Me, or 4-NO_2-6-Cl; and R_2 is an electron-donating or electron-withdrawing group. A crystal structure of one derivative, dimethylbis[2-(4-nitrobenzylidenimino)phenyloxy]tellurane, **74a** will be described in Section XI.C.

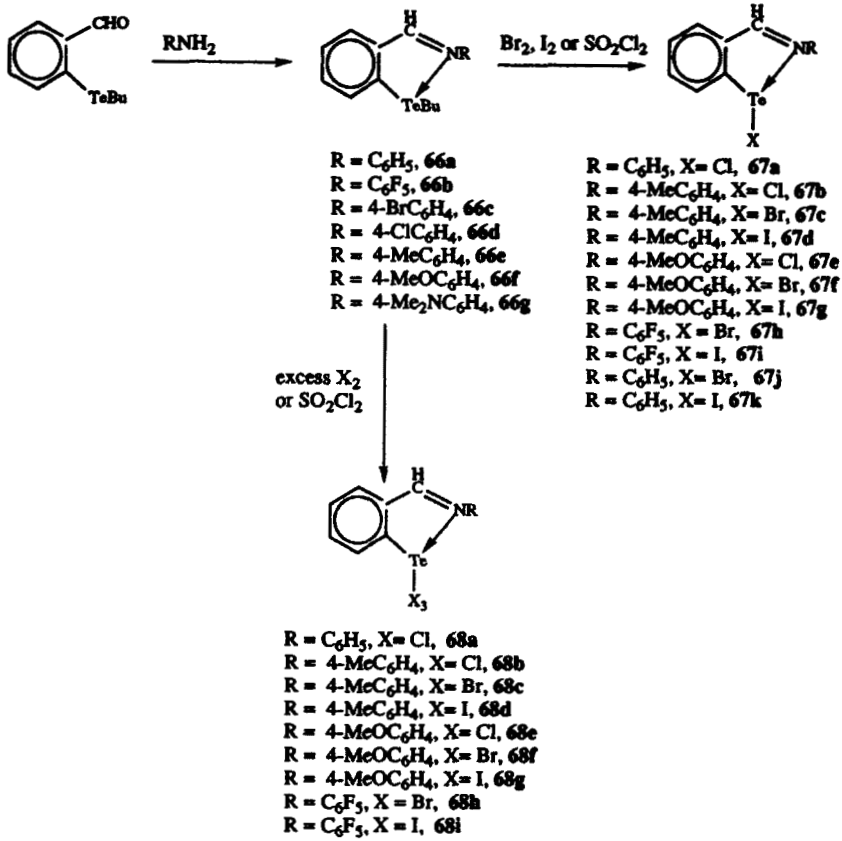

Scheme 27

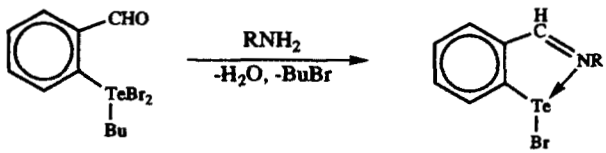

67

Scheme 28

Most recently reported[60] have been the reactions of [2-(*p*-tolyliminomethyl)phenyl-C',N]tellurium tribromide, which result in the formation of further compounds of the same general class, as shown in Scheme 33.

Compound **75** is the first fluoro compound of this type to be isolated. This scheme illustrates another route to **67b**, which was prepared by a different method in Scheme 27.

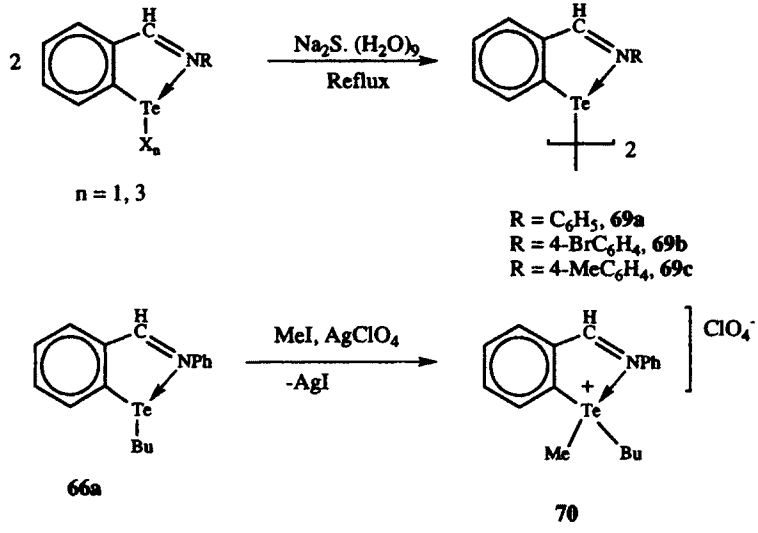

Scheme 29

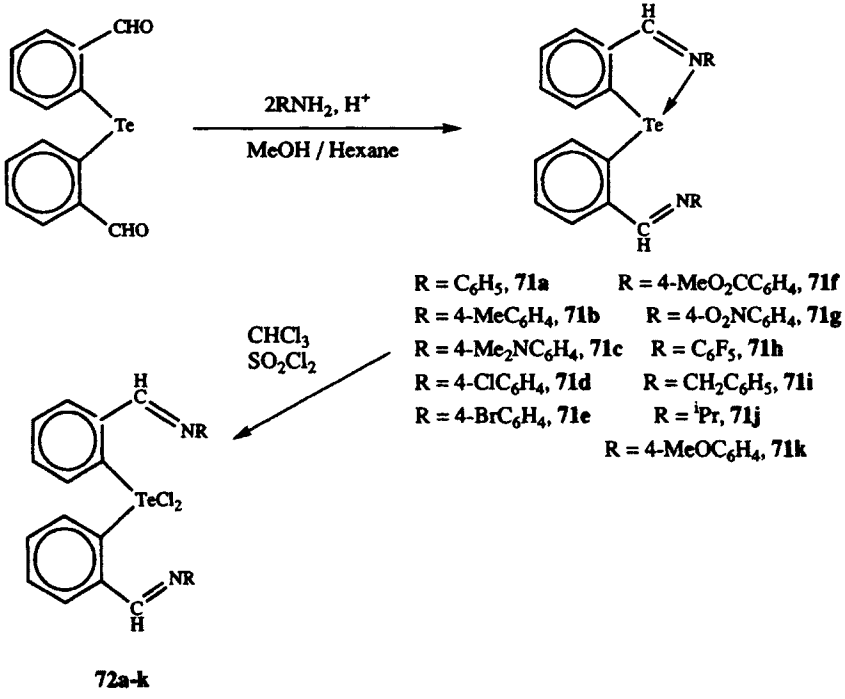

Scheme 30

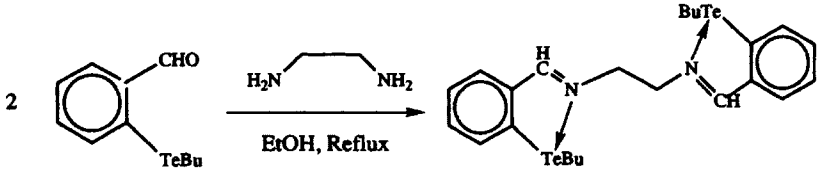

73

Scheme 31

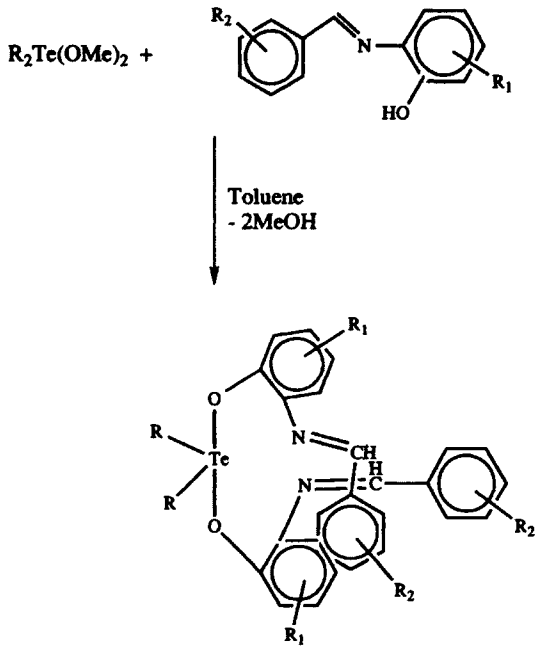

R = Me, R_1 = H, R_2 = NO_2, **74a**
R = Me, R_1 = H, R_2 = 4-Me, **74b**
R = Me, R_1 = 4-Me, R_2 = 4-COMe, **74c**

Scheme 32

B. IR Data on Orthotellurated Azomethine Compounds

The $\nu_{C=N}$ shifts of compounds of type **74** vary between 1593 and 1620 cm^{-1}, which represent shifts of 15–35 cm^{-1} from the values observed for the free ligands, indicating that some interaction with tellurium is taking place.

The only evidence[52] available for the formulation of compounds **63–65** as having Te—N bonds is the $\nu_{C=N}$ bands in the IR spectra. Values are

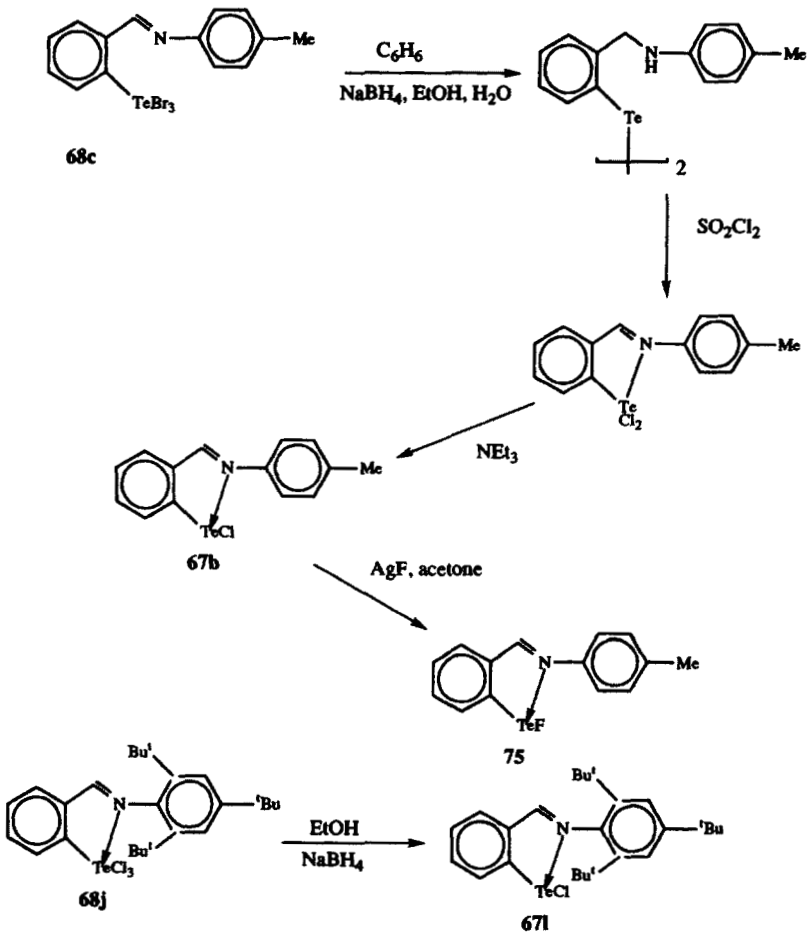

Scheme 33

reproduced in Table 15. As may be seen from the table, shifts of 10 and 34 cm^{-1} are seen relative to the free ligand, indicating that some interaction is occurring between tellurium and the nitrogen of the azomethine group. It appears from compounds that have been crystallographically characterized that shifts in IR bands can be correlated with strengths of the Te—N bond, which would lead one to conclude that **64** has the stronger Te—N interaction.

C. X-Ray Crystal Structures of Orthotellurated Azomethine Compounds

X-ray structure determinations have been carried out for seven of the compounds discussed in this section. The structures of 2-chlorotellurenyl-4′-methylbenzaniline, **67b**[55] and 2-acetatotellurenyl-4′-methylbenzaniline, **76**,[55]

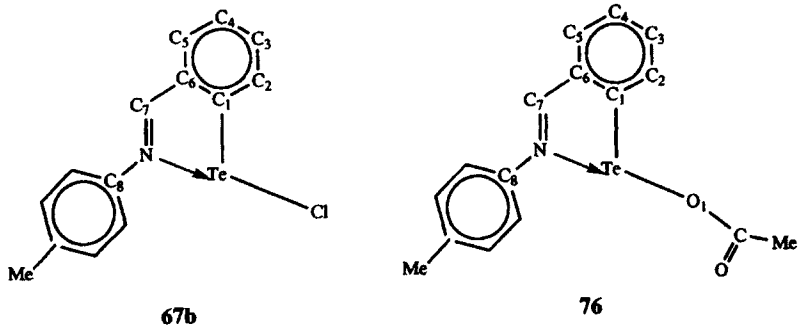

Figure 12. Drawings of **67b** and **76** with non-hydrogen-atom labeling.

are very similar and will be discussed first. Compound **76** is prepared by the reaction of silver acetate with **67c**. Representative drawings are shown in Figure 12 with bond distances and angles in Table 16.

The coordination about Te in both molecules is T-shaped of AB_3E_2 structure, or may also be considered as trigonal bipyramidal if the two lone pairs on Te are counted as ligands. The axial ligands are N and the halide (**67b**) or acetate (**76**). The equatorial sites are occupied by C_1 and the two lone pairs. The T—N distances in both molecules are short; they are close[55] to the sum of the covalent radii of 2.24 Å for axially bonded Te and N. There is a long intermolecular Te—Cl contact of 3.746 Å in **67b** and a long intramolecular Te—O contact with the carbonyl oxygen of the acetate ligand of 3.060 Å in **76**.

The Te—Cl distances are very close to the ideal values for a Te—C(sp^2) single bond (2.11 Å) and therefore are strong single bonds. The Te—Cl distances in the two independent molecules in the unit cell are as expected for Te—Cl bonds. The C7—N bond distance is longer than normal and the C6—C7 bond is shorter, indicating delocalization in the planar ligand system. The N—Te—Cl angle of 168.7° and 168° and the N—Te—O1 angle of 159.2° presumably deviate from 180° as an effect of the two lone pairs of electrons. Similarly, N—Te—C1 angles of 76.7, 77 (**67b**), and 75.8 (**76**) are less than 90° as a result of repulsion away from the lone pairs. As in other T-shaped molecules, the bonding in **67b** and **76** should be considered as having a three-center, four-electron bond between nitrogen, tellurium, and chloride or oxygen.

Structures of two tellurides, bis[2-(4′-methoxyphenyl)iminomethinylphenyl]telluride (**71k**)[55] and bis[2-isopropyliminomethinylphenyl]telluride (**71j**) have been determined. Representative drawings may be found in Figure 13 with bond distances and angles in Table 17.

Both of these molecules have two nitrogen sites that could potentially coordinate to Te. What is observed in both cases is a weak Te—N bond to one azomethine group and no bond to the other, making each molecule a member of the 10-Te-3 class. Tellurium in each case again has a T-shaped, or trigonal bipyramidal coordination about it. Te—C bonds are of normal single-bond

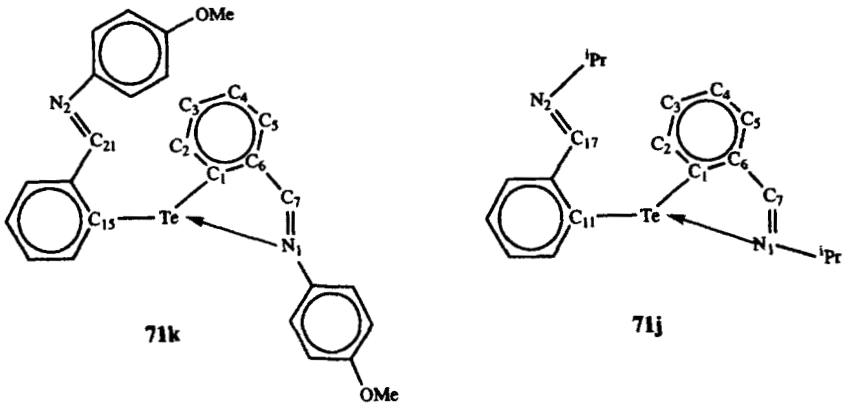

Figure 13. Drawings of **71k** and **71j** with non-hydrogen-atom labeling.

length. The Te—N1 distances are long, at 2.702 Å in **71k** and 2.72 Å in **71j**. An item of interest is the difference in bond distances of the azomethine fragments between the one coordinated to Te and the other. In the "free" azomethine moiety of **71j** (**71k** has comparable values), C16—C17 (1.489 Å) and C17—N2 (1.251 Å) are normal single- and double-bond distances, respectively. Conversely, in the fragment bound to Te, the C6—C7 bond distance is shorter and the C7—N1 distance longer than normal bond distances, as was observed to a greater extent in **67b** and **76**. The smaller differences in **71k** and **71j** are undoubtedly due to weaker Te—N bonds in these molecules.

Two other structures that have weak Te—N interactions have been reported. Methylbutyl(2-phenyliminomethinylphenyl)telluronium perchlorate,[55] **70** has a Te—N distance of 2.75 Å. Dimethylbis[2-(4-nitrobenzylidenimino)phenyloxy]-tellurane,[59] **74a** has two Te—N interactions, of 2.962 and 2.923 Å. Figure 14

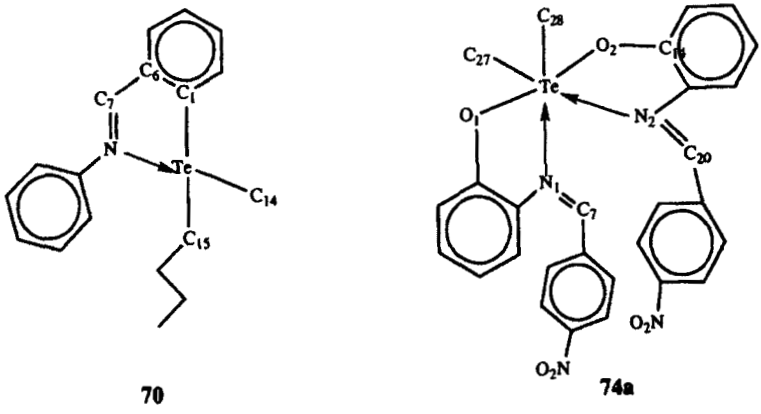

Figure 14. Drawings of **70** and **74a** with non-hydrogen-atom labeling.

shows representative drawings with labeling schemes of **70** and **74a**, with bond distances and angles in Table 18.

Compound **70**, despite bearing a positive charge on Te, has a long Te—N bond. Weak intermolecular contacts are observed between Te and the oxygens of the perchlorate counterion, at 3.33–3.56 Å.

Compound **74a** has pentagonal bipyramidal coordination about Te, if one includes the lone pair of electrons as a ligand, with the aryloxy oxygens occupying the axial positions. Te—O and Te—C bonds are of normal single-bond lengths. The molecule adopts an almost perfectly pentagonal bipyramidal structure as N1—Te—C28 is 146.6° and N2—Te—C27 is 141.3°, very close to the ideal value of 144°.

The crystal structure[57] of **73**, 1,6-bis-2-butyltellurophenyl-2,5-diazahexa-1,5-diene, is represented in Figure 15, and bond distances and angles may be found in Table 19. The molecule is located on an inversion site, so that the two halves are identical. For that reason only half of the molecule is shown in Figure 15.

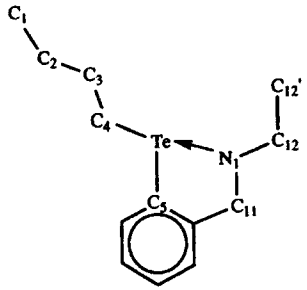

Figure 15. Drawings of 73 with non-hydrogen-atom labeling.

The N1—C11 bond distance is longer than a normal CH=NR bond distance, indicating delocalization. The Te—N1 distance is quite long, at 2.773 Å. The Te—C5 and Te—C4 distances are typical of Te—C(sp^2) and Te—C(sp^3) bonds, respectively. The weak interaction between Te and N may be attributed to the presence of an alkyl ligand on tellurium, *trans* to the nitrogen.

D. NMR Data on Orthotellurated Azomethine Compounds

Compounds of type **74**, **66**, **67**, **69**, **70**, **71**, and **72** have been studied[55,59] by ^{125}Te NMR. The preparation of ^{15}N-labeled samples has allowed the collection of ^{125}Te—^{15}N coupling information. The collected NMR data are shown in Table 20. Spectra were recorded in $CDCl_3$, except in the case of **74b** (benzene) and all were referenced to Me_2Te (0.0 ppm).

The ^{125}Te NMR spectrum of **74a** in $CDCl_3$ showed two signals, while the spectrum of **74b** in benzene showed only one. When the spectrum of **74b** was recorded in $CDCl_3$, two signals were seen, at +1055 and +1108 ppm. In

general, if the spectra of the 24 isolated derivatives were recorded in polar solvents, two signals were observed, while only one was observed in the nonpolar solvent. The presence of two signals indicates that two forms are present in solution. The crystal structure of **74a** showed that both of the nitrogen atoms were coordinated to Te. The two signals are presumed to be due to two structures present in solution, one the same as is observed in the solid state and one with the Te—N bonds broken. Compound **74c** was prepared as the ^{15}N-labeled compound and no ^{125}Te—^{15}N coupling was observed, indicating that the Te—N interaction is weak, as could be inferred from the X-ray crystal structure of **74a**.

^{15}N-labeled compounds were prepared for **66**, **69**–**72** and ^{125}Te—^{15}N coupling was observed. ^{15}N—**67** compounds were also prepared, but no coupling was observed due to quadrupolar broadening from the halogens. Compounds **70** and **71** exhibit smaller couplings, indicating weaker Te—N interactions than in the other cases, a fact verified by X-ray structural data. Larger couplings of 101–141 Hz were observed for the other compounds listed in Table 20, indicating stronger interactions, also confirmed by X-ray crystallography.

E. Reactivity of Orthotellurated Azomethine Compounds

Many of the reactions of compounds of this class have already been described in the section on synthesis, as the products were compounds of the same class. Reaction[61] of **67b** with silver perchlorate in acetone yields *N*-(*p*-tolyl-benzisotellurazolium perchlorate, a Te(II) compound analogous to the Te(IV) compound, **70**. When bromo derivatives of the class **67** are reacted[62] with sodium azide, the products are stable tellurenyl azides. On heating, dinitrogen is evolved to give ditellurides of the type **69**. Reactions of bromo derivatives of **67** with sodium methoxide yield the methoxytellurium compound, **77**, while the reaction with silver acetate gives the acetate derivative, **76**. This compound is also accessible from the aryltellurenic acid anhydride derivatives, on reaction with acetic acid. A summary of this reactivity is shown in Scheme 34.

XII. INTRAMOLECULAR COORDINATION VIA *ORTHO*-CH_2NH_2 GROUPS

A. Synthesis of Compounds

In the last 3 years, reports have begun to appear of aryltellurenyl halides stabilized by interaction with *o*-NH_2 groups or more commonly, *o*-CH_2NR_2 groups. The first compounds were prepared[63] from *N*,*N*-dimethylbenzylamine, as shown in Scheme 35.

The two compounds drawn in brackets are the presumed intermediates in the formation of **78**, but have not been characterized. Scheme 36 illustrates the

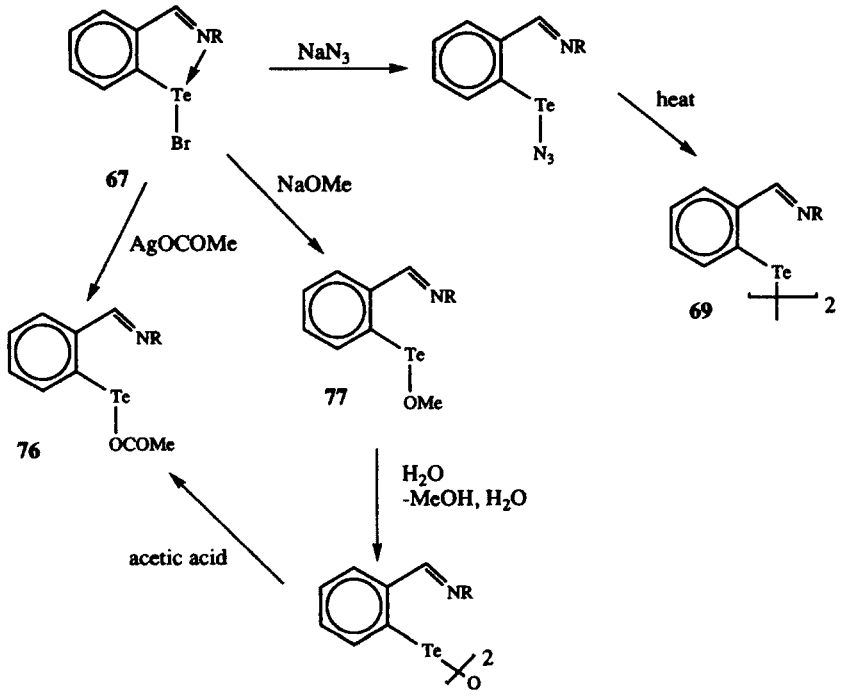

Scheme 34

preparation[63] of similar compounds using *o*-lithio-*N*,*N*-dimethylbenzylamine as the starting material.

The reaction[60] of [2-(*p*-tolyliminomethyl)phenyl-*C*,*N*']tellurium tribomide, **68c** with reducing agent yields 2-bromotelluro-*N*-(*p*-tolyl)benzylamine, **83**, as shown in Scheme 37.

Similarly coordinated compounds have been prepared[64] as shown in Scheme 38.

The preparation of **86a** and **86b** is presumed to proceed through the telluride and its oxidation product, the tellurenic anhydride; $\nu_{Te=O}$ of the anhydride is 650 cm^{-1}.

Ortho-substituted aryltellurenyl halides have recently been reported,[65] with the synthetic route outlined in Scheme 39. To date there is only IR evidence that intramolecular coordination to Te is present.

B. X-Ray Crystal Structures of Compounds with Intramolecular Te—NR_2CH_2 Coordination

X-ray crystal structures have been reported for four of these compounds, **78a**,[63] **82c**,[63] **83**,[60] and **86b**.[64] Figure 16 shows representative drawings of the two 12-Te-5 compounds, **86b** and **78a**, while relevant bond distances and angles are shown in Table 21.

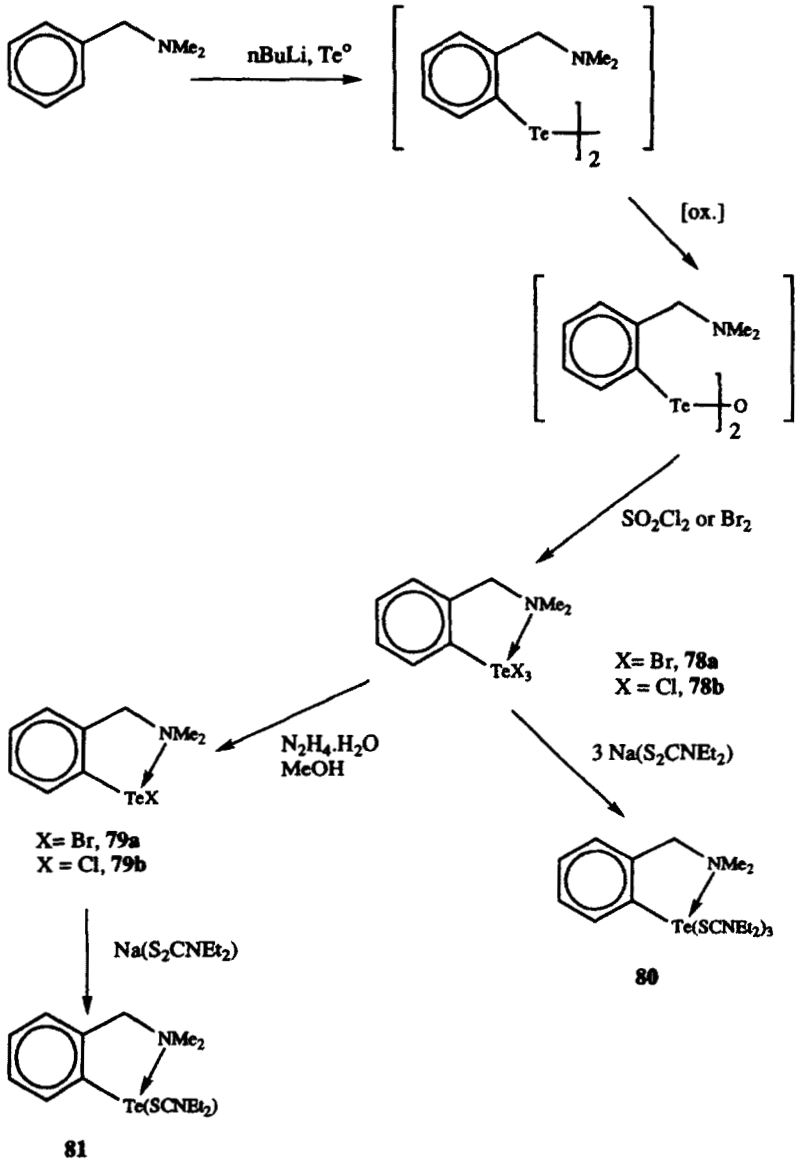

Scheme 35

The coordination about Te in both molecules may be considered as pseudooctahedral, with a lone pair of electrons occupying the fourth equatorial site in both cases. The axial positions are occupied by halide ligands. The Te—Br_{axial} distances are long, as is normally observed. In **78a**, Te—Br1 (2.758 Å) is longer than Te—Br2, and this is presumed to be due to the intermolecular contact observed between Te′ (of another molecule in the asymmetric unit) and Br1. The

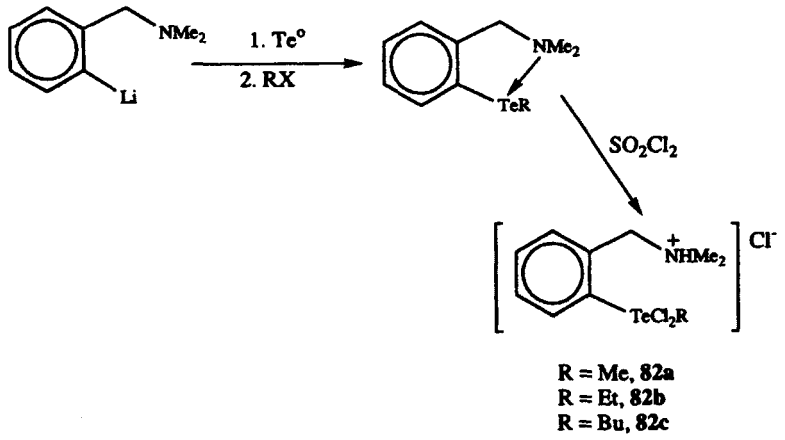

R = Me, 82a
R = Et, 82b
R = Bu, 82c

Scheme 36

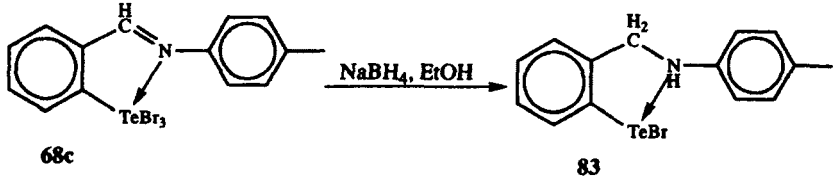

68c **83**

Scheme 37

Te—Cl1 and Te—Cl2 distances in **86b** are longer than Te—Cl3, again as expected. The Te—C1 distances of 2.078 Å (**86b**) and 2.12 Å (**78a**) are close to the value calculated for a tellurium to sp^2 carbon bond. The Te—N bonds in both compounds are longer than the sum of the covalent radii, but are similar to the bond lengths observed for other systems described previously.

The distortion from octahedral geometry in both molecules may be ascribed to the presence of the lone pair of electrons in the equatorial plane. The effect may be noted in the angles Cl3—Te—N (166.8°) and Br3—Te—N (167.4°), which are distorted from the ideal 180° by the repulsion away from the lone pair. The C1—Te—N angle in each case is considerably less than the ideal 90°, as a result of constraint placed on the geometry of the molecule by the five-membered ring.

Figure 17 contains the illustration of the structure[60] of 2-bromotelluro-*N*-(*p*-tolyl)benzylamine, **83** with atom labels while the bond distances and angles are contained in Table 22.

The structure of **83**, a 10-Te-3 compound, has a T-shaped or trigonal bipyramidal environment about Te, with C1 and two lone pairs occupying the equatorial sites. Te—C1 is a normal Te to C(sp^2) single-bond length. Te—N is 2.375 Å, longer than the sum of the covalent radii, but similar to those found in other structures discussed already.

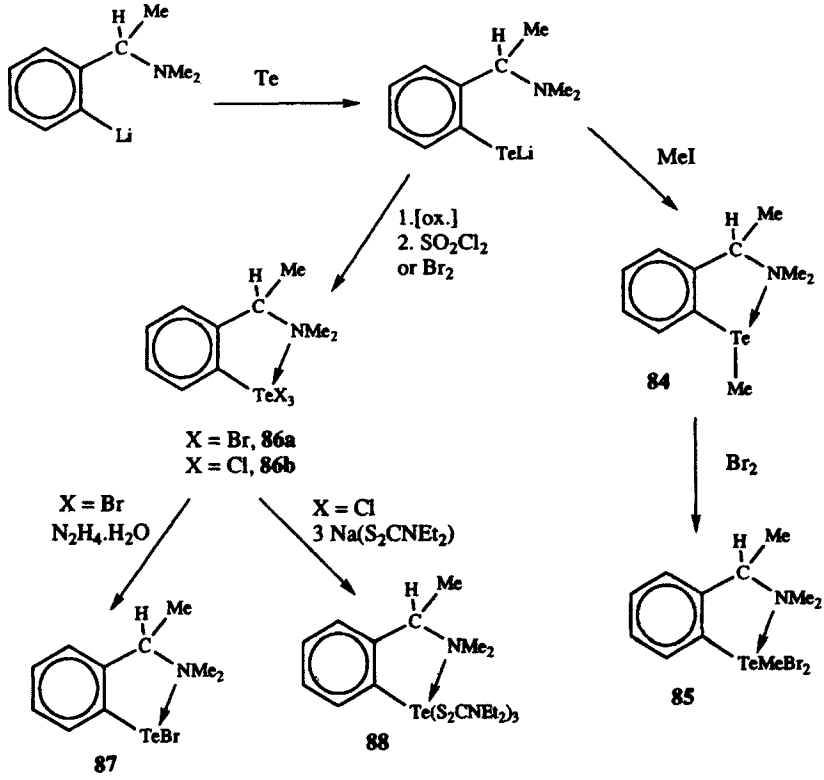

Scheme 38

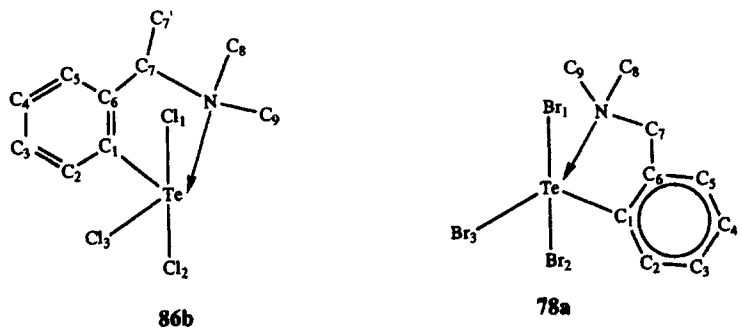

86b 78a

Figure 16. Drawings of **86b** and **78a** with non-hydrogen-atom labeling.

There is an intermolecular contact (3.337 Å) between Te and Cl′ of another molecule of the asymmetric unit in the structure[63] of **82c**. This distance is within the sum of the van der Waals radii. If this contact is considered significant, then the coordination about Te is pseudooctahedral with a lone pair occupying the

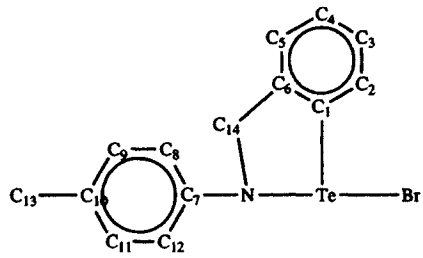

Figure 17. Drawings of **83** with non-hydrogen-atom labeling.

fourth equatorial site. There is no interaction between Te and N (4.380 Å), and the $NHMe_2$ group is bent away from the central tellurium atom. Thus, the effect of protonation of nitrogen is to remove the possibility of its coordination to Te, and hence Te forms a long intermolecular contact with Cl′.

C. NMR Data

The ^{125}Te NMR spectrum[60] of **83** has been measured in $CDCl_3$, relative to Me_2Te. Two signals were observed, at 1511 and 1407 ppm. It is probable that these signals correspond to two structural forms present in solution, one with Te—N coordination, as is seen in the solid-state structure, and one with no Te—N bond. This postulate was confirmed by variable-temperature ^1H NMR experiments.

XIII. INTRAMOLECULAR COORDINATION VIA AZO LINKAGES

A. Preparation of Compounds

The first compound[66] containing a Te—N intramolecular coordination to be structurally characterized was (2-phenylazophenyl-*C,N′*)tellurium chloride, **92**. The syntheses of these types of compounds are outlined in Scheme 40.

It is interesting to note that the formation of the mixed trihalide, **93**, is possible in this system, while in the oxatellurolylium halide system (Scheme 9) only mixtures of homohalides were isolated.

A subsequent paper[67] reported an alternate route to **91a**, which avoided the chloromercuro starting material, as shown in Scheme 41.

A number of derivatives of **92** obtained by metathesis reactions, as illustrated in Scheme 42, have been reported.[68,69]

The Te(IV) analogs of **98** have been isolated by the same route as shown in Scheme 43.

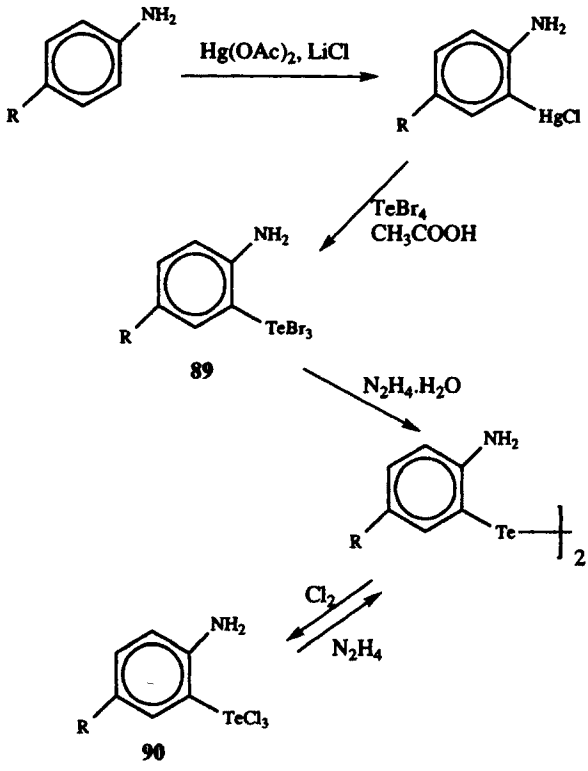

Scheme 39

B. Physical Data on Azo Compounds

X-ray crystal structures have been determined for five compounds of this general class. Figure 18 shows drawings with atom labeling for 2-(phenylazophenyl-*C*,*N*′)tellurium chloride (**92**),[66] 2-(phenylazophenyl-*C*,*N*′)tellurium acetate (**96**),[68] and 2-(phenylazophenyl-*C*,*N*′)tellurium thiocyanate (**97**).[68] Bond distances may be found in Table 23.

The coordination geometries in all three molecules shown are similar, with the ligands about Te in a trigonal bipyramidal coordination. In each case, the carbon ligand and two lone pairs occupy the equatorial positions, so that the molecules have a T-shaped configuration. The angles in each structure defined by N2, Te, and the atoms *trans* to N2 (Cl, Ol, or S1) are less than the ideal 180°, because the axial ligands are bent away from the lone pairs. The N2—Te—C angles are less than 90°, due to the constraints placed on the system by the five-membered ring. The Te—C distances of 2.04 Å (**92**), 2.074 Å (**96**), and 2.073 Å (**97**) are in good agreement with values for other single bonds between Te and an sp^2 carbon. The Te—Cl distance in **92** is slightly longer than a normal single bond because it is *trans* to the electronegative nitrogen. The Te—N distances

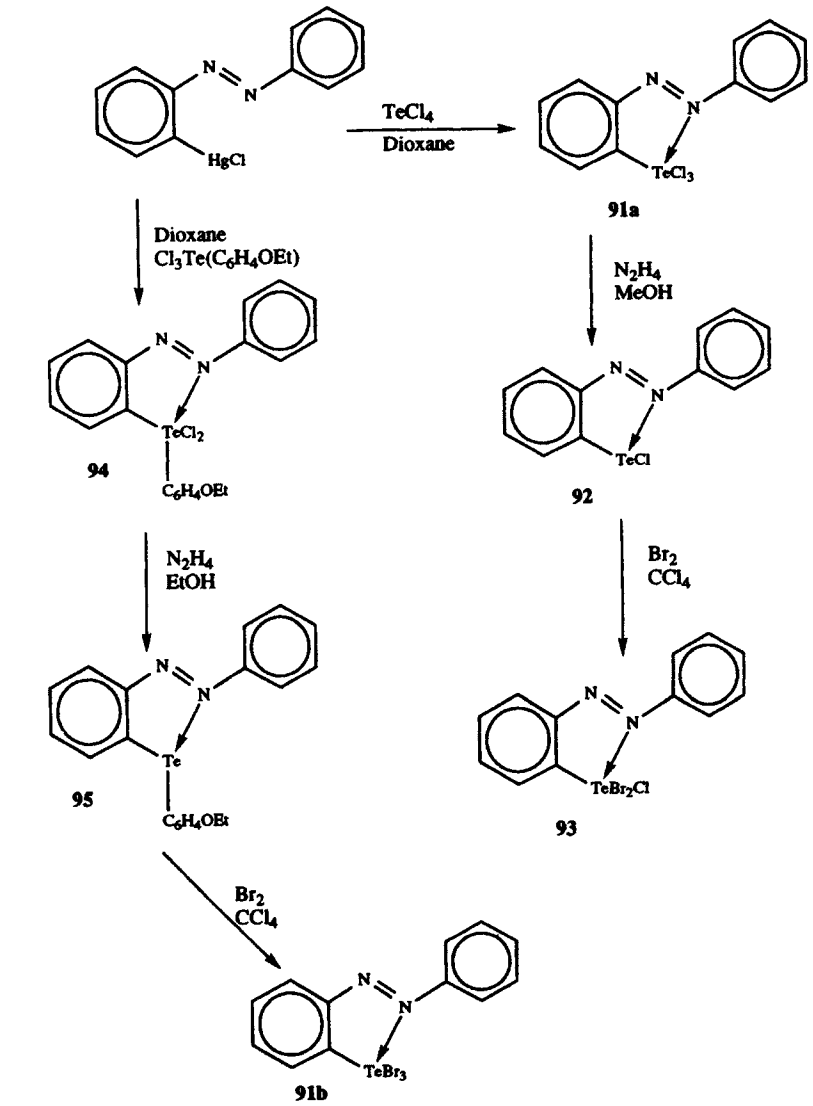

Scheme 40

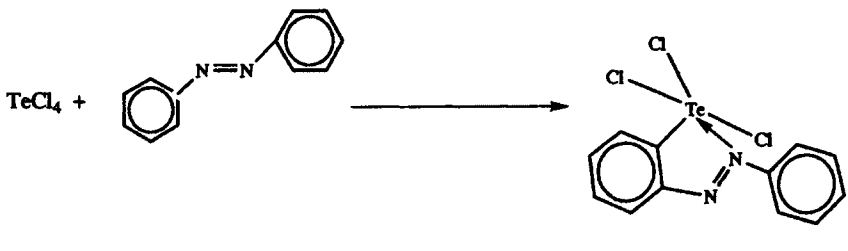

Scheme 41

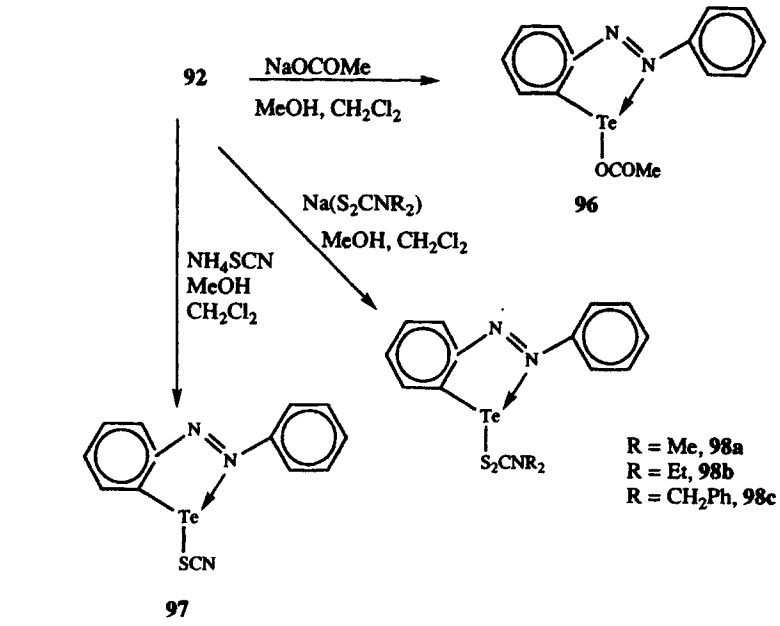

Scheme 42

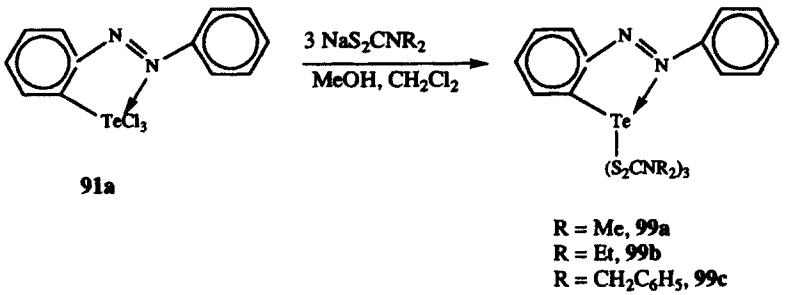

Scheme 43

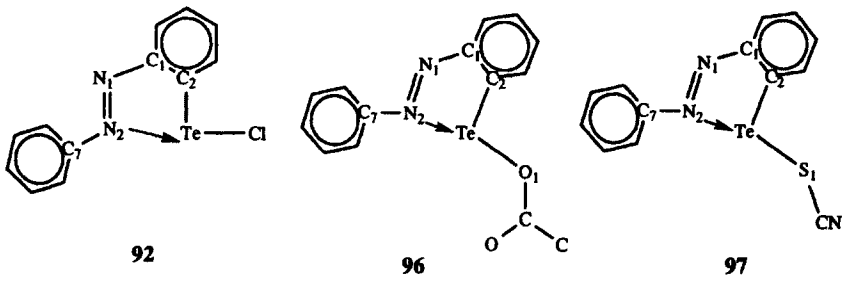

Figure 18. Drawings of 92, 96, and 97 with non-hydrogen-atom labeling.

in all three molecules are similar and are in agreement with the sum of the covalent radii for Te_{axial} and nitrogen, quoted as 2.24 Å.[67] In **92** the N1—N2, C6—N1, and C7—N2 distances are close to those observed[70] for azobenzene, where N—N is 1.243 (3) Å and C—N is 1.433 Å. However, in **96** and **97** the N1—N2 distances are longer than in free azobenzene. The N2—C7 distances are longer than the N1—C1 distances. The lengthening of the N1—N2 bond and shortening of the C1—N1 bond may indicate electron delocalization in the heterocyclic ring. There is a long secondary intramolecular contact of 2.953 (4) Å between Te and the carbonyl oxygen of the acetate ligand in **96**.

A drawing of 2-(phenylazophenyl-*C,N'*)tellurium dimethyldithiocarbamate (**98a**)[69] is shown in Figure 19, with relevant bond distances and angles listed in Table 24.

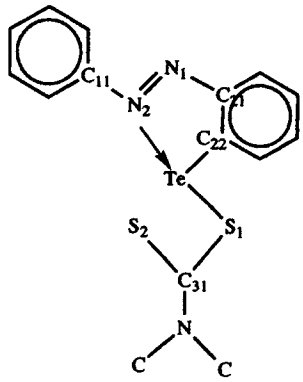

Figure 19. Drawing of **98a** with non-hydrogen-atom-labeling.

The structure of **98a** could also be considered as having a trigonal bipyramidal or T-shaped coordination about tellurium, with the carbon ligand and the two lone pairs forming the equatorial plane. N2 and S1 are the axial ligands, and a weak secondary interaction is present between S2 and Te. The Te—C1 distance is in good agreement with other Te—C(sp^2) single bonds. The Te—S1 bond is a long single bond, while the Te—S2 interaction is weak, resembling that observed in **58** (quin) (Table 14). The Te—N distance is longer than the sum of the covalent radii (2.07 Å), but is comparable to that seen in **91a**.

A drawing of the X-ray crystal structure of **91a**,[67] 2-(phenylazophenyl-*C,N'*)tellurium trichloride, is shown in Figure 20, with atom labels while the bond distances and angles are shown in Table 25.

The coordination about Te in this 12-Te-5 complex is octahedral with the axial sites occupied by Cl ligands and the fourth equatorial site by a lone pair of electrons. The Cl3—Te—N1 angle (165.2°) is distorted from the ideal octahedral angle of 180° as a result of the bending away of bonds from the lone pair. The C2—Te—N1 angle is constrained by the five-membered ring to 72.3°. As is generally observed, the Te—Cl_{axial} distances are longer than the Te—$Cl_{equatorial}$

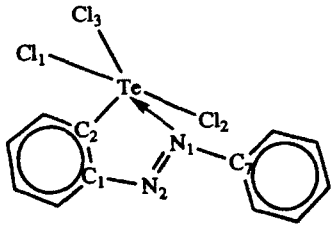

Figure 20. Drawing of **91a** with non-hydrogen-atom labeling.

distances. Te—N1 is long at 2.417 Å, but similar in length to the Te—N bond distances in **78a**, **98a** and **83**, among others described already. ^{125}Te NMR data are collected[69] in Table 26 for this class of compounds. The shift of the Te(II) monochloride, **92**, is downfield from that of the Te(IV) trichloride, **91a**.

Raman spectroscopy has been used[52] to investigate the Te—N interaction in these azo compounds, and $\nu_{(N=N)}$ shifts are listed in Table 27. The shorter Te—N bond distance in **92** is reflected in the move to higher energy of $\nu_{N=N}$ for **92** relative to **91a**.

C. Reactivity of Azo Compounds

Much of the reactivity of these molecules has been reported in Section XII.A, such as the reduction of the trihalides to monohalides and metathetical

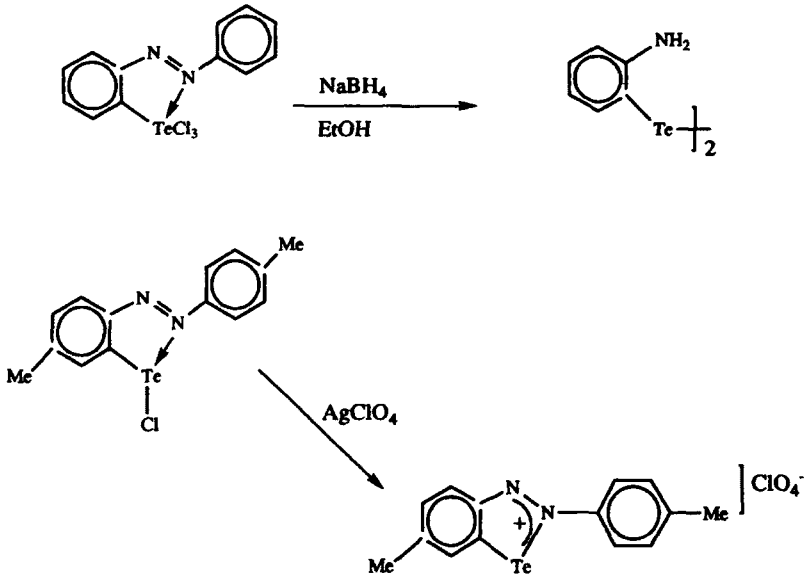

Scheme 44

reactions with alkali metal reagents. Two other reactions[61,71] are shown in Scheme 44.

XIV. INTRAMOLECULAR COORDINATION VIA SULFUR

Little documentation exists of compounds where tellurium is stabilized by intramolecular coordination to sulfur, but a crystal structure shows that there is evidence to suggest the existence of such a contact. This compound does not exhibit the strong intramolecular contact seen in the dioxatellurapentalenes or the phenylazo derivatives, but does suggest that this class of compounds should be explored further.

The X-ray crystal structure[72] of 2-(phenylthiophenyl)tellurium trichloride, **100**, has been determined and shows a long Te—S intramolecular contact. A drawing of **100** is shown in Figure 21, and bond distances and angles may be found in Table 28.

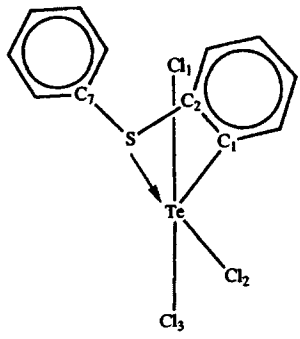

100

Figure 21. Drawing of **100** with non-hydrogen-atom labeling.

The coordination sphere about tellurium is that of a distorted octahedron, if the lone pair of electrons is considered as occupying the fourth equatorial site, with the others taken up by S, Cl2, and Cl. The Te—Cl distance is that of a single bond. The axial Te—Cl bonds are again longer than Te—Cl2. The Te—S contact of 2.972 Å is much longer than the sum of the covalent radii, but is still within the limits of a van der Waals interaction.

XV. OTHER HYPERVALENT COMPOUNDS

Two classic telluranes, one 12-Te-6 and the other 10-Te-4 have been reported by Martin.[73] The preparation of the 10-Te-4 telluranes is outlined in Scheme 45.

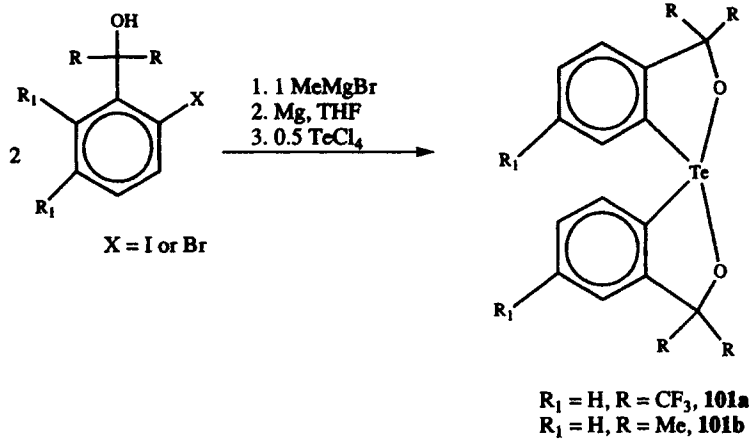

R_1 = H, R = CF_3, **101a**
R_1 = H, R = Me, **101b**

Scheme 45

By a similar procedure, employing *sec*Bu-Li and TMEDA in place of the Grignard reagent, **101c**, where R′ = ^{t}Bu and R = CF_3, may be isolated. Structures of **101a** and **102**, the *cis*-12-Te-6 pertellurane formed by the isomerization of the *trans*-1,1-difluoro-1,1-dihydro-3,3,3′,3′-tetramethyl-1,1′-spirobi[3*H*-2,1-benzoxatellurole], have been determined. The isomerization of the *trans*-12-Te-6 compound (*trans*-**102**) to give *cis*-**102** is acid-catalyzed and postulated to proceed via dissociation of fluoride to give the 10-Te-5 pertelluronium cation, by analogy with the corresponding sulfur system, where the intermediate cation has been isolated.[73] The cation presumably then recombines with fluoride to give *cis*-**102** (or in a degenerate manner to yield *trans*-**102**). This isomerization is also effected by heating a solution of *trans*-**102** at 60°C for 3 days. The thermal isomerization is thought to occur by a intramolecular ligand rearrangement, rather than via a dissociative mechanism. Drawings of the structures of **101a** and *cis*-**102** are shown in Figure 22, and bond distances and angles are given in Table 29.

The structure of **101a** is trigonal bipyramidal about tellurium, with the third equatorial site occupied by a lone pair of electrons. The O—Te—O1 angle of 160.53°, deviating from the ideal value of 180°, is due to bending away of the bonds from the lone pair. The Te—O and Te—C bond distances are normal single bond distances. The structure of the 12-Te-6 compound, *cis*-**102**, is octahedral about tellurium. The angles are all close to ideal values, and bond distances are normal.

A new class of hypervalent tellurium compounds has been documented quite recently. When acetic anhydride is reacted[74] with 12-oxo-5*H*,7*H*-dibenzo-[*b*,*g*][1,5]tellurathiocin as shown in Scheme 46, the product is a 12,12-diacetoxytellurane. The trifluoroacetoxy derivative is prepared in an analogous reaction.

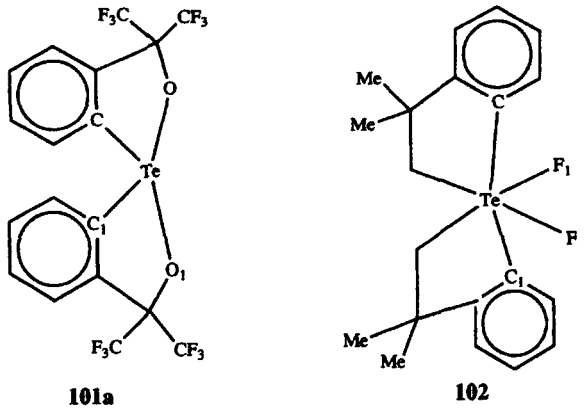

101a **102**

Figure 22. Drawings of **101a** and *cis*-**102** with non-hydrogen-atom labeling.

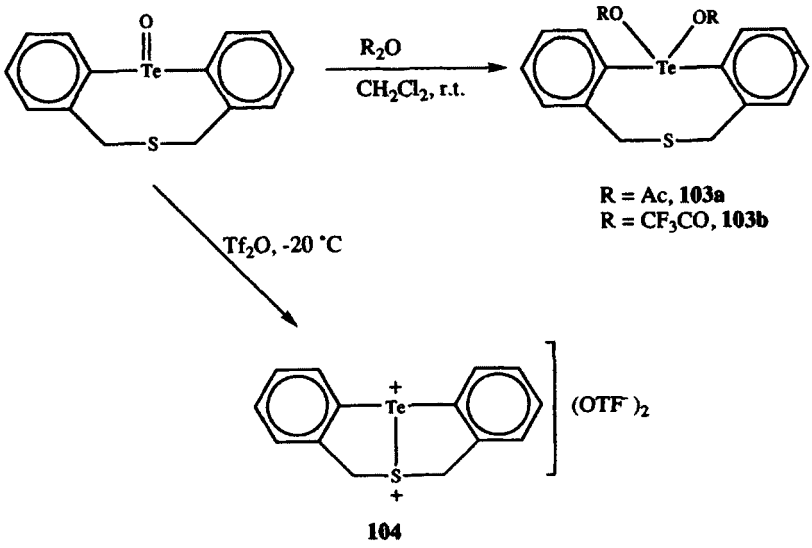

104

Scheme 46

Compound **103a**, on heating in benzene, yields 60% of 5*H*,7*H*-dibenzo[*b*,*g*][1,5]tellurathiocin and 23% of the product where one CH_2 adjacent to S in **103a** bears an acetoxy group. Conversely, **103b** is very stable under reflux conditions and does not yield analogous products.

5*H*,7*H*-Dibenzo[*b*,*g*][1,5]ditellurocin and the analog where one Te is replaced by Se have been prepared and characterized by multinuclear NMR spectroscopy.[75] The routes to these compounds are shown in Scheme 47.

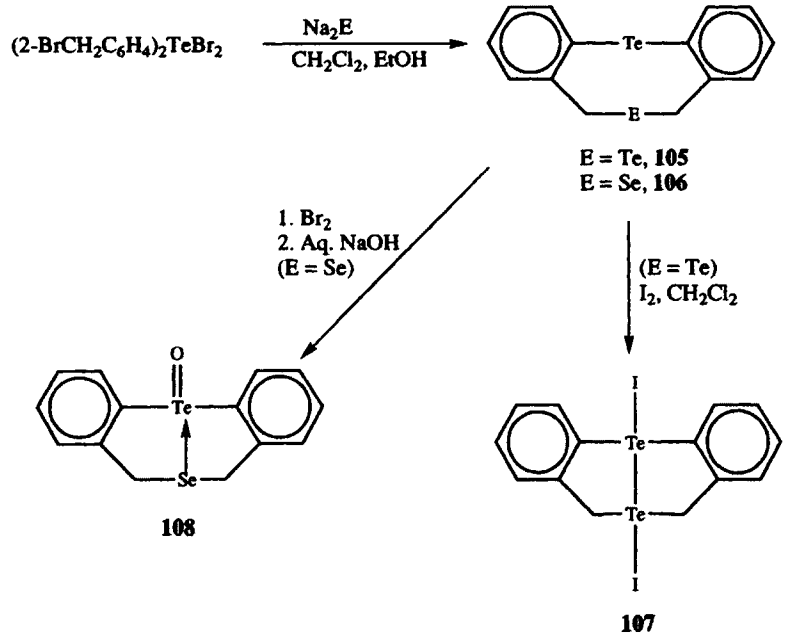

Scheme 47

The reaction of **106** with bromine alone yielded the bromo compound analogous to **107**, but the structure could not be assigned unambiguously by ^{125}Te and ^{77}Se NMR.

The ^{125}Te NMR resonances for this class of compounds are shown in Table 30. The ^{125}Te NMR spectrum of **107** showed two peaks, at 602 and 946 ppm. The peak at 946 is assigned to $PhCH_2$*Te* and the peak at 602 is due to Ph*Te*. A large ^{125}Te—^{125}Te coupling of 1285 Hz is observed, providing strong evidence for the presence of a Te—Te bond. The ^{125}Te spectra of **105** and **106** show the presence in solution of both the chair and boat conformers. Four peaks are present in the spectrum of **105**, two each for the two different tellurium environments in the boat and chair forms. Two peaks are present in the spectrum of **106**, due to the two conformers present in solution. In each pair of resonances the downfield peak is due to $PhCH_2$*Te*.

Compound **109** is a stable compound that exists in solution only in the boat form, as evidenced by variable temperature ^{1}H NMR spectra. Evidence for the intramolecular Se—Te interaction is provided by the ^{77}Se NMR, which showed J_{Se-Te} of 467 Hz.

The same workers have also prepared[76] a diiododitellurane and its dimer by the route shown in Scheme 48.

The ^{125}Te NMR spectrum of **109a** has one peak, at 706 ppm (vs. Me_2Te), and the ^{13}C NMR spectrum has two peaks, confirming the structure as drawn in

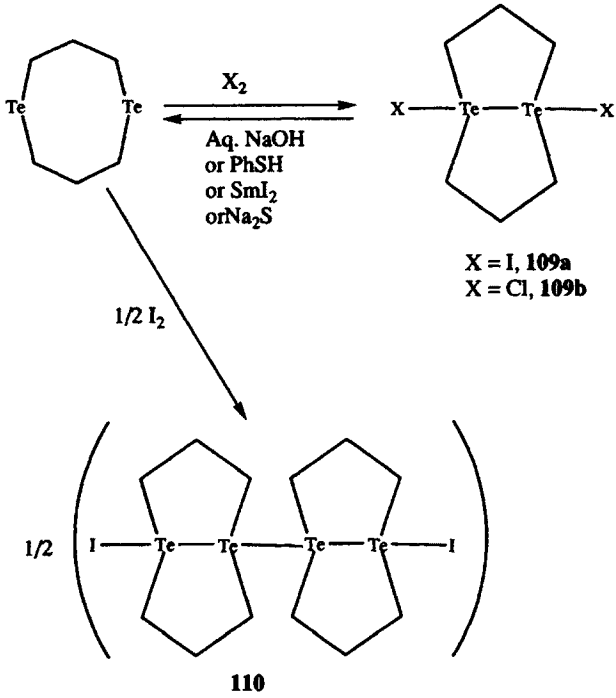

Scheme 48

Scheme 48. The ^{125}Te NMR spectrum of **109b** has a peak at 1008 ppm, and the ^{13}C spectrum again has two peaks. The ^{125}Te NMR spectrum of **110** exhibits two peaks, at 509 and 697 ppm, and the ^{13}C NMR spectrum has three peaks, as it should have if the structure is as drawn in Scheme 48.

TABLES

TABLE 1. BOND DISTANCES (Å) IN **4** AND **6a**

Bond	**4**	**6a**
Te—C3	2.043 (5)	2.11 (1)
Te—O1	2.142 (4)	2.171 (9)
Te—O2	2.130 (4)	2.135 (9)
C1—O1	1.312 (6)	1.27 (1)
C5—O2	1.316 (7)	1.33 (1)
C1—C2	1.390 (7)	1.42 (2)
C2—C3	1.394 (7)	1.42 (2)
C3—C4	1.395 (7)	1.29 (2)
C4—C5	1.404 (7)	1.43 (2)
Te—Br1		2.620 (2)
Te—Br2		2.668 (2)
Te—Br'		3.555 (2)

TABLE 2. XPS STUDY OF DIOXATELLURAPENTALENES

	Binding Energy (eV)	
Compd.	Te ($3d_{5/2}$)	O ($1s$)
4	574.0	531.9
8a	574.5	531.9
8j	574.6	

TABLE 3. ^{125}Te NMR SHIFTS FOR DIOXATELLURAPENTALENES AND PERTELLURANES

Compd.	^{125}Te Shift (ppm)
4	+ 1955
8a	+ 1967
8j	+ 1961
6b	+ 1444
11	+ 1459
H_2TeCl_6	+ 1403[18]
Ph_2Te	+ 688[18]
Me_2Te	0.0[18]

TABLE 4. BOND DISTANCES (Å) AND ANGLES (°) IN **12b** AND **18a**[a]

12b		**18a**	
Te—C7	2.081 (3), 2.080 (3)	Te—C3	2.175 (7)
Te—Cl	2.483 (1), 2.470 (1)	Te—Br1	2.513 (1)
Te—O	2.206 (2), 2.175 (2)	Te—Br2	2.661 (1)
C9—O	1.270, 1.269	Te—Br3	2.659 (1)
C7—C8	1.363, 1.344	Te—O	2.362 (6)
C8—C9	1.419, 1.433	C1—O	1.26 (1)
Cl—Te—O	169.21, 170.97	C2—C3	1.33 (1)
C7—Te—O	76.37, 76.73	C1—C2	1.47 (1)
		C1—O—Te	95.0 (2)

[a] *Note*: Estimated standard deviations (ESDs) were not reported individually for all distances and angles in **12b**, but the average ESDs may be found in reference 19.

TABLE 5. CARBONYL STRETCHING FREQUENCIES OF THE OXATELLUROLYLIUM HALIDES

Compd.	$\nu_{C=O}$ (cm^{-1})	Compd.	$\nu_{C=O}$ (cm^{-1})
12a	1520	**12e**	1530
12b	1530	**12a** (Br)	1540
12c	1532	**13a**	1520
12d	1528	**13a** (Br)	1525
12f	1530	**13b**	1530
12i	1522	**13b** (Br)	1530
14	1535	**15a**	1540
15b	1525	**15c**	1540
16	1540	**17a**	1530
17b	1520	**17c**	1532
18a	1595	**18b**	1595
18c	1590	**18d**	1590
18e	1590	**18f**	1590

TABLE 6. BINDING ENERGIES FOR OXATELLUROLYLIUM HALIDES

Compd.	Te ($3d_{5/2}$) (eV)	O (1*s*) (eV)
13b	574.2	531.9
12a	574.2	531.8
12i	574.3	531.8
16	574.5	531.9
12i (Br)	574.3	532.0
15a	574.0	531.7
18e	576.6	531.9
18b	576.5	531.8
18f	576.4	531.9

TABLE 7. ^{125}Te NMR SHIFTS FOR OXATELLUROLYLIUM HALIDES

Compd.	NMR Shift (ppm)
13b	+ 1726
12a	+ 1697
12i	+ 1692
16	+ 1672
12i (Br)	+ 1650
15a	+ 1501
18e	+ 1365
18b	+ 1359
18f	+ 1386

TABLE 8. BOND DISTANCES (Å) AND ANGLES (°) FOR **19** AND **20**

19		**20**	
C2—O	1.457 (4)	C7—O	1.52 (5)
Te—Cl1	2.505 (1)	Te—Br1	2.653 (8)
Te—Cl2	2.355 (1)	Te—Br2	2.665 (9)
Te—Cl3	2.481 (1)	Te—Br3	2.502 (9)
Te—C1	2.172 (3)	Te—C1	2.29 (4)
C1—C2	1.521 (5)	C1—C7	1.53 (6)
C5—C6	1.310 (7)		
Te—O	2.419 (2)	Te—O1	2.49 (3)
Cl1—Te—Cl3	176.24 (4)	Br1—Te—Br2	172.9 (3)
Cl1—Te—Cl2	91.51 (4)	Br1—Te—Br3	94.7 (3)
Cl1—Te—C1	90.36		

TABLE 9. BOND DISTANCES (Å) AND ANGLES (°) IN **24b**, **30a**, AND **29a**

Bond Length (Å) Bond Angle (°)	**24b**, X = Br R = H	**30a**, X = Cl R = NHMe	**29b**, X = Br R = NH_2
Te—X	2.618 (03)	2.516 (3)	2.646 (1)
C7—O	1.283 (26)	1.28 (2)	1.27 (1)
Te—C2	2.081 (21)	2.133 (10)	2.105 (9)
C1—C7	1.440 (29)	1.58 (2)	1.48 (1)
Te—O	2.31	2.250 (7)	2.237 (8)
C2—Te—X	94.2 (6)	92.7 (3)	95.1 (2)
C2—Te—O	74.4 (7)	78.5 (4)	75.6 (2)
X—Te—O		168.6 (3)	170.7 (2)

TABLE 10. CARBONYL BANDS IN IR SPECTRA OF ORTHOTELLURATED BENZALDEHYDE DERIVATIVES

Compd.	Wavenumber (cm^{-1})	Compd.	Wavenumber (cm^{-1})
24a	1585	**24f**	1698
32a	1660	**28c**	1700
40a	1640	**35b**	1638
40b	1630	**41a**	1520
42c	1625	**41b**	1520
44a	1650	**43a**	1500
		45	1570

TABLE 11. BOND DISTANCES (Å) AND ANGLES (°) IN **54**

Distance	(Å)	Angle	(°)
Te—C1	2.129 (3)	Cl2—Te—Cl1	171.28 (4)
Te—N	2.402 (3)	C1—Te—Cl3	88.4 (1)
Te—O2	2.878 (3)	Cl1—Te—N	85.00 (7)
Te—Cl3	2.438 (2)	C1—Te—N	75.1 (1)
Te—Cl1	2.500 (1)	O2—Te—Cl3	135.56 (6)
Te—Cl2	2.491 (1)	N—Te—Cl3	163.37

TABLE 12. BOND DISTANCES (Å) AND ANGLES (°) OF **56a**

Distance	(Å)	Angle	(°)
Te—Br1	2.673 (3)	Br1—Te—Br2	172.4 (1)
Te—Br2	2.658 (3)	Br1—Te—Br3	93.5 (2)
Te—Br3	2.589 (3)	Br2—Te—Br3	92.8 (1)
Te—C1	2.110 (19)	Br3—Te—C1	92.5 (6)
Te—N1	2.244 (14)	Br1—Te—N1	88.4 (4)
		C1—Te—N1	78.2 (7)
		N1—Te—Br3	170.4 (4)

TABLE 13. BOND DISTANCES (Å) AND ANGLES (°) IN **57a**, **58**, AND **55**[a]

	57	**58**	**55**
Te—X1	2.707 (11)	2.518 (1)	2.144 (6)
Te—C1	2.111 (6)	2.111 (5)	2.138 (6)
Te—N1	2.236 (11)	2.354 (4)	2.695 (4)
X1—Te—C1	93.6 (5)	95.0 (1)	94.8 (2)
C1—Te—N1	75.9 (5)	74.4 (2)	
N1—Te—X1	169.2 (2)	167.6 (1)	

[a] *Note*: X1 = Br1 (**57**), S1 (**58**), C12 (**55**).

TABLE 14. BOND DISTANCES (Å) AND ANGLES (°) IN **58** (QUIN.)

Distance	(Å)	Angle	(°)
Te—C1	2.124 (5)	S1—Te—C1	90.3 (1)
	2.135 (4)		89.0 (1)
Te—N1	2.365 (4)	N1—Te—C1	74.5 (1)
	2.385 (4)		74.0 (1)
Te—S1	2.569 (1)	N1—Te—S1	163.7 (1)
	2.543 (1)		162.8 (1)
Te—S	3.222 (1)		
	3.230 (1)		

TABLE 15. $\nu_{C=N}$ BANDS FOR **63**, **64**, AND **65**

Compound	(cm^{-1})
63	1624
64	1600
4-$MeOC_6H_5$–CH=NPh	1634

TABLE 16. BOND DISTANCES (Å) AND ANGLES (°) IN **67b** AND **76**[a]

	67b	**76**
Te—X	2.582 (2) 2.553 (2)	2.160 (8)
Te—C1	2.107 (7) 2.088 (7)	2.087 (7)
Te—N	2.218 (6) 2.239 (6)	2.297 (7)
C6—C7	1.44 (1) 1.44 (1)	1.434 (13)
C7—N	1.285 (9) 1.300 (9)	1.291 (9)
N—Te—C1	77.0 76.7	75.8 (3)
C1—Te—X	91.7 91.3	84.1 (3)
N—Te—X	168.7 168.0	159.9 (2)

[a] *Note*: X = Cl (**67b**); X = O1 (**76**).

TABLE 17. BOND DISTANCES (Å) AND ANGLES (°) IN **71k** AND **71j**

	71k		**71j**
Te—C15	2.162 (4)	Te—C11	2.163 (2)
Te—C1	2.128 (4)	Te—C1	2.125 (2)
Te—N1	2.702 (3)	Te—N1	2.720 (2)
C6—C7	1.462 (6)	C6—C7	1.462 (3)
		C7—N1	1.270 (3)
C15—Te—N1	165.9	C11—Te—N1	164.7 (6)
C15—Te—C1	96.3	C11—Te—C1	93.5 (7)

TABLE 18. BOND DISTANCES (Å) AND ANGLES (°) IN **70** AND **74a**

	70		**74a**
Te—C1	2.120 (5)	Te—O1	2.129 (2)
Te—C14	2.137 (6)	Te—O2	2.100 (2)
Te—C15	2.147 (5)	Te—C27	2.100 (3)
Te—N	2.750 (4)	Te—C28	2.092 (3)
N—Te—C14	164.9	Te—N1	2.923 (3)
N—Te—C1	71.1	Te—N2	2.962 (3)
C14—Te—C1	96.4	N1—C7	1.269 (3)
C14—Te—C15	92.5	N2—C20	1.269 (3)
C15—Te—N	81.1	O1—Te—O2	164.9 (1)
		O1—Te—C27	85.3 (1)
		C27—Te—C28	96.9 (2)
		N1—Te—O1	64.8(2)
		N1—Te—O2	128.0 (2)
		N2—Te—C27	141.3 (2)
		N1—Te—C28	146.6 (2)

TABLE 19. BOND DISTANCES (Å) AND ANGLES (°) IN **73**

Te—N	2.773
Te—C5	2.111 (8)
Te—C4	2.181 (10)
N1—C11	1.273 (11)
C4—Te—C5	95.2 (4)

TABLE 20. ^{125}Te NMR SHIFTS OF AZOMETHINE COMPOUNDS

Compd.	^{125}Te (ppm)	J (^{125}Te–^{15}N) (Hz)
66a	+ 483.0	101.4
66c	+ 484.8	102.0
69a	+ 1027.0	135.3
69c	+ 1036.0	141.4
67a	+ 1355.0	
67j	+ 1316.0	
67k	+ 1187.0	
70	+ 641.5	62.4
71a	+ 600.0	61.0
72b	+ 636.0	122.0
74a	+ 1056.0, 1076.0	
74b	+ 1100.0	
74c	+ 1100, 1052	
75	+ 1634.8 1633.5	

TABLE 21. BOND DISTANCES (Å) AND ANGLES (°) OF **86b** AND **78a**

	86b (X = Cl)	**78a** (X = Br)
Te—X1	2.538 (4)	2.758 (2)
Te—X2	2.465 (4)	2.633 (3)
Te—X3	2.447 (3)	2.632 (2)
Te—N	2.406 (8)	2.42 (1)
Te—C1	2.078 (10)	2.12 (1)
N—C7	1.495 (17)	1.48 (2)
N—C8	1.485 (18)	1.51 (2)
N—C9	1.511 (12)	1.46 (2)
X1—Te—X2	175.4 (1)	178.7 (1)
X2—Te—X3	88.2 (1)	91.3 (1)
X3—Te—N	166.8 (2)	167.4 (3)
C1—Te—N	75.3 (3)	76.1 (5)
X3—Te—C1	92.6 (3)	92.4 (4)

TABLE 22. BOND DISTANCES (Å) AND ANGLES (°) IN **83**

Distance	(Å)	Angle	(°)
Te—Br	2.633 (3)	Br—Te—N	165.3 (3)
Te—C1	2.125 (16)	Br—Te—C1	91.5 (4)
Te—N	2.375 (13)	N—Te—C1	74.9 (5)
N—C7	1.457 (20)		
N—C14	1.495 (18)		

TABLE 23. BOND DISTANCES (Å) AND ANGLES (°) OF **92**, **96**, AND **97**

	92 (X = Cl)	**96** (X = O1)	**97** (X = S1)
Te—X	2.552 (8)	2.167 (4)	2.672 (1)
Te—C2	2.04 (2)	2.074 (4)	2.073 (4)
Te—N2	2.23 (2)	2.260 (4)	2.243 (3)
N1—N2	1.25 (2)	1.270 (5)	1.270 (5)
C1—N1	1.43 (3)	1.387 (7)	1.379 (6)
C7—N2	1.45 (3)	1.420 (6)	1.436 (6)
N2—Te—X	166.6	159.0 (1)	166.8 (1)
N2—Te—C2	72.8	73.9 (2)	74.2 (2)
C2—Te—X		85.3 (2)	92.6 (1)

TABLE 24. BOND DISTANCES (Å) AND ANGLES (°) IN **98a**

Distance	(Å)	Angle	(°)
Te—S1	2.568 (2)	N2—Te—C22	72.5 (3)
Te—S2	3.225 (3)	S2—TE—S1	60.9 (1)
Te—N2	2.340 (7)	N2—Te—S2	136.3 (2)
Te—C22	2.101 (8)	S1—Te—C22	89.8 (2)
C21—N1	1.384 (10)		
N1—N2	1.265 (9)		
N2—C11	1.396 (10)		

TABLE 25. BOND DISTANCES (Å) AND ANGLES (°) IN **91a**

Distance	(Å)	Angle	(°)
Te—Cl1	2.483 (1)	Cl3—Te—Cl2	92.3 (1)
Te—Cl2	2.491 (1)	Cl3—Te—N1	165.2 (1)
Te—Cl3	2.406 (2)	C2—Te—N1	72.3 (2)
Te—N1	2.417 (4)	Cl1—Te—Cl2	171.7 (1)
Te—C2	2.114 (5)		
C1—N2	1.423 (7)		
N2—N1	1.255 (6)		
N1—C7	1.431 (7)		

TABLE 26. ^{125}Te NMR SHIFTS FOR AZO COMPOUNDS

92	1486.5
91a	1278.2
98a	1228.6
99a	1225.4
98c	1239.1
98	1239.6

TABLE 27. RAMAN SHIFTS (ppm) FOR AZO COMPOUNDS

Azobenzene	1433
91a	1410
92	1375

TABLE 28. BOND DISTANCES (Å) AND ANGLES (°) IN **100**

Distance	(Å)	Angle	(°)
Te—C1	2.108 (4)	Cl1—Te—Cl3	174.97 (4)
Te—Cl1	2.477 (2)	Cl2—Te—S	154.01 (3)
Te—Cl2	2.324 (1)	C1—Te—Cl2	94.1 (1)
Te—Cl3	2.497 (1)		
Te—S	2.972 (1)		
S—C2	1.765 (4)		
S—C7	1.779 (5)		

TABLE 29. BOND DISTANCES (Å) AND ANGLES IN **101a** AND *cis*-**102**

	101a		***cis*-102**
Te—O	2.077 (2)	Te—F	1.942 (2)
Te—O1	2.082 (2)	Te—F1	1.937 (2)
Te—C	2.106 (2)	Te—O	1.939 (2)
Te—C1	2.103 (2)	Te—O1	1.943
O—Te—O1	160.53 (7)	Te—C	2.078 (3)
C—Te—C1	104.58 (10)	Te—C1	2.073 (3)
		F—Te—F1	84.50 (9)
		O—Te—O1	96.91 (9)
		C—Te—C1	172.7 (1)
		F—Te—O	172.28 (9)
		F—Te—O1	89.45 (9)

TABLE 30. ^{125}Te NMR SHIFTS (ppm) FOR **104–108**[a]

104	1111
105	553, 565
	677, 703
106	559, 581
107	602, 946
108	1159

[a] Peaks are referenced to Me_2Te.

REFERENCES

1. Perkins, C. W.; Martin, J. C.; Arduengo, A. J.; Lau, W.; Alegria, A.; Kochi, J. K. *J. Am. Chem. S*
1980, *102*, 7753.
2. Perrier, M; Vialle, J. *Bull. Soc. Chim. Fr.* **1971**, 4591.
3. Perrier, M; Pinel, R.; Vialle, J. *J. Heterocyclic Chem.* **1975**, *12*, 639.
4. Perrier, M.; Vialle, J. *Bull. Soc. Chim. Fr.* **1979**, II-199.
5. Beer, R. J. S.; Hatton, J. R.; Llaguno, E. C.; Paul, I. C. *Chem. Commun.* **1971**, 594.
6. King, F. E.; Felton, D. G. I. *J. Chem. Soc.* **1949**, 274.
7. Perrier, M.; Vialle, J. *Bull. Soc. Chim. Fr.* **1979**, II-205.
8. Detty, M. R.; Luss, H. R. *J. Org. Chem.* **1983**, *48*, 5149.
9. Detty, M. R.; Perlstein, J. *Organometallics* **1987**, *6*, 1597.
10. Pauling, L. *The Nature of the Chemical Bond*, Cornell University Press, Ithaca, NY, 1960.
11. Knobler, C.; McCullough, J. D. *Inorg. Chem.* **1977**, *16*, 612.
12. Gillespie, R. J. *J. Chem. Educ.* **1970**, *47*, 18.
13. Cotton, F. A.; Wilkinson, G. *Advanced Inorganic Chemistry*, 5th edn., Wiley-Interscien
New York, 1988.
14. Foss, O. *Pure Appl. Chem.* **1970**, 31.
15. Detty, M. R.; Lenhart, W. C.; Gassman, P. G.; Callstrom, M. R. *Organometallics* **1989**, *8*, 8
16. Detty, M. R.; Lenhart, W. C.; Gassman, P. G.; Callstrom, M. R. *Organometallics* **1989**, *8*, 8
17. Detty, M. R.; Murray, B. J.; Smith, D. L.; Zumbulyadis, N. *J. Am. Chem. Soc.* **1983**, *105*, 87
18. McFarlane, H. C. E.; McFarlane, W. *NMR of Newly Accessible Nuclei*, Laszlo, P., ed., Acade
Press, New York, 1983, Vol. 2.
19. Detty, M. R.; Murray, B. J.; *J. Am. Chem. Soc.* **1983**, *105*, 883.
20. Detty, M. R.; *Organometallics* **1988**, *7*, 2188.
21. Detty, M. R.; Luss, H. R.; McKelvey, J. M.; Geer, S. M. *J. Org. Chem.* **1986**, *51*, 1692.
22. Bergman, J.; Engman, L. *J. Organomet. Chem.* **1979**, *181*, 335.
23. Cameron, T. S.; Amero, R. B.; Chan, C.; Cordes, R. E. *Cryst. Struct. Commun.* **1980**, *9*, 543.
24. Castellano, E. E.; Zukeman-Schrector, J.; Ferreira, J. T. B.; Comassetto, J. V. *Acta Cryst.* **19**
C42, 44.
25. Bakshi, P. K.; Cameron, T. S.; Sabir Ali, M. E.; Azad Malik, M. A.; Smith, B. C. *Inorgani*
Chimica Acta **1993**, *204*, 27.
26. Sabir Ali, M. E.; Azad Malik, M.; Smith, B. C. *Inorganica Chimica Acta* **1989**, *162*, 157.
27. Husebye, S.; Meyers, E. A.; Zingaro, R. A.; Comasseto, J. V.; Petragnani, N. *Acta Cryst.* **19**
C43, 1147.
28. Gysling, H. J.; Luss, H. R.; Gardner, S. A. *J. Organomet. Chem.* **1980**, *184*, 417.
29. Piette, J.-L.; Renson, M. *Bull. Soc. Chim. Belges* **1971**, *80*, 669.
30. Piette, J.-L.; Lysy, R.; Renson, M. *Bull. Soc. Chim. Fr.* **1972**, 3559.
31. Piette, J.-L.; Pardon, M. C.; Weber, R.; Baiwir, M.; Llabres, G. *Bull. Soc. Chim. Belges* **19**
95, 247.
32. Piette, J.-L.; Talbot. J. M.; Genard, J. C.; Renson, M. *Bull. Soc. Chim. Fr.* **1973**, 2468.
33. Piette, J.-L.; Thibaut, P.; Renson, M. *Tetrahedron* **1978**, *34*, 655.
34. Dereu, N.; Piette, J.-L. *Bull. Soc. Chim. Fr.* **1979**, II-623.
35. Abid, K. Y.; Al-Salim, N.; Greaves, M.; McWhinnie, W. R.; West, A. A.; Hamor, T. A. *J. Ch*
Soc. Dalton Trans. **1989**, 1697.
36. Baiwir, M.; Llabres, G.; Diderberg. O.; Dupont, L.; Piette, J.-L. *Acta Cryst.* **1974**, *B30*, 139.

37. Dupont, L.; Diderberg, O.; Lamotte, J.; Piette, J. L. *Acta Cryst.* **1979**, *B35*, 849.
38. Lamotte, J.; Campsteyn, H.; Dupont, L.; Vermeire, M. *Cryst. Struct. Commun.* **1977**, *6*, 749.
39. Huang, C.-K.; O'Brien, D. H.; Irgolic, K. J.; Meyers, E. A. *Cryst. Struct. Commun.* **1982**, *11*, 1593.
40. Zukerman-Schpector, J.; Castellano, E. E.; Comasseto, J. V.; Stefani, H. A. *Acta Cryst.* **1988**, *C44*, 2182.
41. Talbot, J.-M.; Piette, J.-L.; Renson, M. *Bull. Soc. Fr.* **1976**, 294.
42. Weber, R.; Piette, J. L.; Renson, M. *J. Heterocyclic Chem.* **1978**, *15*, 865.
43. Wiriyachitra, P.; Falcone, J. J.; Cava, M. P. *J. Org. Chem.* **1979**, *44*, 3957.
44. Gunther, W. H. H.; Lok, R. U.S. Patent 4607000, 1986; *Chem. Abstr.* **1986**, *105*, 235722.
45. Przyklek-Elling, R.; Gunther, W. H. H.; Lok, R. U.S. Patent 4661438, 1987; *Chem. Abstr.* **1987**, *106*, 76046.
46. Gunther, W. H. H. U.S. Patent 4599410, 1986; *Chem. Abstr.* **1987**, *106*, 86230.
47. Hamor, T. A.; Al-Salim, N.; West, A. A.; McWhinnie, W. R. *J. Organomet. Chem.* **1986**, *310*, C5.
48. Al-Salim, N.; West, A. A.; McWhinnie, W. R.; Hamor, T. A. *J. Chem. Soc., Dalton Trans.* **1988**, 2363.
49. Singh, H. B.; Sudha, N. *J. Organomet. Chem.* **1990**, *397*, 153.
50. Greaves, M. R.; Hamor, T. A.; Howlin, B. J.; Lobana, T. S.; Mbogo, S. A.; McWhinnie, W. R.; Povey, D. C. *J. Organomet. Chem.* **1991**, *420*, 327.
51. West, A. A.; McWhinnie, W. R.; Hamor, T. A. *J. Organomet. Chem.* **1988**, *356*, 159.
52. Greaves, M. R.; McWhinnie, W. R.; McWhinnie, S. L. W.; Waters, D. N. *J. Organomet. Chem.* **1992**, *430*, 37.
53. Singh, H. B.; McWhinnie, W. R. *J. Chem. Soc., Dalton Trans.* **1985**, 821.
54. Maksimenko, A. A.; Maslakov, A. G.; Mehrotra, G. K.; Abakarov, G. M.; Sadekov, I. D.; Minkin, V. I. *Zh. Obsch. Khim.* **1988**, *58*, 1176 (trans. ed. **1988**, *58*, 1046).
55. Minkin, V. I.; Sadekov, I. D.; Maksimenko, A. A.; Kompan, O. E.; Struchkov, Y. I. *J. Organomet. Chem.* **1991**, *402*, 331.
56. Minkin, V. I.; Sadekov, I. D.; Maksimenko, A. A.; Maslakov, A. G.; Mehrotra, G. K.; Fedotov, M. A. *Zh. Obsch. Khim.* **1988**, *58*, 1684 (trans. ed. **1988**, *58*, 1503).
57. Al-Salim, N.; Hamor, T. A.; McWhinnie, W. R. *J. Chem. Soc., Chem. Commun.* **1986**, 453.
58. Sadekov, I. D.; Maksimenko, A. A.; Mehrotra, G. K.; Minkin, V. I. *Zh. Org. Khim.* **1987**, *23*, 657 (trans. ed. **1987**, *23*, 594).
59. Minkin, V. I.; Maksimenko, A. A.; Mehrotra, G. K.; Maslakov, A. G.; Kompan, O. E.; Sadekov, I. D.; Struchkov, Y. I.; Yufit, D. S. *J. Organomet. Chem.* **1988**, *348*, 63.
60. Maslakov, A. G.; McWhinnie, W. R.; Perry, M. C.; Shaikh, N.; McWhinnie, S. L. W.; Hamor, T. A. *J. Chem. Soc., Dalton Trans.* **1993**, 619.
61. Sadekov, I. D.; Maksimenko, A. A.; Abakarov, G. M.; Maslakov, A. G.; Minkin, V. I. *Khim. Geterot. Soedin.* **1988**, 1426 (trans. ed. **1988**, 1188).
62. Sadekov, I. D.; Maksimenko, A. A.; Maslakov, A. G.; Minkin, V. I. *J. Organomet. Chem.* **1990** *391*, 179.
63. Singh, H. B.; Sudha, N.; West, A. A.; Hamor, T. A. *J. Chem Soc., Dalton Trans.* **1990**, 907.
64. Singh, H. B.; Sudha, N.; Butcher, R. T. *Inorg. Chem.* **1992**, *31*, 1431.
65. Al-Rubaie, A. Z.; Al-Salim, N. I.; Al-Jadaon, S. A. N. *J. Organomet. Chem.* **1993**, *443*, 67.
66. Cobbledick, R. E.; Einstein, F. W. B.; McWhinnie, W. R.; Musa, F. H. J. *J. Chem Research (S)* **1979**; 145. *J. Chem. Research (M)* **1979**, 1901.
67. Ahmed, M. A. K.; McWhinnie, W. R.; Hamor, T. A. *J. Organomet. Chem.* **1985**, *281*, 205.
68. Ahmed, M. A. K.; McWhinnie, W. R.; Hamor, T. A. *J. Organomet. Chem.* **1985**, *293*, 219.
69. Ahmed, M. A. K.; McCarthy, A. E.; McWhinnie, W. R.; Berry, F. J. *J. Chem. Soc., Dalton Trans.* **1986**, 771.

70. Brown, C. J. *Acta Cryst.* **1966**, *21*, 146.

71. Abakarov, G. M.; Shabson, A. A.; Sadekov, I. D.; Garnovskii, X.; Minkin, V. I. *Khim. Geterot. Soedin.* **1988**, 276 (trans. ed. **1988**, 232).

72. Chakravorty, R.; Irgolic, K. J.; Meyers, E. A. *Acta Cryst.* **1985**, *C41*, 1545.

73. Michalak, R. S.; Martin, J. C.; Wilson, S. R. *J. Am. Chem. Soc.* **1984**, *106*, 7529.

74. Fujihara, H.; Takaguchi, Y.; Furukawa, N. *Chem. Lett.* **1992**, 501.

75. Fujihara, H.; Uehara, T.; Erata, T.; Furukawa, N. *Chem. Lett.* **1993**, 263.

76. Fujihara, H.; Takaguchi, Y.; Ninoi, T.; Erata, T.; Furukawa, N. *J. Chem. Soc., Perkin Trans. I* **1992**, 2583.

Chemistry of Heterocyclic Compounds, Volume 53
Michael R. Detty, Marrie B. O'Regan

Index